MOLECULAR MECHANISMS OF NEUROPATHIC PAIN AND NOVEL THERAPEUTIC TARGETS

EDITED BY: Wuping Sun, Yong Chen, Tao Liu and Xiaodong Liu

PUBLISHED IN: Frontiers in Molecular Neuroscience

frontiers Research Topics

frontiers

ISSN 1664-8714
ISBN 978-2-88974-466-4
DOI 10.3389/978-2-88974-466-4

About Frontiers

Frontiers is more than just an open-access publisher of scholarly articles: it is a pioneering approach to the world of academia, radically improving the way scholarly research is managed. The grand vision of Frontiers is a world where all people have an equal opportunity to seek, share and generate knowledge. Frontiers provides immediate and permanent online open access to all its publications, but this alone is not enough to realize our grand goals.

Frontiers Journal Series

The Frontiers Journal Series is a multi-tier and interdisciplinary set of open-access, online journals, promising a paradigm shift from the current review, selection and dissemination processes in academic publishing. All Frontiers journals are driven by researchers for researchers; therefore, they constitute a service to the scholarly community. At the same time, the Frontiers Journal Series operates on a revolutionary invention, the tiered publishing system, initially addressing specific communities of scholars, and gradually climbing up to broader public understanding, thus serving the interests of the lay society, too.

Dedication to Quality

Each Frontiers article is a landmark of the highest quality, thanks to genuinely collaborative interactions between authors and review editors, who include some of the world's best academicians. Research must be certified by peers before entering a stream of knowledge that may eventually reach the public - and shape society; therefore, Frontiers only applies the most rigorous and unbiased reviews.
Frontiers revolutionizes research publishing by freely delivering the most outstanding research, evaluated with no bias from both the academic and social point of view. By applying the most advanced information technologies, Frontiers is catapulting scholarly publishing into a new generation.

What are Frontiers Research Topics?

Frontiers Research Topics are very popular trademarks of the Frontiers Journals Series: they are collections of at least ten articles, all centered on a particular subject. With their unique mix of varied contributions from Original Research to Review Articles, Frontiers Research Topics unify the most influential researchers, the latest key findings and historical advances in a hot research area! Find out more on how to host your own Frontiers Research Topic or contribute to one as an author by contacting the Frontiers Editorial Office: frontiersin.org/about/contact

MOLECULAR MECHANISMS OF NEUROPATHIC PAIN AND NOVEL THERAPEUTIC TARGETS

Topic Editors:
Wuping Sun, Shenzhen University, China
Yong Chen, Duke University, United States
Tao Liu, The First Affiliated Hospital of Nanchang University, China
Xiaodong Liu, The Chinese University of Hong Kong, China

Citation: Sun, W., Chen, Y., Liu, T., Liu, X., eds. (2022). Molecular Mechanisms of Neuropathic Pain and Novel Therapeutic Targets. Lausanne: Frontiers Media SA. doi: 10.3389/978-2-88974-466-4

Table of Contents

frontiers in Molecular Neuroscience

ORIGINAL RESEARCH
published: 17 May 2021
doi: 10.3389/fnmol.2021.665931

Transcriptome Analysis Reveals the Role of Cellular Calcium Disorder in Varicella Zoster Virus-Induced Post-Herpetic Neuralgia

Songbin Wu[1†], Shaomin Yang[1†], Mingxi Ou[2], Jiamin Chen[3], Jiabing Huang[1], Donglin Xiong[1], Wuping Sun[1] and Lizu Xiao[1*]*

[1] Shenzhen Municipal Key Laboratory for Pain Medicine, Department of Pain Medicine, Shenzhen Nanshan People's Hospital, The 6th Affiliated Hospital of Shenzhen University Health Science Center, Shenzhen, China, [2] Department of Chemistry, University of Science and Technology of China, Hefei, China, [3] Vanke Bilingual School (VBS), Shenzhen, China

As a typical neuropathic pain, post-herpetic neuralgia (PHN) is a common complication of herpes zoster (HZ), which seriously affects the normal life and work of patients. The unclear pathogenesis and lack of effective drugs make the clinical efficacy of PHN unsatisfactory. Here, we obtained the transcriptome profile of neuroblastoma cells (SH-SY5Y) and DRG in rats infected with varicella zoster virus (VZV) by transcriptome sequencing (RNA-Seq) combined with publicly available gene array data sets. Next, the data processing of the transcriptome map was analyzed using bioinformatics methods, including the screening of differentially expressed genes (DEGs), Gene Ontology (GO), and the Kyoto Encyclopedia of Genes and Genomes (KEGG) analysis. Finally, real-time fluorescent quantitative PCR (qRT-PCR) was used to detect the expression of calcium-related genes, and calcium fluorescent probes and calcium colorimetry were used to evaluate the distribution and content of calcium ions in cells after VZV infection. Transcriptome data analysis (GO and KEGG enrichment analysis) showed that calcium disorder played an important role in SH-SY5Y cells infected by VZV and dorsal root ganglion (DRG) of the PHN rat model. The results of qRT-PCR showed that the expression levels of calcium-related genes *BHLHA15*, *CACNA1F*, *CACNG1*, *CHRNA9*, and *STC2* were significantly upregulated, while the expression levels of *CHRNA10*, *HRC*, and *TNNT3* were significantly downregulated in SH-SY5Y cells infected with VZV. Our calcium fluorescent probe and calcium colorimetric test results showed that VZV could change the distribution of calcium ions in infected cells and significantly increase the intracellular calcium content. In conclusion, our results revealed that the persistence of calcium disorder caused by VZV in nerve cells might be a crucial cause of herpetic neuralgia, and a potential target for clinical diagnosis and treatment of PHN.

Keywords: post-herpetic neuralgia, RNA-seq, VZV, calcium-related genes, calcium channel, Ca^{2+}

OPEN ACCESS

Edited by:
Guilherme Lucas, University of São Paulo, Brazil

Reviewed by:
Guang-Yin Xu, Soochow University, China
Xiaodong Liu, Beijing University of Chinese Medicine, China

****Correspondence:***
Wuping Sun
wuping.sun@foxmail.com;
wupingsun@email.szu.edu.cn
Lizu Xiao
nsyyjoe@live.cn

† These authors have contributed equally to this work

Specialty section:
This article was submitted to Pain Mechanisms and Modulators, a section of the journal Frontiers in Molecular Neuroscience

Received: *09 February 2021*
Accepted: *09 April 2021*
Published: *17 May 2021*

Citation:
Wu S, Yang S, Ou M, Chen J, Huang J, Xiong D, Sun W and Xiao L (2021) Transcriptome Analysis Reveals the Role of Cellular Calcium Disorder in Varicella Zoster Virus-Induced Post-Herpetic Neuralgia. Front. Mol. Neurosci. 14:665931. doi: 10.3389/fnmol.2021.665931

INTRODUCTION

As a member of the alphaherpesvirinae subfamily, varicella zoster virus (VZV) is a common human pathogen that causes chickenpox during the initial infection, and reactivation from latently infected sensory neurons can cause herpes zoster (HZ) (Oliver et al., 2017; Yang et al., 2017). As a common complication of HZ, neuropathic pain is generally considered to be associated with neuronal

damage and inflammation caused by reactivated VZV (Gilden et al., 2000; Gnann and Whitley, 2002). The outbreak of HZ rash usually precedes neuropathic pain, and after the rash is cured, neuropathic pain and discomfort such as allodynia and itching may develop further, eventually resulting in "post-herpetic neuralgia" (PHN) (Oxman et al., 2008). Herpetic neuralgia is usually defined as persistent pain and often accompanied by burning and hyperalgesia, a type of severe pain that can be triggered by touching or rubbing the affected area (O'Connor and Paauw, 2013; Silva et al., 2017). Although the use of anti-herpes drugs (such as acyclovir and famciclovir) in the early stage of HZ is conducive to shortening the duration of skin lesions and reducing the complications associated with HZ to a certain extent, the pain is unable to be completely cured (Li et al., 2009; Field and Vere Hodge, 2013). In clinics, antidepressants, non-steroidal anti-inflammatory drugs (NSAIDs), and sympathetic nerve blockers are also commonly used to relieve herpetic neuralgia, but these treatments often fail to prevent the development of PHN (Gan et al., 2013). Besides, the HZ virus vaccines cannot completely eliminate the occurrence of PHN, although it achieves some success in preventing the occurrence of shingles and herpetic neuralgia (Walker et al., 2018; Lang and Aspinall, 2019). All in all, the lack of precise pathological mechanism and effective drugs makes the clinical treatment of PHN unsatisfactory.

Central nervous system diseases, including neuropathic pain, are usually associated with abnormal neuronal calcium homeostasis and calcium signaling (Hagenston and Simonetti, 2014). More and more evidence has shown that second messenger calcium and calcium-dependent pathways played an important role in central sensitization (Luo et al., 2008). In fact, several reports have confirmed that abnormal calcium channel physiology and expression are not only associated with neuropathic pain and diabetic neuralgia, but also chronic inflammatory pain and bone cancer pain (Fossat et al., 2010; Naziroglu et al., 2012; Bourinet et al., 2014; Hagenston and Simonetti, 2014; Liu et al., 2018). However, there are many significant differences in the underlying mechanisms of different pain patterns, and there is also diversity in calcium regulation changes in pain models caused by specific injury patterns or diseases (Xu and Yaksh, 2011; Hagenston and Simonetti, 2014). These changes in calcium regulation usually cause the accumulation of calcium ions in cells, and eventually lead to disturbances in the calcium signal activity triggered by synapses (Raymond and Redman, 2006; Hagenston and Bading, 2011; Bading, 2013). Furthermore, calcium signals have been confirmed to be involved in pain signal transduction of cells and functional plasticity changes, ultimately affecting the occurrence and persistence of pain (Hagenston and Simonetti, 2014). However, there is no report about calcium signals in herpetic neuralgia, and the role of calcium signals in the occurrence and development of PHN is still unclear.

Here, we obtained the transcriptome map of VZV-infected neuroblastoma (SH-SY5Y) cells through *in vitro* experiments. By Gene Ontology (GO) enrichment and Kyoto Encyclopedia of Genes and Genomes (KEGG) analysis of the differentially expressed genes (DEGs) produced by VZV infection of SH-SY5Y cells, we have obtained preliminary evidence that calcium signals are involved in nerve cell response to VZV. Next, we combined with the reported gene chip data of DRGs in the rat model of herpetic neuralgia induced by VZV, and further confirmed the important role of calcium signals in the rat model of herpetic neuralgia. Additionally, the VZV-infected SH-SY5Y cell transcriptome profile and the VZV-induced herpetic neuralgia rat DRG gene chip data were compared to obtain 52 identical DEGs. The enrichment results indicated that these identical DEGs were mainly related to the regulation of calcium signals. Finally, qRT-PCR, calcium fluorescence probe, and calcium colorimetric assay were used to reveal the direct evidence of VZV induced intracellular calcium disorder. Therefore, we speculated that the disturbance of intracellular calcium signals caused by VZV might be related to the occurrence of PHN and the maintenance of persistent pain.

MATERIALS AND METHODS

Ethics Statement

This study was approved by the Ethics Committee of Shenzhen Nanshan People's Hospital and The 6th Affiliated Hospital of Shenzhen University Health Science Center.

Cells and Cell Culture

SH-SY5Y (ATCC, CRL-2266) and ARPE-19 (ATCC, CRL-2302) cells were cultured in Dulbecco's Modified Eagle medium (DMEM) with 10% fetal bovine serum (FBS) and penicillin-streptomycin (100 U/ml and 100 μg/ml), all from Gibco/Life Technology. All cells were cultured at 37°C in a 5% CO_2 atmosphere.

Viruses and Infection

Varicella zoster virus recombinant Oka strain carrying GFP reporter gene (rOka-GFP), kindly provided by Tong Cheng (Development in Infectious Diseases, Xiamen University, Xiamen, China), propagated in ARPE-19 cells to generate cell-associated progeny virus. VZV has a distinctive cell-associated nature, and the virus inoculants were prepared from VZV-infected ARPE-19 monolayer cells with marked and equivalent-appearing cytopathic effect (CPE) reaching >80% of cells. As previously reported, a cell-free virus was produced from ARPE-19 cells infected with VZV. Briefly, ARPE-19 cells were infected with the virus and the supernatant and cell pellets were collected when about 80% of the cells developed severe CPEs (Jiang et al., 2017). The cell pellets collected from three T-175 bottles were resuspended in 5 ml of DMEM. The virus particles were released from the cells by ultrasonic treatment (noise isolating chamber; 20 kHz, 45% amplitude, 15 s) and centrifuged at low speed (Beckman microfuge 20R; 1,000 × *g*, 5 min, 4°C) to remove cell debris. The supernatant obtained from cell lysis was combined with cell culture supernatant and centrifuged at high speed (Beckman rotor sw32; 80,000 × *g*, 3 h, 4°C) to concentrate the virus. The centrifuged virus precipitate was resuspended in 200 μl DMEM, and the viral titer was determined by plaque formation in ARPE-19 cells. All the virus experiments were

carried out in a biosafety laboratory under appropriate ethical and safety approval. The study was performed according to the guidelines of the competent national authority.

Total RNA Extraction

Before virus infection, SH-SY5Y (8×10^5 cells/ml) and ARPE-19 (8×10^5 cells) were seeded in a six-well cell plate at an initial seeding density of 80% of the cell-attached area. The next day, cells were infected with 1×10^4 plaque-forming units (PFU)/ml cell-free VZV. The cells were digested with trypsin and harvested at 1×10^3 rpm after 24 and 48 h of virus infection, respectively. The cell pellet harvested by centrifugation was treated with TRIzol Reagent (Invitrogen, United States) according to the manufacturer's manual. RNA precipitation was dissolved in RNase-free water (Thermo Fisher Scientific, United States), and RNA samples were treated with DNase (TaKaRa, Japan). All nucleic acids were quantified on a nanodrop spectrophotometer (Thermo Fisher Scientific, United States), and the OD-(260)/OD-(280) ratio of the total RNA was between 1.8 and 2.0. The total RNA of the samples meeting the above criteria was stored in a freezer at −80°C until use.

RNA Sequence and Data Analysis

SH-SY5Y cells were infected with 1×10^4 PFU/ml cell-free VZV-rOka for 24 h and 48 h, respectively. The cells of each group were harvested and dissolved in TRIzol Reagent ($n = 3$ per group). The mRNA library construction and transcriptome sequencing of each sample was completed by Beijing Genomics Institute (BGI, Shenzhen, China). BGISEQ-500 high-throughput sequencing platform was used to pair sequence the cDNA of the RNA fragment, and 6 G average raw data of each sample were obtained. SOAPnuke (v1.5.2) was used to filter the raw data of sequencing, including removed adapter contamination, low-quality base ratio, and unknown base ("N" base); afterward, clean reads were obtained and stored in FASTQ format (Li et al., 2008). The clean reads were mapped to the human genome (hg19) using HISAT2 (v2.0.4) with Q-value ≤ 0.05 (Kim et al., 2015). Bowtie2 (v2.2.5) was applied to align the clean reads to the reference coding gene set; then, the expression level of the gene was calculated by RSEM (v1.2.12) (Li and Dewey, 2011; Langmead and Salzberg, 2012). According to the quantitative results of gene expression, we screened DEGs among samples based on DEseq2 and edgeR algorithm (Robinson et al., 2010; Love et al., 2014). The gplots R package was used to construct the heatmaps[1], and Draw Venn Diagram online tool was used to generate the Venn diagram[2]. Functional classification of DEGs between groups was performed using the DAVID 6.8[3] (Huang et al., 2009) and KOBAS 3.0[4] (Xie et al., 2011; Shen et al., 2019) online database. The sequencing data set supporting the results of this article has been submitted to the NCBI Gene Expression Omnibus (GEO) database, and the accession number is GSE141932. The transcriptome data set of dorsal root ganglion (DRG) in a rat model of PHN induced by VZV was obtained from GEO, and the access number is GSE64345.

[1]http://cran.r-project.org/web/packages/gplots/index.html

[2]http://bioinformatics.psb.ugent.be/webtools/Venn/

[3]https://david.ncifcrf.gov/

[4]http://kobas.cbi.pku.edu.cn/kobas3

qRT-PCR for mRNA Quantification

Total RNA was extracted by using TRIzol Reagent (Invitrogen, United States), followed by treatment with 10 U of DNase (TaKaRa, Japan). The synthesis of cDNA from 500 ng of total RNA was reverse transcribed using SuperScript® III CellsDirect cDNA Synthesis Kit (Invitrogen, United States). The primers were designed using Primer-BLAST from the National Center for Biotechnology Information (NCBI) (**Table 1**). Gene expression quantification was determined by qRT-PCR using Fast SYBR™ Green Master Mix (Applied Biosystems, United States) following the manufacturer's instructions. Data were collected and analyzed using ABI-7500 software (Applied Biosystems, United States). The results were normalized to a housekeeping gene (*GAPDH*) and relative expression shown as $2^{-\Delta\Delta Ct}$.

Western Blot Analysis

ARPE-19 and SH-SY5Y cells were treated with 1×10^4 PFU/ml of cell-free VZV for 48 h. Using Western and IP cell lysate, we successfully extracted the total cellular protein, and then a 10% sodium dodecyl sulfate-polyacrylamide (SDS-PAGE) gel was used to separate the proteins. The protein was then transferred onto the PVDF membrane (Millipore, United States), which would later be blocked with 5% non-fat dry milk (Bio-Rad, United States) dissolved in TBS-T for 1 h at room temperature. The antibodies were then incubated at 4°C overnight: anti-VZV gE antibody (ab272686) (Abcam, United States; 1:2000) and anti-β-Actin (#4970) (Cell Signaling Technology, United States; 1:2000). The next day, after TBS-T washing three times, HRP-conjugated secondary antibodies (ProteinTech, United States, 1:5000) were performed to be combined with the primary antibodies. Finally, the immunoblots were visualized by using an ECL substrate kit (Millipore, United States).

Assessment of Intracellular Ca^{2+}

The content of Ca^{2+} in the cells was measured by fluorescent Ca^{2+} indicator Rhod-2 AM (#40776ES50, Yeasen, China). According to the manufacturer's manual, ARPE-19 cells were infected with VZV for 72 h, and the medium was removed and the cells were rinsed with 1 × PBS at room temperature three

TABLE 1 | Sequences of the primer for quantitative real-time RT-PCR.

Gene name	Forward primer (5′–3′)	Reverse primer (5′–3′)
ORF61	ACATCCCTGCGTTGTCTTT	TTGAGGTGGTTTCTGGTCTTA
GAPDH	CTGGGCTACACTGAGCACC	AAGTGGTCGTTGAGGGCAATG
BHLHA15	CGGATGCACAAGCTAAATAACG	GCCGTCAGCGATTTGATGTAG
CACNA1F	GGAAGCCCTTCGACATCCTC	GTAGGCCACGATCTTGAGCAC
CACNG1	GACAGCCGTGGTAACCGAC	GCTTGGTACAAATCCGCCAGA
CHRNA9	AAATCTGGCACGATGCCTATC	GCAGGACCACATTGGTGTTCA
CHRNA10	CAGATGCCTACCTACGATGGG	GGGAAGGCTGCTACATCCA
HRC	AGAGAATGGGCATCATTTCTGG	TCATCTCCGACTTTGTGGTCTT
STC2	GCGTGCAGGTTCAGTGTGA	GGCCAGTCTCCCTACTGCT
TNNT3	AGGAGCTGGTCGCTCTCAA	CCTTCTCTGCACGAATCCTCT

times. After staining with 4 μM Rhod-2 AM for 30 min at room temperature (25°C), the fluorescent indicator was removed. The cells were rinsed with 1 × PBS at room temperature three times before observation and then placed in a 37°C, 5% carbon dioxide humidified incubator for 30 min. The images were taken by the laser confocal microscope (Olympus FV3000, Japan) at the excitation wavelength of 549/578 nm.

Calcium Assay

According to the manufacturer's calcium colorimetric assay kit (# S1063S, Beyotime Biotechnology, China) operating manual, we determined the calcium ion content of the VZV-infected ARPE-19 and SH-SY5Y cell lysate and culture supernatant. After VZV infects ARPE-19 and SH-SY5Y cells, the cell culture medium is collected and rinsed with pre-cooled 1 × PBS two to three times. Add 200 μl of pre-cooled sample lysate to each sample to make the sample lysate fully contact the cells. After the cells are fully lysed, collect the cell lysate at 4°C, centrifuge at 12,000 × *g* for 5 min, and aspirate the supernatant. The standard curve of calcium ion content was obtained by calcium standard solution and chromogenic solution, and the absorbance value of each sample was quantified as the corresponding calcium ion concentration.

Statistical Analysis

All quantitative data were presented as mean ± standard deviations (SD) from three or more independent experiments. The quantitative data were analyzed by one-way analysis of variance (ANOVA), and the statistical significance was analyzed by GraphPad Prism 8 (GraphPad Software, La Jolla, CA, United States). Fisher's exact test was used to assess the differential expression of genes (Robinson and Oshlack, 2010). For the screening of DEGs, the genes with *q*-values lower than 0.05 and with a fold change ≥2 are considered to differentially expressed. Data were considered significant if $P < 0.05$ (*), $P < 0.01$ (**), or $P < 0.001$ (***).

RESULTS

ARPE-19 and SH-SY5Y Cells Infected With VZV

Virus infection has strict species specificity, usually requiring to be parasitized in specific types of cells to meet the needs of virus replication. As previously reported, ARPE-19 cells and SH-SY5Y cells showed obvious cytopathic states such as roundness, swelling, and syncytial formation after 48 h of VZV infection compared with normal cells (MOCK group without virus infection) (**Figure 1A**; Jiang et al., 2017; Shakya et al., 2019). To further verify the successful infection of VZV, we measured the expression of *ORF61* gene encoding the virus early phosphorylation protein by qRT-PCR and evaluated the expression of VZV membrane glycoprotein E (gE) by Western blot. As shown in **Figures 1B,C**, the expression of *ORF61* gene

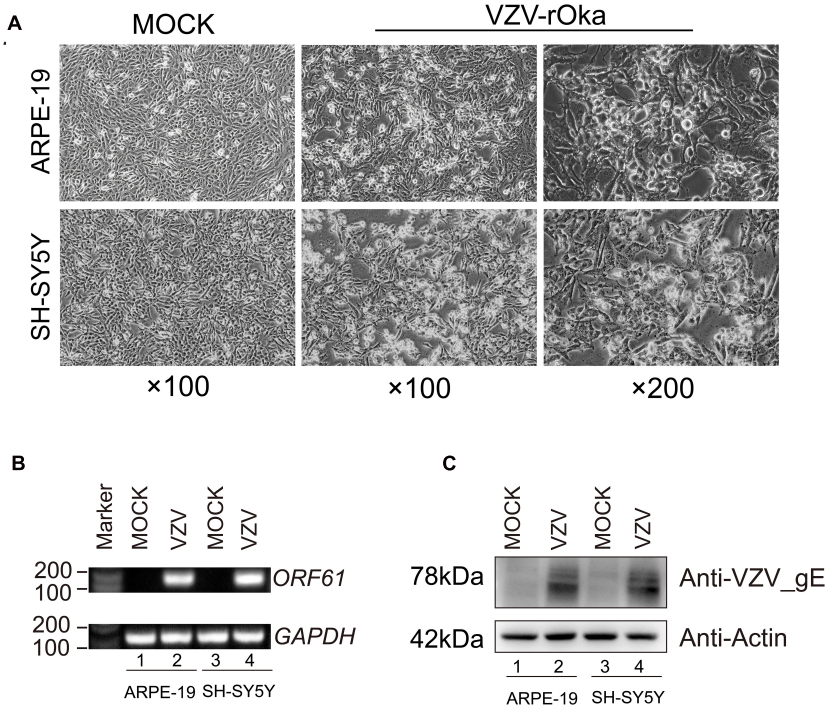

FIGURE 1 | ARPE-19 and SH-SY5Y cells infected with VZV induced obvious cytopathic changes. **(A)** ARPE-19 and SH-SY5Y cells infected with VZV for 48 h induce obvious cytopathic changes, and cells not infected with (MOCK) virus maintain normal morphology and growth. **(B)** Real-time quantitative PCR was used to measure the expression of *ORF61* encoding the early phosphorylation protein of virus in ARPE-19 cells and SH-SY5Y cells after 48 h of VZV infection. **(C)** Western blot was used to evaluate the expression of VZV glycoprotein gE in ARPE-19 cells and SH-SY5Y cells.

and gE protein was observed in ARPE-19 cells and SH-SY5Y cells after 48 h of VZV infection, while no corresponding bands were observed in mock group cells. In conclusion, our results showed that VZV successfully infected ARPE-19 cells and SH-SY5Y cells and expressed viral genes and proteins in infected cells.

Gene Ontology Analysis of DEGs in SH-SY5Y Cells Infected With VZV

To clarify the molecular mechanism of post-herpes neuralgia induced by VZV, we used VZV to infect SH-SY5Y cells to map the transcriptome changes of VZV-infected nerve cells. Transcriptome data were generated by RNA-Seq after infection of SH-SY5Y cells with VZV for 24 and 48 h, respectively. Quantitative expression of all genes was obtained by data quality control, filtering, and mapping, and differential expression genes were generated by deseq2 and edge algorithm. The purpose of obtaining DEGs is to reveal the differences between samples at the level of gene transcription. **Figure 2** shows the representative distribution of upregulated or downregulated genes in SH-SY5Y cells after VZV infection. Our data showed that after 24 h of VZV infection, 1,373 genes were upregulated and 1,000 genes were downregulated in SH-SY5Y cells (**Figure 2A**). After 48 h of virus infection, 1,243 genes were upregulated and 1,661 genes were downregulated in SH-SY5Y cells (**Figure 2B**).

To better explore the related functions of DEGs in SH-SY5Y cells infected with VZV, the GO analysis was used to enrich and classify DEGs (**Figure 3**). **Figure 3** shows the top 20 highly representative GO terms rich in DEG, which contributes to understanding the response of SH-SY5Y cells to VZV. GO analysis clarified the top 20 biological processes of DEGs, including "inflammatory response," "immune response," "response to lipopolysaccharide," "chemotaxis," "positive regulation of cytosolic calcium ion concentration," and "calcium-independent cell–cell adhesion via plasma membrane cell-adhesion molecules," indicating that VZV infection caused strong inflammatory and immune responses in SH-SY5Y cells, and calcium ions might be involved in the pathogenicity of the virus. It identified and enriched the top 20 cellular component terms associated with "extracellular region," "cell junction," "postsynaptic membrane," "secret granule," and "voltage gated potential channel complex," indicating that the response to VZV in SH-SY5Y cells involved sensory neuron signal transduction and intercellular communication. Moreover, enriched molecular functions were defined to be associated with "calcium ion binding," "receptor binding," "cytokine activity," "receptor activity," and "calcium channel activity," implying that cell signal transduction and calcium ion transport were induced in SH-SY5Y cells by VZV infection. In conclusion, GO analysis revealed that inflammatory response, immune response, signal transduction, and calcium channel transport activities were mainly the response of SH-SY5Y cells to VZV infection.

KEGG Analysis of DEGs in SH-SY5Y Cells Infected With VZV

In order to obtain signal pathways and disease classifications enriched by DEGs after VZV infection in SH-SY5Y cells, we used the KOBAS 3.0 online database to annotate the host DEGs produced by the virus. The DEGs produced by VZV are significantly enriched in "neuroactive ligand–receptor interaction," "cytokine–cytokine receptor interaction," "chemokine signaling pathway," and "calcium signaling pathway" (**Figure 4**). These results indicated that VZV infection causes significant signal transduction and calcium signal activity in SH-SY5Y cells. In addition, we further characterized the DEGs through the KEGG DISEASE database. As shown in **Figure 5**, the results of KEGG DISEASE showed that DEGs were mainly enriched in "nervous system diseases," "immune system diseases," "skin diseases," and "other nervous and sensory system diseases." The results showed that the DEGs induced by VZV in SH-SY5Y cells were mainly involved in neurological and sensory diseases. The above results further confirmed that signal transduction, immune response, and calcium signal activity were involved in neurological and sensory diseases induced by VZV.

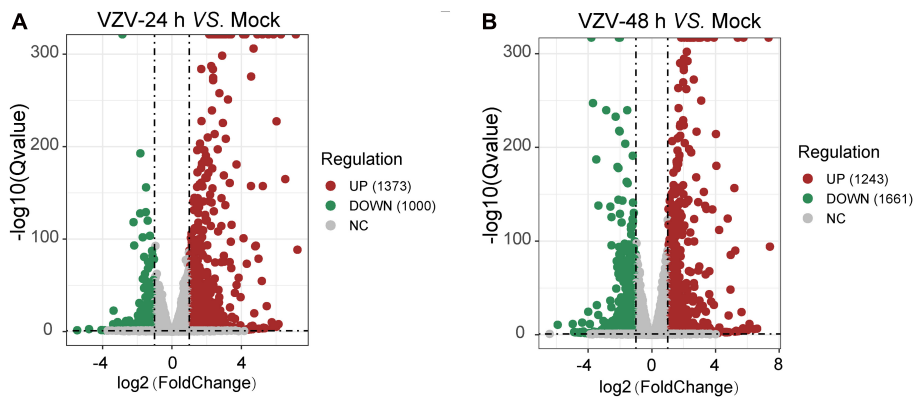

FIGURE 2 | A mass number of DEGs were induced by VZV in SH-SY5Y cells. **(A)** Volcanic map showed the number and distribution of DEGs in SH-SY5Y cells after 24 h of VZV infection. **(B)** Volcanic map showed the number and distribution of DEGs in SH-SY5Y cells after 48 h of VZV infection. Volcano map showed that VZV group had significant mRNA expression compared with mock without VZV infection. Log_2 (Fold change) and log_{10} (Q-value) of DEGs are expressed as abscissa and ordinate, respectively. The significantly upregulated genes are shown in red and the significantly downregulated genes are shown in green.

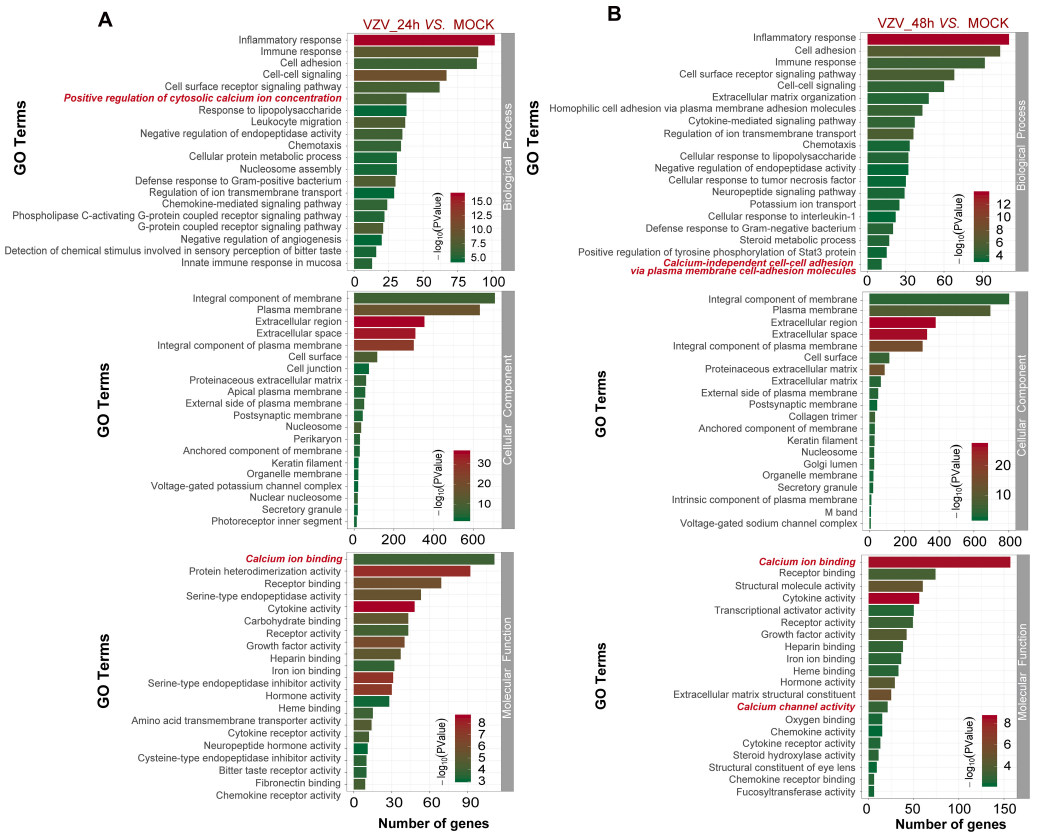

FIGURE 3 | The functional enrichment of DEGs was analyzed by gene ontology classification. **(A)** GO analysis of DEGs in SH-SY5Y cells 24 h after VZV infection. **(B)** GO analysis of DEGs in SH-SY5Y cells 48 h after VZV infection. The number of DEGs was plotted as abscissa and GO terms were plotted as ordinate. It shows the top 20 highly representative GO terms enriched in DEGs, including biological processes, cellular components, and molecular functions.

Transcriptome Comparison Between SH-SY5Y Cells Infected With VZV and DRG in Rats With VZV-Induced PHN

Neuronal damage caused by VZV infection is generally considered to be related to the formation of neuralgia after HZ. Nerve damage is usually accompanied by dysfunction of ion channels. The dysfunction of ion channels causes abnormal ion signals in cells, which will be the cause of pain and persistence. Compared with the mock group without virus infection, our RNA-Seq results showed that the DEGs produced by VZV-infected neuroblastoma cells significantly enriched the biological processes related to calcium channels and calcium signals (**Figures 3**, **4**). To further clarify the role of calcium signals in PHN, as previously reported, we analyzed the gene expression microarray data in the L4–L5 dorsal root ganglia of rats with herpetic neuralgia induced by VZV. As shown in **Supplementary Figure 1**, GO analysis showed that compared with the control group, the DEGs in DRG of herpetic neuralgia rats were mainly enriched in "cellular calcium ion homeostasis," "positive regulation of cytosolic calcium ion concentration," "biological process," "voltage gated calcium channel complex" cell component, and "calcium ion binding" molecular function. Consistent with the results of GO enrichment, KEGG signaling pathway analysis also showed that the DEGs in DRG of herpetic neuralgia rats were mainly enriched in "calcium signaling pathway" (**Supplementary Figure 2**). These results unanimously indicated that the calcium disorder induced by VZV infection may be involved in the occurrence and development of herpetic neuralgia.

Next, we used the Draw Venn Diagram online tool to obtain a total of 52 identical DEGs in VZV-infected SH-SY5Y cells and VZV-induced DRG in herpetic neuralgia rats (**Figure 6A**). In addition, we used a heatmap to show the expression levels of these 52 identical DEGs based on the normalized expression amount (FPKM) of each gene (**Figure 6B**). Interestingly, after GO enrichment and KEGG signal analysis of these 52 identical DEGs, these identical DEGs were also closely related to calcium signaling (**Table 2**). In conclusion, these results further indicated that calcium signaling might play a significant role in post-herpes neuralgia induced by VZV.

VZV Infection Causes Abnormal Expression of Calcium-Related Genes in SH-SY5Y Cells

We obtained the gene expression profile of SH-SY5Y cells after VZV infection by RNA-Seq sequencing and compared with the

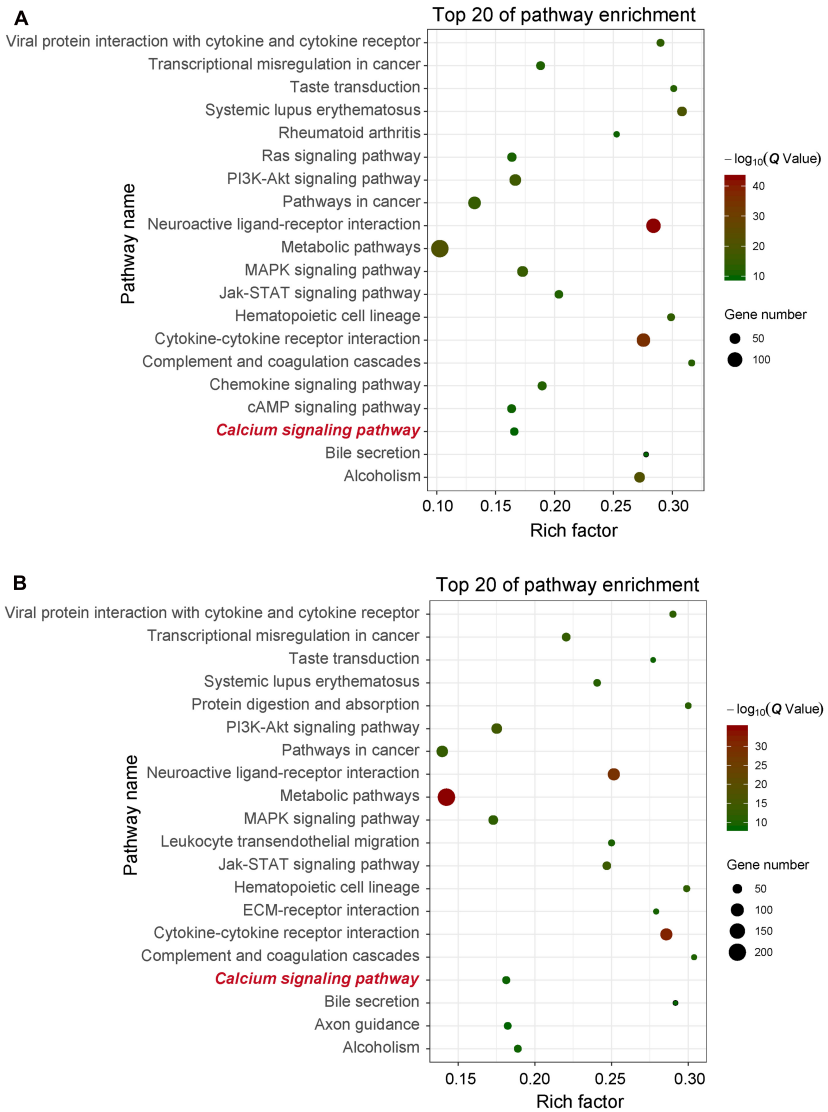

FIGURE 4 | KEGG enrichment of DEGs induced by VZV in SH-SY5Y cells. **(A)** The DEGs enriched KEGG pathway was induced by VZV infection in SH-SY5Y cells for 24 h. **(B)** The DEGs enriched KEGG pathway was induced by VZV infection in SH-SY5Y cells for 48 h. The graph shows the top 20 significantly enriched KEGG pathways by plotting rich factors as abscissa and KEGG terms as ordinates.

DRG gene chip data of PHN rats induced by VZV. These data all indicated that calcium signaling may play an important role in VZV-induced PHN. In **Figure 6**, we have obtained 52 identical DEGs by VZV-infected SH-SY5Y cells and DRG of PHN rats. Using the GeneCards (Fishilevich et al., 2016) online database[5] to annotate these shared DEGs, we got the genes related to calcium signaling as *BHLHA15*, *CACNA1F*, *CACNG1*, *CHRNA9*, *CHRNA10*, *HRC*, *STC2*, and *TNNT3*. We examined the mRNA expression levels of these genes in SH-SY5Y cells 24 h and 48 h after VZV infection. Our results showed that VZV infection of SH-SY5Y cells significantly upregulated the expression of *BHLHA15*, *CACNA1F*, *CACNG1*, *CHRNA9*, and *STC2*, but significantly downregulated the expression of *CHRNA10*, *HRC*, and *TNNT3* (**Figure 7**). These results confirmed the validity of our transcriptome data and suggested that VZV might mediate calcium disorder in SH-SY5Y cells by disrupting the expression of calcium-related proteins. However, the expression patterns of these genes were different in VZV-infected SH-SY5Y cells, suggesting that these genes might be involved in VZV-induced PHN through different mechanisms.

VZV Infection Causes Calcium Signal Disorder in ARPE-19 and SH-SY5Y Cells

In order to obtain further visual evidence that VZV causes calcium disorder in infected cells, we directly assessed the distribution and content of calcium ions in ARPE-19 and SH-SY5Y cells infected with VZV. After 72 h of infecting

[5]https://www.genecards.org/

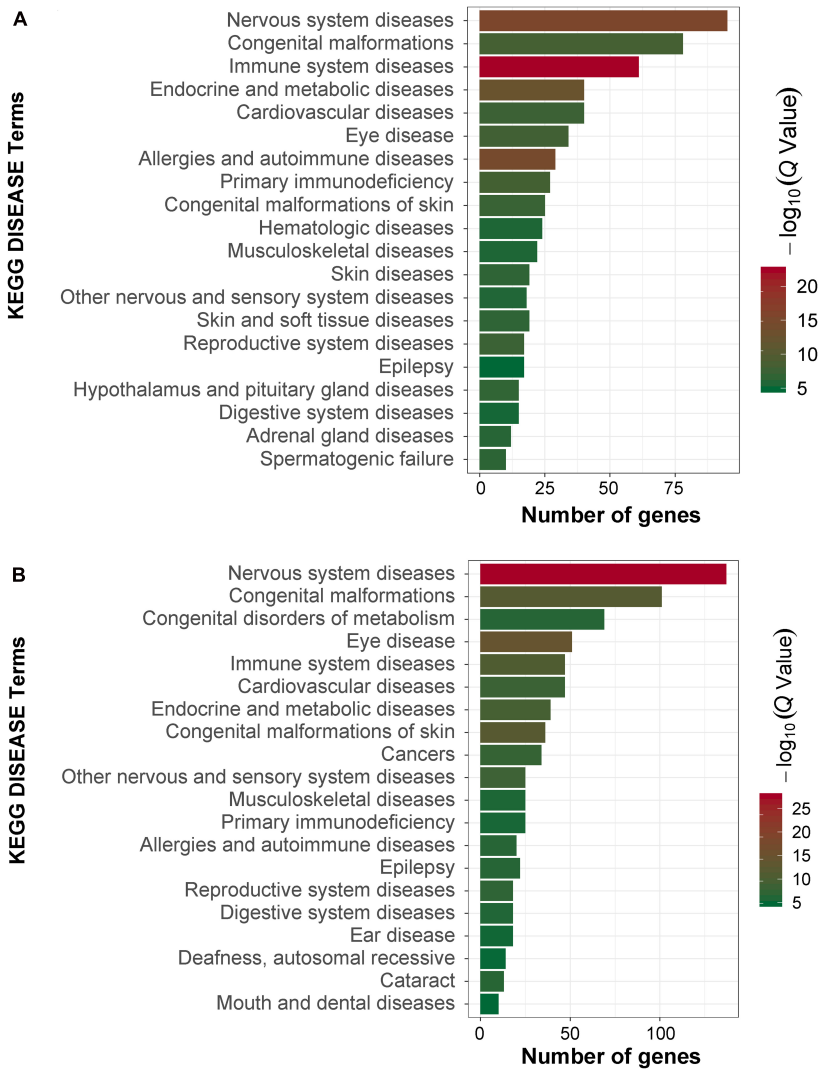

FIGURE 5 | KEGG disease analysis of DEGs in SH-SY5Y cells induced by VZV. **(A)** KEGG disease analysis of DEGs induced by VZV infection of SH-SY5Y cells for 24 h. **(B)** KEGG disease analysis of DEGs induced by VZV infection of SH-SY5Y cells for 48 h. The graph shows the first 20 significantly abundant KEGG diseases by using the number of differentially expressed genes as the abscissa and the KEGG term as the ordinate.

ARPE-19 cells with VZV, we used Rhod-2 AM calcium ion probe to examine the effect of the virus on the distribution of calcium ions in the infected cells. As shown in **Figure 8A**, in ARPE-19 cells without VZV infection, Ca^{2+} was evenly filled into the whole cell (**Figure 8A**, upper part). After infection with VZV for 72 h in ARPE-19 cells, the VZV recombinant strain carrying green fluorescent protein could be clearly observed in ARPE-19 cells (**Figure 8A**, bottom, left). According to the fluorescence images of the nuclear dye Hoechst 33342, we observed that the virus caused ARPE-19 cells to form a significant multi-nucleus syncytial disease state (**Figure 8A**, bottom, right). Interestingly, we found strong Ca^{2+} signals around the cell membrane in VZV-infected cells (**Figure 8A**, bottom, center). These results indicated that VZV might cause intracellular calcium disorder by affecting the distribution of calcium ions in cells.

To clarify the effect of VZV infection on the calcium content in cells, we used the/a calcium colorimetric assay to evaluate the calcium content in cell lysates and cell culture supernatants. The results are shown in **Figures 8B,C**; compared with the mock group, VZV infection significantly increased the calcium content in infected cells (**Figure 8B**, $P < 0.001$), while the calcium ion content in cell culture supernatants did not change significantly before and after the virus infection.

DISCUSSION

The pathogenesis of herpetic neuralgia is complex and unclear, leading to the poor clinical treatment of herpetic neuralgia, especially PHN. In this study, transcriptome sequencing was used to obtain a transcriptional map of neuroblastoma cells

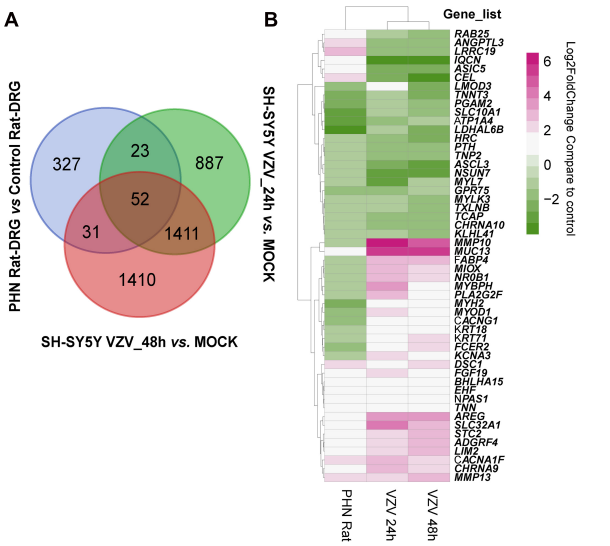

FIGURE 6 | Analysis of the identical DEGs in VZV-infected SH-SY5Y cells and VZV-induced PHN rat DRG. **(A)** The Draw Venn Diagram online tool was used to obtain the identical DEGs in VZV-infected SH-SY5Y cells and VZV-induced PHN rat DRG. **(B)** The Pheatmap package was used to map the gene expression heatmap of the identical DEGs in the DRG of VZV-induced PHN rats and SH-SY5Y cells infected by VZV.

acutely infected with VZV. We tried to reveal the response of nerve cells to VZV infection from the transcription map and explore the evidence that may be related to herpetic neuralgia. Neuroblastoma cells infected with VZV for 48 h showed obvious cytopathic states such as cell rounding, swelling, and syncytial formation (**Figure 1A**). Transcriptome sequencing results demonstrated that thousands of host DEGs were produced in this neurocytopathic state induced by VZV (**Figure 2**). The large number of DEGs induced by VZV also confirmed that VZV in humans would cause great damage to nerve cells from incubation to activation of infection.

The activation and infection of VZV in sensory neurons will cause severe inflammation and immune response, which is the body's defense response to pathogenic microorganisms (Almanzar et al., 2019; Cote-Daigneault et al., 2019). Similarly, our GO enrichment results showed that a large number of VZV-induced DEGs in neuroblastoma cells were mainly related to "inflammatory response," "immune response," "response to lipopolysaccharide," and "chemotaxis" (**Figure 3**). These results indicated that neuroblastoma cells strongly respond to VZV infection. Additionally, we further analyzed and found that the GO enrichment results of these DEGs induced by VZV pointed to "positive regulation of cytosolic calcium ion concentration," "voltage-gated potential channel complex," "calcium ion binding," and "calcium channel activity," suggesting that the intracellular calcium disorder caused by virus might be related to the pathogenicity of virus. KEGG signaling pathway enrichment analysis revealed that the DEGs produced by VZV were mainly enriched in "neuroactive ligand receptor interaction," "cytokine–cytokine receptor interaction," "chemokine signaling pathway," and "calcium signaling pathway"

TABLE 2 | GO enrichment and KEGG pathway analysis of the same DEGs in VZV infected SH-SY5Y cells and VZV induced PHN rats DRG.

Category	Term	Genes
Biological process	Muscle contraction	*MYH2, MYL7, HRC, CACNG1, LMOD3*
	Sarcomere organization	*TCAP, KLHL41, MYLK3*
	Calcium ion transmembrane transport	***CHRNA9, CHRNA10, CACNG1, CACNA1F***
	Muscle filament sliding	*MYH2, TNNT3, TCAP*
	Regulation of striated muscle contraction	*TNNT3, MYBPH*
	Cardiac myofibril assembly	*TCAP, MYLK3*
	Myofibril assembly	*KLHL41, LMOD3*
	Detection of mechanical stimulus involved in sensory perception of sound	*CHRNA9, CHRNA10*
Cellular component	A band	*MYH2, MYL7*
	Myosin filament	*MYH2, MYBPH*
	Pseudopodium	*RAB25, KLHL41*
	M band	*KLHL41, LMOD3*
	Acetylcholine-gated channel complex	*CHRNA9, CHRNA10*
	Extracellular space	*MMP13, PTH, STC2, ANGPTL3, MUC13, CEL, AREG, MMP10*
	Myofibril	*MYH2, MYOD1*
	Voltage-gated calcium channel complex	***CACNG1, CACNA1F***
Molecular function	Integrin binding	*FCER2, TNN, ANGPTL3*
	Tropomyosin binding	*TNNT3, LMOD3*
	Calcium ion binding	***PLA2G2F, MYL7, MMP13, HRC, DSC1, MMP10***
	Acetylcholine-activated cation-selective channel activity	*CHRNA9, CHRNA10*
KEGG pathway	Cardiac muscle contraction	*CACNG1, ATP1A4, CACNA1F, HRC*
	Oxytocin signaling pathway	*CACNG1, MYLK3, CACNA1F, DSC1*
	Pancreatic secretion	*ATP1A4, CEL, PLA2G2F*
	MAPK signaling pathway	*CACNG1, FGF19, CACNA1F, AREG*
	Adrenergic signaling in cardiomyocytes	*CACNG1, ATP1A4, CACNA1F*
	cGMP-PKG signaling pathway	*ATP1A4, MYLK3, CACNA1F*
	Calcium signaling pathway	***CACNA1F, MYLK3, HRC***
	Focal adhesion	*MYL7, TNN, MYLK3*
	Endocrine and other factor-regulated calcium reabsorption	***ATP1A4, PTH***

Bold values represents calcium related items and genes.

(**Figure 4**). Consistently, our transcriptome data suggested that calcium signaling disorders play an important role in VZV-induced neuroblastoma cell lesions. Previous reports have shown that VZV infection induced sensitivity to adrenergic stimulation in cultured nociceptive DRG neurons, causing Ca^{2+} levels to increase after stimulation with norepinephrine or

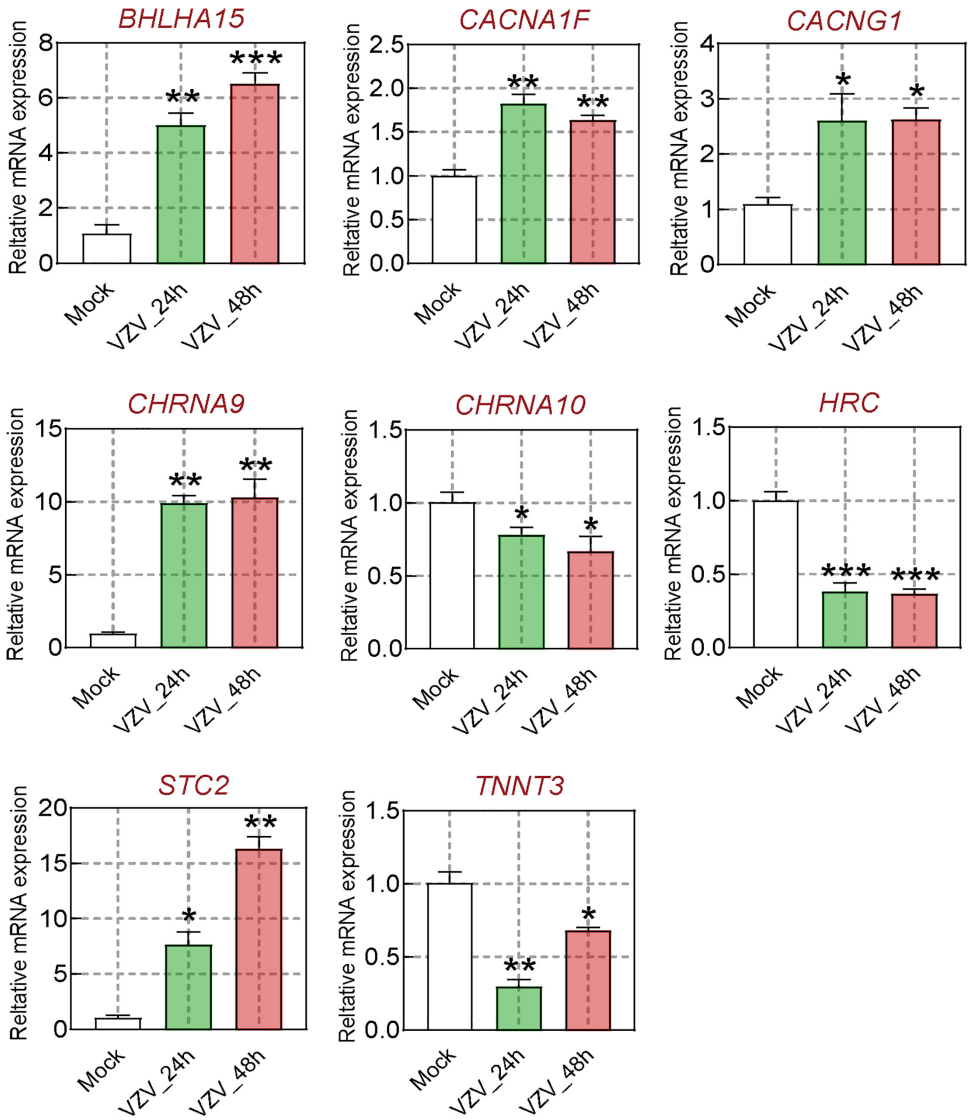

FIGURE 7 | The calcium signal DEGs were verified by qRT-PCR. After VZV-infected SH-SY5Y cells for 24 and 48 h, respectively, qRT-PCR was used to quantify the expression levels of *BHLHA15*, *CACNA1F*, *CACNG1*, *CHRNA9*, *CHRNA10*, *HRC*, *STC2*, and *TNNT3* genes. Data are expressed as the mean ± SD from at least three independent experiments (compared to the Mock group, $^{*}P < 0.05$, $^{**}P < 0.01$, $^{***}P < 0.001$).

adrenergic agonists (Schmidt et al., 2003). The increase in Ca^{2+} is considered to be consistent with pain and hyperalgesia and is also involved in heat sensitization and thermal hyperalgesia of nociceptors (Kress and Guenther, 1999). One of the typical symptoms of HZ pain and PHN is hyperalgesia and thermal hyperalgesia, which may be related to VZV-induced adrenergic stimulation sensitivity and change of calcium signal transduction in nerve cells (Schmidt et al., 2003; Eyigor et al., 2006).

We tried to find evidence that calcium disorder could be involved in the pathogenesis of PHN in rats with HZ neuralgia. We analyzed the previously reported GSE64345 data set, which included microarray profiling from the ipsilateral L4–L5 DRG of PHN rats (Guedon et al., 2015). The results of GO enrichment showed that DEGs from the PHN rat model were mainly concentrated in the biological process of "cellular calcium ion homeostasis," "positive regulation of cytosolic calcium ion concentration," cell component of "voltage gated calcium channel complex," and molecular function of "calcium ion binding" (**Supplementary Figure 1**). Consistent with previous reports, KEGG signaling pathway analysis showed that DEGs in DRG of the PHN rat model were mainly enriched in "calcium signaling pathway," "neuroactive ligand-receptor interaction," and "serotonergic synapse" (**Supplementary Figure 2**; Qiu et al., 2020). Encouragingly, our results further revealed that the GO enrichment and KEGG signaling pathway analysis of 52 identical DEGs (**Figure 6**) obtained from the VZV-infected SH-SY5Y cells and the VZV-induced PHN rat DRG all showed calcium signaling-related items (**Table 2**). Many voltage-gated

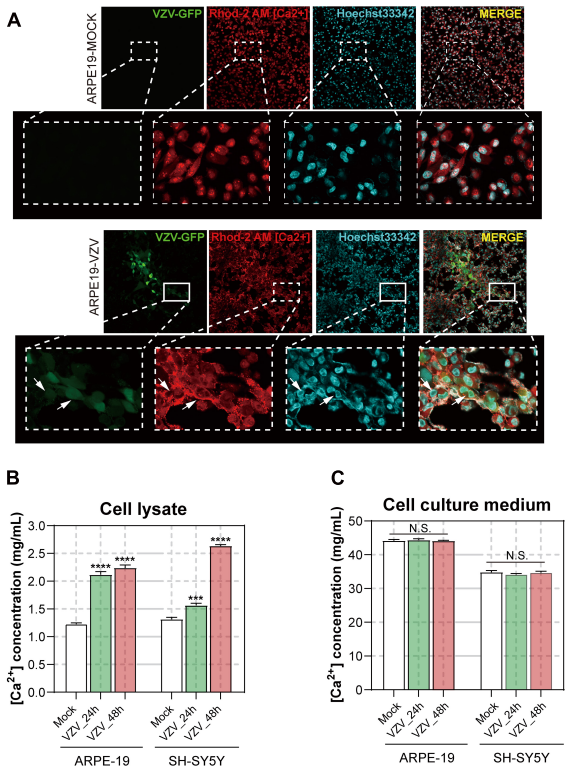

FIGURE 8 | Effect of VZV on Ca^{2+} in ARPE-19 and SH-SY5Y cells. **(A)** The Rhod-2 AM calcium ion probe was used to assess the intracellular calcium ion distribution of ARPE-19 cells 72 h after VZV infection. The calcium colorimetric assay kit was used to evaluate the calcium ion content in the cell lysate **(B)** and cell culture supernatant **(C)** after VZV infection of ARPE-19 and SH-SY5Y cells at 24 h and 48 h, respectively. Data are expressed as the mean ± SD from at least three independent experiments (compared to the Mock group, $^{***}P < 0.001$, $^{****}P < 0.0001$, N.S.; not significant). The white arrows indicate the distribution of calcium ions on the cell membrane surface.

and ligand-gated Ca^{2+} channels are expressed in neurons, which play an important role in the regulation of Ca^{2+} influx in neurons and glia of central nervous system (CNS) (Mei et al., 2018). At the same time, there has been more and more evidence that Ca^{2+} signals are involved in the process of pain and other central nervous system diseases (Gemes et al., 2011; Mei et al., 2018). Therefore, all these results suggest that calcium signaling may play a key role in the progression of PHN disease. These could be attributed to the fact that VZV induces abnormal voltage-gated and ligand-gated Ca^{2+} channel expression in neurons to drive intracellular calcium disorders, thereby maintaining the persistence of pain.

It has already been reported that *BHLHA15*, *CACNA1F*, *CACNG1*, *CHRNA9*, *CHRNA10*, *STC2*, *HRC*, and *TNNT3* participated in calcium ion transport and/or mediate intracellular calcium signals (Burgess et al., 2001; Luo et al., 2005; Zeiger et al., 2011; An et al., 2012; Fasciani et al., 2013; Del Bufalo et al., 2014; Wei and Jin, 2016; Romero et al., 2017). As a member of the basic helix loop helix (bHLH) protein family, *BHLHA15* (also known as *MIST1*) knockout will lead to sustained high levels of cytoplasmic Ca^{2+} in acinar cells and affect the secretion function of cells (Luo et al., 2005; Garside et al., 2010). *CACNA1F* encodes the L-type calcium channel alpha 1 subunit $Ca_v1.4$ protein, which was previously shown to significantly increase its mechanical threshold latency after mutation in rats (An et al., 2012). Ca^{2+} channel γ (*CACNG1*) subunit is a membrane protein, which has been proved to have multiple homologous genes in different tissues and involved in calcium transport (Burgess et al., 1999, 2001). Cholinergic receptor nicotinic alpha 9/10 (*CHRNA9*/*CHRNA* 10, also known as α9α10 nAChR) belongs to the ligand gated ion channel family, which is related to the process of a variety of neuropathic pain (e.g., neuropathy pain, nerve injury, and diabetes pain) (Romero et al., 2017). Stanniocalcin 1 (STC1) proteins have been widely proposed to be regulators of Ca^{2+} homeostasis, and it has been shown to be a negative regulator of store-operated Ca^{2+} entry (SOCE) to regulate intracellular Ca^{2+} levels (Zeiger et al., 2011). Histidine-rich calcium-binding protein (HRC) is a high-capacity, low-affinity calcium-binding protein, which has been confirmed to be involved in the regulation of sarcoplasmic reticulum (SR) release of Ca^{2+} (Kim et al., 2003). Troponin T type 3 (*TNNT3*) encodes the fast skeletal muscle isoform of troponin T (fsTnT), which is required for Ca^{2+}-mediated activation of actomyosin ATPase activity.

Generally, the abnormal expression of many calcium signal-related genes induced by VZV is bound to affect the intracellular calcium homeostasis of infected cells. As shown in **Figure 8**, we directly measured the distribution and content of calcium ions in ARPE-19 and SH-SY5Y cells infected with VZV and found that the virus could change the distribution of calcium ions in infected cells and significantly increase the intracellular calcium content. In fact, the first-line drugs such as gabapentin and pregabalin for the treatment of PHN are calcium channel modulators, which can inhibit hyperalgesia and central sensitization by binding to the α2–δ subunit of voltage-gated calcium channel (VGCC) (McKeage and Keam, 2009; Ifuku et al., 2011; Gudin et al., 2019). However, gabapentin and pregabalin can effectively relieve pain to a certain extent and reduce the occurrence of neuralgia after HZ, but they still cannot fundamentally prevent the occurrence of PHN (Mahn and Baron, 2010). We speculated that activated VZV infection in sensory ganglia could cause abnormal expression of various types of calcium channel proteins. Gabapentin and pregabalin may only regulate one type of calcium channel, but cannot block the intracellular calcium disorder caused by other abnormally expressed calcium channels.

CONCLUSION

Altogether, our results showed that VZV not only changed the expression pattern of calcium signal-related proteins but also disrupted the intracellular calcium ion distribution and calcium ion content, ultimately leading to calcium disorders in infected cells. These findings are unique in VZV infection, which may help to understand the pathogenesis of PHN better. Practically, the persistence of this calcium disorder in nerve cells may become an important cause of PHN and serves as a potential target for clinical diagnosis and treatment of PHN.

DATA AVAILABILITY STATEMENT

Publicly available datasets were analyzed in this study. This data can be found here: Sequencing data set supporting the results of this article has been submitted to the NCBI Gene Expression Omnibus (GEO) database, and the accession number is GSE141932.

ETHICS STATEMENT

This study was approved by the Ethics Committee of Shenzhen Nanshan People's Hospital and The 6th Affiliated Hospital of Shenzhen University Health Science Center.

AUTHOR CONTRIBUTIONS

SW, DX, WS, and LX supervised and coordinated the study and designed the experiments. SW and MO conducted and performed all experiments. SY, MO, JC, and JH assisted various portions of the experiments and analysis of data. SW, SY, MO, and JC wrote the manuscript. All authors contributed to the article and approved the submitted version.

FUNDING

This research has been supported by grants from the Nanshan District Health Bureau on 2019 Health Technology Projects (No. 2019012), Shenzhen Nanshan People's Hospital, and The 6th Affiliated Hospital of Shenzhen University Health Science Center (No. 2020014).

SUPPLEMENTARY MATERIAL

The Supplementary Material for this article can be found online at: https://www.frontiersin.org/articles/10.3389/fnmol.2021.665931/full#supplementary-material

REFERENCES

Almanzar, G., Kienle, F., Schmalzing, M., Maas, A., Tony, H. P., and Prelog, M. (2019). Tofacitinib modulates the VZV-specific CD4+ T cell immune response in vitro in lymphocytes of patients with rheumatoid arthritis. *Rheumatology (Oxford)* 58, 2051–2060. doi: 10.1093/rheumatology/kez175

An, J., Wang, L., Guo, Q., Li, L., Xia, F., and Zhang, Z. (2012). Behavioral phenotypic properties of a natural occurring rat model of congenital stationary night blindness with Cacna1f mutation. *J. Neurogenet.* 26, 363–373. doi: 10.3109/01677063.2012.684416

Bading, H. (2013). Nuclear calcium signalling in the regulation of brain function. *Nat. Rev. Neurosci.* 14, 593–608. doi: 10.1038/nrn3531

Bourinet, E., Altier, C., Hildebrand, M. E., Trang, T., Salter, M. W., and Zamponi, G. W. (2014). Calcium-permeable ion channels in pain signaling. *Physiol. Rev.* 94, 81–140. doi: 10.1152/physrev.00023.2013

Burgess, D. L., Davis, C. F., Gefrides, L. A., and Noebels, J. L. (1999). Identification of three novel Ca(2+) channel gamma subunit genes reveals molecular diversification by tandem and chromosome duplication. *Genome Res.* 9, 1204–1213. doi: 10.1101/gr.9.12.1204

Burgess, D. L., Gefrides, L. A., Foreman, P. J., and Noebels, J. L. (2001). A cluster of three novel Ca2+ channel gamma subunit genes on chromosome 19q13.4: evolution and expression profile of the gamma subunit gene family. *Genomics* 71, 339–350. doi: 10.1006/geno.2000.6440

Cote-Daigneault, J., Bessissow, T., Nicolae, M. V., Nie, R., Bitton, A., Lakatos, P. L., et al. (2019). Herpes zoster incidence in inflammatory bowel disease patients: a population-based study. *Inflamm. Bowel Dis.* 25, 914–918. doi: 10.1093/ibd/izy311

Del Bufalo, A., Cesario, A., Salinaro, G., Fini, M., and Russo, P. (2014). Alpha9 alpha10 nicotinic acetylcholine receptors as target for the treatment of chronic pain. *Curr. Pharm. Des.* 20, 6042–6047. doi: 10.2174/1381612820666140314150634

Eyigor, S., Durmaz, B., and Karapolat, H. (2006). Monoparesis with complex regional pain syndrome-like symptoms due to brachial plexopathy caused by the varicella zoster virus: a case report. *Arch. Phys. Med. Rehabil.* 87, 1653–1655. doi: 10.1016/j.apmr.2006.08.338

Fasciani, I., Temperan, A., Perez-Atencio, L. F., Escudero, A., Martinez-Montero, P., Molano, J., et al. (2013). Regulation of connexin hemichannel activity by membrane potential and the extracellular calcium in health and disease. *Neuropharmacology* 75, 479–490. doi: 10.1016/j.neuropharm.2013.03.040

Field, H. J., and Vere Hodge, R. A. (2013). Recent developments in anti-herpesvirus drugs. *Br. Med. Bull.* 106, 213–249. doi: 10.1093/bmb/ldt011

Fishilevich, S., Zimmerman, S., Kohn, A., Iny Stein, T., Olender, T., Kolker, E., et al. (2016). Genic insights from integrated human proteomics in GeneCards. *Database (Oxford)* 2016, 1–17. doi: 10.1093/database/baw030

Fossat, P., Dobremez, E., Bouali-Benazzouz, R., Favereaux, A., Bertrand, S. S., Kilk, K., et al. (2010). Knockdown of L calcium channel subtypes: differential effects in neuropathic pain. *J. Neurosci.* 30, 1073–1085. doi: 10.1523/JNEUROSCI.3145-09.2010

Gan, E. Y., Tian, E. A., and Tey, H. L. (2013). Management of herpes zoster and post-herpetic neuralgia. *Am. J. Clin. Dermatol.* 14, 77–85. doi: 10.1007/s40257-013-0011-2

Garside, V. C., Kowalik, A. S., Johnson, C. L., DiRenzo, D., Konieczny, S. F., and Pin, C. L. (2010). MIST1 regulates the pancreatic acinar cell expression of Atp2c2, the gene encoding secretory pathway calcium ATPase 2. *Exp. Cell. Res.* 316, 2859–2870. doi: 10.1016/j.yexcr.2010.06.014

Gemes, G., Bangaru, M. L., Wu, H. E., Tang, Q., Weihrauch, D., Koopmeiners, A. S., et al. (2011). Store-operated Ca2+ entry in sensory neurons: functional role and the effect of painful nerve injury. *J. Neurosci.* 31, 3536–3549. doi: 10.1523/JNEUROSCI.5053-10.2011

Gilden, D. H., Kleinschmidt-DeMasters, B. K., LaGuardia, J. J., Mahalingam, R., and Cohrs, R. J. (2000). Neurologic complications of the reactivation of varicella-zoster virus. *N. Engl. J. Med.* 342, 635–645. doi: 10.1056/NEJM200003023420906

Gnann, J. W. Jr., and Whitley, R. J. (2002). Clinical practice. Herpes zoster. *N. Engl. J. Med.* 347, 340–346. doi: 10.1056/NEJMcp013211

Gudin, J., Fudin, J., Wang, E., Haylon, T., Patel, K., and Goss, T. F. (2019). Treatment patterns and medication use in patients with Postherpetic Neuralgia. *J. Manag. Care Spec. Pharm.* 25, 1387–1396. doi: 10.18553/jmcp.2019.19093

Guedon, J. M., Yee, M. B., Zhang, M., Harvey, S. A., Goins, W. F., and Kinchington, P. R. (2015). Neuronal changes induced by Varicella Zoster Virus in a rat model of postherpetic neuralgia. *Virology* 482, 167–180. doi: 10.1016/j.virol.2015.03.046

Hagenston, A. M., and Bading, H. (2011). Calcium signaling in synapse-to-nucleus communication. *Cold Spring Harb. Perspect. Biol.* 3:a004564. doi: 10.1101/cshperspect.a004564

Hagenston, A. M., and Simonetti, M. (2014). Neuronal calcium signaling in chronic pain. *Cell Tissue Res.* 357, 407–426. doi: 10.1007/s00441-014-1942-5

Huang, W. D., Sherman, B. T., and Lempicki, R. A. (2009). Systematic and integrative analysis of large gene lists using DAVID bioinformatics resources. *Nat. Protoc.* 4, 44–57. doi: 10.1038/nprot.2008.211

Ifuku, M., Iseki, M., Hidaka, I., Morita, Y., Komatus, S., and Inada, E. (2011). Replacement of gabapentin with pregabalin in postherpetic neuralgia therapy. *Pain Med.* 12, 1112–1116. doi: 10.1111/j.1526-4637.2011.01162.x

Jiang, H. F., Wang, W., Jiang, X., Zeng, W. B., Shen, Z. Z., Song, Y. G., et al. (2017). ORF7 of varicella-zoster virus is required for viral cytoplasmic envelopment in differentiated neuronal cells. *J. Virol.* 91, e127–e217. doi: 10.1128/JVI.00127-17

Kim, D., Langmead, B., and Salzberg, S. L. (2015). HISAT: a fast spliced aligner with low memory requirements. *Nat. Methods* 12, 357–360. doi: 10.1038/nmeth.3317

Kim, E., Shin, D. W., Hong, C. S., Jeong, D., Kim, D. H., and Park, W. J. (2003). Increased Ca2+ storage capacity in the sarcoplasmic reticulum by overexpression of HRC (histidine-rich Ca2+ binding protein). *Biochem. Biophys. Res. Commun.* 300, 192–196. doi: 10.1016/s0006-291x(02)02829-2

Kress, M., and Guenther, S. (1999). Role of [Ca2+]i in the ATP-induced heat sensitization process of rat nociceptive neurons. *J. Neurophysiol.* 81, 2612–2619. doi: 10.1152/jn.1999.81.6.2612

Lang, P. O., and Aspinall, R. (2019). Vaccination for quality of life: herpes-zoster vaccines. *Aging Clin. Exp. Res. [Online ahead of print]* doi: 10.1007/s40520-019-01374-5

Langmead, B., and Salzberg, S. L. (2012). Fast gapped-read alignment with Bowtie 2. *Nat. Methods* 9, 357–359. doi: 10.1038/nmeth.1923

Li, B., and Dewey, C. N. (2011). RSEM: accurate transcript quantification from RNA-Seq data with or without a reference genome. *BMC Bioinform.* 12:323. doi: 10.1186/1471-2105-12-323

Li, Q., Chen, N., Yang, J., Zhou, M., Zhou, D., Zhang, Q., et al. (2009). Antiviral treatment for preventing postherpetic neuralgia. *Cochrane Database Syst. Rev.* 15:CD006866. doi: 10.1002/14651858.CD006866.pub2

Li, R., Li, Y., Kristiansen, K., and Wang, J. (2008). SOAP: short oligonucleotide alignment program. *Bioinformatics* 24, 713–714. doi: 10.1093/bioinformatics/btn025

Liu, S., Lv, Y., Wan, X. X., Song, Z. J., Liu, Y. P., Miao, S., et al. (2018). Hedgehog signaling contributes to bone cancer pain by regulating sensory neuron excitability in rats. *Mol. Pain* 14, 1–12. doi: 10.1177/1744806918767560

Love, M. I., Huber, W., and Anders, S. (2014). Moderated estimation of fold change and dispersion for RNA-seq data with DESeq2. *Genome Biol.* 15:550. doi: 10.1186/s13059-014-0550-8

Luo, C., Seeburg, P. H., Sprengel, R., and Kuner, R. (2008). Activity-dependent potentiation of calcium signals in spinal sensory networks in inflammatory pain states. *Pain* 140, 358–367. doi: 10.1016/j.pain.2008.09.008

Luo, X., Shin, D. M., Wang, X., Konieczny, S. F., and Muallem, S. (2005). Aberrant localization of intracellular organelles, Ca2+ signaling, and exocytosis in Mist1 null mice. *J. Biol. Chem.* 280, 12668–12675. doi: 10.1074/jbc.M411973200

Mahn, F., and Baron, R. (2010). [Postherpetic neuralgia]. *Klin Monbl Augenheilkd* 227, 379–383. doi: 10.1055/s-0029-1245273

McKeage, K., and Keam, S. J. (2009). Pregabalin: in the treatment of postherpetic neuralgia. *Drugs Aging* 26, 883–892. doi: 10.2165/11203750-000000000-00000

Mei, Y., Barrett, J. E., and Hu, H. (2018). Calcium release-activated calcium channels and pain. *Cell Calcium* 74, 180–185. doi: 10.1016/j.ceca.2018.07.009

Naziroglu, M., Dikici, D. M., and Dursun, S. (2012). Role of oxidative stress and Ca(2)(+) signaling on molecular pathways of neuropathic pain in diabetes: focus on TRP channels. *Neurochem. Res.* 37, 2065–2075. doi: 10.1007/s11064-012-0850-x

O'Connor, K. M., and Paauw, D. S. (2013). Herpes zoster. *Med. Clin. North Am.* 97, 503–522,ix. doi: 10.1016/j.mcna.2013.02.002

Oliver, S. L., Yang, E., and Arvin, A. M. (2017). Dysregulated glycoprotein B-Mediated Cell-Cell fusion disrupts Varicella-Zoster virus and host gene transcription during infection. *J. Virol.* 91, e01613–e01616. doi: 10.1128/JVI.01613-16

Oxman, M. N., Levin, M. J., and Shingles Prevention Study Group (2008). Vaccination against herpes zoster and postherpetic Neuralgia. *J. Infect. Dis.* 197(Suppl. 2), S228–S236. doi: 10.1086/522159

Qiu, Y., Hao, M. L., Cheng, X. T., and Hua, Z. (2020). Bioinformatics analysis of genes and mechanisms in Postherpetic Neuralgia. *Pain Res. Manag.* 2020:1380504. doi: 10.1155/2020/1380504

Raymond, C. R., and Redman, S. J. (2006). Spatial segregation of neuronal calcium signals encodes different forms of LTP in rat hippocampus. *J. Physiol.* 570(Pt 1), 97–111. doi: 10.1113/jphysiol.2005.098947

Robinson, M. D., McCarthy, D. J., and Smyth, G. K. (2010). edgeR: a Bioconductor package for differential expression analysis of digital gene expression data. *Bioinformatics* 26, 139–140. doi: 10.1093/bioinformatics/btp616

Robinson, M. D., and Oshlack, A. (2010). A scaling normalization method for differential expression analysis of RNA-seq data. *Genome Biol.* 11:R25. doi: 10.1186/gb-2010-11-3-r25

Romero, H. K., Christensen, S. B., Di Cesare Mannelli, L., Gajewiak, J., Ramachandra, R., Elmslie, K. S., et al. (2017). Inhibition of alpha9alpha10 nicotinic acetylcholine receptors prevents chemotherapy-induced neuropathic pain. *Proc. Natl. Acad. Sci. U.S.A.* 114, E1825–E1832. doi: 10.1073/pnas.1621433114

Schmidt, M., Kress, M., Heinemann, S., and Fickenscher, H. (2003). Varicella-zoster virus isolates, but not the vaccine strain OKA, induce sensitivity to alpha-1 and beta-1 adrenergic stimulation of sensory neurones in culture. *J. Med. Virol.* 70(Suppl. 1), S82–S89. doi: 10.1002/jmv.10327

Shakya, A. K., O'Callaghan, D. J., and Kim, S. K. (2019). Interferon gamma inhibits varicella-zoster virus replication in a cell line-dependent manner. *J. Virol.* 93, e257–e319. doi: 10.1128/JVI.00257-19

Shen, S., Kong, J., Qiu, Y., Yang, X., Wang, W., and Yan, L. (2019). Identification of core genes and outcomes in hepatocellular carcinoma by bioinformatics analysis. *J. Cell Biochem.* 120, 10069–10081. doi: 10.1002/jcb.28290

Silva, J. R., Lopes, A. H., Talbot, J., Cecilio, N. T., Rossato, M. F., Silva, R. L., et al. (2017). Neuroimmune-Glia interactions in the sensory ganglia account for the development of acute herpetic Neuralgia. *J. Neurosci.* 37, 6408–6422. doi: 10.1523/JNEUROSCI.2233-16.2017

Walker, J. L., Andrews, N. J., Amirthalingam, G., Forbes, H., Langan, S. M., and Thomas, S. L. (2018). Effectiveness of herpes zoster vaccination in an older United Kingdom population. *Vaccine* 36, 2371–2377. doi: 10.1016/j.vaccine.2018.02.021

Wei, B., and Jin, J. P. (2016). TNNT1, TNNT2, and TNNT3: isoform genes, regulation, and structure-function relationships. *Gene* 582, 1–13. doi: 10.1016/j.gene.2016.01.006

Xie, C., Mao, X., Huang, J., Ding, Y., Wu, J., Dong, S., et al. (2011). KOBAS 2.0: a web server for annotation and identification of enriched pathways and diseases. *Nucleic Acids Res.* 39, W316–W322. doi: 10.1093/nar/gkr483

Xu, Q., and Yaksh, T. L. (2011). A brief comparison of the pathophysiology of inflammatory versus neuropathic pain. *Curr. Opin. Anaesthesiol.* 24, 400–407. doi: 10.1097/ACO.0b013e32834871df

Yang, E., Arvin, A. M., and Oliver, S. L. (2017). The glycoprotein B cytoplasmic domain lysine cluster is critical for varicella-zoster virus cell-cell fusion regulation and infection. *J. Virol.* 91, e01707–e01716. doi: 10.1128/JVI.01707-16

Zeiger, W., Ito, D., Swetlik, C., Oh-hora, M., Villereal, M. L., and Thinakaran, G. (2011). Stanniocalcin 2 is a negative modulator of store-operated calcium entry. *Mol. Cell Biol.* 31, 3710–3722. doi: 10.1128/MCB.05140-11

Conflict of Interest: The authors declare that the research was conducted in the absence of any commercial or financial relationships that could be construed as a potential conflict of interest.

frontiers in Molecular Neuroscience

REVIEW
published: 28 May 2021
doi: 10.3389/fnmol.2021.674914

Role of the Ubiquitin System in Chronic Pain

*Jiurong Cheng, Yingdong Deng and Jun Zhou**

Department of Anesthesiology, The Third Affiliated Hospital of Southern Medical University, Guangzhou, China

As a significant public health issue, chronic pain, mainly neuropathic pain (NP) and inflammatory pain, has a severe impact. The underlying mechanisms of chronic pain are enigmatic at present. The roles of ubiquitin have been demonstrated in various physiological and pathological conditions and underscore its potential as therapeutic targets. The dysfunction of the component of the ubiquitin system that occurs during chronic pain is rapidly being discovered. These results provide insight into potential molecular mechanisms of chronic pain. Chronic pain is regulated by ubiquitination, SUMOylation, ubiquitin ligase, and deubiquitinating enzyme (DUB), etc. Insight into the mechanism of the ubiquitin system regulating chronic pain might contribute to relevant therapeutic targets and the development of novel analgesics.

Keywords: chronic pain, deubiquitinases, SUMOylation, ubiquitination, ubiquitin ligase

OPEN ACCESS

Edited by:
Xiaodong Liu,
The Chinese University of Hong Kong, China

Reviewed by:
Shenglan Wang,
Beijing University of Chinese Medicine, China
Huarong Chen,
The Chinese University of Hong Kong, China

***Correspondence:**
Jun Zhou
zhoujun7843@126.com

Specialty section:
This article was submitted to Pain Mechanisms and Modulators, a section of the journal Frontiers in Molecular Neuroscience

Received: *02 March 2021*
Accepted: *12 April 2021*
Published: *28 May 2021*

Citation:
Cheng J, Deng Y and Zhou J (2021) Role of the Ubiquitin System in Chronic Pain. Front. Mol. Neurosci. 14:674914. doi: 10.3389/fnmol.2021.674914

INTRODUCTION

Chronic pain is a compounded problem that lasts or recurs for more than 3 months, which significantly affects physical and psychological health (Treede et al., 2019). It is known that chronic pain can result from many pain syndromes. However, the mechanisms underlying chronic pain are complex and not clarified. Therefore, despite a major long-standing investigation for years, there are no effective therapies for most types of chronic pain. Several recent studies have found that ubiquitin system failure is implicated in chronic pain (Tai and Schuman, 2008), mainly including neuropathic pain (NP) and inflammatory pain (Chen et al., 2011). NP is the pain caused by a lesion or somatosensory system disease (Jensen et al., 2011). Inflammatory pain is caused by an increase in the excitability of peripheral nociceptive fibers due to changes in ion channel activity caused by inflammatory mediators (Linley et al., 2010). During the inflammatory process, the pain is triggered by normally innocuous stimuli and becomes chronic if the inflammation is not resolved. The mechanisms of NP are partly distinct from those of inflammatory pain, and potential therapeutic targets mediated by the ubiquitin system to NP and inflammatory pain are different.

The ubiquitin system is a protein degradation pathway mainly composed of ubiquitin, E1 ubiquitin-activating enzyme, E2 ubiquitin-conjugating enzyme, E3 ubiquitin ligase, deubiquitinating enzyme (DUB), and proteasome, etc. The ubiquitination of proteins is a multistep. First, the E1 activates ubiquitin, which is then transferred to E2. Subsequently, the E2∼Ub subsequently interacts with E3. And then, the E3 ligase transfers the E2-bound ubiquitin to a substrate and mediates the ubiquitination (Pickart, 2001). Interaction with the substrate can be direct or *via* ancillary proteins (Glickman and Ciechanover, 2002), finally leading to the degradation of these substrates by proteasomes. Besides, ubiquitination can be antagonized by DUBs, which remove or trim ubiquitin chains on their substrates (Nakamura, 2018). In addition, studies indicate that the ubiquitin–proteasome system (UPS) influences disease onset and progress

through the timely degradation of various regulatory proteins (Yi and Ehlers, 2007). Hence, a comprehensive understanding of how the ubiquitin system affects chronic pain might be essential for novel therapeutic opportunities for patients.

UBIQUITINATION IN ANIMAL MODELS OF CHRONIC PAIN

The pathogenesis of chronic pain involves many different mechanisms and the etiology is multifactorial. Thus, animal models are essential for exploring molecular mechanisms of chronic pain. Peripheral or central nerve injury is commonly used to induce NP. The common models of NP include spinal nerve ligation (SNL) model, sciatic nerve chronic constriction injury (CCI) model, and spared nerve injury (SNI) model (Kumar et al., 2018), while the formalin-induced and complete Freund's adjuvant (CFA)-induced models are common in inflammatory pain (Muley et al., 2016). Reliable animal models can help understand the mechanisms of the ubiquitin system in chronic pain to develop effective therapeutics.

It is possible that the chronic pain observed in various rodent pain models could be due to an altered ubiquitin system function. Recent studies investigated the expression and function of E3 ubiquitin ligase, deubiquitinase ubiquitin-specific protease 5 (USP5), and Cav3.2 interaction in CCI-triggered NP (García-Caballero et al., 2014). The researchers study the influence of protein ubiquitination on the development of NP and determine mechanical nociception in the pathophysiological processes of NP using a well-characterized rat model of SNL (Lin et al., 2015; Lai et al., 2016, 2018; Liu et al., 2019). SUMOylation disorder after the injury of peripheral nerves, caused by SNI, may alter the Cav3.2 channel activity (Garcia-Caballero et al., 2019; Liu et al., 2019; Tomita et al., 2019). Both formalin and CFA-induced models are valuable experimental methods for inflammatory pain, which provides an empirical basis for understanding the mechanism of the ubiquitin system on inflammatory pain. Altogether, these data indicate that the ubiquitin system is a major determinant of pain response in both inflammatory pain and NP models. Common ubiquitination in animal models of chronic pain is shown in **Table 1**.

ROLE OF THE UBIQUITIN SYSTEM IN NEUROPATHIC PAIN

Mechanism of Ubiquitination in Neuropathic Pain

Protein ubiquitination plays a crucial role in the development of NP (Lai et al., 2016). This function is achieved by ubiquitination-modified protein receptors and ion channels to affect synaptic activity and efficiency.

NP associated with ubiquitination partly works by regulating signal transduction pathways. The transient receptor potential vanilloid-1 (TRPV1), a member of the transient receptor potential (TRP) family, is considered a therapeutic target for pain relief (Caterina et al., 1997). TRPV1 promotes the ubiquitination of epidermal growth factor receptor (EGFR) in cells and regulates EGFR/mitogen-activated protein kinase (MAPK) signaling through the lysosomal degradation pathway, leading to increased cytoplasmic translocation and degradation of EGFR, and then downregulation of EGFR level. It responds to harmful stimuli from afferent nerve terminals and participates in pain and inflammation (Huang et al., 2020). Lysine ubiquitination is a signal for the transport and degradation of G protein-coupled receptors. Short-term stimulation of substance P (SP) can induce the endocytosis and circulation of the neurokinin-1 receptor (NK1R). Chronic stimulation of SP induces the ubiquitination of lysine residues in NK1R cells, which mediates its degradation and downregulation. In this process, tachykinin is released continuously and prevents nociceptive signals (Cottrell et al., 2006). In addition, tumor necrosis factor-alpha (TNF-α) influences the development of NP through the ring finger protein (RNF20)/histone H2B monoubiquitination (H2Bub)/RNA polymerase II (pRNAPII)/metabotropic glutamate receptors (mGluR5) signal transduction cascade. Specifically, TNF-α-induced RNF20-driven H2B monoubiquitination can promote dorsal horn phosphorylated RNAPII-dependent mGluR5 transcription, affecting protein ubiquitination and degradation (Lai et al., 2016). Tumor necrosis factor receptor-associated factor 2 (TRAF2) and NcK-interacting kinase (TNIK) are enhanced, and the TNIK is coupled to glutamate receptor (GluR1) after nerve injury. TRAF2 is regulated by F-box protein 3 (Fbxo3) and ubiquitination of leucine-rich repeat protein 2 (Fbxl2). Thus, Fbxo3-dependent Fbxl2 ubiquitination and degradation participate in the development of NP by upregulating TRAF2/TNIK/GluR1 signaling (Lin et al., 2015). Studies have demonstrated that TRAF6 has E3 ligase activity; the inhibition of TRAF6 expression can effectively relieve SNL-induced NP. Taken together, the results suggest that TRAF6 serves an important role in NP progression and pathogenesis; the exact mechanism remains to be elucidated (Dou et al., 2018).

The other part of ubiquitination mediates the NP process by modifying the activity of synaptic proteins and ion channels. Studies on low voltage-gated calcium channels suggest that Ca^{2+} elevation in sensory neurons is associated with NP (Bourinet et al., 2014; François et al., 2014). Rab3-interactive molecule (RIM) can be associated with N-type voltage-dependent calcium channels. Rab3-interactive molecule-1α (RIM1α) upregulates the expression of CaV2.2 by recruiting and coupling with CaV2.2. This enables the rapid and synchronized release of neurotransmitters at the presynaptic site to mediate NP. Other studies have demonstrated that Fbxo3 affects the activity of CaV2.2 by inhibiting fbxl2-dependent RIM1 ubiquitination. Moreover, Mas-related G-protein-coupled receptor subtype C (MrgC) ubiquitination affects RIM1α/Ca_V2.2 cascade and then reduces intracellular calcium concentration to participate in the occurrence and maintenance of chronic pain (Marangoudakis et al., 2012; Lai et al., 2016; Sun et al., 2019).

Ubiquitination can also regulate NP through nociceptive information modulation and synaptic function regulation in nociceptive neurons (Kiris et al., 2014). TNF-α impedes presynaptic active zone protein (Munc13-1) ubiquitination in the

TABLE 1 | Ubiquitination in animal models of chronic pain.

Animal models	Types of pain	The characteristics	Ubiquitination in models	References
CCI	NP	Produces unilateral peripheral mononeuropathy associated with nerve compression and neuroinflammatory lesions	Investigate the function of E3 ubiquitin ligase, deubiquitinase USP5	García-Caballero et al., 2014; Lai et al., 2018
SNL	NP	More extensive surgery, injury, and separation of intact spinal segments	Study the influence of protein ubiquitination on the development of NP	Lin et al., 2015; Lai et al., 2016; Liu et al., 2019; Tomita et al., 2019
SNI	NP	Much easier independent of the sympathetic system and last for several weeks,	Used to study drugs associated with USP	Caterina et al., 1997; Garcia-Caballero et al., 2019; Huang et al., 2020
Formalin and CFA model	Inflammatory Pain	Simulate inflammatory lesions be used as a disease model of arthritis	Understand the mechanism of the ubiquitin system	Cottrell et al., 2006

Sciatic nerve injury of the peripheral nerve is often used to induce neuropathic pain (NP). Formalin and complete complete Freund's adjuvant (CFA) often induce chronic inflammatory pain. Animal models may help to understand the symptoms and physiology of related pain. Several animal models help in understanding the mechanism by which the ubiquitin system regulates chronic pain.

spinal cord, which promotes the synaptic activity of nociceptive neurotransmission in NP (Lindenlaub et al., 2000; Hsieh et al., 2018). The reduction of ubiquitination of transporter proteins induces the upregulation of glycine transporter 2 (GlyT2) activity, which affects noxious signal conduction (Villarejo-López et al., 2017). Experiments have shown that periaqueductal gray matter (PGM) in the midbrain, which is involved in pain processing and regulation, could be overexcited and dysfunctional in the face of stress. This process is accompanied by the activation of the ubiquitination system, which may contribute to excruciating pain (Quan et al., 2005). Some drug researches are also based on the role of ubiquitination in pain. For example, metformin can eliminate the abundance of ubiquitinated proteins, which can achieve analgesia by inhibiting cell apoptosis (Weng et al., 2019). In brief, these results emphasize that inhibition of the ubiquitination process of proteins or ion channels may achieve adequate chronic pain relief. Therefore, we summarized the possible mechanisms and potential targets of the abovementioned ubiquitination process of NP regulation, aiming to provide new ideas and experimental evidence for the application of strategies to promote the treatment of chronic pain by influencing the ubiquitination process.

SUMOylation and Neuropathic Pain

SUMOylation is a small ubiquitin-like modifier (SUMO) protein family coupled to lysine residues (Yang et al., 2017) and is correlated with ubiquitination. It is an important posttranslational protein modification that participates in NP transmission and modulation (Henley et al., 2014). The members of the collapsin response mediator protein (CRMP) family are an effect of neuronal polarity and synapse dynamics. Dysregulation of CRMP has now been described in numerous diseases (Tan et al., 2014). CRMP2 SUMOylation has been reported as the main factor that mediates chronic pain (Moutal et al., 2019). Studies have shown that CRMP2 SUMOylation can regulate voltage-gated ion channels, especially the sodium channels in the pain signaling process (Dustrude et al., 2013; Baumann and Kursula, 2017; Bennett et al., 2019), which are upregulated to induce NP (Barbosa and Cummins, 2016). Precisely, the combination of CRMP2 and SUMO controls the expression and density of Nav1.7, thus affecting its activity (Dustrude et al., 2016; François-Moutal et al., 2018a; Moutal et al., 2018). In addition, the E2 SUMO conjugating enzyme (Ubc9) is necessary for SUMOylation and interacts with CPMP2 to reduce CRMP2 SUMOylation, which in turn reduces Nav1.7 current to alleviate NP (François-Moutal et al., 2018b; Moutal et al., 2020). Therefore, preventing CRMP2 SUMOylation may be an effective target to reverse NP (Khanna et al., 2020). Thus, further research is necessary before translating preclinical findings into the clinic setting. There are many clinical challenges to developing SUMOylation enzyme inhibitors, notably to determine which specific targets and predictive indicators are targeted, in order to determine what kind of specific mechanisms may be more beneficial.

Ubiquitin Ligase Modulation of Neuropathic Pain

Ubiquitin ligase is the most critical factor in determining specificity during protein ubiquitination. E3 ubiquitin ligase affects the development of pain by promoting protein ubiquitination and degradation. Since E3 ligase determines the specificity of the reaction, they have attracted the most attention. E3 ubiquitin ligase includes three families: HECT (homologous to the E6AP carboxyl terminus), RING (really interesting new gene), and U-box domains (Zheng and Shabek, 2017).

It is well known that E3 ubiquitin ligase can regulate ion channel protein levels through ubiquitination. The late-promoting complex/RING body, anaphase-promoting complex (APC/C), is a cullin-RING-E3 ubiquitin ligase. Its co-activator (Cdh1) is essential for proliferating cells and terminally differentiated neurons. It has been revealed that downregulation of the Cdh1 signal in spinal dorsal horns contributes to the maintenance of mechanical allodynia after nerve injury in rats; thus, it may upregulate the expression of Cdh1 in the spinal cord to induce pain relief (Hu et al., 2016).

Neural precursor cell expressed developmentally downregulated protein 4 (NEDD-4) is a specific E3 ubiquitin ligase regulating N-methyl-D-aspartate (NMDA) receptors (NMDARs) with the GluN2D (NMDAR subtypes) subunit

through ubiquitination-dependent downregulation (Goel et al., 2015). Specifically, NMDARs are a family of glutamate-gated ion channels that can regulate various central nervous system (CNS) functions. The hypo- or hyper-activation of NMDARs is intimately associated with certain neurological diseases (such as chronic pain, neurodegenerative diseases). Nedd4 can attenuate NP *via* ubiquitination-dependent downregulation of the NMDAR of the GluN2D subunit (Gautam et al., 2013). Besides, several studies have revealed that the NEDD4 family of E3 ubiquitin ligase can effectively regulate the Nav channels (Eaton et al., 2010). As mentioned earlier, the upregulation of Nav1.7 and Nav1.8 leads to NP. Each Nav subtype has a PY (PPxY) motif at the end of subunit C, making them a target for the NEDD4 ubiquitin ligase family. NEDD-4 like (NEDD4-2) is a ubiquitin-protein ligase that belongs to the NEDD4 family of E3 ubiquitin ligase. Therefore, NEDD4-2 can ubiquitinate Nav1.7 and Nav1.8 and then regulate the ion channel of the cell membrane (Staub et al., 2000). Specifically, NEDD4-2 exists and acts on Nav1.7 and Nav1.8 in dorsal root ganglion (DRG) neurons. When the peripheral nerve is injured, NEDD4-2 in the neuron is downregulated and then disorders Nav, leading to nervous overexcitement and pain (Ekberg et al., 2014; Laedermann et al., 2014). NEDD4-2 regulates nociceptive sensations, and its dysfunction causes NP occurrence. Therefore, active NEDD4-2 can inhibit the upregulation of sodium channels to cure NP (Bongiorno et al., 2011; Cachemaille et al., 2012; Laedermann et al., 2013, 2014; **Figure 1**).

Cav3.2 channels can be ubiquitinated and are capable of intracellular modification and degradation. The ubiquitination state of Cav3.2 channel in the pain pathway is regulated by the interaction of HECT E3 ligase E3 ubiquitin-protein ligase 1 (WWP1) and USP5, which can regulate the stability of the T-channel protein in the plasma membrane. WWP1 binds to intracellular domains III–IV regions of Cav3.2 T-type and modify specific lysine residues in this region. Preventing the enhancement of this current may potentially combat the development of pain (García-Caballero et al., 2014). The bone morphogenetic protein (BMP) signal downstream of highwire E3 ligase can stimulate nociceptors. The upregulation of the BMP signal leads to a significant increase in Ca^{2+} current, which is based on physiologically sensitized nociceptors and nociceptive behavior (Honjo and TraceyJr., 2018).

Pellino 1, a critical mediator in various immune receptor signaling pathway molecules, forms the conserved E3 ubiquitin ligase family. It can regulate NP by regulating MAPK/nuclear factor kappa B (NF-κB) signaling in the spinal cord (Börner and Kraus, 2013; Wang et al., 2020). Also, E3 ubiquitin ligase Caritas B cell lymphoma (Cbl) is a highly conserved ubiquitin ligase expressed in both normal and tumor cells. Besides, c-Cbl can relieve pain by inhibiting the activation of spinal microglia and reducing the release of inflammatory factors. A study found that nerve injury could downregulate the expression of c-Cbl, which leads to the activation of microglia, the increase of inflammatory factor release, and the occurrence of NP through the extracellular signal-regulated kinase (ERK) pathway (Chen et al., 2014; Zhang et al., 2019a). Therefore, increasing c-Cbl could relieve NP (Xue et al., 2018). Interestingly, when the expression of E3 ubiquitin ligase Cbl family increases, it reduces the analgesic effect of interleukin 2 (IL-2) by increasing ubiquitination of Zeta-chain associated protein 70 (ZAP70) and phospholipase C-γ1 (PLC-γ1) (Jeong et al., 2018). Thus, ubiquitin and E3 ubiquitin ligases c-Cbl can regulate the development of NP by reducing the production of IL-2. These findings indicate that the ubiquitin E3 ligase mainly decreases NP by modulating ion channel activity and influencing different signaling pathways. This mechanism of action illustrates how the interdependence between E3 ubiquitin ligase and its substrate protein can provide new therapeutic targets. Therefore, the effects of E3 ubiquitin ligase should be considered when preventing the development of neuralgia after nerve injury.

Role of the Deubiquitinating Enzyme

Both deubiquitination and ubiquitination are involved in maintaining cell homeostasis. Ubiquitin chain, mediated by DUB, is vital in various cellular processes. USP is a cysteine deubiquitinase and USP5 is recognized to be explicitly polyubiquitin, which is not bound to the target protein and is involved in pain development (Kowalski and Juo, 2012; Ning et al., 2020). Deubiquitination of the channel mediates Cav3.2 T-type calcium by deubiquitinase USP5. When the nerve is damaged, USP5 enhances the deubiquitination of the Cav3.2 channel in the dorsal horn, increasing T-type calcium current, which in turn causes pain hypersensitivity (Gadotti et al., 2015; Gadotti and Zamponi, 2018; Ozaki et al., 2018). Specifically, USP5 is upregulated in NP. Meanwhile, a specific amino acid region in the zinc-finger ubiquitin-specific protease (cUBP) domain of USP5 interacts with the III–IV linker region of the Cav3.2 T-type calcium channel. The reduction of the ubiquitination of the Cav3.2 channel increases the stability of the Cav3.2 channel at the cell surface. Therefore, through disruption, the interaction between USP5 and Cav3.2 channel inhibits the expression of Cav3.2; hence, inhibiting T-type calcium current may alleviate NP (Garcia-Caballero et al., 2016). Some factors also affect the interaction between USP5 and Cav3.2 channels, such as IL-1 recognition (Stemkowski et al., 2017), USP5 SUMOylation disorder (Garcia-Caballero et al., 2019), and TRPV1 nociceptors (Stemkowski et al., 2016). Therefore, these factors also reduce Cav3.2 channel activity by weakening USP5 regulation and increasing channel ubiquitination to achieve the purpose of analgesia (García-Caballero et al., 2014; Joksimovic et al., 2018; **Figure 2**). For therapeutic purposes, interference with USP5/t-type channel interaction will specifically target a process involving abnormal upregulation of channel activity while maintaining normal channel function, thereby reducing the risk of adverse side effects.

Another deubiquitination enzyme, ubiquitin C-terminal hydrolase L1 (UCHL1), is crucial in neurological diseases. As the UCH-L1 activity increases, ubiquitin expression is upregulated. Extracellular ubiquitin is an agonist of CXC motif chemokine receptor type 4 (CXCR4), which is involved in several pathological conditions, such as immunologic, oncologic, and neurologic disorders. Ubiquitin and CXCR4 may lead to microglial activation and NP. Thus, inhibiting spinal cord UCHL1 and suppressing ubiquitin expression and microglial activation may be effective (Cheng et al., 2016). Although there

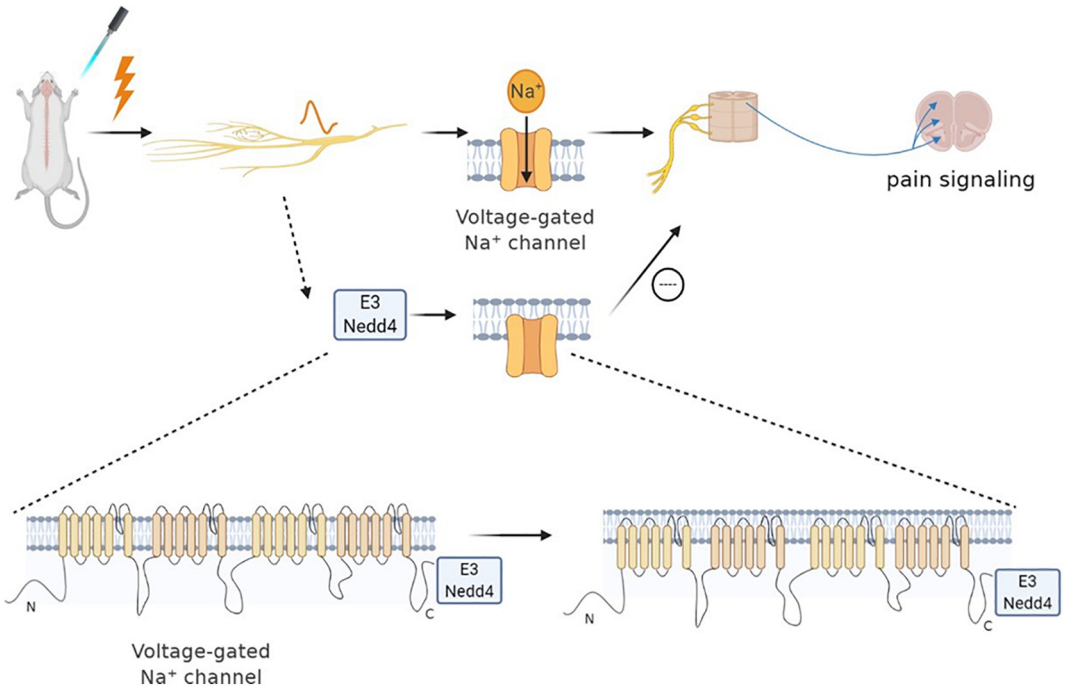

FIGURE 1 | Neural precursor cell expressed developmentally downregulated protein 4 (NEDD4) family of E3 ubiquitin ligase can effectively regulate Nav channels. Sodium channels play an important role in neuropathic pain. When nociceptors are activated, Nav1.7 and Nav1.8 are upregulated, leading to pain. The NEDD4 family of E3 ubiquitin ligase can react on sodium ion channels to ubiquitinate them and promote the channel endocytosis. Specifically, NEDD4 ubiquitin ligase can react with the PY motif at the end of the C subunit of each Nav subtype, thereby regulating the expression of the Nav channel, as well as the current density and neuronal excitability. Therefore, the pain signal of sensory neurons can be reduced indirectly by regulating the activity of NEDD4-2.

is limited information on DUBs in published early preclinical trials, some information can be emphasized. DUB can regulate the stability and degradation of proteins through a variety of cellular pathways. Here, we present evidence that DUBs can act as a potent regulator of chronic pain processing by increasing the stability of the T-channel or promoting the activation of microglia. This may provide a theoretical basis for the development of more effective chronic pain therapeutics.

Ubiquitin–Proteasome System in Neuropathic Pain

UPS is a selective non-lysosomal proteolytic system in which substrates are labeled with ubiquitin and can be degraded by proteasomes (Ji and Kwon, 2017; Caputi et al., 2019). The necessary step in the degradation pathway of the proteasome is the formation of ubiquitin–protein conjugates. Covalent binding of ubiquitin ligase and its target molecule leads to molecular degradation. This system can degrade various cellular proteins that can regulate cell growth or function (**Figure 3**). UPS affects NP by degrading several proteins essential to synaptic plasticity; its downregulation can effectively relieve pain (Hegde, 2010). UPS activity increases during nerve injury, leading to hyperalgesia. Proteasome inhibitors can prevent and reverse NP by concentrating protein systems, including protein systems that control the release of dynorphin A and calcitonin gene-related peptide (CGRP) and the postsynaptic effect of dynorphin A (Moss et al., 2002; Ossipov et al., 2007). Recent studies suggest that reducing proteasome degradation of Cav3.2 T-type calcium channels is associated with persistent pain. When proteasome degradation is inhibited, which subsequently inhibits the upregulation of USP5, the protein level of Cav3.2 in nociceptors is increased (Tomita et al., 2019). In addition, when the UPS was activated, the degradation of glutamate transporters is enhanced, resulting in mechanical hyperalgesia (Manning, 2004; Zavrski et al., 2005; Yang et al., 2008; StocktonJr., Gomes et al., 2015). Accordingly, inhibition of ubiquitin proteasome-mediated degradation of glutamate transporters may offer treatment options for certain neurological diseases and chronic pain. While this methodology deserves further investigation, considering the diversified effects of the proteasome, the use of broad-spectrum proteasome inhibitors may be flawed, and the development of selective inhibitors for chronic pain may be a more effective method. In this sense, developing methods for reducing chronic pain with selective inhibitors could be a more effective approach.

ROLE OF THE UBIQUITIN SYSTEM IN INFLAMMATORY PAIN

The etiology and pathogenesis of NP and inflammatory pain remain inconsistent, and their targets in the ubiquitin system are also different. Therefore, novel therapeutic targets for chronic

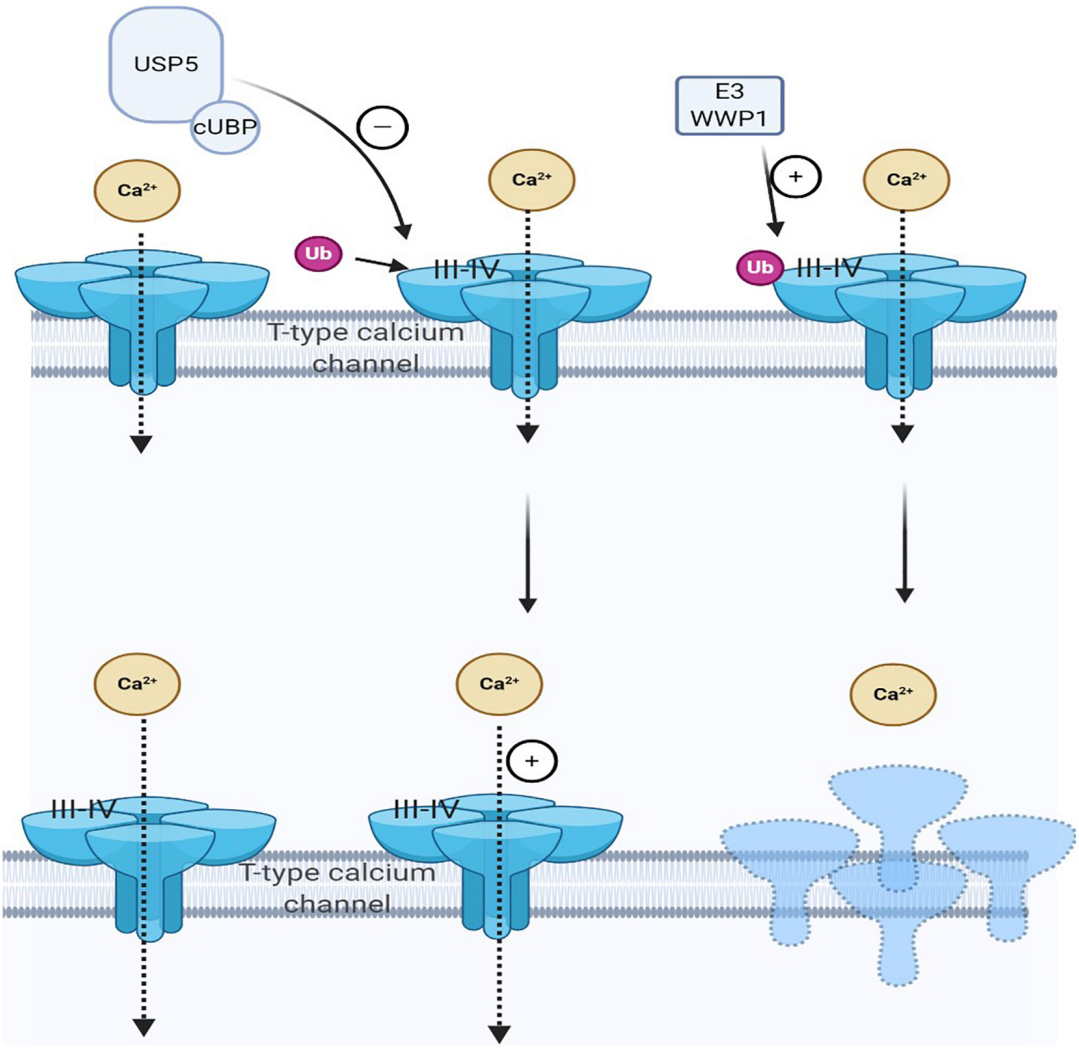

FIGURE 2 | Cav3.2 channel ubiquitination status is regulated by the interaction of E3 ligase and ubiquitin-specific protease 5 (USP5). The ubiquitination state of Cav3.2 channel in the pain pathway is regulated by the interaction of USP5 and HECT E3 ligase HECT E3 ligase E3 ubiquitin-protein ligase 1 (WWP1), which can regulate the stability of the calcium channel protein in the plasma membrane. When pain occurs, USP5 is upregulated and its cUBP domain interacts with the III–IV junction of Cav3.2 T-type calcium channels. This can reduce the ubiquitination of Cav3.2 channels and upregulate Cav3.2 channels, making them more stable on the cell surface. WWP1 also binds to intracellular regions III–IV in the Cav3.2 t-channel junction region and modifies specific lysine residues in this region.

pain states accompanying inflammatory processes are urgently needed. As described below, inflammatory disease models show the relief of inflammatory pain by inhibiting the ubiquitination process of several proteins. Therefore, it is necessary to explore the role of the ubiquitin system that regulates pain signals during chronic inflammation in order to reflect the mediated analgesia in different forms of chronic pain.

Ubiquitination in Inflammatory Pain

Ubiquitination is significant in inflammatory pain. Acute inflammation is a key player in peripheral sensitization and local tissue inflammation-evoked pain. The pain persists and becomes chronic during inflammation resolution. Short-term stimulation of SP induces TRPV1 polyubiquitination, which has an impact on chronic visceral pain. Various pro-inflammatory mediators, such as histamine and bradykinin, express function by regulating TRPV1. The degree of abdominal pain in patients is related to the increased expression of TRPV1. The feedback regulation of TRPV1 by SP also participates in the inflammatory visceral pain. Therefore, drugs that block SP-mediated TRPV1 ubiquitination may reduce chronic pain after inflammation (Lapointe et al., 2015).

The inhibition of glycine is weakened after peripheral tissue damage, which is considered a critical factor in the occurrence of inflammatory pain. The inhibition of glycine can increase the excitability and spontaneous activity of spinal cord nociceptive neurons during inflammatory pain. Studies found that the activity of the glycine receptor subunit (GlyRs-α1) is dependent on ubiquitination, which may help glycinergic inhibition after peripheral inflammation. Therefore, ubiquitin

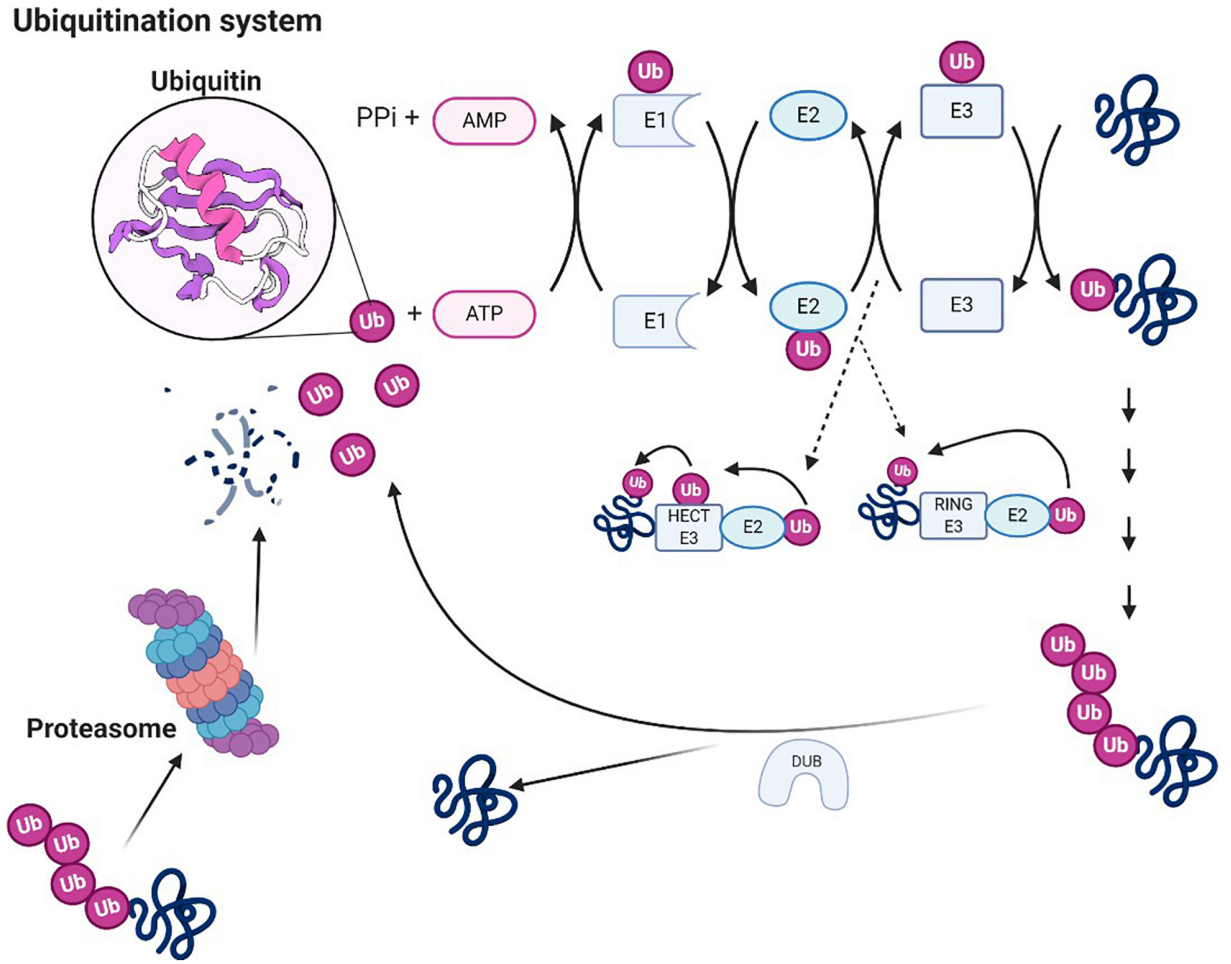

FIGURE 3 | Ubiquitin system. Ubiquitin molecules can be covalently linked to other substrates to form ubiquitin chains. A chain of four or more ubiquitin units constitutes proteasome 26S. Ubiquitin is an ATP-dependent process catalyzed by three enzymes (E1, E2, and E3), which also confer specificity to the process. The first reaction catalyzed by E1 is responsible for the activation of ubiquitin. E1 transfers ubiquitin on cysteine to E2. Through the activity of transferase, E2 transfers the ubiquitin to E3 ligase (two groups of protein ubiquitin ligase, HECT E3 enzymes and ring E3s, the way they transfer ubiquitin is exactly different), which binds ubiquitin to the Lys residue of the target protein. Polyubiquitinated protein can be degraded by 26S proteasome, and ubiquitin can be recovered under the action of the deubiquitinating enzyme.

modification of Glyrs-α1 reduces the spinal glycinergic inhibition in peripheral inflammation. Furthermore, preventing Glyrs-α1 from ubiquitination, restoring Glyrs-α1-mediated synaptic transmission can generate analgesic action (Zhang et al., 2019b). Despite these studies further clarifying the role of ubiquitination in inflammatory pain, more preclinical trials are still necessary. The development of new drugs targeting specific mechanisms may facilitate translation of these findings from bench to bedside.

Role of the Deubiquitinating Enzyme in Inflammatory Pain

As mentioned earlier, USP5 also mediates inflammatory pain by enhancing the Cav3.2 channel activity. Inflammatory mediators, bradykinin, also increase the number of sensory neurons expressing T-type Ca^{2+} channels (Huang et al., 2016; Sekiguchi et al., 2018). USP5 binds to III–IV linkers in Cav3.2 (Garcia-Caballero et al., 2016). Cav3.2 channel ubiquitination is the substrate of USP5, and its association with USP5 leads to changes in Cav3.2 protein level and current density. USP5-mediated regulation of Cav3.2 is abnormally enhanced in chronic pain. These data suggest that USP5 is a regulator of chronic pain associated with inflammatory processes (García-Caballero et al., 2014).

Ubiquitin-specific proteases or deubiquitin enzymes remove ubiquitin groups from the degraded target proteins, thereby improving protein stability. Therefore, USP5 knockout by shRNA can increase Cav3.2 ubiquitination, decrease Cav3.2 protein level, and decrease calcium current. It was found that inhibition of USP5 *in vivo* or decoupling of USP5 from the intrinsic Cav3.2 channel through intrathecal delivery of Tat peptide can protect from inflammatory pain. Therefore, targeting Cav3.2 deubiquitination by USP5 is a potential target for pain conditions associated with inflammatory disorders (Gadotti et al.,

2015). According to data from basic research, combined with experimental pain models, the method of inhibiting DUBs has been studied in preclinical studies. It can be concluded that the mechanisms listed above contribute to relieve chronic pain, especially inflammatory pain.

Ubiquitin Ligase Modulation of Inflammatory Pain

E3 ubiquitin ligase is a key component that generates specific reactions through substrate recognition (Qiu et al., 2011). The substrates of NEDD4-2 mainly include the epithelial sodium channel (ENaC) and neurotrophin receptor (TrkA). NEDD4-2 heterozygous mice can provide a new model for studying inflammatory pain, which causes the mice to be more hyperactive and increase their sensitivity to pain during central sensitization and inflammation. This is likely to be caused by decreased levels of NEDD4-2, leading to increased reactivity of the substrate TrkA to nerve growth factor (NGF). Therefore, a full complement of E3 ubiquitin ligase is necessary for inflammatory pain relief (Yanpallewar et al., 2016).

Ubiquitin protein ligase E3 component n-recognin 5 (UBR5) is a kind of HECT (homologous to E6AP C-terminus), which can recognize another E3 ubiquitin ligase of N-Degrons. It has the catalytic ability to directly identify and link ubiquitin to protein degradation. UBR5 can regulate neuronal plasticity by activating NMDARs in the CNS. It participates in the pathological process of CNS diseases through modified ubiquitination, which is crucial in regulating nociception (Pierre et al., 2008). This adjustment is mainly through the subsequent process. Additionally, for CFA-induced chronic inflammatory pain, the increased expression of circRNA-Filip11 (serine A interacting protein 1-like) in the spinal cord regulates nociception by UBR5. The downregulation of UBR5 significantly reduced the nociceptive response induced by Lenti-Filip11. miRNA-1224-mediated splicing of circRNA-Filip11 regulates chronic inflammatory pain throughout by targeting UBR5. Therefore, the development of inflammatory pain could be reduced by inhibiting UBR5 (Pan et al., 2019).

Myc binding protein 2 (MYCBP2) is another E3 ubiquitin ligase, which can inhibit neuron growth and synapse formation by regulating various signaling pathways. Research has proven that its selective deletion in macrophages can reduce zymogen-induced inflammatory pain and promote the resolution of inflammation (Pierre et al., 2018). Other E3 ubiquitin ligases, such as ligand of numb proteins X1/2 (LNX1/LNX2), are functional regulators of neuronal GlyT2. LNX1 and LNX2 interact with GlyT2 and ubiquitinate the C-terminal cluster of the transporter lysine to control the expression and activity of GlyT2. Changes in the expression or activity of GlyT2 lead to the emptying of synaptic vesicles, which may be related to inflammatory pain pathology (de la Rocha-Munoz et al., 2019). Furthermore, the phosphorylation of E3 ubiquitin ligase Cbl-b weakens its binding and ubiquitination to GLUN2B (a type of NMDAR subunit), thereby inhibiting GLUN2B-mediated synaptic currents and inflammatory pain (Zhang et al., 2020).

HUWE1 (HECT, UBA, and WWE domain contains 1), an E3 ubiquitin ligase located in the spinal cord synapse, specifically interacts with GlyRs-α1. It can reduce the surface expression of GlyRs-α1 by ubiquitinating GlyRs-α1. Ubiquitin modification of GlyRs-α1 is a crucial way to reduce peripheral inflammation inhibited by spinal cord glycine. After the surrounding tissues are injured, the inhibitory effect of glycine is weakened, which leads to the occurrence of inflammatory pain. Previous studies showed that HUWE1 contributed to glycinergic disinhibition.

TABLE 2 | Available potential targets of E3 ubiquitin ligases and DUBs for chronic pain.

Categories	The names of the enzymes	Targets	Pain relief	Types of chronic pain	References
E3 ubiquitin ligases	WWP1	Cav3.2	↑	NP	García-Caballero et al., 2014
	Fbxo3	TRAF2/TNIK/GluR1 Cascade	↓	NP	Lai et al., 2016
	Fbxo45	Munc13-1	↓	NP	Lindenlaub et al., 2000
	APC/C	Cdh1	↑	NP	Goel et al., 2015
	NEDD4-2	GluN2D	↑	NP	Staub et al., 2000; Eaton et al., 2010
		Nav1.7, Nav1.8	↑		
	Peli1	MAPK/NF-κB signal	↓	NP	(Börner and Kraus, 2013
	c-Cbl	microglia	↑	NP	Kowalski and Juo, 2012
		ZAP70, PLC-γ1	↓		
	HUWE1	GlyRs-α1	↓	Inflammatory pain	Sekiguchi et al., 2018
	UBR5	circRNA-Filip11	↓	Inflammatory pain	Pierre et al., 2018
DUBs	USP5	Cav3.2	↓	NP, Inflammatory pain	García-Caballero et al., 2014
	UCHL1	Microglial	↓	NP	Ji and Kwon, 2017

↑ *Represents upregulation of the enzymes can relieve pain.*

↓ *Represents downregulation of the enzymes can relieve pain.*

According to the role of the E3 ubiquitin ligases and DUB in chronic pain. Summarized their targets and specific roles in the pain process. APC/C, anaphase-promoting complex; DUB, deubiquitinating enzymes; Fbxo, F-box protein; HUWE1, HECT, UBA, and WWE domain contains 1; MAPK, mitogen-activated protein kinase; NEDD4, neural precursor cell expressed developmentally downregulated protein 4; NF-κB, nuclear factor kappa B; NIK, NcK-interacting kinase; NP, neuropathic pain; TRAF2, tumor necrosis factor receptor-associated factor 2; UBR5, ubiquitin protein ligase E3 component n-recognin 5; UCHL1, ubiquitin C-terminal hydrolase L1; USP5, ubiquitin-specific protease 5; WWP1, HECT E3 ligase E3 ubiquitin-protein ligase 1.

Additionally, knockout of HUWE1 can attenuate GlyRs-α1 ubiquitination, improve glycinergic synaptic transmission, and reduce inflammatory pain. Therefore, it can interfere with the activity of HUWE1and produce analgesic effects by restoring GlyRs-α1-mediated synaptic transmission (Zhang et al., 2019b). This E3-ubiquitin ligase-mediated protein ubiquitination regulates chronic inflammatory pain *via* controlling the level of substrate proteins and then possibly adjusts synaptic efficacy. The results will offer a basis for future research on the role of protein ubiquitination in inflammatory pain (**Table 2**).

Ubiquitin–Proteasome System in Inflammatory Pain

UPS is a key intracellular regulator of inflammation and pathological pain. Intracellular pathways mediated by UPS affect inflammatory pain. It can affect the expression of sensory neuropeptides, which can regulate pain and inflammation.

UPS inhibitors can prevent inflammatory pain. Proteasome inhibitor MG132 reduces inflammatory pain by targeting the sensory neuropeptide SP of the CNS in arthritis. Specifically, the NF-κB family is a major modulator of immune and inflammatory processes following injury and infection (Napetschnig and Wu, 2013). MG132 can inhibit the activation of NF-κB to reverse the inflammatory pain (Ahmed et al., 2017). The generation of new proteasome inhibitors may represent a new pharmacotherapy for inflammatory pain.

Whether the application of a wide range of proteasome inhibitors may have complex effects in these ubiquitination pathways, even limited to the nervous system, and whether it causes adverse effects require careful consideration.

PERSPECTIVES AND CONCLUSION

A large body of evidence has provided a partial explanation of how changes in the ubiquitin system result in improved chronic pain response.

The examples presented here provide only a glimpse into the expanding role of ubiquitination in regulating chronic pain. The ubiquitin system is essential not only in the process of regulating chronic pain but also in pain treatment. However, understanding the molecular mechanisms underlying pain regulation by ubiquitin remains challenging because more components of the ubiquitin system are linked to chronic pain, such as ubiquitin ligase, UPS, and DUBs. And the differences between NP and inflammatory pain are not reported to be specific in ubiquitination. The underlying specific difference needs to be revealed in future studies.

In the process of pain, the ubiquitin signaling pathway often acts in cascade with other nociceptors, which further complicates chronic pain. Dysregulation of gene expression mediated by epigenetic mechanisms is crucial in the occurrence and maintenance of chronic pain caused by multiple reasons. To understand the dynamics and complexity of such events, it is necessary to conduct comprehensive proteomic and genomic research using various types of chronic pain models.

Understanding how the ubiquitin system affects the development of chronic pain can provide new ideas and strategies for pain treatment. Interfering with the ubiquitin pathway using inhibitors, such as proteasome inhibitors, is an effective strategy to treat chronic pain. The application of these strategies in clinical trials will expand and diversify the scope of chronic pain treatment for more effective therapies of patients in the future. Therefore, a deeper insight into the ubiquitin system will be precious for the future development of chronic pain therapies.

AUTHOR CONTRIBUTIONS

JC, YD, and JZ contributed to conception and design of the study. JC wrote the first draft of the manuscript. YD accessed data. JZ contributed to manuscript revision. All authors contributed to the article and approved the submitted version.

FUNDING

This work was supported by grants from the National Natural Science Foundation of China (81870879), Guangzhou Key Laboratory of Mechanism of Spinal Neuropathic Pain, and the Natural Science Foundation of Guangdong Province (2017A030313534), and Guangzhou Key Laboratory of Neuropathic Pain Mechanism at Spinal Cord Level (202102100005).

REFERENCES

Ahmed, A. S., Ahmed, M., Li, J., Gu, H. F., Bakalkin, G., Stark, A., et al. (2017). Proteasome inhibitor MG132 modulates inflammatory pain by central mechanisms in adjuvant arthritis. *Int. J. Rheumatic Dis.* 20, 25–32. doi: 10.1111/1756-185x.12353

Barbosa, C., and Cummins, T. R. (2016). Unusual voltage-gated sodium currents as targets for pain. *Curr. Topics Membranes* 78, 599–638. doi: 10.1016/bs.ctm.2015.12.005

Baumann, A., and Kursula, P. (2017). SUMO on CRMPs - wrestling for pain? *Channels (Austin, Tex)* 11, 265–267. doi: 10.1080/19336950.2017.1311758

Bennett, D. L., Clark, A. J., Huang, J., Waxman, S. G., and Dib-Hajj, S. D. (2019). The role of voltage-gated sodium channels in pain signaling. *Physiol. Rev.* 99, 1079–1151. doi: 10.1152/physrev.00052.2017

Bongiorno, D., Schuetz, F., Poronnik, P., and Adams, D. J. (2011). Regulation of voltage-gated ion channels in excitable cells by the ubiquitin ligases Nedd4 and Nedd4-2. *Channels (Austin, Tex)* 5, 79–88. doi: 10.4161/chan.5.1.13967

Börner, C., and Kraus, J. (2013). Inhibition of NF-κB by opioids in T cells. *J. Immunol. (Baltimore, Md : 1950)* 191, 4640–4647. doi: 10.4049/jimmunol.1300320

Bourinet, E., Altier, C., Hildebrand, M. E., Trang, T., Salter, M. W., and Zamponi, G. W. (2014). Calcium-permeable ion channels in pain signaling. *Physiol. Rev.* 94, 81–140. doi: 10.1152/physrev.00023.2013

Cachemaille, M., Laedermann, C. J., Pertin, M., Abriel, H., Gosselin, R. D., and Decosterd, I. (2012). Neuronal expression of the ubiquitin ligase Nedd4-2 in rat dorsal root ganglia: modulation in the spared nerve injury model of neuropathic pain. *Neuroscience* 227, 370–380. doi: 10.1016/j.neuroscience.2012.09.044

Caputi, F. F., Rullo, L., Stamatakos, S., Candeletti, S., and Romualdi, P. (2019). Interplay between the endogenous opioid system and proteasome complex: beyond signaling. *Int. J. Mol. Sci.* 20:1441. doi: 10.3390/ijms20061441

Caterina, M. J., Schumacher, M. A., Tominaga, M., Rosen, T. A., Levine, J. D., and Julius, D. (1997). The capsaicin receptor: a heat-activated ion channel in the pain pathway. *Nature* 389, 816–824. doi: 10.1038/39807

Chen, P. C., Bhattacharyya, B. J., Hanna, J., Minkel, H., Wilson, J. A., Finley, D., et al. (2011). Ubiquitin homeostasis is critical for synaptic development and function. *J. Neurosci. : Off. J. Soc. Neurosci.* 31, 17505–17513. doi: 10.1523/jneurosci.2922-11.2011

Chen, Y., Kanju, P., Fang, Q., Lee, S. H., Parekh, P. K., Lee, W., et al. (2014). TRPV4 is necessary for trigeminal irritant pain and functions as a cellular formalin receptor. *Pain* 155, 2662–2672. doi: 10.1016/j.pain.2014.09.033

Cheng, W., Chen, Y. L., Wu, L., Miao, B., Yin, Q., Wang, J. F., et al. (2016). Inhibition of spinal UCHL1 attenuates pain facilitation in a cancer-induced bone pain model by inhibiting ubiquitin and glial activation. *Am. J. Transl. Res.* 8, 3041–3048.

Cottrell, G. S., Padilla, B., Pikios, S., Roosterman, D., Steinhoff, M., Gehringer, D., et al. (2006). Ubiquitin-dependent down-regulation of the neurokinin-1 receptor. *J. Biol. Chem.* 281, 27773–27783. doi: 10.1074/jbc.m603369200

de la Rocha-Munoz, A., Nunez, E., Arribas-Gonzalez, E., Lopez-Corcuera, B., Aragon, C., and de Juan-Sanz, J. (2019). E3 ubiquitin ligases LNX1 and LNX2 are major regulators of the presynaptic glycine transporter GlyT2. *Sci. Rep.* 9:14944.

Dou, Y., Tian, X., Zhang, J., Wang, Z., and Chen, G. (2018). Roles of TRAF6 in central nervous system. *Curr. Neuropharmacol.* 16, 1306–1313. doi: 10.2174/1570159x16666180412094655

Dustrude, E. T., Moutal, A., Yang, X., Wang, Y., Khanna, M., and Khanna, R. (2016). Hierarchical CRMP2 posttranslational modifications control NaV1.7 function. *Proc. Natl. Acad. Sci. U.S.A.* 113, E8443–E8452.

Dustrude, E. T., Wilson, S. M., Ju, W., Xiao, Y., and Khanna, R. (2013). CRMP2 protein SUMOylation modulates NaV1.7 channel trafficking. *J. Biol. Chem.* 288, 24316–24331. doi: 10.1074/jbc.m113.474924

Eaton, D. C., Malik, B., Bao, H. F., Yu, L., and Jain, L. (2010). Regulation of epithelial sodium channel trafficking by ubiquitination. *Proc. Am. Thoracic Soc.* 7, 54–64. doi: 10.1513/pats.200909-096js

Ekberg, J. A., Boase, N. A., Rychkov, G., Manning, J., Poronnik, P., and Kumar, S. (2014). Nedd4-2 (NEDD4L) controls intracellular Na(+)-mediated activity of voltage-gated sodium channels in primary cortical neurons. *Biochem. J.* 457, 27–31. doi: 10.1042/bj20131275

François, A., Laffray, S., Pizzoccaro, A., Eschalier, A., and Bourinet, E. (2014). T-type calcium channels in chronic pain: mouse models and specific blockers. *Pflugers Archiv. : Eur. J. Physiol.* 466, 707–717. doi: 10.1007/s00424-014-1484-4

François-Moutal, L., Dustrude, E. T., Wang, Y., Brustovetsky, T., Dorame, A., Ju, W., et al. (2018a). Inhibition of the Ubc9 E2 SUMO-conjugating enzyme-CRMP2 interaction decreases NaV1.7 currents and reverses experimental neuropathic pain. *Pain* 159, 2115–2127. doi: 10.1097/j.pain.0000000000001294

François-Moutal, L., Scott, D. D., Perez-Miller, S., Gokhale, V., Khanna, M., and Khanna, R. (2018b). Chemical shift perturbation mapping of the Ubc9-CRMP2 interface identifies a pocket in CRMP2 amenable for allosteric modulation of Nav1.7 channels. *Channels (Austin, Tex)* 12, 219–227. doi: 10.1080/19336950.2018.1491244

Gadotti, V. M., Caballero, A. G., Berger, N. D., Gladding, C. M., Chen, L., Pfeifer, T. A., et al. (2015). Small organic molecule disruptors of Cav3.2 - USP5 interactions reverse inflammatory and neuropathic pain. *Mol. Pain* 11:12.

Gadotti, V. M., and Zamponi, G. W. (2018). Disrupting USP5/Cav3.2 interactions protects female mice from mechanical hypersensitivity during peripheral inflammation. *Mol. Brain* 11:60.

Garcia-Caballero, A., Gadotti, V. M., Chen, L., and Zamponi, G. W. (2016). A cell-permeant peptide corresponding to the cUBP domain of USP5 reverses inflammatory and neuropathic pain. *Mol. Pain* 12:1744806916642444. doi: 10.1177/1744806916642444

García-Caballero, A., Gadotti, V. M., Stemkowski, P., Weiss, N., Souza, I. A., Hodgkinson, V., et al. (2014). The deubiquitinating enzyme USP5 modulates neuropathic and inflammatory pain by enhancing Cav3.2 channel activity. *Neuron* 83, 1144–1158. doi: 10.1016/j.neuron.2014.07.036

Garcia-Caballero, A., Zhang, F. X., Chen, L., M'Dahoma, S., Huang, J., and Zamponi, G. W. (2019). SUMOylation regulates USP5-Cav3.2 calcium channel interactions. *Mol. Brain* 12:73.

Gautam, V., Trinidad, J. C., Rimerman, R. A., Costa, B. M., Burlingame, A. L., and Monaghan, D. T. (2013). Nedd4 is a specific E3 ubiquitin ligase for the NMDA receptor subunit GluN2D. *Neuropharmacology* 74, 96–107. doi: 10.1016/j.neuropharm.2013.04.035

Glickman, M. H., and Ciechanover, A. (2002). The ubiquitin-proteasome proteolytic pathway: destruction for the sake of construction. *Physiol. Rev.* 82, 373–428. doi: 10.1152/physrev.00027.2001

Goel, P., Manning, J. A., and Kumar, S. (2015). NEDD4-2 (NEDD4L): the ubiquitin ligase for multiple membrane proteins. *Gene* 557, 1–10. doi: 10.1016/j.gene.2014.11.051

Hegde, A. N. (2010). The ubiquitin-proteasome pathway and synaptic plasticity. *Learn. Memory (Cold Spring Harbor, NY).* 17, 314–327. doi: 10.1101/lm.1504010

Henley, J. M., Craig, T. J., and Wilkinson, K. A. (2014). Neuronal SUMOylation: mechanisms, physiology, and roles in neuronal dysfunction. *Physiol. Rev.* 94, 1249–1285. doi: 10.1152/physrev.00008.2014

Honjo, K., and Tracey, W. D. Jr. (2018). BMP signaling downstream of the Highwire E3 ligase sensitizes nociceptors. *PLoS Genet.* 14:e1007464. doi: 10.1371/journal.pgen.1007464

Hsieh, M. C., Ho, Y. C., Lai, C. Y., Chou, D., Chen, G. D., Lin, T. B., et al. (2018). Spinal TNF-α impedes Fbxo45-dependent Munc13-1 ubiquitination to mediate neuropathic allodynia in rats. *Cell Death Dis.* 9:811.

Hu, R., Li, L., Li, D., Tan, W., Wan, L., Zhu, C., et al. (2016). Downregulation of Cdh1 signalling in spinal dorsal horn contributes to the maintenance of mechanical allodynia after nerve injury in rats. *Mol. Pain* 12:1744806916647376. doi: 10.1177/1744806916647376

Huang, D., Liang, C., Zhang, F., Men, H., Du, X., Gamper, N., et al. (2016). Inflammatory mediator bradykinin increases population of sensory neurons expressing functional T-type Ca(2+) channels. *Biochem. Biophys. Res. Commun.* 473, 396–402. doi: 10.1016/j.bbrc.2016.02.118

Huang, J., Liu, J., and Qiu, L. (2020). Transient receptor potential vanilloid 1 promotes EGFR ubiquitination and modulates EGFR/MAPK signalling in pancreatic cancer cells. *Cell Biochem. Funct.* 38, 401–408. doi: 10.1002/cbf.3483

Jensen, T. S., Baron, R., Haanpää, M., Kalso, E., Loeser, J. D., Rice, A. S., et al. (2011). A new definition of neuropathic pain. *Pain* 152, 2204–2205.

Jeong, J. S., Kim, H. Y., Shin, B. S., Lee, A. R., Yoon, J. H., Hahm, T. S., et al. (2018). Increased expression of the Cbl family of E3 ubiquitin ligases decreases Interleukin-2 production in a rat model of peripheral neuropathy. *BMC Anesthesiol.* 18:87. doi: 10.1186/s12871-018-0555-z

Ji, C. H., and Kwon, Y. T. (2017). Crosstalk and interplay between the ubiquitin-proteasome system and autophagy. *Mol. Cells* 40, 441–449.

Joksimovic, S. L., Joksimovic, S. M., Tesic, V., García-Caballero, A., Feseha, S., Zamponi, G. W., et al. (2018). Selective inhibition of Ca(V)3.2 channels reverses hyperexcitability of peripheral nociceptors and alleviates postsurgical pain. *Sci. Signal.* 11:eaao4425. doi: 10.1126/scisignal.aao4425

Khanna, R., Moutal, A., Perez-Miller, S., Chefdeville, A., Boinon, L., and Patek, M. (2020). Druggability of CRMP2 for neurodegenerative diseases. *ACS Chem. Neurosci.* 11, 2492–2505. doi: 10.1021/acschemneuro.0c00307

Kiris, E., Wang, T., Yanpallewar, S., Dorsey, S. G., Becker, J., Bavari, S., et al. (2014). TrkA in vivo function is negatively regulated by ubiquitination. *J. Neurosci. : Off. J. Soc. Neurosci.* 34, 4090–4098. doi: 10.1523/jneurosci.4294-13.2014

Kowalski, J. R., and Juo, P. (2012). The role of deubiquitinating enzymes in synaptic function and nervous system diseases. *Neural Plasticity* 2012:892749.

Kumar, A., Kaur, H., and Singh, A. (2018). Neuropathic Pain models caused by damage to central or peripheral nervous system. *Pharmacol. Rep. : PR.* 70, 206–216. doi: 10.1016/j.pharep.2017.09.009

Laedermann, C. J., Cachemaille, M., Kirschmann, G., Pertin, M., Gosselin, R. D., Chang, I., et al. (2013). Dysregulation of voltage-gated sodium channels by ubiquitin ligase NEDD4-2 in neuropathic pain. *J. Clin. Investigation* 123, 3002–3013. doi: 10.1172/jci68996

Laedermann, C. J., Decosterd, I., and Abriel, H. (2014). Ubiquitylation of voltage-gated sodium channels. *Handbook Exp. Pharmacol.* 221, 231–250. doi: 10.1007/978-3-642-41588-3_11

Lai, C. Y., Ho, Y. C., Hsieh, M. C., Wang, H. H., Cheng, J. K., Chau, Y. P., et al. (2016). Spinal Fbxo3-Dependent Fbxl2 ubiquitination of active zone protein RIM1α mediates neuropathic allodynia through CaV2.2 activation. *J. Neurosci. : Off. J. Soc. Neurosci.* 36, 9722–9738. doi: 10.1523/jneurosci.1732-16.2016

Lai, C. Y., Hsieh, M. C., Ho, Y. C., Wang, H. H., Chou, D., Wen, Y. C., et al. (2018). Spinal RNF20-mediated histone H2B monoubiquitylation regulates mGluR5 transcription for neuropathic allodynia. *J. Neurosci. : Off. J. Soc. Neurosci.* 38, 9160–9174. doi: 10.1523/jneurosci.1069-18.2018

Lapointe, T. K., Basso, L., Iftinca, M. C., Flynn, R., Chapman, K., Dietrich, G., et al. (2015). TRPV1 sensitization mediates postinflammatory visceral pain following acute colitis. *Am. J. Physiol. Gastrointestinal Liver Physiol.* 309, G87–G99.

Lin, T. B., Hsieh, M. C., Lai, C. Y., Cheng, J. K., Chau, Y. P., Ruan, T., et al. (2015). Fbxo3-dependent Fbxl2 ubiquitination mediates neuropathic allodynia through the TRAF2/TNIK/GluR1 cascade. *J. Neurosci. : Off. J. Soc. Neurosci.* 35, 16545–16560. doi: 10.1523/jneurosci.2301-15.2015

Lindenlaub, T., Teuteberg, P., Hartung, T., and Sommer, C. (2000). Effects of neutralizing antibodies to TNF-alpha on pain-related behavior and nerve regeneration in mice with chronic constriction injury. *Brain Res.* 866, 15–22. doi: 10.1016/s0006-8993(00)02190-9

Linley, J. E., Rose, K., Ooi, L., and Gamper, N. (2010). Understanding inflammatory pain: ion channels contributing to acute and chronic nociception. *Pflugers Archiv. : Eur. J. Physiol.* 459, 657–669. doi: 10.1007/s00424-010-0784-6

Liu, S., Karaganis, S., Mo, R. F., Li, X. X., Wen, R. X., and Song, X. J. I. F. N. (2019). β Treatment inhibits nerve injury-induced mechanical allodynia and MAPK signaling by activating ISG15 in mouse spinal cord. *J. Pain : Off. J. Am. Pain Soc.* 21, 836–847. doi: 10.1016/j.jpain.2019.11.010

Manning, D. C. (2004). New and emerging pharmacological targets for neuropathic pain. *Curr. Pain Headache Rep.* 8, 192–198. doi: 10.1007/s11916-004-0051-7

Marangoudakis, S., Andrade, A., Helton, T. D., Denome, S., Castiglioni, A. J., and Lipscombe, D. (2012). Differential ubiquitination and proteasome regulation of Ca(V)2.2 N-type channel splice isoforms. *J. Neurosci. : Off. J. Soc. Neurosci.* 32, 10365–10369. doi: 10.1523/jneurosci.0851-11.2012

Moss, A., Blackburn-Munro, G., Garry, E. M., Blakemore, J. A., Dickinson, T., Rosie, R., et al. (2002). A role of the ubiquitin-proteasome system in neuropathic pain. *J. Neurosci. : Off. J. Soc. Neurosci.* 22, 1363–1372.

Moutal, A., Cai, S., Yu, J., Stratton, H. J., Chefdeville, A., Gomez, K., et al. (2020). Studies on CRMP2 SUMOylation-deficient transgenic mice identify sex-specific NaV1.7 regulation in the pathogenesis of chronic neuropathic pain. *Pain* 161, 2629–2651. doi: 10.1097/j.pain.0000000000001951

Moutal, A., Dustrude, E. T., Largent-Milnes, T. M., Vanderah, T. W., Khanna, M., and Khanna, R. (2018). Blocking CRMP2 SUMOylation reverses neuropathic pain. *Mol. Psychiatry* 23, 2119–2121. doi: 10.1038/mp.2017.117

Moutal, A., White, K. A., Chefdeville, A., Laufmann, R. N., Vitiello, P. F., Feinstein, D., et al. (2019). Dysregulation of CRMP2 post-translational modifications drive its pathological functions. *Mol. Neurobiol.* 56, 6736–6755. doi: 10.1007/s12035-019-1568-4

Muley, M. M., Krustev, E., and McDougall, J. J. (2016). Preclinical assessment of inflammatory pain. *CNS Neurosci. Therapeutics* 22, 88–101. doi: 10.1111/cns.12486

Nakamura, N. (2018). Ubiquitin system. *Int. J. Mol. Sci.* 19:1080.

Napetschnig, J., and Wu, H. (2013). Molecular basis of NF-κB signaling. *Annu. Rev. Biophys.* 42, 443–468. doi: 10.1146/annurev-biophys-083012-130338

Ning, F., Xin, H., Liu, J., Lv, C., Xu, X., Wang, M., et al. (2020). Structure and function of USP5: insight into physiological and pathophysiological roles. *Pharmacol. Res.* 157:104557. doi: 10.1016/j.phrs.2019.104557

Ossipov, M. H., Bazov, I., Gardell, L. R., Kowal, J., Yakovleva, T., Usynin, I., et al. (2007). Control of chronic pain by the ubiquitin proteasome system in the spinal cord. *J. Neurosci. : Off. J. Soc. Neurosci.* 27, 8226–8237. doi: 10.1523/jneurosci.5126-06.2007

Ozaki, T., Matsuoka, J., Tsubota, M., Tomita, S., Sekiguchi, F., Minami, T., et al. (2018). Zinc deficiency promotes cystitis-related bladder pain by enhancing function and expression of Ca(v)3.2 in mice. *Toxicology* 393, 102–112. doi: 10.1016/j.tox.2017.11.012

Pan, Z., Li, G. F., Sun, M. L., Xie, L., Liu, D., Zhang, Q., et al. (2019). MicroRNA-1224 Splicing CircularRNA-Filip1l in an Ago2-Dependent manner regulates chronic inflammatory pain via targeting Ubr5. *J. Neurosci. : Off. J. Soc. Neurosci.* 39, 2125–2143. doi: 10.1523/jneurosci.1631-18.2018

Pickart, C. M. (2001). Mechanisms underlying ubiquitination. *Annu. Rev. Biochem.* 70, 503–533. doi: 10.1146/annurev.biochem.70.1.503

Pierre, S., Maeurer, C., Coste, O., Becker, W., Schmidtko, A., Holland, S., et al. (2008). Toponomics analysis of functional interactions of the ubiquitin ligase PAM (Protein Associated with Myc) during spinal nociceptive processing. *Mol. Cell. Proteomics : MCP.* 7, 2475–2485. doi: 10.1074/mcp.m800201-mcp200

Pierre, S., Zhang, D. D., Suo, J., Kern, K., Tarighi, N., and Scholich, K. (2018). Myc binding protein 2 suppresses M2-like phenotypes in macrophages during zymosan-induced inflammation in mice. *Eur. J. Immunol.* 48, 239–249. doi: 10.1002/eji.201747129

Qiu, S., Li, X. Y., and Zhuo, M. (2011). Post-translational modification of NMDA receptor GluN2B subunit and its roles in chronic pain and memory. *Seminars Cell Dev. Biol.* 22, 521–529. doi: 10.1016/j.semcdb.2011.06.003

Quan, L., Ishikawa, T., Michiue, T., Li, D. R., Zhao, D., Zhu, B. L., et al. (2005). Quantitative analysis of ubiquitin-immunoreactivity in the midbrain periaqueductal gray matter with regard to the causes of death in forensic autopsy. *Legal Med. (Tokyo, Japan)* 7, 151–156. doi: 10.1016/j.legalmed.2004.11.003

Sekiguchi, F., Tsubota, M., and Kawabata, A. (2018). Involvement of voltage-gated calcium channels in inflammation and inflammatory pain. *Biol. Pharmaceutical Bull.* 41, 1127–1134. doi: 10.1248/bpb.b18-00054

Staub, O., Abriel, H., Plant, P., Ishikawa, T., Kanelis, V., Saleki, R., et al. (2000). Regulation of the epithelial Na+ channel by Nedd4 and ubiquitination. *Kidney Int.* 57, 809–815. doi: 10.1046/j.1523-1755.2000.00919.x

Stemkowski, P., García-Caballero, A., Gadotti, V. M., M'Dahoma, S., Huang, S., Black, S. A. G., et al. (2016). TRPV1 nociceptor activity initiates USP5/T-type channel-mediated plasticity. *Cell Rep.* 17, 2901–2912. doi: 10.1016/j.celrep.2016.11.047

Stemkowski, P. L., Garcia-Caballero, A., Gadotti, V. M., M'Dahoma, S., Chen, L., Souza, I. A., et al. (2017). Identification of interleukin-1 beta as a key mediator in the upregulation of Cav3.2-USP5 interactions in the pain pathway. *Mol. Pain* 13:1744806917724698.

Stockton, S. D. Jr., Gomes, I., Liu, T., Moraje, C., Hipólito, L., Jones, M. R., et al. (2015). Morphine regulated synaptic networks revealed by integrated proteomics and network analysis. *Mol. Cell. Proteomics : MCP.* 14, 2564–2576. doi: 10.1074/mcp.m115.047977

Sun, Y. E., Xu, H. Y., Hao, J., Huo, W. W., Qian, Y., and Hou, B. L. (2019). The ubiquitination of spinal MrgC alleviates bone cancer pain and reduces intracellular calcium concentration in spinal neurons in mice. *Neurochem. Res.* 44, 2527–2535. doi: 10.1007/s11064-019-02869-3

Tai, H. C., and Schuman, E. M. (2008). Ubiquitin, the proteasome and protein degradation in neuronal function and dysfunction. *Nat. Rev. Neurosci.* 9, 826–838. doi: 10.1038/nrn2499

Tan, F., Thiele, C. J., and Li, Z. (2014). Collapsin response mediator proteins: potential diagnostic and prognostic biomarkers in cancers (Review). *Oncol. Lett.* 7, 1333–1340. doi: 10.3892/ol.2014.1909

Tomita, S., Sekiguchi, F., Deguchi, T., Miyazaki, T., Ikeda, Y., Tsubota, M., et al. (2019). Critical role of Ca(v)3.2 T-type calcium channels in the peripheral neuropathy induced by bortezomib, a proteasome-inhibiting chemotherapeutic agent, in mice. *Toxicology* 413, 33–39. doi: 10.1016/j.tox.2018.12.003

Treede, R. D., Rief, W., Barke, A., Aziz, Q., Bennett, M. I., Benoliel, R., et al. (2019). Chronic pain as a symptom or a disease: the IASP Classification of Chronic Pain for the International Classification of Diseases (ICD-11). *Pain* 160, 19–27.

Villarejo-López, L., Jiménez, E., Bartolomé-Martín, D., Zafra, F., Lapunzina, P., Aragón, C., et al. (2017). P2X receptors up-regulate the cell-surface expression of the neuronal glycine transporter GlyT2. *Neuropharmacology* 125, 99–116. doi: 10.1016/j.neuropharm.2017.07.018

Wang, L., Yin, C., Liu, T., Abdul, M., Zhou, Y., Cao, J. L., et al. (2020). Pellino1 regulates neuropathic pain as well as microglial activation through the regulation of MAPK/NF-kappaB signaling in the spinal cord. *J. Neuroinflamm.* 17:83.

Weng, W., Yao, C., Poonit, K., Zhou, X., Sun, C., Zhang, F., et al. (2019). Metformin relieves neuropathic pain after spinal nerve ligation via autophagy flux stimulation. *J. Cell. Mol. Med.* 23, 1313–1324. doi: 10.1111/jcmm.14033

Xue, P., Liu, X., Shen, Y., Ju, Y., Lu, X., Zhang, J., et al. (2018). E3 Ubiquitin Ligase c-cbl inhibits microglia activation after chronic

constriction injury. *Neurochem. Res.* 43, 1631–1640. doi: 10.1007/s11064-018-2578-8

Yang, L., Wang, S., Sung, B., Lim, G., and Mao, J. (2008). Morphine induces ubiquitin-proteasome activity and glutamate transporter degradation. *J. Biol. Chem.* 283, 21703–21713. doi: 10.1074/jbc.m800809200

Yang, Y., He, Y., Wang, X., Liang, Z., He, G., Zhang, P., et al. (2017). Protein SUMOylation modification and its associations with disease. *Open Biol.* 7:170167. doi: 10.1098/rsob.170167

Yanpallewar, S., Wang, T., Koh, D. C., Quarta, E., Fulgenzi, G., and Tessarollo, L. (2016). Nedd4-2 haploinsufficiency causes hyperactivity and increased sensitivity to inflammatory stimuli. *Sci. Rep.* 6:32957.

Yi, J. J., and Ehlers, M. D. (2007). Emerging roles for ubiquitin and protein degradation in neuronal function. *Pharmacol. Rev.* 59, 14–39. doi: 10.1124/pr.59.1.4

Zavrski, I., Krebbel, H., Wildemann, B., Heider, U., Kaiser, M., Possinger, K., et al. (2005). Proteasome inhibitors abrogate osteoclast differentiation and osteoclast function. *Biochem. Biophys. Res. Commun.* 333, 200–205. doi: 10.1016/j.bbrc.2005.05.098

Zhang, Z. Y., Bai, H. H., Guo, Z., Li, H. L., Diao, X. T., Zhang, T. Y., et al. (2020). Ubiquitination and functional modification of GluN2B subunit-containing NMDA receptors by Cbl-b in the spinal cord dorsal horn. *Sci. Signal.* 13:eaaw1519. doi: 10.1126/scisignal.aaw1519

Zhang, Z. Y., Bai, H. H., Guo, Z., Li, H. L., He, Y. T., Duan, X. L., et al. (2019a). mGluR5/ERK signaling regulated the phosphorylation and function of glycine receptor α1ins subunit in spinal dorsal horn of mice. *PLoS Biol.* 17:e3000371. doi: 10.1371/journal.pbio.3000371

Zhang, Z. Y., Guo, Z., Li, H. L., He, Y. T., Duan, X. L., Suo, Z. W., et al. (2019b). Ubiquitination and inhibition of glycine receptor by HUWE1 in spinal cord dorsal horn. *Neuropharmacology* 148, 358–365. doi: 10.1016/j.neuropharm.2019.02.002

Zheng, N., and Shabek, N. (2017). Ubiquitin ligases: structure, function, and regulation. *Annu. Rev. Biochem.* 86, 129–157. doi: 10.1146/annurev-biochem-060815-014922

Conflict of Interest: The authors declare that the research was conducted in the absence of any commercial or financial relationships that could be construed as a potential conflict of interest.

frontiers in Molecular Neuroscience

ORIGINAL RESEARCH
published: 04 June 2021
doi: 10.3389/fnmol.2021.690858

Oxaliplatin Depolarizes the IB4$^-$ Dorsal Root Ganglion Neurons to Drive the Development of Neuropathic Pain Through TRPM8 in Mice

*Bin Wu[1,2†], Xiaolin Su[2,3†], Wentong Zhang[2], Yi-Hong Zhang[2], Xinghua Feng[4], Yong-Hua Ji[5] and Zhi-Yong Tan[2]**

[1] Institute of Special Environment Medicine, Nantong University, Nantong, China, [2] Department of Pharmacology and Toxicology, Stark Neurosciences Research Institute, Indiana University School of Medicine, Indianapolis, IN, United States, [3] Department of Biochemistry and Molecular Biology, Indiana University School of Medicine, Indianapolis, IN, United States, [4] Collaborative Innovation Center of Yangtze River Delta Region Green Pharmaceuticals, College of Pharmaceutical Sciences, Zhejiang University of Technology, Hangzhou, China, [5] Laboratory of Neuropharmacology and Neurotoxicology, Shanghai University, Shanghai, China

OPEN ACCESS

Edited by:
Yong Chen,
Duke University, United States

Reviewed by:
Zilong Wang,
Southern University of Science and Technology, China
Changyu Jiang,
Duke University, United States

***Correspondence:**
Zhi-Yong Tan
zt2@iupui.edu

† These authors have contributed equally to this work

Specialty section:
This article was submitted to Pain Mechanisms and Modulators, a section of the journal Frontiers in Molecular Neuroscience

Received: 04 April 2021
Accepted: 10 May 2021
Published: 04 June 2021

Citation:
Wu B, Su X, Zhang W, Zhang Y-H, Feng X, Ji Y-H and Tan Z-Y (2021) Oxaliplatin Depolarizes the IB4$^-$ Dorsal Root Ganglion Neurons to Drive the Development of Neuropathic Pain Through TRPM8 in Mice.
Front. Mol. Neurosci. 14:690858.
doi: 10.3389/fnmol.2021.690858

Use of chemotherapy drug oxaliplatin is associated with painful peripheral neuropathy that is exacerbated by cold. Remodeling of ion channels including TRP channels in dorsal root ganglion (DRG) neurons contribute to the sensory hypersensitivity following oxaliplatin treatment in animal models. However, it has not been studied if TRP channels and membrane depolarization of DRG neurons serve as the initial ionic/membrane drives (such as within an hour) that contribute to the development of oxaliplatin-induced neuropathic pain. In the current study, we studied in mice (1) *in vitro* acute effects of oxaliplatin on the membrane excitability of IB4$^+$ and IB4$^-$ subpopulations of DRG neurons using a perforated patch clamping, (2) the preventative effects of a membrane-hyperpolarizing drug retigabine on oxaliplatin-induced sensory hypersensitivity, and (3) the preventative effects of TRP channel antagonists on the oxaliplatin-induced membrane hyperexcitability and sensory hypersensitivity. We found (1) IB4$^+$ and IB4$^-$ subpopulations of small DRG neurons displayed previously undiscovered, substantially different membrane excitability, (2) oxaliplatin selectively depolarized IB4$^-$ DRG neurons, (3) pretreatment of retigabine largely prevented oxaliplatin-induced sensory hypersensitivity, (4) antagonists of TRPA1 and TRPM8 channels prevented oxaliplatin-induced membrane depolarization, and (5) the antagonist of TRPM8 largely prevented oxaliplatin-induced sensory hypersensitivity. These results suggest that oxaliplatin depolarizes IB4$^-$ neurons through TRPM8 channels to drive the development of neuropathic pain and targeting the initial drives of TRPM8 and/or membrane depolarization may prevent oxaliplatin-induce neuropathic pain.

Keywords: oxaliplatin, neuropathic pain, dorsal root ganglion, IB4, initial drive, membrane depolarization, TRPM8

INTRODUCTION

The third-generation platinum drug oxaliplatin is the most common used drug for locally advanced and metastatic cancer of the colon, rectum, or pancreas. Compared to classic platinum agents, such as cisplatin, oxaliplatin has lower hematotoxicity and gastrointestinal toxicity (de Gramont et al., 2000). However, unlike other platinum agents which cause the chronic neuropathy, oxaliplatin specifically induced acute painful chemotherapy-induced peripheral neuropathy (CIPN) during or within hours after its first infusion in almost 90% patients (Leonard et al., 2005; Gebremedhn et al., 2018). The acute pain may become increasingly severe in the subsequent cycles and can become chronic that lasts for months and years (Beijers et al., 2014; Briani et al., 2014). The oxaliplatin-induced CIPN is evoked or exacerbated by cold, with symptoms including throat discomfort, paresthesia and dysesthesia of the hands, feet, and perioral region; these symptoms often lead to reduction or discontinued use of oxaliplatin treatment (Argyriou et al., 2010; Kerckhove et al., 2017).

The mechanisms of oxaliplatin-induced CIPN include DNA damage, mitochondrial dysfunction, calcium chelation, reactive oxygen species (ROS) production, and ion channel remodeling in dorsal root ganglion (DRG) neurons (Joseph et al., 2008; Descoeur et al., 2011; Boyette-Davis et al., 2015; Viatchenko-Karpinski et al., 2018; Rovini, 2019; Trecarichi and Flatters, 2019). For instance, transient receptor potential (TRP) channels expressed on DRG neurons such as TRPV1, TRPA1, and TRPM8 have been studied following the treatment of oxaliplatin (Chukyo et al., 2018). Several studies have shown that the mRNA expression level of TRPA1 and TRPM8, but not TRPV1 were upregulated within several days after oxaliplatin treatment (Gauchan et al., 2009; Ta et al., 2010; Yamamoto et al., 2015; Nakagawa and Kaneko, 2017). More importantly, mechanical allodynia and cold hypersensitivity induced by single or repeated administration of oxaliplatin was abolished by pharmacological inhibition or a gene deficiency of TRPA1 or TRPM8 (Gauchan et al., 2009; Nassini et al., 2011). These findings suggest that TRPA1 and/or TRPM8 channels play important role in the maintaining of oxaliplatin-induced neuropathic pain several days following oxaliplatin treatment. On the other hand, it has not been studied if TRP channels and membrane depolarization of DRG neurons serve as the initial ionic/membrane drives (such as within an hour) that contribute to the development of oxaliplatin-induced neuropathic pain. In the current study, we investigated the role of TRP channels and membrane depolarization in the initial pain-driving process following oxaliplatin treatment using *in vitro* and *in vivo* mouse models. We characterized the membrane excitability of IB4$^+$ and IB4$^-$ subpopulations of small DRG neurons, examined the responses of IB4$^+$ and IB4$^-$ DRG neurons to acute oxaliplatin, and studied the effects of antagonists of membrane depolarization and subtypes of TRP channels on the membrane hyperexcitability and/or pain behaviors induced by oxaliplatin. We found that IB4$^+$ and IB4$^-$ subpopulations of small DRG neurons displayed large differences in membrane excitability and that oxaliplatin selectively depolarized IB4$^-$ neurons. Antagonists of TRPA1 or TRPM8 prevented oxaliplatin-induced membrane depolarization and that targeting membrane depolarization or TRPM8 prevented oxaliplatin-induced neuropathic pain behaviors. There results suggest that TRPM8 and membrane depolarization in IB4$^-$ neurons might serve as the initial ionic/membrane drives that contribute to the development of oxaliplatin-induced neuropathic pain.

MATERIALS AND METHODS

Animals

Male C57BL/6 mice at the age of 8 weeks (Jackson Laboratory, Bar Harbor, ME, United States) were used for cell culture and behavior experiments. Mice were housed five or less per cage at a temperature-controlled room (22 $\pm$ 0.5°C, 12 h/12 h light/dark cycle) and were with free access to water and pellet diet. All experimental protocols were approved by the Institutional Animal Care and Use Committees of the Indiana University School of Medicine, Indianapolis, IN, United States. All procedures were conducted in accordance with the Guide for Care and Use of Laboratory Animals published by the National Institutes of Health and the ethical guidelines established by the International Association for the Study of Pain.

Drugs and Their Administration

Oxaliplatin and Capsazepine were purchased from Sigma-Aldrich (St. Louis, MO, United States). Retigabine was purchased from Alomone Labs (Jerusalem, Israel), A-967079 was purchased from MedChemExpress (Monmouth Junction, NJ, United States), and TC-I was purchased from Tocris, Bio-Techne Corporation (Minneapolis, MN, United States). For electrophysiology, stock solutions were made in distilled water (oxaliplatin, 10 mM) or DMSO (A-967079, capsazepine, and TC-I). The stock solutions were diluted by bath solution to reach the final concentration of chemicals including oxaliplatin (50 μM), A-967079 (1 μM), capsazepine (10 μM) and TC-1 (10 nM). For chemicals diluted from DMSO stocks, the final solution contains 0.1% DMSO. All these drugs were pre-treated in the bath solution for 15–60 min before electrophysiological recordings. For behavior test, stock solutions of oxaliplatin in distilled water (5 mg/ml), were further diluted in 5% glucose to give the final concentration of 1.25 mg/ml. Retigabine, A-967079, TC-1 were dissolved in DMSO and further diluted in saline (to give 2% DMSO) for different final concentrations. A single intraperitoneal (i.p.) injection of oxaliplatin (5 mg/kg) was conducted and retigabine (10 mg/kg, i.p.), TC-I (10 mg/kg, i.p.) and A-967079 (100 mg/kg, p.o.) were administrated daily for 5 days from 2 days before to 2 days after the injection of oxaliplatin. Chemicals without specified sources were from Sigma-Aldrich (St. Louis, MO, United States).

Behavior Test

All the testing was carried out in accordance with the approved guidelines. All behavioral measurements were performed in conscious, unrestrained, and age-matched adult male mice.

Mechanical Nociceptor Assay

As described previously, the von Frey assay of "simplified up-down" method was used to assess mechanical sensitivity (Su et al., 2019). Mice were placed in Plexiglas cubicle containers on a metal mesh wire platform to allow access to the plantar hindpaw. A set of eight calibrated von Frey filaments ranging from 0.008 to 6 g (North Coast Medical, Morgan Hill, CA, United States) were applied alternately to the plantar surface of each hindpaw until they bent. The duration of each stimulus was approximately 1 s and nociceptive behaviors included retraction/lifting, rapid shaking, and/or licking of the hindpaw.

Heat Nociceptor Assay

The thermal sensitivity was assessed by applying infrared heating to the plantar surface of hindpaw and the response latency was read from an automated device (IITC model 400, Woodland Hills, CA, United States), as described previously (Zhou et al., 2019). Each hindpaw was tested five times with 5 min interval, and the withdrawal latency was averaged. To avoid tissue damage by prolonged thermal stimuli, cut off latency was set as 20 s.

Cold Nociceptor Assay

The acetone test was performed as previously described (Su et al., 2019). Mice were placed to the same setting described above for the von Frey test. Fifty microliter of acetone was applied to the center of the ventral side of the hindpaw and responses were observed. In the first 20 s following acetone application, if the mouse did not withdraw, flick or stamp of the paw then 0 points were recorded for the trial. However, if within this 20 s period the animal responded to acetone, then the animal's response was assessed for an additional 20 s. Responses to acetone were graded according to the following 4-point scale: 0, no response; 1, quick withdrawal, flick or stamp of the paw; 2, prolonged withdrawal or repeated flicking of the paw; 3, repeated flicking of the paw with licking directed at the paw. Acetone test was applied alternately three times to each paw and the responses scored categorically.

Rotarod Test

The rotarod test was conducted according to the previous publication (Liu et al., 2014). The animals had two sessions of training tests before the first scheduled test. At each training or scheduled test, three levels of rotating speed were used: 1–18 rpm, 3–30 rpm, and 4–40 rpm. The time for the animal to stay on the rod from the beginning of rod-rotation to the falling of the animal to the ground was recorded. A cut-off time of 120 s was used.

Cell Culture

Dorsal root ganglion neurons were dissociated and prepared from adult mice using a similar protocol as previously described (Su et al., 2019). Briefly, mice were sacrificed by exposure to CO_2 and decapitated. DRG were rapidly removed and placed in Puck's solution containing digesting enzymes. The DRGs were digested with Liberase TM (0.35 U/ml; Sigma-Aldrich, St. Louis, MO, United States) for 35–40 min before another 10 min with Liberase TL (0.25 U/ml; Sigma-Aldrich, St. Louis, MO, United States) and papain (30 U/ml, Worthington Biochemical) at 37°C. The ganglia were then triturated with fire-polished Pasteur pipettes. The dispersed cells were resuspended in F12 (Thermo Fisher Scientific, Waltham, MA, United States) medium supplemented with 10% FBS (Thermo Fisher Scientific, Waltham, MA, United States) and 1% penicillin/streptomycin (MediaTech, Inc., Manassas, VA, United States) and plated on coverslips coated with polyornithine (Neuvitro Corporation, Vancouver, WA, United States) and laminin. Cell cultures were maintained in regular 95% air and 5% CO_2 at 37°C in an incubator.

Electrophysiological Recordings

Dorsal root ganglion neurons were recording 16–24 h after dissociation as described previously (Su et al., 2019; Wu et al., 2019). Small diameter DRG neurons (<25 μm) were chosen for whole-cell patch clamp recording in the current-clamp mode at room temperature. A perforated whole-cell patch clamp recording was conducted by including 240 μg/mL Amphotericin B in the pipette solution (Tan et al., 2010). The bath solution consisted of 140 mM NaCl, 3 mM KCl, 2 mM MgCl2, 2 mM CaCl2, 10 mM HEPES, pH 7.3. DRG neurons were recorded with fire-polished, borosilicate glass patch pipettes (5–8 MΩ), which were pulled from borosilicate glass capillaries (Harvard Apparatus, Holliston, MA, United States) using a Sutter P-97 puller (Sutter Instrument, Novato, CA, United States). The pipette solution contained 30 mM KCl, 110 mM potassium gluconate, 0.5 mM EGTA, 5 mM HEPES, and 3 mM Mg-ATP, pH 7.3. Data were acquired using Axopatch 200B patch-clamp amplifier (Molecular Devices Corporation, Sunnyvale, CA, United States) driven by a personal computer in conjunction with an A/D and D/A board (DigiData 1320 A series interface, Molecular Devices Corporation). The action potential (AP) was evoked by depolarizing current steps with long or short time durations (1,000 ms or 5 ms). The long current steps were used to test AP rheobases and AP numbers. The short current steps were used to trigger single action potential that was used to calculate the shape properties of APs. Signals were low-pass filtered at 5 kHz, sampled at 20 kHz and analyzed offline. To avoid the confounding effects of IB4 staining on the forming of Giga-seal for patch clamp recording and potentially on the electrophysiological properties of DRG neuron, DRG neurons were stained by IB4-FITC (5 μg/ml, incubated for 10 min) immediately after recording to distinguish IB4$^+$ and IB4$^-$ neurons (Dirajlal et al., 2003; Vilceanu et al., 2010).

Quantification and Statistics

GraphPad Prism v5.0 was used for statistical analyses. All the results were presented as mean ± SEM. The behavioral data were analyzed by two-way repeated measures (RM) ANOVA followed by Bonferroni test. The electrophysical recording data were analyzed by Student's *t*-test or two-way RM ANOVA followed by Bonferroni test. For all experiments, $P < 0.05$ was considered to be significant ($^*P < 0.05$, $^{**}P < 0.01$, and $^{***}P < 0.001$).

RESULTS

IB4$^+$ and IB4$^-$ Neurons Showed Substantially Different Electrophysiological Properties

IB4$^+$ and IB4$^-$ neurons are two major cell types of small diameter (<25 μm) DRG neurons, most of which are nociceptive. To begin with the study, we compared the electrophysiological properties of small IB4$^+$ (n = 21) and IB4$^-$ (n = 38) DRG neurons using a perforated current-clamp whole-cell recording (**Figure 1A**). As shown in **Figure 1**, the membrane capacitance (Cm, **Figure 1B**) and membrane resistance (Rm, **Figure 1C**) were similar between IB4$^+$ and IB4$^-$ neurons. Compared to IB4$^-$ neurons, the resting membrane potentials in IB4$^+$ neurons were significantly depolarized and the rheobase currents were lower (**Figures 1D–F**). Although the number of action potentials, triggered by current injections from 20 to 100 pA were not significantly different (**Figure 1G**), a suprathreshold current injection (at 3 × rheobase) elicited significantly more action potentials in IB4$^-$ neurons than those in IB4$^+$ ones (**Figure 1H**).

We further compared the properties of single action potentials elicited in IB4$^+$ (n = 17) and IB4$^-$ (n = 24) neurons (**Figure 1I**). Although the amplitude (**Figure 1J**), duration (**Figure 1K**), the maximal rising slope (68.8 ± 4.3 mV/ms in IB4$^+$ cells and 70.9 ± 4.0 mV/ms in IB4$^-$ cells) or decaying slope of action potentials (−55.7 ± 3.3 mV/ms in IB4$^+$ cells and −64.0 ± 2.9 mV/ms in IB4$^-$ cells) were not significantly different between these two cell subtypes, the afterhyperpolarization of action potentials in IB4$^+$ was nearly doubled compared to that in IB4$^-$ neurons (**Figure 1L**). Moreover, the action potential in IB4$^+$ neurons exhibited an apparent afterdepolarization

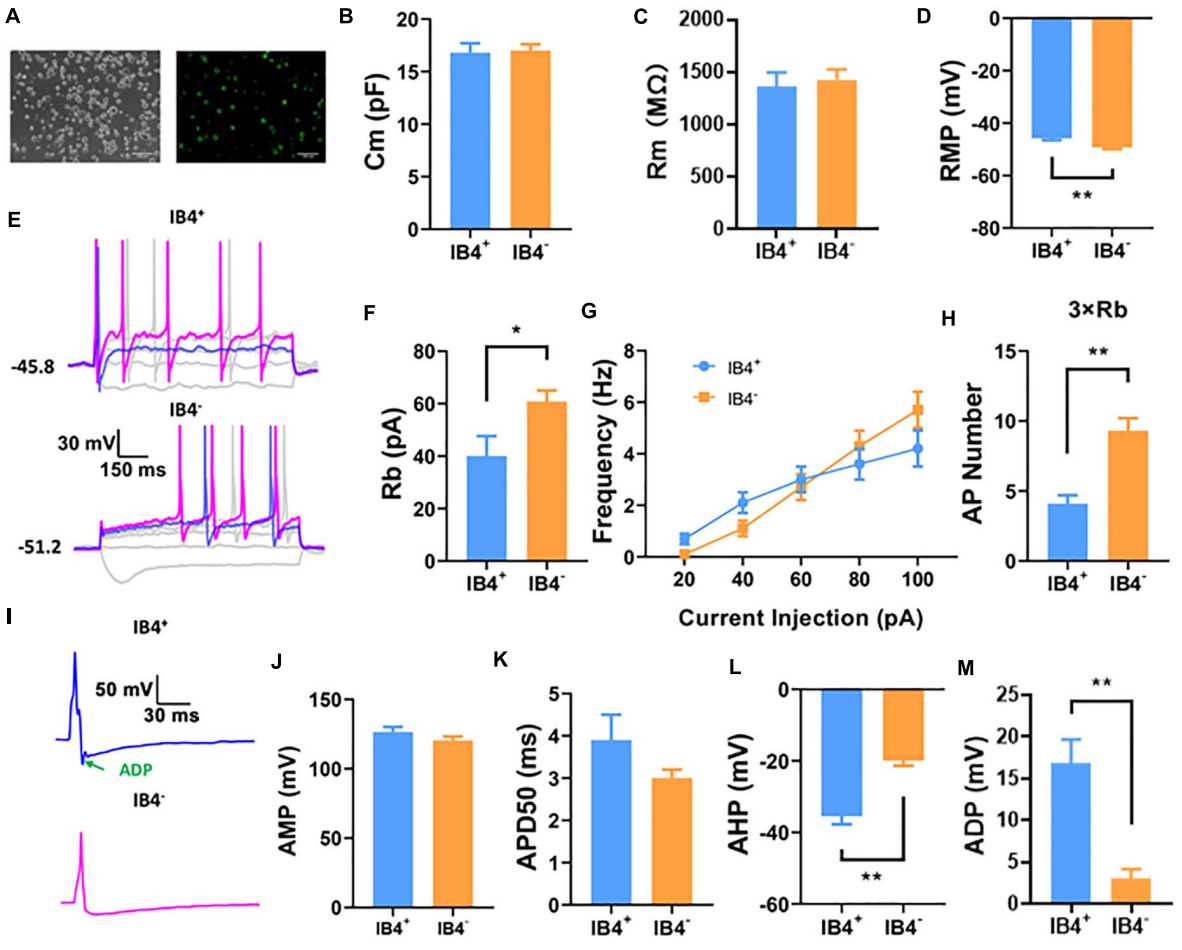

FIGURE 1 | Comparison of passive and active properties of IB4$^+$ and IB4$^-$ subpopulations of small DRG neurons in mouse. IB4$^+$ and IB4$^-$ subpopulations of small DRG neurons (<25 μm), separated by the staining of IB4-FITC **(A)**. Small DRG neurons were recorded in current-clamp mode using a perforated configuration of whole-cell patch clamping. To avoid the confounding effects of IB4 staining on the forming of Giga-seal for patch clamp recording and potentially on the electrophysiological properties of DRG neurons, the DRG neurons were stained immediately after recording. Representative recordings using a long (1,000 ms) or short (5 ms) step current protocol were shown in **(E,I)**, respectively. Passive properties including membrane capacitance [Cm, **(B)**], membrane resistance [Rm, **(C)**], resting membrane potential [RMP,**(D)**], and active properties including rheobase [Rb, **(F)**], frequency **(G)**, number at 3x rheobase **(H)**, amplitude [AMP, **(J)**], half duration [APD50, **(K)**], afterhyperpolarization [AHP, **(L)**], and afterdepolarization [ADP, **(I,M)**] of action potentials were compared between IB4$^+$ and IB4$^-$ neurons. n = 17–38 for each groups (see detailed numbers for each group in results). *, $P < 0.05$; **, $P < 0.01$; Student's t-test.

potential (ADP) spike, which is often absent in IB4$^-$ neurons (**Figures 1I,M**). Taken together, our results suggest that the electrophysiological properties between mouse IB4$^+$ and IB4$^-$ neurons are substantially different.

Oxaliplatin Selectively Depolarized IB4$^-$ Neurons, but Not IB4$^+$ Neurons

To assess the effects of oxaliplatin on the electrophysiological properties in the two subgroups of small DRG neurons, IB4$^+$ and IB4$^-$ DRG neurons were recorded after 15–60 min pre-treatment of oxaliplatin (50 μM) *in vitro*. The cells in control (n = 12 and 13 for IB4$^+$ and IB4$^-$ neurons, respectively) and oxaliplatin (n = 8 and 14 for IB4$^+$ and IB4$^-$ neurons, respectively) groups have similar membrane capacitance for both IB4$^+$ and IB4$^-$ groups (**Figure 2A**). In addition, oxaliplatin did not change the membrane resistance (**Figure 2B**), resting membrane potential (**Figure 2C**), the rheobase and the firing frequency of action potentials in IB4$^+$ neurons significantly (**Figures 2D,F,G**). In contrast, the membrane resistances of IB4$^-$ neurons deceased by ∼500 MΩ after oxaliplatin treatment (**Figure 2B**). Meanwhile, the resting potentials of IB4$^-$ neurons were depolarized by ∼5.6 mV following oxaliplatin treatment (**Figure 2C**), which consequently reduced the rheobase current and increased the firing frequency of action potentials trigged by 60–100 pA of injection currents (**Figures 2E,F,H**). The other parameters of action potentials such as AP threshold, amplitude, half-width, and afterhyperpolarization were not significantly changed by oxaliplatin in both cell subtypes (**Table 1**). Overall, these results indicate that the excitability of IB4$^-$ neurons, but not IB4$^+$ neurons, were selectively enhanced by acute oxaliplatin treatment *in vitro*.

Retigabine Prevented Oxaliplatin-Induced Nociceptive Behavior

To test if the oxaliplatin-induced membrane depolarization of DRG neurons might serve as an initial drive that contributes to the development of oxaliplatin-induced sensory hypersensitivity, we examined the potential preventative effects of retigabine, an opener of potassium channel Kv7 that hyperpolarizes the resting potential of DRG neurons (Corbin-Leftwich et al., 2016), on the sensory and motor behaviors in oxaliplatin treated mice.

TABLE 1 | Shape properties of action potentials in the absence and presence of oxaliplatin.

IB4$^+$	Vt (mV)	AMP (mV)	AHP (mV)	APD50 (ms)
Control (n = 12)	−13.8 ± 4.2	125.9 ± 4.6	−37.8 ± 2.8	3.4 ± 0.2
Oxaliplatin (n = 8)	−18.1 ± 3.0	128.7 ± 6.5	−30.5 ± 1.4	3.6 ± 0.6
IB4$^-$				
Control (n = 13)	−17.0 ± 2.5	118.4 ± 5.0	−21.9 ± 2.4	3.4 ± 0.3
Oxaliplatin (n = 14)	−12.2 ± 2.8	112.3 ± 2.3	−20.6 ± 2.3	3.5 ± 0.3

Vt, voltage threshold; AMP, amplitude; AHP, afterhyperpolarization; APD50, half duration.

As shown in **Figure 3** (n = 6 for all groups), oxaliplatin significantly reduced the paw withdrawal threshold to mechanical stimuli (**Figure 3A**) and increased withdrawal score to cold stimuli (**Figure 3B**) 3 days after oxaliplatin treatment (5 mg/kg, ip). In contrast to the mechanical allodynia and cold hyperalgesia, oxaliplatin did not change the paw withdrawal latency to heat stimuli (**Figure 3C**) or time stayed on rod for the rotarod test (**Figure 3D**) 4 days following oxaliplatin, in the same groups of animals that had their mechanical and cold tests on Day 3 (**Figures 3A,B**). Although heat and motor behaviors were tested at Day 4 in these groups of animals in order to compare different types of behaviors in same groups of animals, separate experiments found that heat and motor behaviors were not changed by oxaliplatin at Day 3 as well (data not shown).

To test the potential preventative effects on oxaliplatin-induced sensory hypersensitivity, retigabine (10 mg/kg, ip, daily) was administrated at Day −2, Day −1, Day 0, Day 1, and Day 2. Oxaliplatin was injected at Day 0. As shown in **Figure 3**, retigabine largely prevented mechanical allodynia (**Figure 3A**) and significantly attenuated cold hyperalgesia (**Figure 3B**) caused by oxaliplatin. On the other hand, retigabine did not change heat or motor behaviors significantly (**Figures 3C,D**).

TRP Channels Mediated the Depolarization Induced by Oxaliplatin

As the membrane depolarization may be the key electrophysiological effect caused by oxaliplatin that consequently results in the neuronal hyperexcitability (**Figure 2**), we further studied the possible ion channels that may be involved in the oxaliplatin-induced membrane depolarization. Because the membrane resistance of IB4$^-$ neurons was significantly reduced by oxaliplatin along with the membrane depolarization, it is suggested that oxaliplatin increased the permeability of extracellular cations, such as sodium and calcium, at resting state. As TRP channels are a major family of non-selective cation channels expressed in DRG neurons that are directly involved in a variety of chemical and thermal sensing, we tested whether some of the major TRP channel subtypes are involved in the oxaliplatin-induced membrane depolarization. Specific channel antagonists including A-967079 (1 μM) (**Figure 4A**), Capsazepine (10 μM) (**Figure 4B**), and TC-I (10 nM) (**Figure 4C**), were used to block TRPA1, TRPV1, and TRPM8 channels, respectively.

As shown in **Figure 4**, pre-treatment of Capsazepine (n = 10 and 11 for control and oxaliplatin groups, respectively) did not prevent the oxaliplatin-induced changes in membrane resistance (**Figure 4D**), resting membrane potential (**Figure 4E**), AP rheobase (**Figure 4F**). However, in the presence of A-967079 (n = 12 and 10 for control and oxaliplatin groups, respectively) or TC-I (n = 6 and 12 for control and oxaliplatin groups, respectively), there were no significant changes in these parameters between control and oxaliplatin groups (**Figures 4D–F**). These results indicate that TRPA1 and/or TRPM8, but not TRPV1, may contribute to the oxaliplatin-induced membrane depolarization and neuronal sensitization, which might contribute to the initiation of sensory hypersensitivity induced by oxaliplatin.

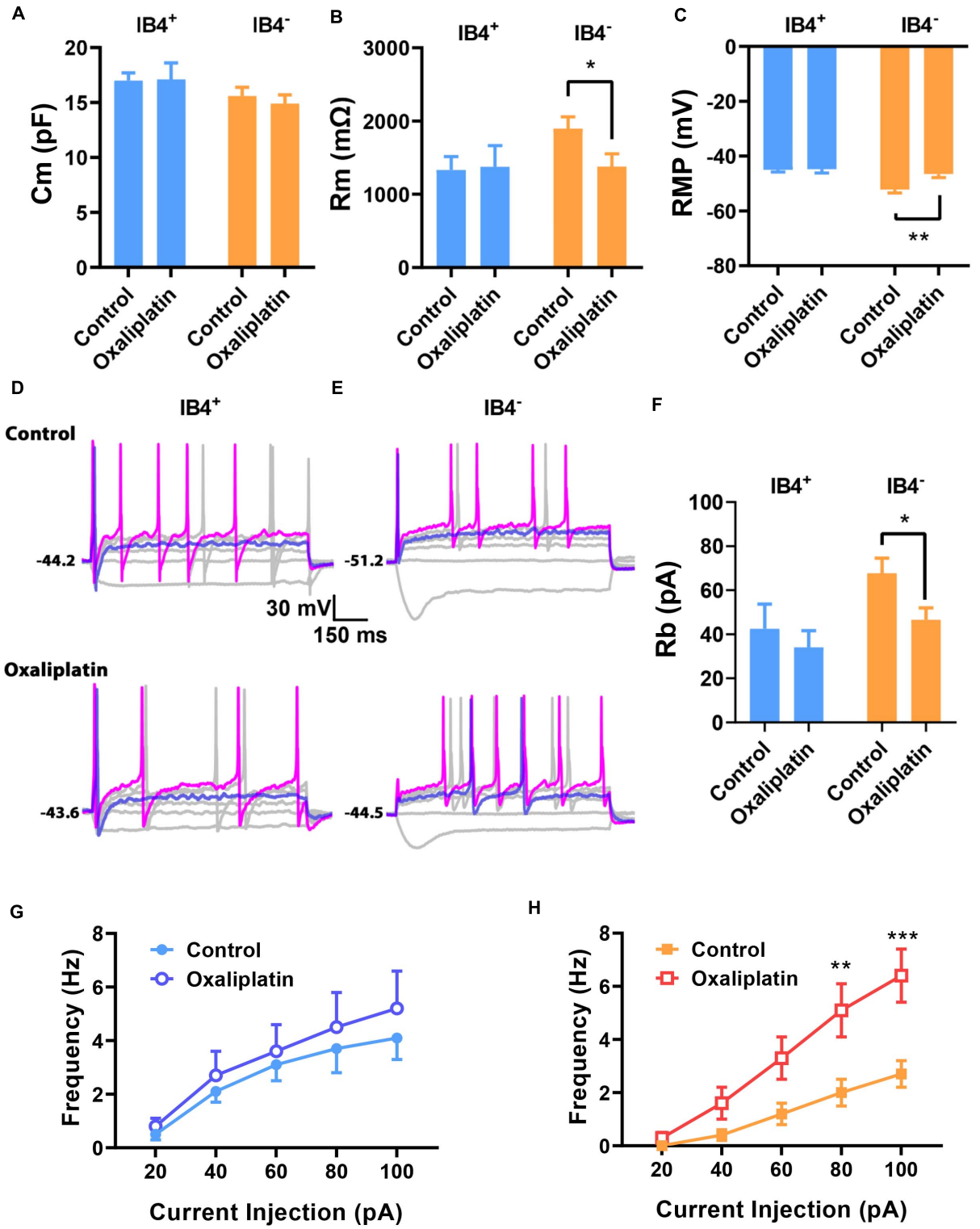

FIGURE 2 | Effects of oxaliplatin on the electrophysiological properties of IB4$^+$ and IB4$^-$ subpopulations of small DRG neurons. Oxaliplatin (50 μM) was pre-treated in the recording chamber for 15–60 min. The passive and active properties of IB4$^+$ and IB4$^-$ subpopulations of small DRG neurons were recorded and presented in the same way described in the legend of **Figure 1**. Oxaliplatin did not change the Cm of both IB4$^+$ and IB4$^-$ neurons **(A)** but decreased the Rm **(B)** and depolarized the RMP **(C)** in IB4$^-$ neurons; **(D,E)** Representative recordings from IB4$^+$ or IB4$^-$ DRG neurons in the absence or presence of oxaliplatin, respectively. **(F)** The effect of oxaliplatin on rheobase of IB4$^+$ and IB4$^-$ neurons. **(G,H)** The effect of oxaliplatin on the firing frequency of IB4$^+$ (G) and IB4$^-$ (H) neurons, respectively. n = 8–14 for each group (see detailed numbers for each group in results). $^*P < 0.05$, $^{**}P < 0.01$, $^{***}P < 0.001$, Student's t-test **(B,C,F)** or Two-way repeated measure ANOVA **(H)**.

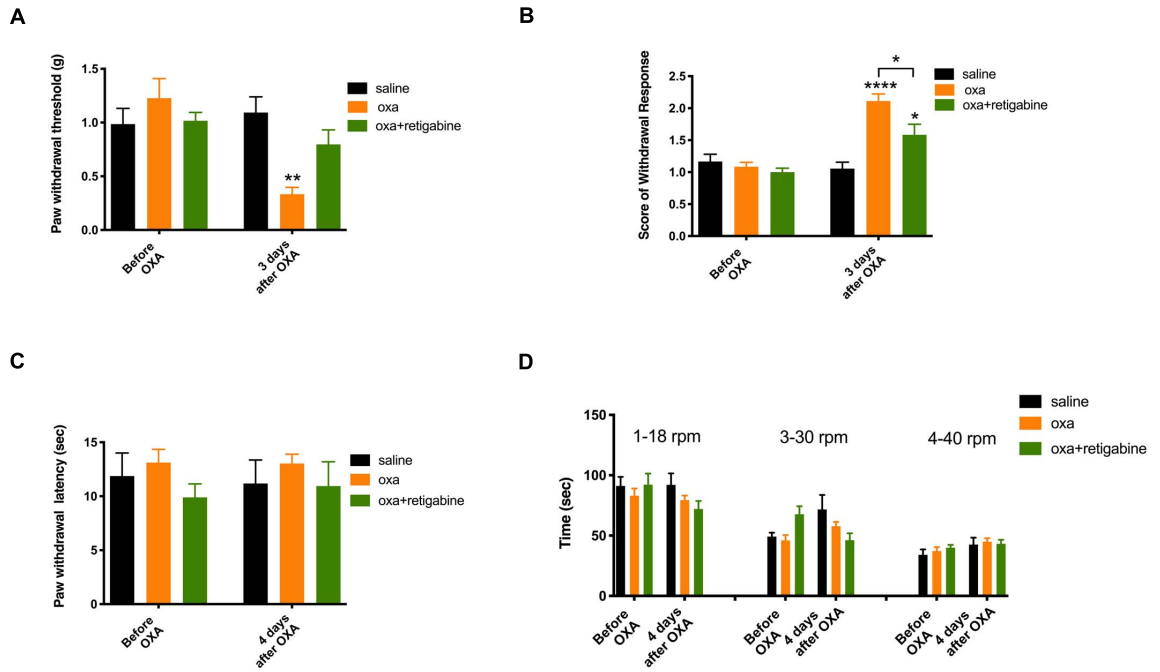

FIGURE 3 | Effects of retigabine on the sensory and motor behaviors following oxaliplatin treatment. Oxaliplatin (oxa, 5 mg/kg, ip) was administrated at Day 0. Retigabine (10 mg/kg, ip, daily) was treated at Day –2, Day –1, Day 0, Day 1, and Day 2. The same groups of animals were tested for mechanical and cold behaviors at Day 3, and were tested for heat and motor behaviors at Day 4. **(A)** Paw withdrawal threshold to Von-Frey filament; **(B)** Score of withdrawal response to acetone; **(C)** Paw withdrawal latency to radiant heat; and **(D)** Time stayed on rod at different speeds in rotarod tests (n = 6 for all groups). *, $P < 0.05$; **, $P < 0.01$; ****, $P < 0.0001$; two-way repeated measure ANOVA.

TC-I, but Not A-967079, Prevented Oxaliplatin-Induced Nociceptive Behavior

To test if TRPM8 and TRPA1 might be involved in the initial pain-driving process of the oxaliplatin-induced sensory hypersensitivity, we examined the potential preventative effects of TC-I and A-967079 on the sensory and motor behaviors in oxaliplatin treated mice.

As shown in **Figure 5** (n = 6 for all groups), daily treatment of 10 mg/kg TC-I (ip, administrated at Day −2, Day −1, Day 0, Day 1, and Day 2) largely prevented mechanical and cold hypersensitivity induced by oxaliplatin administrated at Day 0 (**Figures 5A,B**) without causing any changes in the heat and motor behaviors tested (**Figures 5C,D**). In contrast, the treatment of 100 mg/kg A-967079 (po) with the same schedule of TC-I did not change any behaviors following oxaliplatin administration (**Figure 6**) (n = 6 for all groups). These results suggest that TRPM8 may play a critical role in the initiation of sensory hypersensitivity induced by oxaliplatin.

DISCUSSION

In the present study, we found that there were previously undiscovered, substantial differences in membrane excitability between IB4$^+$ and IB4$^-$ subpopulations of small-sized DRG neurons in mice. These differences included depolarized resting membrane potential, lower rheobase of the action potential, overwhelmingly larger afterdepolarization, and nearly doubled afterhyperpolarization in IB4$^+$ neurons compared to IB4$^-$ neurons (**Figure 1**). Differential properties of membrane excitability have been reported previously between IB4$^+$ and IB4$^-$ subpopulations of small DRG neurons of rats and mice (Stucky and Lewin, 1999; Wu and Pan, 2004; Choi et al., 2007; Zhang et al., 2010). These differences, in IB4$^+$ compared to IB4$^-$ subpopulation of neurons, included a longer duration of the action potential in both rat and mouse neurons, a hyperpolarized resting membrane potential and/or higher rheobases of action potentials in rat neurons, and a smaller afterhyperpolarization in cutaneous rat neurons. Interestingly, none of the major findings in the present study have been reported previously. A possible reason for the different findings between previous and current studies could be due to the different recording configuration of whole-cell patch clamping. Typical whole-cell recordings were used in the previous studies while a perforated whole-cell recording was used in the present study. As the perforation introduced by amphotericin B does not allow the exchange of ions and molecules larger than monovalent ions between patch pipettes and cytosols of cells, divalent ions such as intracellular Ca^{2+}, and other cytosolic molecules might contribute to these differences. For example, a predominant expression of large conductance, calcium activated potassium currents (BK_{Ca}) was discovered in IB4$^+$ cutaneous DRG neurons which would result

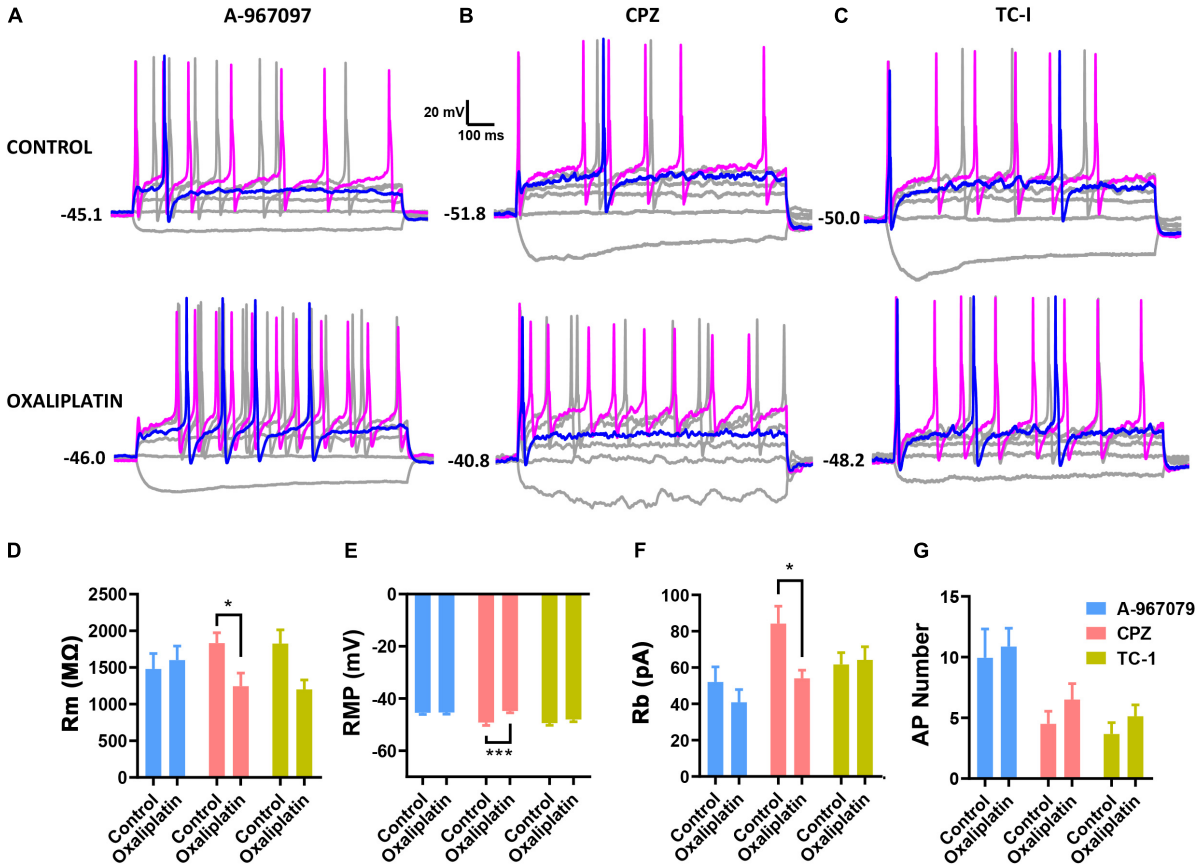

FIGURE 4 | Effects of selective TRP channel antagonists on the electrophysiological properties of IB4$^+$ and IB4$^-$ subpopulations of small DRG neurons. Selective antagonists for TRPA1 (1 μM A-967097), TRPV1 (10 μM Capsazepine, CPZ), or TRPM8 (10 nM TC-I) were pre-treated in the recording chamber for 15 min before the addition of 50 μM oxaliplatin. The passive and active properties of IB4$^+$ and IB4$^-$ subpopulations of small DRG neurons were recorded and presented in the same way described in the legend of **Figure 1**. **(A-C)** Representative recordings in the absence or presence of oxaliplatin, and in the presence of A-967097, Capsazepine, and TC-I, respectively. Effect of oxaliplatin on Rm **(D)**, RMP **(E)** and Rb **(F)** in each group of TRP antagonists. **(G)** Number of action potentials evoked by 100 pA current injection in each group of cells. n = 6–12 for each group (see detailed numbers for each group in results). $^*P < 0.05$, $^{***}P < 0.001$, Student's t-test.

in a larger afterhyperpolarization in these neurons (Zhang et al., 2010). However, a smaller afterhyperpolarization was actually observed in these neurons using typical whole-cell recording (Zhang et al., 2010). On the other hand, using perforated whole-cell recording, we found that there were a nearly doubled afterhyperpolarization expressed in the IB4$^+$ DRG neurons (**Figures 1I,L**). Therefore, the revealing of the larger afterhyperpolarization in IB4$^+$ neurons is likely due to the perforated whole-cell recording used in the current study that allowed the endogenous Ca^{2+} dynamics unbuffered by the Ca^{2+} chelators included in the patch pipette. In addition to the different configurations of whole-cell recordings, other factors such as species of rodents, mouse strains, culture protocols could also contribute to the differences among previous and current studies.

Among the major differential membrane properties between IB4$^+$ and IB4$^-$ neurons found in the current study, the afterdepolarization recorded in the small DRG neurons has not been reported (**Figures 1I,M**). Previously a different type of afterdepolarization was reported in the subpopulations of medium, or small-to-medium DRG neurons that are enriched with T-type calcium channels (Ca_T) in rats (White et al., 1989; Nelson et al., 2005). However, the afterdepolarization recorded from Ca_T-enriched neurons did not appear at the resting membrane potential and a membrane hyperpolarization was needed to induce this type of afterdepolarization. On the other hand, afterdepolarization recorded in the small mouse neurons of the present study was induced at normal resting membrane potential. Moreover, the afterdepolarization was much shorter in the present study compared to that recorded in the previous studies. It has been reported that a variety of ion currents can contribute to afterdepolarization in neurons. These ionic mechanisms include low threshold sodium currents, non-selective cationic currents, KCNQ/M channels, calcium-activated chloride currents, and sodium-calcium exchanger (Higashi et al., 1993; Linden et al., 1994; Azouz et al., 1996; Haj-Dahmane and Andrade, 1998; Yue and Yaari, 2004; Ghitani et al., 2016). As it would beyond the scope of the current study, future studies are needed to study the ionic mechanism of the novel afterdepolarization recorded in the present study.

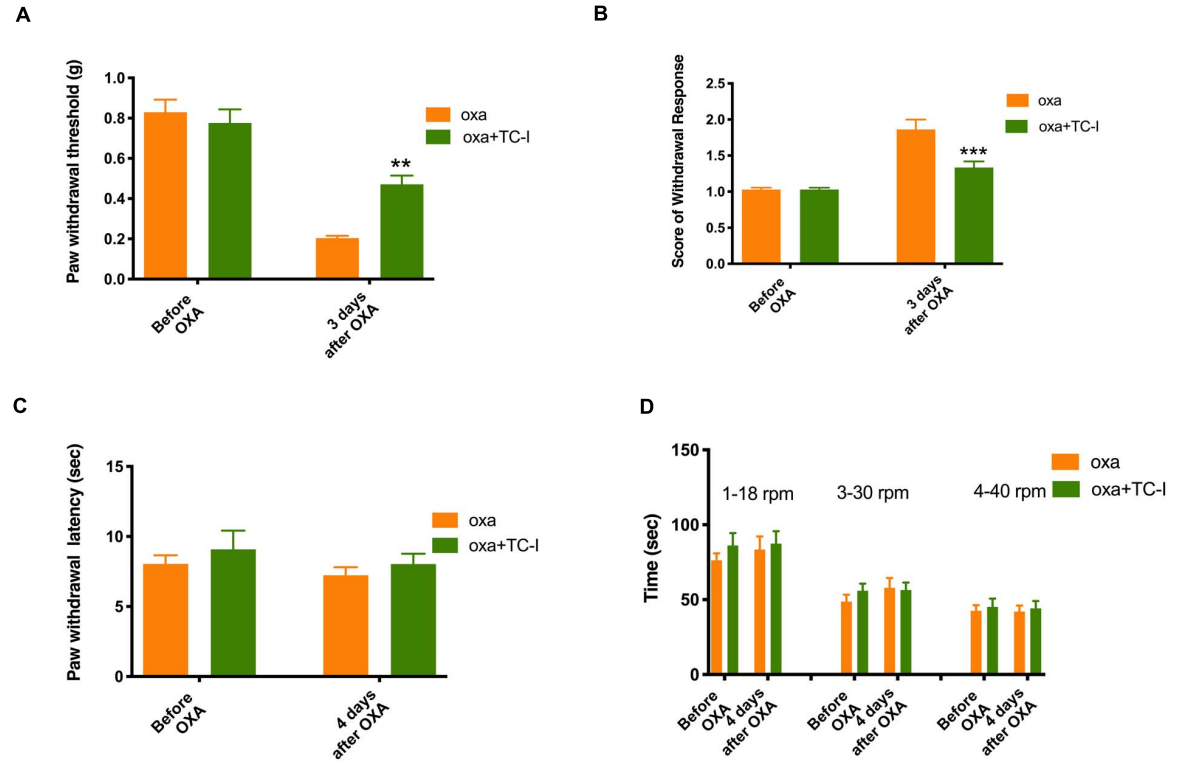

FIGURE 5 | Effects of TC-I on the sensory and motor behaviors following oxaliplatin treatment. The administration of oxaliplatin, the schedule for TC-I (10 mg/kg, ip) treatment (same to the Retigabine treatment), the testing schedule for different types of behaviors were described in the Legend of **Figure 3**. **(A)** Paw withdrawal threshold to Von-Frey filament; **(B)** Score of withdrawal response to acetone; **(C)** Paw withdrawal latency to radiant heat; and **(D)** Time stayed on rod at different speeds in rotarod tests (n = 6 for all groups). **, $P < 0.01$; ****, $P < 0.0001$; two-way repeated measure ANOVA.

One major finding of this study is that *in vitro* oxaliplatin selectively depolarized and increased the membrane excitability of the IB4$^-$, but not IB4$^+$ small DRG neurons. Previously, membrane depolarization and reduction in rheobases induced by *in vitro* oxaliplatin have been reported (Cerles et al., 2019; Zhang et al., 2021). However, a selective effect of *in vitro* oxaliplatin on the membrane excitability of IB4$^-$ over IB4$^+$ neurons has not been reported. As the two major subpopulations of DRG neurons, IB4$^-$ and IB4$^+$ neurons are largely different in their expression of neuronal peptides, peripheral innervation and central projection in spinal cord, modulation by growth factors, expression of ion channels and membrane receptors, and physiological function (Verge et al., 1989; Silverman and Kruger, 1990; Molliver et al., 1997; Zylka et al., 2005; Jankowski et al., 2009; Chiu et al., 2014). Therefore, a selective excitatory effect of oxaliplatin on the IB4$^-$ subpopulation of small DRG neurons would selectively activate peptidergic innervation at periphery and therefore their central projections at Lamina I and outer Lamina II in the spinal cord.

In the present study, we found that a membrane-hyperpolarizing drug retigabine largely prevented the oxaliplatin-induced mechanical and cold hyperalgesia (Du et al., 2014). A previous study also showed that retigabine prevented oxaliplatin-induced orofacial cold hyperalgesia that is likely involved with TRP channels also (Abd-Elsayed et al., 2015; Luo et al., 2021). As retigabine opens potassium channels at resting membrane potential leading to membrane hyperpolarization, these results suggest that targeting oxaliplatin-induced membrane depolarization might be a useful strategy to prevent oxaliplatin-induced sensory hyperalgesia.

Another finding of the *in vitro* study is that blockade of TRPA1 and TRPM8, but not TRPV1 prevented the oxaliplatin-induced membrane depolarization and reduction in the rheobase of action potentials (**Figure 4**). These results suggest that TRPA1 and TRPM8, but not TRPV1 contribute to oxaliplatin-induced membrane depolarization in IB4$^-$ subpopulation of small DRG neurons in mice. Previous it has been reported that *in vitro* oxaliplatin potentiates the increasing effects of agonists of TRPA1 and TRPV1, but not TRPM8 on intracellular Ca^{2+} in DRG neurons (Anand et al., 2010; Nassini et al., 2011; Zhao et al., 2012). The consistent (for TRPA1) and different (for TRPV1 and TRPM8) effects of TRP channel agonists on the membrane excitability compared to intracellular Ca^{2+} suggest that oxaliplatin might induce membrane hyperexcitability and increased intracellular Ca^{2+} through partially overlapping mechanisms in RG neurons.

Upregulation of multiple TRP channel isoforms (TRPA1, TRPV1, and TRPM8) have been reported following oxaliplatin treatment (Chukyo et al., 2018). The upregulation of these

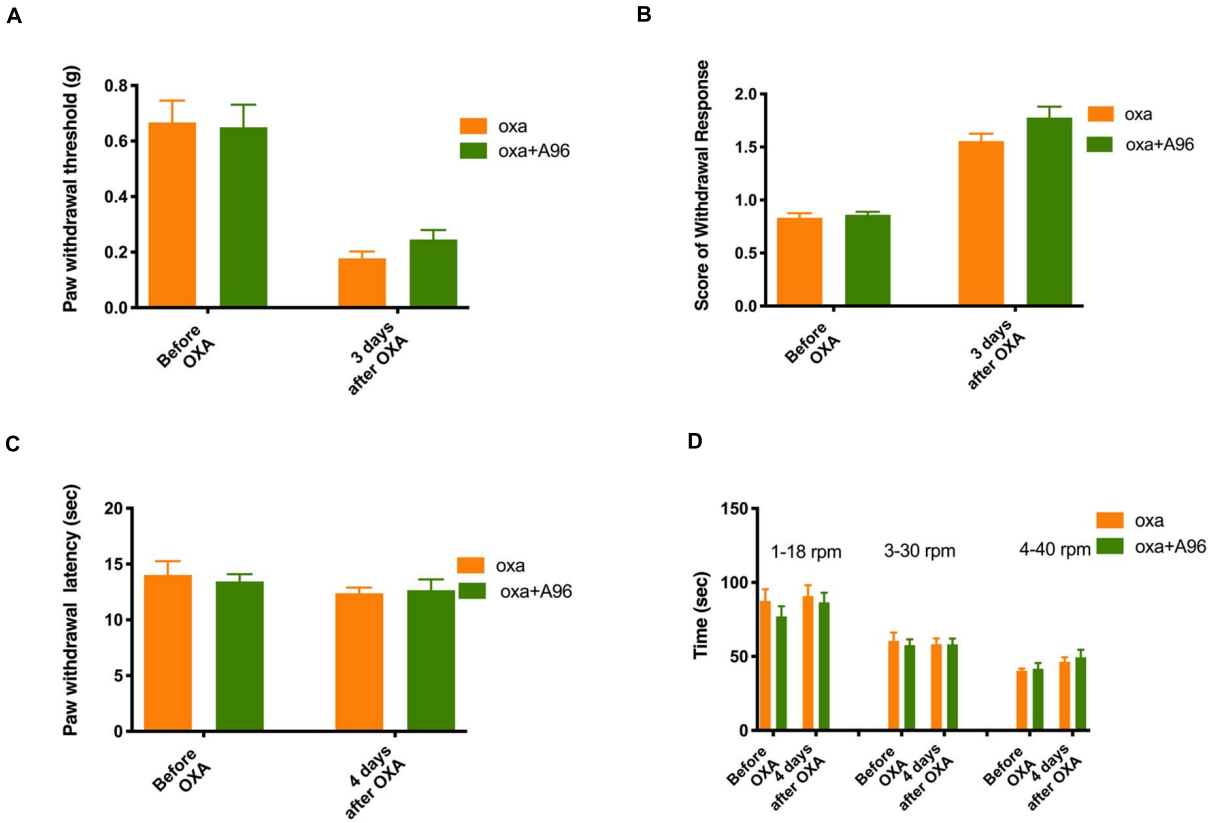

FIGURE 6 | Effects of A-967079 on the sensory and motor behaviors following oxaliplatin treatment. The administration of oxaliplatin, the schedule for A-967079 (A-96, 100 mg/kg, po) treatment (same to the Retigabine and TC-I treatment), the testing schedule for different types of behaviors were described in the Legend of **Figure 3**. **(A)** Paw withdrawal threshold to Von-Frey filament; **(B)** Score of withdrawal response to acetone; **(C)** Paw withdrawal latency to radiant heat; and **(D)** Time stayed on rod at different speeds in rotarod tests (n = 6 for all groups).

TRP channels following oxaliplatin treatment may or may not contribute to the oxaliplatin-induced mechanical and/or cold hyperalgesia (Gauchan et al., 2009; Mizuno et al., 2014; Chen et al., 2015; Yamamoto et al., 2015). Different from previous studies, the current study is focused on the potential role of TRP channels and membrane depolarization as the initial ionic/membrane drives (such as within an hour) that contribute to the development of oxaliplatin-induced neuropathic pain. Our results suggest that TRPM8 and TRPM8-mediated membrane depolarization, but not TRPA1 or TRPV1, serve as the initial ionic/membrane drives that contribute to the development of oxaliplatin-induced neuropathic pain. On the other hand, although the current study might provide some new suggestion on the role of TRPM8 as the initial ionic drive for the development of oxaliplatin-induced acute pain, we fully recognize that the potential TRPM8 involvement in Oxaliplatin-induced neurotoxicity has been reported by other researchers previously (Gauchan et al., 2009; Ta et al., 2010; Descoeur et al., 2011; Kono et al., 2012; Mizuno et al., 2014; Hsieh et al., 2017; Chukyo et al., 2018).

Although most studies of TRPM8 and allodynia have been focused on the cold allodynia, the involvement of TRPM8 in mechanical allodynia has been reported in multiple inflammatory and neuropathic pain conditions (Gao et al., 2013; Caceres et al., 2017; De Caro et al., 2018). The current manuscript showed that TRPM8 also participant in the oxaliplatin induced mechanical allodynia in addition to the cold allodynia. However, a previous study found that knockout of TRPM8 did not prevent the development of mechanical hyperalgesia induced by oxaliplatin (Descoeur et al., 2011). This discrepancy might be due to the different mechanical force used for the von-Frey tests. The previous study used 1.4 g as the stimulating force while the current study found that the mechanical threshold changed from about 0.2 to 0.45 g in the absence and presence of TC-I pre-treatment. Moreover, it has been reported that a selective reduction of TRPM8, but not TRPV1 is associated with the transcutaneous ultrasound nerve stimulation-induced inhibition of mechanical and cold allodynia following oxaliplatin treatment (Hsieh et al., 2017). Therefore, it might be suggested that TRPM8 is more involved in the mechanical allodynia compared to mechanical hyperalgesia induced by oxaliplatin.

One inconsistence in results in the present study is that the TRPA1 antagonist prevented oxaliplatin-induced membrane depolarization in DRG neurons *in vitro* but did not prevent the oxaliplatin-induced neuropathic pain behaviors *in vivo*.

One possibility for this discrepancy could be due to the dissociated cell culture of DRG neurons. It has been suggested that dissociation of DRG neurons might induce hyperexcitability that is caused by increased PKA and PKG signaling (Zheng et al., 2007). As PKA can sensitize TRPA1 channels, the TRPA1 *in vitro* might become more sensitive to oxaliplatin through ROS or other mechanisms compared to *in vivo* (Meents et al., 2017; Zheng et al., 2019). Another possibility might be that TRPA1 and TRPM8 are functionally coupled in the dissociated DRG neurons but not *in vivo*, as association of different types of TRP channels has been reported in DRG neurons (Patil et al., 2020). Nevertheless, other possibilities can not be excluded and future studies are needed to address this difference.

The present study suggests that oxaliplatin depolarizes IB4$^-$ DRG neurons through activation of TRPM8 channels to drive the development of neuropathic pain in mice. However, a previous study suggested that oxaliplatin acts on IB4$^+$ nociceptors to induce peripheral sensory neuropathy (Joseph et al., 2008). Specifically, the previous study found that intrathecal IB4-saporin prevented mechanical hyperalgesia induced by oxaliplatin while the present study found that the antagonist of TRPM8 (not expressed in IB4$^+$ neurons) prevented both mechanical and cold hyperalgesia induced by oxaliplatin. Taken these results together, it is possible that oxaliplatin-induced mechanical hyperalgesia might be dependent on the activation of both IB4$^+$ and IB4$^-$ subpopulations of DRG neurons. On the other hand, in addition to the different blocking approach, there are multiple other conditions that might contribute to the different suggestions made from the previous and current studies. These differences include species of experimental animals (rat vs. mouse), route of administration of oxaliplatin (iv vs. ip), types of relevant behavioral tests (mechanical vs. mechanical and cold), and time points of relevant behavioral tests (6–10 vs. 3 days following oxaliplatin treatment).

DATA AVAILABILITY STATEMENT

The original contributions presented in the study are included in the article/supplementary material, further inquiries can be directed to the corresponding author/s.

ETHICS STATEMENT

The animal study was reviewed and approved by the Institutional Animal Care and Use Committees of the Indiana University School of Medicine.

AUTHOR CONTRIBUTIONS

BW, XF, Y-HJ, and Z-YT conceived the idea. BW, XS, and Z-YT designed the experiments, analyzed the data, and wrote the manuscript. BW, XS, WZ, and Y-HZ conducted the experiments. All authors were involved in the discussion of the project.

FUNDING

Z-YT was supported by a DoD PRMRP DA grant (W81XWH-20-1-0138), and an NIH R01 grant (#NS102415). This publication was partially supported by an award from the Indiana University School of Medicine.

ACKNOWLEDGMENTS

The authors thank Drs. Naikui Liu and Heqiao Dai from Dr. Xiao-Ming Xu's lab for the assistance of rotarod test.

REFERENCES

Abd-Elsayed, A. A., Ikeda, R., Jia, Z., Ling, J., Zuo, X., Li, M., et al. (2015). KCNQ channels in nociceptive cold-sensing trigeminal ganglion neurons as therapeutic targets for treating orofacial cold hyperalgesia. *Mol. Pain* 11:45. doi: 10.1186/s12990-015-0048-8

Anand, U., Otto, W. R., and Anand, P. (2010). Sensitization of capsaicin and icilin responses in oxaliplatin treated adult rat DRG neurons. *Mol. Pain* 6:82. doi: 10.1186/1744-8069-6-82

Argyriou, A. A., Zolota, V., Kyriakopoulou, O., and Kalofonos, H. P. (2010). Toxic peripheral neuropathy associated with commonly used chemotherapeutic agents. *J. BUON.* 15, 435–446.

Azouz, R., Jensen, M. S., and Yaari, Y. (1996). Ionic basis of spike after-depolarization and burst generation in adult rat hippocampal CA1 pyramidal cells. *J. Physiol.* 492(Pt 1), 211–223. doi: 10.1113/jphysiol.1996.sp021302

Beijers, A. J., Mols, F., and Vreugdenhil, G. A. (2014). systematic review on chronic oxaliplatin-induced peripheral neuropathy and the relation with oxaliplatin administration. *Support Care Cancer* 22, 1999–2007. doi: 10.1007/s00520-014-2242-z

Boyette-Davis, J. A., Walters, E. T., and Dougherty, P. M. (2015). Mechanisms involved in the development of chemotherapy-induced neuropathy. *Pain Manag.* 5, 285–296. doi: 10.2217/pmt.15.19

Briani, C., Argyriou, A. A., Izquierdo, C., Velasco, R., Campagnolo, M., Alberti, P., et al. (2014). Long-term course of oxaliplatin-induced polyneuropathy: a prospective 2-year follow-up study. *J. Peripher. Nerv. Syst.* 19, 299–306. doi: 10.1111/jns.12097

Caceres, A. I., Liu, B., Jabba, S. V., Achanta, S., Morris, J. B., and Jordt, S. E. (2017). Transient Receptor Potential Cation Channel Subfamily M Member 8 channels mediate the anti-inflammatory effects of eucalyptol. *Br. J. Pharmacol.* 174, 867–879. doi: 10.1111/bph.13760

Cerles, O., Goncalves, T. C., Chouzenoux, S., Benoit, E., Schmitt, A., Bennett Saidu, N. E., et al. (2019). Preventive action of benztropine on platinum-induced peripheral neuropathies and tumor growth. *Acta Neuropathol. Commun.* 7:9. doi: 10.1186/s40478-019-0657-y

Chen, K., Zhang, Z. F., Liao, M. F., Yao, W. L., Wang, J., and Wang, X. R. (2015). Blocking PAR2 attenuates oxaliplatin-induced neuropathic pain via TRPV1 and releases of substance P and CGRP in superficial dorsal horn of spinal cord. *J. Neurol. Sci.* 352, 62–67. doi: 10.1016/j.jns.2015.03.029

Chiu, I. M., Barrett, L. B., Williams, E. K., Strochlic, D. E., Lee, S., Weyer, A. D., et al. (2014). Transcriptional profiling at whole population and single cell levels reveals somatosensory neuron molecular diversity. *Elife* 3:4660. doi: 10.7554/eLife.04660

Choi, J. S., Dib-Hajj, S. D., and Waxman, S. G. (2007). Differential slow inactivation and use-dependent inhibition of Nav1.8 channels contribute to distinct firing properties in IB4+ and IB4- DRG neurons. *J. Neurophysiol.* 97, 1258–1265. doi: 10.1152/jn.01033.2006

Chukyo, A., Chiba, T., Kambe, T., Yamamoto, K., Kawakami, K., Taguchi, K., et al. (2018). Oxaliplatin-induced changes in expression of transient receptor potential channels in the dorsal root ganglion as a neuropathic mechanism

for cold hypersensitivity. *Neuropeptides* 67, 95–101. doi: 10.1016/j.npep.2017.12.002

Corbin-Leftwich, A., Mossadeq, S. M., Ha, J., Ruchala, I., Le, A. H., and Villalba-Galea, C. A. (2016). Retigabine holds KV7 channels open and stabilizes the resting potential. *J. Gen. Physiol.* 147, 229–241. doi: 10.1085/jgp.201511517

De Caro, C., Russo, R., Avagliano, C., Cristiano, C., Calignano, A., Aramini, A., et al. (2018). Antinociceptive effect of two novel transient receptor potential melastatin 8 antagonists in acute and chronic pain models in rat. *Br. J. Pharmacol.* 175, 1691–1706. doi: 10.1111/bph.14177

de Gramont, A., Figer, A., Seymour, M., Homerin, M., Hmissi, A., Cassidy, J., et al. (2000). Leucovorin and fluorouracil with or without oxaliplatin as first-line treatment in advanced colorectal cancer. *J. Clin. Oncol.* 18, 2938–2947. doi: 10.1200/JCO.2000.18.16.2938

Descoeur, J., Pereira, V., Pizzoccaro, A., Francois, A., Ling, B., Maffre, V., et al. (2011). Oxaliplatin-induced cold hypersensitivity is due to remodelling of ion channel expression in nociceptors. *EMBO Mol. Med.* 3, 266–278. doi: 10.1002/emmm.201100134

Dirajlal, S., Pauers, L. E., and Stucky, C. L. (2003). Differential response properties of IB(4)-positive and -negative unmyelinated sensory neurons to protons and capsaicin. *J. Neurophysiol.* 89, 513–524. doi: 10.1152/jn.00371.2002

Du, X., Hao, H., Gigout, S., Huang, D., Yang, Y., Li, L., et al. (2014). Control of somatic membrane potential in nociceptive neurons and its implications for peripheral nociceptive transmission. *Pain* 155, 2306–2322. doi: 10.1016/j.pain.2014.08.025

Gao, T., Hao, J., Wiesenfeld-Hallin, Z., and Xu, X. J. (2013). Activation of TRPM8 cold receptor triggers allodynia-like behavior in spinally injured rats. *Scand. J. Pain* 4, 33–37. doi: 10.1016/j.sjpain.2012.09.007

Gauchan, P., Andoh, T., Kato, A., and Kuraishi, Y. (2009). Involvement of increased expression of transient receptor potential melastatin 8 in oxaliplatin-induced cold allodynia in mice. *Neurosci. Lett.* 458, 93–95. doi: 10.1016/j.neulet.2009.04.029

Gebremedhn, E. G., Shortland, P. J., and Mahns, D. A. (2018). The incidence of acute oxaliplatin-induced neuropathy and its impact on treatment in the first cycle: a systematic review. *BMC Cancer* 18:410. doi: 10.1186/s12885-018-4185-0

Ghitani, N., Bayguinov, P. O., Basso, M. A., and Jackson, M. B. A. (2016). sodium afterdepolarization in rat superior colliculus neurons and its contribution to population activity. *J. Neurophysiol.* 116, 191–200. doi: 10.1152/jn.01138.2015

Haj-Dahmane, S., and Andrade, R. (1998). Ionic mechanism of the slow afterdepolarization induced by muscarinic receptor activation in rat prefrontal cortex. *J. Neurophysiol.* 80, 1197–1210. doi: 10.1152/jn.1998.80.3.1197

Higashi, H., Tanaka, E., Inokuchi, H., and Nishi, S. (1993). Ionic mechanisms underlying the depolarizing and hyperpolarizing afterpotentials of single spike in guinea-pig cingulate cortical neurons. *Neuroscience* 55, 129–138. doi: 10.1016/0306-4522(93)90460-w

Hsieh, Y. L., Chen, H. Y., Yang, C. H., and Yang, C. C. (2017). Analgesic Effects of Transcutaneous Ultrasound Nerve Stimulation in a Rat Model of Oxaliplatin-Induced Mechanical Hyperalgesia and Cold Allodynia. *Ultrasound Med. Biol.* 43, 1466–1475. doi: 10.1016/j.ultrasmedbio.2017.03.002

Jankowski, M. P., Lawson, J. J., McIlwrath, S. L., Rau, K. K., Anderson, C. E., Albers, K. M., et al. (2009). Sensitization of cutaneous nociceptors after nerve transection and regeneration: possible role of target-derived neurotrophic factor signaling. *J. Neurosci.* 29, 1636–1647. doi: 10.1523/JNEUROSCI.3474-08.2009

Joseph, E. K., Chen, X., Bogen, O., and Levine, J. D. (2008). Oxaliplatin acts on IB4-positive nociceptors to induce an oxidative stress-dependent acute painful peripheral neuropathy. *J. Pain* 9, 463–472. doi: 10.1016/j.jpain.2008.01.335

Kerckhove, N., Collin, A., Conde, S., Chaleteix, C., Pezet, D., and Balayssac, D. (2017). Long-Term Effects, Pathophysiological Mechanisms, and Risk Factors of Chemotherapy-Induced Peripheral Neuropathies: A Comprehensive Literature Review. *Front. Pharmacol.* 8:86. doi: 10.3389/fphar.2017.00086

Kono, T., Satomi, M., Suno, M., Kimura, N., Yamazaki, H., Furukawa, H., et al. (2012). Oxaliplatin-induced neurotoxicity involves TRPM8 in the mechanism of acute hypersensitivity to cold sensation. *Brain Behav.* 2, 68–73. doi: 10.1002/brb3.34

Leonard, G. D., Wright, M. A., Quinn, M. G., Fioravanti, S., Harold, N., Schuler, B., et al. (2005). Survey of oxaliplatin-associated neurotoxicity using an interview-based questionnaire in patients with metastatic colorectal cancer. *BMC Cancer* 5:116. doi: 10.1186/1471-2407-5-116

Linden, D. J., Smeyne, M., and Connor, J. A. (1994). Trans-ACPD, a metabotropic receptor agonist, produces calcium mobilization and an inward current in cultured cerebellar Purkinje neurons. *J. Neurophysiol.* 71, 1992–1998. doi: 10.1152/jn.1994.71.5.1992

Liu, N. K., Zhang, Y. P., Zou, J., Verhovshek, T., Chen, C., Lu, Q. B., et al. (2014). A semicircular controlled cortical impact produces long-term motor and cognitive dysfunction that correlates well with damage to both the sensorimotor cortex and hippocampus. *Brain Res.* 1576, 18–26. doi: 10.1016/j.brainres.2014.05.042

Luo, Y., Suttle, A., Zhang, Q., Wang, P., and Chen, Y. (2021). Transient Receptor Potential (TRP) Ion Channels in Orofacial Pain. *Mol. Neurobiol.* [preprint]. doi: 10.1007/s12035-021-02284-2

Meents, J. E., Fischer, M. J., and McNaughton, P. A. (2017). Sensitization of TRPA1 by Protein Kinase A. *PLoS One* 12:e0170097. doi: 10.1371/journal.pone.0170097

Mizuno, K., Kono, T., Suzuki, Y., Miyagi, C., Omiya, Y., Miyano, K., et al. (2014). Goshajinkigan, a traditional Japanese medicine, prevents oxaliplatin-induced acute peripheral neuropathy by suppressing functional alteration of TRP channels in rat. *J. Pharmacol. Sci.* 125, 91–98. doi: 10.1254/jphs.13244fp

Molliver, D. C., Wright, D. E., Leitner, M. L., Parsadanian, A. S., Doster, K., Wen, D., et al. (1997). IB4-binding DRG neurons switch from NGF to GDNF dependence in early postnatal life. *Neuron* 19, 849–861. doi: 10.1016/s0896-6273(00)80966-6

Nakagawa, T., and Kaneko, S. (2017). Roles of Transient Receptor Potential Ankyrin 1 in Oxaliplatin-Induced Peripheral Neuropathy. *Biol. Pharm. Bull.* 40, 947–953. doi: 10.1248/bpb.b17-00243

Nassini, R., Gees, M., Harrison, S., De Siena, G., Materazzi, S., Moretto, N., et al. (2011). Oxaliplatin elicits mechanical and cold allodynia in rodents via TRPA1 receptor stimulation. *Pain* 152, 1621–1631. doi: 10.1016/j.pain.2011.02.051

Nelson, M. T., Joksovic, P. M., Perez-Reyes, E., and Todorovic, S. M. (2005). The endogenous redox agent L-cysteine induces T-type Ca2+ channel-dependent sensitization of a novel subpopulation of rat peripheral nociceptors. *J. Neurosci.* 25, 8766–8775. doi: 10.1523/JNEUROSCI.2527-05.2005

Patil, M. J., Salas, M., Bialuhin, S., Boyd, J. T., Jeske, N. A., and Akopian, A. N. (2020). Sensitization of small-diameter sensory neurons is controlled by TRPV1 and TRPA1 association. *FASEB J.* 34, 287–302. doi: 10.1096/fj.201902026R

Rovini, A. (2019). Tubulin-VDAC Interaction: Molecular Basis for Mitochondrial Dysfunction in Chemotherapy-Induced Peripheral Neuropathy. *Front. Physiol.* 10:671. doi: 10.3389/fphys.2019.00671

Silverman, J. D., and Kruger, L. (1990). Selective neuronal glycoconjugate expression in sensory and autonomic ganglia: relation of lectin reactivity to peptide and enzyme markers. *J. Neurocytol.* 19, 789–801. doi: 10.1007/BF01188046

Stucky, C. L., and Lewin, G. R. (1999). Isolectin B(4)-positive and -negative nociceptors are functionally distinct. *J. Neurosci.* 19, 6497–6505. doi: 10.1523/jneurosci.19-15-06497.1999

Su, X., Wu, B., Zhang, W., Ji, Y. H., Wang, Q., and Tan, Z. Y. (2019). Inhibitory Effects of Columbianadin on Nociceptive Behaviors in a Neuropathic Pain Model, and on Voltage-Gated Calcium Currents in Dorsal Root Ganglion Neurons in Mice. *Front. Pharmacol.* 10:1522. doi: 10.3389/fphar.2019.01522

Ta, L. E., Bieber, A. J., Carlton, S. M., Loprinzi, C. L., Low, P. A., and Windebank, A. J. (2010). Transient Receptor Potential Vanilloid 1 is essential for cisplatin-induced heat hyperalgesia in mice. *Mol. Pain* 6:15. doi: 10.1186/1744-8069-6-15

Tan, Z. Y., Lu, Y., Whiteis, C. A., Simms, A. E., Paton, J. F., Chapleau, M. W., et al. (2010). Chemoreceptor hypersensitivity, sympathetic excitation, and overexpression of ASIC and TASK channels before the onset of hypertension in SHR. *Circ. Res.* 106, 536–545. doi: 10.1161/CIRCRESAHA.109.206946

Trecarichi, A., and Flatters, S. J. L. (2019). Mitochondrial dysfunction in the pathogenesis of chemotherapy-induced peripheral neuropathy. *Int. Rev. Neurobiol.* 145, 83–126. doi: 10.1016/bs.irn.2019.05.001

Verge, V. M., Richardson, P. M., Benoit, R., and Riopelle, R. J. (1989). Histochemical characterization of sensory neurons with high-affinity receptors for nerve growth factor. *J. Neurocytol.* 18, 583–591. doi: 10.1007/BF01187079

Viatchenko-Karpinski, V., Ling, J., and Gu, J. G. (2018). Down-regulation of Kv4.3 channels and a-type K(+) currents in V2 trigeminal ganglion neurons of rats following oxaliplatin treatment. *Mol. Pain* 14:1744806917750995. doi: 10.1177/1744806917750995

Vilceanu, D., Honore, P., Hogan, Q. H., and Stucky, C. L. (2010). Spinal nerve ligation in mouse upregulates TRPV1 heat function in injured IB4-positive nociceptors. *J. Pain* 11, 588–599. doi: 10.1016/j.jpain.2009.09.018

White, G., Lovinger, D. M., and Weight, F. F. (1989). Transient low-threshold Ca2+ current triggers burst firing through an afterdepolarizing potential in an adult mammalian neuron. *Proc. Natl. Acad. Sci. U S A.* 86, 6802–6806. doi: 10.1073/pnas.86.17.6802

Wu, B., McDermott, J. S., Krajewski, J. L., Knopp, K. L., Nisenbaum, E. S., Cummins, T. R., et al. (2019). Extracellular signal-regulated kinases mediate the enhancing effects of inflammatory mediators on resurgent currents in dorsal root ganglion neurons. *Mol. Pain* 15:1744806919837104. doi: 10.1177/1744806919837104

Wu, Z. Z., and Pan, H. L. (2004). Tetrodotoxin-sensitive and -resistant Na+ channel currents in subsets of small sensory neurons of rats. *Brain Res.* 1029, 251–258. doi: 10.1016/j.brainres.2004.09.051

Yamamoto, K., Chiba, N., Chiba, T., Kambe, T., Abe, K., Kawakami, K., et al. (2015). Transient receptor potential ankyrin 1 that is induced in dorsal root ganglion neurons contributes to acute cold hypersensitivity after oxaliplatin administration. *Mol. Pain* 11:69. doi: 10.1186/s12990-015-0072-8

Yue, C., and Yaari, Y. K. C. N. Q. (2004). /M channels control spike afterdepolarization and burst generation in hippocampal neurons. *J. Neurosci.* 24, 4614–4624. doi: 10.1523/JNEUROSCI.0765-04.2004

Zhang, X. L., Mok, L. P., Katz, E. J., and Gold, M. S. (2010). BKCa currents are enriched in a subpopulation of adult rat cutaneous nociceptive dorsal root ganglion neurons. *Eur. J. Neurosci.* 31, 450–462. doi: 10.1111/j.1460-9568.2009.07060.x

Zhang, Y., Zhang, Y., Wang, Z., Sun, Y., Jiang, X., Xue, M., et al. (2021). Suppression of delayed rectifier K(+) channels by gentamicin induces membrane hyperexcitability through JNK and PKA signaling pathways in vestibular ganglion neurons. *Biomed. Pharmacother.* 135:111185. doi: 10.1016/j.biopha.2020.111185

Zhao, M., Isami, K., Nakamura, S., Shirakawa, H., Nakagawa, T., and Kaneko, S. (2012). Acute cold hypersensitivity characteristically induced by oxaliplatin is caused by the enhanced responsiveness of TRPA1 in mice. *Mol. Pain* 8:55. doi: 10.1186/1744-8069-8-55

Zheng, J. H., Walters, E. T., and Song, X. J. (2007). Dissociation of dorsal root ganglion neurons induces hyperexcitability that is maintained by increased responsiveness to cAMP and cGMP. *J. Neurophysiol.* 97, 15–25. doi: 10.1152/jn.00559.2006

Zheng, X., Tai, Y., He, D., Liu, B., Wang, C., Shao, X., et al. (2019). ETAR and protein kinase A pathway mediate ET-1 sensitization of TRPA1 channel: A molecular mechanism of ET-1-induced mechanical hyperalgesia. *Mol. Pain* 15:1744806919842473. doi: 10.1177/1744806919842473

Zhou, J., Zhang, X., Zhou, Y., Wu, B., and Tan, Z. Y. (2019). Up-regulation of P2X7 Receptors Contributes to Spinal Microglial Activation and the Development of Pain Induced by BmK-I. *Neurosci. Bull.* 35, 624–636. doi: 10.1007/s12264-019-00345-0

Zylka, M. J., Rice, F. L., and Anderson, D. J. (2005). Topographically distinct epidermal nociceptive circuits revealed by axonal tracers targeted to Mrgprd. *Neuron* 45, 17–25. doi: 10.1016/j.neuron.2004.12.015

Conflict of Interest: The authors declare that the research was conducted in the absence of any commercial or financial relationships that could be construed as a potential conflict of interest.

frontiers in Molecular Neuroscience

ORIGINAL RESEARCH
published: 07 June 2021
doi: 10.3389/fnmol.2021.663649

The $P2X_7$ Receptor Is Involved in Diabetic Neuropathic Pain Hypersensitivity Mediated by TRPV1 in the Rat Dorsal Root Ganglion

*Anhui Wang[1], Xiangchao Shi[2], Ruoyang Yu[2], Bao Qiao[2], Runan Yang[1] and Changshui Xu[1,3]**

[1] Department of Physiology, Basic Medical College of Nanchang University, Nanchang, China, [2] Medical Department, Queen Mary School, Nanchang University, Nanchang, China, [3] Jiangxi Provincial Key Laboratory of Autonomic Nervous Function and Disease, Nanchang, China

The purinergic $2X_7$ ($P2X_7$) receptor expressed in satellite glial cells (SGCs) is involved in the inflammatory response, and transient receptor potential vanilloid 1 (TRPV1) participates in the process of neurogenic inflammation, such as that in diabetic neuropathic pain (DNP) and peripheral neuralgia. The main purpose of this study was to explore the role of the $P2X_7$ receptor in DNP hypersensitivity mediated by TRPV1 in the rat and its possible mechanism. A rat model of type 2 diabetes mellitus-related neuropathic pain (NPP) named the DNP rat model was established in this study. The mechanical withdrawal threshold (MWT) and thermal withdrawal latency (TWL) of DNP rats were increased after intrathecal injection of the $P2X_7$ receptor antagonist A438079, and the mRNA and protein levels of TRPV1 in the dorsal root ganglion (DRG) were decreased in DNP rats treated with A438079 compared to untreated DNP rats; in addition, A438079 also decreased the phosphorylation of p38 and extracellular signal-regulated kinase 1/2 (ERK1/2) in the DNP group. Based on these results, the $P2X_7$ receptor might be involved in DNP mediated by TRPV1.

Keywords: diabetic neuropathic pain, $P2X_7$ receptors, TRPV1, dorsal root ganglion, satellite glial cells, neurons

OPEN ACCESS

Edited by:
Wuping Sun,
Shenzhen University, China

Reviewed by:
Celina Lotufo,
Federal University of Uberlândia, Brazil
Koichi Iwata,
Nihon University, Japan

****Correspondence:***
Changshui Xu
xuchangshui@ncu.edu.cn

Received: *03 February 2021*
Accepted: *05 May 2021*
Published: *07 June 2021*

Citation:
Wang A, Shi X, Yu R, Qiao B, Yang R and Xu C (2021) The $P2X_7$ Receptor Is Involved in Diabetic Neuropathic Pain Hypersensitivity Mediated by TRPV1 in the Rat Dorsal Root Ganglion. Front. Mol. Neurosci. 14:663649. doi: 10.3389/fnmol.2021.663649

INTRODUCTION

Diabetic neuropathic pain (DNP) is one of the most common chronic complications of diabetes and one of the most common types of neuropathic pain (NPP) treated in the clinic (Galuppo et al., 2014; Lu et al., 2017; Pan et al., 2018). DNP, a type of chronic pain with a morbidity rate that is increasing annually, is associated with severe and long-lasting clinical symptoms that seriously affect patient quality of life. Additionally, effective clinical treatments are lacking, which has drawn increased attention to this difficult topic in the field of pain research in recent years (Vinik et al., 2013; Sloan et al., 2018).

The purinergic $2X_7$ ($P2X_7$) receptor is an ion channel gated by the purine ATP involved in the transmission of pain information (Boue-Grabot and Pankratov, 2017; Burnstock, 2017; Ugur and Ugur, 2019). The release of ATP from the vesicles of injured neurons during acute injury

further triggers the release of ATP from surrounding glial cells, thereby activating P2X$_7$ receptors on adjacent glial cells and allowing glial cells to release ATP in an autocrine manner. Through this cascade reaction, the ATP signal is amplified (Volonté et al., 2012; Wei et al., 2016). The effect of a large dose of ATP on P2X$_7$ receptors for an extended period of time promotes the formation and opening of plasma membrane pores and release of cytokines such as IL-1β, plasminogen and TNF-α, which further activate glial cells and aggravate neuronal damage (Zou et al., 2016; Janks et al., 2018). The P2X$_7$ receptor is expressed on satellite glial cells (SGCs) of the dorsal root ganglion (DRG) (Kobayashi et al., 2013), and mechanical and thermal hyperalgesia are related to the activation of SGCs (Zou et al., 2019). Thus, the P2X$_7$ receptor is involved in the pathogenesis of inflammation and NPP (Skaper et al., 2010; Ni et al., 2020).

Transient receptor potential vanilloid 1 (TRPV1), also known as the capsaicin receptor, is mainly distributed in medium- and small-diameter neurons of the DRG and the trigeminal ganglion (Kaneko and Szallasi, 2014) and plays an important role in enhancing of pain sensitivity caused by heat and chemicals in a model of diabetes-induced NPP (Gunthorpe and Szallasi, 2008; Hsu et al., 2014; Zhang et al., 2020). Moreover, primary sensory neurons play a key role in the process of pain generation and conduction, and TRPV1 is expressed in pain transmission pathways.

Studies have found that glial cells of the central nervous system could regulate the activity of spinal neurons and play a vital role in chronic pain (Milligan and Watkins, 2009; Tsuda et al., 2012; Ji et al., 2013). Studies have also shown that the activation of DRG SGCs is involved in NPP in some cases of peripheral neuropathy and that neurons in the sensory ganglia interact with glial cells (Gu et al., 2010; Jarvis, 2010). Therefore, the purpose of this study was to determine whether the P2X$_7$ receptor plays a role in DNP mediated by TRPV1 in the rat DRG.

MATERIALS AND METHODS

Animals and Ethics

Healthy and clean male Sprague-Dawley rats (weight, 180–220 g) were obtained from the Center of Laboratory Animal Science of Nanchang University, and the use of animals was approved by the Animal Protection and Use Committee of Nanchang University. All rats were housed in a clean room (22 ± 2°C, 50% relative humidity, and a 12-h light/12-h dark cycle) according to the Animal Care and Use Guidelines developed by the Ethics Committee of Nanchang University and provided free access to food and water and carried out in accordance with the National Institute of Health Guide for the Care and Use of Laboratory Animals.

Animal Modeling and Groups

Rats were fed a high-sugar and high-fat diet (the high-sugar and high-fat diet was composed of 77.8% ordinary feed, 2% cholesterol, 0.2% sodium cholate, 10% lard, and 10% sucrose mixed with water, kneaded into balls, and placed in a constant temperature oven for baking) for 4 weeks and then intraperitoneally injected with a solution of streptozotocin (35 mg/kg), which can cause impaired pancreatic β-cell function. One week after the injection of streptozotocin, rats with a fasting blood glucose level > 7.8 mM or a non-fasting blood glucose level > 11.1 mM accompanied by a marked increase in behavioral sensitivity to pain were identified as successful DNP models.

In this experiment, the rats were divided into a control group (control group), DNP model group (DNP group), P2X$_7$ receptor antagonist A438079 (S7705; Selleckchem)-treated DNP group (DNP + A438079 group), and normal saline (NS)-treated DNP group (DNP + NS group). Each group contained six rats and all rats participated in all procedures. The rats in the control group were not administered any treatment, the rats in the DNP + A438079 group were intrathecally injected with A438079, the rats in the DNP + NS group were injected intrathecally with an equal volume of NS, rats of the DNP + A438079 group and DNP + NS group were given A438079 (10 μM, 10 μl; dissolved in NS) and NS (10 μl) intrathecal injection once a day for 7 days (Ying et al., 2014), respectively. All treatments were administered starting when all experimental rats had become DNP model rats (namely, the first day of the eighth week). After the A438079 treatment, the blood glucose levels in type 2 diabetic rats were decreased compared with those in the untreated type 2 diabetic rats. Besides, a total of 20 rats were successfully modeled with diabetes. After successful modeling, two rats died during the observation period. Therefore, the success rate of DNP modeling is about 90%. After the last behavioral test, the rats were euthanized and the L4-6 DRGs of all experimental rats were isolated for later experiments.

Intrathecal injection was performed as described to previous studies (Mestre et al., 1994), and it is briefly described as follows: the rats were anesthetized with intraperitoneal injection of chloral hydrate with a volume fraction of 10% (30 mg kg^{-1}); one hand was positioned at the spinous process of L4-6, and the other hand held a 25 μl micro sampler to pierce the subarachnoid space; there was a clear sense of breakthrough, and the needle was continuously injected until a typical rat tail lateral shake and jitter was considered as the puncture was successful.

Mechanical Withdrawal Threshold (MWT)

Rats from each group were placed on a stainless-steel wire mesh (1 × 1 cm grid) in a transparent plastic chamber (22 × 12 × 22 cm) for 30 min. The environment was kept quiet, and the room temperature was maintained at 20–25°C. The rats were tested after adapting to the environment and exhibiting a quiet state (rats were tested at the same time of day). An electronic mechanical pain meter (BME-404; Tianjin, China) was used to test pain hypersensitivity thresholds. A filament with a random bending force was applied to the bottom of the left hind paw of rats from each group (the center of the foot was stimulated, the location of each stimulation was consistent throughout the experiment, and the intensity gradually increased) until each rat showed a significant contraction response of the stimulated foot. The test was repeated 6 times with an interval of 10 s between each test. The mechanical reflex threshold was read, and the average of 6 trials was recorded to obtain the final value (Liu C. et al., 2018).

Thermal Withdrawal Latency (TWL)

The method for measuring the thermal withdrawal reflex latency of rats was similar to the procedure used to determine the mechanical withdrawal reflex threshold. Rats from each group were placed on a glass plate under a transparent bottomless square acrylic box (22 × 12 × 22 cm) for 30 min. The environment was kept quiet, and the room temperature was maintained at 20–25°C. The test did not start until the rats had adapted to the environment and exhibited a quiet state. An automatic thermal pain stimulator (BME-410C; Tianjin, China) was used to stimulate the midpoint of the left hind paw of the rat with a tungsten lamp. The light stimulus was approximately 0.5 cm in diameter to ensure a continuous thermal radiation stimulation for the specified duration. The length of time from the start of thermal stimulation to the point at which the rats raised their paws was observed, and the test was repeated 6 times with an interval of 2 min between each test. The thermal radiation stimulation time did not exceed 30 s. The time point at which each rat exhibit a contractile reflex was observed, the data were recorded, and the values from the 6 trials were averaged (Deng et al., 2018).

Quantitative Real-Time Reverse Transcription Polymerase Chain Reaction

The DRG were isolated and then immediately placed in a glass homogenizer that had been soaked with prepared diethylpyrocarbonate. An appropriate volume of Transzol Up (ER501; TransGen Biotechnology Co., Ltd., Beijing, China) was added to every homogenizer and the DRGs were completely ground and lysed on ice. Then, total RNA was collected according to the instructions of the RNA extraction kit (ER501; TransGen Biotechnology Co., Ltd., Beijing, China). Next, total extracted RNA was reverse transcribed into cDNA using the First Strand cDNA Synthesis Kit (AE301; TransGen Biotechnology Co., Ltd., Beijing, China) according to the manufacturer's instructions (a PCR amplification apparatus was used to incubate the samples at 42°C for 15 min and then heat them to 85°C for 5 s to deactivate the EasyScript® RT/RI). At the same time, a NanoDrop2000 ultraviolet spectrophotometer (Thermo Fisher Scientific Inc., United States) was used to detect the cDNA concentration. The cDNA templates were mixed with Tip Green qPCR SuperMix kit reagent (AQ141; TransGen Biotechnology Co., Ltd., Beijing, China) in a 20-μl reaction, and qPCR was performed using an ABI PRISM system with the help of the StepOnePlus real-time PCR system (Applied Biosystems, Inc., Foster City, CA, United States). PCR specificity was determined by constructing a fusion curve, and the results were analyzed using the aforementioned software. Using the $2^{-\Delta\Delta CT}$ data analysis method, the average threshold cycle (CT) values of the target genes (TRPV1 and P2X$_7$) were normalized to the average CT value of the internal control gene (β-actin) to calculate ΔCT values (ΔCT = CT target-CT internal reference), and the ΔCT value of the control group was used to normalize the ΔCT values of the experimental groups to calculate ΔΔCT values (ΔΔCT = ΔCT experimental group-ΔCT control group); expression data are presented in terms of relative mRNA quantity (RQ; RQ = $2^{-\Delta\Delta CT}$) (Liu et al., 2017). The sequences of the primers were as follows: TRPV1 forward, 5′-ATGACACCATCGCTCTGCTC-3′, and reverse, 5′-GTGCTGTCTGGCCCTTGTAG-3′; and β-actin forward, 5′-CCTAAGGCCAACCGTGAAAAGA-3′, and reverse, 5′-GGTACGACCAGAGGCATACA-3′.

Western Blotting

The DRG were isolated and immediately rinsed in ice-cold PBS, and DRGs were placed in a pretreatment homogenizer to be mechanically dry-milled and crushed until homogenized. Next, an appropriate volume of protein lysis buffer [50 mM Tris-HCl (pH 7.4), 150 mM NaCl, 0.1% sodium dodecyl sulfate (SDS), 1% Nonidet P-40 (NP-40), 1% protein phosphatase inhibitor, and 1% protease inhibitor] was added to each sample, and the samples were then placed on ice for 30 min to ensure complete lysis. Afterward, the homogenates were centrifuged at 12,000 × g for 10 min at 4°C, the volume of supernatant was measured, and the supernatant was transferred to a new centrifuge tube. An aliquot of the supernatant was used to measure the protein concentration; then, an appropriate amount of protein loading buffer (DL101; TransGen Biotechnology Co., Ltd., Beijing, China) was added to the remaining supernatant, and the mixture was boiled in a 95°C water bath for 5 min to denature the proteins. The protein samples were separated on SDS-PAGE gels and then transferred to polyvinylidene fluoride membranes. The transfer time was adjusted according to the molecular weight of the protein. Afterward, each polyvinylidene fluoride membrane was incubated with a 5% blocking solution to block non-specific binding sites. The membrane subsequently was incubated with the following primary antibodies: rabbit anti-TRPV1 (Abcam, United Kingdom, 1:500); mouse anti-β-actin (TA-09; Beijing Zhongshan Biotech CO., CN, 1:800); rabbit anti-ERK1/2 (4695S; Cell Signaling Technology, United States, 1:1,000), rabbit anti-p-ERK1/2 (4370S; Cell Signaling Technology, United States, 1:1,000); rabbit anti-p38 (8690S; Cell Signaling Technology, United States, 1:800), rabbit anti-p-p38 (4511S; Cell Signaling Technology, United States, 1:800); rabbit anti-IL-1β and mouse anti-IL-10 (Abcam, United States, 1:500). Then, the membrane was incubated with a horseradish peroxidase-conjugated goat anti-rabbit or goat anti-mouse antibody. Finally, the membrane was subjected to exposure with hypersensitive ECL luminescent solution (FD8020; Fude Biotechnology Co., Ltd, Hangzhou, China) and signal detection. The integrated optical density (IOD) values of the detected proteins were analyzed by Image-Pro Plus software (Media Cybernetics Inc., Rockville, MD) (Dan et al., 2020).

Immunofluorescence Staining

Double immunofluorescence staining was performed to show the coexpression of TRPV1 and neuronal nuclear protein (NeuN) and the coexpression of P2X$_7$ receptor and glial fibrillary acidic protein (GFAP) in the DRGs of rats from each group. The L_{4-6} DRGs were fixed in 4% paraformaldehyde solution for 24 h. Then, the DRGs were removed and placed in 20% glucose solution overnight for dehydration at 4°C. The DRGs were

embedded in OCT, and 8–10-μm-thick sections were prepared with a freezing microtome and subsequently fixed on slides at room temperature overnight before being stored at −20°C. Several slices were selected from each group and washed three times with 1 × PBS for 5 min each. The slices were fixed with 4% paraformaldehyde and then permeabilized with 0.3% Triton X-100 for 15 min (T8200; Beijing Solarbio Science Technology Co., Ltd.). Next, the slides were washed 3 times and dried. Afterward, a working solution of goat serum (ZLI-9022; Beijing Zhongshan Biotech CO., CN) was added dropwise to the ganglia to block non-specific binding sites and incubated in a water bath at 37°C for 1 h. Antibodies against TRPV1 (rabbit anti-TRPV1, 1:100, Abcam), NeuN (mouse anti-NeuN, 1:200), P2X$_7$ (APR-004; rabbit anti-P2X$_7$, 1:100, Israel Alomone) and GFAP (mouse anti-GFAP, 1:200) were diluted to the appropriate concentrations and then uniformly added to the slices dropwise. The slices were incubated at 4°C over night. The slices were brought to room temperature, washed 3 times and dried. Thereafter, secondary antibodies (TRITC-conjugated goat anti-rabbit, 1:200, Beijing Zhongshan Biotech Co., and FITC-conjugated goat anti-mouse, 1:200, Beijing Zhongshan Biotech Co., ZF-0312) were incubated with the sections at 37°C for 1 h. An antifluorescence quenching agent (AR1109; Boster Biological Technology Co., Ltd.) was applied, and then a coverglass was carefully placed on the slides. Finally, an inverted fluorescence microscope (Olympus, Tokyo, Japan) was used for imaging (Ge et al., 2019).

Molecular Docking

AutoDock 4.2 was used for molecular docking experiments (Yang et al., 2019). Molecular docking is a computer simulation tool that attempts to predict the binding mode and affinity of ligands at the active sites of proteins and is a theoretical method used to simulate intermolecular interactions by selecting ligands that are close to the natural conformation and have the best affinity for the receptor through a scoring function. Molecular docking is also an important approach for structure-based drug design because it allows researchers to study the interactions between ligand molecules and receptor biomolecules and predict their affinity. The aim of docking technology is to determine the location of ligands in the binding sites in different directions and conformations to calculate the optimal binding geometry and energy. In this experiment, we used docking technology to determine whether two molecules have binding sites and bind one another, namely, whether A438079 bind to the TRPV1 receptor.

According the rat TRPV1 (PDB ID: 3J5P.1) protein sequence NP_114188.1 as target proteins, the structure of the TRPV1 protein 3D file was obtained by homology modeling via online SWISS-MODEL website[1] (Hollopeter et al., 2001). A438079 (PubChem CID: 11673921) was used as the ligand. The protein and ligand structures were prepared using AutoDock Tools and Python scripts, named prepare_ligand4.py and prepare_receptor4.py, which are associated with the AutoDock 4.2 program. The binding pocket position in the target protein was specified with the AutoDock Tools molecular viewer. The parameters were maintained at their default values. Finally, the output files were viewed using MGL tools and PyMol[2].

Statistical Analyses

Statistical analyses were performed using Excel, SPSS 21.0 (IBM, United States) and GraphPad Prism 6.01 (GraphPad Software Inc., United States) software. The experimental data from each group are presented as the mean ± standard error of the mean (SEM). The data were analyzed by one-way analysis of variance (ANOVA) followed by Fisher's least significant difference (LSD) test. For the behavioral test, two-way repeated-measures ANOVA followed by Bonferroni's *post-hoc* test was carried out. The results were statistically significant when $P < 0.05$.

RESULTS

Intrathecal Injection of A438079 Attenuated the Mechanical and Thermal Sensitivity of DNP Rats

The MWT and TWL of the DNP group were lower than those of the control group ($p < 0.01$; **Figures 1A,B**); the MWT and TWL of DNP rats treated with the P2X$_7$ receptor antagonist A438079 were higher than those of untreated DNP rats ($p < 0.01$), but a significant difference was not observed between the results obtained from the DNP group and DNP + NS group ($p > 0.05$). Thus, the P2X$_7$ receptor antagonist A438079 reduced mechanical and thermal hyperalgesia in DNP rats, indicating that treatment with the P2X$_7$ receptor antagonist A438079 may alleviate DNP in rats.

A438079 Reduced TRPV1 mRNA Level in the DRGs of DNP Rats

The mRNA level of TRPV1 in the DRGs of experimental rats in each group was detected by qPCR. A significantly lower level of the TRPV1 mRNA was detected in the control group than in the DNP group ($P < 0.01$; **Figure 2A**), but no obvious difference was detected between the control group and DNP + A438079 group ($P > 0.05$). A significant difference in the mRNA expression of TRPV1 was not observed between the DNP + NS group and DNP group ($P > 0.05$). Based on these results, A438079, a P2X$_7$ receptor antagonist, might reduce the upregulation of TRPV1 mRNA in the DRGs of DNP rats.

A438079 Decreased Level of the TRPV1 Protein in the DRGs of DNP Rats

Western blotting was performed to analyze protein levels in each group of experimental rats. Noticeably lower levels of the TRPV1 protein were observed in the control group than in the DNP group ($P < 0.01$; **Figures 2B,C**). In contrast, no fundamental difference in TRPV1 protein expression was observed between the control group and the DNP + A438079 group ($P > 0.05$). Expression of the TRPV1 protein was also not

[1]https://swissmodel.expasy.org/

[2]http://www.pymol.org/

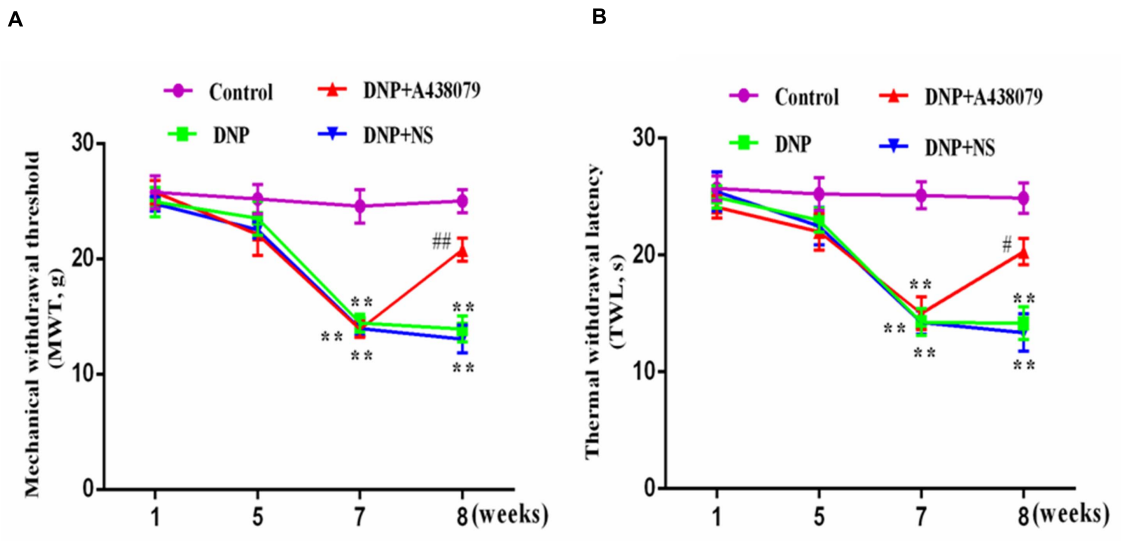

FIGURE 1 | The effect of A438079 on the mechanical withdrawal threshold (MWT) and the thermal withdrawal latency (TWL) of DNP rats. **(A)** Changes in the MWTs of rats from each group. **(B)** Changes in the TWLs of rats from each group. The MWTs and TWLs of rats from the DNP group were significantly lower than the values of rats from the control group (namely, the sensitivity was increased). At the end of the 8th week, the MWTs and TWLs of rats in the DNP group treated with an intrathecal injection of the P2X$_7$ receptor antagonist A438079 (DNP + A438079 group) were significantly higher than those of rats in the DNP group (i.e., decreased sensitivity). The data are presented as the mean ± SEM for the six animals in each group; compared with the control group, $^{**}P < 0.01$; compared with the DNP group, $^{\#}P < 0.05$, $^{\#\#}P < 0.01$.

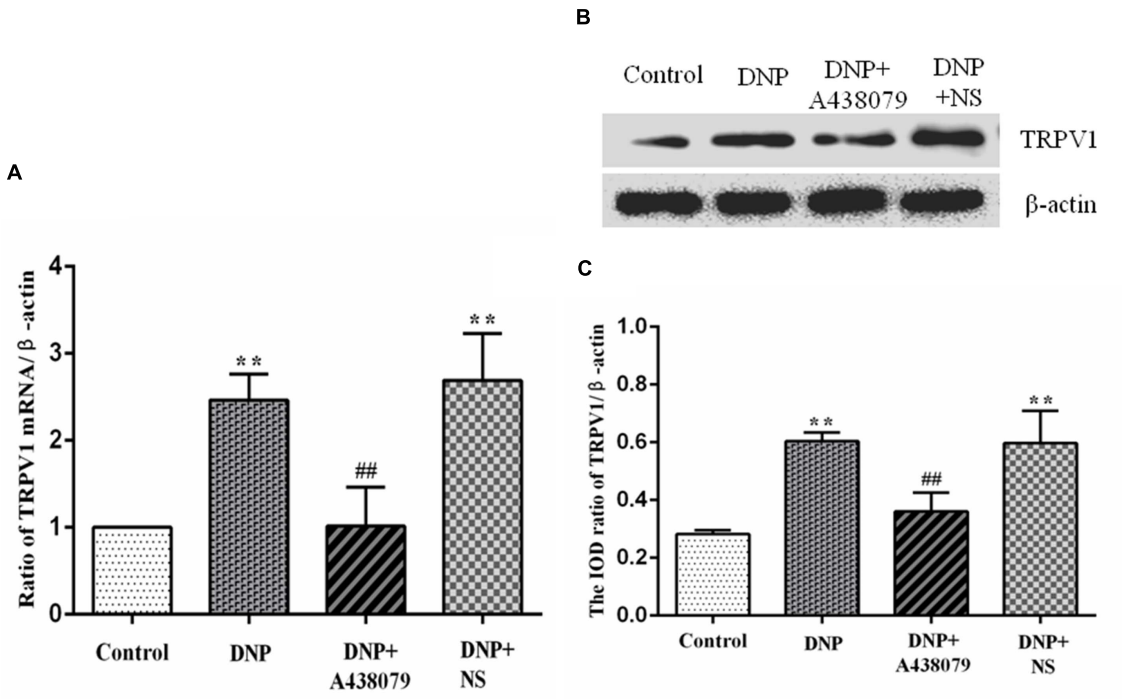

FIGURE 2 | The levels of the TRPV1 mRNA and protein in the DRG were detected. **(A)** The level of the TRPV1 mRNA in the DRG from each group. **(B)** SDS-PAGE band of the TRPV1 protein in the DRG from each group of experimental rats. **(C)** Analysis of the relative level of the TRPV1 protein in the DRG from each group of experimental rats. Higher levels of the TRPV1 mRNA and protein were detected in the DRG in the DNP group than in the control group, while lower levels of the TRPV1 mRNA and protein were observed in the DRG in the DNP + A438079 group than in the DNP group. The data are presented as the mean ± SEM, $n = 6$; compared with the control group, $^{**}P < 0.01$; compared with the DNP group, $^{\#\#}P < 0.01$.

significantly different between the DNP + NS group and DNP group ($P > 0.05$). The above results demonstrate that A438079, a P2X$_7$ receptor antagonist, might inhibit the increase in the levels of the TRPV1 protein in the DRGs of DNP rats.

Coexpression of TRPV1 With NeuN and P2X$_7$ Receptor With GFAP

NeuN is a neuronal marker, a higher level of TRPV1 with NeuN coexpression was observed in the DNP group than in the control group. A lower level of coexpression was observed in the DNP + A438079 group than in the DNP group. A significant change was not detected between the DNP group and the DNP + NS group. Therefore, we speculate that the P2X$_7$ receptor antagonist A438079 may inhibit coexpression of the TRPV1 receptor and NeuN in neurons in the DRG (**Figures 3A,B**).

Similarly, the marker for SGCs is GFAP, and its upregulation indicates the activation of SGCs. The coexpression of P2X$_7$ with GFAP in the SGCs of each group followed a trend consistent with that for the coexpression of TRPV1 with NeuN in neuronal cells. Consequently, we concluded that the P2X$_7$ receptor antagonist A438079 might inhibit the upregulation of the P2X$_7$ receptor expression associated with the activation of SGCs in the DRG (**Figures 3C,D**).

Effect of A438079 on the Levels of IL-1β and IL-10 in the DRGs of DNP Rats

An increase in cytokine expression is another characteristic of SGC activation, and IL-1β released from SGCs is believed to initiate and maintain DNP. The IL-1β protein was expressed at significantly lower levels in the control group than in the DNP group ($P < 0.01$; **Figures 4A,B**) but a significant difference was not observed between the expression level in the DNP + A438079 group and control group ($P > 0.05$). A significant difference in the level of the IL-1β protein was not observed between the DNP + NS group and DNP group ($P > 0.05$). Based on the

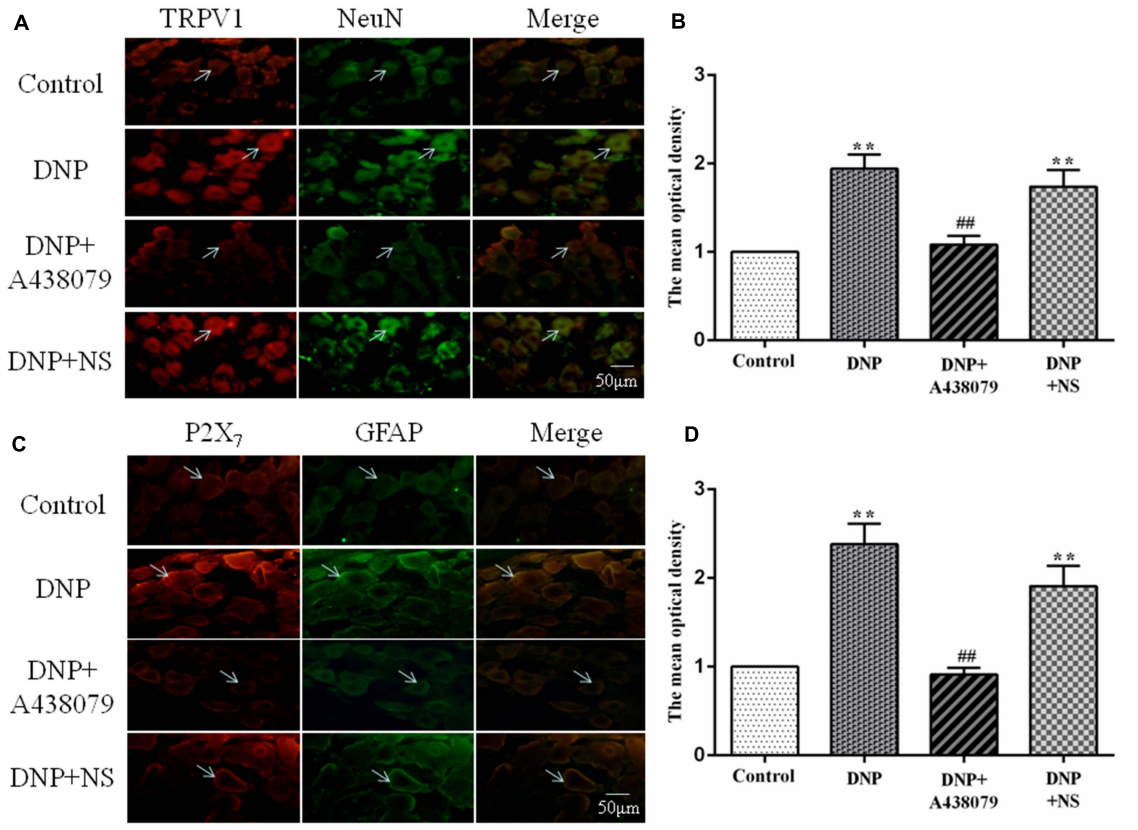

FIGURE 3 | The coexpression of TRPV1 with NeuN and P2X$_7$ receptor with GFAP was detected by immunofluorescence staining. **(A)** Levels of TRPV1 with NeuN coexpression in neurons in the rat DRG ($n = 6$ rats for each group). **(B)** The histogram shows the mean optical density of the coexpression of TRPV1 with NeuN. **(C)** Levels of P2X$_7$ with GFAP coexpression in SGCs in the rat DRG ($n = 6$ rats for each group). **(D)** The histogram shows the mean optical density of the coexpression of the P2X$_7$ receptor with GFAP. In the DNP group, the coexpression of TRPV1 with NeuN in the DRG was increased compared with that in the control group, while the coexpression of TRPV1 with NeuN in the DNP + A438079 group was decreased compared with that in the DNP group. Furthermore, the coexpression of P2X$_7$ receptor with GFAP in the DRG was consistent with the coexpression trend described above. The green signal is fluorescein isothiocyanate (FITC)-labeled NeuN and FITC-labeled GFAP; the red signal is tetramethylrhodamine isothiocyanate (TRITC)-labeled TRPV1 and TRITC-labeled P2X$_7$; and the yellow signal is the combination of the green and red signals. The arrow indicates activated neuronal cells and SGCs in the DRG. The scale bar represents 50 μm. The data are presented as the mean ± SEM; compared with the control group, $^{**}P < 0.01$; compared with the DNP group, $^{\#\#}P < 0.01$.

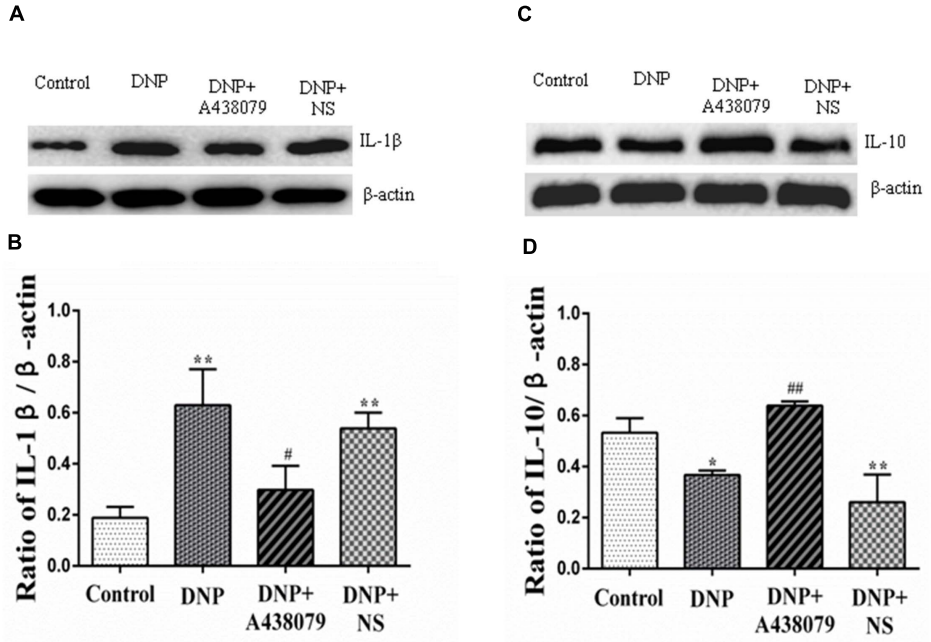

FIGURE 4 | The relative levels of IL-1β and IL-10 in the DRG were detected by Western blotting. **(A)** SDS-PAGE band of IL-1β in the DRG in each group of experimental rats. **(B)** The relative levels of IL-1β in the DRG from each group of experimental rats. **(C)** SDS-PAGE band of IL-10 in the DRG in each group of experimental rats. **(D)** The relative levels of IL-10 protein in the DRG from each group of experimental rats. The relative level of the IL-1β protein in the DRG from the DNP group was higher than that in the control group, while a lower level of IL-1β was observed in the DRG from the DNP + A438079 group than in the DNP group. In contrast, the relative level of the IL-10 protein in the DRG from the DNP group was lower than that in the control group, while a higher level of IL-10 was detected in the DRG in the DNP + A438079 group than in the DNP group. The data are presented as the mean ± SEM, $n = 6$; compared with the control group, $^{*}P < 0.05$, $^{**}P < 0.01$; compared with the DNP group, $^{\#}P < 0.05$, $^{\#\#}P < 0.01$.

results described above, the P2X$_7$ receptor antagonist A438079 may inhibit expression of the IL-1β protein in DNP rats.

IL-10, an anti-inflammatory cytokine, may provide protection for the body. The expression of the IL-10 protein was different from that of IL-1β protein. That is, the expression of IL-10 protein was decreased in the DNP group compared to the control group, and A438079 inhibited this downregulation (**Figures 4C,D**), suggesting that the P2X$_7$ receptor antagonist A438079 may induce expression of the IL-10 protein in rats presenting a state of NPP.

A438079 Inhibited the Phosphorylation of p38 and ERK1/2 in the DRGs of DNP Rats

Western blot analysis was used to detect the levels of p-p38 and p38 in the DRG as an indication of the phosphorylation of proteins in the p38 mitogen-activated protein kinase (p38MAPK) signaling pathway. The electrophoretic protein bands (**Figure 5A**) and the ratio of the IOD of the target protein to that of β-actin (**Figures 5B,C**) are shown. A significantly lower level of the p-p38 protein was detected in the control group than in the DNP group ($P < 0.01$); the level of the p-p38 protein in the DNP + A438079 group was significantly lower than in the DNP group ($P < 0.05$), but no significant difference was observed between the control group and DNP + A438079 group ($P > 0.05$). Similarly, a significant difference in the level of the p-p38 protein was not observed between the DNP + NS group and DNP group ($P > 0.05$). The levels of phosphorylated proteins involved in the MAPK-ERK1/2 signaling pathway were also measured in the groups described above, and the trend in the levels of these proteins was highly consistent with that of proteins involved in the p38 signaling pathway (**Figures 5D–F**). This finding indicates that the P2X$_7$ receptor antagonist A438079 inhibits the phosphorylation of p38 and ERK1/2, which may inhibit the expression of TRPV1 and P2X$_7$ receptors in the DRGs of DNP rats.

Molecular Docking of A438079 With the P2X$_7$ Receptor and TRPV1

The molecular docking of A438079 with the TRPV1 protein was performed by AutoDock4.2. The result showed that the P2X$_7$ receptor antagonist A438079 does not form a hydrogen bond with TRPV1 (**Figure 6**). The result of this experiment indicates that the effect of A438079 on TRPV1-mediated DNP is mediated by its interaction with the P2X$_7$ receptor, but this compound does not exert a direct effect on TRPV1.

DISCUSSION

Pain is a complex physiological process including many components, while chronic pain is a pathological state (Nazıroğlu et al., 2020). DNP is one of the common chronic complications

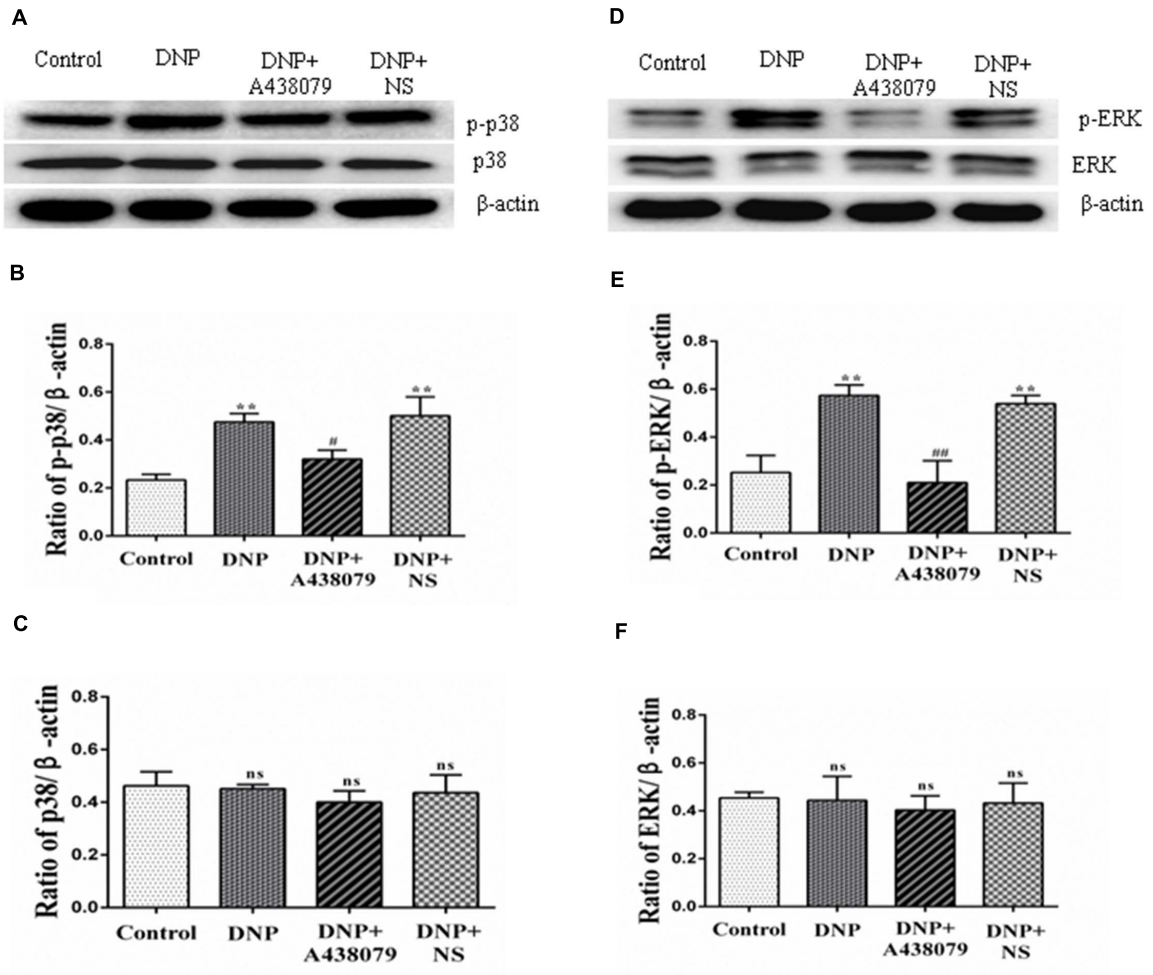

FIGURE 5 | Western blotting was performed to detect the levels of proteins related to the p38 and ERK1/2 signaling pathways in the DRG. **(A)** SDS-PAGE bands of the p-p38 and p38 proteins in each group. **(B)** The ratio of the optical density of p-p38 to that of the internal reference. **(C)** The ratio of the optical density of p38 to that of the internal reference. **(D)** SDS-PAGE bands of p-ERK1/2 and ERK1/2 in each group. **(E)** The ratio of the optical density of p-ERK1/2 to that of the internal reference. **(F)** The ratio of the optical density of ERK1/2 to that of the internal reference. The data are presented as the mean ± SEM, $n = 6$; compared with the control group, $^{**}P < 0.01$; compared with the DNP group, $^{\#}P < 0.05$, $^{\#\#}P < 0.01$; ns indicates a non-significant difference.

of diabetes and an early symptom of diabetic neuropathy, which is also related to metabolic disorders, neurotrophic disorders, and autoimmune and inflammatory responses caused by hyperglycemia (Sierra-Silvestre et al., 2018). Currently, DNP is difficult to treat, partially because the underlying mechanism of pain is not completely understood (Desai et al., 2014). For many years, pain treatment methods have focused on neurons, but with progress in research, glial cells may become a new target for pain management. Purinergic receptors can be divided into P1 and P2 receptors, and P2 receptors are further divided into ligand-gated ion channel type P2X receptors (including P2X$_{1-7}$) and G-protein-coupled P2Y receptors (Kuan and Shyu, 2016; Burnstock and Gentile, 2018; Alarcon-Vila et al., 2019). Studies have confirmed that P2X$_7$ receptors on SGCs are involved in the pathogenesis of NPP and inflammatory pain (Alarcon-Vila et al., 2019; Ni et al., 2020). Our experimental results showed that the MWT and TWL of DNP model rats were significantly reduced compared to those of control rats, indicating that the mechanical and heat hypersensitivity enhanced in DNP model rats. However, after treatment with the P2X$_7$ receptor antagonist A438079, the mechanical and heat hypersensitivity decreased in DNP model rats, indicating that the P2X$_7$ receptor is involved in the pathogenesis of DNP.

The transient receptor potential (TRP) channel is a non-selective cation channel that is expressed in various tissues and organs of the human body, participates in various sensory processes in the body, and plays an important role in maintaining the normal physiological function of the body (Kaneko and Szallasi, 2014; Yue et al., 2015). At least 6 TRPV subtypes, namely, TRPV1-6 (Nilius and Szallasi, 2014) have been identified to date. TRPV1-4 is heat-sensitive ion channel, while TRPV5 and TRPV6 are ion channels with a high selectivity for calcium ions (Mickle et al., 2016). Many factors cause pain, such as capsaicin and its analogs, bradykinin, ATP, TNF-α, H^+, fatty

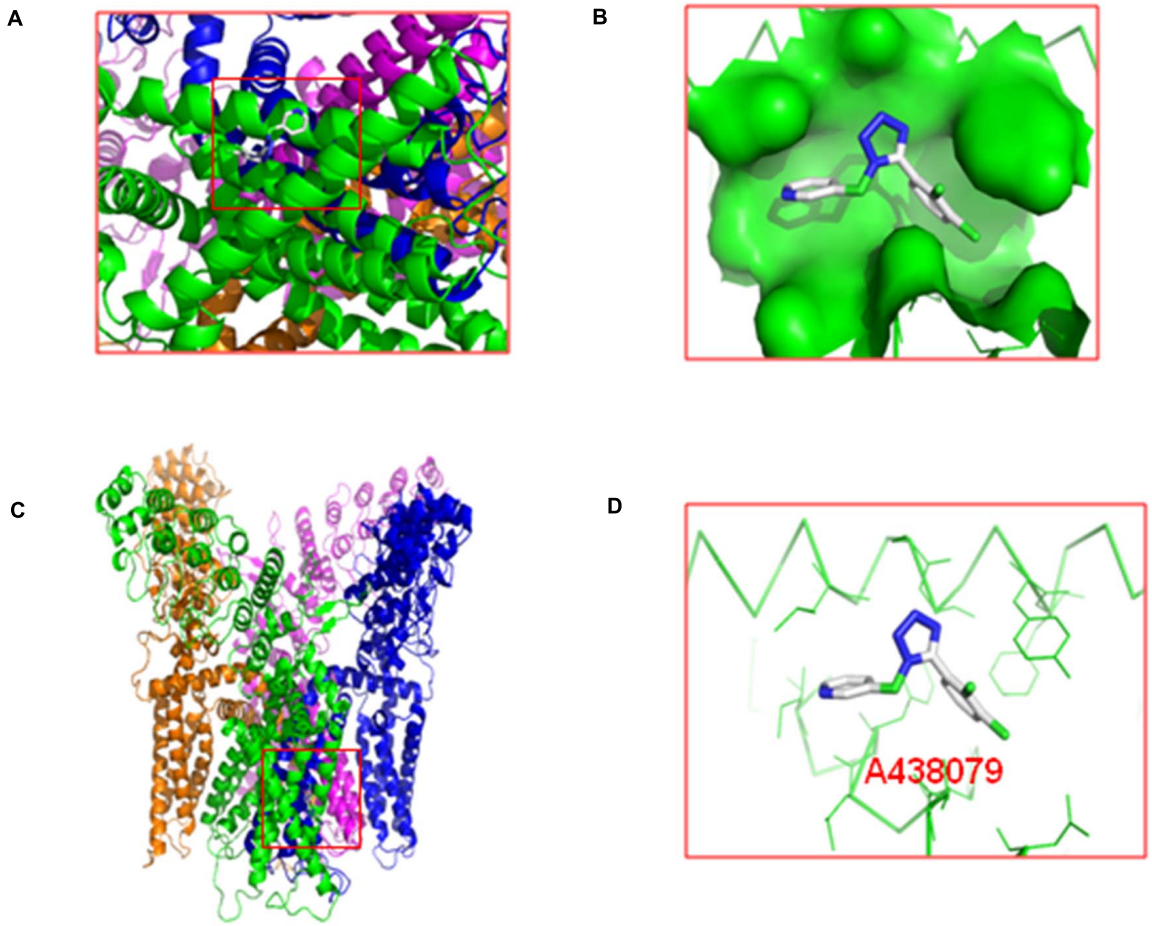

FIGURE 6 | Molecular docking of A438079 with the TRPV1. **(A)**, top view. **(B)**, the docking pocket between A438079 and TRPV1. **(C)**, front view. **(D)**, A438079 does not form a hydrogen bond with TRPV1, and A438079 is in the middle.

acid derivatives, and PGE2, and can directly or indirectly upregulate the expression of TRPV1 or activate TRPV1 to cause various types of pain, particularly inflammatory pain and thermal hyperalgesia (Alawi and Keeble, 2010; Luo et al., 2011; Hsu et al., 2014; Ferreira et al., 2019), suggesting that TRPV1 is involved in the processes of inflammation and immune activation. In the present study, mRNA and protein levels of TRPV1 in DRG neurons in DNP model rats were significantly increased compared to those in control rats. The mRNA and protein levels of TRPV1 were decreased after intrathecal injection of the P2X$_7$ receptor antagonist A438079, indicating that TRPV1 is involved in the hypersensitivity associated with DNP. Based on the interaction between neurons and glial cells in the sensory ganglia (Gu et al., 2010) and the results described above, we speculated that the P2X$_7$ receptor may have a certain role in TRPV1-mediated DNP in rats.

GFAP is a marker of SGCs, and its upregulation indicates the activation of SGCs (Feldman-Goriachnik et al., 2018; Liu H. et al., 2018), while NeuN is a neuronal marker (Halene et al., 2016). The expression of NeuN and GFAP in the DRG was detected in our study. The results of double immunofluorescence staining showed a significant increase in the coexpression of TRPV1 and NeuN in DRG neurons from the model group compared to the control group and that the coexpression of the P2X$_7$ receptor and GFAP in SGCs was also significantly increased; the coexpression of TRPV1 and NeuN and coexpression of the P2X$_7$ receptor and GFAP was decreased in the model group after treatment with the P2X$_7$ receptor antagonist A438079. Therefore, DRG neurons and SGCs are activated during DNP, along with the corresponding TRPV1 and P2X$_7$ receptors. Additionally, the P2X$_7$ receptor antagonist A438079 can inhibit the activation of P2X$_7$ receptors, which can reduce the release of cytokines, etc., thereby reducing the damage to neurons and the activation of TRPV1.

Upregulation of cytokine expression is another feature of activated SGCs and may play an important role in information exchange between ganglion cells. The release of cytokines by SGCs is increased under pathological conditions, thus affecting the activity of neurons (Otoshi et al., 2010; Berta et al., 2012; Cairns et al., 2015; Afroz et al., 2019). Exciting P2X$_7$ receptors can increase the release of cytokines such as IL-1β in glial cells, which cause chronic pain. Peripheral tissue inflammation significantly increased the expression of COX-1 and COX-2

in DRG cells. IL-1β induces the expression of COX-2, and subsequently increases prostaglandin synthesis in different cells including DRG cells. The prostaglandins released in DRG activate an autocrine signaling mechanism in primary afferent neurons to sensitize them and directly or indirectly activate TRPV1 to induce various pain sensations (Yaksh et al., 2001; Amaya et al., 2009; Araldi et al., 2013). Our results showed that the expression of IL-1β was upregulated and that the relative level of the IL-10 protein was decreased in the DRGs of DNP model rats compared to those of control rats, while the P2X$_7$ receptor antagonist A438079 reduced the upregulation of IL-1β expression and increased the relative level of IL-10. This suggests that inflammatory factors may be involved in the pathophysiological mechanism by which P2X$_7$ receptor participates in DNP mediated by TRPV1.

Additionally, the p38MAPK and ERK pathways are involved in the regulation of the pathophysiological functions of various related diseases mediated by TRPV1 (Shin et al., 2016; Hong et al., 2017) and the pathogenesis of inflammatory and neurodegenerative diseases mediated by the P2X$_7$ receptor (Ji et al., 2018; Yu et al., 2018; Pérez de Lara et al., 2019). In our study, we detected changes in the levels of proteins involved in the p-p38MAPK and p-ERK1/2 signaling pathways in each group of rats using western blotting. The levels of p-p38 and p-ERK1/2 in the DNP group were increased compared to those in the control group, but the levels of these proteins in the DNP + A438079 group were significantly decreased compared to those in the DNP group. The detection of changes in the phosphorylation of cell signal transduction molecules showed that the P2X$_7$ receptor antagonist A438079 inhibited the activation of p38MAPK and ERK1/2 mediated via TRPV1 and P2X$_7$ receptor in DRG, which provides experimental evidence for the possible mechanism underlying the role of the P2X$_7$ receptor in TRPV1-mediated DNP.

We used AutoDock4.2 for molecular docking experiments to further confirm that the P2X$_7$ receptor antagonist A438079 directly binds to the P2X$_7$ receptor and then interacts with TRPV1 rather than directly acting on TRPV1. The results showed that A438079 does not form a hydrogen bond with the TRPV1. Thus, A438079 modulates TRPV1-mediated DNP by binding the P2X$_7$ receptor but has no direct effect on TRPV1.

CONCLUSION

In summary, the P2X$_7$ receptor antagonist A438079 alleviates nociception, as measured by the behavioral responses of DNP rats, and reduces the upregulation of TRPV1; activation of the P2X$_7$ receptor also increases the release of IL-1β and inhibits the release of IL-10, and A438079 has no direct effect on TRPV1, suggesting that the P2X$_7$ receptor is involved in the maintenance and development of DNP mediated by TRPV1, and the mechanism may involve reducing the activation of p38MAPK and ERK1/2.

DATA AVAILABILITY STATEMENT

The original contributions presented in the study are included in the article/supplementary material, further inquiries can be directed to the corresponding author.

ETHICS STATEMENT

The animal study was reviewed and approved by the Ethics Committee of Nanchang University.

AUTHOR CONTRIBUTIONS

AW: methodology, validation, formal analysis, investigation, data curation, writing—original draft, writing—review and editing, and visualization. XS: methodology and writing—original draft. RYu, BQ, and RYa: methodology. CX: conceptualization, investigation, writing—review and editing, supervision, and project administration. All authors read and approved the final manuscript.

FUNDING

This work was supported by grants from the National Natural Science Foundation of China (No. 82060247), the Cultivating Foundation of Young Scientists (Star of Jing gang) of Jiangxi Province (No. 20153BCB23033), the Youth Science Foundation of the Educational Department of Jiangxi Province (No. GJJ14146), and the Innovation Foundation of the Graduate School of Nanchang University (No. CX2019148).

ACKNOWLEDGMENTS

We sincerely appreciate those who contributed to our research. We would extend our gratitude to the Laboratory Animal Science Department of Nanchang University for providing experimental animals. We also convey our heartfelt thanks to Shangdong Liang, in Nanchang University who participated in this study.

REFERENCES

Afroz, S., Arakaki, R., Iwasa, T., Oshima, M., Hosoki, M., Inoue, M., et al. (2019). CGRP induces differential regulation of cytokines from satellite glial cells in trigeminal ganglia and Orofacial Nociception. *Int. J. Mol. Sci.* 20:3. doi: 10.3390/ijms20030711

Alarcon-Vila, C., Pizzuto, M., and Pelegrin, P. (2019). Purinergic receptors and the inflammatory response mediated by lipids. *Curr. Opin. Pharmacol.* 47, 90–96. doi: 10.1016/j.coph.2019.02.004

Alawi, K., and Keeble, J. (2010). The paradoxical role of the transient receptor potential vanilloid 1 receptor in inflammation. *Pharmacol. Ther.* 125, 181–195. doi: 10.1016/j.pharmthera.2009.10.005

Amaya, F., Samad, T. A., Barrett, L., and Broom, D. C. (2009). Woolf CJ. Periganglionic inflammation elicits a distally radiating pain hypersensitivity by promoting COX-2 induction in the dorsal root ganglion. *Pain* 142, 59–67. doi: 10.1016/j.pain.2008.11.013

Araldi, D., Ferrari, L. F., Lotufo, C. M., Vieira, A. S., Athie, M. C., Figueiredo, J. G., et al. (2013). Peripheral inflammatory hyperalgesia depends on the COX

increase in the dorsal root ganglion. *Proc. Natl. Acad. Sci. USA* 110, 3603–3608. doi: 10.1073/pnas.1220668110

Berta, T., Liu, T., Liu, Y. C., Xu, Z. Z., and Ji, R. R. (2012). Acute morphine activates satellite glial cells and up-regulates IL-1beta in dorsal root ganglia in mice via matrix metalloprotease-9. *Mol. Pain* 8:18. doi: 10.1186/1744-8069-8-18

Boue-Grabot, E., and Pankratov, Y. (2017). Modulation of central synapses by astrocyte-released ATP and Postsynaptic P2X Receptors. *Neural. Plast* 2017:9454275. doi: 10.1155/2017/9454275

Burnstock, G. (2017). Purinergic signalling and neurological diseases: an update. *CNS Neurol. Disord. Drug Targets* 16, 257–265. doi: 10.2174/1871527315666160922104848

Burnstock, G., and Gentile, D. (2018). The involvement of purinergic signalling in obesity. *Purinergic Signal* 14, 97–108. doi: 10.1007/s11302-018-9605-8

Cairns, B. E., Arendt-Nielsen, L., and Sacerdote, P. (2015). Perspectives in pain research 2014: Neuroinflammation and glial cell activation: the cause of transition from acute to chronic pain? *Scand J. Pain* 6, 3–6. doi: 10.1016/j.sjpain.2014.10.002

Dan, Y., Guo, H., Zheng, C., Wu, B., Guo, J., and Li, G. (2020). Neferine alleviates P2X3 receptor in rat dorsal root ganglia mediated neuropathic pain. *Neurosci. Res.* 2020, 30424–30427. doi: 10.1016/j.neures.2020.08.004

Deng, Z., Li, C., Du, E., Liu, C., Xia, B., Chen, H., et al. (2018). Catestatin enhances neuropathic pain mediated by P2X4 receptor of dorsal root ganglia in a Rat Model of Chronic Constriction injury. *Cell. Physiol. Biochem.* 51, 812–826. doi: 10.1159/000495334

Desai, B., Freeman, E., Huang, E., Hung, A., Knapp, E., Breunig, I. M., et al. (2014). Clinical value of tapentadol extended-release in painful diabetic peripheral neuropathy. *Expert. Rev. Clin. Pharmacol.* 7, 203–209. doi: 10.1586/17512433.2014.889562

Feldman-Goriachnik, R., Wu, B., and Hanani, M. (2018). Cholinergic responses of satellite glial cells in the superior cervical ganglia. *Neurosci. Lett.* 671, 19–24. doi: 10.1016/j.neulet.2018.01.051

Ferreira, L. G. B., Prevatto, J. P., Freitas, H. R., Reis, R. A. M., Silva, P. M. R., Martins, M. A., et al. (2019). Capsaicin inhibits lipopolysaccharide-induced adrenal steroidogenesis by raising intracellular calcium levels. *Endocrine* 64, 169–175. doi: 10.1007/s12020-019-01849-5

Galuppo, M., Giacoppo, S., Bramanti, P., and Mazzon, E. (2014). Use of natural compounds in the management of diabetic peripheral neuropathy. *Molecules* 19, 2877–2895. doi: 10.3390/molecules19032877

Ge, H., Guan, S., Shen, Y., Sun, M., Hao, Y., He, L., et al. (2019). Dihydromyricetin affects BDNF levels in the nervous system in rats with comorbid diabetic neuropathic pain and depression. *Sci. Rep.* 9:14619. doi: 10.1038/s41598-019-51124-w

Gu, Y., Chen, Y., Zhang, X., Li, G. W., Wang, C., and Huang, L. Y. (2010). Neuronal soma-satellite glial cell interactions in sensory ganglia and the participation of purinergic receptors. *Neuron. Glia. Biol.* 6, 53–62. doi: 10.1017/s1740925x10000116

Gunthorpe, M. J., and Szallasi, A. (2008). Peripheral TRPV1 receptors as targets for drug development: new molecules and mechanisms. *Curr. Pharm. Des.* 14, 32–41. doi: 10.2174/138161208783330754

Halene, T. B., Kozlenkov, A., Jiang, Y., Mitchell, A. C., Javidfar, B., Dincer, A., et al. (2016). NeuN+ neuronal nuclei in non-human primate prefrontal cortex and subcortical white matter after clozapine exposure. *Schizophr Res.* 170, 235–244. doi: 10.1016/j.schres.2015.12.016

Hollopeter, G., Jantzen, H. M., Vincent, D., Li, G., England, L., Ramakrishnan, V., et al. (2001). Identification of the platelet ADP receptor targeted by antithrombotic drugs. *Nature* 409, 202–207. doi: 10.1038/35051599

Hong, S. I., Nguyen, T. L., Ma, S. X., Kim, H. C., Lee, S. Y., and Jang, C. G. (2017). TRPV1 modulates morphine-induced conditioned place preference via p38 MAPK in the nucleus accumbens. *Behav. Brain Res.* 334, 26–33. doi: 10.1016/j.bbr.2017.07.017

Hsu, H. C., Tang, N. Y., Lin, Y. W., Li, T. C., Liu, H. J., and Hsieh, C. L. (2014). Effect of electroacupuncture on rats with chronic constriction injury-induced neuropathic pain. *Sci. World J.* 14:129875. doi: 10.1155/2014/129875

Janks, L., Sharma, C. V. R., and Egan, T. M. (2018). A central role for P2X7 receptors in human microglia. *J. Neuroinflam.* 15:325. doi: 10.1186/s12974-018-1353-8

Jarvis, M. F. (2010). The neural-glial purinergic receptor ensemble in chronic pain states. *Trends Neurosci.* 33, 48–57. doi: 10.1016/j.tins.2009.10.003

Ji, R. R., Berta, T., and Nedergaard, M. (2013). Glia and pain: is chronic pain a gliopathy? *Pain* 154, S10–S28. doi: 10.1016/j.pain.2013.06.022

Ji, Z., Xie, Y., Guan, Y., Zhang, Y., Cho, K. S., Ji, M., et al. (2018). Involvement of P2X(7) receptor in proliferation and migration of human glioma cells. *Biomed. Res. Int.* 2018:8591397. doi: 10.1155/2018/8591397

Kaneko, Y., and Szallasi, A. (2014). Transient receptor potential (TRP) channels: a clinical perspective. *Br. J. Pharmacol.* 171, 2474–2507. doi: 10.1111/bph.2014.171.issue-10

Kobayashi, K., Yamanaka, H., and Noguchi, K. (2013). Expression of ATP receptors in the rat dorsal root ganglion and spinal cord. *Anat. Sci. Int.* 88, 10–16. doi: 10.1007/s12565-012-0163-9

Kuan, Y. H., and Shyu, B. C. (2016). Nociceptive transmission and modulation via P2X receptors in central pain syndrome. *Mol. Brain* 9:58. doi: 10.1186/s13041-016-0240-4

Liu, C., Li, C., Deng, Z., Du, E., and Xu, C. (2018). Long Non-coding RNA BC168687 is involved in TRPV1-mediated Diabetic Neuropathic Pain in Rats. *Neuroscience* 374, 214–222. doi: 10.1016/j.neuroscience.2018.01.049

Liu, C., Tao, J., Wu, H., Yang, Y., Chen, Q., Deng, Z., et al. (2017). Effects of LncRNA BC168687 siRNA on diabetic neuropathic pain mediated by P2X7 receptor on SGCs in DRG of Rats. *Biomed. Res. Int.* 2017:7831251. doi: 10.1155/2017/7831251

Liu, H., Zhao, L., Gu, W., Liu, Q., Gao, Z., Zhu, X., et al. (2018). Activation of satellite glial cells in trigeminal ganglion following dental injury and inflammation. *J. Mol. Histol.* 49, 257–263. doi: 10.1007/s10735-018-9765-4

Lu, J., Luo, Y., Wang, J., Hu, C., Zhang, R., Wang, C., et al. (2017). Association of type 2 diabetes susceptibility loci with peripheral nerve function in a Chinese population with diabetes. *J. Diabetes Investig.* 8, 115–120. doi: 10.1111/jdi.12546

Luo, X. J., Peng, J., and Li, Y. J. (2011). Recent advances in the study on capsaicinoids and capsinoids. *Eur. J. Pharmacol.* 650, 1–7. doi: 10.1016/j.ejphar.2010.09.074

Mestre, C., Pélissier, T., Fialip, J., Wilcox, G., and Eschalier, A. (1994). A method to perform direct transcutaneous intrathecal injection in rats. *J. Pharmacol. Toxicol. Methods* 32, 197–200. doi: 10.1016/1056-8719(94)90087-6

Mickle, A. D., Shepherd, A. J., and Mohapatra, D. P. (2016). Nociceptive TRP Channels: sensory detectors and transducers in multiple pain pathologies. *Pharmaceuticals (Basel)* 9:72. doi: 10.3390/ph9040072

Milligan, E. D., and Watkins, L. R. (2009). Pathological and protective roles of glia in chronic pain. *Nat. Rev. Neurosci.* 10, 23–36. doi: 10.1038/nrn2533

Nazıroğlu, M., Öz, A., and Yıldızhan, K. (2020). Selenium and neurological diseases: focus on peripheral pain and TRP channels. *Curr. Neuropharmacol.* 18, 501–517. doi: 10.2174/1570159x18666200106152631

Ni, C. M., Sun, H. P., Xu, X., Ling, B. Y., Jin, H., Zhang, Y. Q., et al. (2020). Spinal P2X7R contributes to streptozotocin-induced mechanical allodynia in mice. *J. Zhejiang Univ. Sci. B* 21, 155–165. doi: 10.1631/jzus.B1900456

Nilius, B., and Szallasi, A. (2014). Transient receptor potential channels as drug targets: from the science of basic research to the art of medicine. *Pharmacol. Rev.* 66, 676–814. doi: 10.1124/pr.113.008268

Otoshi, K., Kikuchi, S., Konno, S., and Sekiguchi, M. (2010). The reactions of glial cells and endoneurial macrophages in the dorsal root ganglion and their contribution to pain-related behavior after application of nucleus pulposus onto the nerve root in rats. *Spine (Phila Pa 1976)* 35, 264–271. doi: 10.1097/BRS.0b013e3181b8b04f

Pan, B., Ding, H., Cheng, Z., Song, Z., Xiao, D., and Guo, Q. (2018). Vascular endothelial growth factor antibody attenuates diabetic peripheral neuropathic pain in rats. *Zhong Nan Da Xue Xue Bao Yi Xue Ban* 43, 1097–1102. doi: 10.11817/j.issn.1672-7347.2018.10.009

Pérez de Lara, M. J., Avilés-Trigueros, M., Guzmán-Aránguez, A., Valiente-Soriano, F. J., de la Villa, P., Vidal-Sanz, M., et al. (2019). Potential role of P2X7 receptor in neurodegenerative processes in a murine model of glaucoma. *Brain Res. Bull.* 150, 61–74. doi: 10.1016/j.brainresbull.2019.05.006

Shin, Y. H., Kim, J. M., and Park, K. (2016). The effect of capsaicin on salivary gland dysfunction. *Molecules* 21:835. doi: 10.3390/molecules21070835

Sierra-Silvestre, E., Bisset, L., and Coppieters, M. W. (2018). Altered pain processing in people with type I and II diabetes: a protocol for a systematic review and meta-analysis of pain threshold and pain modulation mechanisms. *Syst. Rev.* 7:222. doi: 10.1186/s13643-018-0895-2

Skaper, S. D., Debetto, P., and Giusti, P. (2010). The P2X7 purinergic receptor: from physiology to neurological disorders. *Faseb J.* 24, 337–345. doi: 10.1096/fj.09-138883

Sloan, G., Shillo, P., Selvarajah, D., Wu, J., Wilkinson, I. D., Tracey, I., et al. (2018). A new look at painful diabetic neuropathy. *Diabetes Res. Clin. Pract.* 144, 177–191. doi: 10.1016/j.diabres.2018.08.020

Tsuda, M., Tozaki-Saitoh, H., and Inoue, K. (2012). Purinergic system, microglia and neuropathic pain. *Curr. Opin. Pharmacol.* 12, 74–79. doi: 10.1016/j.coph.2011.10.014

Ugur, M., and Ugur, O. (2019). How does P2X7 receptor work? a mechanism based approach to P2X7 receptor action. *Mol. Pharmacol.* 95, 442–450. doi: 10.1124/mol.118.115022

Vinik, A. I., Nevoret, M. L., Casellini, C., and Parson, H. (2013). Diabetic neuropathy. *Endocrinol. Metab. Clin. North Am.* 42, 747–787. doi: 10.1016/j.ecl.2013.06.001

Volonté, C., Apolloni, S., Skaper, S. D., and Burnstock, G. (2012). P2X7 receptors: channels, pores and more. *CNS Neurol. Disord. Drug Targets* 11, 705–721. doi: 10.2174/187152712803581137

Wei, L., Caseley, E., Li, D., and Jiang, L. H. (2016). ATP-induced P2X receptor-dependent large pore formation: how much do we know? *Front. Pharmacol.* 7:5. doi: 10.3389/fphar.2016.00005

Yaksh, T. L., Dirig, D. M., Conway, C. M., Svensson, C., Luo, Z. D., and Isakson, P. C. (2001). The acute antihyperalgesic action of nonsteroidal, anti-inflammatory drugs and release of spinal prostaglandin E2 is mediated by the inhibition of constitutive spinal cyclooxygenase-2 (COX-2) but not COX-1. *J. Neurosci.* 21, 5847–5853. doi: 10.1523/JNEUROSCI.21-16-05847

Yang, R., Li, L., Yuan, H., Liu, H., Gong, Y., Zou, L., et al. (2019). Quercetin relieved diabetic neuropathic pain by inhibiting upregulated P2X4 receptor in dorsal root ganglia. *J. Cell. Physiol.* 234, 2756–2764. doi: 10.1002/jcp.27091

Ying, Y. L., Wei, X. H., Xu, X. B., She, S. Z., Zhou, L. J., Lv, J., et al. (2014). Over-expression of P2X7 receptors in spinal glial cells contributes to the development of chronic postsurgical pain induced by skin/muscle incision and retraction (SMIR) in rats. *Exp. Neurol.* 261, 836–843. doi: 10.1016/j.expneurol.2014.09.007

Yu, M., Su, B., and Zhang, X. (2018). Gardenoside suppresses the pain in rats model of chronic constriction injury by regulating the P2X3 and P2X7 receptors. *J. Recept. Signal Transduct. Res.* 38, 198–203. doi: 10.1080/10799893.2018.1468782

Yue, Z., Xie, J., Yu, A. S., Stock, J., Du, J., and Yue, L. (2015). Role of TRP channels in the cardiovascular system. *Am. J. Physiol. Heart Circ. Physiol.* 308, H157–H182. doi: 10.1152/ajpheart.00457.2014

Zhang, B. Y., Zhang, Y. L., Sun, Q., Zhang, P. A., Wang, X. X., Xu, G. Y., et al. (2020). Alpha-lipoic acid downregulates TRPV1 receptor via NF-κB and attenuates neuropathic pain in rats with diabetes. *CNS Neurosci. Ther.* 26, 762–772. doi: 10.1111/cns.13303

Zou, L., Tu, G., Xie, W., Wen, S., Xie, Q., Liu, S., et al. (2016). LncRNA NONRATT021972 involved the pathophysiologic processes mediated by P2X7 receptors in stellate ganglia after myocardial ischemic injury. *Purinergic. Signal.* 12, 127–137. doi: 10.1007/s11302-015-9486-z

Zou, L., Yu, K., Fan, Y., Cao, S., Liu, S., Shi, L., et al. (2019). The inhibition by guanfu base A of neuropathic pain mediated by P2Y12 receptor in dorsal root ganglia. *ACS Chem. Neurosci.* 10, 1318–1325. doi: 10.1021/acschemneuro.8b00399

Conflict of Interest: The authors declare that the research was conducted in the absence of any commercial or financial relationships that could be construed as a potential conflict of interest.

frontiers in Molecular Neuroscience

ORIGINAL RESEARCH
published: 21 June 2021
doi: 10.3389/fnmol.2021.673669

Long Non-coding RNA LINC01119 Promotes Neuropathic Pain by Stabilizing BDNF Transcript

Le Zhang[1], Hao Feng[1], Yanwu Jin[1], Yufeng Zhan[2], Qi Han[1], Xin Zhao[1] and Peilong Li[3]**

[1] Department of Anesthesiology, The Second Hospital, Cheeloo College of Medicine, Shandong University, Jinan, China, [2] Department of Anesthesiology, Affiliated Hangzhou First People's Hospital, Zhejiang University School of Medicine, Hangzhou, China, [3] Department of Clinical Laboratory, The Second Hospital, Cheeloo College of Medicine, Shandong University, Jinan, China*

Neuropathic pain (NP) is caused by primary injury or dysfunction of the peripheral and the central nervous system. Long non-coding RNAs were critical regulators involved in nervous system diseases, however, the precise regulatory mechanism remains unclear. This study aims to uncover the essential role of LINC01119 in NP progression and further clarify the underlying regulatory mechanism at post-transcriptional level. LINC01119 was significantly upregulated in rats of spare nerve injury (SNI) group compared to sham group. Functionally, silencing of LINC01119 significantly alleviated the neuropathic pain-induced hypersensitivity and reduced the increase in IL−6, IL−1β, and TNF−α caused by SNI. Mechanistically, Brain-derived neurotrophic factor (BDNF) was identified as the functional target of LINC01119. Besides, an RNA binding protein, ELAVL1 could directly interact with LINC01119, and this formed LINC01119- ELAVL1 complex binds to BDNF mRNA, strengthening its RNA stability and increasing the expression level of BDNF at both transcript and protein levels. Clinically, serum LINC01119 was verified as a promising diagnostic biomarker for NP patients. LINC01119 induces NP progression via binding with ELAVL1 and increasing BDNF mRNA stability and expression level. Therefore, LINC01119 may serve as a promising diagnostic marker and therapeutic target for NP treatment.

Keywords: neuropathic pain, LINC01119, BDNF, ELAVL1, spare nerve injury

OPEN ACCESS

Edited by:
Tao Liu,
The First Affiliated Hospital of Nanchang University, China

Reviewed by:
Arkady Khoutorsky,
McGill University, Canada
Zhiyao Wang,
Fudan University, China

****Correspondence:***
Xin Zhao
lujnzx@sohu.com
Peilong Li
lipeilong@whu.edu.cn

Specialty section:
This article was submitted to Pain Mechanisms and Modulators, a section of the journal Frontiers in Molecular Neuroscience

Received: *28 February 2021*
Accepted: *19 May 2021*
Published: *21 June 2021*

Citation:
Zhang L, Feng H, Jin Y, Zhan Y, Han Q, Zhao X and Li P (2021) Long Non-coding RNA LINC01119 Promotes Neuropathic Pain by Stabilizing BDNF Transcript. Front. Mol. Neurosci. 14:673669. doi: 10.3389/fnmol.2021.673669

INTRODUCTION

Neuropathic pain (NP) is a complicated, chronic pain state that is generally caused by tissue damage that affects the somatosensory nervous system (Nagpal et al., 2020). Neuropathic pain is linked with multiple diseases, commonly caused by Shingles (postherpetic neuralgia, PHN), diabetes (painful diabetic neuropathy, PDN) and others including trauma, stroke or cancer (Vuka et al., 2020). Pathologically, NP is tightly associated with peripheral and spinal

Abbreviations: AREs, AU-rich elements; BDNF, Brain-derived neurotrophic factor; ELAVL1, embryonic lethal abnormal version like RNA binding protein 1; ELISA, Enzyme-linked immunosorbent assay; IHC, Immunohistochemistry; lncRNAs, Long non-coding RNAs; mRNA, messenger RNA; NP, Neuropathic pain; PWT, Paw withdrawal threshold; PWL, paw withdrawal latency; RBPs, RNA-binding proteins; RIP, RNA immunoprecipitation; RNA-FISH, RNA fluorescent *in situ* hybridization; ROC, Receiver operator characteristic; SCI, spinal cord injury; SNI, spare nerve injury.

cord injury and is a common clinical disease in orthopedics (Soler et al., 2021). However, the therapeutic approaches for NP are not satisfactory mainly due to the lack of effective molecular targets. Therefore, finding novel predictive markers and new targets to cure NP are urgently needed.

Long non-coding RNAs (lncRNAs) is characterized with the transcripts more than 200 nucleotides without protein coding potential (Serghiou et al., 2016). In recent years, lncRNAs were reported to play essential roles in various diseases, including cancer, cardiovascular, diabetes and neuropathy-related affaires; especially during the pathophysiological changes, such as cell growth and migration, autophagy and aging, et al. (Herrera-Solorio et al., 2017). Importantly, mountain evidence supports that a group of lncRNAs are involved in the central nervous system of rats and affects the development of nerves, and is closely related to many nervous system diseases (Pang et al., 2019; Song et al., 2020). However, the expression pattern, biological function, and underlying mechanism of lncRNAs in NP remains unclear.

RNA-binding proteins (RBPs) are playing wide roles in various diseases by the regulation of stability and splicing of mRNAs (Pereira et al., 2017). RNA-binding proteins regulate the processes of RNA maturation and decay to control the initiation and development of diseases (Upadhyay et al., 2013). For instance, ELAVL1 RBP (HuR) could stabilize matrix metalloproteinase-9 mRNA during seizure-induced mmp-9 expression in neurons, participating in the neuron lesions (Zybura-Broda et al., 2018). In addition, HuR was a critical regulator of autophagy during the process of myocardial ischemia-reperfusion injury, resulting in the progression of ferroptosis (Chen et al., 2021). Moreover, increasing studies suggested that lncRNAs could play essential roles in disease progression through the interaction with RBPs (Wu et al., 2016; Choi and Nam, 2018). However, whether lncRNAs promotes NP progression via binding with RBPs is not well known, and the related studies are very limited. Uncovering the regulatory mechanism of lncRNA-RBP interactions during NP progression could provide better understanding of NP treatment.

Brain-derived neurotrophic factor (BDNF) serves as a transducer, has been shown to contribute to the maintenance and development of NP by activating astrocytes and microglia as well as sensitizing neurons (Chow et al., 2020; Halloway et al., 2020). Previously, we identified the essential role of BDNF in NP progression (Zhang et al., 2016; Wang et al., 2017). However, how BDNF was regulated and the functional link between lncRNA and BDNF was not defined. In this study, we detected the expression of LINC01119 in NP model, and determined its role in NP progression. We revealed that LINC01119 was upregulated in rats with NP. Moreover, LINC01119 caused NP through upregulating BDNF expression via binding with ELVAL1.

MATERIALS AND METHODS

Patient Samples

A total of 45 NP (postherpetic neuralgia, PHN) patients caused by Shingles and 49 healthy people were included from June 2018 to October 2020, to determine the predictive role of serum LINC01119. Serum samples were obtained and centrifuged at 3000 r/min for 10 min under 4°C. Included patients, aged from 24 to 78 years, had peripheral NP and a score $\geq$4/10 on pain VAS score (a 10-point VAS in which 0 indicated no pain and 10 indicated the worst possible pain). Evidences of neuropathy attributable to hypothyroidism, vitamin B12 deficiency, connective tissue disease, and amyloidosis were excluded. The study protocol was approved and written informed consent was obtained from all participants by the Research Scientific Ethics Committee of The Second Hospital of Shandong University.

Animals

A total of 90 male Sprague-Dawley rats weighing 200–220 g were purchased from the Experimental Animal Center of Shandong University. Rats were housed in separated cages with a light/dark cycle of 12 h with free access to food and water. The room temperature was maintained at 26 ± 1℃, and the humidity was controlled at 40–50%. As previously described (Zhang et al., 2016), NP model in rats was constructed by performing SNI experiments. Rats were randomly divided into 9 groups: ① Sham (17 rats), ② Sham + +sh-LINC01119 (8 rats), ③ SNI (17 rats), ④ SNI-sh-NC (8 rats), ⑤ SNI-sh-LINC01119 (8 rats), ⑥ SNI-sh-LINC01119 + Lv-BDNF (8 rats), ⑦ SNI-Lv-NC (8 rats), ⑧ SNI-Lv-LINC01119 (8 rats), ⑨ SNI-Lv-LINC01119 + sh-ELAVL1 (8 rats). Among the above groups, five rats were used for evaluation of pain behaviors, and the rest were used for detection of LINC01119, BDNF, and ELAVL1 expression levels after behavioral test at day 14. The animal studies were carried out in accordance with NIH Guidelines for the Care and Use of Laboratory Animals and approved by the Animal Care Committee of the Second Hospital of Shandong University.

Cell Culture

Rat microglial cells were purchased from Scien-cell Research Laboratories (Carlsbad, CA). Cells were cultured in Dulbecco's Modified Eagle medium (DMEM; Lonza Inc. United States) supplemented with 10% FBS (Gibco, Carlsbad, CA) and 1% penicillin/streptomycin (Gibco) in an incubator at 37°C with humidified atmosphere of 5% CO_2. Cells were authenticated by short tandem repeat (STR) profiling. Actinomycin D (ActD) was used for testing RNA stability and used for triplicates.

Spare Nerve Injury (SNI) Surgery

Spare Nerve Injury models were established as previously described (Decosterd and Woolf, 2000). All rats were anesthetized with an intraperitoneal injection of 10% chloral hydrate (300 mg/kg). By incising the skin directly on the outside of the thigh and deep in the biceps femoris, the sciatic nerve and its three terminal branches were exposed. The tibia and common peroneal nerve were tightly ligated with 5–0 silk and cut 2–4 mm when present. The skin and muscle were sutured in two layers, and after this operation, the nerve remained completely flat and transparent. Sham-operated rats that underwent the

same surgical procedure but nerves not damaged were used as a control group.

Intrathecal Catheter Implantation and Lentivirus Injection

To stably overexpress or silencing LINC01119, BDNF, and ELAVL1, lentivirus-based vectors containing respective oligonucleotides were constructed by GenePharma (Shanghai, China). For cell transfection, the above-mentioned lentivirus vectors were mixed with 6 μg/ml polybrene and co-cultured for 24 h. For rat injection, we used an intrathecal catheter implantation method as previously described. Briefly, a PE-10 polyethylene catheter was inserted into the epidural space between the L5 and L6 vertebrae. After the anesthesia was completely restored, the 2% lidocaine (0.2 mL) was injected, and the dragging or paralysis of the hind limbs were observed to determine the correct implantation. The inside of the catheter is fixed with paraspinal muscles. After the wound is closed, the outside of the catheter is inserted and fixed on the skin and sutured to the head. The lentivirus vectors were injected via the above established intrathecal catheter. Brain-derived neurotrophic factor and ELAVL1 vectors were injected at day 3 while LINC01119-related vectors were injected at day 7 after SNI induction. The pain behaviors influenced by above injections were observed at day 14, 17, and 21 and repeated five times. Expression detection of respective genes were performed in day 14 and repeated in triplicates.

NP Assessment

Mechanical sensitivity was assessed by determining paw withdrawal threshold (PWT). Rats were exposed in a transparent plastic box (22 × 12 × 22 cm) with a metal mesh at the bottom. Calibrated von Frey filament (IITC, Woodland Hills, CA, United States) was used to apply pressure on the plantar surface of the hind paw. The diameter of the filament is recorded when paw is pulled. Paw Withdrawal Latency (PWL) to noxious cold (0°C) was examined to evaluate cold allodynia. It was recorded by the length of time between the placement of the hind paw on the plate and a flinching of the paw. To avoid tissue damage, a cut off time of 40s for rats was used. Tests were performed 1 day before and 3, 7, 10, 14, 17, and 21 days after surgery, and all tests were repeated five times.

RNA Extraction and qRT-PCR Analysis

Total RNAs was extracted by using L4-L5 spinal cord tissues or dorsal root ganglia (DRGs) or cells by using TRIzol reagent (Invitrogen, Carlsbad, CA) according to the manufacture's guidelines. The quality and concentration of RNA were measured on a Nanodrop spectrophotometer (ND-1000, Nanodrop Technologies). cDNA was synthesized using Transcriptor First Strand cDNA Synthesis Kit (ROCHE, Basel, Switzerland) with corresponding specific primers. FastStart Essential DNA Green Master (ROCHE, Basel, Switzerland) was used for qRT-PCR on a LightCycler480 machine (ROCHE, Basel, Switzerland). GAPDH was used as the internal control to normalize lncRNA and mRNA expressions. The relative expression levels were determined by the $2^{-\Delta\Delta Ct}$ method and performed in triplicates. Related primers were detailed in **Table 1**.

RNA Immunoprecipitation (RIP)

RNA Immunoprecipitation experiments were performed with a Magna RIP RNA-Binding Protein Immunoprecipitation Kit (Cat. 17-700) (Millipore, Cambridge, MA) following the manufacturer's instructions. In brief, total RNA was extracted from L4 to L5 spinal cord tissues using TRIZOL reagent (Invitrogen) and then fragmented using 2μL fragmentation buffer later. The fragmented RNA was then incubated with antibodies against ELAVL1 (cat. no. ab200342, Abcam, Cambridge, MA) and IgG (cat. no. 12-371, EMD Millipore, Cambridge, MA) conjugated with A/G magnetic beads in IP buffer at 4°C for 2 h for immunoprecipitation. Next, the bound RNA was eluted from the beads in IP buffer. SuperScript^{TM} III Reverse Transcriptase (Invitrogen) was applicated for reverse transcription of the eluted RNA after purification. qRT-PCR was conducted using qPCR SYBR Green Master Mix (CloudSeq, Shanghai, China) in QuantStudio 5 real-time PCR System (Thermo Fisher, Waltham, MA, United States). The CT difference between input and the immunoprecipitated RNA was identified, and the relative enrichment was calculated using the $2^{-\Delta\Delta Ct}$ method. The experiments were repeated in triplicates.

RNA Pulldown

LINC01119 was transcribed using T7 RNA polymerase or T3 RNA polymerase to obtain sense and antisense RNA. RNA Pull down assay for investigating RNA-protein interaction was performed by Pierce Magnetic RNA-Protein Pull-Down Kit (Thermo Fisher Scientific). Then the biotin-labeled RNA was mixed with 50 μl streptavidin magnetic beads 65801D (Invitrogen) which were pre-washed twice with Tris-Buffer. After incubation at room temperature for 30 min, the RNA-labeled beads were washed twice with tris-buffer. Then, 1 mg protein was added to the RNA-labeled beads in 1X Protein-RNA binding buffer. The mixture was incubated at 4°C with rotation overnight. Then the RNA-labeled beads with proteins were washed twice with wash buffer. RNA-interacting proteins were eluted with 50 μl elution buffer by incubation at 37°C

TABLE 1 | Information of the sequences of qPCR primer sequences.

Primer name	Sequence (5'-3')
LINC01119 (Forward)	CCAGGCCCATCAATCACCTT
LINC01119 (Reverse)	GGCCTGTGTTCTGGCTACAT
BDNF (Forward)	GCCAGGGGCAACTCATCTTC
BDNF (Reverse)	GGTTGAAAGGCGCAGATGTC
ELAVL1 (Forward)	TTCCGCCATGTGGTCTTCAT
ELAVL1 (Reverse)	ATACACTGACTGTGGCAAGGT
GAPDH (Forward)	AGTTAATGCCGCCCCTTACC
GAPDH (Reverse)	CAGGGCTGACTACAAACCCA
U6 (Forward)	CTCGCTTCGGCAGCACA
U6 (Reverse)	AACGCTTCACGAATTTGCGT

for 30 min. Proteins were then run in an SDS-PAGE gels. Experiments were repeated in triplicates.

RNA Fluorescent *in situ* Hybridization (RNA-FISH)

Oligonucleotide-modified probe sequence for LINC01119 was synthesized from GenePharma (Shanghai, China). Tissues were fixed by 4% paraformaldehyde followed by permeabilization with 0.5% Triton at room temperature for 15 min. The probe is pre-denatured at 73℃ for 5 min. Then hybridization was performed with 2μM probe at 37°C overnight in a dark moist chamber. After being washed twice in 2 × SSC for 5 min, the slices were incubated with rabbit anti-BDNF antibody (Abcam, cat. no. ab108319). The images were acquired using a fluorescence microscopy ZFM-700 (Carl Zeiss AG, Oberkochen, Germany) rabbit anti-ELAVL1 antibody (1:1000, cat. no. ab200342, Abcam, Cambridge, MA). Experiments were repeated in triplicates.

Immunofluorescence Staining Analysis

Immunofluorescence staining was performed on frozen coronal sections of L4–L5 rat spinal cords. For marker/BDNF or ELAVL1/BDNF double immunofluorescence, slides were incubated with a series of primary antibodies mixed with rabbit anti-BDNF antibody (1:500, cat. no. ab108319, Abcam, Cambridge, MA), and rabbit anti-ELAVL1 antibody (1:500, cat. no. ab200342, Abcam, Cambridge, MA), or anti-Iba1 antibody (1:500, cat. no. ab178846, Abcam, Cambridge, MA), or anti-NeuN (1:300, cat. no. ab177487, Abcam, Cambridge, MA) or anti-GFAP (1:500, cat. no. ab7260, Abcam, Cambridge, MA) overnight at 4°C. Then, tissues were incubated with same-origin secondary antibodies conjugated by FITC or GFP for 1 h at 37°C. Finally, the staining slides were pictured using a laser confocal microscope (TCS SP2 AOBS), and the related analysis were repeated in triplicates.

Enzyme-Linked Immunosorbent Assay (ELISA)

Enzyme-linked immunosorbent assay (R&D System, United States) was performed according to the instructions to measure the protein expression level of IL-6, TNF-α, and IL-1β in the L4–L5 rat spinal cord tissue (obtained 14 days after the establish of SNI model). Tissue samples were centrifuged for 10 min at 10000 rpm, and the supernatants were collected and stored at -80°C for future analysis. The experimental steps were strictly performed according to the manufacturer's manual and repeated in triplicates.

Western Blot Analysis

Western blot was performed to measure protein expression levels in L4–L5 rat spinal cords and microglial cells. The following primary antibodies were used: rabbit anti-BDNF antibody (1:1000, cat. no. ab108319, Abcam, Cambridge, MA), rabbit anti-ELAVL1 antibody (1:1000, cat. no. ab200342, Abcam, Cambridge, MA), rabbit anti-α-Tubulin (1:1000, cat. no. ab7291, Abcam, Cambridge, MA), rabbit anti-GAPDH (1:1000, cat. no. ab8245, Abcam, Cambridge, MA), secondary antibody goat anti-rabbit IgG (1:5000, cat. no. ab6721, Abcam, Cambridge, MA). Proteins were extracted using RIPA buffer (Beyotime, Shanghai, China). Protein extracts were separated with 10% SDS-PAGE, and then electro-transferred to polyvinylidene difluoride membrane. The membrane was then blocked with 5% fat-free milk followed by incubation with respective primary antibodies at 4°C overnight. The detection of proteins was carried out using ECL reagent. Experiments were repeated in triplicates.

Statistical Analysis

Statistics were presented as mean ± SD. Comparisons between two groups were carried out via paired or unpaired Student's *t*-test accordingly. Comparisons among multiple groups were performed using one-way analysis of variance with Tuker-*post hoc* test. Fisher exact testing was performed to evaluate the difference of proportions between different groups. Statistical analyses were performed using GraphPad Prism (v8.0.1, GraphPad Software Inc., San Diego, CA, United States). $P < 0.05$ was used for the indication of statistical significance.

RESULTS

LINC01119 Is Upregulated in the Spinal Cord of SNI-NP Rat Model

Firstly, we established NP rats by using SNI model. No significant difference in PWL and PWT between groups prior to the operation was identified. In response to the operation, PWL and PWT were significantly decreased in SNI rats while no significant change was identified in sham rats (**Figures 1A,B**). Previously, it has been reported that LINC01119 may be bio-molecules that are closely related to NP (Zhao et al., 2021). To validate the expression mode of LINC01119 in NP rats, we performed qRT-PCR using L4–L5 spinal cord and DRGs samples from SNI rats and sham rats. **Figure 1C** showed that LINC01119 expression was significantly higher in the spinal cord tissues of NP rats compared to controls. However, LINC01119 was unchanged in DRGs of SNI rats (**Figure 1D**), suggesting that LINC01119 may participated in NP in spinal cord areas.

Silencing of LINC01119 Attenuates NP at Spinal Cord of Rats Undergoing SNI

To verify the functional role of LINC01119 in NP, LINC01119-silencing vector (sh-LINC01119) and a negative control vector (sh-NC) were injected intrathecally at day 7 after SNI induction. The expression of LINC01119 at day 14 was significantly decreased after intrathecal administration of sh-LINC01119 in both spinal cord and DRGs tissues (**Figures 2A,B**). In addition, silencing of LINC01119 significantly attenuated NP behaviors as evidenced with restored PWL and PWT (**Figure 2C**). It is well known that inflammation-associated cytokines, including IL-6, TNF-α, and IL-1β, were closely associated with neuropathic pain, hence we determined their expression levels via ELISA at day 14 in SNI rats after intrathecal injection of sh-LINC01119 at day 7. Results showed that the concentrations of IL-6, TNF-α, and IL-1β were upregulated in SNI rats and significantly

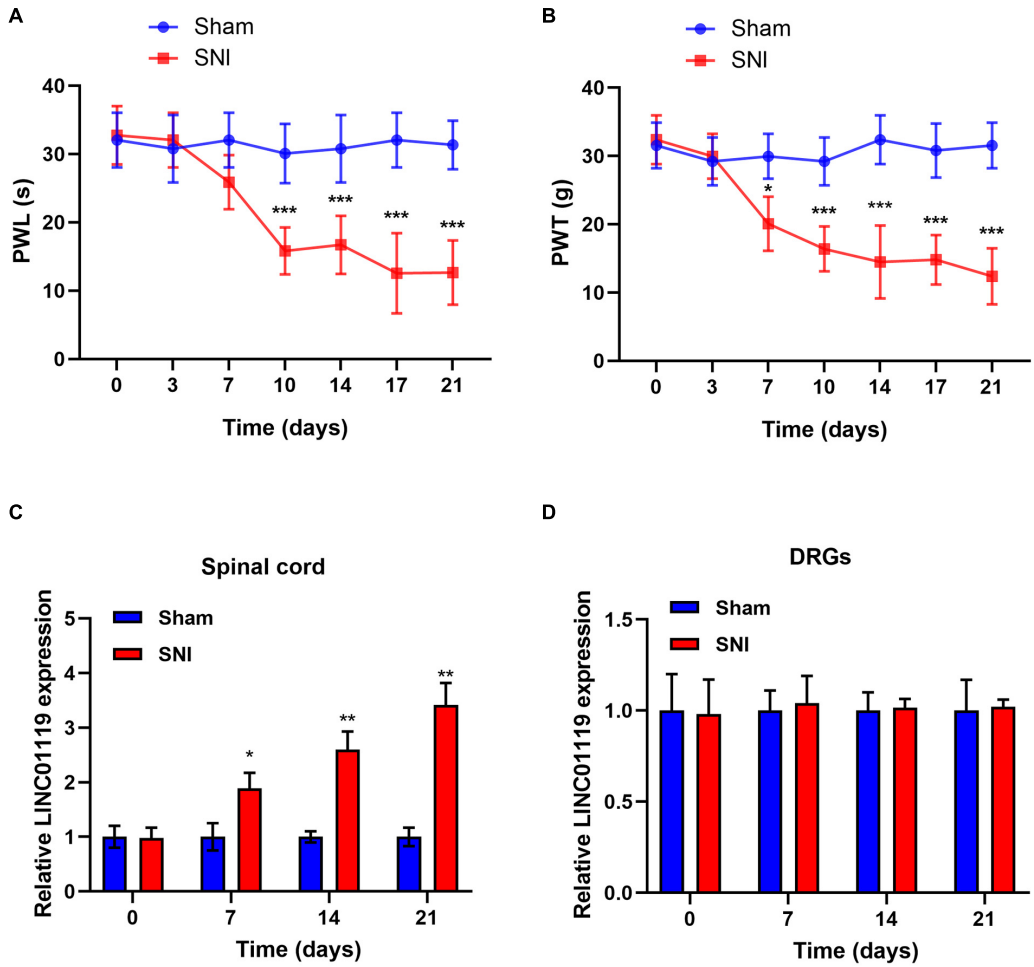

FIGURE 1 | LINC01119 was upregulated in rats with SNI **(A,B)** PWL **(A)** and PWT **(B)** in rats of Sham group and SNI group, $^{*}P < 0.05$, $^{***}P < 0.001$ compared to Sham group, $n = 5$/group. **(C,D)** The expression level of LINC01119 were detected in rats of SNI and control group from spinal cord **(C)** and DRGs **(D)** at day 0, 7, 14, and 21. $^{*}P < 0.05$, $^{**}P < 0.01$ compared to Sham group, $n = 3$/group.

reversed by the inhibition of LINC01119 in spinal cord tissues (**Figure 2D**), however, this inhibition of inflammatory cytokines by LINC01119 was not observed in DRGs (**Figure 2E**), suggesting that LINC01119 may regulate neuroinflammation in spinal cord area but not in DRGs. Moreover, this functional of LINC01119 in NP was not observed in sham rats without SNI surgery (**Figure 2F**). Therefore, the above data suggested that LINC01119 play critical roles in neuroinflammation and NP behaviors in spinal cord area of SNI rats.

BDNF Mediates the LINC01119-Induced NP in Spinal Cord of SNI Rats

Brain-derived neurotrophic factor (BDNF) has been well accepted as an activity-dependent neuronal regulator in the nervous system via enhancing neuronal excitability. Previously, we demonstrated that BDNF contributes to neuropathic spontaneous pain in SNI rats (Zhang et al., 2016; Wang et al., 2017). In this study, we sought to define whether LINC01119 regulates NP progression via modulating BDNF expression. Brain-derived neurotrophic factor was downregulated in spinal cord tissues, but was not altered in DRGs after injection of sh-LINC01119 (**Figures 3A,B**), suggesting that LINC01119 may influence NP via regulating BDNF expression in spinal cord areas. We then detected BDNF distribution via performing double immunofluorescence assay. **Figure 3C** showed that BDNF was co-localized with NeuN (a neuronal marker), Ibal (a microglial marker), and GFAP (an astrocytic marker), indicating that BDNF was diffusely located in both glial cells and neurons of spinal cord. With specific LINC01119 probe, we also verified the co-localization of LINC01119 and BDNF (**Figure 3D**). In addition, BDNF was also suppressed by silencing of LINC01119 in rat microglia cells (**Figure 3E**). Subsequently, we overexpressed BDNF in LINC01119-silenced SNI rats by intrathecal injection of Lv-BDNF (**Figure 3F**). LINC01119 and BDNF expression in spinal cord was successfully manipulated at day 14 in respective groups (**Figures 3G,H**). Analysis with ELISA showed that BDNF overexpression could partially attenuate the

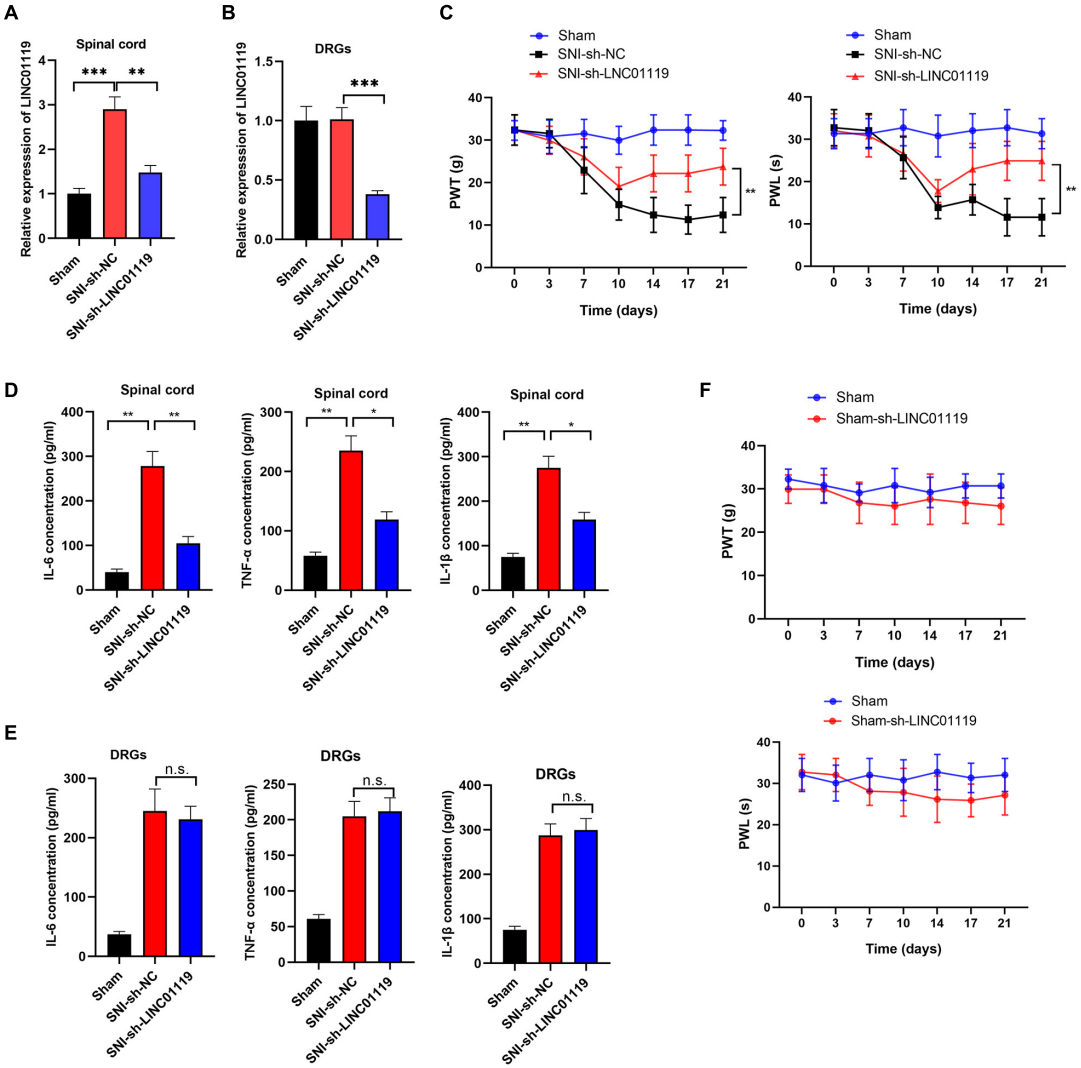

FIGURE 2 | LINC01119 causes NP in rats undergoing SNI **(A,B)**. LINC01119 was silenced in SNI rats after intrathecal injection of sh-LINC01119 vector in both spinal cord **(A)** and DRGs **(B)**, $^{**}P < 0.01$, $^{***}P < 0.001$, $n = 3$/group. **(C)** PWT (left) and PWL (right) were assessed in rats silenced with LINC01119, $^{**}P < 0.01$, $n = 5$/group. **(D,E)** The concentrations of IL–6, TNF–α, and IL-1β in spinal cord **(D)** and DRGs tissues **(E)** of rats were detected by ELISA at day 14, $^{*}P < 0.05$, $^{**}P < 0.01$, $n = 3$/group. **(F)** PWL and PWT were not altered by LINC01119 knockdown in sham rats without SNI surgery, $n = 5$/group.

suppressive effect of sh-LINC01119 on the expressions of IL-6, TNF-α, and IL-1β in SNI rats (**Figure 3I**). Consistently, the effects on NP-like behaviors caused by knockdown of LINC01119 were also abrogated by overexpression of BDNF (**Figure 3J**). Above results clearly showed that BDNF was essential for LINC01119-induced NP in spinal cord of SNI rats.

LINC01119 Directly Interacts With ELAVL1

To verify the RBPs of LINC01119, we performed bioinformatic analysis with *POSTAR*[1] and revealed the interacting networks (**Figure 4A**). Six binding sites of embryonic lethal abnormal version like RNA binding protein 1 (ELAVL1) were predicted at the function region (chr2:46833952-46834811) of LINC01119 (**Table 2**, **Figure 4B**). Then, we analyzed the structure of binding area of LINC01119 on *RNAfold* online software (Lorenz et al., 2011), and revealed that the targeted area could form a stem-loop, which is essential for the binding with RBPs (**Figure 4C**). Furthermore, by performing serial deletion analysis, we verified that the region of chr2:46834785-46834811 of LINC01119 was essential for binding with ELAVL1 (**Figure 4D**). Take a step further, we verified that ELAVL1 could directly bind with LINC01119 in spinal cord tissues by performing western blotting after RNA pulldown (**Figure 4E**). RIP assay also proved the direct binding between ELAVL1 with LINC01119 (**Figure 4F**). RNA Fluorescent *in situ* Hybridization using spinal cord tissues showed that LINC01119 and ELAVL1 were co-expressed, which strengthens our conclusion (**Figure 4G**). Collectively, our results

[1]http://lulab.life.tsinghua.edu.cn/postar/index.php

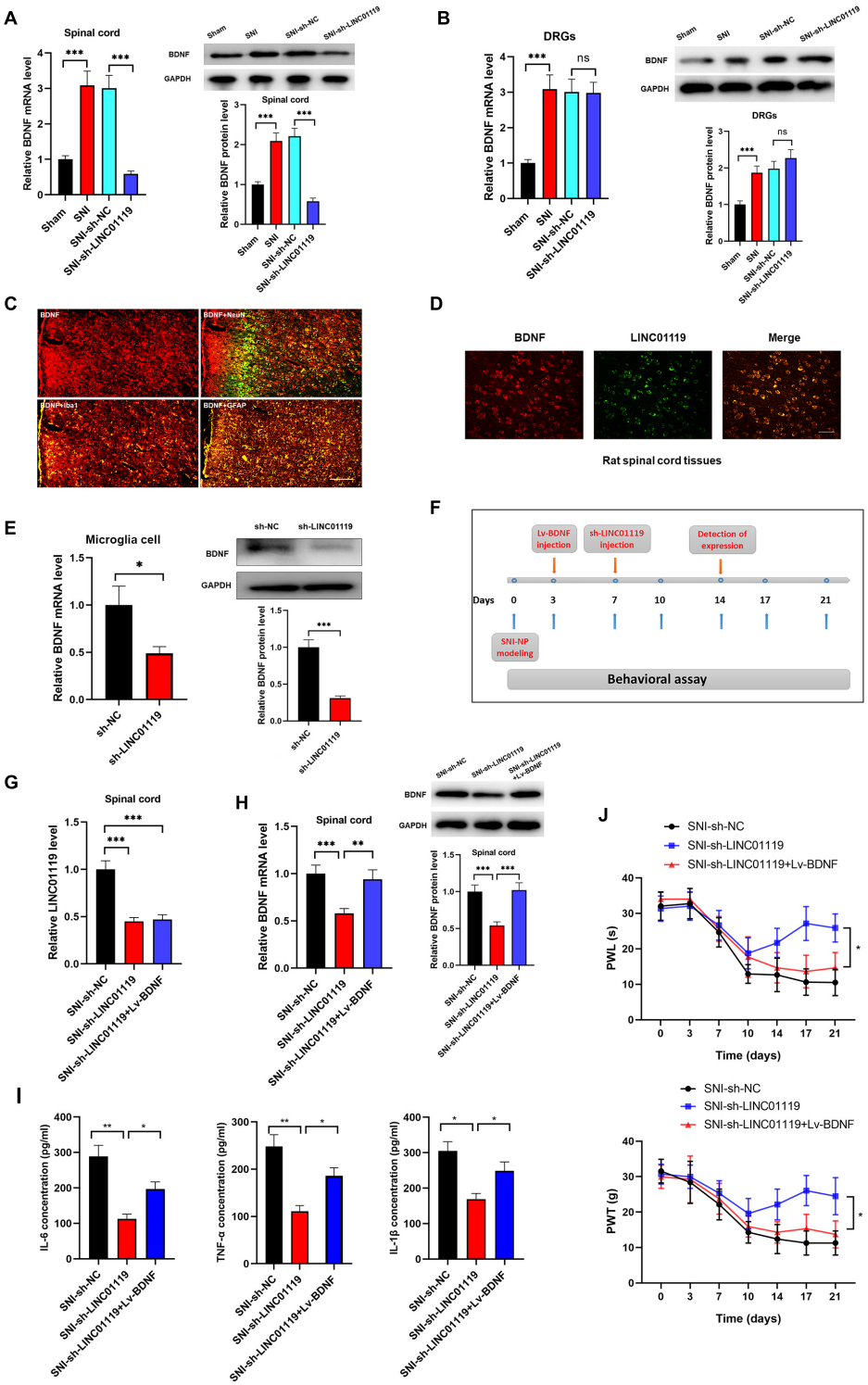

FIGURE 3 | LINC01119 mediated NP progression via targeting BDNF. **(A)** BDNF mRNA (left panel) and protein (right panel) were upregulated in spinal cord tissue of SNI rats and downregulated by intrathecal injection of sh-LINC01119 in contrast to sham rats, ***$P < 0.001$, $n = 3$/group. **(B)** BDNF mRNA (left panel) and protein (right panel) were upregulated in DRGs of SNI rats, but was not regulated by sh-LINC01119, ***$P < 0.001$, $n = 3$/group. **(C)** Localization of BDNF in the spinal cord of SNI rats by double immunofluorescence of BDNF (red) with NeuN (marker of neuron, merged as yellow), Iba1 (marker of microglia, merged as yellow), and GFAP (marker of astrocyte, merged as yellow). Scare bar = 100μm. **(D)** FISH analysis revealed a co-localization of LINC01119 and BDNF in spinal cord. Scare bar = 100μm. **(E)** BDNF was downregulated in microglia cells silenced with LINC01119 at both transcript and protein levels compared to control group, *$P < 0.05$,

(Continued)

FIGURE 3 | Continued
$^{***}P < 0.001$, $n = 3$/group. **(F)** The procedure of intrathecal injection of respective lentivirus vectors. **(G,H)** Expressions of LINC01119 **(G)** and BDNF **(H)** were shown in respective groups with different manipulations, $^{**}P < 0.01$, $^{***}P < 0.001$, $n = 3$/group. **(I)** The concentrations of IL–6, TNF–α, and IL-1β in the spinal cord tissue of rats were downregulated by LINC01119 knockdown, however, this effect was abrogated by overexpression of BDNF, $^{*}P < 0.05$, $^{**}P < 0.01$, $n = 3$/group. **(J)** PWL and PWT was evaluated in SNI rats which were silenced of LINC01119 with or without BDNF overexpression, $^{*}P < 0.05$, $n = 5$/group.

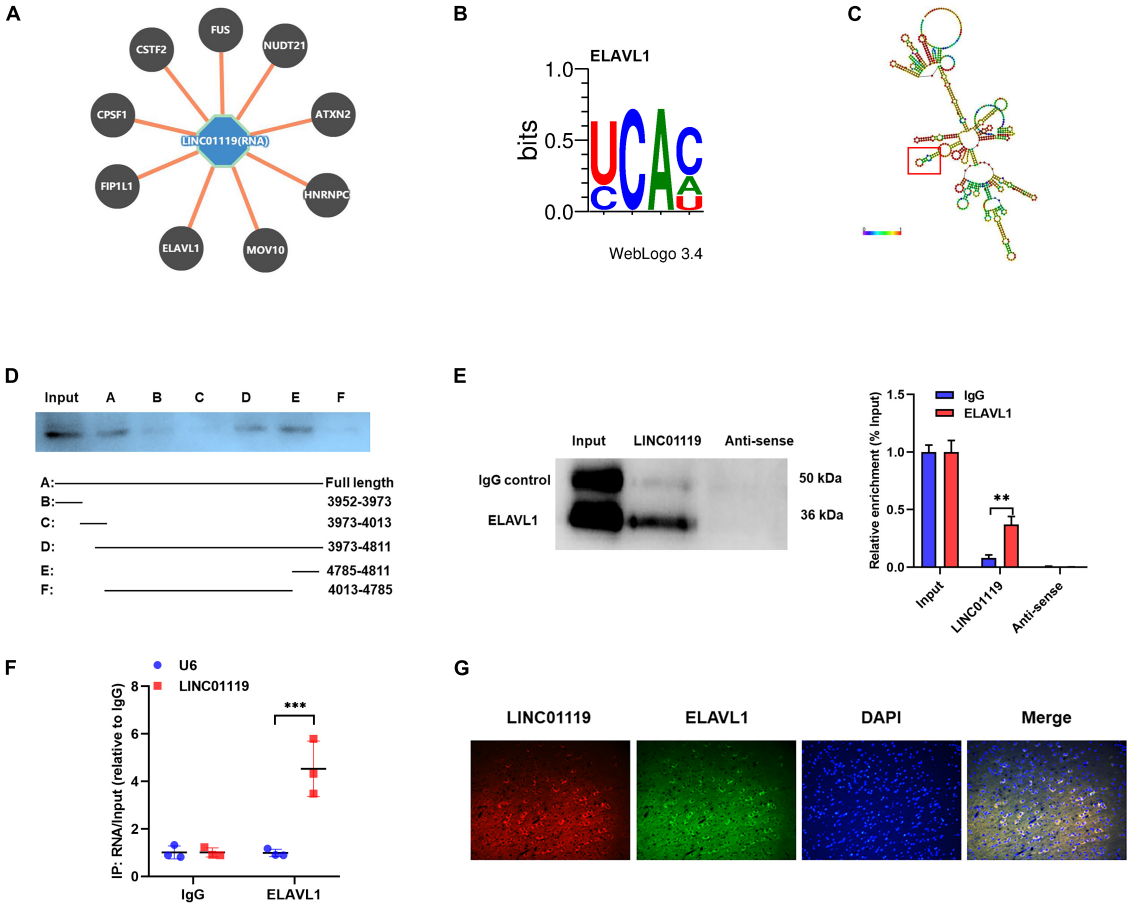

FIGURE 4 | LINC01119 directly interacts with ELAVL1. **(A)** The potential binding proteins of LINC01119 predicted by POSTAR (http://lulab.life.tsinghua.edu.cn/postar/index.php). **(B)** Predicted motif sequence of ELAVL1 was shown according to POSTAR. **(C)** The region of chr2:46834785-46834811 formed a stem-loop structure as predicted according to RNAfold (http://rna.tbi.univie.ac.at//cgi-bin/RNAWebSuite/RNAfold.cgi?). **(D)** Serial deletion analysis revealed that the chr2:46834785-46834811 region of LINC01119 was essential for binding with ELAVL1. **(E)** RNA pulldown assay using biotinylated *LINC01119* and antisense control were performed using spinal cord of SNI rats, $^{**}P < 0.01$, $n = 3$/group. **(F)** RIP assay with ELAVL1 antibody further confirmed the direct interaction between LINC01119 and ELAVL1 in SNI rats, $^{***}P < 0.001$, $n = 3$/group. **(G)** RNA-FISH with specific probe using SNI rats verified that LINC01119 and ELAVL1 protein colocalized mostly in the cytoplasm section ($n = 3$/group). Scare bar = 100μm.

clearly showed that LINC01119 could directly interact with ELAVL1, suggesting a potential regulatory role of LINC01119-ELAVL1 complex in NP progression in SNI rats.

LINC01119-ELAVL1 Complex Stabilizes BDNF mRNA, Thereby Inducing NP in SNI Rats

Previous literatures demonstrated that ELAVL1 was a critical regulator in stabilizing mRNAs by linking with AU-rich elements (AREs) (Bakheet et al., 2018). To confirm the LINC01119-ELAVL1 complex could increase BDNF level via stabilizing BDNF transcript, we knocked out ELAVL1 by intrathecally injection of sh-ELAVL1 (**Figure 5A**). As shown in **Figure 5B**, downregulation of ELAVL1 induced decreased expression of BDNF in spinal cord at both transcript and protein levels, suggesting that ELAVL1 may function synchronously with the interaction of LINC01119. In rat microglial cells, silencing of ELAVL1 also induced decreased expression of BDNF at both transcript and protein level (**Figure 5C**). By performing immunofluorescence assay, we observed a co-expression of ELAVL1 and BDNF (**Figure 5D**) in spinal cord. RNA pulldown and RIP assay with ELAVL1 antibody provided direct evidence supporting the

TABLE 2 | Predicted targeted sites of LINC01119 by ELAVL1 in *POSTAR*.

Targeted site	Location	Score	PhastCons	Phylop
1	chr2:46833952-46833973	0.703464	0.0638095	0.219905
2	chr2:46833952-46833973	0.703464	0.0638095	0.219905
3	chr2:46833987-46834013	0.800532	0.430038	0.337692
4	chr2:46833987-46834013	0.800532	0.430038	0.337692
5	chr2:46834785-46834811	0.742447	0.00226923	–0.0092692
6	chr2:46834785-46834811	0.742447	0.00226923	–0.0092692

interaction between ELAVL1 and BDNF mRNA in NP rats (**Figures 5E,F**).

To verify the role of ELAVL1 in the regulation of BDNF stability, we blocked RNA transcription process by treating with actinomycin D (ActD) in rat microglial cells, the stability of BDNF RNA was dramatically suppressed by the silencing of ELAVL1 (**Figure 5G**). Moreover, enhanced expression of LINC01119 prevented the decay process of BDNF mRNA, however, this effect was significantly abrogated when ELAVL1 was knocked out, suggesting that ELAVL1 is essential for LINC01119-induced BDNF mRNA stability (**Figure 5H**). To demonstrate whether silenced ELAVL1 reverses LINC01119-mediated NP production, Lv-LINC01119 and sh-ELAVL1 vectors were injected intrathecally into SNI rats at day 7 and day 3, respectively (**Figure 5I**). The manipulations of LINC01119 and ELAVL1 were confirmed (**Figures 5J,K**). The results showed that silencing ELAVL1 abrogated the LINC01119-mediated NP behaviors (**Figure 5L**). Taken together, the above data suggests that LINC01119-ELAVL1 complex may directly bind to BDNF mRNA and regulate its stability, thereby causing NP progression.

LINC01119 Is a Useful Biomarker for NP Diagnosis and Prognosis

We also explored the clinical role of LINC01119 in patients with Shingles-induced NP; the detailed patient information showed that no statistical bias was identified between NP patients and controlled people (**Table 3**). By detecting the expression level of LINC01119 in serum samples, we verified that LINC01119 was significantly upregulated in NP patients compared to healthy individuals (**Figure 6A**). Receiver operator characteristic (ROC) analysis indicated a high diagnostic potential of serum LINC01119 in differentiating NP and healthy population, with sensitivity, specificity and AUC reaching 80.0%, 67.3%, and 0.799, respectively (**Figure 6B**). By stratifying all populations into a high and a low LINC01119-level group based on the stratification criterion of 1.32 according to the ROC curve, we revealed that the proportion of NP patients was much higher in high LINC01119-level group when compared to that of low LINC01119 group (**Figure 6C**), which further indicates LINC01119 is a promising diagnostic marker. We then defined the expression level of LINC01119 in NP patients in remission after treatment, and found that LINC01119 was dramatically downregulated in contrast to the level before treatment (**Figure 6D**). Therefore, our study provided a preliminary data showing the potential value of circulating LINC01119 in diagnostic and efficacy monitoring of NP patients.

DISCUSSION

Despite current therapeutic regimens that evidently improved the prognosis of patients experienced nerve injury, nearly all those patients finally develop pain, which indirectly influence the quality of life (Fink et al., 2017; Nickel et al., 2001). Long non-coding RNAs are dysregulated in various diseases, and mediate biological process by interacting with RNA and proteins (Huang et al., 2018). However, the detailed regulatory pathways that involved in lncRNA-mediated NP progression is still not clearly defined. In this work, we explored the potential role of LINC01119 in NP via the post-transcriptional regulation of BDNF expression. We proved that LINC01119 accelerated NP formation via increasing BDNF expression. Mechanistically, LINC01119 directly interacted with ELAVL1 and the LINC01119-ELAVL1 complex could bind to and stabilize BDNF mRNA (**Figure 6E**).

NP remains a clinically challenging problem and the mechanisms are still unclear. The rat model of NP provides an appropriate system for preclinical study of pain (Kc et al., 2020). Previously, Zhao et al. compares lncRNA and mRNA expression and screens disease-related biomarkers related to NP after spinal cord injury (SCI) in peripheral blood samples of patients (Zhao et al., 2021). They revealed two lncRNAs, LINC01119, and LINC02447, are directly involved in the pain pathway and may be important for NP. In this study, we focused on those lncRNAs and eventually identified LINC01119 as a critical regulator of NP. In addition, LINC01119 was reported as a potential regulatory gene involved in cervical cancer (Ding et al., 2020), colorectal cancer (Han et al., 2019), and adipocyte differentiation (Chen et al., 2019). However, its detailed functional role and regulatory mechanism in NP and other diseases are still not well known. Our study determined that LINC01119 was upregulated in NP rat model in spinal cord area but not in DRGs. Furthermore, knockdown of LINC01119 significantly decreased the expression of IL-6, TNF-α, and IL-1β and partly reversed NP, suggesting an essential role of LINC01119 in the formation of NP in spinal cord. To the best of our knowledge, this is the first study to identify the functional role of LINC01119 in NP.

Another finding of this study is the identification of the RBP, ELAVL1 (also known as Hu Antigen R, HuR), which could directly bind to LINC01119. ELAVL1 is a ubiquitously expressed member of the embryonic lethal abnormal vision (ELAV)-like/Hu-protein family of RNA-binding proteins (Zhang et al., 2017). ELAVL1 selectively binds to target mRNAs bearing specific sequence elements, often U- and AU-rich, and generally found in the mRNA 3'-UTR, and plays a critical role in their posttranscriptional regulation (Chang and Hla, 2014). Multiple studies have demonstrated the essential role of ELAVL1 in the development of biological progression via the modulation at post-transcriptional mode, such as cancer metastasis, autophagy and others (Zhang et al., 2018; Palomo-Irigoyen et al., 2020). More importantly, Li et al. reported that

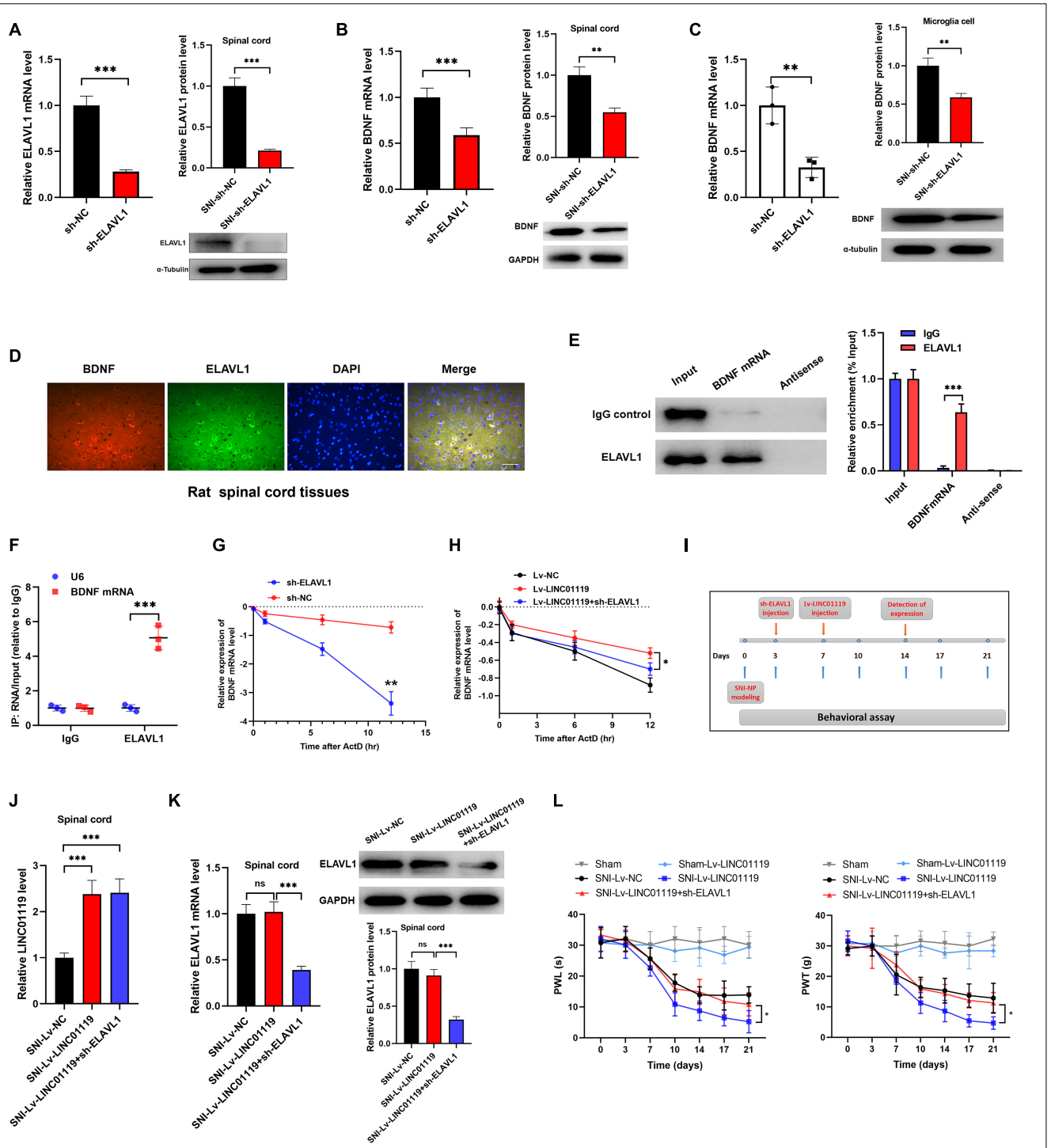

FIGURE 5 | LINC01119-ELAVL1 complex stabilizes BDNF mRNA, thereby inducing NP in SNI rats. **(A)** ELAVL1 was silenced in spinal cord tissue of SNI rats at both transcript and protein levels, $^{***}P < 0.001$, $n = 8$/group. **(B)** BDNF was downregulated in spinal cord tissue of SNI rats silenced with ELAVL1 at both transcript and protein levels, $^{***}P < 0.001$, $n = 3$/group. **(C)** Knockdown of ELAVL1 induced inhibition of BDNF expression in rat microglial cells, $^{**}P < 0.01$. **(D)** Immunofluorescence showed the co-expression of ELAVL1 and BDNF protein in spinal cord tissue of SNI rats. Scare bar = 100μm. **(E)** RNA pulldown assay showed that ELAVL1 protein was interacted with BDNF mRNA in spinal cord tissues, $^{***}P < 0.001$, $n = 3$/group. **(F)** RIP assay with ELAVL1 antibody in spinal cord showed a significantly higher enrichment of BDNF mRNA compared to U6, $^{***}P < 0.001$, $n = 3$/group. **(G)** The half-life of BDNF RNA was dramatically decreased in ELAVL1-silenced cells compared to that in control cells, $^{***}P < 0.001$. **(H)** Knockdown of ELAVL1 reversed the LINC01119-mediated RNA stability of BDNF in microglia cells, $^{*}P < 0.05$. **(I)** The flow chart of manipulations of respective lentivirus vectors in SNI rats. **(J,K)** Expressions of LINC01119 **(J)** and ELAVL1 **(K)** in groups received respective manipulations, $^{***}P < 0.001$, $n = 3$/group. **(L)** PWL and PWT assays showed that knockdown of ELAVL1 abrogated LINC01119-induced NP behaviors, $^{*}P < 0.05$, $n = 5$/group.

TABLE 3 | Characteristics of patients with NP and the healthy control group (CG).

Characteristic	NP (*N* = 45)	CG (*N* = 49)	Statistical significance
Age (y; mean ± SD)	57.4 ± 12.4	56 ± 12.8	$P > 0.05$
Gender (n; female/male)	26/19	29/20	$P > 0.05$
BMI (kg/m^2; mean ± SD)	23.1 ± 3.1	22.6 ± 3.6	$P > 0.05$
HZ Location (n/N)			
•Thorax	21/45	-	-
•Abdomen	9/45	-	-
•Extremities	7/45	-	-
•Other	8/45	-	-
Pain VAS (0–10; mean ± SD)	6.0 ± 1.7	-	-

ELAVL1 was involved in the lncRNA MALAT1-regulated renal tubular epithelial pyroptosis in diabetic nephropathy, revealing its potential role NP (Li et al., 2017). Our results suggest that there exists a direct interaction between LINC01119 and ELAVL1 protein, and the formed LINC01119-ELAVL1 complex further binds to BDNF mRNA, inducing stabilization of BDNF and increased expression. Reciprocally, overexpression of ELAVL1 partly reversed the LINC01119-caused NP effect, indicating that LINC01119 functions dependent on the interaction with ELAVL1. Our results also suggest that both LINC01119 and BDNF mRNA were interacted by ELAVL1 protein, however, the direct interaction between LINC01119 and BDNF mRNA were not observed, suggesting that ELAVL1 protein may function as a scaffold to form the LINC01119-ELAVL1-BDNF complex.

Brain-derived neurotrophic factor (BDNF) is a well-studied growth factor that serves many critical functions within the central nervous system (Almeida et al., 2021). It is a member of a unique family of polypeptide growth factors, neurotrophies, which influence the proliferation, differentiation, survival, and death of neuronal and non-neuronal cells (Cappoli et al., 2020; Su et al., 2020). Despite this, BDNF has been implicated in several injury-induced maladaptive processes including pain, spasticity and convulsive activity (Smith, 2014). Our previous

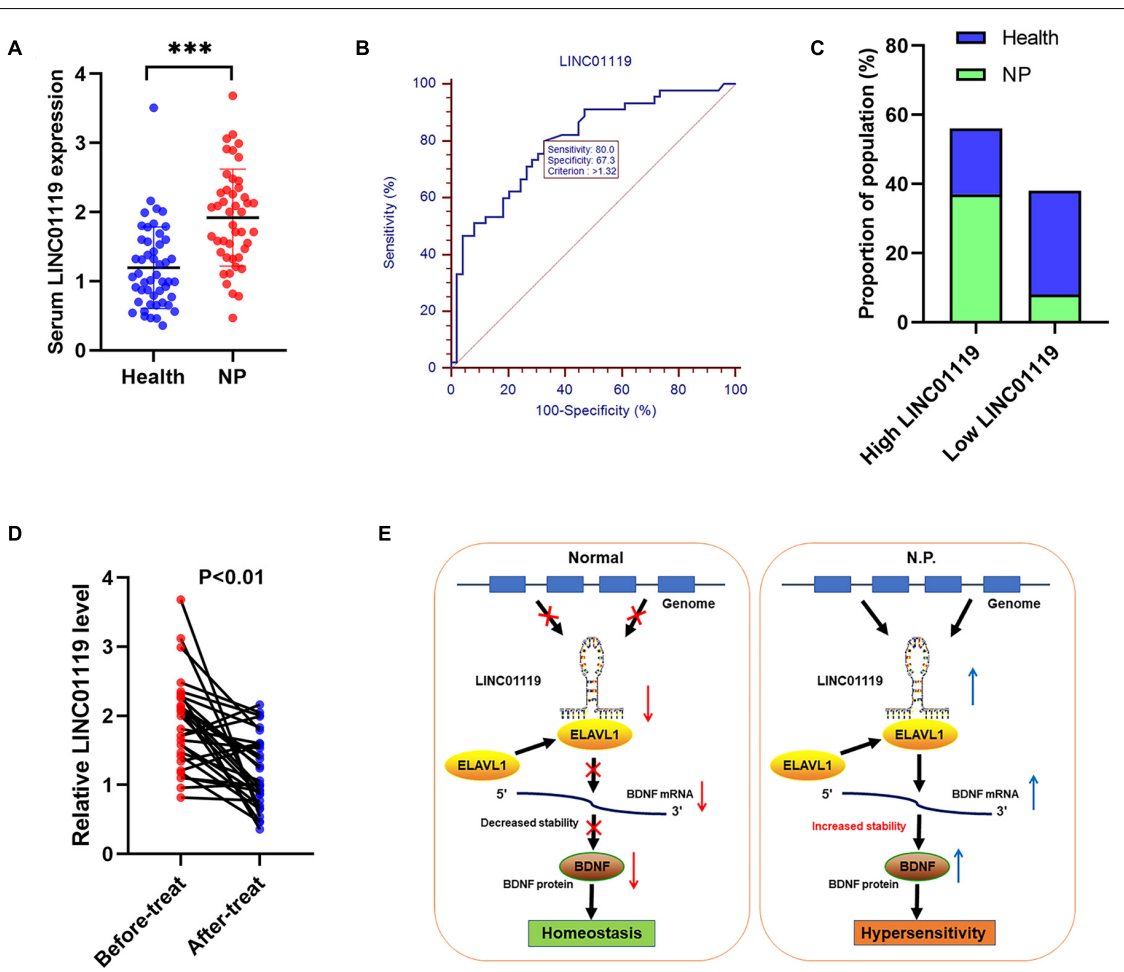

FIGURE 6 | LINC01119 is a promising diagnostic marker for NP patients. **(A)** LINC01119 expression was detected in serum samples from 45 NP patients (PHN) and 49 healthy people by qRT-PCR, ***$P < 0.001$. **(B)** ROC curve was established to evaluate the diagnostic performance of serum LINC01119 level. **(C)** The proportions of NP patients and healthy people in high or low-LINC01119 groups were shown. **(D)** Serum LINC01119 level were determined in 45 NP patients before and after treatment. **(E)** Schematic diagram of LINC01119 induces NP through regulating BDNF expression in an ELAVL1-dependent manner.

study has well addressed the role of BDNF in neuropathic spontaneous pain-related aversion via NR2B receptors (Zhang et al., 2016). Other studies also reported the contribution of BDNF in NP (Fiore and Austin, 2019). This study further revealed how BDNF was regulated during NP and the direct association between LINC01119-ELAVL1 complex. Gain- and -loss functional assays showed that BDNF was essential for LINC01119-mediated NP. Moreover, dysregulation of BDNF expression could only partially reversed the LINC01119-induced NP and neuroinflammation, suggesting that there are other pathways targeted by LINC01119 involved in NP and neuroinflammation.

Finally, we also investigated the clinical role of LINC01119 as crucial biomarker used for NP diagnosis and curative effect monitoring. Currently, the clinical tools used for diagnosing NP are very limited (Jonsson et al., 2021). Finding effective clinical biomarkers for NP is an urgent issue. By detecting the serum LINC01119 level in NP patients, we revealed its clinical significance, suggesting that LINC01119 is a promising biomarker for the diagnosis and prognosis of NP. We need to point out the limitations of this study. First, experimental and preliminary clinical role of LINC01119 was identified in NP, however, a large cohort multicenter study was needed before clinical application. Second, although the functional role of LINC01119 and the underlying regulation pathway of LINC01119/ELAVL1/BDNF were identified, the detailed elements that participated in the initiation and progression of NP, such as other pain-related factors in the microenvironment involved in signaling transmission need to be defined in following studies.

CONCLUSION

To conclude, our study revealed the novel contribution of LINC01119/ELALV1/BDNF axis in NP progression. Our discovery not only help us get a better understanding on the regulatory potential of LINC01119 in NP, but also useful for finding promising drug targets and developing novel therapeutic strategies to overcome NP.

DATA AVAILABILITY STATEMENT

The original contributions presented in the study are included in the article/ Supplementary Material, further inquiries can be directed to the corresponding authors.

ETHICS STATEMENT

The studies involving human participants were reviewed and approved by the Research Scientific Ethics Committee of The Second Hospital of Shandong University. The patients/participants provided their written informed consent to participate in this study. The animal study was reviewed and approved by the Animal Use and Care Committee of Shandong University.

AUTHOR CONTRIBUTIONS

LZ, HF, and PL acquired date and draft of the manuscript. LZ, YJ, and XZ established NP models and performed the experimental assays. LZ and YZ analyzed and interpreted date and statistical analysis. QH and YZ provide technical and material support. XZ and PL approved the final version of the manuscript. All authors contributed to the article and approved the submitted version.

FUNDING

This study is supported by the National Natural Science Foundation of China (82002228) and Natural Science Foundation of Shandong Province (ZR2020QH280).

REFERENCES

Almeida, F. B., Barros, H. M. T., and Pinna, G. (2021). Neurosteroids and Neurotrophic Factors: What Is Their Promise as Biomarkers for Major Depression and PTSD? *Int. J. Mol. Sci.* 2021:22.

Bakheet, T., Hitti, E., Al-Saif, M., Moghrabi, W. N., and Khabar, K. S. A. (2018). The AU-rich element landscape across human transcriptome reveals a large proportion in introns and regulation by ELAVL1/HuR. Biochimica et biophysica acta. *Gene Regulat. Mechan.* 1861, 167–177. doi: 10.1016/j.bbagrm.2017.12.006

Cappoli, N., Tabolacci, E., Aceto, P., and Dello Russo, C. (2020). The emerging role of the BDNF-TrkB signaling pathway in the modulation of pain perception. *J. Neuroimmunol.* 349:577406. doi: 10.1016/j.jneuroim.2020.577406

Chang, S. H., and Hla, T. (2014). Post-transcriptional gene regulation by HuR and microRNAs in angiogenesis. *Curr. Opin. Hematol.* 21, 235–240. doi: 10.1097/moh.0000000000000040

Chen, H. Y., Xiao, Z. Z., Ling, X., Xu, R. N., Zhu, P., and Zheng, S. Y. (2021). ELAVL1 is transcriptionally activated by FOXC1 and promotes ferroptosis in myocardial ischemia/reperfusion injury by regulating autophagy. *Mol. Med.* 27:14.

Chen, K., Xie, S., and Jin, W. (2019). Crucial lncRNAs associated with adipocyte differentiation from human adipose-derived stem cells based on co-expression and ceRNA network analyses. *PeerJ.* 7:e7544. doi: 10.7717/peerj.7544

Choi, S. W., and Nam, J. W. (2018). TERIUS: accurate prediction of lncRNA via high-throughput sequencing data representing RNA-binding protein association. *BMC Bioinform.* 19:41.

Chow, R., Wessels, J. M., and Foster, W. G. (2020). Brain-derived neurotrophic factor (BDNF) expression and function in the mammalian reproductive Tract. *Hum. Reprod, Update* 26, 545–564. doi: 10.1093/humupd/dmaa008

Decosterd, I., and Woolf, C. J. (2000). Spared nerve injury: an animal model of persistent peripheral neuropathic pain. *Pain* 87, 149–158. doi: 10.1016/s0304-3959(00)00276-1

Ding, H., Zhang, L., Zhang, C., Song, J., and Jiang, Y. (2020). Screening of significant biomarkers related with prognosis of cervical cancer and functional study based on lncRNA-associated ceRNA regulatory network. *Comb Chem High Throughput Screen* 24, 472–482.

Fink, C., Uhlmann, L., Enk, A., and Gholam, P. (2017). Pain management in photodynamic therapy using a nitrous oxide/oxygen mixture: a prospective, within-patient, controlled clinical trial. *J. Eur. Acad. Dermatol. Venereol.* 31, 70–74. doi: 10.1111/jdv.13788

Fiore, N. T., and Austin, P. J. (2019). Peripheral Nerve Injury Triggers Neuroinflammation in the Medial Prefrontal Cortex and Ventral Hippocampus in a Subgroup of Rats with Coincident Affective Behavioural Changes. *Neuroscience* 416, 147–167. doi: 10.1016/j.neuroscience.2019.08.005

Halloway, S., Jung, M., Yeh, A. Y., Liu, J., McAdams, E., Barley, M., et al. (2020). An Integrative Review of Brain-Derived Neurotrophic Factor and Serious Cardiovascular Conditions. *Nurs. Res.* 69, 376–390. doi: 10.1097/nnr.0000000000000454

Han, Y., Wang, X., Mao, E., Shen, B., and Huang, L. (2019). Analysis of Differentially Expressed lncRNAs and mRNAs for the Identification of Hypoxia-Regulated Angiogenic Genes in Colorectal Cancer by RNA-Seq. *Med. Sci. Monit.* 25, 2009–2015. doi: 10.12659/msm.915179

Herrera-Solorio, A. M., Armas-Lopez, L., Arrieta, O., Zuniga, J., Pina-Sanchez, P., and vila-Moreno, F. A. (2017). Histone code and long non-coding RNAs (lncRNAs) aberrations in lung cancer: implications in the therapy response. *Clin. Epigenet.* 9:98.

Huang, P., Li, F., Li, L., You, Y., Luo, S., Dong, Z., et al. (2018). lncRNA profile study reveals the mRNAs and lncRNAs associated with docetaxel resistance in breast cancer cells. *Sci. Rep.* 8:17970.

Jonsson, M., Gerdle, B., Ghafouri, B., and Backryd, E. (2021). The inflammatory profile of cerebrospinal fluid, plasma, and saliva from patients with severe neuropathic pain and healthy controls-a pilot study. *BMC Neurosci.* 22:6.

Kc, E., Moon, H. C., Kim, S., Kim, H. K., Won, S. Y., Hyun, S. H., et al. (2020). Optical Modulation on the Nucleus Accumbens Core in the Alleviation of Neuropathic Pain in Chronic Dorsal Root Ganglion Compression Rat Model. *Neuromodulation* 23, 167–176. doi: 10.1111/ner.13059

Li, X., Zeng, L., Cao, C., Lu, C., Lian, W., Han, J., et al. (2017). Long noncoding RNA MALAT1 regulates renal tubular epithelial pyroptosis by modulated miR-23c targeting of ELAVL1 in diabetic nephropathy. *Exp. Cell Res.* 350, 327–335. doi: 10.1016/j.yexcr.2016.12.006

Lorenz, R., Bernhart, S. H., Honer, C., Tafer, H., Flamm, C., Stadler, P. F., et al. (2011). ViennaRNA Package 2.0. Algorithms for molecular biology. *AMB* 6:26.

Nagpal, A., Clements, N., Duszynski, B., and Boies, B. (2020). The Effectiveness of Dorsal Root Ganglion Neurostimulation for the Treatment of Chronic Pelvic Pain and Chronic Neuropathic Pain of the Lower Extremity: A Comprehensive Review of the Published Data. *Pain Med.* 22, 49–59. doi: 10.1093/pm/pnaa369

Nickel, J. C., Downey, J., Johnston, B., Clark, J., and Canadian, G. (2001). Prostatitis Research, Predictors of patient response to antibiotic therapy for the chronic prostatitis/chronic pelvic pain syndrome: a prospective multicenter clinical trial. *J. Urol.* 165, 1539–1544. doi: 10.1016/s0022-5347(05)66344-6

Palomo-Irigoyen, M., Perez-Andres, E., Iruarrizaga-Lejarreta, M., Barreira-Manrique, A., Tamayo-Caro, M., Vila-Vecilla, L., et al. (2020). HuR/ELAVL1 drives malignant peripheral nerve sheath tumor growth and metastasis. *J. Clin. Invest.* 130, 3848–3864.

Pang, H., Ren, Y., Li, H., Chen, C., and Zheng, X. (2019). LncRNAs linc00311 and AK141205 are identified as new regulators in STAT3-mediated neuropathic pain in bCCI rats. *Eur. J. Pharmacol.* 868:172880. doi: 10.1016/j.ejphar.2019.172880

Pereira, B., Billaud, M., and Almeida, R. (2017). RNA-Binding Proteins in Cancer: Old Players and New Actors. *Trends Cancer* 3, 506–528. doi: 10.1016/j.trecan.2017.05.003

Serghiou, S., Kyriakopoulou, A., and Ioannidis, J. P. (2016). Long noncoding RNAs as novel predictors of survival in human cancer: a systematic review and meta-analysis. *Mole. Cancer* 15:50.

Smith, P. A. (2014). BDNF: no gain without pain? *Neuroscience* 283, 107–123. doi: 10.1016/j.neuroscience.2014.05.044

Soler, D., Morina, D., Kumru, H., Vidal, J., and Navarro, X. (2021). Transcranial Direct Current Stimulation and Visual Illusion Effect According to Sensory Phenotypes in Patients With Spinal Cord Injury and Neuropathic Pain. *J. Pain* 22, 86–96. doi: 10.1016/j.jpain.2020.06.004

Song, G., Yang, Z., Guo, J., Zheng, Y., Su, X., and Wang, X. (2020). Interactions Among lncRNAs/circRNAs, miRNAs, and mRNAs in Neuropathic Pain. *Neurotherapeutics* 17, 917–931. doi: 10.1007/s13311-020-00881-y

Su, J., Liu, P., Liu, B., and Zhang, Y. (2020). BDNF polymorphisms across the spectrum of psychiatric morbidity: A protocol for a systematic review and meta-analysis. *Medicine* 99:e22875. doi: 10.1097/md.0000000000022875

Upadhyay, R., Sanduja, S., Kaza, V., and Dixon, D. A. (2013). Genetic polymorphisms in RNA binding proteins contribute to breast cancer survival. *Intern. J. Cancer* 132, E128–E138.

Vuka, I., Dosenovic, S., Marcius, T., Ferhatovic Hamzic, L., Vucic, K., Sapunar, D., et al. (2020). Efficacy and safety of pulsed radiofrequency as a method of dorsal root ganglia stimulation for treatment of non-neuropathic pain: a systematic review. *BMC Anesthesiol.* 20:105.

Wang, X., Zhang, L., Zhan, Y., Li, D., Zhang, Y., Wang, G., et al. (2017). Contribution of BDNF/TrkB signalling in the rACC to the development of pain-related aversion via activation of ERK in rats with spared nerve injury. *Brain Res.* 1671, 111–120. doi: 10.1016/j.brainres.2017.07.010

Wu, H., Yin, Q. F., Luo, Z., Yao, R. W., Zheng, C. C., Zhang, J., et al. (2016). Unusual Processing Generates SPA LncRNAs that Sequester Multiple RNA Binding Proteins. *Mol. Cell* 64, 534–548. doi: 10.1016/j.molcel.2016.10.007

Zhang, J., Kong, L., Guo, S., Bu, M., Guo, Q., Xiong, Y., et al. (2017). hnRNPs and ELAVL1 cooperate with uORFs to inhibit protein translation. *Nucleic Acids Res.* 45, 2849–2864.

Zhang, L., Wang, G., Ma, J., Liu, C., Liu, X., Zhan, Y., et al. (2016). Brain-derived neurotrophic factor (BDNF) in the rostral anterior cingulate cortex (rACC) contributes to neuropathic spontaneous pain-related aversion via NR2B receptors. *Brain Res. Bull.* 127, 56–65. doi: 10.1016/j.brainresbull.2016.08.016

Zhang, Z., Yao, Z., Wang, L., Ding, H., Shao, J., Chen, A., et al. (2018). Activation of ferritinophagy is required for the RNA-binding protein ELAVL1/HuR to regulate ferroptosis in hepatic stellate cells. *Autophagy* 14, 2083–2103. doi: 10.1080/15548627.2018.1503146

Zhao, J., Yang, L., Huang, L., and Li, Z. (2021). Screening of disease-related biomarkers related to neuropathic pain (NP) after spinal cord injury (SCI). *Hum. Genom.* 15:5.

Zybura-Broda, K., Wolder-Gontarek, M., Ambrozek-Latecka, M., Choros, A., Bogusz, A., Wilemska-Dziaduszycka, J., et al. (2018). HuR (Elavl1) and HuB (Elavl2) Stabilize Matrix Metalloproteinase-9 mRNA During Seizure-Induced Mmp-9 Expression in Neurons. *Front. Neurosci.* 12:224.

Conflict of Interest: The authors declare that the research was conducted in the absence of any commercial or financial relationships that could be construed as a potential conflict of interest.

frontiers in Molecular Neuroscience

REVIEW
published: 06 July 2021
doi: 10.3389/fnmol.2021.691396

Orofacial Neuropathic Pain-Basic Research and Their Clinical Relevancies

*Masamichi Shinoda[1], Yoshiki Imamura[2], Yoshinori Hayashi[1], Noboru Noma[2], Akiko Okada-Ogawa[2], Suzuro Hitomi[1] and Koichi Iwata[1]**

[1] Department of Physiology, Nihon University School of Dentistry, Tokyo, Japan, [2] Department of Oral Diagnostic Sciences, Nihon University School of Dentistry, Tokyo, Japan

Trigeminal nerve injury is known to cause severe persistent pain in the orofacial region. This pain is difficult to diagnose and treat. Recently, many animal studies have reported that rewiring of the peripheral and central nervous systems, non-neuronal cell activation, and up- and down-regulation of various molecules in non-neuronal cells are involved in the development of this pain following trigeminal nerve injury. However, there are many unknown mechanisms underlying the persistent orofacial pain associated with trigeminal nerve injury. In this review, we address recent animal data regarding the involvement of various molecules in the communication of neuronal and non-neuronal cells and examine the possible involvement of ascending pathways in processing pathological orofacial pain. We also address the clinical observations of persistent orofacial pain associated with trigeminal nerve injury and clinical approaches to their diagnosis and treatment.

Keywords: trigeminal nerve injury, trigeminal ganglion, trigeminal spinal subnucleus caudalis, craniofacial pain, oral diagnosis, treatment

OPEN ACCESS

Edited by:
Xiaodong Liu, The Chinese University of Hong Kong, China

Reviewed by:
Carsten Theiss, Ruhr University Bochum, Germany
Yongchul Bae, Kyungpook National University, South Korea

****Correspondence:***
Koichi Iwata
iwata.kouichi@nihon-u.ac.jp

Specialty section:
This article was submitted to Pain Mechanisms and Modulators, a section of the journal Frontiers in Molecular Neuroscience

Received: *06 April 2021*
Accepted: *21 May 2021*
Published: *06 July 2021*

Citation:
Shinoda M, Imamura Y, Hayashi Y, Noma N, Okada-Ogawa A, Hitomi S and Iwata K (2021) Orofacial Neuropathic Pain-Basic Research and Their Clinical Relevancies. Front. Mol. Neurosci. 14:691396. doi: 10.3389/fnmol.2021.691396

INTRODUCTION

Peripheral nerve injury produces high-frequency injury discharges in the injured nerve fibers. These high-frequency injury discharges in the primary afferent neurons are conveyed to the central nervous system via dorsal root ganglion neurons, resulting in the enhancement of nociceptive neurons in the spinal dorsal horn. In the trigeminal system, injury discharges are conveyed to the trigeminal spinal subnucleus caudalis (Vc) and upper cervical spinal cord (C1-C2) via trigeminal ganglion (TG) neurons, resulting in severe persistent pain in the orofacial region (Dubner and Ren, 2004). In association with hyperactivation of TG, Vc and C1-C2 nociceptive neurons, non-neuronal glial cells and macrophages are activated and accumulated, respectively in the TG, Vc, and C1-C2

Abbreviations: AMPA, alpha amino-3-hydroxy-5-methyl-4-isoxazole-propionate; BDNF, brain-derived neurotrophic factor; CCI, Chronic Constriction Injury; CCL2, the chemokine C-C motif ligand 2; C1-C2, the upper cervical spinal cord; Cx43, Connexin 43; HZ, herpes zoster; IASP, International Association for the Study of Pain; IGF-1, insulin-like growth factor-1; IL, interleukin; KCC2, K^+-Cl^- cotransporter; MCP-1, monocyte chemoattractant protein-1; MRA, magnetic resonance angiography; MRI, magnetic resonance imaging; MT, medial thalamic nuclei; Nav1.8, voltage-gated sodium channels 1.8; NMDA, *N*-methyl-D-aspartate; PBN, parabrachial nucleus; QST, quantitative sensory testing; sEPSCs, spontaneous excitatory postsynaptic currents; sIPSCs, spontaneous inhibitory postsynaptic currents; SNRIs, serotonin-norepinephrine reuptake inhibitors; SP, Substance P; PHTN, Postherpetic trigeminal neuralgia; PPTTN, peripheral, painful, traumatic trigeminal neuropathy; TCAs, tricyclic antidepressants; TG, trigeminal ganglion; TN, trigeminal neuralgia; TNFR, TNF receptor; TNFα, tumor necrosis factor alpha; TrkB, tropomyosin-related kinase B; Vc, trigeminal spinal subnucleus caudalis.

regions. Neuron-non-neuronal cell communication is thought to be involved in the enhancement of macrophage accumulation and activation of non-neuronal glial cells, and further causes the increase of neuronal cell activation. It is also known that activated satellite cells, microglial cells, and accumulated macrophages generate a variety of cytokines, neurotrophic factors, and tumor necrosis factors in Vc and C1-C2 regions and are released from non-neuronal glial cells and macrophages (Liu et al., 2000; Ristoiu, 2013).

These neuron-non-neuronal cell communications are also considered to be involved in the acceleration of spreading of the neuronal activation in TG, Vc, and C1-C2 regions. Activated satellite glial cells and accumulated macrophages release various cytokines and cause further enhancement of the excitability of uninjured TG neurons, resulting in the spreading of the activation of TG neurons. Further, in Vc and C1-C2 regions, microglia-astrocyte interaction is thought to be involved in the spreading of the excitability of nociceptive neurons in Vc and C1-C2 (Shibuta et al., 2012; Asano et al., 2020).

Noxious information from the brain stem neurons is further conveyed to the higher CNS areas (Iwata et al., 2017b). Three major CNS areas receiving noxious inputs from Vc and C1-C2 regions are known to be involved in processing orofacial pathological pain, ventral posteromedial thalamic nucleus (VPM), medial thalamic nuclei (MT), and parabrachial nucleus (PBN) (Saito et al., 2017). It has recently been shown that these ascending pathways are functionally modulated after trigeminal nerve injury (Okada et al., 2019).

Trigeminal nerve injury is known to causes long-lasting, widely spreading, and persistent pathological pain in orofacial regions in humans. However, we do not have an appropriate strategy to diagnose and treat these orofacial pain because detailed mechanisms underlying pathological pain associated with trigeminal nerve injury are not fully understood. It is essential to know the mechanisms underlying these pain for the development of the appropriate treatment of orofacial neuropathic pain patients.

In this review, we address recent animal data regarding the involvement of neuron-non-neuronal cell communication and related various molecules and also address possible involvement of ascending pathways for processing of the orofacial pathological pain associated with trigeminal nerve injury. We also demonstrate the clinical observations of orofacial neuropathic pain and trigeminal neuralgia patients and their clinical approaches to diagnose and treat these orofacial neuropathic pain patients.

PERIPHERAL MECHANISMS OF OROFACIAL NEUROPATHIC PAIN

Trigeminal nerve injury results in pain hypersensitivity categorized as persistent orofacial pain, allodynia, and hyperalgesia (Kaji et al., 2016; Batbold et al., 2017; Sugawara et al., 2019). When the peripheral nerves are damaged, the cellular response is induced by via various molecules at the site of nerve damage. In the first place, nerve inflammatory response is triggered in relation to several changes in the microenvironment of immune cells surrounding the damaged peripheral nerves. Concurrent with immune cells infiltration to the injury site, some inflammatory molecules which cause the hypersensitivity of the peripheral nerve are released from the damaged neurons and Schwann cells. Moreover, changes in neuronal excitability with regard to threshold decrease and spontaneous firing are caused in the damaged neurons (Peng et al., 2016). For example, in greater detail: the levels of proinflammatory mediators like tumor necrosis factor-alpha (TNFα) or nerve growth factor are upregulated at the sites of peripheral nerve injury (Chu et al., 2020). TNFα binds to TNF receptor (TNFR), expressed in non-injured nerve endings, which results in a change in the excitatory potential of voltage-gated sodium channels 1.8 (Nav1.8), via activation of protein kinase C, leading to neuronal hyperexcitation (Leo et al., 2015). Another pathway to hyperexcitation can be found in tongue mucosa collected from patients with burning mouth syndrome, which is thought to have neuropathic involvement at various levels of the neuraxis: the mRNA expression in artemin, which is one of the glial cell line-derived neurotrophic factor, is upregulated (Shinoda et al., 2015). The upregulated artemin signaling leads to the hyperexpression of TRPV1 in tongue nociceptors via the p38 mitogen-activated protein kinase phosphorylation, producing heat hypersensitivity in the tongue (Shinoda et al., 2015). Many monocyte-derived macrophages are known to infiltrate at the nerve injury site following peripheral nerve injury. These blood-borne macrophages accumulate especially around injured axons, the accumulation is caused by monocyte chemoattractant protein-1 (MCP-1) signaling, that modulates the development of neuropathy (Kanamori et al., 2007). Reportedly, peripheral nerve injury induces infiltration and proliferation of macrophages which release insulin-like growth factor-1 (IGF-1) (Liu et al., 2000). Via TRPV2, the signaling of IGF-1 that is released by macrophages which accumulate in the site of infraorbital nerve injury, increases TRPV4 expression in neurons of the TG, innervating the facial skin. This results in mechanical hypersensitivity in the facial skin (Sugawara et al., 2019). Many molecules released from the injured axons, the infiltrating macrophages, and Schwann cells activate non-injured axons after peripheral nerve injury. The activation of non-injured axons might play an important role in peripheral neuronal hyperexcitability, closely correlated with neuropathic pain.

TRANSCELLULAR COMMUNICATION BETWEEN NEURONS AND INFLAMMATORY CELLS IN TG

Satellite glial cells, lymphocytes, macrophages, and the somata of the primary afferent neurons, are known to be present in TG. The satellite glial cells surround the sensory neuronal soma, and these cells communicate with each other via neurotransmitters. Nerve injury is reported to activate cell-to-cell communication in TG, via humoral factors, including cytokines, neuropeptides, and gas. Interestingly, macrophages accumulate at the site of peripheral nerve injury and in TG, where the somata of the injured primary

afferent neurons are found (Shinoda et al., 2019). Additionally, trigeminal nerve injury leads to infiltration of inflammatory cells, including macrophages, into TG and their subsequent accelerated activation. Following peripheral nerve injury in the orofacial region, TNFα or Substance P (SP) is released from the accumulated macrophages in TG, which leads to TG neuronal hyperexcitability followed by orofacial pain hypersensitivity (Batbold et al., 2017). The proliferation of resident macrophages is accelerated in sensory ganglia following peripheral nerve injury (Donegan et al., 2013). Some orofacial pathological conditions induce characteristic morphological changes in the infiltrated and resident macrophages (thicker ramifications and a larger soma), accelerating the release of various neurotransmitters. Thus, it is presumed that changes in the morphological appearance indicate activation of the macrophages.

Additionally, macrophages can be divided into two histological types, depending on their specific functional properties. First, the classically activated phenotype known as the M1 macrophage, which releases a variety of proinflammatory mediators, plays an essential role in the early stages of inflammatory reaction. Second, the alternatively activated phenotype is known as the M2 macrophage which has an anti-inflammatory effect and is associated with the tissue repair process. Peripheral nerve injury elicits infiltration and activation of M1 and M2 macrophages at the site of nerve damage and in the sensory ganglion where the somata of the injured neurons lie (Komori et al., 2011). In TG, transcellular communication between neurons and macrophages, via various biochemical mediators, regulates the excitability of TG neurons following peripheral nerve injury in the orofacial region (Iwata et al., 2017a). Trigeminal nerve injury induces infiltration of macrophages which release TNFα into TG. The TNFα signaling contributes to TG neuronal hypersensitivity, resulting in orofacial neuropathic pain (Batbold et al., 2017). Following peripheral nerve injury, a wide variety of biochemical mediators released from TG neurons also mediate the accumulation and activation of M1 and M2 macrophages. For example, the chemokine C-C motif ligand 2 (CCL2) is released from the somata of injured TG neurons, and the CCL2 signaling activates macrophages that accumulate in TG (Kim et al., 2011; Liu et al., 2016).

COMMUNICATION BETWEEN SATELLITE CELLS IN TG

Recent studies have indicated that peripheral nerve injury leads to functional and morphological changes in satellite cells (swelling of soma and shortening of processes), and these changes confer the primary neuronal hyperactivity (Li and Zhou, 2001). Moreover, satellite cells communicate with each other via gap junctions, which allow various molecules to pass between cells (Hansson and Skioldebrand, 2015).

Connexin 43 (Cx43), a gap junction protein, regulates the transport of several molecules between satellite glial cells (Chen et al., 2012). In TG, morphological changes of satellite glial cells are induced by inferior alveolar nerve injury via Cx43, resulting in extensive orofacial mechanical hypersensitivity (Kaji et al., 2016). These reports indicate that satellite glial cells are activated via Cx43 throughout TG, playing an essential role in ectopic orofacial pain via the enhancement of trigeminal neuronal excitability.

Thus, non-neuronal cell mechanisms in the TG might induce ectopic or extraterritorial pain hypersensitivity associated with peripheral nerve injury in the orofacial region. The orofacial ectopic pain can easily lead to misdiagnosis as dental pain and unnecessary and irreversible dental treatment such as pulpectomy or tooth extraction. Further elucidation of these mechanisms might make management of orofacial neuropathic pain and avoidance of misdiagnosis much easier for the clinician treating orofacial neuropathic pain.

BRAINSTEM AND CERVICAL SPINAL CORD MECHANISMS

The trigeminal spinal nucleus is an elongated structure that is divided into three subnuclei: oralis, interpolaris, and caudalis. The bulk of the trigeminal spinal nucleus is taken up with Vc, which has a laminated structure similar to that of the spinal cord. Nociceptive information arising from the craniofacial region is conveyed to the Vc, and the C1-C2, via primary afferent fibers, the somata of which lie in TG. Projection neurons, carrying nociceptive information from the craniofacial region, are found in the branches of the trigeminal nerve. The ophthalmic and mandibular branches of the trigeminal nerve project to the ventral and dorsal portion of both C1-C2 and Vc, respectively. The maxillary branch projects between the ventral and dorsal. Noxious information from brainstem neurons is further conveyed to the higher CNS areas (Iwata et al., 2017b). Three major CNS areas receiving noxious inputs from Vc and C1-C2 regions are known to be involved in processing orofacial pathological pain: posterior medial thalamic nucleus, MT, and PBN (Saito et al., 2017). The orofacial noxious pathway projecting to VPM is thought to be involved in the sensory discriminative aspect of pain. In contrast, the MT and PBN pathways are considered to be involved in the motivational and affective aspects of pain (Saito et al., 2017). Recently, these two ascending pathways have been functionally altered after trigeminal nerve injury (Okada et al., 2019). In response to trigeminal nerve injury, increased activity in *N*-methyl-D-aspartate (NMDA) and alpha amino-3-hydroxy-5-methyl-4-isoxazole-propionate (AMPA) receptors were found to facilitate synaptic transmission (Dubner and Ren, 2004). GABAergic and glycinergic inhibitory neurotransmission have also been seen to change following trigeminal nerve injury (Okada-Ogawa et al., 2013). In recent years, accumulated evidence has clarified that glial cells in the central nervous system are essential factors in inducing a wide variety of changes in neuronal function in the Vc following trigeminal nerve injury. Microglia and astrocytes are key players in neuropathic pain and are activated in response to trigeminal nerve injury as well as inflammation in the orofacial region (Okada-Ogawa et al., 2009; **Figure 1**). It is generally believed that microglia are activated in the early phase of nerve injury and that astrocytic

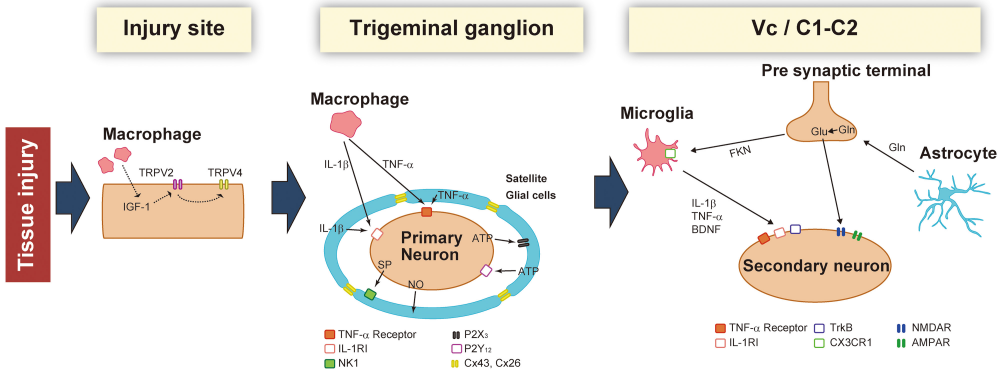

FIGURE 1 | Schematic illustration of the changes that occur in the injured site, trigeminal ganglion (TG), and Vc/C1-C2 following trigeminal nerve injury. After nerve injury, macrophages sensitize TG neurons by activating peripheral nerves and the soma. In the TG, neuronal activity is potentiated by secretory factors from satellite glial cells. Activated glial cells such as microglia and astrocytes further enhance synaptic transmission in the Vc and C1-C2.

activation occurs subsequently. Microglia are macrophage-like immune cells, secrete several proinflammatory cytokines, including interleukin (IL)-1β, IL-6, and TNFα. These cytokines can enhance both the frequency and amplitude of spontaneous excitatory postsynaptic currents (sEPSCs) in lamina II spinal neurons (Kawasaki et al., 2008). Among these cytokines, the target of IL-1β is the phosphorylation of NMDA receptors (Guo et al., 2007). Proinflammatory cytokines inhibit both GABA- and glycine-mediated spontaneous inhibitory postsynaptic currents (sIPSCs) in lamina II spinal neurons (Kawasaki et al., 2008). Another secretory molecule from microglia is the brain-derived neurotrophic factor (BDNF), which plays an essential role in neuropathic pain. BDNF binds to tropomyosin-related kinase B (TrkB), and in turn, leads to a reduction in expression levels of K^+-Cl^- cotransporter (KCC2). Due to the accumulation of intracellular Cl^-, GABA receptor-mediated Cl^- influx changes to Cl^- efflux, resulting in the excitatory response by GABA (Coull et al., 2005). Down-regulation of KCC2 in the Vc is observed after 21 days of inferior alveolar nerve injury in rat model of inferior alveolar transection, which results in hyperalgesia in regions innervated by the second branch of the trigeminal nerve (Okada-Ogawa et al., 2013). In addition, intracisternal injection of R-DIOA, an inhibitor of KCC2, induces hyperalgesia in naïve rats (Okada-Ogawa et al., 2013). Na^+-K^+-Cl^- cotransporter 1 (NKCC1), known as another regulator of intracellular Cl^-, does not influence its expression in the medullary dorsal horn after formalin injection in the vibrissa pad (Wu et al., 2009). Thus, besides regulating the excitatory transmission, BDNF also can affect the GABAergic effect by reducing the inhibition or even reversing to excitation. The reports that pharmacological inhibition of α6GABAA receptors, a subunit of GABA receptor, reduced the enhanced pain threshold in chronic constriction injury (CCI) model rats strongly suggest that GABAergic disinhibition plays an important role in neuropathic pain. BDNF secreted from microglia can phosphorylate GluN2B via Fyn kinase, downstream signaling of TrkB (Hildebrand et al., 2016). Furthermore, it activates NMDA receptors in presynaptic terminals of primary afferent fibers, facilitating glutamate release (Chen et al., 2014). More recently, BDNF from microglia has been shown to cause an increase in the number of synaptic terminals in CGRP positive primary sensory fibers, leading to long-term potentiation in the spinal cord during neuropathic pain (Zhou et al., 2019). Thus, BDNF can regulate both excitatory and inhibitory neurotransmission. The activation of microglia is not restricted to episodes of trigeminal nerve injury. Microglia release cathepsin S, a lysosomal cysteine protease, which induces fractalkine expression on the membrane surface of neurons. Fractalkine binds to CX3CR1, a receptor exclusively expressed in microglia, and sustains their activation state (Clark et al., 2007). Prolonged release of proinflammatory cytokines from microglia leads to severe pain. It is widely accepted that microglia are involved in the development of neuropathic pain. However, minocycline, an inhibitor of microglial activation, has little effect on existing pain. This might be due to the phase shift of glial activation after nerve injury. Prominent astrocytic activation can be seen after microglial activation. In fact, intracisternal injection of fluoroacetate, an inhibitor of reactive astrocytes, attenuates neuropathic pain caused by inferior alveolar nerve injury (Okada-Ogawa et al., 2009). Physiologically, astrocytes are known to modulate neuronal function as follows: glutamate, an essential factor in excitatory neurotransmission, is synthesized from glutamine derived from astrocytes in the presynaptic terminal. Adjacent astrocytes in the gap junction synchronize their activity as neuronal assemblies (Allen and Eroglu, 2017). Suppression of excessive astrocyte activity by methionine sulfoximine, an inhibitor of glutamine synthetase, or carbenoxolone, a gap junction blocker, significantly attenuates nociceptive behavior caused by pulpitis, or infraorbital nerve transection, respectively (Tsuboi et al., 2011). The involvement of astrocyte-derived D-serine in orofacial pain is as follows: D-serine works as a co-agonist of NMDA receptors, facilitating C-fiber-mediated long-term potentiation (Kronschlager et al., 2016). D-amino acid oxidase attenuates neuropathic pain caused by infraorbital nerve injury (Dieb and Hafidi, 2013). Together, abnormal regulation of neuronal function by glial cells contributes to the induction and maintenance of orofacial pain (**Figure 2**).

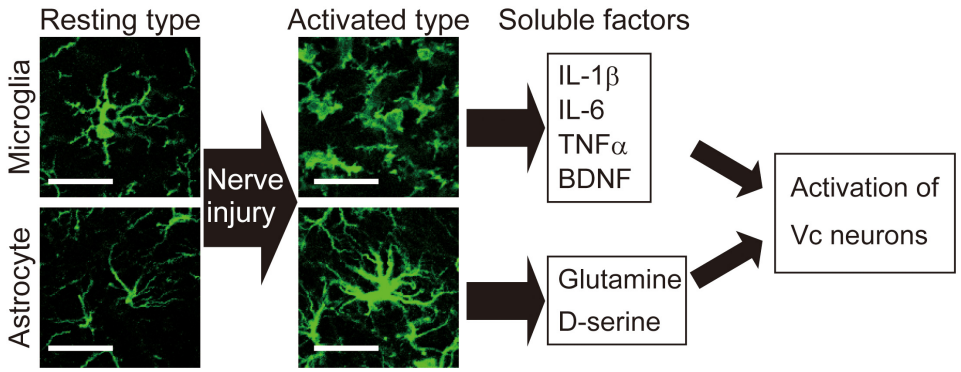

FIGURE 2 | Activation of microglia and astrocytes is observed in the Vc following peripheral nerve injury. Images show microglia and astrocytes in the Vc of normal rat or rat with infraorbital nerve injury (IONI). In the physiological situation, both microglia and astrocytes exhibit highly branched and thin processes, which is called resting type. Seven days after IONI, hypertrophic morphology of microglia and astrocytes, which is called activated type, is observed in the Vc. Activated types of glial cells release multiple factors that enhance neuronal activity in the Vc. Scale bar: 50 μm.

After trigeminal nerve injuries, such as the inferior alveolar nerve, mental nerve, and infraorbital nerve transection, the primary afferent neurons become hyperexcitable, resulting in satellite glial cell activation within TG. After hyperactivation of Vc and C1-C2 nociceptive neurons, microglial cells and astrocytes are further activated (Iwata and Sessle, 2019). As mentioned earlier, minocycline is known to inhibit the activation of microglia, and bioactive substances and other cytokines, such as nitric oxide, prostaglandin, IL-1, IL-1β, IL-6, are involved in the modulation of microglial activities in the central nervous system (Iwata and Sessle, 2019). A recent study demonstrated that minocycline administration relieves orofacial neuropathic pain and partially recovers cortical activity changes induced by the partial ligation of the infraorbital nerve (Zama et al., 2019).

Therefore, in the near future, minocycline may be used as a therapeutic agent for orofacial neuropathic pain. Additionally, clinical research should focus on developing drugs for orofacial neuropathic pain with relatively few side effects.

DIAGNOSIS OF OROFACIAL NEUROPATHIC PAIN

Recently, the International Classification of orofacial pain (ICOP) was described that orofacial neuropathic pain as "Orofacial pain attributed to lesion or disease of the cranial nerves" (ICOP, 2020). Neuropathic pain in the orofacial area has unique problems compared to neuropathic pain in the spinal cord. The international headache society reported that anatomical boundaries and associated medical specialty demarcations in the orofacial area contributed to the problem (ICOP, 2020). For example, the symptoms of neuropathic pain in the orofacial area often mimic odontogenic toothache, and it can easily be misdiagnosed and misdirected treatment (Christoforou et al., 2015; Christoforou, 2018). The orofacial area consists of many kinds of structures innervated by the trigeminal system, head, sinus, masticatory musculature, temporomandibular joint, jaw, teeth, and gingiva, and the complexity induces many kinds of non-odontogenic toothache (Schames et al., 2016). Besides, the measurement of orofacial pain is difficult because of its subjective nature. Therefore, accurate diagnosis of the cause of the pain is critical to avoid unnecessary dental treatment.

Orofacial neuropathic pain is thought to be classified into two types: episodic or continuous. The typical example of episodic neuropathic pain is trigeminal neuralgia (TN). TN involving the mandibular nerve, the third branch of the trigeminal nerve, is the most common type of TN, and paroxysmal pain is often felt in the tooth and can lead to the diagnosis of endodontic pain and unnecessary endodontic treatment (Antonaci et al., 2020). Diagnosis of TN is based on the patient's history and description of the symptoms. Therefore, a detailed interview with the patient is essential to obtain an accurate diagnosis. The pain of TN is characterized by sudden and severe attacks of electric shock-like shooting pain, lasting from a few seconds up to 2 min. These can be precipitated by mild stimulation of the orofacial region from eating, brushing the teeth, speech, or putting on makeup. Classical TN is associated with chronic vascular compression of the trigeminal nerve at the root entry zone of the brainstem. Other morphological changes, such as multiple sclerosis and space-occupying lesions, can cause secondary TN (ICOP, 2020). Therefore, to diagnose TN, investigations, as well as detailed interviews, are necessary. These include cranial nerve examination, magnetic resonance imaging (MRI), and magnetic resonance angiography (MRA) of the brain.

The typical example of continuous neuropathic pain is post-traumatic trigeminal neuropathic pain, although some cases may be episodic, from minutes to days. The orofacial area may be caused by third molar extractions, implants, root canal therapy, orthognathic surgery, or facial fractures. The typical description of pain is continuous burning and/or shooting pain in the area of injury or in the distal dermatome of the affected nerve. In its early stages, intraoral post-traumatic trigeminal neuropathic pain is also often misdiagnosed as odontogenic pain (Baad-Hansen and Benoliel, 2017). Therefore, the detailed history of trauma and the classical signs of post-traumatic trigeminal neuropathic pain lead to an accurate diagnosis as well. Therefore, in order

to diagnose post-traumatic trigeminal neuropathic pain, it is essential to know the patient's specific medical history and to perform chairside sensory testing, including quantitative sensory testing (QST) (Devine et al., 2018; Jaaskelainen, 2019). Post-traumatic trigeminal neuropathic pain is defined as a "unilateral or bilateral facial or oral pain following and caused by trauma to the trigeminal nerve (s), with other symptoms and/or clinical signs of trigeminal nerve dysfunction, and persisting or recurring for more than 3 months" (ICOP, 2020). Trigeminal postherpetic neuralgia is another typical example of continuous neuropathic pain. It is a complication of herpes zoster (HZ), and occurred following trigeminal neuropathic pain attributed to herpes zoster, that is also easily mistaken for toothache and induces unnecessary dental treatment in the early stage (Paquin et al., 2017). Although the lesions heal within a few months, the infection by HZ induces painful trigeminal neuropathy. Overall, approximately 10–15% of HZ patients will develop trigeminal postherpetic neuralgia. In patients older than 60 years, trigeminal postherpetic neuralgia occurs in more than 50% (Bayat et al., 2015). It has similar clinical features to post-traumatic trigeminal neuropathic pain: allodynia and hyperalgesia to mechanical and thermal stimuli, and burning, shooting, or electric shock-like pain. Accordingly, details of the patient's history, and sensory testing are also necessary for the diagnosis of trigeminal postherpetic neuralgia (ICOP, 2020).

There are many other neuropathic pains such as painful polyneuropathy, post-stroke pain, peripheral neuritis, glossopharyngeal neuralgia, occipital peripheral neuralgia, superior laryngeal neuralgia, and nervous intermedius neuralgia. These latter neuropathic pains are not common but need an appropriate strategy for diagnosis.

Neuropathic pain induces ectopic or extraterritorial pain upon nerve injury in the spinal area and orofacial area. However, in the orofacial area, the referred pain can easily lead to misdiagnosis as dental pain and unnecessary and irreversible dental treatment such as pulpectomy or tooth extraction. The referred pain has been explained by neuronal convergence and sensitization theories (Woolf, 2011; Markman, 2014), but it is difficult to clarify all the phenomena by referred pain. Recently, the mechanism of referred pain has been explained by various molecular and cellular changes in peripheral and central neuronal and non-neuronal cells, as above stated. The use of inhibitors and modulators for these cells in clinical trials has shown some encouraging results but still inconsistent levels of efficacy (Sainoh et al., 2016; Roerink et al., 2017). Further developments of these medications might make management of orofacial neuropathic pain and avoidance of mistreatment much easier for the clinician in orofacial neuropathic pain.

CLINICAL TREATMENT OF OROFACIAL NEUROPATHIC PAIN

In comparison with other neuropathic pain conditions such as post-herpetic neuralgia, painful diabetic neuropathy, and painful spinal traumatic neuropathy with a drug response rate of 20–40% (Bates et al., 2019), the response rate of PTTN is reported to be low, at approximately 11% (Haviv et al., 2014). However, the most common orofacial neuropathic pain syndromes are PPTTN as well as trigeminal neuralgia and PHTN. PPTTN is caused by trigeminal nerve injury, following procedures such as pulp extirpation, apicectomy, tooth extraction, or routine endodontic treatment. It is estimated that 3–5% of all such treatments lead to PPTTN (Baad-Hansen and Benoliel, 2017). PPTTN typically causes unilateral, continuous burning pain, at the site of injury or distal to the site, possibly with an additional sharp, shooting quality (Okada-Ogawa et al., 2015). Sensory loss may also be present. The peripheral nervous system seems to be involved at first, with additional CNS involvement over time. To manage this condition, it may be desirable to administer topical and/or systemic therapy to target the peripheral or central nervous system or both.

TOPICAL THERAPY

The topical application of medication is a relatively new method to treat neuropathic pain. Local drug delivery has advantages over centrally acting drugs that must taper up to adequate levels: it is less likely to induce systemic side effects or interact with other medications and can provide faster relief (Nasri-Heir et al., 2013). Discontinuation of centrally acting medications can also cause side effects, a phenomenon far less common with topically applied medications. Abrupt discontinuation of systemic medication can sometimes be dangerous, occurring when refills are not done on time or when patient instructions are ignored, misunderstood, forgotten, or not given (Sheikh et al., 2013). Topical medications are usually used to treat a specific peripheral target, making them useful for PPTTN, which involves peripheral nerve sensitization (Padilla et al., 2000). For severe pain, a combination of systemic and topical medications is often required. Topical lidocaine can desensitize a painful site by blocking a peripheral ectopic generator, such as a triggering zone near the tissue surface, in trigeminal neuralgia (Zakrzewska, 2010). It has also been shown to provide pain relief for PHTN patients (Derry et al., 2014). Five-percent lidocaine patches offer excellent comfort from allodynia in patients with slight sensory loss, but not in those with profound sensory loss.

With only preliminary evidence of benefit, another topical medication is orally applied capsaicin (Zostrix 0.025 or 0.075%) recommended for patients with orofacial neuropathic pain (Padilla et al., 2000). Initially, most patients complain of a burning sensation that wears off within 1–2 days. Repeated capsaicin applications alleviate pain by depleting SP in C-fiber primary afferents, thereby reducing the peripheral noxious inputs. A combination of capsaicin and Orabase (a paste containing gelatin 16.7%, pectin 16.7%, carboxymethylcellulose Sodium 16.7%) can be applied topically to the injured area using a neurosensory stent (Padilla et al., 2000). If sympathetic involvement is suspected, clonidine, an alpha-2-adrenergic agonist, can be added to the formulation (Epstein et al., 1997). This drug causes the suppression of the norepinephrine release from sympathetic terminals. Some clinicians have reported that

a topically-applied formulation containing amitriptyline 2% and ketamine 1% has an analgesic effect against orofacial neuropathic pain (Sawynok and Zinger, 2016).

SYSTEMIC PHARMACOTHERAPY

International and regional professional associations have published clinical practice guidelines on the pharmacological management of neuropathic pain. The most commonly recommended, centrally targeted analgesics are tricyclic antidepressants (TCAs; e.g., amitriptyline and nortriptyline), serotonin-norepinephrine reuptake inhibitors (SNRIs; e.g., venlafaxine and duloxetine), gabapentin and pregabalin, the latter two being the first drugs used for PPTTN (Lewis et al., 2007). The combination therapy of duloxetine or amitriptyline plus gabapentin or pregabalin should be the second choice for PPTTN. If the above strategy fails, opioids and opioid combinations may be a viable alternative. Pregabalin and gabapentin are classified as anticonvulsants. These two drugs inhibit the release of excitatory neurotransmitters such as glutamate and SP by combining with the α2δ subunit of the voltage-gated calcium channel in the central nervous system. Clinically, pregabalin and gabapentin are useful for persistent pain and numbness associated with PHTN, and diabetic neuropathy (Snedecor et al., 2014). Large clinical trials of pregabalin and gabapentin on PHTN patients demonstrated significant effects on PHTN pain; this analgesic effect is similar to that found in studies involving antidepressants. Mirogabalin is a newly synthesized, potent, and selective α2δ ligand, another gabapentinoid. It has been approved in Japan for the treatment of peripheral neuropathic pain, including painful diabetic peripheral neuropathy and PHTN (Kato et al., 2019). An animal study demonstrated that mirogabalin alleviated tactile allodynia in CCI of the sciatic nerve in rats (Murasawa et al., 2020). The effects of mirogabalin may be partly mediated by reducing ectopic afferent activity, thus directly reducing or eliminating the nociceptive afferent input to the medullary dorsal horn. A recent study demonstrated that the pain-inhibitory system became less sensitive to drugs in PPTTN patients over time (Nasri-Heir et al., 2015). Therefore, impaired inhibitory pain modulation should be considered a target in the management of PPTTN patients. TCAs or SNRIs are thought to block the reuptake of norepinephrine and serotonin (Nasri-Heir et al., 2015). Some clinicians have reported that among the various analgesic drugs available for treating neuropathic pain, TCAs provide the greatest benefit for patients with PPTTN (Nasri-Heir et al., 2015). SNRIs, such as duloxetine and venlafaxine, have also been used for orofacial neuropathic pain management. The central pain modulation, aided by TCAs or SNRIs, originates from brainstem neurons, mediated by the noradrenergic or serotonergic systems, and results in the enhancement of the pain inhibitory system.

On the contrary, carbamazepine, and oxcarbazepine, the first-line recommended medications in a systematic review, reduce pain in approximately 90% of patients with trigeminal neuralgia. Baclofen, lamotrigine, pregabalin, and gabapentin are included in the treatment for classical trigeminal neuralgia as a second-line treatment (Moore et al., 2019). To improve the effectiveness of oral anticonvulsants and abort an acute attack, the use of topical, injected, or intravenous lidocaine, intravenous fosphenytoin, and topical or injected sumatriptan are recommended in the current practice (Moore et al., 2019).

Pre-emptive analgesia is the possible treatment wherein preoperative treatment is designed to prevent the development of orofacial neuropathic pain. This treatment aims primarily to avoid the initial injury-induced afferent volley and central sensitization by using local anesthetic blocks during invasive dental procedures or oral surgery and diminishing the production of inflammatory mediators. Preventive analgesia focuses on the relative timing of preemptive analgesia or anesthetic interventions. It attenuates the impact of the peripheral nociceptive transduction associated with noxious stimuli preoperatively, intraoperatively, and/or postoperatively (Korczeniewska et al., 2020). In the dental setting, clinicians should consider using local analgesia during invasive dental procedures or using preemptive analgesics and/or anti-inflammatory drugs to prevent postoperative pain.

CONCLUSION

Following trigeminal nerve injury, non-neuronal cells, astrocytes, microglial cells, and astroglial cells, are activated, and macrophages are accumulated. The various molecules are generated in these non-neuronal cells and released from them, and these molecules are involved in the enhancement of the noxious neuronal activity. The glial cell-neuron and glial cell-glial cell interactions in TG, Vc, and C1/C2 regions are crucial mechanisms underlying orofacial neuropathic pain. According to the recent findings obtained from basic animal studies, appropriate diagnostic parameters and a variety of new treatments were developed for orofacial neuropathic pain and trigeminal neuropathy patients. More detailed mechanisms of non-neuronal cell function need to be evaluated in future studies, and the basic data hope to be applied for the appropriate diagnosis and treatment of orofacial neuropathic pain patients.

AUTHOR CONTRIBUTIONS

MS, YH, SH, and KI contributed to conception, design, analysis, interpretation, drafted and critically revised the manuscript. YI contributed to the concept, design, analysis, interpretation, drafted and critically revised the manuscript. NN and AO-O contributed to conception, analysis, interpretation, drafted about clinical treatment of orofacial neuropathic pain or diagnosis of orofacial neuropathic pain, respectively, and critically revised the manuscript. All authors gave their final approval and agreed to be accountable for all aspects of the work.

FUNDING

This work was supported in part by research grants from Sato Fund, Uemura Fund, Dental Research Center, Nihon University

School of Dentistry, KAKENHI [Grant-in-Aid for Scientific Research (C) 17K11654, 18K09732, and 19K10049]. The authors declare no potential conflicts of interest with the authorship and/or publication of this article.

ACKNOWLEDGMENTS

We would like to thank Editage (www.editage.jp) for English language editing.

REFERENCES

Allen, N. J., and Eroglu, C. (2017). Cell biology of astrocyte-synapse interactions. *Neuron* 96, 697–708. doi: 10.1016/j.neuron.2017.09.056

Antonaci, F., Arceri, S., Rakusa, M., Mitsikostas, D. D., Milanov, I., Todorov, V., et al. (2020). Pitfals in recognition and management of trigeminal neuralgia. *J. Headache Pain* 21:82. doi: 10.1186/s10194-020-01149-8

Asano, S., Hayashi, Y., Iwata, K., Okada-Ogawa, A., Hitomi, S., Shibuta, I., et al. (2020). Microglia-astrocyte communication via C1q contributes to orofacial neuropathic pain associated with infraorbital nerve injury. *Int. J. Mol. Sci.* 21:6384. doi: 10.3390/ijms21186834

Baad-Hansen, L., and Benoliel, R. (2017). Neuropathic orofacial pain: facts and fiction. *Cephalalgia* 37, 670–679. doi: 10.1177/0333102417706310

Batbold, D., Shinoda, M., Honda, K., Furukawa, A., Koizumi, M., Akasaka, R., et al. (2017). Macrophages in trigeminal ganglion contribute to ectopic mechanical hypersensitivity following inferior alveolar nerve injury in rats. *J. Neuroinflammation* 14:249. doi: 10.1186/s12974-017-1022-3

Bates, D., Schultheis, B. C., Hanes, M. C., Jolly, S. M., Chakravarthy, K. V., Deer, T. R., et al. (2019). A comprehensive algorithm for management of neuropathic pain. *Pain Med.* 20(Suppl. 1), S2–S12. doi: 10.1093/pm/pnz075

Bayat, A., Burbelo, P. D., Browne, S. K., Quinlivan, M., Martinez, B., Holland, S. M., et al. (2015). Anti-cytokine autoantibodies in postherpetic neuralgia. *J. Transl. Med.* 13:333. doi: 10.1186/s12967-015-0695-6

Chen, M. J., Kress, B., Han, X., Moll, K., Peng, W., Ji, R. R., et al. (2012). Astrocytic CX43 hemichannels and gap junctions play a crucial role in development of chronic neuropathic pain following spinal cord injury. *Glia* 60, 1660–1670. doi: 10.1002/glia.22384

Chen, W., Walwyn, W., Ennes, H. S., Kim, H., McRoberts, J. A., and Marvizon, J. C. (2014). BDNF released during neuropathic pain potentiates NMDA receptors in primary afferent terminals. *Eur. J. Neurosci.* 39, 1439–1454. doi: 10.1111/ejn.12516

Christoforou, J. (2018). Neuropathic orofacial pain. *Dent. Clin. North Am.* 62, 565–584. doi: 10.1016/j.cden.2018.05.005

Christoforou, J., Balasubramaniam, R., and Klasser, G. D. (2015). Neuropathic orofacial pain. *Curr. Oral Health Rep.* 2, 148–157.

Chu, L. W., Cheng, K. I., Chen, J. Y., Cheng, Y. C., Chang, Y. C., Yeh, J. L., et al. (2020). Loganin prevents chronic constriction injury-provoked neuropathic pain by reducing TNF-alpha/IL-1beta-mediated NF-kappaB activation and Schwann cell demyelination. *Phytomedicine* 67:153166. doi: 10.1016/j.phymed.2019.153166

Clark, A. K., Yip, P. K., Grist, J., Gentry, C., Staniland, A. A., Marchand, F., et al. (2007). Inhibition of spinal microglial cathepsin S for the reversal of neuropathic pain. *Proc. Natl. Acad. Sci. U.S.A* 104, 10655–10660. doi: 10.1073/pnas.0610811104

Coull, J. A., Beggs, S., Boudreau, D., Boivin, D., Tsuda, M., Inoue, K., et al. (2005). BDNF from microglia causes the shift in neuronal anion gradient underlying neuropathic pain. *Nature* 438, 1017–1021. doi: 10.1038/nature04223

Derry, S., Wiffen, P. J., Moore, R. A., and Quinlan, J. (2014). Topical lidocaine for neuropathic pain in adults. *Cochrane Database Syst. Rev.* 2014:CD010958. doi: 10.1002/14651858.CD010958.pub2

Devine, M., Hirani, M., Durham, J., Nixdorf, D. R., and Renton, T. (2018). Identifying criteria for diagnosis of post-traumatic pain and altered sensation of the maxillary and mandibular branches of the trigeminal nerve: a systematic review. *Oral Surg. Oral Med. Oral Pathol. Oral Radiol.* 125, 526–540. doi: 10.1016/j.oooo.2017.12.020

Dieb, W., and Hafidi, A. (2013). Astrocytes are involved in trigeminal dynamic mechanical allodynia: potential role of D-serine. *J. Dent. Res.* 92, 808–813. doi: 10.1177/0022034513498898

Donegan, M., Kernisant, M., Cua, C., Jasmin, L., and Ohara, P. T. (2013). Satellite glial cell proliferation in the trigeminal ganglia after chronic constriction injury of the infraorbital nerve. *Glia* 61, 2000–2008. doi: 10.1002/glia.22571

Dubner, R., and Ren, K. (2004). Brainstem mechanisms of persistent pain following injury. *J. Orofac. Pain* 18, 299–305.

Epstein, J. B., Grushka, M., and Le, N. (1997). Topical clonidine for orofacial pain: a pilot study. *J. Orofac. Pain* 11, 346–352.

Guo, W., Wang, H., Watanabe, M., Shimizu, K., Zou, S., LaGraize, S. C., et al. (2007). Glial-cytokine-neuronal interactions underlying the mechanisms of persistent pain. *J. Neurosci.* 27, 6006–6018. doi: 10.1523/JNEUROSCI.0176-07.2007

Hansson, E., and Skioldebrand, E. (2015). Coupled cell networks are target cells of inflammation, which can spread between different body organs and develop into systemic chronic inflammation. *J. Inflamm. (Lond.)* 12:44. doi: 10.1186/s12950-015-0091-2

Haviv, Y., Zadik, Y., Sharav, Y., and Benoliel, R. (2014). Painful traumatic trigeminal neuropathy: an open study on the pharmacotherapeutic response to stepped treatment. *J. Oral Facial Pain Headache* 28, 52–60. doi: 10.11607/jop.1154

Hildebrand, M. E., Xu, J., Dedek, A., Li, Y., Sengar, A. S., Beggs, S., et al. (2016). Potentiation of synaptic GluN2B NMDAR currents by fyn kinase ss gated through BDNF-mediated disinhibition in spinal pain processing. *Cell Rep.* 17, 2753–2765. doi: 10.1016/j.celrep.2016.11.024

ICOP (2020). International classification of orofacial pain, 1st edition (ICOP). *Cephalalgia* 40, 129–221. doi: 10.1177/0333102419893823

Iwata, K., and Sessle, B. J. (2019). The Evolution of neuroscience as a research field relevant to dentistry. *J. Dent. Res.* 98, 1407–1417. doi: 10.1177/0022034519875724

Iwata, K., Katagiri, A., and Shinoda, M. (2017a). Neuron-glia interaction is a key mechanism underlying persistent orofacial pain. *J. Oral Sci.* 59, 173–175. doi: 10.2334/josnusd.16-0858

Iwata, K., Takeda, M., Oh, S. B., and Shinoda, M. (2017b). "Neurophysiology of orofacial pain," in *Contemporary Oral Medicine*, eds C. Farah, R. Balasubramaniam, and M. McCullough (Cham: Springer). doi: 10.1007/978-3-319-28100-1_8-3

Jaaskelainen, S. K. (2019). Differential diagnosis of chronic neuropathic orofacial pain: role of clinical neurophysiology. *J. Clin. Neurophysiol.* 36, 422–429. doi: 10.1097/WNP.0000000000000583

Kaji, K., Shinoda, M., Honda, K., Unno, S., Shimizu, N., and Iwata, K. (2016). Connexin 43 contributes to ectopic orofacial pain following inferior alveolar nerve injury. *Mol. Pain* 12:1744806916633704. doi: 10.1177/1744806916633704

Kanamori, H., Matsubara, T., Mima, A., Sumi, E., Nagai, K., Takahashi, T., et al. (2007). Inhibition of MCP-1/CCR2 pathway ameliorates the development of diabetic nephropathy. *Biochem. Biophys. Res. Commun.* 360, 772–777. doi: 10.1016/j.bbrc.2007.06.148

Kato, J., Matsui, N., Kakehi, Y., Murayama, E., Ohwada, S., and Sugihara, M. (2019). Mirogabalin for the management of postherpetic neuralgia: a randomized, double-blind, placebo-controlled phase 3 study in Asian patients. *Pain* 160, 1175–1185. doi: 10.1097/j.pain.0000000000001501

Kawasaki, Y., Zhang, L., Cheng, J. K., and Ji, R. R. (2008). Cytokine mechanisms of central sensitization: distinct and overlapping role of interleukin-1beta, interleukin-6, and tumor necrosis factor-alpha in regulating synaptic and neuronal activity in the superficial spinal cord. *J. Neurosci.* 28, 5189–5194. doi: 10.1523/JNEUROSCI.3338-07.2008

Kim, D., You, B., Lim, H., and Lee, S. J. (2011). Toll-like receptor 2 contributes to chemokine gene expression and macrophage infiltration in the dorsal root ganglia after peripheral nerve injury. *Mol. Pain* 7:74. doi: 10.1186/1744-8069-7-74

Komori, T., Morikawa, Y., Inada, T., Hisaoka, T., and Senba, E. (2011). Site-specific subtypes of macrophages recruited after peripheral nerve injury. *Neuroreport* 22, 911–917. doi: 10.1097/WNR.0b013e32834cd76a

Korczeniewska, O. A., Khan, J., Eliav, E., and Benoliel, R. (2020). Molecular mechanisms of painful traumatic trigeminal neuropathy-Evidence from animal research and clinical correlates. *J. Oral Pathol. Med.* 49, 580–589. doi: 10.1111/jop.13078

Kronschlager, M. T., Drdla-Schutting, R., Gassner, M., Honsek, S. D., Teuchmann, H. L., and Sandkuhler, J. (2016). Gliogenic LTP spreads widely in nociceptive pathways. *Science* 354, 1144–1148. doi: 10.1126/science.aah5715

Leo, M., Argalski, S., Schafers, M., and Hagenacker, T. (2015). Modulation of voltage-gated sodium channels by activation of tumor necrosis factor receptor-1 and receptor-2 in small DRG neurons of rats. *Mediators Inflamm.* 2015:124942. doi: 10.1155/2015/124942

Lewis, M. A., Sankar, V., De Laat, A., and Benoliel, R. (2007). Management of neuropathic orofacial pain. *Oral Surg. Oral Med. Oral Pathol. Oral Radiol. Endod.* 103(Suppl. S32), e1–e24. doi: 10.1016/j.tripleo.2006.10.014

Li, L., and Zhou, X. F. (2001). Pericellular Griffonia simplicifolia I isolectin B4-binding ring structures in the dorsal root ganglia following peripheral nerve injury in rats. *J. Comp. Neurol.* 439, 259–274. doi: 10.1002/cne.1349

Liu, T., van Rooijen, N., and Tracey, D. J. (2000). Depletion of macrophages reduces axonal degeneration and hyperalgesia following nerve injury. *Pain* 86, 25–32. doi: 10.1016/s0304-3959(99)00306-1

Liu, X. J., Liu, T., Chen, G., Wang, B., Yu, X. L., Yin, C., et al. (2016). TLR signaling adaptor protein MyD88 in primary sensory neurons contributes to persistent inflammatory and neuropathic pain and neuroinflammation. *Sci. Rep.* 6:28188. doi: 10.1038/srep28188

Markman, S. (2014). Referred pain. *J. N. J. Dent. Assoc.* 85, 26–29.

Moore, D., Chong, M. S., Shetty, A., and Zakrzewska, J. M. (2019). A systematic review of rescue analgesic strategies in acute exacerbations of primary trigeminal neuralgia. *Br. J. Anaesth.* 123, e385–e396. doi: 10.1016/j.bja.2019.05.026

Murasawa, H., Kobayashi, H., Saeki, K., and Kitano, Y. (2020). Anxiolytic effects of the novel alpha2delta ligand mirogabalin in a rat model of chronic constriction injury, an experimental model of neuropathic pain. *Psychopharmacology (Berl.)* 237, 189–197. doi: 10.1007/s00213-019-05356-3

Nasri-Heir, C., Khan, J., and Heir, G. M. (2013). Topical medications as treatment of neuropathic orofacial pain. *Dent. Clin. North Am.* 57, 541–553. doi: 10.1016/j.cden.2013.04.011

Nasri-Heir, C., Khan, J., Benoliel, R., Feng, C., Yarnitsky, D., Kuo, F., et al. (2015). Altered pain modulation in patients with persistent postendodontic pain. *Pain* 156, 2032–2041. doi: 10.1097/j.pain.0000000000000265

Okada, S., Katagiri, A., Saito, H., Lee, J., Ohara, K., Iinuma, T., et al. (2019). Differential activation of ascending noxious pathways associated with trigeminal nerve injury. *Pain* 160, 1342–1360. doi: 10.1097/j.pain.0000000000001521

Okada-Ogawa, A., Nakaya, Y., Imamura, Y., Kobayashi, M., Shinoda, M., Kita, K., et al. (2015). Involvement of medullary GABAergic system in extraterritorial neuropathic pain mechanisms associated with inferior alveolar nerve transection. *Exp. Neurol.* 267, 42–52. doi: 10.1016/j.expneurol.2015.02.030

Okada-Ogawa, A., Suzuki, I., Nakaya, Y., Kobayashi, M., Ebihara, K., Imamura, Y., et al. (2013). Involvement of GABAergic interneurons in orofacial neuropathic pain following trigeminal nerve transection in rats. *Pain Res.* 28, 33–41. doi: 10.11154/pain.28.33

Okada-Ogawa, A., Suzuki, I., Sessle, B. J., Chiang, C. Y., Salter, M. W., Dostrovsky, J. O., et al. (2009). Astroglia in medullary dorsal horn (trigeminal spinal subnucleus caudalis) are involved in trigeminal neuropathic pain mechanisms. *J. Neurosci.* 29, 11161–11171. doi: 10.1523/JNEUROSCI.3365-09.2009

Padilla, M., Clark, G. T., and Merrill, R. L. (2000). Topical medications for orofacial neuropathic pain: a review. *J. Am. Dent. Assoc.* 131, 184–195. doi: 10.14219/jada.archive.2000.0146

Paquin, R., Susin, L. F., Welch, G., Barnes, J. B., Stevens, M. R., and Tay, F. R. (2017). Herpes zoster involving the second division of the trigeminal nerve: case report and literature review. *J. Endod.* 43, 1569–1573. doi: 10.1016/j.joen.2017.03.004

Peng, J., Gu, N., Zhou, L., Ukpong, B. E., Murugan, M., Gan, W. B., et al. (2016). Microglia and monocytes synergistically promote the transition from acute to chronic pain after nerve injury. *Nat. Commun.* 7:12029. doi: 10.1038/ncomms12029

Ristoiu, V. (2013). Contribution of macrophages to peripheral neuropathic pain pathogenesis. *Life Sci.* 93, 870–881. doi: 10.1016/j.lfs.2013.10.005

Roerink, M. E., Bredie, S. J. H., Heijnen, M., Dinarello, C. A., Knoop, H., and Van der Meer, J. W. M. (2017). Cytokine inhibition in patients with chronic fatigue syndrome: a randomized trial. *Ann. Intern. Med.* 166, 557–564. doi: 10.7326/M16-2391

Sainoh, T., Orita, S., Miyagi, M., Inoue, G., Kamoda, H., Ishikawa, T., et al. (2016). Single intradiscal administration of the tumor necrosis factor-alpha inhibitor, Etanercept, for patients with discogenic low back pain. *Pain Med.* 17, 40–45. doi: 10.1111/pme.12892

Saito, H., Katagiri, A., Okada, S., Mikuzuki, L., Kubo, A., Suzuki, T., et al. (2017). Ascending projections of nociceptive neurons from trigeminal subnucleus caudalis: a population approach. *Exp Neurol* 293, 124–136. doi: 10.1016/j.expneurol.2017.03.024

Sawynok, J., and Zinger, C. (2016). Topical amitriptyline and ketamine for post-herpetic neuralgia and other forms of neuropathic pain. *Expert Opin. Pharmacother.* 17, 601–609. doi: 10.1517/14656566.2016.1146691

Schames, S. E., Jordan, M., Robbins, H., Katz, L., and Tarbert, K. (2016). Nonodontogenic sources of dental pain. *J. Calif. Dent. Assoc.* 44, 507–513.

Sheikh, S., Gupta, D., Pallagatti, S., Singla, I., Gupta, R., and Goel, V. (2013). Role of topical drugs in treatment of oral mucosal diseases. A literature review. *N. Y. State Dent. J.* 79, 58–64.

Shibuta, K., Suzuki, I., Shinoda, M., Tsuboi, Y., Honda, K., Shimizu, N., et al. (2012). Organization of hyperactive microglial cells in trigeminal spinal subnucleus caudalis and upper cervical spinal cord associated with orofacial neuropathic pain. *Brain Res.* 1451, 74–86. doi: 10.1016/j.brainres.2012.02.023

Shinoda, M., Kubo, A., Hayashi, Y., and Iwata, K. (2019). Peripheral and central mechanisms of persistent orofacial pain. *Front. Neurosci.* 13:1227. doi: 10.3389/fnins.2019.01227

Shinoda, M., Takeda, M., Honda, K., Maruno, M., Katagiri, A., Satoh-Kuriwada, S., et al. (2015). Involvement of peripheral artemin signaling in tongue pain: possible mechanism in burning mouth syndrome. *Pain* 156, 2528–2537. doi: 10.1097/j.pain.0000000000000322

Snedecor, S. J., Sudharshan, L., Cappelleri, J. C., Sadosky, A., Mehta, S., and Botteman, M. (2014). Systematic review and meta-analysis of pharmacological therapies for painful diabetic peripheral neuropathy. *Pain Pract.* 14, 167–184. doi: 10.1111/papr.12054

Sugawara, S., Shinoda, M., Hayashi, Y., Saito, H., Asano, S., Kubo, A., et al. (2019). Increase in IGF-1 expression in the injured infraorbital nerve and possible implications for orofacial neuropathic pain. *Int. J. Mol. Sci.* 20:6360. doi: 10.3390/ijms20246360

Tsuboi, Y., Iwata, K., Dostrovsky, J. O., Chiang, C. Y., Sessle, B. J., and Hu, J. W. (2011). Modulation of astroglial glutamine synthetase activity affects nociceptive behaviour and central sensitization of medullary dorsal horn nociceptive neurons in a rat model of chronic pulpitis. *Eur. J. Neurosci.* 34, 292–302. doi: 10.1111/j.1460-9568.2011.07747.x

Woolf, C. J. (2011). Central sensitization: implications for the diagnosis and treatment of pain. *Pain* 152(Suppl. 3), S2–S15. doi: 10.1016/j.pain.2010.09.030

Wu, L. A., Huang, J., Wang, W., Wang, W., Wang, X. J., and Wu, S. X. (2009). Down-regulation of K+ -Cl- co-transporter 2 in mouse medullary dorsal horn contributes to the formalin-induced inflammatory orofacial pain. *Neurosci. Lett.* 457, 36–40. doi: 10.1016/j.neulet.2009.03.107

Zakrzewska, J. M. (2010). Medical management of trigeminal neuropathic pains. *Expert Opin. Pharmacother.* 11, 1239–1254. doi: 10.1517/14656561003767449

Zama, M., Fujita, S., Nakaya, Y., Tonogi, M., and Kobayashi, M. (2019). Preceding administration of minocycline suppresses plastic changes in cortical excitatory propagation in the model rat with partial infraorbital nerve ligation. *Front. Neurol.* 10:1150. doi: 10.3389/fneur.2019.01150

Zhou, L. J., Peng, J., Xu, Y. N., Zeng, W. J., Zhang, J., Wei, X., et al. (2019). Microglia are indispensable for synaptic plasticity in the spinal dorsal horn and chronic pain. *Cell Rep.* 27, 3844–3859.e3846. doi: 10.1016/j.celrep.2019.05.087.

Conflict of Interest: The authors declare that the research was conducted in the absence of any commercial or financial relationships that could be construed as a potential conflict of interest.

frontiers in Molecular Neuroscience

ORIGINAL RESEARCH
published: 27 August 2021
doi: 10.3389/fnmol.2021.723395

Elevated Expression and Activity of Sodium Leak Channel Contributes to Neuronal Sensitization of Inflammatory Pain in Rats

Jia Li[1,2,3†], Yali Chen[1,2†], Jin Liu[1,2], Donghang Zhang[1,2], Peng Liang[1], Peilin Lu[1], Jiefei Shen[4], Changhong Miao[5], Yunxia Zuo[1,2] and Cheng Zhou[1,2*]*

[1] Department of Anesthesiology, West China Hospital, Sichuan University, Chengdu, China, [2] Laboratory of Anaesthesia and Critical Care Medicine, Translational Neuroscience Center, West China Hospital, Sichuan University, Chengdu, China, [3] Department of Anesthesiology, Xi'an Jiaotong University-Affiliated Honghui Hospital, Xi'an, China, [4] Laboratory of Oral Diseases & National Clinical Research Center for Oral Diseases and Department of Prosthodontics, West China Stomatology Hospital of Sichuan University, Chengdu, China, [5] Department of Anesthesiology, Zhongshan Hospital, Fudan University, Shanghai, China

OPEN ACCESS

Edited by:
Wuping Sun,
Shenzhen University, China

Reviewed by:
Olga Kopach,
University College London, United Kingdom
Lingli Liang,
Xi'an Jiaotong University, China
Chao Ma,
Chinese Academy of Medical Sciences and Peking Union Medical College, China

***Correspondence:**
Donghang Zhang
zhangdhscu@163.com
Cheng Zhou
zhouc@163.com

[†] These authors have contributed equally to this study

Specialty section:
This article was submitted to Pain Mechanisms and Modulators, a section of the journal Frontiers in Molecular Neuroscience

Received: 10 June 2021
Accepted: 02 August 2021
Published: 27 August 2021

Citation:
Li J, Chen Y, Liu J, Zhang D, Liang P, Lu P, Shen J, Miao C, Zuo Y and Zhou C (2021) Elevated Expression and Activity of Sodium Leak Channel Contributes to Neuronal Sensitization of Inflammatory Pain in Rats.
Front. Mol. Neurosci. 14:723395.
doi: 10.3389/fnmol.2021.723395

Inflammatory pain encompasses many clinical symptoms, and there is no satisfactory therapeutic target. Neuronal hyperexcitability and/or sensitization of the primary nociceptive neurons in the dorsal root ganglion (DRG) and spinal dorsal horn are critical to the development and maintenance of inflammatory pain. The sodium leak channel (NALCN), a non-selective cation channel, mediates the background Na^+ leak conductance and controls neuronal excitability. It is unknown whether abnormal activity of NALCN mediates the pathological process of inflammatory pain. Complete Freund's adjuvant (CFA) was injected into the left footpad of rats to induce inflammatory pain. The thresholds of mechanical and thermal sensation and spontaneous pain behaviors were assessed. The expression of NALCN in DRG and spinal dorsal cord was measured. NALCN currents and the contribution of NALCN to neuronal excitability in the DRG and spinal dorsal cord were recorded using whole-cell patch-clamping recording. NALCN was abundantly expressed in neurons of the DRG and spinal dorsal cord. In acutely isolated DRG neurons and spinal cord slices from rats with CFA-induced inflammatory pain, NALCN currents and neuronal excitability were increased. Subsequently, intrathecal and sciatic nerve injection of NALCN-small interfering RNA (siRNA) decreased NALCN mRNA and reverted NALCN currents to normal levels, and then reduced CFA-induced neuronal excitability and alleviated pain symptoms. Furthermore, pain-related symptoms were significantly prevented by the NALCN-shRNA-mediated NALCN knockdown in DRG and spinal cord. Therefore, increased expression and activity of NALCN contributed to neuronal sensitization in CFA-induced inflammatory pain. NALCN may be a novel molecular target for the control of inflammatory pain.

Keywords: NALCN, electrophysiology, inflammatory pain, neuronal sensitization, substance P

Abbreviations: NALCN, sodium leak channel; CFA, complete Freund's adjuvant; PCR, polymerase chain reaction; DRG, dorsal root ganglion; SP, substance P; NK1, neurokinin 1; TRPV1, transient receptor potential cation channel subfamily V member 1; TTX, tetrodotoxin; PVDF, polyvinyl difluoride; NF200, neurofilament 200; IB4, isolectin B4; Gd^{3+}, gadolinium; RMP, resting membrane potential; siRNA, small interfering RNA.

INTRODUCTION

Inflammatory pain is induced by neural injury or disease that affects approximately 20% of the general population; however, a large proportion of patients with inflammatory pain is treated ineffectively (Goldberg and McGee, 2011). Several causes may contribute to the development of inflammatory pain. Current therapeutics for inflammatory pain mainly include non-steroidal anti-inflammatory drugs and opioids, but the effects are not satisfactory and their use are also limited because of side effects (Weinblatt, 1991; Mehta, 2007; Carter et al., 2014). Therefore, the development of novel drugs is clinically important for the treatment of inflammatory pain.

Neuronal hyperexcitability and/or sensitization of the primary nociceptive neurons in the dorsal root ganglion (DRG) and spinal dorsal horn is critical to the development and maintenance of inflammatory pain (Herrmann et al., 2017; Amsalem et al., 2018). However, the key molecular target that regulates the intrinsic excitability of neurons in DRG and spinal dorsal horn during the development of inflammatory pain has yet to be identified.

The sodium leak channel (NALCN), a non-selective background leak cation channel, is widely expressed in the nervous system, including the DRG and spinal cord (Lu et al., 2007; Zhang et al., 2021). NALCN can regulate the neuronal resting membrane potential (RMP; Lu et al., 2007; Cochet-Bissuel et al., 2014), which is associated with neuronal excitability and rhythm in the central nervous system (Lu et al., 2007). Abnormal function of NALCN induces many physiological dysfunctions, such as respiratory failure in mice (Yeh et al., 2017), disrupted circadian rhythm in *Drosophila melanogaster* (Flourakis et al., 2015), motor dysfunction in *Caenorhabditis elegans* (Gao et al., 2015), and cognitive defects in humans (Bend et al., 2016; Lozic et al., 2016). For sensory functions, NALCN can regulate the excitability of spinal cord projection neurons (Ford et al., 2018). Overexpression of NALCN in nociceptors of African highveld mole-rat-induced depolarization of the neuronal RMP (Eigenbrod et al., 2019). However, it is unclear whether the expression and the function of NALCN in the DRG and spinal cord contribute to the initiation and maintenance of inflammatory pain.

Substance P (SP), a neuropeptide and neurotransmitter, is synthesized in cell bodies of pain-sensing fibers of DRG, and then it is transported and released in the spinal dorsal horn (Hökfelt et al., 1975). SP exerts its effects via neurokinin 1 (NK1) receptors, which is involved in the transmission of nociceptive sensations (Andoh et al., 1996; Man et al., 2012). SP-NK1 receptor signaling also modulates the activity of many ion channels, including $Na_v1.8$ (Cang et al., 2009), transient receptor potential cation channel subfamily V member 1 (TRPV1) (Zhang et al., 2007; Lapointe et al., 2015), and potassium channels (Sculptoreanu et al., 2009). Interestingly, NALCN is activated by SP in the neurons of both hippocampus and ventral tegmental area in mice (Lu et al., 2007, 2009; Ou et al., 2020). SP enhances respiration by activating NALCN in the pre-Bötzinger complex and the retrotrapezoid nucleus (Ren, 2011; Yeh et al., 2017). However, it is still not known whether NALCN in DRG and spinal cord neurons is the molecular target of SP in inflammatory pain.

In the present study, we hypothesized that the NALCN is a potent regulator of neuronal activity in the DRG and spinal dorsal cord in a rat model of complete Freund's adjuvant (CFA)-induced inflammatory pain. Our findings suggest that NALCN might be an important molecular target for the control of pain induced by inflammation.

MATERIALS AND METHODS

Animals

All the study protocols were approved by the Animal Ethics Committee of West China Hospital of Sichuan University (Chengdu, Sichuan, China) (Approval No. 2018181A). The protocols were conducted in accordance with the Animal Research: Reporting of *in vivo* Experiments (ARRIVE) guidelines. Neonatal (postnatal days 7–10, PD7∼10, male and female) Sprague-Dawley rats and adult (∼6 weeks, male) rats were used for electrophysiological recordings. Adult (6–8 weeks, male) rats were used for behavioral tests. All rats were housed under controlled conditions (temperature 22–24°C; humidity, 45–55%; and a 12/12-h light–dark cycle) with free access to food and water. Neonatal rats were kept with their mothers. Every effort was made to minimize the number of rats used and to minimize their pain.

Chemicals

Substance P (MedChemExpress LLC, Monmouth Junction, NJ, United States) was dissolved in saline and intrathecally injected at a concentration of 1 μg/μl. The NK1 receptor antagonist L-703606 (Sigma-Aldrich, St. Louis, MO, United States) was dissolved in saline and intrathecally injected at a concentration of 6 μg/μl.

The CFA-Induced Inflammatory Pain Model in Rats

Under 2% isoflurane anesthesia, the rats were subcutaneously injected with CFA (Sigma-Aldrich, St. Louis, MO, United States, 1 mg ml^{-1}) in the left footpad, using a 28-gauge needle. The injected volumes were 100 and 10 μl for adult and neonatal rats, respectively.

Injection of Interventions

Small interfering RNAs (siRNA), modified by 3′-AlexaFluor488 (QIAGEN, Germantown, MD, United States), were dissolved in RNase-free water (NALCN-siRNA: 5′-UUGGCGUUGGUAUCUUCGCTT-3′; control-siRNA: catalog No. 1027419, QIAGEN, United States). *In vivo* SilenceMag^{TM} transfection reagent (OZ Biosciences, Marseille, France) was mixed with NALCN-siRNA or control-siRNA to a concentration of 1 μg/μl. Then, NALCN-siRNA or control-siRNA was injected into the sciatic nerve (1 μl for neonatal and 2 μl for adult rats) and subarachnoid space between L5 and L6 (5 μl for neonatal and 10 μl for adults). Briefly, rats were anesthetized with 2% isoflurane. Intraneural injection was at mid-part of sciatic nerve, using a glass micropipette connected to a Hamilton syringe. Then a magnet (SilenceMag^{TM} kit) was placed at the body

surface that corresponded to the targeted site for at least 1 h after injection. For intrathecal injection, the rats were restrained in the horizontal position, and a 25-gauge needle connected to a Hamilton syringe was slowly inserted through punctured skin into the subarachnoid space between L5 and L6. A sudden flick of the tail indicates a successful puncture into the subarachnoid space. The needle was kept in place for at least 60 s after the injection to avoid an outflow.

Dorsal root ganglion microinjection was performed as described previously (Zhao et al., 2013). Laminectomy was performed to expose the DRG (left L4-L5), and 2 μl pAAV2-H1-shRNA-(NALCN)-CAG-eGFP or pAAV2-scrambled-CAG-eGFP virus (2×10^{13} TU/ml) (Taitool Bioscience, Shanghai, China) was unilaterally injected into each DRG at a constant speed of 0.2 μl/min with a glass micropipette connected to a Hamilton syringe affixed by a stereotaxic syringe holder (SYS-Micro4, WPI, Sarasota, FL, United States). The injection needle was carefully removed after 10 min. The experiments were performed in all rats 4 weeks after the injection. The intrathecal injection method of AAV was the same with that of siRNA.

Behavioral Tests

Von Frey filaments and the Hargreaves test (heat) were used to measure mechanical and thermal hyperalgesia. For von Frey test, rats were placed individually in a Plexiglas chamber on an elevated metal mesh floor and habituated for 30 min. The plantar surface of the hind limb was stimulated with a series of von Frey filaments (0.07, 0.16, 0.4, 0.6, 1, 1.4, 2, 4, 6, 8, 10, and 15 g). The absolute withdrawal threshold was determined using the up-down method (Dixon, 1991). In Hargreaves test, rats were habituated in glass chambers on an elevated transparent glass platform. A beam of radiant heat from a thermal stimulator was focused on the plantar surface of the hind limb. The latency from the onset of radiant heat to an aversive response was defined as the thermal withdrawal latency. The cut-off time of radiant heat was set at 20 s to prevent tissue damage. The withdrawal threshold in the von Frey test and the thermal withdrawal latency in the Hargreaves test were measured three times daily, and the averages were calculated (with at least 10-min intervals between measurements). The behavioral tests were performed before the injection of CFA (baseline) and at 2 h, 8 h, and day 1 to day 12 daily after the injection of CFA. The experimenter was blinded to the groups of rats.

For the evaluation of CFA and SP-induced spontaneous aversive behaviors, the rats were firstly acclimated in the transparent recording chamber for 30 min. After intrathecal injection of SP or intraplantar injection of CFA, nociceptive behaviors were recorded, including paw licking, lifting, and shaking, and the duration of nociceptive behaviors (Rivat et al., 2018). The experimenter was blinded to the groups of rats.

Preparation of Spinal Cord Slices for Patch-Clamp Recording

Neonatal rats (PD7∼10) were anesthetized by inhalation of 2% isoflurane. The lumbar enlargement of the spinal cord was quickly excised, fixed in agarose gel (2%), and mounted on the chamber of a vibratome (VT1000A; Leica, Wetzlar, Germany). The chamber was filled with chilled (0–4°C) cutting solution containing (in mM): 260 sucrose, 3 KCl, 5 $MgCl_2$, 1 $CaCl_2$, 1.25 NaH_2PO_4, 26 $NaHCO_3$, 10 glucose, and 1 kynurenic acid (pH 7.4). Sagittal 300-μm thick spinal cord slices were cut and incubated at 36–37°C for 1 h, and then stored at room temperature (24–26°C) with incubation solution containing (in mM): 130 NaCl, 3 KCl, 2 $MgCl_2$, 2 $CaCl_2$, 1.25 NaH_2PO_4, 26 $NaHCO_3$, and 10 glucose (pH 7.4). The incubation solution was equilibrated with 95% O_2/5% CO_2. After incubation, spinal cord slices were placed in the recording chamber at room temperature.

Acutely Isolated DRG Neurons

Acutely isolated DRG neurons were prepared as previously reported (Xu and Huang, 2002). Briefly, the rats were anesthetized with 2% isoflurane. L4-L6 DRGs were removed and digested sequentially in 2% papain for 30 min and 2% collagenase I for 30 min at 37°C. Isolated neurons were then plated on glass coverslips coated with poly-D-lysine and laminin, and incubated with neuronal culture medium (Neurobasal medium, 2% B27, 1% Glutamax), aerated with 95% O_2/5% CO_2. Patch-clamp recordings were performed ∼2 h later.

Patch-Clamp Recordings

Spinal cord slices or acutely isolated DRG neurons with coverslips were mounted in a recording chamber and submerged in continuously perfused incubation solution (∼2 ml/min), bubbled with 95% O_2/5% CO_2. The incubation solution contained (in mM): 130 NaCl, 3 KCl, 2 $MgCl_2$, 2 $CaCl_2$, 1.25 NaH_2PO_4, 26 $NaHCO_3$, and 10 glucose (pH 7.4). L4-L6 DRG and spinal dorsal horn (lamina I-II) neurons were visualized and identified by the shape using infrared differential interference contrast microscopy. Electrophysiological recordings were conducted using an Axopatch 700B amplifier and a Digidata 1440 digitizer linked to a computer running pClamp 10.2 software (Molecular Devices, Sunnyvale, CA, United States). Recordings were sampled at 20 kHz and filtered at 10 kHz. All recordings were performed in the whole-cell configuration. The resistance of patch electrodes was 4–6 MΩ. Current-clamp recordings were performed to record action potentials using an internal solution containing (in mM): 120 KCH_3SO_3, 4 NaCl, 1 $MgCl_2$hin $CaCl_2$, 10 HEPES, 10 EGTA, 3 Mg-ATP, and 0.3 GTP-Tris, pH 7.3 (adjusted with KOH). For the recordings in the current-clamp mode, the rheobase was determined by applying a series of short depolarizing current steps (from −10 to 300 pA for DRG, from −5 to 200 pA for spinal dorsal cord) until a single action potential was generated. The duration of depolarizing current was 800 ms for each current step, and the interval was 5 pA for spinal dorsal cord and 10 pA for DRG. Voltage-clamp recordings were established to measure NMDG- (140 mM), Gd^{3+}- (50 μM), and SP-sensitive (10 μM) holding currents using an internal solution containing (in mM): 104 $CsCH_3SO_3$, 1 $MgCl_2$, 0.5 $CaCl_2$, 30 TEA-Cl, 10 EGTA, 3 Mg-ATP, 0.3 GTP-Tris, 10 HEPES, pH 7.3 (adjusted with CsOH). The series resistance was compensated by 70–75%, and data were rejected if the series resistance exceeded 20 MΩ. To block K^+ channels, synaptic GABAergic and AMPA inputs, 25-mM TEA, 5-mM 4-Aminopyridine (4-AP), 10-μM

CNQX, and 10-μM bicuculline were added to the incubation solution. For NALCN current recording, 500-nM tetrodotoxin (TTX) was added to the incubation solution as previously described (Yang et al., 2020).

Real-Time Polymerase Chain Reaction

Total RNA was extracted using an Eastep® Super RNA extraction kit (Promega, Shanghai, China), and reverse transcription of total RNA was performed with a GoScript™ Reverse Transcription Kit (Promega, Shanghai, China). Real-time polymerase chain reaction (PCR) was performed using GoTaq® qPCR Master Mix (Promega, Shanghai, China) and specific primers (Sangon Biotech, Shanghai, China) according to the instructions of the manufacturer. PCR cycling parameters were set as follows: 40 cycles at 95°C for 30 s, 60°C for 30 s, and then 72°C for 30 s. The Ct values of test genes were normalized to the value for GAPDH. The primers used to detect NALCN, SP, and GAPDH mRNA were:

NALCN forward (5′-GTCCTGACGAATCTCTGTCAGA-3′);
NALCN reverse (5′- CTGAGATGACGCTGATGATGG-3′);
SP forward (5′-GACAGTGACCAAATCAAGGAGG -3′);
SP reverse (5′-GAGGAATCAGCATCCCGTTTG-3′);
GAPDH forward (5′-GACATGCCGCCTGGAGAAAC-3′); and
GAPDH reverse (5′-AGCCCAGGATGCCCTTTAGT-3′).

Western Blotting

The lumbar enlargement of the spinal cord and L4-L6 DRGs were rapidly homogenized and lysed on ice. The protein concentration was determined with a BCA protein assay kit (Beyotime, Shanghai, China). The protein was electrophoresed on a 7.5% sodium dodecyl sulfate polyacrylamide gel and then transferred to polyvinyl difluoride (PVDF) membranes (Bio-Rad, Hercules, CA, United States). The PVDF membranes were incubated overnight at 4°C with primary antibodies against NALCN (1:1,000, Alomone Labs, Jerusalem, Israel) and β-actin (1:5,000, Abcam, Cambridge, United Kingdom). Then, membranes were incubated with the secondary antibody (1:4,000, Cell Signaling Technology, Beverly, MA, United States) at ambient temperature for 2 h. The protein bands were quantified using ImageJ software (National Institutes of Health, Bethesda, MD, United States).

Immunofluorescence Staining

The rats were deeply anesthetized by inhalation of 2% isoflurane and transcardially perfused with phosphate-buffered saline (PBS, pH 7.4) for 5 min, and then followed by 4% paraformaldehyde until muscle twitching stopped and liver tissue was hardened (5 min) as previously described (Chalermpalanupap et al., 2018; Kumar et al., 2019). L4–L6 DRGs and the lumbar enlargement of the spinal cord were removed and soaked in 4% formalin overnight at 4°C and then in 30% sucrose until the tissue sank to the bottom. The spinal cords and DRGs were cut into 12-μm-thick sequential sections using a freezing microtome (CM1850; Leica, Buffalo Grove, IL, United States). Sections were double labeled by incubating them overnight at 4°C with primary antibodies against NALCN (1:400, Alomone Labs, Jerusalem, Israel), TRPV1 (1:800, Abcam, Cambridge, United Kingdom), SP (1:200, Abcam, Cambridge, United Kingdom), neurofilament 200 (NF200, 1:800, Millipore, Burlington, MA, United States), isolectin B4 (IB4)-FITC-conjugated 488 (1:400, Sigma, St. Louis, MO, United States), NeuN (1:400, Sigma, St. Louis, MO, United States), and vesicular glutamate transporter 2 (VGLUT2, 1:200, Novus, Centennial, CO, United States). Fluorescent secondary antibodies (1:400, Jackson Immuno Research, West Grove, PA, United States) were added to 5% bovine serum albumin and incubated for 2 h at room temperature. For cell-counting analysis, five rats were included in each group. Twenty sections of L4–L6 DRGs of each rat were randomly selected for statistical analysis. The percent of co-expression of NALCN and SP, TRPV1, NF200, or IB4-positive cells was obtained. All images were captured using a Zeiss Axio Imager Z.2.

Statistical Analysis

All figures were prepared using GraphPad Prism 8.0 software (GraphPad Software, San Diego, CA, United States). Statistical tests were carried out using SPSS 22.0 software (IBM, Armonk, NY, United States). A Shapiro–Wilk normality test was used to assess the normality of the data distribution. Normally distributed data were presented as the mean ± standard deviation (SD) and were analyzed with student's *t*-test. Non-normally distributed data were presented as median (quartile), and the Mann–Whitney *U* test was used. The behavioral experiment data were analyzed by two-way repeated measures ANOVA; if significance was established, *post hoc* Holm–Sidak multiple comparisons were performed. The real-time PCR data were analyzed by paired, unpaired student's *t*-tests or two-way ANOVA; if significance was established, *post hoc* Holm–Sidak multiple comparisons were performed. The Western blotting data were analyzed by two-way (compared between groups) ANOVA; if significance was established, *post hoc* Holm–Sidak multiple comparisons were performed. The electrophysiology data were analyzed by paired, unpaired Student's *t*-tests, or two-way ANOVA; if significance was established, *post hoc* Holm–Sidak multiple comparisons were performed. All statistical methods used for individual analyses were indicated in the figure legends. The level of significance was set as $p < 0.05$.

RESULTS

Relative Expression of NALCN and SP Increased After the Injection of CFA in Adult Rats

Spontaneous aversive behaviors were observed for 30 min after the injection of CFA, including lifting and licking of the injected foot (**Figure 1A**, $n = 10$, $p < 0.05$). Compared with the CFA-contralateral side, thermal hyperalgesia and mechanical allodynia were detected in the CFA-ipsilateral side from 2 h to day 10 after the CFA injection (**Figures 1B,C**, $n = 10$, $p < 0.05$, respectively). The most pronounced mechanical allodynia and/or thermal hyperalgesia was detected on day 1 after CFA injection. The relative mRNA level of NALCN (**Figure 1D**) and SP (**Figure 1F**) in the DRG from the CFA-ipsilateral side was increased at 2 h

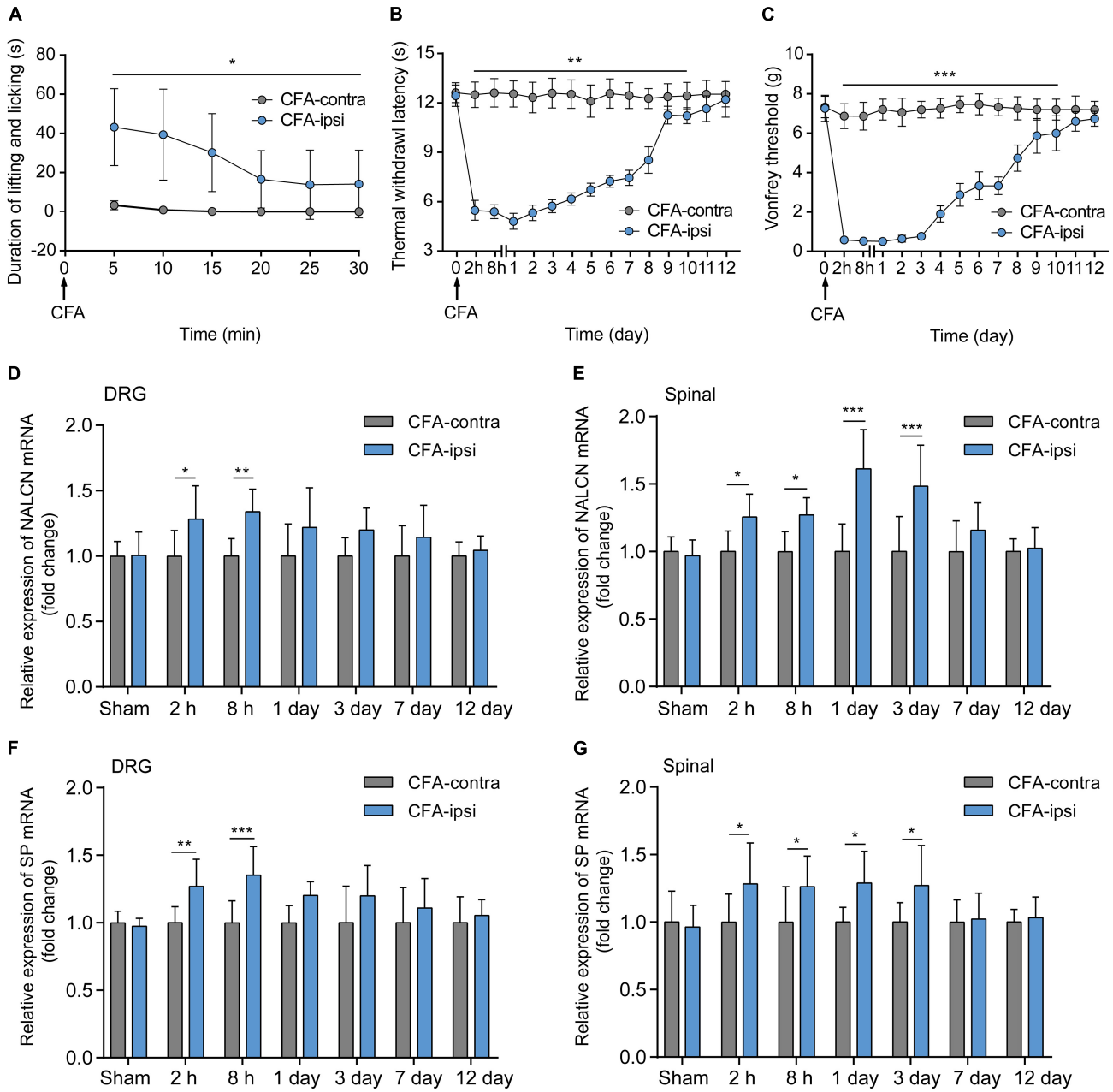

FIGURE 1 | Relative expression of sodium leak channel (NALCN) and substance P (SP) increase after injection of CFA. **(A)** Time course of spontaneous pain behavior (lifting/licking/flinching behaviors), following CFA injection (n = 10, by two-way repeated measures ANOVA, Holm–Sidak test). **(B)** Time course of thermal hyperalgesia following CFA injection (n = 10, by two-way repeated measures ANOVA, Holm–Sidak test). **(C)** Time course of mechanical allodynia, following CFA injection (n = 10, by two-way repeated measures ANOVA, Holm–Sidak test). **(D)** Changes in NALCN mRNA level in DRG (n = 10, by two-way ANOVA, Holm–Sidak test). **(E)** Changes in NALCN mRNA in spinal dorsal horn (n = 10, by two-way ANOVA, Holm–Sidak test). **(F)** Changes in SP mRNA in DRG (n = 10, by two-way ANOVA, Holm–Sidak test). **(G)** Changes in SP mRNA expression in spinal dorsal horn (n = 10, by two-way ANOVA, Holm–Sidak test). CFA-contra: CFA-contralateral side; CFA-ipsi: CFA-ipsilateral side; DRG: dorsal root ganglion; SP: substance P. Data are presented as mean ± SD. *$p < 0.05$, **$p < 0.01$, ***$p < 0.001$.

(n = 10, p = 0.011 for NALCN; p = 0.008 for SP) and 8 h (n = 10, p = 0.001 for NALCN; $p < 0.001$ for SP) after CFA injection, compared to the CFA-contralateral side. In the spinal dorsal horn, NALCN (**Figure 1E**) and SP (**Figure 1G**) mRNA levels were increased at 2 h (n = 6, P = 0.026 for NALCN; P = 0.021 for SP), 8 h (n = 10, P = 0.015 for NALCN; P = 0.037 for SP), day 1 (n = 10, $p < 0.001$ for NALCN; P = 0.016 for SP) and day 3 (n = 10, $p < 0.001$ for NALCN; P = 0.029 for SP) after CFA injection.

The NALCN non-selective protein was also evaluated at the highest mRNA expression time point. Expression of NALCN protein was 6.3 ± 2.4-fold greater in the CFA-ipsilateral side than that in the CFA-contralateral side in the DRG at 8 h after

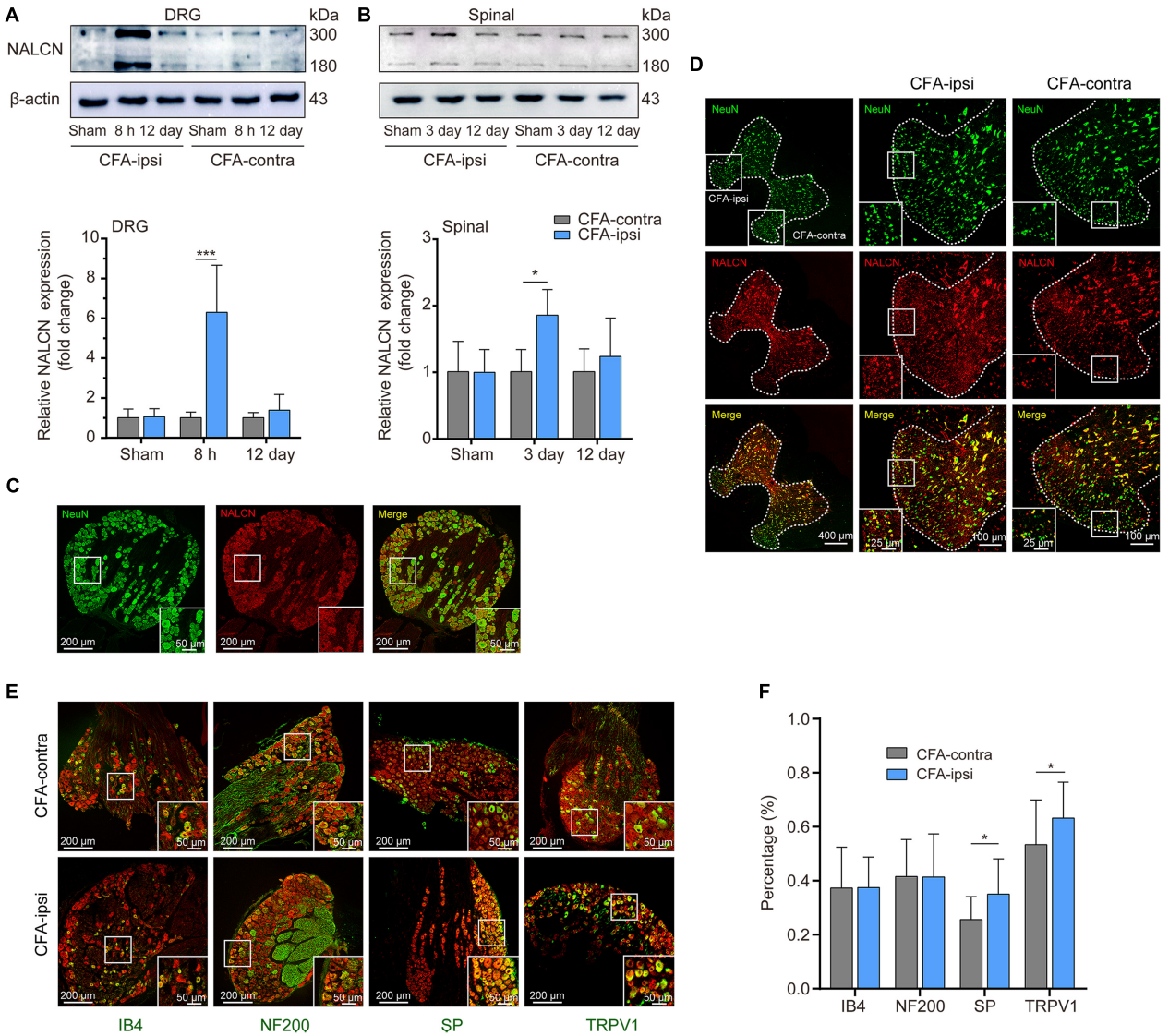

FIGURE 2 | Expression of NALCN increases in DRG and spinal dorsal horn after CFA injection in rats. **(A)** Representative immunoblotting image and statistical analysis indicated that the level of NALCN protein in DRG was upregulated at 8 h after CFA injection (n = 5, by two-way ANOVA, Holm–Sidak test). **(B)** The level of NALCN protein in spinal cord was upregulated at day 3 after CFA injection (n = 5, by two-way ANOVA, Holm–Sidak test). **(C)** Double immunofluorescence staining performed with an NALCN antibody in DRG at 8 h after CFA injection. NALCN (red) and neuronal marker NeuN (green) immunoreactivity showed NALCN mostly colocalized with NeuN. **(D)** Double immunofluorescence staining of spinal cord at day 3 after CFA injection showed NALCN immunoreactivity mostly colocalized with NeuN. **(E)** Double immunostaining shows colocalization of NALCN (red) with IB4 (green), NF200 (green), SP (green), and TRPV1 (green) in DRG neurons. **(F)** Percent of neuronal markers of the total population of DRG neurons. Five animals were used to obtain counts (unpaired t-test). IB4, isolectin B4; NF200, neurofilament 200 kDa; SP, substance P; TRPV1, transient receptor potential vanilloid 1. Data are presented as mean ± SD. $^{*}p < 0.05$, $^{***}p < 0.001$.

CFA injection (**Figure 2A**, n = 5, $p < 0.001$) and 1.8 ± 0.4-fold greater in the spinal dorsal cord at day 3 after CFA injection (**Figure 2B**, n = 5, P = 0.01). By fluorescence staining, NALCN was widely expressed in nearly all neurons of the DRG (**Figure 2C**) and spinal dorsal cord (**Figure 2D**). NALCN was widely co-expressed with SP, NF200, IB4, and TRPV1 in the DRG (**Figure 2E**). The percent of DRG neurons that co-expressed SP and NALCN (25.7% ± 8.5% vs. 35% ± 13.1%, n = 11–16 sections, P = 0.032) and co-expressed TRPV1 and NALCN (53.4% ± 16.6% vs. 63.2% ± 13.3%, n = 30–29 sections, P = 0.015) were increased on the CFA-ipsilateral side (**Figure 2F**). In the spinal dorsal cord, NALCN was widely expressed in the SP-positive area (**Supplementary Figure 1**). Notably, the specificity of the NALCN primary antibody was confirmed by both Western blotting and fluorescence staining (**Supplementary Figure 2**).

Na^+-Mediated Currents in DRG Neurons Functionally Increase After CFA Injection

To determine the function of NALCN in CFA-induced pain, we intrathecally and intraneurally injected NALCN-siRNA and/or

control-siRNA in adult rats at day 3 after CFA injection. The Na^+-mediated current ($I_{holding}$) was recorded at a holding potential of −60 mV by replacing extracellular Na^+ with NMDG (**Figures 3A,C**). For the adult rats that received control-siRNA, the total change in $I_{holding}$ was larger in small- and medium-sized DRG neurons from the CFA-ipsilateral side compared with the CFA-contralateral side (**Figures 3B,E**, left, 21.8 ± 9. vs. 11.2 ± 4.3 pA, n = 9, P = 0.001). Treatment of NALCN-siRNA

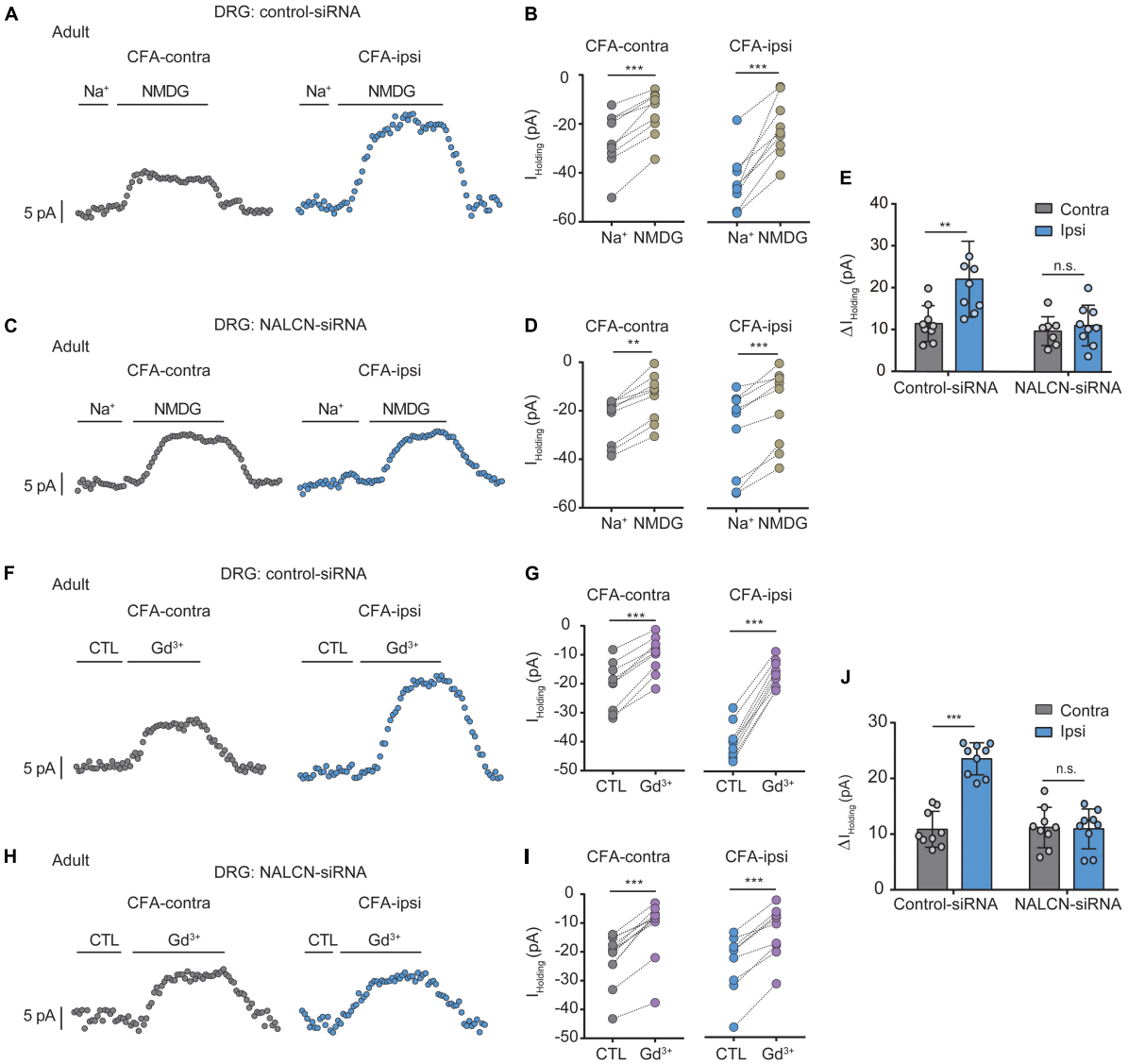

FIGURE 3 | Na^+-mediated currents ($I_{holding}$) and gadolinium (Gd^{3+})-inhibited $I_{holding}$ increase in small and medium neurons of DRG after injection of CFA in adult rats. Currents were recorded at holding potential of –60 mV. **(A)** Representative real-time analysis of $I_{holding}$ in small and medium DRG neurons from the rats that received control-siRNA combined with injection of CFA. $I_{holding}$ was extracted by replacing extracellular Na^+ with NMDG. **(B)** The $I_{holding}$ in small and medium DRG neurons of control siRNA-treated rats were analyzed before and after replacement with NMDG. **(C)** Representative real-time analysis of holding currents in small and medium DRG neurons from the rats that received NALCN-siRNA combined with injection of CFA. $I_{holding}$ was extracted by replacing extracellular Na^+ with NMDG. **(D)** The $I_{holding}$ in small and medium DRG neurons of NALCN siRNA-treated rats were analyzed before and after replacement with NMDG. **(E)** The $I_{holding}$ increased more in the DRG neurons of CFA-ipsi side than those of CFA-contra side from the control-siRNA-treated rats; treatment of NALCN-siRNA diminished the difference in $I_{holding}$ between CFA-ipsi and CFA-contra sides (n = 9, by two-way ANOVA, Holm–Sidak test). **(F)** Representative real-time analysis of Gd^{3+}-inhibited $I_{holding}$ in small and medium DRG neurons from the rats that received control-siRNA combined with injection of CFA. **(G)** The $I_{holding}$ in small and medium DRG neurons of control siRNA-treated rats was analyzed before and after perfusion of Gd^{3+}. **(H)** Representative real-time analysis of Gd^{3+}-inhibited $I_{holding}$ in small and medium DRG neurons from the rats that received NALCN-siRNA combined with injection of CFA. **(I)** The $I_{holding}$ in small and medium DRG neurons of NALCN siRNA-treated rats was analyzed before and after perfusion of Gd^{3+}. **(J)** Gd^{3+}-inhibited $I_{holding}$ increased more in the DRG neurons of CFA-ipsi side than those of CFA-contra side from the control-siRNA-treated rats; treatment of NALCN-siRNA diminished the difference in Gd^{3+}-inhibited $I_{holding}$ between CFA-ipsi and CFA-contra sides (n = 9, by two-way ANOVA, Holm–Sidak test). CFA-contra: CFA-contralateral side; CFA-ipsi: CFA-ipsilateral side; CTL: control, before perfusion of Gd^{3+}; DRG: dorsal root ganglion. Data are present as mean ± SD. $^{**}p < 0.01$, $^{***}p < 0.001$, n.s.: no significance.

diminished the difference in $I_{holding}$ between the CFA-ipsilateral and CFA-contralateral sides in small- and medium-sized DRG neurons (**Figures 3D,E**, right, 10.9 ± 4.9 vs. 9.6 ± 3.4 pA, $n = 9$, $P = 0.865$). Gadolinium (Gd^{3+}) is a non-selective blocker of NALCN. The $I_{holding}$ was blocked by Gd^{3+} (**Figures 3F,H**). The total change of Gd^{3+}-mediated inhibition of $I_{holding}$ was greater in small- and medium-sized DRG neurons of the CFA-ipsilateral side compared with the CFA-contralateral side in rats that received control-siRNA (**Figures 3G,J**, left, 23.1 ± 2.9 vs. 10.6 ± 3.2 pA, $n = 9$, $p < 0.001$). Treatment of NALCN-siRNA diminished the difference in Gd^{3+}-inhibited $I_{holding}$ between the CFA-ipsilateral and CFA-contralateral sides in small- and medium-sized DRG neurons (**Figures 3I,J**, right, 10.6 ± 3.5 vs. 10.9 ± 3.6 pA, $n = 9$, $P = 0.984$). No difference was found between Gd^{3+}-mediated current inhibition and that produced by siRNA (**Supplementary Figure 3A**, 12.45 ± 2.27 vs. 10.89 ± 5.31 pA, $n = 9$, $P = 0.431$).

Similar experiments were also performed in neonatal rats (PD7∼10). We intrathecally and intraneurally injected NALCN-siRNA and/or control-siRNA in neonatal rats at day 3 after CFA injection. Change of NALCN mRNA was confirmed in neonatal rats after CFA injection. The level of NALCN mRNA was increased at 8 h in the DRG after injection of CFA in neonatal rats (**Supplementary Figure 4A**, left, $n = 9$, $P = 0.040$). The level of NALCN mRNA was decreased on day 3 in the DRG after injection of NALCN-siRNA (**Supplementary Figure 4B**, left, $n = 12$, $p < 0.001$). Whole-cell patch-clamp recordings were performed on acutely isolated small and medium neurons of DRG (8 h after CFA injection). The $I_{holding}$ was recorded at a holding potential of −60 mV by replacing normal extracellular Na^+ with NMDG (**Figures 4A,C**). For the rats that received control-siRNA, the total change in $I_{holding}$ was larger in the neurons of DRG from the CFA-ipsilateral side, compared with the CFA-contralateral side (**Figures 4B**, left; **Figures 4E**, left, 24.6 ± 8.5 vs. 7. ± 2.8 pA, $n = 9$, $p < 0.001$). Treatment of NALCN-siRNA diminished the difference of $I_{holding}$ between the CFA-ipsilateral and CFA-contralateral sides in DRG neurons (**Figure 4D**, right; **Figure 4E**, right, 7.2 ± 2.5 vs. 7.1 ± 2.4 pA, $n = 9$, $P = 0.997$). The $I_{holding}$ was blocked by Gd^{3+} (**Figures 4F,H**). The total change of Gd^{3+}-mediated inhibition of $I_{holding}$ was greater in small- and medium-sized DRG neurons of the CFA-ipsilateral side, compared with the CFA-contralateral side in rats that received control-siRNA (**Figures 4G,J**, left, 15.2 ± 5.6 vs. 7.4 ± 3.8 pA, $n = 9$, $p < 0.001$). Treatment with NALCN-siRNA diminished the difference in Gd^{3+}-inhibited $I_{holding}$ between the two sides in small- and medium-sized DRG neurons (**Figures 4I,J**, right, 3.5 ± 2.5 vs. 4. ± 0.9 pA, $n = 9$–8, $P = 0.952$). No difference was found between Gd^{3+}-mediated current inhibition and that produced by siRNA [**Supplementary Figure 3B**, 9.96 (9.54, 12.51) vs. 13.42 (8.82, 14.64) pA, $n = 8$, $P = 0.382$].

Elevated Activity of NALCN Contributes to Excitability of DRG Neurons

NALCN-siRNA was used to test whether NALCN contributes to the excitability of DRG neurons after CFA injection. For adult rats, representative traces of action potentials of DRG neurons were shown in **Figures 5B,E**. With treatment of control-siRNA, small- and medium-sized neurons in the DRG from the CFA-ipsilateral side were hyperactive, as evidenced by depolarized RMP (**Figure 5A**, left, −46.4 ± 3.9 vs. −54.9 ± 8.1 mV, $n = 15$, $P = 0.001$), decreased rheobase (**Figure 5D**, left, 32.7 ± 12.2 vs. 85.3 ± 61.3 pA, $n = 15$, $p < 0.001$), and increased the number of AP spikes (**Figure 5C**). With treatment of NALCN-siRNA, the RMP (**Figure 5A**, right, −55.4 ± 6.1 vs. −53.7 ± 5.1 mV, $n = 14$–15, $P = 0.417$), rheobase (**Figure 5D**, right, 98.6 ± 69.9 vs. 94.7 ± 61.9 pA, $n = 14$–15, $P = 0.940$), and the number of AP spikes (**Figure 5F**) did not differ between the CFA-ipsilateral and CFA-contralateral sides for small- and medium-sized DRG neurons.

For neonatal rats, representative traces of action potentials of small, medium, large DRG neurons were shown in **Figures 5H,K,N,Q**. With treatment of control-siRNA, the small neurons in DRG from the CFA-ipsilateral side were hyperactive, as evidenced by depolarized RMPs (**Figure 5G**, left, −48.3 ± 1.9 vs. −57.5 ± 6.5 mV, $n = 12$, $p < 0.001$), decreased rheobase (**Figure 5G**, right, 58.3 ± 40.5 vs. 121.7 ± 72 pA, $n = 12$, $P = 0.015$) and increased the number of AP spikes (**Figure 5I**). The medium-sized neurons in DRG from the CFA-ipsilateral side were also hyperactive (RMP in **Figure 5M**, left, −50.4 ± 4. vs. −56.4 ± 4.6 mV, $n = 12$–14, $P = 0.002$; rheobase in **Figure 5M**, right, 48.6 ± 22.1 vs. 134.2 ± 59.2 pA, $n = 12$–14, $p < 0.001$), with the increased number of AP spikes (**Figure 5O**). However, for large neurons, the RMP (**Supplementary Figure 5A**, left, $n = 13$, $P = 0.870$), rheobase (**Supplementary Figure 5A**, right, $n = 13$, $P = 0.773$) and the number of AP spikes (**Supplementary Figure 5C**) did not significantly differ between the CFA-ipsilateral and CFA-contralateral sides. With treatment of NALCN-siRNA, the RMP, rheobase, and the number of AP spikes did not differ between the two sides for small (**Figure 5J**, $n = 14$, $P = 0.184$; $P = 0.171$, respectively, **Figure 5L**), medium (**Figure 5P**, $n = 13$, $P = 0.538$; $P = 0.912$, respectively, **Figure 5R**) or large neurons (**Supplementary Figure 5D**, $n = 13$, $P = 0.482$; $P = 0.771$, respectively, **Supplementary Figure 5F**). These results indicated that the increased excitability of small- and medium-sized neurons in the DRG of the CFA-ipsilateral side, at least partly, resulted from the increased NALCN activity.

Na^+-Mediated Currents in Spinal Dorsal Horn Are Increased After CFA Injection

The level of NALCN mRNA was increased on day 1 after injection of CFA in the spinal dorsal cord of neonatal rats (**Supplementary Figure 4A**, right, $n = 9$, $P = 0.003$). Injection of NALCN-siRNA led to a decreased level of NALCN mRNA on day 3 in the spinal dorsal cord of neonatal rats (**Supplementary Figure 4B**, right, $n = 11$, $p < 0.001$). Whole-cell patch-clamp recordings were performed on acutely isolated spinal cord slices on day 1 after injection of CFA. The $I_{holding}$ was recorded at a holding potential of −60 mV and measured by replacing normal extracellular Na^+ with NMDG (**Figures 6A,C**). With treatment of control-siRNA, the change of $I_{holding}$ was larger in the neurons from spinal dorsal cord (**Figures 6B,E**,

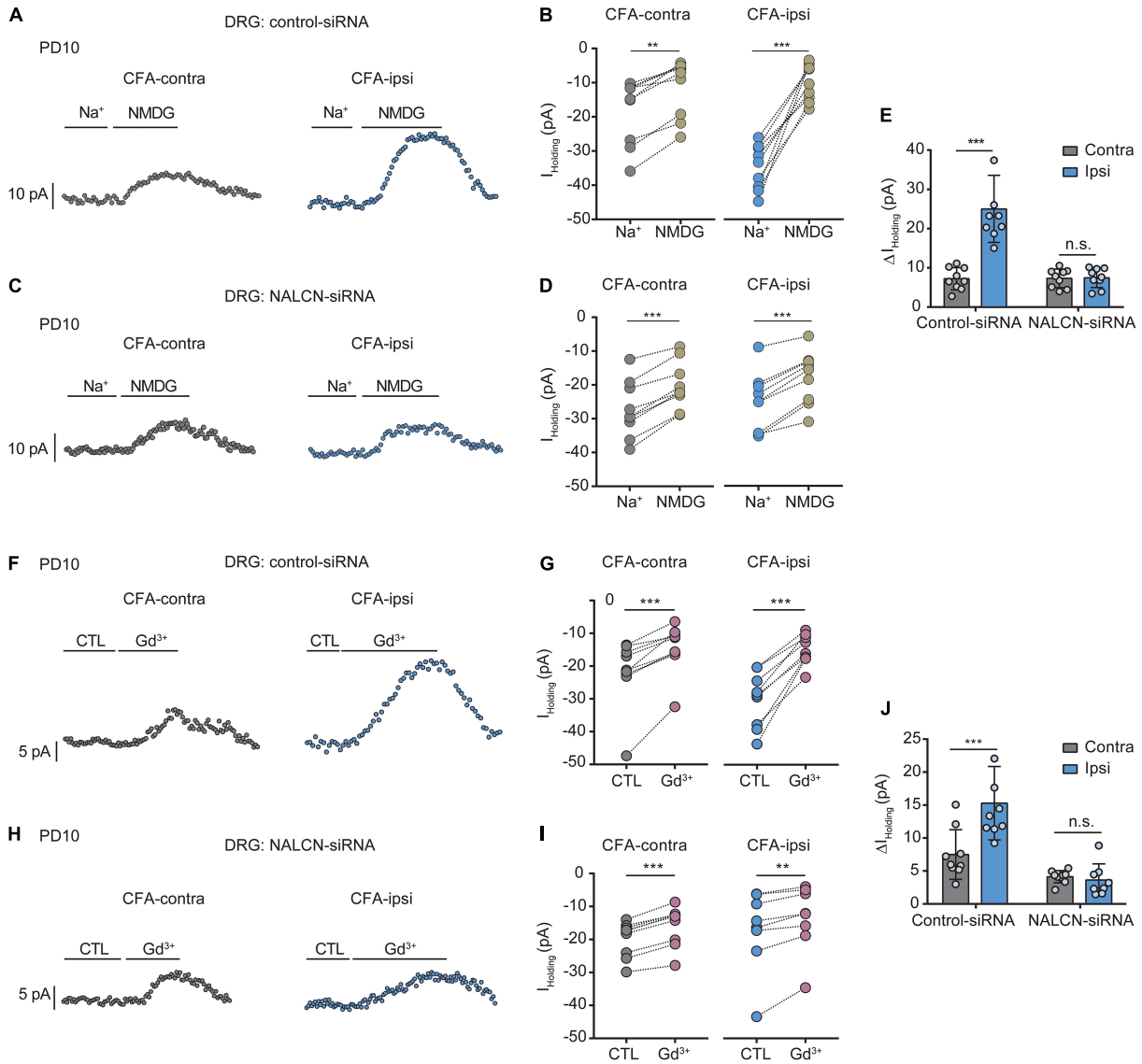

FIGURE 4 | Na^+-mediated currents and gadolinium (Gd^{3+})-inhibited holding currents in DRG neurons increase after injection of CFA in neonatal rats. NALCN-siRNA and/or control-siRNA were intrathecally and intraneurally injected into the subarachnoid space and sciatic nerve in P7 rats; CFA was injected 2 days later. **(A)** Representative real-time analysis of $I_{holding}$ in small and medium neurons from the rats that received control-siRNA combined with injection of CFA. The $I_{holding}$ was recorded at holding potential of –60 mV and extracted by replacing extracellular Na^+ with NMDG. **(B)** The $I_{holding}$ in small and medium DRG neurons of control siRNA-treated rats was analyzed before and after replacement with NMDG. **(C)** Representative real-time analysis of $I_{holding}$ in small and medium neurons from the rats that received NALCN-siRNA combined with an injection of CFA. **(D)** The $I_{holding}$ in small and medium DRG neurons of NALCN siRNA-treated rats was analyzed before and after replacement with NMDG. **(E)** The $I_{holding}$ increased more in the DRG neurons of CFA-ipsi side than those of CFA-contra side from the control-siRNA-treated rats; treatment of NALCN-siRNA diminished the difference of $I_{holding}$ between CFA-ipsi and CFA-contra side (n = 9, by two-way ANOVA, Holm–Sidak test). **(F)** Representative real-time analysis of Gd^{3+}-inhibited $I_{holding}$ in small and medium DRG neurons from the rats that received control-siRNA combined with injection of CFA. **(G)** The $I_{holding}$ in small and medium DRG neurons of control siRNA-treated rats was analyzed before and after perfusion of Gd^{3+}. **(H)** Representative real-time analysis of Gd^{3+}-inhibited $I_{holding}$ in small and medium DRG neurons from the rats that received NALCN-siRNA combined with injection of CFA. **(I)** The $I_{holding}$ in small and medium DRG neurons of NALCN siRNA-treated rats was analyzed before and after perfusion of Gd^{3+}. **(J)** Gd^{3+}-inhibited $I_{holding}$ was increased in DRG neurons of CFA-ipsi side than those of CFA-contra side from control siRNA-treated rats, but no difference was shown between CFA-ipsi side and CFA-contra sides from the NALCN-siRNA-treated rats (n = 9, by two-way ANOVA, Holm–Sidak test). CFA-contra: CFA-contralateral side; CFA-ipsi: CFA-ipsilateral side; CTL: control, before perfusion of Gd^{3+}; DRG: dorsal root ganglion; RMP: rest membrane potential; AP: action potential. Data are presented as mean ± SD. $^{**}p < 0.01$, $^{***}p < 0.001$, n.s.: no significance.

left, 24. ± 6.3 vs. 10.4 ± 5 pA, n = 9, $p < 0.001$) of the CFA-ipsilateral side, compared with the CFA-contralateral side. Treatment of NALCN-siRNA diminished the difference in $I_{holding}$ between the two sides in spinal dorsal horn neurons (**Figures 6D,E**, right, 10.8 ± 4.2 vs.10.2 ± 4.2 pA, n = 9, $P = 0.957$).

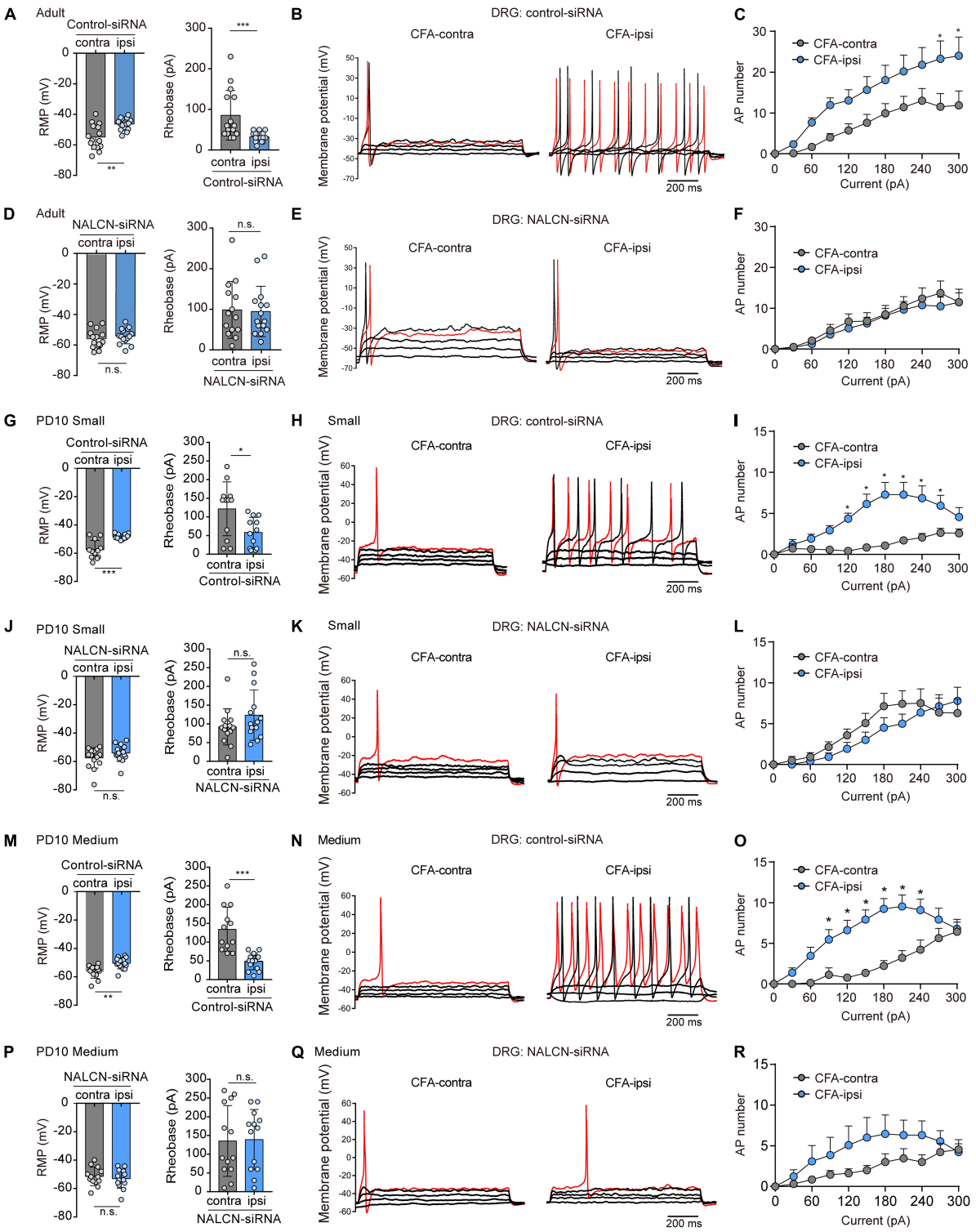

FIGURE 5 | Sodium leak channel enhances the excitability of small- and medium-sized DRG neurons after CFA injection in adult and neonatal rats. **(A,D)** Excitability of small and medium neurons in DRG compared between CFA-contralateral and CFA-ipsilateral sides based on RMP and rheobase from the rats that received control-siRNA and/or NALCN-siRNA combined with injection of CFA in adult rats (n = 14–15, unpaired t-test). **(B,E)** Representative traces of action potentials in the DRG neurons in control-siRNA and/or NALCN siRNA-treated rats. Red traces were the action potentials when receiving the same current injection. **(C,F)** Numbers of APs were increased more in small and medium DRG neurons of CFA-ipsi side than those of CFA-contra side from control siRNA-treated rats [**(C)**, n = 14, by two-way ANOVA, Holm–Sidak test], but no difference was shown between CFA-ipsi side and CFA-contra side from the NALCN-siRNA-treated rats [**(F)**, n = 15, by

(Continued)

FIGURE 5 | Continued
two-way ANOVA, Holm–Sidak test], respectively. **(G,J)** Excitability of small neurons in DRG compared between CFA-contralateral and CFA-ipsilateral sides based on RMP and rheobase from the rats that received control-siRNA and/or NALCN-siRNA combined with injection of CFA (n = 12, unpaired t-test). **(H,K)** Representative traces of action potentials in the small neurons of DRG from the rats that received control-siRNA and/or NALCN-siRNA combined with injection of CFA. Red trace was the action potential when receiving the same current injection. **(I,L)** Numbers of APs were increased more in small DRG neurons of CFA-ipsi side than those of CFA-contra side from control siRNA-treated rats [**(I)**, n = 12, by two-way ANOVA, Holm–Sidak test], but no difference was shown between CFA-ipsi side and CFA-contra side from the NALCN-siRNA-treated rats [**(L)**, n = 12, by two-way ANOVA, Holm–Sidak test], respectively. **(M,P)** Excitability of medium neurons in DRG compared between CFA-contralateral and CFA-ipsilateral sides based on RMP and rheobase from the rats that received control-siRNA and/or NALCN-siRNA combined with injection of CFA (n = 12–14, unpaired t-test). **(N,Q)** Action potential traces of medium neurons of DRG from the rats that received control-siRNA and/or NALCN-siRNA combined with injection of CFA. Red trace was the action potential when receiving the same current injection. **(O,R)** Numbers of APs increased more in medium DRG neurons of CFA-ipsi side than those of CFA-contra side from control siRNA-treated rats [**(O)**, n = 12, by two-way ANOVA, Holm–Sidak test], but no difference was shown between CFA-ipsi side and CFA-contra side from the NALCN-siRNA-treated rats [**(R)**, n = 14, by two-way ANOVA, Holm–Sidak test], respectively. CFA-contra: CFA-contralateral side; CFA-ipsi: CFA-ipsilateral side; DRG: dorsal root ganglion; RMP: rest membrane potential; AP: action potential. Data are presented as mean ± SD. $^{*}p < 0.05$, $^{***}p < 0.001$, n.s.: no significance.

The $I_{holding}$ was enhanced by perfusion of SP onto neurons of the spinal dorsal horn and was blocked by the NK1 receptor antagonist L703606 (**Figures 6F,H**). After control-siRNA treatment, the SP-evoked $I_{holding}$ was larger in spinal dorsal horn neurons of the CFA-ipsilateral side (**Figures 6G,J**, left, −22.1 ± 5.4 vs. −8.2 ± 5 pA, n = 9–8, $p < 0.001$). Treatment with NALCN-siRNA diminished the difference in SP-evoked $I_{holding}$ of neurons of the spinal dorsal horn between the CFA-ipsilateral and CFA-contralateral sides (**Figures 6I,J**, right, −4.7 ± 2.8 vs. −4.7 ± 2.8 pA, n = 8–9, $p > 0.999$). These results indicated that the NALCN-mediated current was increased after CFA injection, which may strengthen the response to SP in the spinal dorsal horn neurons but can be reduced by NALCN-siRNA.

Next, the $I_{holding}$ was blocked with Gd^{3+}in spinal cord neurons (**Figures 6K,M**). The Gd^{3+}-mediated inhibition of $I_{holding}$ was greater in spinal dorsal cord neurons on the CFA-ipsilateral side of rats that treated with control-siRNA (**Figures 6L,O**, left, 20.8 ± 4.6 vs. 10.2 ± 4.4 pA, n = 9, $p < 0.001$). For the rats that treated with NALCN-siRNA, no difference was found in Gd^{3+}-inhibited $I_{holding}$ of spinal dorsal cord neurons between the CFA-ipsilateral and the CFA-contralateral sides (**Figures 6N,O**, right, 9.6 ± 2.9 vs. 10.4 ± 5.8 pA, n = 9, P = 0.919). No difference was found between Gd^{3+}-mediated current inhibition and that produced by siRNA (**Supplementary Figure 3C**, 10.36 ± 2.04 vs. 12.63 ± 2.38 pA, n = 8–9, P = 0.052).

Elevated Activity of NALCN Contributes to Excitability of Sensory Neurons in the Spinal Dorsal Horn

Representative traces of action potentials of spinal dorsal horn neurons were shown in **Figures 7B,E**. The neurons from the CFA-ipsilateral side were hyperactive in rats treated with control-siRNA (depolarized RMP, **Figure 7A**, left, −47.7 ± 2.6 vs. −55.2 ± 5.3 mV, n = 11, $p < 0.001$; decreased rheobase, **Figure 7D**, left, 5 (5,5) vs. 10 (10,15) pA, n = 11, P = 0.002; the increased number of AP spikes, **Figure 7C**). However, the RMP (**Figure 7A**, right, −57.3 ± 4.5 vs. −56.5 ± 2.8 mV, n = 10–11, P = 0.654), rheobase (**Figure 7D**, right, 15.9 ± 6.3 vs. 17. ± 11.8 pA, n = 10–11, P = 0.792), and the number of AP spikes (**Figure 7F**) did not differ between the CFA-ipsilateral and CFA-contralateral sides in NALCN-siRNA-treated rats. Thus, the increased excitability of neurons in the spinal dorsal horn of the CFA-ipsilateral side, at least partly, resulted from the increased NALCN activity.

Knockdown Expression of NALCN in the DRG and Spinal Cord Reduces SP- and CFA-Induced Pain Behaviors

To investigate whether NALCN was involved in SP- and CFA-induced pain behaviors *in vivo*, NALCN-siRNA and/or control-siRNA was injected intrathecally and intraneurally into the subarachnoid space and sciatic nerve of adult rats (**Figure 8A**). Alexa Fluor 488-positive fluorescence was detected in the sciatic nerve, DRG, and spinal dorsal cord on day 2 after siRNA injection (**Figure 8B**). NALCN-siRNA-treated rats did not display any difference in the mechanical sensation threshold [**Figure 8C**, n = 10, before NALCN-siRNA vs. after NALCN-siRNA (P = 0.707 for contralateral side; P = 0.856 for ipsilateral side)] or thermal sensation threshold [**Figure 8C**, n = 10, before NALCN-siRNA vs. after NALCN-siRNA (P = 0.999 for contralateral side; P = 0.833 for ipsilateral side)] on day 3 after injection of NALCN-siRNA. SP-induced acute aversive behaviors in normal rats (**Figure 8D**, n = 10, $p < 0.001$), whereas the knockdown of NALCN expression in the DRG and spinal cord reduced the duration that the rats spent biting, licking, and scratching within the first 5 min after intrathecal injection of SP (**Figure 8E**, n = 10, $p < 0.001$). Intrathecal injection of the NK1 receptor antagonist L703606 also reduced the duration of aversive behaviors after SP injection (**Figure 8E**, n = 10, P = 0.001), but L703606 did not further decrease the duration of aversive responses in rats that had received NALCN-siRNA (**Figure 8E**, $p > 0.999$). Accordingly, expression of NALCN mRNA was decreased with 20.97% ± 15.95% in the DRG (**Figure 8F**, left, n = 8, P = 0.022) and with 27.46% ± 11.99% in the spinal dorsal horn (**Figure 8F**, right, n = 6, P = 0.008) on day 3 after injection of NALCN-siRNA.

To determine whether NALCN was involved in CFA-induced pain *via* the NK1 receptor, NALCN-siRNA and/or control-siRNA was injected into the subarachnoid space and sciatic nerve of adult rats. Two days later, 100 μLCFA was injected into the left hind foot (**Figure 8G**). Spontaneous pain within the first 25 min (**Figure 8H**, n = 10, $p < 0.05$), thermal hyperalgesia (**Figure 8I**, n = 10, $p < 0.05$) and mechanical allodynia (**Figure 8J**, n = 10, $p < 0.05$) of the injected hind foot were alleviated by preinjection

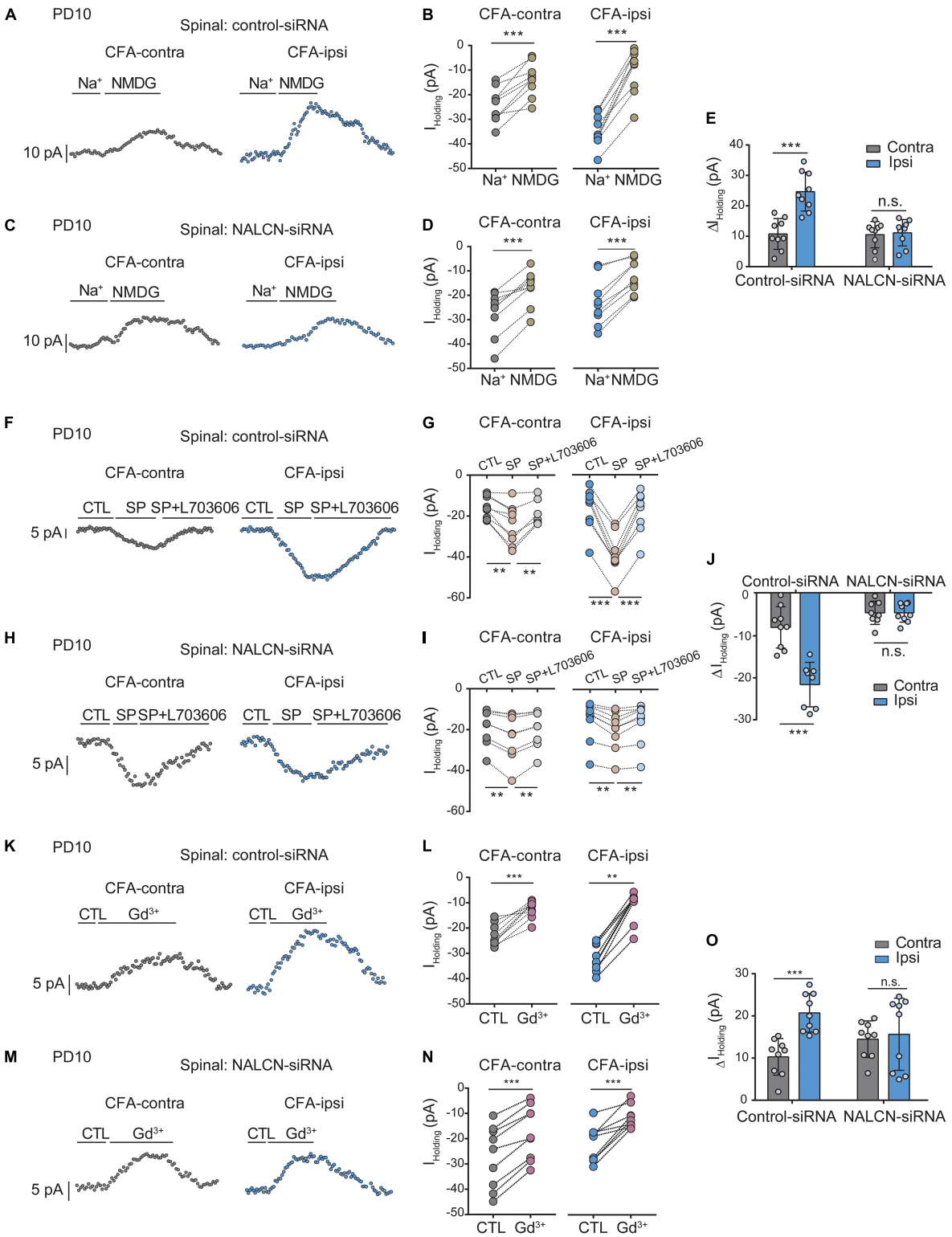

FIGURE 6 | Na^+-mediated currents and gadolinium (Gd^{3+})-inhibited $I_{holding}$ in neurons of spinal cord increase after injection of CFA. Sensory neurons of spinal dorsal cord were recorded at holding potential of –60 mV. **(A)** The representative real-time analysis of $I_{holding}$ in neurons from the rats that received control-siRNA combined with injection of CFA. The $I_{holding}$ was extracted by replacing extracellular Na^+ with NMDG. **(B)** The $I_{holding}$ in spinal cord neurons of control siRNA-treated rats was analyzed before and after replacement with NMDG. **(C)** The representative real-time analysis of holding currents in neurons from the rats that received NALCN-siRNA combined with injection of CFA. The $I_{holding}$ was extracted by replacing extracellular Na^+ with NMDG. **(D)** The $I_{holding}$ in spinal cord neurons of NALCN siRNA-treated

(Continued)

FIGURE 6 | Continued
rats was analyzed before and after replacement with NMDG. **(E)** The $I_{holding}$ increased more in the spinal cord neurons of CFA-ipsi side than those of CFA-contra side from the control-siRNA-treated rats; treatment of NALCN-siRNA diminished the difference in $I_{holding}$ between CFA-ipsi and CFA-contra sides (n = 9, by two-way ANOVA, Holm–Sidak test). **(F)** The representative real-time analysis of $I_{holding}$ in neurons from the rats that received control-siRNA combined with injection of CFA. SP-evoked $I_{holding}$ was recorded at holding potential of –60 mV. L703606 (10 μM) blocked SP-evoked $I_{holding}$. **(G)** The $I_{holding}$ in spinal dorsal horn neurons of control siRNA-treated rats was analyzed before and after perfusion of SP and L703606. **(H)** The representative real-time analysis of $I_{holding}$ in neurons from the rats that received NALCN-siRNA combined with injection of CFA. SP-evoked $I_{holding}$ was recorded at holding potential of –60 mV. L703606 (10 μM) blocked SP-evoked $I_{holding}$. **(I)** The $I_{holding}$ in spinal dorsal horn neurons of NALCN siRNA-treated rats was analyzed before and after perfusion of SP and L703606. **(J)** SP-evoked $I_{holding}$ increased more in the spinal cord neurons of CFA-ipsi side than those of CFA-contra side from the control-siRNA-treated rats; treatment of NALCN-siRNA diminished the difference in SP-evoked $I_{holding}$ between CFA-ipsi and CFA-contra side (n = 8–9, by two-way ANOVA, Holm–Sidak test). **(K)** Representative real-time analysis of Gd^{3+}-inhibited $I_{holding}$ in neurons of dorsal spinal cord from the rats that received control-siRNA combined with injection of CFA. **(L)** The $I_{holding}$ in neurons of dorsal spinal cord of control siRNA-treated rats was analyzed before and after perfusion of Gd^{3+}. **(M)** Representative real-time analysis of Gd^{3+}-inhibited $I_{holding}$ in neurons of dorsal spinal cord from the rats that received NALCN-siRNA combined with injection of CFA. **(N)** The $I_{holding}$ in neurons of dorsal spinal cord of NALCN siRNA-treated rats was analyzed before and after perfusion of Gd^{3+}. **(O)** Gd^{3+}-inhibited $I_{holding}$ increased more in neurons of dorsal spinal cord of CFA-ipsi side than those of CFA-contra side from control siRNA-treated rats, but no difference was shown between CFA-ipsi side and CFA-contra side from the NALCN-siRNA-treated rats (n = 9, by two-way ANOVA, Holm–Sidak test). CFA-contra: CFA-contralateral side; CFA-ipsi: CFA-ipsilateral side; DRG: dorsal root ganglion; CTL: control, before perfusion of SP or Gd^{3+}; RMP: rest membrane potential. Data are present as mean ± SD. $^{**}p < 0.01$, $^{***}p < 0.001$, n.s.: no significance.

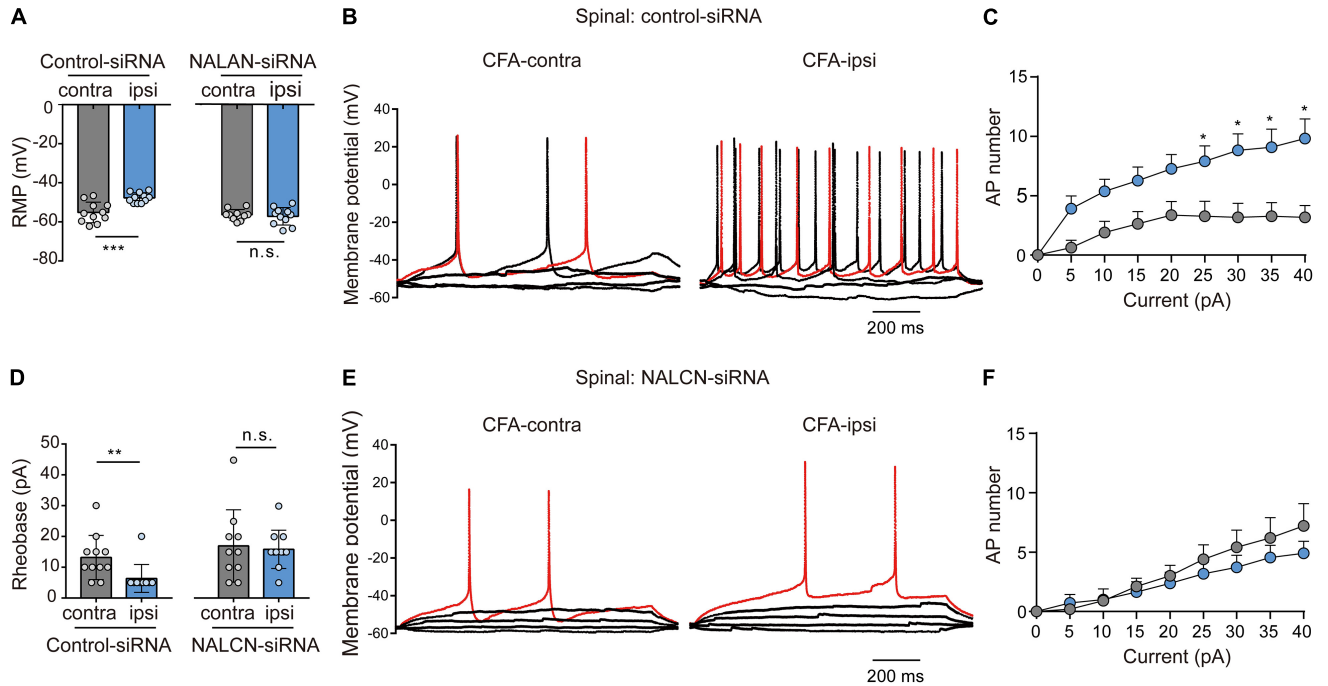

FIGURE 7 | Sodium leak channel enhances the excitability of sensory neurons of spinal dorsal horn after injection of CFA. **(A,D)** Excitability of spinal neurons compared between CFA-contralateral and CFA-ipsilateral sides based on RMP and rheobase from the rats that received control-siRNA and/or NALCN-siRNA combined with injection of CFA (n = 11, unpaired t-test; n = 11, Mann–Whitney U test, unpaired t-test, respectively). **(B,E)** Representative traces of action potentials in the neurons of spinal dorsal horn from the rats that received control-siRNA and/or NALCN-siRNA combined with injection of CFA. Red trace was the action potentials when receiving the same current injection. **(C,F)** Numbers of APs increased more in spinal dorsal horn neurons of CFA-ipsi side than those of CFA-contra side from control siRNA-treated rats [**(C)**, n = 12, by two-way ANOVA, Holm–Sidak test], but no difference was shown between CFA-ipsi side and CFA-contra sides from the NALCN-siRNA-treated rats [**(F)**, n = 14, by two-way ANOVA, Holm–Sidak test, respectively]. CFA-contra: CFA-contralateral side; CFA-ipsi: CFA-ipsilateral side; RMP: rest membrane potential. Data are present as mean ± SD. $^{*}p < 0.05$, $^{**}p < 0.01$, $^{***}p < 0.001$, n.s.: no significance.

of NALCN-siRNA compared with preinjection of control-siRNA-treated rats. The therapeutic effects of NALCN-siRNA lasted until day 3 after the CFA injection. Preinjection of the NK1 receptor antagonist L703606 also reduced spontaneous pain (**Figure 8H**, n = 10, $p < 0.05$), thermal hyperalgesia (**Figure 8I**, n = 10, $p < 0.05$), and mechanical allodynia (**Figure 8J**, n = 10, $p < 0.05$) until day 2 in the rats compared with preinjection of vehicle rats. However, L703606 did not further alleviate spontaneous pain (**Figure 8H**, n = 10, $p > 0.05$), thermal hyperalgesia (**Figure 8I**, n = 10, $p > 0.05$) or mechanical allodynia (**Figure 8J**, n = 10, $p > 0.05$) in rats that had received NALCN-siRNA.

The degradation of NALCN-siRNA is fast, and the action time of NALCN-siRNA is short after injection. To test the role of NALCN in maintenance of CFA-induced pain, pAAV2-H1-shRNA-(NALCN)-CAG-eGFP (AAV-NALCN-shRNA) or pAAV2-scrambled-CAG-eGFP (AAV-scrambled-shRNA) virus was injected into DRG and subarachnoid space of adult rats (**Figure 8K**). The NALCN mRNA level was also significantly

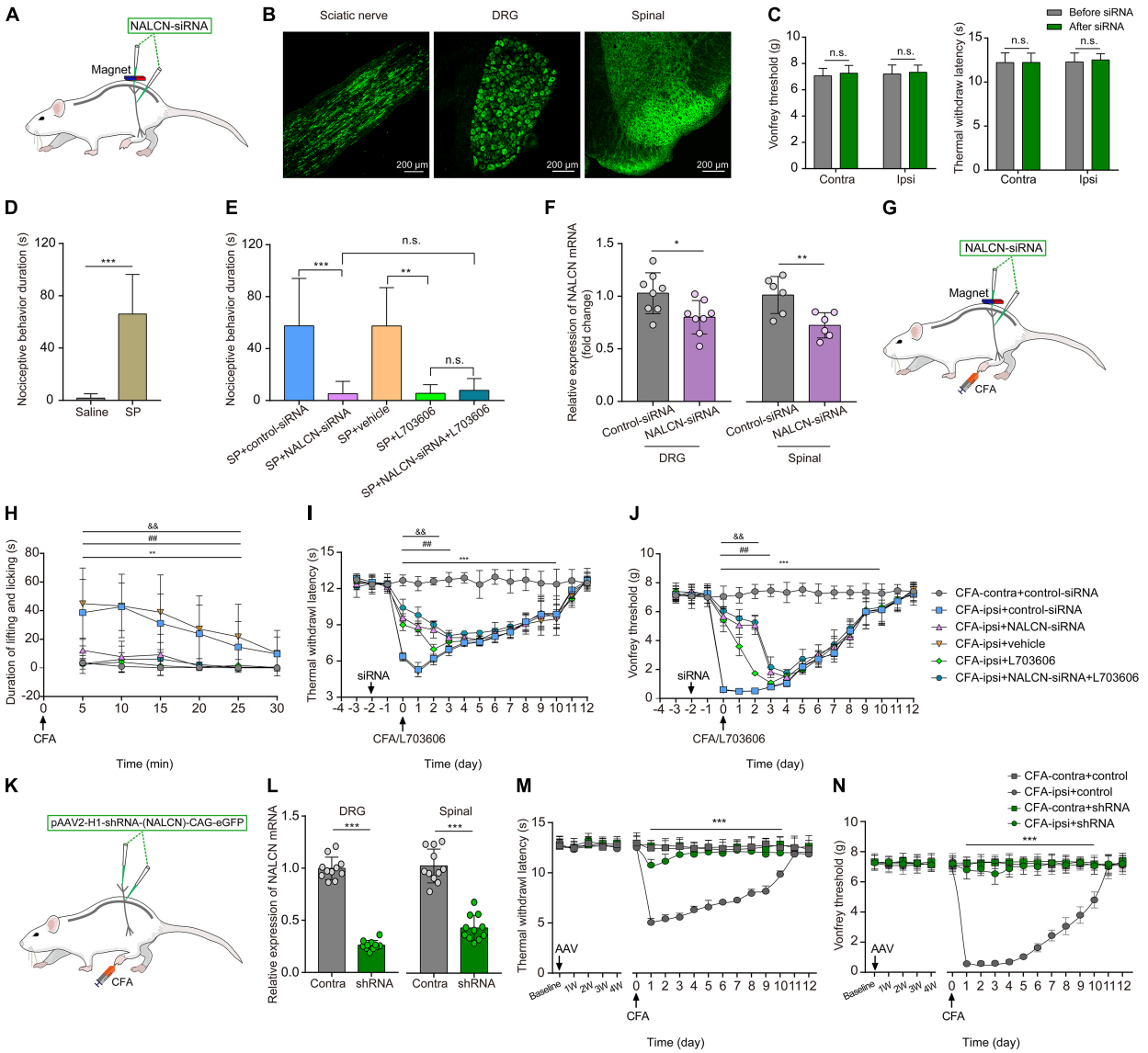

FIGURE 8 | The knockdown of expression of NALCN in DRG and spinal cord alleviates pain behaviors induced by SP or CFA. **(A)** siRNA administration methods used in adult rats. NALCN-siRNA and/or control-siRNA were intrathecally and intraneurally injected into the subarachnoid space and sciatic nerve in adult rats. **(B)** Alexa Fluor 488-positive fluorescence was found in sciatic nerve, DRG, and spinal dorsal cord after injection of NALCN-siRNA. **(C)** NALCN-siRNA did not affect the thermal hyperalgesia and mechanical allodynia of normal rats. **(D)** Intrathecal injection of SP induced pain-related behaviors in rats, including biting, licking, and scratching at the abdomen and hind portions of the body ($n = 10$, unpaired t-test). **(E)** The duration of biting, licking, and scratching within the first 5 min after injection of SP decreased in the rats that received NALCN-siRNA, L703606, siRNA + L703606 ($n = 10$, by two-way ANOVA, Holm–Sidak test). **(F)** The level of NALCN mRNA was decreased at day 3 after injection of NALCN-siRNA in DRG and spinal cord compared with control-siRNA ($n = 8$–6, unpaired t-test). **(G)** Modeling and siRNA administration methods used in adult rats. NALCN-siRNA and/or control-siRNA were intrathecally and intraneurally injected into the subarachnoid space and sciatic nerve in adult rats. **(H)** NALCN-siRNA, L703606, and siRNA + L703606 alleviated spontaneous pain behavior (lifting/licking/flinching behaviors) within the first 25 min, following CFA injection ($n = 10$, two-way repeated measures ANOVA, Holm–Sidak test). **(I)** NALCN-siRNA, L703606, and siRNA + L703606 alleviated thermal hyperalgesia at day 0–3 after CFA injection ($n = 10$, two-way repeated measures ANOVA, Holm–Sidak test). **(J)** NALCN-siRNA, L703606, and siRNA + L703606 alleviated mechanical allodynia at day 0–3 after CFA injection ($n = 10$, two-way repeated measures ANOVA, Holm–Sidak test). **(K)** Representative cartoons of pAAV2-H1-shRNA-(NALCN)-CAG-eGFP injection. **(L)** NALCN mRNA was decreased in DRG of the AAV-NALCN-shRNA group as compared with AAV-scrambled-shRNA group (left panel, $n = 11$, unpaired t-test). NALCN mRNA was decreased in dorsal spinal cord of the AAV-NALCN-shRNA group as compared with the AAV-scrambled-shRNA group (right panel, $n = 11$, unpaired t-test). **(M,N)** Normal sensory function in thermal test [**(M)**, left panel, $n = 10$] or von Frey [**(N)**, left panel, $n = 10$] was unchanged during the 4 weeks after AAV-NALCN-shRNA injection, compared with AAV-scrambled-shRNA or baseline. NALCN-shRNA alleviated thermal hyperalgesia [**(M)**, right panel, $n = 10$, CFA-ipsi + shRNA vs. CFA-ipsi + control, two-way repeated measures ANOVA, Holm–Sidak test] and mechanical allodynia [**(N)**, right panel, $n = 10$, CFA-ipsi + shRNA vs. CFA-ipsi + control, two-way repeated measures ANOVA, Holm–Sidak test] throughout after CFA, compared with scrambled shRNA. DRG: dorsal root ganglion; SP: substance P; CFA-contra: CFA-contralateral side; CFA-ipsi: CFA-ipsilateral side; ANOVA: analysis of variance. Data are presented as mean ± SD. $^{*}p < 0.05$, $^{**}p < 0.01$, $^{***}p < 0.001$ CFA-contra + control-siRNA vs. CFA-ipsi + control-siRNA; $^{\#\#}p < 0.01$ CFA-ipsi + control-siRNA vs. CFA-ipsi + NALCN-siRNA; $^{\&\&}p < 0.01$ CFA-ipsi + vehicle vs. CFA-ipsi + L703606.

decreased both in the DRG (**Figure 8L**, left, $n = 11$, $p < 0.001$) and the dorsal spinal cord (**Figure 8L**, right, $n = 11$, $p < 0.001$) by AAV-NALCN-shRNA at 4 weeks after injection. Accordingly, CFA-induced thermal hyperalgesia (**Figure 8M**, $n = 10$, $p < 0.05$) and mechanical allodynia (**Figure 8N**, $n = 10$, $p < 0.05$) were prevented throughout by the AAV-NALCN-shRNA but not the AAV-scrambled-shRNA.

DISCUSSION

The present study suggests that increased expression and function of NALCN in the DRG and spinal dorsal horn were associated with the behavioral hyperalgesia induced by inflammatory pain. The knockdown of NALCN expression relieved CFA-induced pain behaviors and suppressed the excitability of sensory neurons in the DRG and spinal cord. Our findings indicate that NALCN regulates the excitability of sensory neurons and thus may cause inflammatory pain. Therefore, NALCN is suggested to be a potential molecular target for the control of inflammatory pain. Considering the important functions of NALCN in neuronal rhythms, such as respiration, peripherally restricted NALCN blockers might be a novel potential therapy for inflammatory pain.

Despite the fundamental roles of the DRG and spinal dorsal horn neurons in inflammatory pain, it is still poorly known about the ionic mechanisms that modulate neuronal excitability after inflammation. Sensitization of nociceptive neurons by enhancing the activity of various ion channels can contribute to inflammatory pain (Djouhri et al., 2015; Bennett et al., 2019; Hu et al., 2019; Pitake et al., 2019). Here, we have demonstrated that NALCN enhanced the intrinsic excitability of sensory neurons of the DRG and spinal dorsal horn. Similarly, in other studies, NALCN produced a small background leak Na^+ current that affected the RMP and regulated neuronal excitability and rhythmic behaviors (Lu et al., 2007; Lu and Feng, 2012; Xie et al., 2013). NALCN increased neuronal excitability and modulated a number of physiological functions, including respiratory rhythms in mice (Lu et al., 2007), locomotion of *C. elegans* (Jospin et al., 2007; Yeh et al., 2008), hypotonia, growth retardation, and the intellectual disability of NALCN mutant children (Cochet-Bissuel et al., 2014; Fukai et al., 2016; Campbell et al., 2018). Ford et al. (2018) reported that NALCN may contribute to neuronal excitability of spinal projection neurons. Additionally, the *C. elegans* NALCN gene, NCA-1, controls the thermal sensitivity of thermo-nociceptor and NCA-2 functions in thermal sensitivity, sensory gain maintenance, and signal kinetics during thermal stimuli termination (Saro et al., 2020). Eigenbrod et al. (2019) showed that highveld mole-rat cells that expressed the NALCN gene produced a depolarized RMP to about −20 mV, which may induce a state unresponsive to normal stimuli. In the present study, relatively small upregulation of NALCN can also lead to depolarization of the RMP by ∼5 mV, which can cause a hyperactive state. Overall, all these studies have provided evidence that NALCN in nociceptors might play a key function in pain processing.

Sodium leak channel and SP are widely expressed and distributed in the DRG and spinal dorsal horn neurons. Lu et al. (2009) reported that SP activated NALCN in the neurons of ventral tegmental area and the hippocampus. Furthermore, SP modulated the stability of the respiratory network and retrotrapezoid nucleus network activity in a NALCN-dependent manner (Yeh et al., 2017). Kim et al. (2012) found that activation of NALCN by SP caused depolarized pacemaking activity in interstitial cells of Cajal. SP is a peptide, produced in peptidergic neurons of the DRG and spinal dorsal horn, which modulates transmission of nociceptive signals (PERNOW, 1953). Spinal dorsal horn neurons also express the NK1 receptor (PERNOW, 1953; Todd, 2002), and the secretion of SP is increased during inflammation. SP increases neuronal excitability through action at NK1 receptors and elicits pain (Navratilova and Porreca, 2019). Like the findings of other studies, we found that SP elicited acute pain-related behaviors after intrathecal injection (Dobry et al., 1981; Share and Rackham, 1981; Partridge et al., 1998; Hua et al., 1999). However, what is the critical target responsible for SP-induced aversive behaviors? Here, we have shown that the pain-related behaviors induced by intrathecal injection of SP were greatly alleviated after the knockdown of the expression of NALCN. Thus, NALCN may be an important molecular target triggering SP-induced aversive behaviors. Our electrophysiology recordings showed that SP-activated NALCN currents were blocked by NK1 receptor antagonist in spinal dorsal horn neurons. These data are in line with the study by Lu et al. in which SP was shown to enhance NALCN conductance via the NK1 receptor (Lu et al., 2009). Our results here show that SP inhibitor and/or NALCN-siRNA produced similar effects for pain relief. Because SP inhibitor was intrathecally injected, therefore, the actions of SP inhibitor or NALCN-siRNA were likely due to a transsynaptic effect of SP from DRG to spinal neurons. Overall, our findings have demonstrated that NALCN is an important background channel for modulating neuronal excitability and is a downstream target for SP-evoked signaling of inflammatory pain. However, further studies are needed to split the changes between NALCN and NK1 receptors and test their specific contribution during inflammatory pain.

Because it is difficult to patch spinal slices of adult animals, we chose to do electrophysiology analysis in the neonate rats. By this design, we can use the rats for both DRG and spinal cord recordings. We also recorded DRG neurons from the adult rats, which is technically available. However, it should be noticed that the physiological function within the sensory circuitry changes with development and the comparison of the recordings from single-isolated DRG neurons at different ages cannot directly apply to the recordings made in the spinal cord. Here, we have proved that NALCN was widely expressed in DRG and spinal cord at both neonatal and adult rats; and NALCN expression was increased in DRG and spinal cord at both ages after CFA injection. All these facts suggests that the comparation between adult and neonatal rats is comparable. Therefore, although electrophysiological recordings in spinal cord slices and *in vivo* therapeutic experiments were not performed in the same rats, the conclusions were deemed reliable.

Small interfering RNA is rapidly effective, but its action duration is short. In our therapeutic experiments, the effects of NALCN-siRNA persisted for 4 days after injection and then the pain behaviors reproduced, most likely because of the degradation of the siRNA. Because the therapeutic efficacy of NALCN-siRNA lasted for ∼3 days, rats at postnatal day 7 were injected with NALCN-siRNA and subsequently injected with CFA3 days later. Then, activity of neurons in the DRG and spinal cord dorsal horn was assayed at 8 and 24 h after CFA injection. Notably, the knockdown of NALCN expression did not change baseline sensory thresholds before injection of CFA, which indicated that baseline NALCN currents in a physiological state might be small and may not have affected normal sensation. Alternatively, the efficacy of the NALCN-siRNA knockdown in the present study may not have been sufficient to change normal sensation. However, NALCN currents were increased after the injection of CFA, and the difference was diminished after treatment of NALCN-siRNA, which indicated that NALCN was probably a target for inflammatory pain.

Western blotting was further used to confirm the change of the NALCN expression level in our study; therefore, the choice of time points for testing the NALCN protein expression was according to the PCR results. In the DRG, the relative mRNA level of NALCN from the CFA-ipsilateral side was significantly increased at 2 h, 8 h, and reached the highest level at 8 h after CFA injection. Therefore, NALCN protein was tested at the 8 h after CFA injection in DRG. For the spinal cord, the relative mRNA level of NALCN from the CFA-ipsilateral side was significantly increased at 2 h, 8 h, 1 day, 3 days, and reached the highest levels at 1 and 3 days after CFA injection; therefore, NALCN protein was evaluated at the 3-day time point after CFA injection in spinal cord.

Our experimental protocols used for recording the NALCN current are according to the previous studies (Yang et al., 2020; Zhang et al., 2021), which are currently the most commonly used. Briefly, extracellular Na^+ was replaced by NMDG to determine NALCN-mediated background currents, although this cannot completely rule out other Na^+ currents or other cation currents mediated by NALCN due to our experimental design. Moreover, because of no specific modulators, substances P and Gd^{3+} are widely used as the activator and inhibitor of NALCN conductance, respectively. Nevertheless, we used the siRNA-mediated knockdown of NALCN to further determine the role of NALCN-mediated background currents. In summary, these protocols are typically used to measure NALCN currents.

In this study, we did not use Ca^{2+} channel blockers in patch-clamp recording because the Ca^{2+} channel antagonist is suggested to be a potent blocker of NALCN (Eigenbrod et al., 2019), which may disturb the recording. Besides, Ca_v channels were typically activated within the membrane voltage between −40 and +40 mV (Pan et al., 2014; Leo et al., 2017), while, in this study, NALCN currents were mainly recorded at a holding potential of −60 mV. Perhaps, for the same reason, there were also no Ca_v blockers used for NALCN currents recordings in previous studies (Lu et al., 2009; Yang et al., 2020; Zhang et al., 2021). However, the low-voltage T-type channels Ca2 + currents, which can be activated from −60 mV, may not be completely ruled out due to our experimental design. For NMDA receptors, it is better to add the NMDA receptor blockers when recording neuronal intrinsic excitability. It is commonly known that NMDAR-mediated excitatory postsynaptic currents were recorded at +40 mV (significant depolarization) in the presence of Mg^{2+} or in the absence of Mg^{2+} (Chen et al., 2016; Ferreira et al., 2017). In our protocol here, the membrane test was recorded at −60 mV with 2 mM Mg^{2+}; therefore, it was unlikely to be affected by NMDA receptors even without NMDA blockers in the recording of isolated DRG neurons. However, voltage clamping may not be consistent along with the axon in the spinal cord slices; therefore, only membrane potential cannot fully exclude NMDAR contribution in this network. However, although no Ca^{2+} channel blockers and NMDA receptor blockers were used, we believe that our conclusions make sense by NALCN-siRNA to knockdown the NALCN mRNA. The comparison results between control siRNA and NALCN-siRNA should be contributed by NALCN, although other ion channels and/or receptors can still contribute to both conditions.

In **Figure 2C**, we aimed to show a morphological profile of NALCN expression in DRG. The results indicated that NALCN was widely expressed in almost all neurons. Therefore, we did not quantify the NALCN fluorescence intensity here because it may be not accurate. Instead, we combined PCR and Western blotting to fully access the expressional level of NALCN. As a result, we did not know the expressional level of NALCN in neuronal subtypes. Also, it may be not necessary to determine the percentage of NALCN positive neurons in different sizes of DRG neurons, because NALCN was present in almost all DRG neurons. Moreover, it is difficult to quantitatively evaluate the difference of the NALCN between different spinal laminae only by immunostaining (e.g., **Figure 2D**). Future studies that used genetic mice may well determine contribution of NALCN in neuronal subtypes to inflammatory pain.

The present study also has several limitations. Because global NALCN knockout mice cannot survive for behavioral tests, we did not use NALCN knockout mice. Further studies with conditional NALCN knockout mice may better evaluate the function of NALCN in inflammatory pain. In addition, we did not determine which subtype of neurons in the DRG and/or spinal dorsal horn directly accounts for inflammatory pain. Finally, we did not investigate whether NALCN modulates the SP expression in the DRG and/or spinal dorsal horn after inflammatory pain. The underlying interaction between SP expression and NALCN function needs to be further determined.

In summary, this study demonstrated that NALCN is a pivotal ion channel involved in CFA-induced inflammatory pain and neuronal sensitization. Peripheral NALCN may be an effective therapeutic target for inflammatory pain.

DATA AVAILABILITY STATEMENT

The original contributions presented in the study are included in the article/**Supplementary Material**, further inquiries can be directed to the corresponding authors.

ETHICS STATEMENT

The animal study was reviewed and approved by the Animal Ethics Committee of West China Hospital of Sichuan University (Chengdu, Sichuan, China) (Approval No. 2018181A).

AUTHOR CONTRIBUTIONS

CZ, PL, YZ, and JinL designed the research. JiaL and YC performed the research. DZ, PLL, and JS analyzed the data. JiaL, YC, CM, and CZ wrote the manuscript. All authors read and approved the final manuscript.

FUNDING

This work was supported by the National Key Research and Development Program of China (Project Nos. 2020YFC2008400 and 2020YFC2008402) (CZ); Grant Nos. 81974164 (CZ) and 81801117 (PLL) from the National Natural Science Foundation of China (Beijing, China); and 1, 3, 5 Project for Excellence of West China Hospital (Zy2016101).

SUPPLEMENTARY MATERIAL

The Supplementary Material for this article can be found online at: https://www.frontiersin.org/articles/10.3389/fnmol.2021.723395/full#supplementary-material

Supplementary Figure 1 | Co-staining of NALCN (red) and SP (green) in spinal dorsal horn after injection of CFA. SP: substance P.

Supplementary Figure 2 | The specificity of the NALCN primary antibody was confirmed by Western blotting and fluorescence staining. **(A)** The specificity of the NALCN primary antibody was confirmed by Western blotting. The tissue of spinal dorsal horn was used. Left: spinal dorsal horn was incubated with the NALCN primary antibody. Right: spinal dorsal horn was preincubated with NALCN antigen before the NALCN primary antibody. No specific protein bands were found after preincubation with the NALCN antigen. **(B)** The specificity of the NALCN primary antibody was confirmed by fluorescence staining. The tissue of DRG was used. Left: DRG was incubated with the NALCN primary antibody in the control-siRNA group. Middle: DRG was preincubated with the NALCN antigen before the NALCN primary antibody in the control-siRNA group. No specific staining was observed. Right: DRG was incubated with the NALCN primary antibody in the NALCN-siRNA group. After NALCN-siRNA treatment, the NALCN fluorescence intensity was weaker compared with control-siRNA-treated animals. **(C)** The specificity of the NALCN primary antibody was confirmed by fluorescence staining. The tissue of spinal dorsal horn was used. Left: spinal dorsal horn was incubated with the *n*'s NALCN primary antibody in the control-siRNA group. Middle: spinal dorsal horn was preincubated with the NALCN antigen before the NALCN primary antibody in the control-siRNA group. Right: spinal dorsal horn was incubated with the NALCN primary antibody in the NALCN-siRNA group. After NALCN-siRNA treatment, the NALCN fluorescence intensity was weaker compared with control-siRNA-treated animals. DRG: dorsal root ganglion.

Supplementary Figure 3 | Gd^{3+}-mediated current inhibition and that produced by siRNA. **(A)** Gd^{3+}-mediated current inhibition and that produced by siRNA in adult rats DRG (n = 9, by unpaired t-test). **(B)** Gd^{3+}-mediated current inhibition and that produced by siRNA in PD10 rats DRG (n = 9, by Mann–Whitney U test). **(C)** Gd^{3+}-mediated current inhibition and that produced by siRNA in the spinal cord of PD10 rats (n = 9, by unpaired t-test). siRNA: NALCN-siRNA. n.s.: no significance.

Supplementary Figure 4 | The relative expression of NALCN mRNA in DRG and/or spinal dorsal horn in neonatal rats after injection of CFA (refer to **Figures 4–7**). **(A)** Similar to adult rats, the level of NALCN mRNA in CFA-ipsilateral side was increased in both DRG (8 h later, n = 9, by paired t-test) and spinal cord (1 day later, n = 9, by paired t-test) after injection of CFA in footpad. **(B)** Compared to the rats that received control-siRNA, levels of NALCN mRNA were lower in DRG (n = 12, by paired t-test) and/or spinal cord (n = 11, by Mann–Whitney U test) at day 3 after injection of NALCN-siRNA. CFA-contra: CFA-contralateral side; CFA-ipsi: CFA-ipsilateral side; DRG: dorsal root ganglion; data are presented as mean ± SD. $^{*}p < 0.05$, $^{**}p < 0.01$, $^{***}p < 0.001$.

Supplementary Figure 5 | Sodium leak channel does not enhance the excitability of large-sized DRG neurons after CFA injection in neonatal rats. **(A,D)** Excitability of large neurons in DRG was compared between CFA-contralateral and CFA-ipsilateral sides based on RMP and rheobase from the rats that received control-siRNA and/or NALCN-siRNA combined with injection of CFA (n = 13, Mann–Whitney U test). **(B,E)** Action potential in the large neurons of DRG from the rats that received control-siRNA and/or NALCN-siRNA combined with injection of CFA. Red trace is the action potential when receiving the same current injection. **(C,F)** Numbers of APs increased more in small and medium DRG neurons of CFA-ipsi side than those of CFA-contra side from control siRNA-treated rats [**(C)**, n = 13, by two-way ANOVA, Holm–Sidak test], but no difference was shown between CFA-ipsi side and CFA-contra side from the NALCN-siRNA-treated rats [**(F)**, n = 13, by two-way ANOVA, Holm–Sidak test], respectively. CFA-contra: CFA-contralateral side; CFA-ipsi: CFA-ipsilateral side; DRG: dorsal root ganglion; RMP: rest membrane potential; AP: action potential. Data are presented as mean ± SD or median (first quartile-third quartile). $^{*}p < 0.05$, $^{**}p < 0.01$, $^{***}p < 0.001$, n.s.: no significance.

REFERENCES

Amsalem, M., Poilbout, C., Ferracci, G., Delmas, P., and Padilla, F. (2018). Membrane cholesterol depletion as a trigger of Nav1.9 channel-mediated inflammatory pain. *EMBO J.* 37:e97349.

Andoh, T., Nagasawa, T., and Kuraishi, Y. (1996). Expression of tachykinin NK1 receptor mRNA in dorsal root ganglia of the mouse. *Brain Res. Mol. Brain Res.* 35, 329–332. doi: 10.1016/0169-328x(95)00244-m

Bend, E. G., Si, Y., Stevenson, D. A., Bayrak-Toydemir, P., Newcomb, T. M., Jorgensen, E. M., et al. (2016). NALCN channelopathies: Distinguishing gain-of-function and loss-of-function mutations. *Neurology* 87, 1131–1139. doi: 10.1212/wnl.0000000000003095

Bennett, D., Clark, A., Huang, J., Waxman, S., and Dib-Hajj, S. (2019). The role of voltage-gated sodium channels in pain signaling. *Phys. Rev.* 99, 1079–1151. doi: 10.1152/physrev.00052.2017

Campbell, j, fitzpatrick, D., Azam, T., Gibson, N., Somerville, L., Joss, S., et al. (2018). NALCN dysfunction as a cause of disordered respiratory rhythm with central apnea. *Pediatrics* 141, S485–S490.

Cang, C., Zhang, H., Zhang, Y., and Zhao, Z. (2009). PKCepsilon-dependent potentiation of TTX-resistant Nav1.8 current by neurokinin-1 receptor activation in rat dorsal root ganglion neurons. *Mol. Pain* 5:33.

Carter, G., Duong, V., Ho, S., Ngo, K., Greer, C., and Weeks, D. (2014). Side effects of commonly prescribed analgesic medications. *Phys. Med. Rehabil. Clin. North Am.* 25, 457–470. doi: 10.1016/j.pmr.2014.01.007

Chalermpalanupap, T., Schroeder, J. P., Rorabaugh, J. M., Liles, L. C., Lah, J. J., Levey, A. I., et al. (2018). Locus coeruleus ablation exacerbates cognitive deficits, neuropathology, and lethality in P301S tau transgenic mice. *J. Neurosci.* 38, 74–92. doi: 10.1523/jneurosci.1483-17.2017

Chen, G., Xie, R., Gao, Y., Xu, Z., Zhao, L., Bang, S., et al. (2016). β-arrestin-2 regulates NMDA receptor function in spinal lamina II neurons and duration of persistent pain. *Nat. Commun.* 7:12531.

Cochet-Bissuel, M., Lory, P., and Monteil, A. (2014). The sodium leak channel, NALCN, in health and disease. *Front. Cell. Neurosci.* 8:132. doi: 10.3389/fncel.2014.00132

Dixon, W. (1991). Staircase bioassay: the up-and-down method. *Neurosci. Biobehav. Rev.* 15, 47–50. doi: 10.1016/s0149-7634(05)80090-9

Djouhri, L., Otaibi, M. A., Kahlat, K., Smith, T., Sathish, J., and Weng, X. (2015). Persistent hindlimb inflammation induces changes in activation properties of hyperpolarization-activated current (Ih) in rat C-fiber nociceptors in vivo. *Neuroscience* 301, 121–133. doi: 10.1016/j.neuroscience.2015.05.074

Dobry, P., Piercey, M., and Schroeder, L. (1981). Pharmacological characterization of scratching behaviour induced by intracranial injection of substance P and somatostatin. *Neuropharmacology* 20, 267–272. doi: 10.1016/0028-3908(81)90132-5

Eigenbrod, O., Debus, K., Reznick, J., Bennett, N., Sánchez-Carranza, O., Omerbašić, D., et al. (2019). Rapid molecular evolution of pain insensitivity in multiple African rodents. *Science* 364, 852–859. doi: 10.1126/science.aau0236

Ferreira, J., Papouin, T., Ladépêche, L., Yao, A., Langlais, V., Bouchet, D., et al. (2017). Co-agonists differentially tune GluN2B-NMDA receptor trafficking at hippocampal synapses. *eLife* 6:e25492.

Flourakis, M., Kula-Eversole, E., Hutchison, A., Han, T., Aranda, K., Moose, D., et al. (2015). A conserved bicycle model for circadian clock control of membrane excitability. *Cell* 162, 836–848. doi: 10.1016/j.cell.2015.07.036

Ford, N., Ren, D., and Baccei, M. (2018). NALCN channels enhance the intrinsic excitability of spinal projection neurons. *Pain* 159, 1719–1730. doi: 10.1097/j.pain.0000000000001258

Fukai, R., Saitsu, H., Okamoto, N., Sakai, Y., Fattal-Valevski, A., Masaaki, S., et al. (2016). De novo missense mutations in NALCN cause developmental and intellectual impairment with hypotonia. *J. Hum. Genet.* 61, 451–455. doi: 10.1038/jhg.2015.163

Gao, S., Xie, L., Kawano, T., Po, M., Guan, S., Zhen, M., et al. (2015). The NCA sodium leak channel is required for persistent motor circuit activity that sustains locomotion. *Nat. Commun.* 6:6323.

Goldberg, D., and McGee, S. (2011). Pain as a global public health priority. *BMC Public Health* 11:770. doi: 10.1186/1471-2458-11-770

Herrmann, S., Rajab, H., Christ, I., Schirdewahn, C., Höfler, D., Fischer, M., et al. (2017). Protein kinase A regulates inflammatory pain sensitization by modulating HCN2 channel activity in nociceptive sensory neurons. *Pain* 158, 2012–2024. doi: 10.1097/j.pain.0000000000001005

Hökfelt, T., Kellerth, J., Nilsson, G., and Pernow, B. (1975). Substance p: localization in the central nervous system and in some primary sensory neurons. *Science* 190, 889–890. doi: 10.1126/science.242075

Hu, F., Liu, H., Su, D., Chen, H., Chan, S., Wang, Y., et al. (2019). Nogo-A promotes inflammatory heat hyperalgesia by maintaining TRPV-1 function in the rat dorsal root ganglion neuron. *FASEB J.* 33, 668–682. doi: 10.1096/fj.201800382rr

Hua, X., Chen, P., Marsala, M., and Yaksh, T. (1999). Intrathecal substance P-induced thermal hyperalgesia and spinal release of prostaglandin E2 and amino acids. *Neuroscience* 89, 525–534. doi: 10.1016/s0306-4522(98)00488-6

Jospin, M., Watanabe, S., Joshi, D., Young, S., Hamming, K., Thacker, C., et al. (2007). UNC-80 and the NCA ion channels contribute to endocytosis defects in synaptojanin mutants. *Curr. Boil.* 17, 1595–1600. doi: 10.1016/j.cub.2007.08.036

Kim, B., Chang, I., Choi, S., Jun, J., Jeon, J., Xu, W., et al. (2012). Involvement of Na(+)-leak channel in substance P-induced depolarization of pacemaking activity in interstitial cells of Cajal. *Cell. Physiol. Biochem.* 29, 501–510. doi: 10.1159/000338504

Kumar, M., Ojha, S., Rai, P., Joshi, A., Kamat, S. S., and Mallik, R. (2019). Insulin activates intracellular transport of lipid droplets to release triglycerides from the liver. *J. Cell. Biol.* 218, 3697–3713. doi: 10.1083/jcb.201903102

Lapointe, T., Basso, L., Iftinca, M., Flynn, R., Chapman, K., Dietrich, G., et al. (2015). TRPV1 sensitization mediates postinflammatory visceral pain following acute colitis. *Am. J. Physiol. Gastrointest. Liver Physiol.* 309, G87–G99.

Leo, M., Schmitt, L., Erkel, M., Melnikova, M., Thomale, J., and Hagenacker, T. (2017). Cisplatin-induced neuropathic pain is mediated by upregulation of N-type voltage-gated calcium channels in dorsal root ganglion neurons. *Exper. Neurol.* 288, 62–74. doi: 10.1016/j.expneurol.2016.11.003

Lozic, B., Johansson, S., Kojundzic, S. L., Markic, J., Knappskog, P., Hahn, A., et al. (2016). Novel NALCN variant: altered respiratory and circadian rhythm, anesthetic sensitivity. *Ann. Clin. Transl. Neurol.* 3, 876–883. doi: 10.1002/acn3.362

Lu, B., Su, Y., Das, S., Liu, J., Xia, J., and Ren, D. (2007). The neuronal channel NALCN contributes resting sodium permeability and is required for normal respiratory rhythm. *Cell* 129, 371–383. doi: 10.1016/j.cell.2007.02.041

Lu, B., Su, Y., Das, S., Wang, H., Wang, Y., Liu, J., et al. (2009). Peptide neurotransmitters activate a cation channel complex of NALCN and UNC-80. *Nature* 457, 741–744. doi: 10.1038/nature07579

Lu, T., and Feng, Z. (2012). NALCN: a regulator of pacemaker activity. *Mol. Neurobiol.* 45, 415–423. doi: 10.1007/s12035-012-8260-2

Man, S., Géranton, S., and Hunt, S. (2012). Lamina I NK1 expressing projection neurones are functional in early postnatal rats and contribute to the setting up of adult mechanical sensory thresholds. *Mol. Pain* 8, 35.

Mehta, T. (2007). Fundamental problem with opioid trials for chronic pain. *Can. Med. Assoc. J.* 176, 1307–1308. doi: 10.1503/cmaj.1060140

Navratilova, E., and Porreca, F. (2019). Substance P and inflammatory pain: getting it wrong and right simultaneously. *Neuron* 101, 353–355. doi: 10.1016/j.neuron.2019.01.034

Ou, M., Zhao, W., Liu, J., Liang, P., Huang, H., Yu, H., et al. (2020). The general anesthetic isoflurane bilaterally modulates neuronal excitability. *iScience* 23:100760. doi: 10.1016/j.isci.2019.100760

Pan, B., Guo, Y., Kwok, W., Hogan, Q., and Wu, H. (2014). Sigma-1 receptor antagonism restores injury-induced decrease of voltage-gated Ca2+ current in sensory neurons. *J. Pharmacol. Exper. Therapeutics* 350, 290–300. doi: 10.1124/jpet.114.214320

Partridge, B., Chaplan, S., Sakamoto, E., and Yaksh, T. (1998). Characterization of the effects of gabapentin and 3-isobutyl-gamma-aminobutyric acid on substance P-induced thermal hyperalgesia. *Anesthesiology* 88, 196–205. doi: 10.1097/00000542-199801000-00028

PERNOW, B. (1953). Distribution of substance P in the central and peripheral nervous system. *Nature* 171:746. doi: 10.1038/171746a0

Pitake, S., Middleton, L., Abdus-Saboor, I., and Mishra, S. (2019). Inflammation induced sensory nerve growth and pain hypersensitivity requires the N-Type calcium channel Cav2.2. *Front. Neurosci.* 13:1009. doi: 10.3389/fnins.2019.01009

Ren, D. (2011). Sodium leak channels in neuronal excitability and rhythmic behaviors. *Neuron* 72, 899–911. doi: 10.1016/j.neuron.2011.12.007

Rivat, C., Sar, C., Mechaly, I., Leyris, J., Diouloufet, L., Sonrier, C., et al. (2018). Inhibition of neuronal FLT3 receptor tyrosine kinase alleviates peripheral neuropathic pain in mice. *Nat. Commun.* 9:1042.

Saro, G., Lia, A., Thapliyal, S., Marques, F., Busch, K., and Glauser, D. (2020). Specific ion channels control sensory gain, sensitivity, and kinetics in a tonic thermonociceptor. *Cell. Rep.* 30, 397–408. doi: 10.1016/j.celrep.2019.12.029

Sculptoreanu, A., Artim, D., and Groat, W. D. (2009). Neurokinins inhibit low threshold inactivating K+ currents in capsaicin responsive DRG neurons. *Exper. Neurol.* 219, 562–573. doi: 10.1016/j.expneurol.2009.07.016

Share, N., and Rackham, A. (1981). Intracerebral substance P in mice: behavioral effects and narcotic agents. *Brain Res.* 211, 379–386. doi: 10.1016/0006-8993(81)90709-5

Todd, A. (2002). Anatomy of primary afferents and projection neurones in the rat spinal dorsal horn with particular emphasis on substance P and the neurokinin 1 receptor. *Exper. Physiol.* 87, 245–249. doi: 10.1113/eph8702351

Weinblatt, M. (1991). Nonsteroidal anti-inflammatory drug toxicity: increased risk in the elderly. *Scand. J. Rheumatol. Suppl.* 91, 9–17. doi: 10.3109/03009749109096946

Xie, L., Gao, S., Alcaire, S., Aoyagi, K., Wang, Y., Griffin, J., et al. (2013). NLF-1 delivers a sodium leak channel to regulate neuronal excitability and modulate rhythmic locomotion. *Neuron* 77, 1069–1082. doi: 10.1016/j.neuron.2013.01.018

Xu, G., and Huang, L. (2002). Peripheral inflammation sensitizes P2X receptor-mediated responses in rat dorsal root ganglion neurons. *J. Neurosci.* 22, 93–102. doi: 10.1523/jneurosci.22-01-00093.2002

Yang, Y., Ou, M., Liu, J., Zhao, W., Zhuoma, L., Liang, Y., et al. (2020). Volatile anesthetics activate a leak sodium conductance in retrotrapezoid nucleus neurons to maintain breathing during anesthesia in mice. *Anesthesiology* 133, 824–838.

Yeh, E., Ng, S., Zhang, M., Bouhours, M., Wang, Y., Wang, M., et al. (2008). A putative cation channel, NCA-1, and a novel protein, UNC-80, transmit neuronal activity in C. elegans. *PLoS Biol.* 6:e55. doi: 10.1371/journal.pbio.0060055

Yeh, S., Huang, W., Wang, W., Ward, C., Chao, E., Wu, Z., et al. (2017). Respiratory network stability and modulatory response to substance P Require Nalcn. *Neuron* 94, 294–303. doi: 10.1016/j.neuron.2017.03.024

Zhang, D., Zhao, W., Liu, J., Ou, M., Liang, P., Li, J., et al. (2021). Sodium leak channel contributes to neuronal sensitization in neuropathic pain. *Prog. Neurobiol.* 202:102041. doi: 10.1016/j.pneurobio.2021.102041

Zhang, H., Cang, C., Kawasaki, Y., Liang, L., Zhang, Y., Ji, R., et al. (2007). Neurokinin-1 receptor enhances TRPV1 activity in primary sensory neurons via PKCepsilon: a novel pathway for heat hyperalgesia. *J. Neurosci.* 27, 12067–12077. doi: 10.1523/jneurosci.0496-07.2007

Zhao, X., Tang, Z., Zhang, H., Atianjoh, F., Zhao, J., Liang, L., et al. (2013). A long noncoding RNA contributes to neuropathic pain by silencing Kcna2 in primary afferent neurons. *Nat. Neurosci.* 16, 1024–1031. doi: 10.1038/nn.3438

Conflict of Interest: The authors declare that the research was conducted in the absence of any commercial or financial relationships that could be construed as a potential conflict of interest.

frontiers in Molecular Neuroscience

REVIEW
published: 23 November 2021
doi: 10.3389/fnmol.2021.760964

Roles of Long Non-coding RNAs in the Development of Chronic Pain

Zheng Li[1,2], Xiongjuan Li[1,2], Wenling Jian[1,2], Qingsheng Xue[3] and Zhiheng Liu[1,2]**

[1] Department of Anesthesiology, The First Affiliated Hospital of Shenzhen University, Shenzhen Second People's Hospital, Shenzhen, China, [2] Department of Geriatric & Spinal Pain Multi-Department Treatment, The First Affiliated Hospital of Shenzhen University, Shenzhen Second People's Hospital, Shenzhen, China, [3] Department of Anesthesiology, Ruijin Hospital, School of Medicine, Shanghai Jiao Tong University, Shanghai, China

Chronic pain, a severe public health issue, affects the quality of life of patients and results in a major socioeconomic burden. Only limited drug treatments for chronic pain are available, and they have insufficient efficacy. Recent studies have found that the expression of long non-coding RNAs (lncRNAs) is dysregulated in various chronic pain models, including chronic neuropathic pain, chronic inflammatory pain, and chronic cancer-related pain. Studies have also explored the effect of these dysregulated lncRNAs on the activation of microRNAs, inflammatory cytokines, and so on. These mechanisms have been widely demonstrated to play a critical role in the development of chronic pain. The findings of these studies indicate the significant roles of dysregulated lncRNAs in chronic pain in the dorsal root ganglion and spinal cord, following peripheral or central nerve lesions. This review summarizes the mechanism underlying the abnormal expression of lncRNAs in the development of chronic pain induced by peripheral nerve injury, diabetic neuropathy, inflammatory response, trigeminal neuralgia, spinal cord injury, cancer metastasis, and other conditions. Understanding the effect of lncRNAs may provide a novel insight that targeting lncRNAs could be a potential candidate for therapeutic intervention in chronic pain.

Keywords: long non-coding RNA, chronic neuropathic pain, chronic cancer-related pain, dorsal root ganglion, spinal cord

OPEN ACCESS

Edited by:
Xiaodong Liu,
The Chinese University of Hong Kong, Hong Kong SAR, China

Reviewed by:
Mian Peng,
Wuhan University, China
Chamini Perera,
University of New South Wales, Australia
Yu-Qing Wu,
Xuzhou Medical University, China

****Correspondence:***
Qingsheng Xue
xqs11260@rjh.com.cn
Zhiheng Liu
zhiheng_liu_tongji@163.com

Specialty section:
This article was submitted to Pain Mechanisms and Modulators, a section of the journal Frontiers in Molecular Neuroscience

Received: *19 August 2021*
Accepted: *21 October 2021*
Published: *23 November 2021*

Citation:
Li Z, Li X, Jian W, Xue Q and Liu Z (2021) Roles of Long Non-coding RNAs in the Development of Chronic Pain. Front. Mol. Neurosci. 14:760964. doi: 10.3389/fnmol.2021.760964

Abbreviations: AQP4, Aquaporin 4; BCP, bone cancer pain; BDNF, brain-derived neurotrophic factor; CCRP, chronic cancer-related pain; CCI, chronic constriction injury; CDK, cyclin-dependent kinase; ceRNA, competitive endogenous RNA; CFA, Complete Freund's Adjuvant; CGRP, calcitonin gene-related peptide; CIP, cancer-induced pain; CIPN, chemotherapy-induced peripheral neuropathy; CNP, chronic neuropathic pain; CRNDE, colorectal neoplasia differentially expressed; CRPS, complex regional pain syndrome; CXCL13, chemokine ligand 13; CXCL9, chemokine ligand 9; CXCR5, chemokine receptor 5; DGCR5, DiGeorge syndrome critical region gene 5; DILC, downregulated in liver cancer stem cells; DLEU1, deleted in lymphocytic leukemia 1; DNP, diabetic neuropathic pain; DRG, dorsal root ganglion; ELAVL1, embryonic lethal abnormal version-like RNA-binding protein 1; ERK 1/2, extracellular regulated protein kinases 1/2; exo-lncRNA H19, exosome containing lncRNA H19; FIRRE, functional intergenic repeating RNA element; GAS5, growth-arrest-specific 5; GO, Gene ontology; HMGB1, high-mobility group box 1; IL-1β, Interleukin-1β; IL-6, Interleukin-6; IL-12, Interleukin-12; JAK, Janus kinase; KCNA2-AS, KCNA antisense RNA; KEGG, Kyoto Encyclopedia of Genes and Genomes; lncRNAs, long non-coding RNAs; MALAT1, Metastasis-associated lung adenocarcinoma transcript (MALAT)1; MAPK, mitogen-activated protein kinases; MEG3, maternally expressed gene 3; miR, miRNA; NEAT1, nuclear paraspeckle assembly transcript 1; NF-κB, nuclear factor-kappaB; NO, nitric oxide; OA, osteoarthritis; $P2X_3R$, $P2X_3$ receptor; $P2X_7R$, $P2X_7$ receptor; PNI, peripheral nerve injury; PVT1, plasmacytoma variant translocation 1; SC, spinal cord; SCI, spinal cord injury; SGCs, satellite glial cells; siRNA, small interference RNA; SNHG1, small nucleolar RNA host gene 1; SNHG5, small nucleolar RNA host gene 5; SNI, spared sciatic nerve injury; SNL, spinal nerve ligation; STAT3, signal transducer and activator of transcription 3; TG, trigeminal ganglia; TN, trigeminal neuralgia; TNF-α, tumor necrosis factor; TRPV1, transient receptor potential vanilloid type 1; UCBMSCs, umbilical cord blood mesenchymal stem cells; XIST, X-inactive specific transcript; YY1, Yin-Yang 1.

INTRODUCTION

Chronic pain is an extremely prevalent healthcare issue that affects the quality of life of patients, resulting in an annual financial impact (van Hecke et al., 2014; Hamood et al., 2018). It can be generally categorized as chronic cancer-related pain or chronic non-cancer-related pain, such as chronic neuropathic pain (CNP) and chronic postsurgical or posttraumatic pain (Treede et al., 2019). Although many studies have elucidated the mechanisms underlying the development of chronic pain, only a few currently available clinical therapeutic strategies effectively alleviate pain symptoms in patients with limited unwanted side effects. Thus, it is imperative to explore novel targets for the treatment of chronic pain.

Long non-coding RNA, which consists of more than 200 nucleotides, is a non-coding RNA that lacks a complete open reading frame (Batista and Chang, 2013). Although they cannot translate into detectable proteins individually, long non-coding RNAs (lncRNAs) can play a crucial role in the expression and translation of other genes and whole gene networks by interacting with DNA, proteins, and other RNAs (Wang and Chang, 2011). Accumulating evidence indicates that lncRNAs are potent regulators of physiological and pathological processes, such as embryonic development, cancer, inflammation, and neurological diseases (Ulitsky and Bartel, 2013). Recently, many studies have identified changes in the expression and important role of lncRNAs in chronic pain models. Therefore, this review aimed to explore the roles and mechanisms of lncRNAs in the development of chronic pain, including CNP and chronic cancer-related pain (CCRP).

THE ROLE OF lncRNAs IN THE NERVOUS SYSTEM AND THE PAIN-SIGNALING PATHWAY

Dysregulated lncRNA expression has been found in damaged nerves, primary sensory dorsal root ganglion neurons, spinal cord, and postsynaptic dorsal horn after peripheral nerve lesions or spinal cord injury (SCI). Under these conditions, accumulating evidence has shown the effect of the interaction between lncRNAs and miRNAs in the development of chronic pain. As a competitive endogenous RNA (ceRNA) (Chen et al., 2017; Sun et al., 2019), lncRNAs can competitively bind miRNAs, inhibit the interaction between miRNAs and downstream genes, and regulate the transcription and expression of downstream genes. For example, lncRNA MALAT1 can sponge miR-129-5p as a ceRNA and upregulate the expression of high-mobility group box 1 (HMGB1) in the spinal cord, promoting the development of CNP (Zhao et al., 2016). lncRNA CRNDE can upregulate the expression of IL-6 receptors in chronic pain by interacting with miR-136 (Zhang et al., 2019). In addition, lncRNA Linc01119 can interact with embryonic lethal abnormal version-like RNA-binding protein 1 (ELAVL1), upregulate the expression of brain-derived neurotrophic factor (BDNF) at the mRNA and protein levels, and induce chronic pain in the spinal cord and DRG (Zhang L. et al., 2021). In summary, lncRNAs can interact with miRNA or RNA-associated proteins and regulate the different downstream mechanisms involved in chronic pain.

In addition, some lncRNAs have been reported to mediate the activation of signaling pathways (Ren et al., 2020) and participate in the development of chronic pain. lncRNA LOC100911498 small interfering RNA (siRNA) treatment can decrease the phosphorylation of the p38 pathway in the spinal cord induced by chronic pain (Tang et al., 2021). Another study suggested that activation of the ERK1/2 pathway in the DRG is regulated by lncRNA uc.48+ (Wang et al., 2016). p38 and ERK1/2 can participate in the development of chronic pain (Lin et al., 2014; Qian et al., 2019). In addition, $P2X_3$ and $P2X_7$ receptors have been found to be regulated by lncRNAs (Seino et al., 2006; Peng H. et al., 2017). The two receptors play a role in the development of chronic pain (Wu et al., 2021; Xia et al., 2021). Furthermore, the levels of pro-inflammatory factors, such as IL-1β, IL-6, IL-12, and TNF-α (Xia et al., 2018; Li Z. et al., 2020; Pan et al., 2020), have been found to change in chronic pain after lncRNA downregulation. Neuroinflammation plays a significant role in chronic pain. Thus, the effect of lncRNAs on the development of chronic pain may involve various mechanisms (**Figure 1**).

lncRNAs AND CHRONIC NEUROPATHIC PAIN

Chronic neuropathic pain (CNP), a major public health concern worldwide, affects the quality of life of 6.9–10% of the general population (van Hecke et al., 2014). CNP is characterized by spontaneous ongoing or evoked by sensory stimuli (hyperalgesia and allodynia). It is mainly observed in peripheral nerve lesions [diabetic neuropathy, peripheral nerve injury (PNI), and trigeminal neuralgia (TN)] or central nerve lesions (SCI) (Scholz et al., 2019). Various animal models of peripheral neuropathic pain and central neuropathic pain have been established to explore the mechanisms underlying the development of CNP (Tian et al., 2020; Zhang P. et al., 2021). However, the treatment of CNP remains a major challenge. Recent accumulating evidence has shown that lncRNAs are related to the development of peripheral neuropathic pain and central neuropathic pain (Liu et al., 2018; Sun et al., 2018; Tian et al., 2020; Xu et al., 2020).

lncRNAs and Peripheral Neuropathic Pain

lncRNAs and Peripheral Nerve Injury

Peripheral nerve injury, which induces CNP, is a common clinical cause of peripheral nerve lesions. PNI can cause excitability of the primary sensory ganglia or the spinal cord in the nervous system (Tsuda et al., 2009), which plays a role in pain-signaling transmission. Most animal models, such as those of chronic constriction injury (CCI), spinal nerve ligation (SNL), and spared sciatic nerve injury (SNI), have been used to investigate the relationship between lncRNAs and CNP in the nervous system (**Table 1** and **Figure 2**). Zhao et al. (2013) were the first to show that the expression of a new native lncRNA was upregulated in mammalian DRG neurons of SNL and CCI model mice. Since the sequence of this lncRNA was found to be complementary

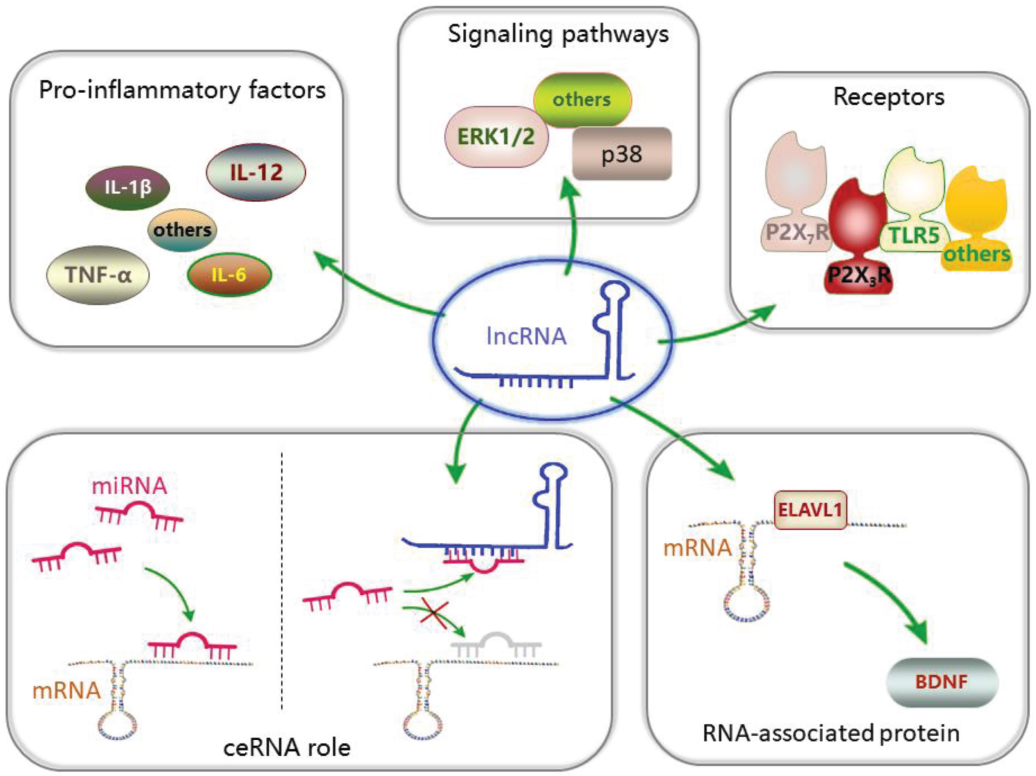

FIGURE 1 | Long non-coding RNA (lncRNAs) and their mechanism in pain transmission: lncRNAs can participate in pain transmission through various mechanisms.

to that of KCNA2 RNA, the researchers named it as KCNA antisense (KCNA2-AS). KCNA2-AS was identified to trigger the downregulation of KCNA2 in the DRG and participate in the development of neuropathic pain by using KCNA2-AS siRNA, indicating the important role of lncRNAs in CNP development. The following studies were performed to explore the roles and mechanisms of lncRNAs in the development of PNI-induced CNP. lncRNAs, such as MALAT1, DILC, FIRRE, XIST, H19, and DGCR5 in the spinal cord, have been found to have a continuous effect on CNP (Wei et al., 2018; Peng et al., 2019; Li K. et al., 2020; Liu et al., 2020; Wu et al., 2020; Wen et al., 2021). lncRNAs, such as H19, SNHG5, and MRAK009713 in DRG, have also been identified to play important roles in the development of CNP (Li et al., 2017; Chen et al., 2020; Wen et al., 2020). Since numerous lncRNAs are involved, we have summarized the following points:

(1) Most lncRNAs interacted with miRNAs, and MALAT1 and XIST were the most common among these lncRNAs. miRNA downregulation triggered by these lncRNAs could influence the downstream mechanism and induce mechanical and cold hypersensitivity and the symptoms of PNI-associated CNP. In addition, other mechanisms of lncRNAs have been investigated in PNI models. DILC, Linc00311, AK141205, and KCNA2-AS have been reported to participate in CNP by regulating the JAK/STAT3-signaling pathway (Mao et al., 2018; Kong et al., 2020; Liu et al., 2020). MRAK009713-mediated CNP development is involved in $P2X_3$ receptor activation (Li et al., 2017). Cyclin-dependent kinases 4 and 6 (CDK4 and CDK6) have been found to be regulated by lncRNA SNHG1 and PKIA-AS1, respectively (Hu et al., 2019; Zhang J.Y. et al., 2020). Notably, changes in the levels of pro-inflammatory cytokines (IL-1β, IL-6, and TNF-α) have been found in most PNI models (Li Z. et al., 2020; Pan et al., 2020), indicating that lncRNA-mediated CNP development may be involved in neuroinflammation.

(2) The same issue could express various lncRNAs, which may be different expression levels or play opposite effect on the PNI model. In the spinal cord of CCI rats, DLEU1 expression was upregulated (Li Z. et al., 2020), whereas GAS5 expression was downregulated (Tian et al., 2020). Thus, the two lncRNAs played opposite roles in the development of PNI-induced CNP. In addition, the expression of the same lncRNA in different conditions or models may display opposite changes. MALAT1 expression was increased in the L4-L6 spinal cord of male CCI rats (Ma et al., 2020), while its expression was reduced in the C5-T1 spinal cord of male complete brachial plexus avulsion rats (Meng et al., 2019).

(3) Owing to the sex difference in pain sensitivity (Fullerton et al., 2018), clinical and experimental findings have suggested that women are more sensitive to pain than men (Fillingim et al., 2009). lncRNA XIST, which mediates

TABLE 1 | lncRNAs and peripheral nerve injury.

Model	lncRNAs	Distribution	Expression	Mechanism	References
CCI	MALAT1	SC of female rat	↑	MALAT1/miR-154-5p/AQP9 axis	Wu et al., 2020
		SC of female rat	↑	MALAT1/miR-206/ZEB2 axis	Chen Z.L. et al., 2019
		SC of male rat	↑	MALAT1/miR-129-5p/HMGB1 axis	Ma et al., 2020
	DILC	SC of male rat	↑	SOCS3/JAK2/STAT3 pathway	Liu et al., 2020
	FIRRE	SC of female mouse	↑	HMGB1	Wen et al., 2021
	CRNDE	SC of rat	↑	CRNDE/miR-136/IL6R axis, IL-1, IL-6, IL-10, TNF-α	Zhang et al., 2019
	XIST	SC of female rat	↑	XIST/miR-154-5p/TLR5 axis	Wei et al., 2018
		SC of female rat	↑	XIST/miR-150/ZEB1 axis	Yan et al., 2018
		SC of female rat	↑	XIST/miR-544/STAT3 axis, TNF-α, IL-1β, IL-6	Jin et al., 2018
		SC of female rat	↑	XIST/miR-137/TNFAIP1 axis	Zhao et al., 2018
	Linc00657	SC of female rat	↑	Linc00657/miR-136/ZEB1 axis	Shen et al., 2019
	NEAT1	SC of female rat	↑	NEAT1/miR-381/HMGB1 axis, IL-6, IL-1β, TNF-α	Xia et al., 2018
	uc.153	SC of male mouse	↑	uc.153/miR-182-5p/EphB1-NMDA receptors	Zhang C. et al., 2020
	Linc00311, AK141205	SC of male rat	↑	STAT3, IL-6, IL-1β	Pang et al., 2020
	SNHG16	SC of female rat	↑	SNHG16/miR-124-3p, miR-141-3p/JAG1 axis, IL- 6, TNF-α, IL-1β	Li H. et al., 2020
	GAS5	SC of female rat	↓	GAS5/miR-452-5p/CELF2 axis	Tian et al., 2020
	DLEU1	SC of female rat	↑	DLEU1/miR-133a-3p/SRPK1 axis, IL-6, TNF-α, IL-1β	Li Z. et al., 2020
	H19	SC of rat	↑	H19/miR-196a-5p/CDK5 axis, p-CREB	Li K. et al., 2020
	HAGLR	SC of female rat	↑	HAGLR/miR-182-5p/ATAT1 axis, NLRP3	Zhang Q. et al., 2021
	CCAT1	Hippocampus, SC, DRG of male rat	↓	miR155, SGK3	Dou et al., 2017
	MRAK009713	DRG of male rat	↑	$P2X_3$ receptor	Li et al., 2017
SNL, CCI	Kcna2-AS	DRG neuron of male rat	↑	MZF1/Kcna2-AS/Kcna2	Zhao et al., 2013
SNL	PKIA-AS1	SC of male rat	↑	CDK6	Hu et al., 2019
	SNHG1	SC of male rat	↑	CDK4	Zhang J.Y. et al., 2020
	SNHG4	SC of male rat	↑	miR-423-5p, IL-6, IL-12, TNF-α	Pan et al., 2020
	SNHG5	L5 DRG of male mouse	↑	SNHG5/miR-154-5p/CXCL13 axis	Chen et al., 2020
	P21	SC of male rat	↑	P21/miR-181b/Tnfaip1, AKT/CREB axis	Liu et al., 2021
	Linc00052	SC of male rat	↑	Linc00052/miR-448/JAK1 axis, IL-6, TNF-α	Wang L. et al., 2020
	H19	DRG of male mouse	↑	Unknown	Wen et al., 2020
	Lncenc1	DRG of male mouse	↑	Lncenc1/EZH2/BAI1 TNF-α, IL-1β, IL-10	Zhang Z. et al., 2021
SNI	AC111653.1	DRG of male rat	↑	Unknown	Mao et al., 2018
	DGCR5	SC of female rat	↓	DGCR5/miR-330-3p/PDCD4 axis	Peng et al., 2019
	LOC100911498	L4, L5 SC of male rat	↑	$P2X_4R$, BDNF, p38	Tang et al., 2021
	Slc6a19os, Sox11	L3-L5 DRG of male mouse	↑	miR-125a-5p, miR-125b-5p, miR-351-5p	Chen et al., 2021
	Linc01119	L4-L5 SC and DRGs of male rats	↑	Linc01119/ELAVL1/BDNF axis	Zhang L. et al., 2021
Complete brachial plexus avulsion	MALAT1	cytoplasm of neurons in male rat C5-T1 SC	↓	Unknown	Meng et al., 2019
PHN	Kcna2-AS	L4, L5 SC of female rat	↑	STAT3, astrocyte	Kong et al., 2020

CCI, chronic constriction injury, SNL, spinal nerve ligation; SNI, spared sciatic nerve injury; SCI, spinal cord injury; SC, spinal cord; DRG, dorsal root ganglion; PHN, postherpetic neuralgia; ↑, upregulated expression; ↓, downregulated expression.

X-chromosome inactivation or reactivation in female cells (Vacca et al., 2016), has been found to play an important role in female PNI models (Jin et al., 2018; Wei et al., 2018; Yan et al., 2018; Zhao et al., 2018). However, most lncRNAs exert their effect on all PNI models, regardless of sex, indicating that most lncRNAs can play an important role

in the development of PNI-induced CNP in both female and male models.

(4) Many studies have paid attention to the effect of lncRNAs on spinal cord and DRG. However, various specific brain regions, such as hippocampus, periaqueductal gray (PAG), anterior cingulate cortex (ACC), can also exert their effect on the development of chronic pain (Bliss et al., 2016; Ong et al., 2019). Dou et al. (2017) found the decrease of the lncRNA CCAT1 level in hippocampus and ACC of the CCI model. Overexpression of CCAT1 could alleviate CNP and inhibit the increased miR-155. As a role of ceRNA, CCAT1 could inhibit miRNA expression, and the researcher further identified the role of serum and glucocorticoid-regulated protein kinase 3 (SGK3) in CCAT1-mediated miR-155 expression and CCAT1-induced CNP. These results indicated the significant role of lncRNA in hippocampus and ACC. However, the effect of lncRNAs on specific brain regions needs to be explored in the future.

lncRNAs and Diabetic Neuropathic Pain

Diabetic neuropathic pain (DNP), a painful diabetic peripheral neuropathy, is one of the most common types of neuropathic pain (de Vos et al., 2014), and it commonly manifests as allodynia, hyperalgesia, or spontaneous pain (Wang et al., 2014). Approximately, 40–50% of patients with diabetes experience DNP (Schreiber et al., 2015), whereas effective therapies for DNP remain elusive. Recently, genome-wide expression patterns of lncRNAs have been identified, and RT-qPCR validated the dysregulation of lncRNAs in the spinal cord of DNP mice (Du et al., 2019). Bioinformatics analysis results have shown that these lncRNA-related genes are involved in calcium ion transport, which participates in neuropathic pain development (Baba et al., 2016). However, the speculation that lncRNA exerts an effect on the ion channel in DNP needs to be further explored (**Table 2**).

Liu et al. (2018) identified the role of lncRNAs in DNP by regulating transient receptor potential vanilloid type 1 (TRPV1) activation in the rat DRG. Using western blot analysis, they found that high TRPV1 receptor expression in DRG neurons of DNP rats could be substantially decreased by lncRNA BC168687 siRNA, which could alleviate TRPV1-mediated diabetic neuropathic pain (Zhang B.Y. et al., 2020), indicating that lncRNA BC168687 may regulate the ion channel of DRG neurons and participate in the development of DNP. In addition, Liu et al. (2018) found that $P2X_7$ receptor expression was downregulated after BC168687 siRNA treatment. The $P2X_7$ receptor is mainly expressed in satellite glial cells (SGCs) (Chen et al., 2012; Puchałowicz et al., 2015), which tightly enwrap the DRG (Costa and Moreira Neto, 2015). Previous studies have suggested that SGC $P2X_7$ receptors play an important role in neuropathic pain (Kuan and Shyu, 2016; Bernier et al., 2018). Liu et al. (2017) found that treatment with BC168687 siRNA decreased the serum level of oxidative injury factors (e.g., NO) released by SGCs in a DNP model. NO can strengthen the sensitivity of neurons to noxious stimulation in the DRG (Thippeswamy et al., 2005). NO has been reported to be involved in the development of neuropathic pain (Rondón et al., 2018). Thus, BC168687 may promote interaction with neurons and glia in the DRG during DNP. These data indicate that lncRNA BC168687 in DRG may participate in the development of DNP by regulating the activation of both neurons and glia.

Long non-coding RNA NONRATT021972 has also been validated to play an important role in the development of DNP (Liu et al., 2016). Using lncRNA siRNA, $P2X_7$ antagonist, and electrophysiological recordings of neurons, this lncRNA was found to regulate $P2X_7$ receptor expression in the SGCs of the DRG during DNP. Peng H. et al. (2017) explored the direct effect of this lncRNA on DRG neurons. NONRATT021972 siRNA inhibited the expression and activation of the $P2X_3$ receptor and its downstream ERK1/2-signaling pathway in neurons and relieved DNP. The ERK1/2-signaling pathway is involved in neuropathic pain transmission (Seino et al., 2006). These results indicate that lncRNA NONRATT021972 in the DRG may participate in the development of DNP by regulating the activation of both neurons and glia.

Similarly, the $P2X_3$ receptor and ERK1/2-signaling pathway in the DRG are regulated by another lncRNA uc.48+ (Wang et al., 2016). In addition, lncRNA uc.48+ siRNA can significantly suppress the expression of calcitonin gene-related peptide (CGRP), IL-1β, and TNF-α in the spinal cord (Xiong et al., 2017). The expression of CGRP, IL-1β, and TNF-α in the spinal cord may contribute to pain responses (Brown et al., 2008; Hansen et al., 2016). Thus, lncRNA uc.48+ may participate in the development of DNP by regulating the expression of the three factors in the spinal cord. The findings from the aforementioned studies suggest a role for lncRNA uc.48+ in the progression of DNP and provide various lines of evidence to explain the lncRNA-mediated mechanisms underlying the development of DNP.

lncRNAs and Trigeminal Neuralgia

Trigeminal neuralgia is a common type of neuropathic pain, and many treatments for TN, including medical therapy and microvascular decompression, have been found to be ineffective (Bick and Eskandar, 2017). Recently, lncRNA Gm14461 expression has been found to be increased in the trigeminal ganglia (TG) of TN mice (Xu et al., 2020). The Gm14461 knockdown increased the mechanical withdrawal threshold of TN mice, indicating that Gm14461 may play a regulatory role in mechanical hyperalgesia in TN mice. Western blot analysis results suggested that the Gm14461 knockdown could downregulate the expression of CGRP and $P2X_{3/7}$ receptors at the protein level in TN mice. The three proteins are reported to participate in the development of neuropathic pain (Hansen et al., 2016; Wu et al., 2021; Xia et al., 2021). Moreover, Gm14461 upregulates the expression of TNF-α, IL-1β, and IL-6 (Xu et al., 2020). Another lncRNA uc.48+ interacts with the $P2X_7$ receptor and promotes the expression of the $P2X_7$ receptor in TG (Xiong et al., 2019). Western blot analysis results suggests that the ERK-signaling pathway may be involved in this interaction between uc.48+ and $P2X_7$ receptor. These findings suggest that lncRNAs may play an important role in the development of TN through various mechanisms.

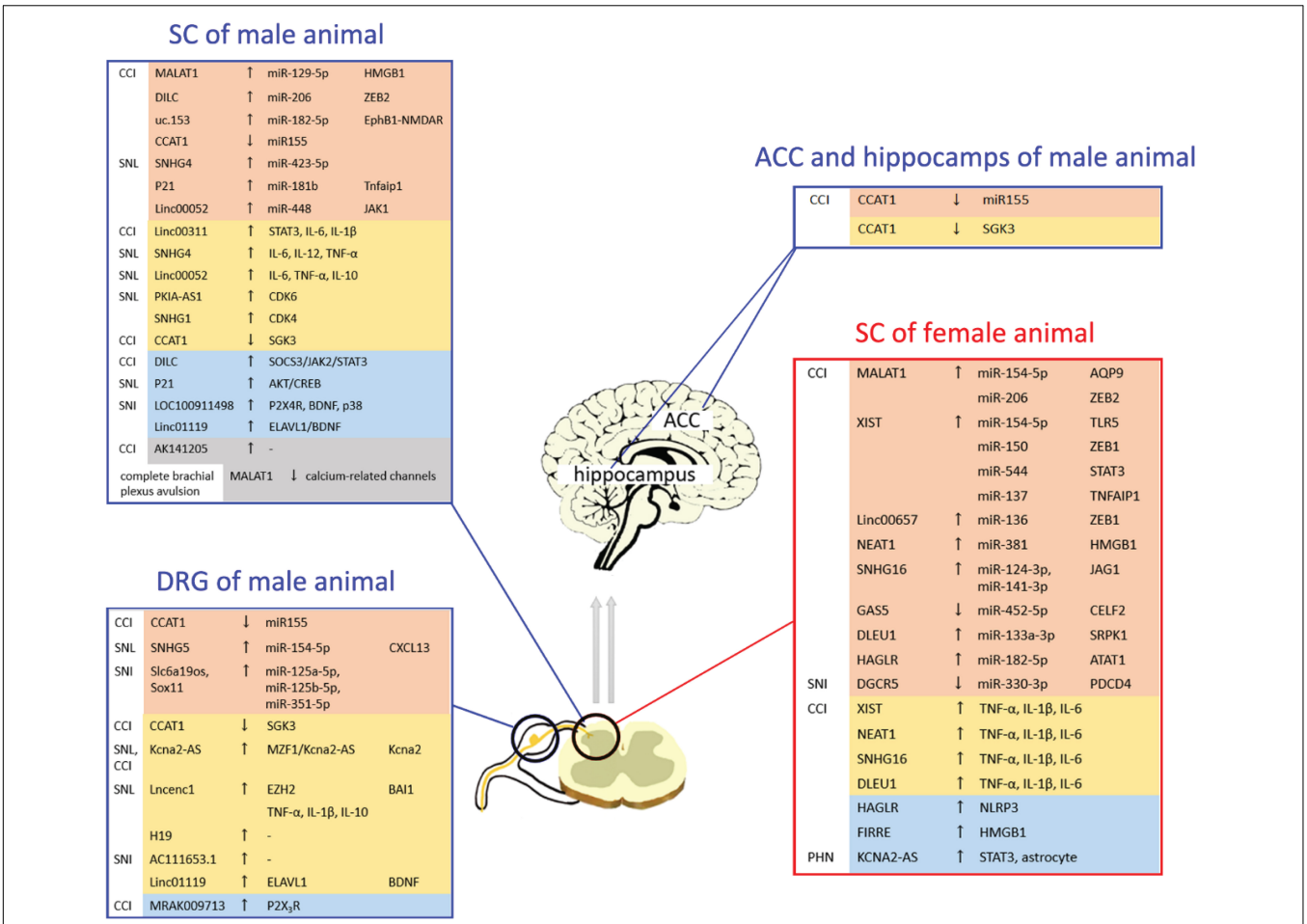

FIGURE 2 | Distribution of deregulated long non-coding RNAs (lncRNAs) with the respective associated mechanisms in peripheral nerve injury (PNI): lncRNAs can participate in the development of PNI-induced chronic neuropathic pain (CNP) through various mechanisms. The same lncRNA displays different expressions in different models or issues. Most lncRNAs can play an important role in the development of PNI-induced CNP in both female and male models. ACC, anterior cingulate cortex; DRG, dorsal root ganglion; SC, spinal cord.

lncRNAs and Central Neuropathic Pain Associated With Spinal Cord Injury

Chronic neuropathic pain is one of the most common complications of SCI that severely influences the quality of life of patients with SCI (Bouhassira et al., 2008). A bioinformatics analysis was performed to determine the dysregulation of lncRNA expression associated with pain transmission in blood samples from patients with SCI (Zhao et al., 2021). Two lncRNAs (Linc01119 and Linc02447) involved in the pain pathway indicated that lncRNA-mediated pain transmission may play a role in the development of SCI-induced CNP. Xian et al. (2021) confirmed the role of lncRNAs in the spinal cord of the CNP model. lncRNA NEAT1 expression was increased in the spinal cord of SCI rats, and NEAT1 inhibition alleviated SCI-induced CNP. miR-128-3p was downregulated by NEAT1 overexpression, as it played the role of its ceRNA, and the levels of AQP4, IL-6, IL-1β, and TNFα were increased after miR-128-3p inhibition. Another study suggested that upregulated lncRNA PVT1 could alleviate SCI-induced CNP by targeting the miR-186-5p/CXCL13/CXCR5 axis (Zhang P. et al., 2021). CXCL13, CXCR5, and AQP4 are vital regulators of the inflammatory response in the nervous system (Liang et al., 2016; Bu et al., 2019). Thus, these two studies indicated the role and the mechanism of lncRNAs in the development of SCI-induced CNP, including their interaction with miRNAs or indirect regulation of the inflammatory response.

lncRNAs AND COMPLEX REGIONAL PAIN SYNDROME-INDUCED INFLAMMATORY PAIN

Complex regional pain syndrome (CRPS) is a chronic pain disorder characterized by intense pain, inflammation, and altered autonomic function (de Mos et al., 2007). The mechanism underlying the development of CRPS remains unclear (Birklein and Schlereth, 2015). Since women are about four times more likely than men to develop CRPS (Schwartzman et al., 2009),

TABLE 2 | lncRNAs and diabetic neuropathic pain.

Model	lncRNAs	Distribution	Expression	Mechanism	References
DNP	BC168687	DRG of male rat	↑	TRPV1, ERK1/2, p38, TNF-α, IL-1β	Liu et al., 2018
		DRG of male rat	↑	$P2X_7R$, NO	Liu et al., 2017
	NONRATT021972	DRG of rat	↑	$P2X_7R$, TNF-α, astrocyte	Liu et al., 2016
		DRG of male rat	↑	$P2X_3R$, ERK1/2	Peng H. et al., 2017
		Blood sample of male rat	↑	TNF-α	Yu et al., 2017
	uc.48+	DRG of male rat	↑	$P2X_3R$, ERK1/2	Wang et al., 2016
		SC of male rat	↑	CGRP, ERK1/2, p38	Xiong et al., 2017

DNP, diabetic neuropathic pain; ↑, upregulated expression.

Shenoda et al. (2018) investigated the role of lncRNA XIST in the development of CRPS. XIST promotes and maintains X-chromosome inactivation (Wang et al., 2021), which refers to the random selection and transcriptional silencing of one of the two X-chromosomes in females, indicating the association of its effect with sex differences. RT-qPCR analysis results suggested that the expression of XIST was increased, and the upstream expression of miR-34a was decreased in the blood samples of patients with CRPS (Shenoda et al., 2018). As a role of a ceRNA, XIST in blood was identified to be directly regulated by miR-34a in a complete Freund's adjuvant (CFA)-induced inflammatory pain model. The pro-inflammatory transcription factor, Yin-Yang 1 (YY1), was found to participate in miR-34a-mediated XIST expression. Thus, miRNA-mediated downregulation of XIST expression in the blood may be a potential strategy for relieving CRPS-induced inflammatory pain. Another study found that XIST expression in the DRG was increased in a CFA-induced inflammatory pain model, and the XIST knockdown inhibited activated the Nav1.7 channel and levels of IL-6 and TNF-α in the DRG and attenuated inflammatory pain (Sun et al., 2018). These studies indicate that XIST is regulated by miRNAs and mediates the release of pro-inflammatory factors, participating in the development of inflammatory pain, demonstrating a new mechanism underlying inflammatory pain. However, the mechanism underlying CRPS-induced inflammatory pain in male patients needs to be further explored.

lncRNAs AND OSTEOARTHRITIS-INDUCED INFLAMMATORY PAIN

Osteoarthritis is one of the most common forms of arthritis (Sellam and Berenbaum, 2010). Its clinical manifestations include joint swelling, synovitis, and inflammatory pain, which cause pain to the patient. Many studies have indicated the regulatory role of lncRNAs in the inflammatory process of OA. Many lncRNAs can attenuate OA through the interaction between lncRNAs and miRNAs (Xie et al., 2020), MAPK pathway (Xiao et al., 2019), and pro-inflammatory factors (Li et al., 2018a). However, the role of lncRNAs in OA-induced inflammatory pain remains unclear. This review focused on lncRNAs involved in this type of pain. Similar to lncRNAs in the PNI model, various lncRNAs may be differentially expressed and exert opposite effects in the pathogenesis of OA (Abbasifard et al., 2020; Xie et al., 2020). Li et al. (2018b) first found that the levels of lncRNA MEG3 increased in the articular tissue of an OA model after treatment with methylene blue, which improved pain sensitivity and reduced inflammatory pain in the OA model. MEG3 has been reported to play a protective role in chondrocytes against IL-1β-induced inflammation in an OA model (Huang et al., 2021). IL-1β, IL-6, and TNFα levels were decreased in a methylene blue-treated OA model, and MEG3 siRNA increased the expression of IL-1β, IL-6, and TNF-α reduced, following methylene blue treatment (Li et al., 2018b), indicating that lncRNA MEG3 may alleviate OA-induced pain by regulating inflammation. Subsequently, research was performed to investigate the effect of lncRNAs on the nervous system (Yang et al., 2021). Umbilical cord blood mesenchymal stem cells, which can release exosomes containing lncRNA H19, were intravenously, intracavitary, or intrathecally administered to an OA model, and all three types of administrations improved the pain sensitization of advanced OA. RT-qPCR analysis results suggested that serum IL-1α, IL-2, IL-6, and TNF-αlevels were decreased by treatment with exo-lncRNA H19. In addition, activation of the ERK-signaling pathway in the spinal dorsal horn was inhibited by exo-lncRNA H19. These results indicate that lncRNAs may regulate the development of OA-induced pain *via* different mechanisms. Notably, different lncRNAs may play opposite roles in the inflammatory process of OA (Abbasifard et al., 2020; Xie et al., 2020); a similar phenomenon may appear in the development of OA-induced pain. The roles and mechanisms of different lncRNAs need to be validated.

lncRNA AND CHRONIC CANCER-RELATED PAIN

Chronic cancer-related pain, another type of chronic pain, similarly deteriorates the quality of life of patients. It can be caused by cancer itself (primary tumor or metastases) or by its treatment (surgery, chemotherapy, and radiotherapy) (Bennett et al., 2019). CCRP is characterized by symptoms of syndromes, including neuropathic and musculoskeletal pain (Treede et al., 2019). Many lncRNAs have been found to play a significant role in cancer, cancer metastasis, and cancer-associated treatment (Li et al., 2016, 2021; Peng W.X. et al., 2017). Recently, accumulating

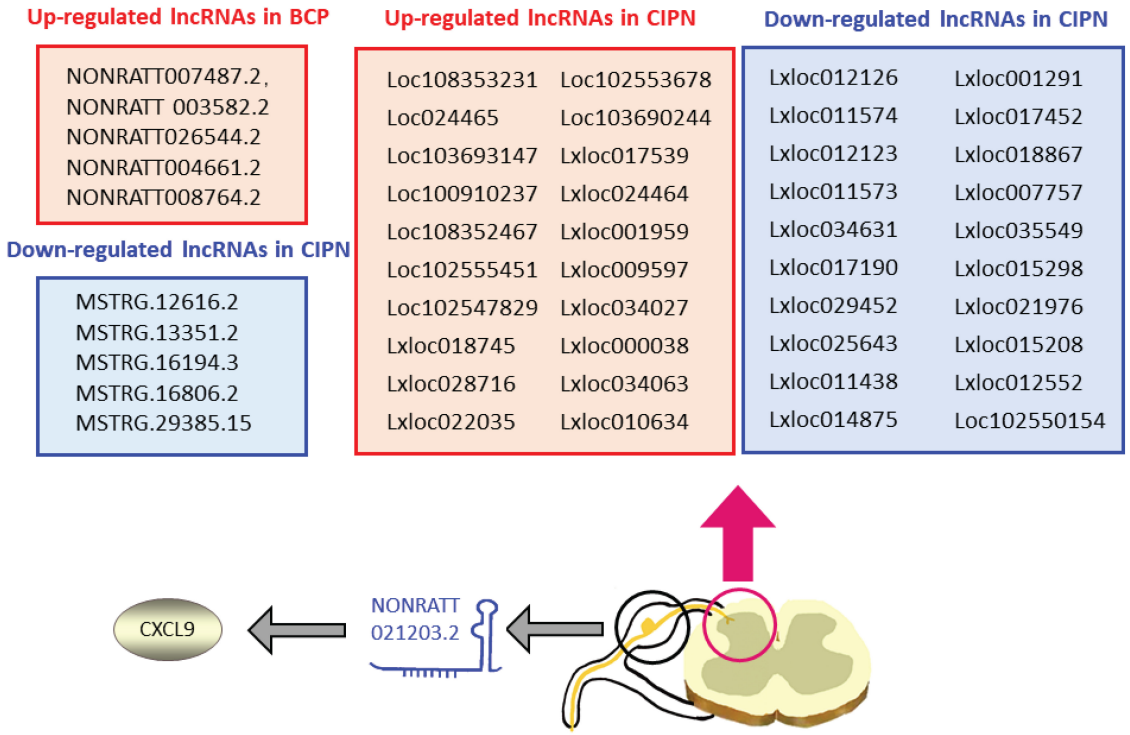

FIGURE 3 | Expression changes and mechanisms of long non-coding RNAs (lncRNAs) in CCRP: many lncRNAs are dysregulated by tumor metastasis and chemotherapy treatment. lncRNA NONRATT021203.2 can exert its effect on BCP by mediating CXCL9 release. BCP, bone cancer pain; CCRP, chronic cancer-related pain; CIPN, chemotherapy-induced peripheral neuropathy.

evidence has shown that lncRNAs are related to the development of CCRP (**Figure 3**).

lncRNAs and Cancer-Induced Pain

More than 50% of patients with cancer experience cancer-induced pain (CIP) (van den Beuken-van et al., 2016). Bone cancer pain (BCP) is the most common type of CIP and is mainly caused by metastatic tumors (Bennett et al., 2019). Many studies have focused on the role of lncRNAs in tumor metastasis (Weidle et al., 2017). This review focuses on the latest research findings on the effect of lncRNAs on CIP and identifies the roles of lncRNAs in metastatic tumor-induced pain. Transcriptome sequencing and RT-qPCR validated the change in the expression of 10 lncRNAs (five upregulated and five downregulated) in the ipsilateral lumbar spinal cord in a rat BCP model (Hou et al., 2020). Gene Ontology (GO) and Kyoto Encyclopedia of Genes and Genomes (KEGG) analysis of the dysregulated lncRNAs (NONRATT007487.2, NONRATT 003582.2, NONRATT026544.2, NONRATT004661.2, NONRATT008764.2, MSTRG.12616.2, MSTRG.13351.2, MSTRG.16194.3, MSTRG.16806.2, and MSTRG.29385.15) indicated that they were mainly involved in inflammatory and immunological responses. Inflammation in the nervous system has been reported to play an important role in BCP, and inhibiting this response could significantly attenuate BCP (Song et al., 2015; Chen S.P. et al., 2019), indicating the potential role of lncRNAs in the development of BCP. Another study further confirmed the link between lncRNAs and neuroinflammation in a BCP model (Sun et al., 2020). The researchers relieved hyperalgesia in BCP rats by treatment with lncRNA NONRATT021203.2 siRNA. In addition, the increased expression of C-X-C motif chemokine ligand 9 (CXCL9) in the DRG was inhibited by this siRNA. CXCL9 has been reported to play a pro-neuroinflammation role in the nervous system (Koper et al., 2018), and inhibiting CXCL9 expression could relieve hyperalgesia in BCP rats (Sun et al., 2020), indicating that NONRATT021203.2 could target CXCL9 and result in CIP in the BCP model. The findings from the two studies indicate that the lncRNA-neuroinflammation axis may be a potential target for the treatment of CIP.

lncRNA and Chemotherapy-Induced Pain

Chemotherapy-induced peripheral neuropathy is a neurotoxic adverse effect of many chemotherapeutic agents (Banach et al., 2017). Chronic pain is a major symptom of chemotherapy-induced peripheral neuropathy (CIPN) (Brewer et al., 2016). The mechanism underlying chemotherapy-induced pain remains unclear, and many medical treatments are usually insufficient for pain management (Sisignano et al., 2014). In a recent study, RNA sequencing (RNA-Seq) and bioinformatics analysis have been performed to explore lncRNA expression profiles in the spinal cord dorsal horn of rats treated with paclitaxel (Li et al., 2021),

one of the most commonly used chemotherapeutic agents (Mody et al., 2016). These results suggest that dysregulated lncRNAs were primarily involved in the neurotrophin-signaling pathway. Neurotrophin signaling could result in the recruitment of signaling proteins (Scott-Solomon and Kuruvilla, 2018), which activate downstream intracellular-signaling pathways, including the ERK1/2 and NF-κB pathways. ERK1/2 and NF-κB signaling have been found to participate in paclitaxel-induced peripheral neuropathy (Wang G. J. et al., 2020; Zhao et al., 2020). These two signaling pathways have been identified downstream of lncRNAs (Peng H. et al., 2017; Zhao et al., 2018). This study indicated that lncRNAs may play an important role in the process of chemotherapy-induced pain by mediating the two signaling pathways; however, this needs to be further validated.

CONCLUSION

In recent years, an increasing number of studies have addressed the change in expression of lncRNAs in humans with chronic pain and preclinical pain models. The vital role of lncRNAs in chronic pain, including CNP, inflammatory pain, and CCRP, has been identified. These lncRNAs can participate in the development of chronic pain by interacting with miRNAs, regulating pro-inflammatory cytokine levels, and mediating signaling pathways. However, the regulatory effects of lncRNAs may be contradictory in different models or different issues. Some lncRNAs, such as XIST, are associated with sex-related differences. Thus, it is necessary to take these factors into account while exploring strategies for alleviating chronic pain. In addition, the same lncRNA could exert its effect on different types of chronic pain, indicating the existence of a similar mechanism underlying the development of different types of pain. Although lncRNA-based clinical agents for chronic pain have not been clearly determined, this preclinical exploration of the mechanism may provide novel and evidential insights for exploring effective strategies for lncRNA-based treatments for chronic pain. However, the clinical efficacy and risks involved in lncRNA therapy need to be systematically evaluated.

AUTHOR CONTRIBUTIONS

ZL wrote the first draft of the manuscript. XL and WJ accessed the data. QX and ZHL contributed to the manuscript revision. All authors contributed to the conception and design of the study, contributed to the article, and approved the submitted version.

FUNDING

This study was supported by grants from the National Natural Science Foundation of China (81901984) and the Shenzhen Science and Technology Innovation Committee (GJHZ20180926170402056).

REFERENCES

Abbasifard, M., Kamiab, Z., Bagheri-Hosseinabadi, Z., and Sadeghi, I. (2020). The role and function of long non-coding RNAs in osteoarthritis. *Exp. Mol. Pathol.* 114:104407. doi: 10.1016/j.yexmp.2020.104407

Baba, H., Petrenko, A. B., and Fujiwara, N. (2016). Clinically relevant concentration of pregabalin has no acute inhibitory effect on excitation of dorsal horn neurons under normal or neuropathic pain conditions: an intracellular calcium-imaging study in spinal cord slices from adult rats. *Brain Res.* 1648, 445–458. doi: 10.1016/j.brainres.2016.08.018

Banach, M., Juranek, J. K., and Zygulska, A. L. (2017). Chemotherapy-induced neuropathies-a growing problem for patients and health care providers. *Brain Behav.* 7:e00558. doi: 10.1002/brb3.558

Batista, P. J., and Chang, H. Y. (2013). Long noncoding RNAs: cellular address codes in development and disease. *Cell* 152, 1298–1307. doi: 10.1016/j.cell.2013.02.012

Bennett, M. I., Kaasa, S., Barke, A., Korwisi, B., Rief, W., and Treede, R. D. (2019). The IASP classification of chronic pain for ICD-11: chronic cancer-related pain. *Pain* 160, 38–44. doi: 10.1097/j.pain.0000000000001363

Bernier, L. P., Ase, A. R., and Séguéla, P. (2018). P2X receptor channels in chronic pain pathways. *Br. J. Pharmacol.* 175, 2219–2230. doi: 10.1111/bph.13957

Bick, S. K. B., and Eskandar, E. N. (2017). Surgical treatment of trigeminal neuralgia. *Neurosurg. Clin. N. Am.* 28, 429–438.

Birklein, F., and Schlereth, T. (2015). Complex regional pain syndrome-significant progress in understanding. *Pain* 156(Suppl. 1), S94–S103. doi: 10.1097/01.j.pain.0000460344.54470.20

Bliss, T. V., Collingridge, G. L., Kaang, B. K., and Zhuo, M. (2016). Synaptic plasticity in the anterior cingulate cortex in acute and chronic pain. *Nat. Rev. Neurosci.* 17, 485–496. doi: 10.1038/nrn.2016.68

Bouhassira, D., Lantéri-Minet, M., Attal, N., Laurent, B., and Touboul, C. (2008). Prevalence of chronic pain with neuropathic characteristics in the general population. *Pain* 136, 380–387. doi: 10.1016/j.pain.2007.08.013

Brewer, J. R., Morrison, G., Dolan, M. E., and Fleming, G. F. (2016). Chemotherapy-induced peripheral neuropathy: current status and progress. *Gynecol. Oncol.* 140, 176–183. doi: 10.1016/j.ygyno.2015.11.011

Brown, K. K., Heitmeyer, S. A., Hookfin, E. B., Hsieh, L., Buchalova, M., Taiwo, Y. O., et al. (2008). P38 MAP kinase inhibitors as potential therapeutics for the treatment of joint degeneration and pain associated with osteoarthritis. *J. Inflamm.* 5:22. doi: 10.1186/1476-9255-5-22

Bu, H. L., Xia, Y. Z., Liu, P. M., Guo, H. M., Yuan, C., Fan, X. C., et al. (2019). The roles of chemokine CXCL13 in the development of bone cancer pain and the regulation of morphine analgesia in rats. *Neuroscience* 406, 62–72. doi: 10.1016/j.neuroscience.2019.02.025

Chen, M., Yang, Y., Zhang, W., Li, X., Wu, J., Zou, X., et al. (2020). Long noncoding RNA SNHG5 knockdown alleviates neuropathic pain by targeting the miR-154-5p/CXCL13 axis. *Neurochem. Res.* 45, 1566–1575. doi: 10.1007/s11064-020-03021-2

Chen, P., Wang, C., Lin, D., Li, B., Ye, S., Qu, J., et al. (2021). Identification of Slc6a19os and SOX11 as two novel essential genes in neuropathic pain using integrated bioinformatic analysis and experimental verification. *Front. Neurosci.* 15:627945. doi: 10.3389/fnins.2021.627945

Chen, S. P., Zhou, Y. Q., Wang, X. M., Sun, J., Cao, F., HaiSam, S., et al. (2019). Pharmacological inhibition of the NLRP3 inflammasome as a potential target for cancer-induced bone pain. *Pharmacol. Res.* 147:104339. doi: 10.1016/j.phrs.2019.104339

Chen, W. K., Yu, X. H., Yang, W., Wang, C., He, W. S., Yan, Y. G., et al. (2017). lncRNAs: novel players in intervertebral disc degeneration and osteoarthritis. *Cell Prolif.* 50:e12313 doi: 10.1111/cpr.12313

Chen, Y., Li, G., and Huang, L. Y. (2012). P2X7 receptors in satellite glial cells mediate high functional expression of P2X3 receptors in immature dorsal root ganglion neurons. *Mol. Pain* 8:9. doi: 10.1186/1744-8069-8-9

Chen, Z. L., Liu, J. Y., Wang, F., and Jing, X. (2019). Suppression of MALAT1 ameliorates chronic constriction injury-induced neuropathic pain in rats *via*

modulating miR-206 and ZEB2. *J Cell Physiol.* Online ahead of print. doi: 10.1002/jcp.28213

Costa, F. A., and Moreira Neto, F. L. (2015). [Satellite glial cells in sensory ganglia: its role in pain]. *Rev. Bras. Anestesiol.* 65, 73–81. doi: 10.1016/j.bjane.2013.07.013

de Mos, M., de Bruijn, A. G., Huygen, F. J., Dieleman, J. P., Stricker, B. H., and Sturkenboom, M. C. (2007). The incidence of complex regional pain syndrome: a population-based study. *Pain* 129, 12–20. doi: 10.1016/j.pain.2006.09.008

de Vos, C. C., Meier, K., Zaalberg, P. B., Nijhuis, H. J., Duyvendak, W., Vesper, J., et al. (2014). Spinal cord stimulation in patients with painful diabetic neuropathy: a multicentre randomized clinical trial. *Pain* 155, 2426–2431. doi: 10.1016/j.pain.2014.08.031

Dou, L., Lin, H., Wang, K., Zhu, G., Zou, X., Chang, E., et al. (2017). Long non-coding RNA CCAT1 modulates neuropathic pain progression through sponging miR-155. *Oncotarget* 8, 89949–89957. doi: 10.18632/oncotarget.21192

Du, H., Liu, Z., Tan, X., Ma, Y., and Gong, Q. (2019). Identification of the genome-wide expression patterns of long non-coding RNAs and mRNAs in mice with streptozotocin-induced diabetic neuropathic pain. *Neuroscience* 402, 90–103. doi: 10.1016/j.neuroscience.2018.12.040

Fillingim, R. B., King, C. D., Ribeiro-Dasilva, M. C., Rahim-Williams, B., et al. (2009). Sex, gender, and pain: a review of recent clinical and experimental findings. *J. Pain* 10, 447–485. doi: 10.1016/j.jpain.2008.12.001

Fullerton, E. F., Doyle, H. H., and Murphy, A. Z. (2018). Impact of sex on pain and opioid analgesia: a review. *Curr. Opin. Behav. Sci.* 23, 183–190. doi: 10.1016/j.cobeha.2018.08.001

Hamood, R., Hamood, H., Merhasin, I., and Keinan-Boker, L. (2018). Chronic pain and other symptoms among breast cancer survivors: prevalence, predictors, and effects on quality of life. *Breast Cancer Res. Treat.* 167, 157–169. doi: 10.1007/s10549-017-4485-0

Hansen, R. R., Vacca, V., Pitcher, T., Clark, A. K., and Malcangio, M. (2016). Role of extracellular calcitonin gene-related peptide in spinal cord mechanisms of cancer-induced bone pain. *Pain* 157, 666–676. doi: 10.1097/j.pain.0000000000000416

Hou, X., Weng, Y., Guo, Q., Ding, Z., Wang, J., Dai, J., et al. (2020). Transcriptomic analysis of long noncoding RNAs and mRNAs expression profiles in the spinal cord of bone cancer pain rats. *Mol. Brain* 13:47. doi: 10.1186/s13041-020-00589-2

Hu, J. Z., Rong, Z. J., Li, M., Li, P., Jiang, L. Y., Luo, Z. X., et al. (2019). Silencing of lncRNA PKIA-AS1 attenuates spinal nerve ligation-induced neuropathic pain through epigenetic downregulation of CDK6 Expression. *Front. Cell Neurosci.* 13:50. doi: 10.3389/fncel.2019.00050

Huang, Y., Chen, D., Yan, Z., Zhan, J., Xue, X., Pan, X., et al. (2021). LncRNA MEG3 protects chondrocytes from IL-1β-induced inflammation *via* regulating miR-9-5p/KLF4 Axis. *Front. Physiol.* 12:617654. doi: 10.3389/fphys.2021.617654

Jin, H., Du, X. J., Zhao, Y., and Xia, D. L. (2018). XIST/miR-544 axis induces neuropathic pain by activating STAT3 in a rat model. *J. Cell. Physiol.* 233, 5847–5855. doi: 10.1002/jcp.26376

Kong, C., Du, J., Bu, H., Huang, C., Xu, F., and Ren, H. (2020). LncRNA KCNA2-AS regulates spinal astrocyte activation through STAT3 to affect postherpetic neuralgia. *Mol. Med.* 26:113. doi: 10.1186/s10020-020-00232-9

Koper, O. M., Kamińska, J., Sawicki, K., and Kemona, H. (2018). CXCL9, CXCL10, CXCL11, and their receptor (CXCR3) in neuroinflammation and neurodegeneration. *Adv. Clin. Exp. Med.* 27, 849–856. doi: 10.17219/acem/68846

Kuan, Y. H., and Shyu, B. C. (2016). Nociceptive transmission and modulation *via* P2X receptors in central pain syndrome. *Mol. Brain* 9:58. doi: 10.1186/s13041-016-0240-4

Li, G., Jiang, H., Zheng, C., Zhu, G., Xu, Y., Sheng, X., et al. (2017). Long noncoding RNA MRAK009713 is a novel regulator of neuropathic pain in rats. *Pain* 158, 2042–2052.

Li, H., Fan, L., Zhang, Y., Cao, Y., and Liu, X. (2020). SNHG16 aggravates chronic constriction injury-induced neuropathic pain in rats *via* binding with miR-124-3p and miR-141-3p to upregulate JAG1. *Brain Res. Bull.* 165, 228–237. doi: 10.1016/j.brainresbull.2020.09.025

Li, J., Meng, H., Bai, Y., and Wang, K. (2016). Regulation of lncRNA and its role in cancer metastasis. *Oncol. Res.* 23, 205–217. doi: 10.3727/096504016x14549667334007

Li, K., Jiao, Y., Ren, X., You, D., and Cao, R. (2020). Long noncoding RNA H19 induces neuropathic pain by upregulating cyclin-dependent Kinase 5-mediated phosphorylation of cAMP response element binding protein. *J. Pain Res.* 13, 2113–2124.

Li, X., Ren, W., Xiao, Z. Y., Wu, L. F., Wang, H., and Guo, P. Y. (2018a). GACAT3 promoted proliferation of osteoarthritis synoviocytes by IL-6/STAT3 signaling pathway. *Eur. Rev. Med. Pharmacol. Sci.* 22, 5114–5120. doi: 10.26355/eurrev_201808_15705

Li, X., Tang, C., Wang, J., Guo, P., Wang, C., Wang, Y., et al. (2018b). Methylene blue relieves the development of osteoarthritis by upregulating lncRNA MEG3. *Exp. Ther. Med.* 15, 3856–3864. doi: 10.3892/etm.2018.5918

Li, Y., Yin, C., Liu, B., Nie, H., Wang, J., Zeng, D., et al. (2021). Transcriptome profiling of long noncoding RNAs and mRNAs in spinal cord of a rat model of paclitaxel-induced peripheral neuropathy identifies potential mechanisms mediating neuroinflammation and pain. *J. Neuroinflamm.* 18:48. doi: 10.1186/s12974-021-02098-y

Li, Z., Li, A., Yan, L., Yang, T., Xu, W., and Fan, P. (2020). Downregulation of long noncoding RNA DLEU1 attenuates hypersensitivity in chronic constriction injury-induced neuropathic pain in rats by targeting miR-133a-3p/SRPK1 axis. *Mol. Med.* 26:104. doi: 10.1186/s10020-020-00235-6

Liang, R., Yong, S., Huang, X., Kong, H., Hu, G., and Fan, Y. (2016). Aquaporin-4 mediates the suppressive effect of lipopolysaccharide on hippocampal neurogenesis. *Neuroimmunomodulation* 23, 309–317. doi: 10.1159/000467141

Lin, X., Wang, M., Zhang, J., and Xu, R. (2014). p38 MAPK: a potential target of chronic pain. *Curr. Med. Chem.* 21, 4405–4418.

Liu, C., Li, C., Deng, Z., Du, E., and Xu, C. (2018). Long non-coding RNA BC168687 is involved in TRPV1-mediated diabetic neuropathic pain in rats. *Neuroscience* 374, 214–222. doi: 10.1016/j.neuroscience.2018.01.049

Liu, C., Tao, J., Wu, H., Yang, Y., Chen, Q., Deng, Z., et al. (2017). Effects of LncRNA BC168687 siRNA on diabetic neuropathic pain mediated by P2X(7) receptor on SGCs in DRG of rats. *Biomed. Res. Int.* 2017:7831251. doi: 10.1155/2017/7831251

Liu, S., Zou, L., Xie, J., Xie, W., Wen, S., Xie, Q., et al. (2016). LncRNA NONRATT021972 siRNA regulates neuropathic pain behaviors in type 2 diabetic rats through the P2X7 receptor in dorsal root ganglia. *Mol. Brain* 9:44. doi: 10.1186/s13041-016-0226-2

Liu, Y., Feng, L., Ren, S., Zhang, Y., and Xue, J. (2020). Inhibition of lncRNA DILC attenuates neuropathic pain *via* the SOCS3/JAK2/STAT3 pathway. *Biosci. Rep.* 40:BSR20194486. doi: 10.1042/BSR20194486

Liu, Y., Sun, H., and Sun, Y. (2021). LncRNA p21, downregulating miR-181b, aggravates neuropathic pain by upregulating Tnfaip1 and inhibit the AKT/CREB axis. *Brain Res. Bull.* 171, 150–161. doi: 10.1016/j.brainresbull.2021.03.005

Ma, X., Wang, H., Song, T., Wang, W., and Zhang, Z. (2020). lncRNA MALAT1 contributes to neuropathic pain development through regulating miR-129-5p/HMGB1 axis in a rat model of chronic constriction injury. *Int. J. Neurosci.* 130, 1215–1224. doi: 10.1080/00207454.2020.1731508

Mao, P., Li, C. R., Zhang, S. Z., Zhang, Y., Liu, B. T., and Fan, B. F. (2018). Transcriptomic differential lncRNA expression is involved in neuropathic pain in rat dorsal root ganglion after spared sciatic nerve injury. *Braz. J. Med. Biol. Res.* 51:e7113. doi: 10.1590/1414-431X20187113

Meng, C., Yang, X., Liu, Y., Zhou, Y., Rui, J., Li, S., et al. (2019). Decreased expression of lncRNA Malat1 in rat spinal cord contributes to neuropathic pain by increasing neuron excitability after brachial plexus avulsion. *J. Pain Res.* 12, 1297–1310. doi: 10.2147/JPR.S195117

Mody, M. D., Gill, H. S., and Saba, N. F. (2016). The evolving and future role of taxanes in squamous cell carcinomas of the head and neck: a review. *JAMA Otolaryngol. Head Neck Surg.* 142, 898–905. doi: 10.1001/jamaoto.2016.1238

Ong, W. Y., Stohler, C. S., and Herr, D. R. (2019). Role of the prefrontal cortex in pain processing. *Mol. Neurobiol.* 56, 1137–1166. doi: 10.1007/s12035-018-1130-9

Pan, X., Shen, C., Huang, Y., Wang, L., and Xia, Z. (2020). Loss of SNHG4 attenuated spinal nerve ligation-triggered neuropathic pain through sponging miR-423-5p. *Mediators Inflamm.* 2020:2094948.

Pang, H., Ren, Y., Li, H., Chen, C., and Zheng, X. (2020). LncRNAs linc00311 and AK141205 are identified as new regulators in STAT3-mediated neuropathic pain in bCCI rats. *Eur. J. Pharmacol.* 868:172880. doi: 10.1016/j.ejphar.2019.172880

Peng, C., Zhang, C., Su, Z., and Lin, D. (2019). DGCR5 attenuates neuropathic pain through sponging miR-330-3p and regulating PDCD4 in CCI rat models. *J. Cell. Physiol.* 234, 7292–7300. doi: 10.1002/jcp.27487

Peng, H., Zou, L., Xie, J., Wu, H., Wu, B., Zhu, G., et al. (2017). lncRNA NONRATT021972 siRNA decreases diabetic neuropathic pain mediated by the P2X(3) receptor in dorsal root ganglia. *Mol. Neurobiol.* 54, 511–523. doi: 10.1007/s12035-015-9632-1

Peng, W. X., Koirala, P., and Mo, Y. Y. (2017). LncRNA-mediated regulation of cell signaling in cancer. *Oncogene* 36, 5661–5667. doi: 10.1038/onc.2017.184

Puchałowicz, K., Baranowska-Bosiacka, I., Dziedziejko, V., and Chlubek, D. (2015). Purinergic signaling and the functioning of the nervous system cells. *Cell Mol. Biol. Lett.* 20, 867–918.

Qian, Y., Wang, Q., Jiao, J., Wang, G., Gu, Z., Huang, D., et al. (2019). Intrathecal injection of dexmedetomidine ameliorates chronic neuropathic pain *via* the modulation of MPK3/ERK1/2 in a mouse model of chronic neuropathic pain. *Neurol. Res.* 41, 1059–1068. doi: 10.1080/01616412.2019.1672391

Ren, X., Yang, R., Li, L., Xu, X., and Liang, S. (2020). Long non coding RNAs involved in MAPK pathway mechanism mediates diabetic neuropathic pain. *Cell Biol. Int.* 44, 2372–2379. doi: 10.1002/cbin.11457

Rondón, L. J., Farges, M. C., Davin, N., Sion, B., Privat, A. M., Vasson, M. P., et al. (2018). L-Arginine supplementation prevents allodynia and hyperalgesia in painful diabetic neuropathic rats by normalizing plasma nitric oxide concentration and increasing plasma agmatine concentration. *Eur. J. Nutr.* 57, 2353–2363. doi: 10.1007/s00394-017-1508-x

Scholz, J., Finnerup, N. B., Attal, N., Aziz, Q., Baron, R., Bennett, M. I., et al. (2019). The IASP classification of chronic pain for ICD-11: chronic neuropathic pain. *Pain* 160, 53–59.

Schreiber, A. K., Nones, C. F., Reis, R. C., Chichorro, J. G., and Cunha, J. M. (2015). Diabetic neuropathic pain: physiopathology and treatment. *World J. Diabetes* 6, 432–444.

Schwartzman, R. J., Erwin, K. L., and Alexander, G. M. (2009). The natural history of complex regional pain syndrome. *Clin. J. Pain* 25, 273–280.

Scott-Solomon, E., and Kuruvilla, R. (2018). Mechanisms of neurotrophin trafficking *via* Trk receptors. *Mol. Cell. Neurosci.* 91, 25–33. doi: 10.1016/j.mcn.2018.03.013

Seino, D., Tokunaga, A., Tachibana, T., Yoshiya, S., Dai, Y., Obata, K., et al. (2006). The role of ERK signaling and the P2X receptor on mechanical pain evoked by movement of inflamed knee joint. *Pain* 123, 193–203. doi: 10.1016/j.pain.2006.02.032

Sellam, J., and Berenbaum, F. (2010). The role of synovitis in pathophysiology and clinical symptoms of osteoarthritis. *Nat. Rev. Rheumatol.* 6, 625–635. doi: 10.1038/nrrheum.2010.159

Shen, F., Zheng, H., Zhou, L., Li, W., Zhang, Y., and Xu, X. (2019). LINC00657 expedites neuropathic pain development by modulating miR-136/ZEB1 axis in a rat model. *J. Cell. Biochem.* 120, 1000–1010. doi: 10.1002/jcb.27466

Shenoda, B. B., Tian, Y., Alexander, G. M., Aradillas-Lopez, E., Schwartzman, R. J., and Ajit, S. K. (2018). miR-34a-mediated regulation of XIST in female cells under inflammation. *J. Pain Res.* 11, 935–945. doi: 10.2147/JPR.S159458

Sisignano, M., Baron, R., Scholich, K., and Geisslinger, G. (2014). Mechanism-based treatment for chemotherapy-induced peripheral neuropathic pain. *Nat. Rev. Neurol.* 10, 694–707.

Song, H., Han, Y., Pan, C., Deng, X., Dai, W., Hu, L., et al. (2015). Activation of adenosine monophosphate-activated protein kinase suppresses neuroinflammation and ameliorates bone cancer pain: involvement of inhibition on mitogen-activated protein kinase. *Anesthesiology* 123, 1170–1185. doi: 10.1097/ALN.0000000000000856

Sun, H., Peng, G., Ning, X., Wang, J., Yang, H., and Deng, J. (2019). Emerging roles of long noncoding RNA in chondrogenesis, osteogenesis, and osteoarthritis. *Am. J. Transl. Res.* 11, 16–30.

Sun, R. M., Wei, J., Wang, S. S., Xu, G. Y., and Jiang, G. Q. (2020). Upregulation of lncRNA-NONRATT021203.2 in the dorsal root ganglion contributes to cancer-induced pain *via* CXCL9 in rats. *Biochem. Biophys. Res. Commun.* 524, 983–989. doi: 10.1016/j.bbrc.2020.01.163

Sun, W., Ma, M., Yu, H., and Yu, H. (2018). Inhibition of lncRNA X inactivate-specific transcript ameliorates inflammatory pain by suppressing satellite glial cell activation and inflammation by acting as a sponge of miR-146a to inhibit Na(v) 1.7. *J. Cell Biochem.* 119, 9888–9898. doi: 10.1002/jcb.27310

Tang, W., Zhang, L., and Li, Z. (2021). Long noncoding RNA LOC100911498 is a novel regulator of neuropathic pain in rats. *Brain Behav.* 11:e01966. doi: 10.1002/brb3.1966

Thippeswamy, T., McKay, J. S., Morris, R., Quinn, J., Wong, L. F., and Murphy, D. (2005). Glial-mediated neuroprotection: evidence for the protective role of the NO-cGMP pathway *via* neuron-glial communication in the peripheral nervous system. *Glia* 49, 197–210. doi: 10.1002/glia.20105

Tian, Y., Sun, L., and Qi, T. (2020). Long noncoding RNA GAS5 ameliorates chronic constriction injury induced neuropathic pain in rats by modulation of the miR-452-5p/CELF2 axis. *Can. J. Physiol. Pharmacol.* 98, 870–877. doi: 10.1139/cjpp-2020-0036

Treede, R. D., Rief, W., Barke, A., Aziz, Q., Bennett, M. I., Benoliel, R., et al. (2019). Chronic pain as a symptom or a disease: the IASP classification of chronic pain for the International Classification of Diseases (ICD-11). *Pain* 160, 19–27.

Tsuda, M., Masuda, T., Kitano, J., Shimoyama, H., Tozaki-Saitoh, H., and Inoue, K. (2009). IFN-gamma receptor signaling mediates spinal microglia activation driving neuropathic pain. *Proc. Natl. Acad. Sci. U.S.A.* 106, 8032–8037. doi: 10.1073/pnas.0810420106

Ulitsky, I., and Bartel, D. P. (2013). lincRNAs: genomics, evolution, and mechanisms. *Cell* 154, 26–46. doi: 10.1016/j.cell.2013.06.020

Vacca, M., Della Ragione, F., Scalabrì, F., and D'Esposito, M. (2016). X inactivation and reactivation in X-linked diseases. *Semin. Cell Dev. Biol.* 56, 78–87. doi: 10.1016/j.semcdb.2016.03.009

van den Beuken-van, Everdingen, M. H., Hochstenbach, L. M., Joosten, E. A., Tjan-Heijnen, V. C., and Janssen, D. J. (2016). Update on prevalence of pain in patients with cancer: systematic review and meta-analysis. *J. Pain Symptom Manage.* 51, 1070–1090.e1079.

van Hecke, O., Austin, S. K., Khan, R. A., Smith, B. H., and Torrance, N. (2014). Neuropathic pain in the general population: a systematic review of epidemiological studies. *Pain* 155, 654–662. doi: 10.1016/j.pain.2013.11.013

Wang, D., Couture, R., and Hong, Y. (2014). Activated microglia in the spinal cord underlies diabetic neuropathic pain. *Eur. J. Pharmacol.* 728, 59–66.

Wang, G. J., Zhang, X., Huang, L. D., and Xiao, Y. (2020). Involvement of the sodium channel Nav1.7 in paclitaxel-induced peripheral neuropathy through ERK1/2 signaling in rats. *Curr. Neurovasc. Res.* 17, 267–274. doi: 10.2174/1567202617666200514113441

Wang, K. C., and Chang, H. Y. (2011). Molecular mechanisms of long noncoding RNAs. *Mol. Cell.* 43, 904–914. doi: 10.1016/j.molcel.2011.08.018

Wang, L., Zhu, K., Yang, B., and Cai, Y. (2020). Knockdown of Linc00052 alleviated spinal nerve ligation-triggered neuropathic pain through regulating miR-448 and JAK1. *J. Cell. Physiol.* 235, 6528–6535. doi: 10.1002/jcp.29465

Wang, S., Xu, H., Zou, L., Xie, J., Wu, H., Wu, B., et al. (2016). LncRNA uc.*48*+ is involved in diabetic neuropathic pain mediated by the P2X3 receptor in the dorsal root ganglia. *Purinergic Signal.* 12, 139–148. doi: 10.1007/s11302-015-9488-x

Wang, W., Min, L., Qiu, X., Wu, X., Liu, C., Ma, J., et al. (2021). Biological function of long non-coding RNA (LncRNA) Xist. *Front. Cell Dev. Biol.* 9:645647.

Wei, M., Li, L., Zhang, Y., Zhang, Z. J., Liu, H. L., and Bao, H. G. (2018). LncRNA X inactive specific transcript contributes to neuropathic pain development by sponging miR-154-5p *via* inducing toll-like receptor 5 in CCI rat models. *J. Cell Biochem.* Online ahead of print. doi: 10.1002/jcb.27088

Weidle, U. H., Birzele, F., Kollmorgen, G., and Rüger, R. (2017). Long non-coding RNAs and their role in metastasis. *Cancer Genomics Proteom.* 14, 143–160.

Wen, J., Yang, Y., Wu, S., Wei, G., Jia, S., Hannaford, S., et al. (2020). Long noncoding RNA H19 in the injured dorsal root ganglion contributes to peripheral nerve injury-induced pain hypersensitivity. *Transl. Perioper. Pain Med.* 7, 176–184.

Wen, Y., Fan, X., Bu, H., Ma, L., Kong, C., Huang, C., et al. (2021). Downregulation of lncRNA FIRRE relieved the neuropathic pain of female mice by suppressing HMGB1 expression. *Mol. Cell. Biochem.* 476, 841–852. doi: 10.1007/s11010-020-03949-7

Wu, J., Wang, C., and Ding, H. (2020). LncRNA MALAT1 promotes neuropathic pain progression through the miR-154-5p/AQP9 axis in CCI rat models. *Mol. Med. Rep.* 21, 291–303. doi: 10.3892/mmr.2019.10829

Wu, Y., Shen, Z., Xu, H., Zhang, K., Guo, M., Wang, F., et al. (2021). BDNF Participates in chronic constriction injury-induced neuropathic pain *via* transcriptionally activating P2X(7) in primary sensory neurons. *Mol. Neurobiol.* 58, 4226–4236. doi: 10.1007/s12035-021-02410-0

Xia, L. P., Luo, H., Ma, Q., Xie, Y. K., Li, W., Hu, H., et al. (2021). GPR151 in nociceptors modulates neuropathic pain *via* regulating P2X3 function and microglial activation. *Brain* doi: 10.1093/brain/awab245 [Epub ahead of print].

Xia, L. X., Ke, C., and Lu, J. M. (2018). NEAT1 contributes to neuropathic pain development through targeting miR-381/HMGB1 axis in CCI rat models. *J. Cell. Physiol.* 233, 7103–7111. doi: 10.1002/jcp.26526

Xian, S., Ding, R., Li, M., and Chen, F. (2021). LncRNA NEAT1/miR-128-3p/AQP4 axis regulating spinal cord injury-induced neuropathic pain progression. *J. Neuroimmunol.* 351:577457. doi: 10.1016/j.jneuroim.2020.577457

Xiao, Y., Yan, X., Yang, Y., and Ma, X. (2019). Downregulation of long noncoding RNA HOTAIRM1 variant 1 contributes to osteoarthritis *via* regulating miR-125b/BMPR2 axis and activating JNK/MAPK/ERK pathway. *Biomed. Pharmacother.* 109, 1569–1577. doi: 10.1016/j.biopha.2018.10.181

Xie, F., Liu, Y. L., Chen, X. Y., Li, Q., Zhong, J., Dai, B. Y., et al. (2020). Role of MicroRNA, LncRNA, and exosomes in the progression of osteoarthritis: a review of recent literature. *Orthop. Surg.* 12, 708–716. doi: 10.1111/os.12690

Xiong, W., Huang, L., Shen, Y., Guan, S., He, L., Tong, Z., et al. (2017). Effects of lncRNA uc.*48*+ siRNA on the release of CGRP in the spinal cords of rats with diabetic neuropathic pain. *Int. J. Clin. Exp. Pathol.* 10, 9960–9969.

Xiong, W., Tan, M., Tong, Z., Yin, C., He, L., Liu, L., et al. (2019). Effects of long non-coding RNA uc.*48*+ on pain transmission in trigeminal neuralgia. *Brain Res. Bull.* 147, 92–100. doi: 10.1016/j.brainresbull.2019.02.009

Xu, M., Yan, Y., Zhu, M., Wang, Z., Zhang, X., and Zhang, D. (2020). Effects of long non-coding RNA Gm14461 on pain transmission in trigeminal neuralgia. *J. Inflamm.* 17:1. doi: 10.1186/s12950-019-0231-1

Yan, X. T., Lu, J. M., Wang, Y., Cheng, X. L., He, X. H., Zheng, W. Z., et al. (2018). XIST accelerates neuropathic pain progression through regulation of miR-150 and ZEB1 in CCI rat models. *J. Cell. Physiol.* 233, 6098–6106. doi: 10.1002/jcp.26453

Yang, Q., Yao, Y., Zhao, D., Zou, H., Lai, C., Xiang, G., et al. (2021). LncRNA H19 secreted by umbilical cord blood mesenchymal stem cells through microRNA-29a-3p/FOS axis for central sensitization of pain in advanced osteoarthritis. *Am. J. Transl. Res.* 13, 1245–1256.

Yu, W., Zhao, G. Q., Cao, R. J., Zhu, Z. H., and Li, K. (2017). LncRNA NONRATT021972 was associated with neuropathic pain scoring in patients with type 2 diabetes. *Behav. Neurol.* 2017:2941297. doi: 10.1155/2017/2941297

Zhang, B. Y., Zhang, Y. L., Sun, Q., Zhang, P. A., Wang, X. X., Xu, G. Y., et al. (2020). Alpha-lipoic acid downregulates TRPV1 receptor *via* NF-κB and attenuates neuropathic pain in rats with diabetes. *CNS Neurosci. Ther.* 26, 762–772. doi: 10.1111/cns.13303

Zhang, C., Peng, Y., Wang, Y., Xu, H., and Zhou, X. (2020). Transcribed ultraconserved noncoding RNA uc.*153* is a new player in neuropathic pain. *Pain* 161, 1744–1754. doi: 10.1097/j.pain.0000000000001868

Zhang, D., Mou, J. Y., Wang, F., Liu, J., and Hu, X. (2019). CRNDE enhances neuropathic pain *via* modulating miR-136/IL6R axis in CCI rat models. *J. Cell. Physiol.* 234, 22234–22241. doi: 10.1002/jcp.28790

Zhang, J. Y., Lv, D. B., Su, Y. N., Wang, X. L., Sheng, W. C., Yang, G., et al. (2020). LncRNA SNHG1 attenuates neuropathic pain following spinal cord injury by regulating CDK4 level. *Eur. Rev. Med. Pharmacol. Sci.* 24, 12034–12040. doi: 10.26355/eurrev_202012_23992

Zhang, L., Feng, H., Jin, Y., Zhan, Y., Han, Q., Zhao, X., et al. (2021). Long Non-coding RNA LINC01119 promotes neuropathic pain by stabilizing BDNF transcript. *Front. Mol. Neurosci.* 14:673669. doi: 10.3389/fnmol.2021.673669

Zhang, P., Sun, H., and Ji, Z. (2021). Downregulating lncRNA PVT1 relieves astrocyte overactivation induced neuropathic pain through targeting miR-186-5p/CXCL13/CXCR5 axis. *Neurochem. Res.* 46, 1457–1469. doi: 10.1007/s11064-021-03287-0

Zhang, Q., Zhou, L., Xie, H., Zhang, H., and Gao, X. (2021). HAGLR aggravates neuropathic pain and promotes inflammatory response and apoptosis of lipopolysaccharide-treated SH-SY5Y cells by sequestering miR-182-5p from ATAT1 and activating NLRP3 inflammasome. *Neurochem. Int.* 145:105001. doi: 10.1016/j.neuint.2021.105001

Zhang, Z., Sun, X., Zhao, G., Ma, Y., and Zeng, G. (2021). LncRNA embryonic stem cells expressed 1 (Lncenc1) is identified as a novel regulator in neuropathic pain by interacting with EZH2 and downregulating the expression of Bai1 in mouse microglia. *Exp. Cell Res.* 399:112435. doi: 10.1016/j.yexcr.2020.112435

Zhao, J., Yang, L., Huang, L., and Li, Z. (2021). Screening of disease-related biomarkers related to neuropathic pain (NP) after spinal cord injury (SCI). *Hum. Genom.* 15:5. doi: 10.1186/s40246-021-00303-w

Zhao, X., Shen, L., Xu, L., Wang, Z., Ma, C., and Huang, Y. (2016). Inhibition of CaMKIV relieves streptozotocin-induced diabetic neuropathic pain through regulation of HMGB1. *BMC Anesthesiol.* 16:27. doi: 10.1186/s12871-016-0191-4

Zhao, X., Tang, Z., Zhang, H., Atianjoh, F. E., Zhao, J. Y., Liang, L., et al. (2013). A long noncoding RNA contributes to neuropathic pain by silencing Kcna2 in primary afferent neurons. *Nat. Neurosci.* 16, 1024–1031. doi: 10.1038/nn.3438

Zhao, Y. X., Yao, M. J., Liu, Q., Xin, J. J., Gao, J. H., and Yu, X. C. (2020). Electroacupuncture treatment attenuates paclitaxel-induced neuropathic pain in rats *via* inhibiting spinal glia and the TLR4/NF-κB pathway. *J. Pain Res.* 13, 239–250. doi: 10.2147/JPR.S241101

Zhao, Y., Li, S., Xia, N., Shi, Y., and Zhao, C. M. (2018). Effects of XIST/miR-137 axis on neuropathic pain by targeting TNFAIP1 in a rat model. *J. Cell. Physiol.* 233, 4307–4316. doi: 10.1002/jcp.26254

Conflict of Interest: The authors declare that the research was conducted in the absence of any commercial or financial relationships that could be construed as a potential conflict of interest.

Publisher's Note: All claims expressed in this article are solely those of the authors and do not necessarily represent those of their affiliated organizations, or those of the publisher, the editors and the reviewers. Any product that may be evaluated in this article, or claim that may be made by its manufacturer, is not guaranteed or endorsed by the publisher.

frontiers in Molecular Neuroscience

REVIEW
published: 14 December 2021
doi: 10.3389/fnmol.2021.705023

Kampo Formulae for the Treatment of Neuropathic Pain ~ Especially the Mechanism of Action of *Yokukansan* ~

Masataka Sunagawa[1], Yasunori Takayama[1], Mami Kato[1], Midori Tanaka[1,2], Seiya Fukuoka[1,3], Takayuki Okumo[1], Mana Tsukada[1] and Kojiro Yamaguchi[1]*

[1] Department of Physiology, School of Medicine, Showa University, Tokyo, Japan, [2] Department of Rehabilitation Medicine, School of Medicine, Showa University, Tokyo, Japan, [3] Department of Ophthalmology, School of Medicine, Showa University, Tokyo, Japan

Kampo medicine has been practiced as traditional medicine (TM) in Japan. Kampo medicine uses Kampo formulae that are composed of multiple crude drugs to make Kampo formulae. In Japan, Kampo formulae are commonly used instead of or combined with Western medicines. If drug therapy that follows the guidelines for neuropathic pain does not work or cannot be taken due to side effects, various Kampo formulae are considered as the next line of treatment. Since Kampo formulae are composed of two or more kinds of natural crude drugs, and their extracts contain many ingredients with pharmacological effects, one Kampo formula usually has multiple effects. Therefore, when selecting a formula, we consider symptoms other than pain. This review outlines the Kampo formulae that are frequently used for pain treatment and their crude drugs and the basic usage of each component. In recent years, Yokukansan (YKS) has become one of the most used Kampo formulae for pain treatment with an increasing body of baseline research available. We outline the known and possible mechanisms by which YKS exerts its pharmacologic benefits as an example of Kampo formulae's potency and holistic healing properties.

Keywords: neuropathic pain, analgesic effect, Kampo formula, Kampo medicine, Yokukansan

OPEN ACCESS

Edited by:
Wuping Sun,
Shenzhen University, China

Reviewed by:
Toshiaki Makino,
Nagoya City University, Japan
Yasuhito Uezono,
Jikei University School of Medicine, Japan

****Correspondence:***
Masataka Sunagawa
suna@med.showa-u.ac.jp

Specialty section:
This article was submitted to Pain Mechanisms and Modulators, a section of the journal Frontiers in Molecular Neuroscience

Received: *04 May 2021*
Accepted: *22 November 2021*
Published: *14 December 2021*

Citation:
Sunagawa M, Takayama Y, Kato M, Tanaka M, Fukuoka S, Okumo T, Tsukada M and Yamaguchi K (2021) Kampo Formulae for the Treatment of Neuropathic Pain ~ Especially the Mechanism of Action of Yokukansan ~. Front. Mol. Neurosci. 14:705023. doi: 10.3389/fnmol.2021.705023

INTRODUCTION

Tricyclic antidepressants, calcium channel α2δ ligands such as gabapentin and pregabalin, and serotonin noradrenaline reuptake inhibitors (SNRIs) are the first choices for treating neuropathic pain according to the Japan Pain Clinic Society's guidelines for drug therapy (Sumitani et al., 2018). An extract from inflammatory rabbit skin inoculated with vaccinia virus, Neurotropin, and tramadol are second-line treatments. The third-line treatment is potent opioids, such as morphine, fentanyl, and oxycodone. Carbamazepine is the first choice for trigeminal neuralgia,

Abbreviations: SNRI, serotonin noradrenaline reuptake inhibitor; GJG, Goshajinkigan; EJT, Eppikajutsuto; KBG, Keishibukuryogan; GRS, Goreisan; YKS, Yokukansan; JTT, Juzentaihoto; KJT, Keishikajutsubuto; SKT, Saikokeishito; CRPS, complex regional pain syndrome; CCI, chronic constriction injury; PSL, partial sciatic nerve ligation; NMDA, *N*-methyl-D-aspartate.

while lamotrigine and baclofen are the second choices. However, the actual efficacy rates of these drugs are low (Finnerup et al., 2015). In many cases, patients have been unable to take them due to side effects. In such cases, Kampo formulae are used as a treatment option in Japan. The Japanese Ministry of Health, Labor, and Welfare has officially approved the clinical use of Kampo formulae as an ethical pharmaceutical. Kampo medicine has been practiced as traditional medicine (TM) in Japan. Kampo medicine uses Kampo formulae that are composed of multiple crude drugs to make Kampo formulae. In recent years, the need for Kampo medicine has increased, and more than 80% of doctors prescribe Kampo formulae clinically (Ito et al., 2012; Moschik et al., 2012). We herein review examples of the clinical uses of Kampo formulae for neuropathic pain and their action mechanisms based on findings in the literature.

KAMPO FORMULAE FOR NEUROPATHIC PAIN

Kampo formulae are composed of two or more kinds of natural crude drugs, and the decoctions of their mixtures are generally administered. One of the characteristics of Kampo formulae is that they are multi-component formulations, unlike most Western medicines. A single medicine has an analgesic effect along with various other effects such as improving blood flow and coldness while reducing swelling and stress. Therefore, when selecting a Kampo formula, we check for symptoms other than pain.

Table 1 shows examples. For example, patients whose pain is exacerbated by cold stimulation require medicine that relieves pain and simultaneously warms the body. Patients with an impaired blood flow receive medicine that improves the blood flow while reducing pain. Since the factors that make the pain worse can also be improved simultaneously, the therapeutic effect is higher than the administration of analgesics alone. The second feature is that almost no side effects are developed. Kampo medicines have a long history (Kuchta, 2019), and in the process, ineffective and poisonous components have been naturally eliminated. At present, only potent and safe Kampo formulae are cataloged.

Table 2 lists the Kampo formulae frequently used to treat chronic pain, their crude drugs, and each crude drug's main actions and components, classified according to their effects based on Kampo medicine. (TM) has been added to certain terms to indicate that their meaning in this content is in relation to traditional Kampo medicine. Crude drugs with mainly analgesic and anti-inflammatory effects are assigned to Class 1, those with anti-stress effects are assigned to Class 2, and those that improve blood (TM) disturbances are assigned to Class 3. Blood (TM) is a red fluid that supports the nutrition and metabolism of the body, and its disturbance patterns include static blood (TM) and blood (TM) deficiency (The Editing Committee for the Dictionary of Kampo Medicine, the Japan Society for Oriental Medicine, 2020). In addition, crude drugs that enhance the digestive function and improve physical strength are assigned to Class 4, whereas those that improve water metabolism, suppress swelling, and confer a diuretic effect are assigned to Class 5. Class 4 includes crude drugs that have a qi (TM)-tonifying effect. Qi is a fundamental energy required for life activities. Class 5 includes drugs that have a fluid (TM)-regulating effect. Fluid is a colorless fluid that supports nutrition and metabolism including interstitial fluid and lymph. Weights (g) indicate the amount of each crude drug used to produce each Kampo formula, and the drugs marked with (*) are those that play the most central role in each Kampo formula (Takayama, 2019). Aside from Goshajinkigan (GJG) and Yokukansan (YKS), the contents of crude drugs differ depending on the manufacturers, so some patterns were shown. These doses of crude drugs are mixed, and the decoction is administered.

Goshajinkigan (Chinese Name: Niu Che Sen Qi Wan)

Goshajinkigan was first described in *Ji Sheng Fang* published in 1253 in China (Yan and Liu, 2012). It is a well-balanced combination of Class 3–5 crude drugs plus Aconiti radix processa and Cinnamomi cortex, which have strong analgesic and warming effects. This combination is suitable for patients who have a decreased physical function, are extremely tired, and complain of coldness, especially in the lower limbs, a dry mouth, and dysuria. GJG is often prescribed for inferior limb pain and lower back pain (Hamaguchi et al., 2017). Recent reports have suggested that GJG may prevent chemotherapy-induced peripheral neuropathy (Nishioka et al., 2011; Cascella and Muzio, 2017).

Eppikajutsuto (Yue Bi Jia Zhu Tang)

Eppikajutsuto (EJT) was first described in *Jin Gui Yao Lue* published around 200 AD in China (Zhang, 2020). EJT mainly includes Class 1 crude drugs, such as Ephedrae Herba, Gypsum fibrosum, and Glycyrrhizae radix, which have anti-inflammatory activities, and Atractylodis lanceae rhizoma, which improves an uneven distribution of water, such as in case of edema. EJT is useful for relieving edema and knee effusion caused by allergies and inflammation, especially rheumatoid arthritis (Kogure et al., 2013). Since EJT has a very strong anti-inflammatory effect, it is an alternative to non-steroidal anti-inflammatory drugs in patients with gastrointestinal disorders.

Keishibukuryogan (Gui Zhi Fu Ling Wan)

Keishibukuryogan (KBG), which was first described in *Jin Gui Yao Lue* (Zhang, 2020), is a Kampo formula that improves various symptoms caused by a decreased blood flow and stagnation (Nozaki et al., 2007; Tomita et al., 2017). It is composed of Persicae semen and Moutan cortex, which belong to Class 3, and Paeoniae radix, which improves the blood flow. In addition, the analgesic and anti-inflammatory effects of Paeoniae radix and Cinnamomi cortex, which belong to Class 1, are also present. The administration of KBG is reported to warm diseased limbs and improve post-stroke cold sensations and numbness in the affected body parts by increasing the peripheral blood flow (Fujita et al., 2010).

TABLE 1 | Treatment strategies and examples of drug selection in Kampo medicine.

Characteristic symptoms other than pain	Treatment strategies	Representative example of Kampo formulae	References
Cold	Warm	Goshajinkigan (GJG)	Takayama et al., 2018; Matsubara et al., 2021
Heat/inflammation	Cool/anti-inflammatory	Eppikajutsuto (EJT)	Kogure et al., 2013; Shinkai et al., 2017
Microangiopathy	Improving blood flow	Keishibukuryogan (KBG)	Endo et al., 2008; Fujita et al., 2010
Dropsy/abnormal water metabolism	Improving water metabolism	Goreisan (GRS)	Yano et al., 2017; Murakami et al., 2021
Stress/anxiety	Antistress/antianxiety	Yokukansan (YKS)	Katahira et al., 2017; Wada et al., 2017
Decreased physical strength/immune deficiency	Improving physical fitness/improving immunity	Juzentaihoto (JTT)	Ishikawa et al., 2017; Takaku et al., 2020

Goreisan (Wu Ling San)

Goreisan (GRS) was first described in *Jin Gui Yao Lue* (Zhang, 2020) and *Shang Hang Lun* published around 200 AD in China (Zhang, 1999). GRS consists of Atractylodis lanceae rhizoma (or Atractylodis rhizoma), Alismatis tuber, Poria, and Polyporus (Class 5), which relieve water retention in such conditions as edema, oliguria, and diarrhea and Cinnamomi cortex, which has analgesic, anti-inflammatory, and warming effects. GRS is administered to patients with exacerbated pain due to swelling. Changes in barometric pressure that accompany weather changes can exacerbate pain, and GRS is effective in such cases (Kurihara et al., 2018).

Yokukansan (Yi Gan San)

YKS was first described in a Chinese medical book *Bao Ying Cuo Yao* published in 1556 (Kai and Ji, 2016). One characteristic of YKS is that it is mainly composed of Bupleuri radix and Uncariae uncis cum ramulus (Class 2), which have anti-stress effects. In addition, it contains crude drugs from Classes 3 to 5. It is useful for patients with a weak constitution, especially those with frustration and anger due to increased sensitivity to stress. Originally, YKS was administered to patients with symptoms of emotional irritability, neurosis, and insomnia and to infants suffering from night crying and convulsions (de Caires and Steenkamp, 2010). The crude drug components of YKS, including Glycyrrhizae radix, Bupleuri radix, Uncariae uncis cum ramulus, and Cnidii rhizome, have analgesic effects. Thus, YKS is also used to treat various pain disorders, including fibromyalgia, post-herpetic neuralgia, phantom-limb pain, headache, and trigeminal neuralgia (Nakamura et al., 2009; Yamaguchi, 2015; Sugasawa, 2016; Akiyama and Hasegawa, 2019). Many studies have been published concerning the mechanism of analgesic action of YKS. Chronic pain causes stress, and stress further promotes and exacerbates pain (Hannibal and Bishop, 2014). YKS is effective in such cases.

Juzentaihoto (Shi Quan Da Bu Tang)

Juzentaihoto (JTT) was first described in *Taiping Huimin Heji Ju Fang* published (1151) in China (Ping et al., 2017). Long-lasting pain deprives patients of physical strength and reduces their willingness to fight illness. Chronic pain may alter immune response, which can affect recovery from chronic pain (Herzberg et al., 1994; Sunagawa et al., 2000; Bethea and Fischer, 2021). The main components of JTT, Ginseng radix, and Astragali radix (Class 4) improve fatigue, malaise, loss of appetite, and weakened immunity. JTT should improve physical strength to fight illness (Yamakawa et al., 2016). In addition, JTT contains crude drugs from Classes 3 to 5. Glycyrrhizae radix, Paeoniae radix, and Cinnamomi cortex, which have analgesic effects, contribute to a well-balanced formula. JTT is frequently used for cancer patients because it enhances immune function (Saiki et al., 2017; Ogawa-Ochiai et al., 2021).

Keishikajutsubuto (Gui Zhi Jia Zhu Fu Tang)

Keishikajutsubuto (KJT) was produced by Japanese doctor Todo Yoshimasu (1702–1773) and described in *Hoki* (Yoshimasu, 1181). KJT is mainly composed of Class 1 drugs with anti-inflammatory and analgesic effects. In addition to its strong analgesic effect, Aconiti radix processa, Atractylodis lanceae rhizoma (Class 5), Cinnamomi cortex (Class 1), and Zingiberis rhizoma (Class 4) variously offer warming and diuretic effects. KJT is effective for joint pain and neuralgia associated with coldness and swelling (Nakanishi et al., 2012). Although the crude constituent drugs are similar to EJT, EJT contains Gypsum fibrosum and Ephedrae Herba, which have strong anti-inflammatory effects, and treats cases without coldness.

KAMPO FORMULAE FOR TRIGEMINAL AND GLOSSOPHARYNGEAL NEURALGIAS

In Western medicine, treatment strategies differ between trigeminal neuralgia and neuralgia in other parts of the body. Similarly, the drugs used in Kampo medicine are slightly different. Trigeminal neuralgia is divided into idiopathic trigeminal neuralgia caused by the compression of blood vessels around the nerve and symptomatic trigeminal neuralgia caused by organic diseases, such as tumors, other than vascular compression. Drug treatment is less invasive than surgery and is often the first treatment choice, including to achieve pain relief before surgery. In addition, drug administration is performed when surgical therapy, radiation therapy, and nerve block cannot be performed, or when symptoms recur. As mentioned above, the first-line drug is carbamazepine, an antiepileptic drug, but its number needed to harm is 3.4 (Cruccu et al., 2008). Its side effects, including gastrointestinal symptoms, light-headedness,

TABLE 2 | Kampo formulae for chronic pain and crude constituent drugs.

Classification	Crude drugs				Kampo formulae														References
	Latin name	English name	Main effects	Major component	GJG	EJT		KBG		GRS			YKS	JTT		KJT	SKT			
						(1)	(2)	(1)	(2)	(1)	(2)	(3)		(1)	(2)		(1)	(2)	(3)	
1	Aconiti radix processa	Processed Aconiti root	Analgesia, cardiotonic, warm	Aconitine	1.0											0.5 or 1.0				Yu et al., 2012; Deng et al., 2021; Qiu et al., 2021.
	Glycyrrhizae radix	Glycyrrhiza	Analgesia, antiinflammation, antitussive	Glycyrrhizin		2.0	2.0						1.5	1.0	1.5	2.0	1.5	1.5	2.0	Kamei et al., 2005; Wang et al., 2015
	Paeoniae radix	Peony root	Analgesia, antiinflammation, improving static blood (TM), sedation	Paeoniflorin				3.0	4.0					3.0	3.0	4.0	2.0	2.5	2.0	Li et al., 2014; Yin et al., 2016; Xin et al., 2019.
	Cinnamomi cortex	Cinnamon bark	Analgesia, antiinflammation, perspiration, warm	Cinnamaldehyde	1.0			3.0	4.0	3.0	2.0	1.5		3.0	3.0	**4.0***	2.5	2.5	2.0	Iwasaki et al., 2008; Churihar et al., 2016; Lee et al., 2018.
	Gypsum fibrosum	Gypsum	Antiinflammation, sedation	Calcium sulfate		8.0	8.0													Liu et al., 2021.
	Ephedrae Herba	Ephedrae Herb	Antiinflammation, perspiration, antitussive	Ephedrine		**6.0***	**6.0***													Miyagoshi et al., 1986; Wu et al., 2014; Cheng et al., 2017.
	Scutellariae radix	Scutellaria root	Antiinflammation	Baicalin													2.0	2.0	2.0	Shimizu et al., 2018.
2	Pinelliae tuber	Pinellia tuber	Antistress, sedation, antitussive	Homogentisic acid													4.0	4.0	4.0	Goto et al., 2013; Lin et al., 2019.
	Bupleuri radix	Bupleurum root	Antistress, antiinflammation, analgesia	Saikosaponin									2.0				**5.0***	**5.0***	**5.0***	Shin et al., 2019; Guo et al., 2020; Xu et al., 2021.
	Uncariae uncis cum ramulus	Uncaria hook	Antistress, vasodilation, analgesia	Rhynchophylline									**3.0***							Pengsuparp et al., 2001; Loh et al., 2017; Qiao et al., 2021.

(Continued)

TABLE 2 | (Continued)

Classification	Crude drugs				Kampo formulae														References
	Latin name	English name	Main effects	Major component	GJG	EJT		KBG		GRS			YKS	JTT		KJT	SKT			
						(1)	(2)	(1)	(2)	(1)	(2)	(3)		(1)	(2)		(1)	(2)	(3)	
3	Persicae semen	Peach kernel	Improving static blood (TM), antiinflammation	Amygdalin				**3.0***	**4.0***											Hao et al., 2019; He et al., 2020.
	Moutan cortex	Moutan bark	Improving static blood (TM)	Paeonol	3.0			**3.0***	**4.0***											Hirai et al., 1983.
	Rehmanniae radix	Rehmannia root	Tonifying blood (TM), analeptic	Catalpol	**5.0***									3.5	3.0					Leong et al., 2018; Wu et al., 2019.
	Angelicae acutilobae radix	Japanese angelica root	Tonifying blood (TM), analeptic	Ligustilide									3.0	3.5	3.0					Shimizu et al., 1991; Hatano et al., 2004.
	Achyranthis radix	Achyranthes root	Improving static blood (TM), improving of fluid (TM), analgesia	Ecdysterone	3.0															Luo et al., 2009; Jung et al., 2015; He et al., 2017.
	Cnidii rhizoma	Cnidium rhizome	Tonifying blood (TM), analgesia, analeptic	Cnidilide									3.0	3.0	3.0					Choi et al., 2016; Lee et al., 2016; Ningsih et al., 2020.
4	Ginseng radix	Ginseng	Tonifying qi (TM), analeptic, stomachic	Ginsenoside										**2.5***	**3.0***		2.0	2.0	2.0	Zhang et al., 2019; Fan et al., 2021; Qu et al., 2021.
	Corni fructus	Cornus fruit	Tonifying qi (TM), analeptic	Loganin	3.0															Dong et al., 2018.
	Dioscoreae rhizoma	Dioscorea rhizome	Tonifying qi (TM), analeptic, antitussive	Diosgenin	3.0															Kim et al., 2012.
	Zizyphi fructus	Jujube	Tonifying qi (TM), analeptic, antistress	Zizyphus saponin		3.0	3.0									4.0	2.0	2.0	2.0	Peng et al., 2000; Irshad et al., 2020; Wang et al., 2020.
	Zingiberis rhizoma	Ginger	Stomachic, warm	Gingerol		1.0	0.8									1.0	0.5 or 1.0	1.0	2.0	Yoshikawa et al., 1994; Chang et al., 1995; Chrubasik et al., 2005.
	Astragali radix	Astragalus root	Tonifying qi (TM), analeptic, cardiotonic	Formononetin										2.5	3.0					Zhang et al., 2011; Wei et al., 2021.

(Continued)

TABLE 2 | (Continued)

Classification	Crude drugs				Kampo formulae														References
	Latin name	English name	Main effects	Major component	GJG	EJT		KBG		GRS			YKS	JTT		KJT	SKT			
						(1)	(2)	(1)	(2)	(1)	(2)	(3)		(1)	(2)		(1)	(2)	(3)	
5	Atractylodis rhizoma	Atractylodes rhizome	Improving static blood (TM), anti-edema, stomachic	Atractylon						4.5[#]	3.0		4.0[#]	3.5	3.0[#]					Hwang et al., 1996; Shi et al., 2019; Zhang et al., 2021.
	Atractylodis lanceae rhizoma	Atractylodes lancea rhizome	Improving of fluid (TM), anti-edema, stomachic, perspiration	Atractylodin		4.0	4.0			4.5[#]		3.0	4.0[#]		3.0[#]	4.0				Yamahara et al., 1990; Koonrungsesomboon et al., 2014; Yu et al., 2017.
	Alismatis tuber	Alisma tuber	Improving of fluid (TM), anti-edema	Alisol	3.0					6.0	5.0	4.0								Makino et al., 2002; Han et al., 2013.
	Poria	Poria sclerotium	Improving of fluid (TM), anti-edema, stomachic, antistress	Eburicoic acid	3.0			3.0	4.0	**4.5***	**3.0***	**3.0***	4.0	3.5	3.0					Nukaya et al., 1996; Lee et al., 2012; Lu et al., 2021.
	Polyporus	Polyporus sclerotium	Improving of fluid (TM), anti-edema, antiinflammation	Ergosterol						4.5	3.0	3.0								Sun and Yasukawa, 2008; Zhang et al., 2010.
	Plantaginis semen	Plantago seed	Improving of fluid (TM), anti-edema, antiinflammation, antitussive	Aucubin	3.0															Park and Chang, 2004; Tzeng et al., 2016; Li et al., 2020.

All crude drugs are listed in the 17th edition of the Japanese Pharmacopeia (Pharmaceutical and Medical Device Regulatory Science Society of Japan, 2017). Class 1, crude drugs with analgesic and anti-inflammatory effects; Class 2, drugs with anti-stress effects; Class 3, drugs with blood flow-improving effects; Class 4, drugs that enhance the digestive function and improve physical strength; and Class 5, drugs that improve water metabolism, suppress swelling, and confer a diuretic effect. Traditional medicine (TM) is added to the terms used in the content of traditional Kampo medicine. Weights (g) indicate the amount of each crude drug to produce each Kampo formula, and the crude drugs marked with (*) and bold are the most active components of each medicine (Takayama, 2019). Except for GJG and YKS, the contents of crude drugs differ depending on the manufacturers, so some patterns were shown. One of the crude drugs marked with (#) (Atractylodis rhizoma or Atractylodis lanceae rhizoa) is used. GJG, Goshajinkigan; EJT, Eppikajutsuto; KBG, Keishibukuryogan; GRS, Goreisan; YKS, Yokukansan; JTT, Juzentaihoto; KJT, Keishikajutsubuto; SKT, Saikokeishito.

drowsiness, drug eruption, and myelosuppression, also cause dose reduction or discontinuation of administration. In such cases, the carbamazepine dosage may be reduced by concomitant use of Kampo formulae. Kampo formula treatment is a useful countermeasure against side effects caused by long-term carbamazepine use. Frequent treatments for trigeminal neuralgia include GRS (Kido et al., 2017), Saikokeshito (SKT) and KJT.

Glossopharyngeal neuralgia is paroxysmal pain induced by coughing, swallowing, mastication, conversation, and yawning. It occurs mainly in the back of the ear, behind the tongue, tonsils, and pharynx and just below the lower jaw angle. The incidence is reportedly 0.2/100,000, making it a very rare disease. GRS is a common glossopharyngeal neuralgia treatment that it seems to confer anti-inflammatory effects and helps reduce edema around the nerve.

The reason GRS works for trigeminal and glossopharyngeal neuralgias is unclear. However, according to oriental medical theory, neuralgia is caused by the swelling of nerves. Therefore, GRS, which has a diuretic effect, is effective against these neuralgias. KJT would be better for cases with strong symptoms of coldness.

Saikokeshito (Chai Hu Gui Zhi Tang)

Saikokeshito was first described in *Jin Gui Yao Lue* (Zhang, 2020) and *Shang Hang Lun* (Zhang, 1999). SKT is usually given to patients with cold accompanied by gastrointestinal symptoms. Still, most crude drugs such as Glycyrrhizae radix, Paeoniae radix, Cinnamomi cortex, Scutellariae radix, and Bupleuri radix have analgesic and anti-inflammatory effects. SKT has been reported to exert analgesic activity in a rat trigeminal neuralgia model (Sunagawa et al., 2001). Some reports indicate the efficacy of SKT for epilepsy (Aimi et al., 1976). Therefore, SKT may have an anticonvulsant effect and may be effective for trigeminal neuralgia.

ACTION MECHANISMS OF YOKUKANSAN FOR NEUROPATHIC PAIN

Kampo medicines have a long history, and although their effectiveness has been empirically recognized, their mechanisms of action have not been completely clarified. However, in recent years, basic research on the Kampo formula has been actively conducted, and evidence based Kampo medicine treatments are also being carried out. For physicians who are trained under Western medicine, evidence-based drug selection is more familiar and easier to understand than narrative-based ones. In this section we will consider the mechanism through which Kampo formulae exert their analgesic effects, using YKS as an example.

YKS has been found clinically effective for diseases with chronic pain, including post-herpetic neuralgia, central post-stroke pain, post-traumatic spinal cord injury pain, thalamic syndrome, complex regional pain syndrome (CRPS; Nakamura et al., 2009), trigeminal neuralgia (Yamaguchi, 2015; Takinami et al., 2017), phantom pain (Sugasawa, 2016), migraine (Akiyama and Hasegawa, 2019), and headache (Kimura et al., 2008). Mitsuhata et al. (2010) administered YKS to 121 patients with chronic pain who did not respond to conventional drug therapy or nerve block treatment and found it effective in 73 patients (60%). They also found YKS to be effective in 25 of 47 chronic lumbar and inferior limb pain cases (53%), 3 of 6 cervical or lumbar post-surgery syndrome cases (50%), 13 of 20 post-herpetic neuralgia cases (65%), 6 of 8 herpes zoster neuralgia cases (75%), 7 of 15 cervical spondylosis/cervical spondylotic radiculopathy cases (47%), 2 of 4 perineal pain cases (50%), and 6 of 6 CRPS cases (100%). Considering that all of these entities are intractable painful diseases, the efficacy rate seems to be relatively high.

The analgesic effect of YKS has been proven in some animal models, including a chronic constriction injury (CCI) model (Suzuki et al., 2012; Suga et al., 2015), partial sciatic nerve ligation (PSL) model (Ebisawa et al., 2015), bone metastasis model (Nakao et al., 2019), and adjuvant arthritis model (Honda et al., 2013). Several factors are involved in the complex development and promotion of neuropathic pain. Increased reactivity of the dorsal horn of the spinal cord, i.e., central sensitization, is considered one cause of hyperalgesia and allodynia. Central sensitization includes the following: (1) enhancement of excitatory synaptic transmission, (2) attenuation of inhibitory synaptic transmission, (3) activation of glial cells, and (4) dysfunction of the descending pain modulatory system.

Enhancement of Excitatory Synaptic Transmission and Yokukansan

From the terminal of the primary afferent nerve C-fiber, neurotransmitters like glutamate and substance P act on each receptor in the dorsal horn of the spinal cord. Continuous or repetitive stimulation from the primary nerve promotes excitatory synaptic transmission by activating and phosphorylating the glutamate receptor, *N*-methyl-D-aspartate (NMDA) receptor.

YKS was observed to attenuate excessive glutamate release from presynaptic sites (Takeda et al., 2008). The removal of glutamate in the synaptic cleft is mainly carried out by the two glutamate transporters in astrocytes: glutamate transporter 1 (GLT- 1) and glutamate/aspartate transporter. YKS has been reported to promote the GLT-1-mediated uptake of glutamate using cultured astrocytes (Ueki et al., 2018). This action appears to be due to Glycyrrhizin and its metabolite, 18β-glycyrrhetinic acid, as well as a compound found in Glycyrrhizae radix (Kawakami et al., 2010). Furthermore, YKS has an antagonistic effect on the NMDA receptor. Isoliquiritigenin, a component of Glycyrrhizae radix, acts as the antagonist (Kawakami et al., 2011). Thus, YKS may suppress excessive neurotransmission mediated by glutamate. Suzuki et al. (2012) reported that YKS inhibited mechanical and cold allodynia in the rat CCI model and reduced the cerebrospinal fluid dialyzate level of glutamate increased by stimulation with a brush or acetone.

Attenuation of Inhibitory Synaptic Transmission and Yokukansan

The hypofunctions of GABAergic neurons, which are inhibitory interneurons in the spinal dorsal horn, occurred in rodents with chronic pain (Fu et al., 2017). YKS has been reported to reverse

the reduction in pentobarbital-induced sleep durations in socially isolated mice (Egashira et al., 2011). It also exhibited anxiolytic effects (Kamei et al., 2009), which are thought to be mediated by $GABA_A$ receptors. Liao et al. (1995) reported that the water extract of Angelicae acutilobae radix binds to $GABA_A$ receptors *in vitro*. These findings suggest that YKS can be expected to exert an inhibitory effect on synaptic transmissions *via* the GABAergic neuron.

Activation of Glial Cells and Yokukansan

In animal models of schizophrenia (Furuya et al., 2013), multiple sclerosis (Nomura et al., 2017), and behavioral and psychological symptoms of dementia (Ikarashi et al., 2009), YKS suppresses glial cell (microglia and astrocytes) activity. The activation of these glial cells is associated with the development and persistence of neuropathic pain (Tsuda, 2018), so glial cells and their associated molecules became the targets of YKS treatment. Suga et al. (2015) reported that the administration of YKS inhibited the expression of activated astrocytes and astrogliosis in the CCI rat model. Ebisawa et al. (2015) reported that YKS inhibited the increased expression of interleukin-6 mRNA in the dorsal horn of the spinal cord in the PSL mouse model, and the expression was confirmed in astrocytes and/or microglia, not in neurons. Furthermore, only the administration of Atratylodis Lanceae rhizoma exhibited the same effect. These studies suggest that YKS is effective against neuropathic pain, as evidenced by the regulation of microglial and astrocytic functions, which indicate the formula's potential mechanisms.

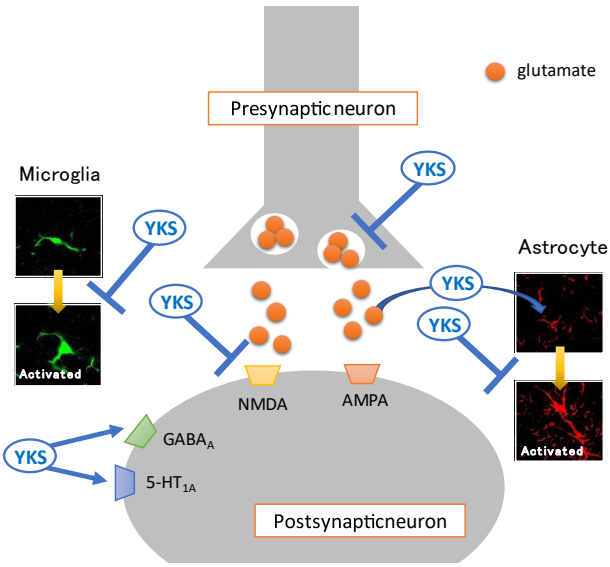

FIGURE 1 | Mechanisms of action of Yokukansan for neuropathic pain. Several different mechanisms of action may act on neurotransmission in the spinal dorsal horn. (1) Attenuation of excessive glutamate release from presynaptic neurons. (2) Promotion of the uptake of glutamate into astrocytes. (3) Antagonistic effect on the glutamate receptor, *N*-methyl-D-aspartate (NMDA) receptor. (4) Agonistic effect on the $GABA_A$ receptor. (5) Inhibition of the activation of glia cells (microglia and astrocyte). (6) Agonistic effect on the serotonin 5-HT_{1A} receptor. YKS, Yokukansan; AMPA, α-amino-3-hydroxy-5-methyl-4-isoxazolepropionic acid receptor.

Dysfunction of the Descending Pain Modulatory System and Yokukansan

Descending neurons from the rostral ventromedial medulla mainly secrete serotonin. In contrast, neurons from the locus ceruleus secrete noradrenaline. Serotonin acts on 5-HT_{1A} and 5-HT_{1B} receptors, which are suppressive serotonin receptors in spinal dorsal horn neurons. Noradrenaline acts on α2 receptors, which suppress synaptic transmission. SNRI treats chronic pain with the expectation that this effect will be enhanced. Dysfunction of the descending pain modulatory system reportedly involves the development of chronic pain (Ossipov et al., 2014). YKS acts as an agonist of the 5-HT_{1A} receptor; geissoschizine methyl ether, an alkaloid synthesized by the YKS component Uncariae uncis cum ramulus, is believed to play this role (Nishi et al., 2012; Yamaguchi et al., 2012). However, whether or not YKS improves the dysfunction of the descending pain modulatory system is unclear, so further studies are needed.

Other Actions of Yokukansan

The pre-administration of YKS attenuated the development of morphine antinociceptive tolerance, and suppression of glial cell activation may be one mechanism underlying this phenomenon (Takemoto et al., 2016; Katayama et al., 2018). A study that investigated orexin secretion found that orexin secretion was significantly increased in rats with morphine tolerance; however, YKS administration significantly suppressed it (Katayama et al., 2018). Orexin is a neuropeptide secreted from the hypothalamus. It has an analgesic effect (Yamamoto et al., 2003), but under pathological conditions of chronic pain, the excessive secretion of orexin may disrupt the pain modulatory system. The administration of an orexin receptor antagonist to rats with morphine tolerance, therefore suppressed the decrease in the pain threshold (Erami et al., 2012) and also exerted analgesic effects against acute and chronic pain (McDonald et al., 2016). We also found that YKS suppressed orexin secretion in a dose-dependent manner in healthy rats (Katahira et al., 2017). These findings suggest that the analgesic effect of YKS is partly involved in the inhibition of orexin secretion.

Oxytocin is also a neuropeptide secreted from the hypothalamus and has been reported to have a central-acting analgesic effect (Sun et al., 2018; González-Hernández et al., 2019). YKS administration also increased oxytocin secretion in rats (Kanada et al., 2018). The analgesic effect of YKS may be related to the secretagogue effect of oxytocin. Future studies should be conducted using pain model animals. **Figure 1** summarizes the main actions of YKS.

CONCLUSION

The multiple ingredients that comprise Kampo formulae exert various beneficial effects. Although the individual pharmacological action of the components might be weak, the combination of these actions confers a holistic effect on

intractable pain. This is an important point to consider in future pain treatment strategies. Multiple central sensitizations cause chronic pain; therefore, multi-component drugs, such as Kampo formulae, are more beneficial than seeking a strong analgesic effect with a single agent. In addition, identifying the active ingredients in the drugs used in traditional medicine can lead to the development of new drugs.

AUTHOR CONTRIBUTIONS

YT and MS participated in the conception and design. KY and MS wrote the draft. All authors retrieved and reviewed the literature and accepted responsibility for the entire content of this manuscript and approved its submission.

REFERENCES

Aimi, S., Saito, T., and Matsuda, T. (1976). The effect of Saiko-Keishi-to on the treatment of epilepsy, referring to the improvement of the electroencephalogram of them [in Japanese, English abstract]. *J. Jpn. Soc. Orient. Med.* 27, 99–116.

Akiyama, H., and Hasegawa, Y. (2019). Effectiveness of the traditional Japanese Kampo medicine Yokukansan for chronic migraine: A case report. *Med* 98:e17000. doi: 10.1097/MD.0000000000017000

Bethea, J. R., and Fischer, R. (2021). Role of Peripheral Immune Cells for Development and Recovery of Chronic Pain. *Front. Immunol.* 12:641588. doi: 10.3389/fimmu.2021.641588

Cascella, M., and Muzio, M. R. (2017). Potential application of the Kampo medicine goshajinkigan for prevention of chemotherapy-induced peripheral neuropathy. *J. Integr. Med.* 15, 77–87. doi: 10.1016/S2095-4964(17)60313-3

Chang, C. P., Chang, J. Y., Wang, F. Y., and Chang, J. G. (1995). The effect of Chinese medicinal herb Zingiberis rhizoma extract on cytokine secretion by human peripheral blood mononuclear cells. *J. Ethnopharmacol.* 48, 13–19. doi: 10.1016/0378-8741(95)01275-i

Cheng, Y., Zhang, Y., Xing, H., Qian, K., Zhao, L., and Chen, X. (2017). Comparative Pharmacokinetics and Bioavailability of Three Ephedrines in Rat after Oral Administration of Unprocessed and Honey-Fried Ephedra Extract by Response Surface Experimental Design. *Evid. Based Complement. Alternat. Med.* 2017:2802193. doi: 10.1155/2017/2802193

Choi, T. Y., Jun, J. H., Park, B., Lee, J. A., You, S., Jung, J., et al. (2016). Concept of blood stasis in Chinese medical textbooks: a systematic review. *Eur. J. Integr. Med.* 8, 158–164. doi: 10.1016/j.eujim.2015.09.137

Chrubasik, S., Pittler, M. H., and Roufogalis, B. D. (2005). Zingiberis rhizoma: a comprehensive review on the ginger effect and efficacy profiles. *Phytomedicine* 12, 684–701. doi: 10.1016/j.phymed.2004.07.009

Churihar, R., Solanki, P., Vyas, S., Hemant Tanwani, H., and Shubham Atal, S. (2016). Analgesic activity of cinnamaldehyde per se and it's interaction with diclofenac sodium and pentazocine in swiss albino mice. *Int. J. Phamacog.* 3, 97–102. doi: 10.13040/IJPSR.0975-8232.IJP.3(2).97-102

Cruccu, G., Gronseth, G., Alksne, J., Argoff, C., Brainin, M., Burchiel, K., et al. (2008). AAN-EFNS guidelines on trigeminal neuralgia management. *Eur. J. Neurol.* 15, 1013–1028. doi: 10.1111/j.1468-1331.2008.02185.x

de Caires, S., and Steenkamp, V. (2010). Use of Yokukansan (TJ-54) in the treatment of neurological disorders: a review. *Phytother. Res.* 24, 1265–1270. doi: 10.1002/ptr.3146

Deng, J., Han, J., Chen, J., Zhang, Y., Huang, Q., Wang, Y., et al. (2021). Comparison of analgesic activities of aconitine in different mice pain models. *PLoS One* 16:e0249276. doi: 10.1371/journal.pone.0249276

Dong, Y., Feng, Z. L., Chen, H. B., Wang, F. S., and Lu, J. H. (2018). *Corni Fructus*: a review of chemical constituents and pharmacological activities. *Chin. Med.* 13, 1–20. doi: 10.1186/s13020-018-0191-z

Ebisawa, S., Andoh, T., Shimada, Y., and Kuraishi, Y. (2015). Yokukansan improves mechanical allodynia through the regulation of interleukin-6 expression in the spinal cord in mice with neuropathic pain. *Evid. Based Complement. Alternat. Med.* 2015:870687. doi: 10.1155/2015/870687

Egashira, N., Nogami, A., Iwasaki, K., Ishibashi, A., Uchida, N., Takasaki, K., et al. (2011). Yokukansan enhances pentobarbital-induced sleep in socially isolated mice: possible involvement of GABA(A)-benzodiazepine receptor complex. *J. Pharmacol. Sci.* 116, 316–320. doi: 10.1254/jphs.11079SC

Endo, F., Oguchi, T., Ikeda, M., Sugimura, T., Shiga, Y., Yashi, M., et al. (2008). Prospective clinical study of keishibukuryogan on pain caused by varicocele. *J. Trad. Med.* 25, 52–54. doi: 10.11339/jtm.25.52

Erami, E., Azhdari-Zarmehri, H., Rahmani, A., Ghasemi-Dashkhasan, E., Semnanian, S., and Haghparast, A. (2012). Blockade of orexin receptor 1 attenuates the development of morphine tolerance and physical dependence in rats. *Pharmacol. Biochem. Behav.* 103, 212–219. doi: 10.1016/j.pbb.2012.08.010

Fan, J., Liu, S., Ai, Z., Chen, Y., Wang, Y., Li, Y., et al. (2021). Fermented ginseng attenuates lipopolysaccharide-induced inflammatory responses by activating the TLR4/MAPK signaling pathway and remediating gut barrier. *Food Funct.* 12, 852–861. doi: 10.1039/d0fo02404j

Finnerup, N. B., Attal, N., Haroutounian, S., McNicol, E., Baron, R., Dworkin, R. H., et al. (2015). Pharmacotherapy for neuropathic pain in adults: a systematic review and meta-analysis. *Lancet Neurol.* 14, 162–173.

Fu, H., Li, F., Thomas, S., and Yang, Z. (2017). Hyperbaric oxygenation alleviates chronic constriction injury (CCI)-induced neuropathic pain and inhibits GABAergic neuron apoptosis in the spinal cord. *Scand. J. Pain* 17, 330–338. doi: 10.1016/j.sjpain.2017.08.014

Fujita, K., Yamamoto, T., Kamezaki, T., and Matsumura, A. (2010). Efficacy of keishibukuryogan, a traditional Japanese herbal medicine, in treating cold sensation and numbness after stroke: clinical improvement and skin temperature normalization in 22 stroke patients. *Neurol. Med. Chir.* 50, 1–6. doi: 10.2176/nmc.50.1

Furuya, M., Miyaoka, T., Tsumori, T., Liaury, K., Hashioka, S., Wake, R., et al. (2013). Yokukansan promotes hippocampal neurogenesis associated with the suppression of activated microglia in Gunn rat. *J. Neuroinflamm.* 10:145.

González-Hernández, A., Espinosa, De Los Monteros-Zuñiga, A. E., Martínez-Lorenzana, G., and Condés-Lara, M. (2019). Recurrent antinociception induced by intrathecal or peripheral oxytocin in a neuropathic pain rat model. *Exp. Brain Res.* 237, 2995–3010. doi: 10.1007/s00221-019-05651-7

Goto, F., Morimoto, N., Taiji, H., Tsutumi, T., and Ogawa, K. (2013). Treating pediatric psychogenic dizziness with a Japanese herbal medicine. *Explore* 9, 41–43. doi: 10.1016/j.explore.2012.10.005

Guo, J., Zhang, F., Gao, J., Guan, X., Liu, B., Wang, X., et al. (2020). Proteomics-based screening of the target proteins associated with antidepressant-like effect and mechanism of Saikosaponin A. *J. Cell Mol. Med.* 24, 174–188. doi: 10.1111/jcmm.14695

Hamaguchi, T., Yoshino, T., Horiba, Y., and Watanabe, K. (2017). Goshajinkigan for low back pain: an observational study. *J. Altern. Complement. Med.* 23, 208–213. doi: 10.1089/acm.2016.0276

Han, C. W., Kwun, M. J., Kim, K. H., Choi, J. Y., Oh, S. R., Ahn, K. S., et al. (2013). Ethanol extract of Alismatis Rhizoma reduces acute lung inflammation by suppressing NF-κB and activating Nrf2. *J. Ethnopharmacol.* 146, 402–410. doi: 10.1016/j.jep.2013.01.010

Hannibal, K. E., and Bishop, M. D. (2014). Chronic stress, cortisol dysfunction, and pain: A psychoneuroendocrine rationale for stress management in pain rehabilitation. *Phys. Ther.* 94, 1816–1825. doi: 10.2522/ptj.20130597

Hao, E., Pang, G., Du, Z., Lai, Y.-H., Chen, J.-R., Xie, J., et al. (2019). Peach Kernel Oil Downregulates Expression of Tissue Factor and Reduces Atherosclerosis in ApoE knockout Mice. *Int. J. Mol. Sci.* 20:405. doi: 10.3390/ijms20020405

Hatano, R., Takano, F., Fushiya, S., Michimata, M., Tanaka, T., Kazama, I., et al. (2004). Water-soluble extracts from Angelica acutiloba Kitagawa enhance hematopoiesis by activating immature erythroid cells in mice with 5-fluorouracil-induced anemia. *Exp. Hematol.* 32, 918–924. doi: 10.1016/j.exphem.2004.07.003

He, X. Y., Wu, L. J., Wang, W. X., Xie, P. J., Chen, Y. H., and Wang, F. (2020). Amygdalin-A pharmacological and toxicological review. *J. Ethnopharmacol.* 254:112717. doi: 10.1016/j.jep.2020.112717

He, X., Wang, X., Fang, J., Chang, Y., Ning, N., Guo, H., et al. (2017). The genus Achyranthes: A review on traditional uses, phytochemistry, and pharmacological activities. *J. Ethnopharmacol.* 203, 260–278. doi: 10.1016/j.jep.2017.03.035

Herzberg, U., Murtaugh, M., and Beitz, A. J. (1994). Chronic pain and immunity: mononeuropathy alters immune responses in rats. *Pain* 59, 219–225. doi: 10.1016/0304-3959(94)90074-4

Hirai, A., Terano, T., Hamazaki, T., Sajiki, J., Saito, H., Tahara, K., et al. (1983). Studies on the mechanism of antiaggregatory effect of Moutan Cortex. *Thromb. Res.* 3, 29–40. doi: 10.1016/0049-3848(83)90005-1

Honda, Y., Sunagawa, M., Yoneyama, S., Ikemoto, H., Nakanishi, T., Iwanami, H., et al. (2013). Analgesic and anti-stress effects of Yokukansan in rats with adjuvant arthritis. *Kampo Med.* 64, 78–85. doi: 10.3937/kampomed.64.78

Hwang, J. M., Tseng, T. H., Hsieh, Y. S., Chou, F. P., Wang, C. J., and Chu, C. Y. (1996). Inhibitory effect of atractylon on tert-butyl hydroperoxide induced DNA damage and hepatic toxicity in rat hepatocytes. *Arch. Toxicol.* 70, 640–644. doi: 10.1007/s002040050323

Ikarashi, Y., Iizuka, S., Imamura, S., Yamaguchi, T., Sekiguchi, K., Kanno, H., et al. (2009). Effects of yokukansan, a traditional Japanese medicine, on memory disturbance and behavioral and psychological symptoms of dementia in thiamine-deficient rats. *Biol. Pharm. Bull.* 32, 1701–1709. doi: 10.1248/bpb.32.1701

Irshad, Z., Hanif, M. A., Ayub, M. A., Hanif, A., and Afridi, H. I. (2020). "Jujube," in *Medicinal Plants of South Asia*, eds M. A. Hanif, H. Nawaz, M. M. Khan, and H. J. Byrne (Amsterdam: Elsevier), 451–463.

Ishikawa, S., Ishikawa, T., Tezuka, C., Asano, K., Sunagawa, M., and Hisamitsu, T. (2017). Efficacy of Juzentaihoto for Tumor Immunotherapy in B16 Melanoma Metastasis Model. *Evid. Based Complement. Alternat. Med.* 2017:6054706. doi: 10.1155/2017/6054706

Ito, A., Munakata, K., Imazu, Y., and Watanabe, K. (2012). First nationwide attitude survey of Japanese physicians on the use of traditional Japanese medicine (kampo) in cancer treatment. *Evid. Based Complement. Alternat. Med.* 2012:957082. doi: 10.1155/2012/957082

Iwasaki, Y., Tanabe, M., Kobata, K., and Watanabe, T. (2008). TRPA1 agonists—allyl isothiocyanate and cinnamaldehyde—induce adrenaline secretion. *Biosci. Biotechnol. Biochem.* 72, 2608–2614. doi: 10.1271/bbb.80289

Jung, S. K., Choi, D. W., Kwon, D. A., Kim, M. J., Seong, K. S., and Shon, D. H. (2015). Oral administration of achyranthis radix extract prevents TMA-induced allergic contact dermatitis by regulating th2 cytokine and chemokine production in vivo. *Molecules* 20, 21584–21596. doi: 10.3390/molecules201219788

Kai, X., and Ji, X. (2016). *Bao ying cuo yao*. Beijing: China Press of Traditional Chinese Medicine.

Kamei, J., Miyata, S., and Ohsawa, M. (2009). Involvement of the benzodiazepine system in the anxiolytic-like effect of Yokukansan (Yi-gan san). *Prog. Neuropsychopharmacol. Biol. Psychiatry* 33, 1431–1437. doi: 10.1016/j.pnpbp.2009.07.023

Kamei, J., Saitoh, A., Asano, T., Nakamura, R., Ichiki, H., Iiduka, A., et al. (2005). Pharmacokinetic and pharmacodynamic profiles of the antitussive principles of Glycyrrhizae radix (licorice), a main component of the Kampo preparation Bakumondo-to (Mai-men-dong-tang). *Eur. J. Pharmacol.* 507, 163–168. doi: 10.1016/j.ejphar.2004.11.042

Kanada, Y., Katayama, A., Ikemoto, H., Takahashi, K., Tsukada, M., Nakamura, A., et al. (2018). Inhibitory effect of the Kampo medicinal formula Yokukansan on acute stress-induced defecation in rats. *Neuropsychiatr. Dis. Treat.* 14, 937–944. doi: 10.2147/NDT.S156795

Katahira, H., Sunagawa, M., Watanabe, D., Kanada, Y., Katayama, A., Yamauchi, R., et al. (2017). Antistress effects of Kampo medicine "Yokukansan" via regulation of orexin secretion. *Neuropsychiatr. Dis. Treat.* 13, 863–872. doi: 10.2147/NDT.S129418

Katayama, A., Kanada, Y., Tsukada, M., Akanuma, Y., Takemura, H., Ono, T., et al. (2018). Yokukansan (Kampo medicinal formula) prevents the development of morphine tolerance by inhibiting the secretion of orexin A. *Integr. Med. Res.* 7, 141–148. doi: 10.1016/j.imr.2018.02.005

Kawakami, Z., Ikarashi, Y., and Kase, Y. (2010). Glycyrrhizin and its metabolite 18β-glycyrrhetinic acid in Glycyrrhiza, a constituent herb of yokukansan, ameliorate thiamine deficiency-induced dysfunction of glutamate transport in cultured rat cortical astrocytes. *Eur. J. Pharmacol.* 626, 154–158. doi: 10.1016/j.ejphar.2009.09.046

Kawakami, Z., Ikarashi, Y., and Kase, Y. (2011). Isoliquiritigenin is a novel NMDA receptor antagonist in Kampo medicine yokukansan. *Cell. Mol. Neurobiol.* 31, 1203–1212. doi: 10.1007/s10571-011-9722-1

Kido, H., Komasawa, N., Fujiwara, S., and Minami, T. (2017). Efficacy of go-rei-san for pain management in four patients with intractable trigeminal neuralgia [In Japanese, English Abstract]. *Masui* 66, 184–186.

Kim, S., Shin, S., Hyun, B., Kong, H., Han, S., Lee, A., et al. (2012). Immunomodulatory Effects of Dioscoreae Rhizome Against Inflammation through Suppressed Production of Cytokines Via Inhibition of the NF-κB Pathway. *Immune Netw.* 12, 181–188. doi: 10.4110/in.2012.12.5.181

Kimura, Y., Shimizu, S., Tanaka, A., Suzuki, M., Kinebuchi, A., Inaki, K., et al. (2008). Efficacy of yokukansan-based prescriptions for the treatment of patients with headache [In Japanese, English Abstract]. *Kampo Med.* 59, 265–271. doi: 10.3937/kampomed.59.265

Kogure, T., Harada, N., Tatsumi, T., and Fujinaga, H. (2013). Persistent undifferentiated arthritis successfully treated with the Japanese herbal medicine "Eppikajutsuto". *Eur. J. Integr. Med.* 5, 184–188. doi: 10.1016/j.eujim.2012.11.001

Koonrungsesomboon, N., Na-Bangchang, K., and Karbwang, J. (2014). Therapeutic potential and pharmacological activities of Atractylodes lancea (Thunb.) DC. *Asian Pac. J. Trop. Med.* 7, 421–428. doi: 10.1016/S1995-7645(14)60069-9

Kuchta, K. (2019). Traditional Japanese kampo medicine–history of ideas and practice; Part 1: from ancient shamanic practice to the medical academies of Edo. *Trad. Kampo Med.* 6, 49–56. doi: 10.1002/tkm2.1209

Kurihara, Y., Han, C., Harada, Y., and Kobayashi, H. (2018). General introduction to Kampo medicine - the nuts and bolts of Kampo -. *Juntendo Med. J.* 64, 258–263. doi: 10.14789/jmj.2018.64.JMJ18-R09

Lee, S. C., Wang, S. Y., Li, C. C., and Liu, C. T. (2018). Anti-inflammatory effect of cinnamaldehyde and linalool from the leaf essential oil of Cinnamomum osmophloeum Kanehira in endotoxin-induced mice. *J. Food Drug Anal.* 26, 211–220. doi: 10.1016/j.jfda.2017.03.006

Lee, S. M., Lee, Y. J., Yoon, J. J., Kang, D. G., and Lee, H. S. (2012). Effect of Poria cocos on hypertonic stress-induced water channel expression and apoptosis in renal collecting duct cells. *J. Ethnopharmacol.* 141, 368–376. doi: 10.1016/j.jep.2012.02.048

Lee, W. S., Shin, J. S., Jang, D. S., and Lee, K. T. (2016). Cnidilide, an alkylphthalide isolated from the roots of Cnidium officinale, suppresses LPS-induced NO, PGE2, IL-1β, IL-6 and TNF-α production by AP-1 and NF-κB inactivation in RAW 264.7 macrophages. *Int. Immunopharmacol.* 40, 146–155. doi: 10.1016/j.intimp.2016.08.021

Leong, P. K., Chen, J., and Ko, K. M. (2018). "Development of Chinese Herbal Health Products for the Prevention of Aging-Associated Diseases," in *Natural Products and Drug Discovery*, eds S. C. Mandal, V. Mandal, and T. Konishi (Amsterdam: Elsevier), 73–104. doi: 10.1016/B978-0-08-102081-4.00004-6

Li, C., Wen, R., Liu, W., Liu, Q., Yan, L. P., Wu, J. X., et al. (2020). Diuretic Effect and Metabolomics Analysis of Crude and Salt-Processed Plantaginis Semen. *Front. Pharmacol.* 11:563157. doi: 10.3389/fphar.2020.563157

Li, Y., Wu, P., Ning, Y., Yan, X., Zhu, T., Ma, C., et al. (2014). Sedative and hypnotic effect of freeze-dried paeoniflorin and Sini San freeze-dried powder in pentobarbital sodium-induced mice. *J. Tradit. Chin. Med.* 34, 184–187. doi: 10.1016/s0254-6272(14)60076-5

Liao, J. F., Jan, Y. M., Huang, S. Y., Wang, H. H., Yu, L. L., and Chen, C. F. (1995). Evaluation with receptor binding assay on the water extracts of ten CNS-active Chinese herbal drugs. *Proc. Natl. Sci. Counc. Repub. China B* 19, 151–158.

Lin, S., Nie, B., Yao, G., Yang, H., Ye, R., and Yuan, Z. (2019). Pinellia ternata (Thunb.) Makino Preparation promotes sleep by increasing REM sleep. *Nat. Prod. Res.* 33, 3326–3329. doi: 10.1080/14786419.2018.1474466

Liu, K., Han, S., Gao, W., Tang, Y., Han, X., Liu, Z., et al. (2021). Changes of Mineralogical Properties and Biological Activities of Gypsum and Its Calcined Products with Different Phase Structures. *Evid. Based Complement. Alternat. Med.* 2021:6676797. doi: 10.1155/2021/6676797

Loh, Y. C., Ch'ng, Y. S., Tan, C. S., Ahmad, M., Asmawi, M. Z., and Yam, M. F. (2017). Mechanisms of action of Uncaria rhynchophylla ethanolic extract for its vasodilatory effects. *J. Med. Food* 20, 895–911. doi: 10.1089/jmf.2016.3804

Lu, J., Tian, J., Zhou, L., Meng, L., Chen, S., Ma, C., et al. (2021). Phytochemistry and Biological Activities of *Poria*. *J. Chem.* 2021:6659775. doi: 10.1155/2021/6659775

Luo, C., Zhang, Y., Chi, L., Li, L., and Chen, K. (2009). Protective effect and mechanism of ecdysterone on injury of focal cerebral infarct in rats. *Medical J. Natl. Defend. Forces Southwest China* 19, 176–178.

Makino, B., Kobayashi, M., Kimura, K., Ishimatsu, M., Sakakibara, I., Higuchi, M., et al. (2002). Local variation in the content of angiotensin II and arginine vasopressin receptor antagonistic terpenoids in the rhizomes of Alisma orientale. *Planta Med.* 68, 226–231. doi: 10.1055/s-2002-23129

Matsubara, Y., Okuda, H., Harada, K. H., Youssefian, S., and Koizumi, A. (2021). Mechanical allodynia triggered by cold exposure in mice with the Scn11a p.R222S mutation: a novel model of drug therapy for neuropathic pain related to NaV1.9. *Naunyn Schmiedeberg's Arch. Pharmacol.* 394, 299–306. doi: 10.1007/s00210-020-01978-z

McDonald, T., Liang, H. A., Sanoja, R., Gotter, A. L., Kuduk, S. D., Coleman, P. J., et al. (2016). Pharmacological evaluation of orexin receptor antagonists in preclinical animal models of pain. *J. Neurogenet.* 30, 32–41. doi: 10.3109/01677063.2016.1171862

Mitsuhata, H., Nakamura, Y., Kawagoe, I., Tajima, K., Kanai, M., Konishi, R., et al. (2010). Efficacy of yokukansan against neuropathic pain: clinical reports and the animal study [In Japanese, English Abstract]. *Pain Kampo Med.* 20, 13–19.

Miyagoshi, M., Amagaya, S., and Ogihara, Y. (1986). Antitussive effects of L-ephedrine, amygdalin, and makyokansekito (Chinese traditional medicine) using a cough model induced by sulfur dioxide gas in mice. *Planta Med.* 52, 275–278. doi: 10.1055/s-2007-969151

Moschik, E. C., Mercado, C., Yoshino, T., Matsuura, K., and Watanabe, K. (2012). Usage and attitudes of physicians in Japan concerning traditional Japanese medicine (kampo medicine): a descriptive evaluation of a representative questionnaire-based survey. *Evid. Based Complement. Alternat. Med.* 2012:139818. doi: 10.1155/2012/139818

Murakami, K., Horie, I., Hara-Chikuma, M., Shimizu, T., Matsumoto, C., and Isohama, Y. (2021). Goreisan regulates AQP3 expression and improves diarrhea. *Tradit. Kampo Med.* 8, 91–99. doi: 10.1002/tkm2.1276

Nakamura, Y., Tajima, K., Kawagoe, I., Kanai, M., and Mitsuhata, H. (2009). Efficacy of traditional herbal medicine, Yokukansan on patients with neuropathic pain [In Japanese, English Abstract]. *Masui* 58, 1248–1255.

Nakanishi, M., Arimitsu, J., Kageyama, M., Otsuka, S., Inoue, T., Nishida, S., et al. (2012). Efficacy of traditional Japanese herbal medicines—Keishikajutsubuto (TJ-18) and Bushi-matsu (TJ-3022)—against post-herpetic neuralgia aggravated by self-reported cold stimulation: a case series. *J. Altern. Complement. Med.* 18, 686–692. doi: 10.1089/acm.2010.0745

Nakao, K., Fujiwara, A., Komasawa, N., Jin, D., Kitano, M., Matsunami, S., et al. (2019). Yokukansan alleviates cancer pain by suppressing matrix metalloproteinase-9 in a mouse bone metastasis model. *Evid. Based Complement. Alternat. Med.* 2019:3513064. doi: 10.1155/2019/2956920

Ningsih, F. N., Okuyama, T., To, S., Nishidono, Y., Okumura, T., Tanaka, K., et al. (2020). Comparative Analysis of Anti-inflammatory Activity of the Constituents of the Rhizome of Cnidium officinale Using Rat Hepatocytes. *Biol. Pharm. Bull.* 43, 1867–1875. doi: 10.1248/bpb.b20-00416

Nishi, A., Yamaguchi, T., Sekiguchi, K., Imamura, S., Tabuchi, M., Kanno, H., et al. (2012). Geissoschizine methyl ether, an alkaloid in Uncaria hook, is a potent serotonin1A receptor agonist and candidate for amelioration of aggressiveness and sociality by yokukansan. *Neuroscience* 207, 124–136. doi: 10.1016/j.neuroscience.2012.01.037

Nishioka, M., Shimada, M., Kurita, N., Iwata, T., Morimoto, S., Yoshikawa, K., et al. (2011). The Kampo medicine, Goshajinkigan, prevents neuropathy in patients treated by FOLFOX regimen. *Int. J. Clin. Oncol.* 16, 322–327. doi: 10.1007/s10147-010-0183-1

Nomura, T., Bando, Y., You, H., Tanaka, T., and Yoshida, S. (2017). Yokukansan reduces cuprizone-induced demyelination in the corpus callosum through anti-inflammatory effects on microglia. *Neurochem. Res.* 42, 3525–3536. doi: 10.1007/s11064-017-2400-z

Nozaki, K., Goto, H., Nakagawa, T., Hikiami, H., Koizumi, K., Shibahara, N., et al. (2007). Effects of keishibukuryogan on vascular function in adjuvant-induced arthritis rats. *Biol. Pharm. Bull.* 30, 1042–1047. doi: 10.1248/bpb.30.1042

Nukaya, H., Yamashiro, H., Fukazawa, H., Ishida, H., and Tsuji, K. (1996). Isolation of inhibitors of TPA-induced mouse ear edema from Hoelen, Poria cocos. *Chem. Pharm. Bull.* 44, 847–849. doi: 10.1248/cpb.44.847

Ogawa-Ochiai, K., Katagiri, T., Sato, Y., Shirai, A., Ishiyama, K., Takami, A., et al. (2021). Natural killer cell function changes by the Japanese Kampo Medicine juzentaihoto in General fatigue patients. *Adv. Integr. Med.* 8, 33–43. doi: 10.1016/j.aimed.2019.12.003

Ossipov, M. H., Morimura, K., and Porreca, F. (2014). Descending pain modulation and chronification of pain. *Curr. Opin. Support. Palliat. Care* 8, 143–151. doi: 10.1097/SPC.0000000000000055

Park, K. S., and Chang, I. M. (2004). Anti-inflammatory activity of aucubin by inhibition of tumor necrosis factor-α production in RAW 264.7 cells. *Planta Med.* 70, 778–779. doi: 10.1055/s-2004-827211

Peng, W. H., Hsieh, M. T., Lee, Y. S., Lin, Y. C., and Liao, J. (2000). Anxiolytic effect of seed of Ziziphus jujuba in mouse models of anxiety. *J. Ethnopharmacol.* 72, 435–441. doi: 10.1016/s0378-8741(00)00255-5

Pengsuparp, T., Indra, B., Nakagawasai, O., Tadano, T., Mimaki, Y., Sashida, Y., et al. (2001). Pharmacological studies of geissoschizine methyl ether, isolated from Uncaria sinensis Oliv., in the central nervous system. *Eur. J. Pharmacol.* 425, 211–218. doi: 10.1016/s0014-2999(01)01195-5

Pharmaceutical and Medical Device Regulatory Science Society of Japan (2017). *Japanese pharmacopoeia seventeenth edition (JP XVII) English version*. Tokyo: Yakuji Nippo.

Ping, T., Min, H., Ji, H., and Bian, J. (2017). *Taiping Huimin Heji Ju Fang*. Beijin: People's Health Publisher.

Qiao, Y. L., Zhou, J. J., Liang, J. H., Deng, X. P., Zhang, Z. J., Huang, H. L., et al. (2021). Uncaria rhynchophylla ameliorates unpredictable chronic mild stress-induced depression in mice via activating 5-HT1A receptor: Insights from transcriptomics. *Phytomedicine* 81:153436. doi: 10.1016/j.phymed.2020.153436

Qiu, L. Z., Zhou, W., Yue, L. X., Wang, Y. H., Hao, F. R., Li, P. Y., et al. (2021). Repeated Aconitine Treatment Induced the Remodeling of Mitochondrial Function via AMPK–OPA1–ATP5A1 Pathway. *Front. Pharmacol.* 12:646121. doi: 10.3389/fphar.2021.646121

Qu, Q., Yang, F., Zhao, C., Liu, X., Yang, P., Li, Z., et al. (2021). Effects of fermented ginseng on the gut microbiota and immunity of rats with antibiotic-associated diarrhea. *J. Ethnopharmacol.* 267:113594. doi: 10.1016/j.jep.2020.113594

Saiki, I., Yokoyama, S., and Hayakawa, Y. (2017). Effect of juzentaihoto/Shi-Quan-Da-Bu-Tang on malignant progression and metastasis of tumor cells. *World J. Trad. Chin. Med.* 3, 26–45. doi: 10.1248/bpb.23.677

Shi, K., Qu, L., Lin, X., Xie, Y., Tu, J., Liu, X., et al. (2019). Deep-Fried Atractylodis Rhizoma Protects against Spleen Deficiency-Induced Diarrhea through Regulating Intestinal Inflammatory Response and Gut Microbiota. *Int. J. Mol. Sci.* 21:124. doi: 10.3390/ijms21010124

Shimizu, M., Matsuzawa, T., Suzuki, S., Yoshizaki, M., and Morita, N. (1991). Evaluation of Angelicae Radix (Touki) by the inhibitory effect on platelet aggregation. *Chem. Pharm. Bull.* 39, 2046–2048. doi: 10.1248/cpb.39.2046

Shimizu, T., Shibuya, N., Narukawa, Y., Oshima, N., Hada, N., and Kiuchi, F. (2018). Synergistic effect of baicalein, wogonin and oroxylin A mixture: multistep inhibition of the NF-κB signalling pathway contributes to an anti-inflammatory effect of Scutellaria root flavonoids. *J. Nat. Med.* 72, 181–191. doi: 10.1007/s11418-017-1129-y

Shin, J. S., Im, H. T., and Lee, K. T. (2019). Saikosaponin B2 Suppresses Inflammatory Responses Through IKK/IκBα/NF-κB Signaling Inactivation in LPS-Induced RAW 264.7 Macrophages. *Inflammation* 42, 342–353. doi: 10.1007/s10753-018-0898-0

Shinkai, T., Masumoto, K., Chiba, F., and Tanaka, N. (2017). A large retroperitoneal lymphatic malformation successfully treated with traditional Japanese Kampo medicine in combination with surgery. *Surg. Case Rep.* 3, 1–4. doi: 10.1186/s40792-017-0358-3

Suga, H., Sunagawa, M., Ikemoto, H., Nakanishi, T., Fujiwara, A., and Okada, M. (2015). The analgesic and anti-stress effects of a Kampo medicine (Yokukansan) in rats with chronic constriction injury–a comparative study with kamishoyosan. *J. Integr. Ther.* 2:5. doi: 10.13188/2378-1343.1000009

Sugasawa, Y. (2016). Effect of yokukansan, Japanese herbal medicine, on phantom-limb pain. *Middle East J. Anaesthesiol.* 23, 499–500.

Sumitani, M., Sakai, T., Matsuda, Y., Abe, H., Yamaguchi, S., Hosokawa, T., et al. (2018). Executive summary of the clinical guidelines of pharmacotherapy for

neuropathic pain: by the Japanese Society of Pain Clinicians. *J. Anesth.* 32, 463–478. doi: 10.1007/s00540-018-2501-0

Sun, W., Zhou, Q., Ba, X., Feng, X., Hu, X., Cheng, X., et al. (2018). Oxytocin relieves neuropathic pain through GABA release and presynaptic TRPV1 inhibition in spinal cord. *Front. Mol. Neurosci.* 11:248. doi: 10.3389/fnmol.2018.00248

Sun, Y., and Yasukawa, K. (2008). New anti-inflammatory ergostane-type ecdysteroids from the sclerotium of Polyporus umbellatus. *Bioorg. Med. Chem. Lett.* 18, 3417–3420. doi: 10.1016/j.bmcl.2008.04.008

Sunagawa, M., Okada, M., Guo, S. Y., and Hisamitsu, T. (2000). Splenic natural killer cell activity is suppressed by ligation of unilateral mental nerve in rats [In Japanese, English abstract]. *Masui Jap. J. Anesthesiol.* 49, 250–254.

Sunagawa, M., Okada, M., Guo, S. Y., and Hisamitsu, T. (2001). Effectiveness of Saiko-Keishi-To (TJ-10, a Kampo herbal medicine) for trigeminal neuralgia in rats [In Japanese, English abstract]. *Masui Jap. J. Anesthesiol.* 50, 486–490.

Suzuki, Y., Mitsuhata, H., Yuzurihara, M., and Kase, Y. (2012). Antiallodynic effect of herbal medicine yokukansan on peripheral neuropathy in rats with chronic constriction injury. *Evid. Based Complement. Alternat. Med.* 2012:953459. doi: 10.1155/2012/953459

Takaku, S., Shimizu, M., and Takahashi, H. (2020). Japanese Kampo Medicine Juzentaihoto Enhances Antitumor Immunity in CD1d-/- Mice Lacking NKT Cells. *Integr. Cancer Ther.* 19:1534735419900798. doi: 10.1177/1534735419900798

Takayama, K. (2019). *Kampo Joyoshohou Kaisetsu*, edition 2nd Edn. Chiba: Toyo Gakujutsu Shuppansha.

Takayama, S., Arita, R., Kikuchi, A., Ohsawa, M., Kaneko, S., and Ishii, T. (2018). Clinical practice guidelines and evidence for the efficacy of traditional Japanese herbal medicine (Kampo) in treating geriatric patients. *Front. Nutr.* 5:66. doi: 10.3389/fnut.2018.00066

Takeda, A., Itoh, H., Tamano, H., Yuzurihara, M., and Oku, N. (2008). Suppressive effect of Yokukansan on excessive release of glutamate and aspartate in the hippocampus of zinc-deficient rats. *Nutr. Neurosci.* 11, 41–46. doi: 10.1179/147683008X301414

Takemoto, M., Sunagawa, M., Okada, M., Ikemoto, H., Suga, H., Katayama, A., et al. (2016). Yokukansan, a Kampo medicine, prevents the development of morphine tolerance through the inhibition of spinal glial cell activation in rats. *Integr. Med. Res.* 5, 41–47. doi: 10.1016/j.imr.2015.12.003

Takinami, Y., Mita, K., Nagai, A., Yamakawa, J., and Ohara, H. (2017). A case of trigeminal neuralgia successfully treated with yokukansan [in Japanese, English abstract]. *Kampo Med.* 68, 358–361. doi: 10.3937/kampomed.68.358

The Editing Committee for the Dictionary of Kampo Medicine, the Japan Society for Oriental Medicine (2020). *The Dictionary of Kampo Medicine -Basic terms-*. Kyoto: Medical Yukon.

Tomita, T., Hirayama, A., Matsui, H., and Aoyagi, K. (2017). Effect of keishibukuryogan, a Japanese traditional Kampo prescription, on improvement of microcirculation and Oketsu and induction of endothelial nitric oxide: A live imaging study. *Evid. Based Complement. Alternat. Med.* 2017:3620130. doi: 10.1155/2017/3620130

Tsuda, M. (2018). Modulation of pain and itch by spinal glia. *Neurosci. Bull.* 34, 178–185. doi: 10.1007/s12264-017-0129-y

Tzeng, T. F., Liu, W. Y., Liou, S. S., Hong, T. Y., and Liu, I. M. (2016). Antioxidant-rich extract from plantaginis semen ameliorates diabetic retinal injury in a streptozotocin-induced diabetic rat model. *Nutrients* 8:572. doi: 10.3390/nu8090572

Ueki, T., Kawakami, Z., Kanno, H., Omiya, Y., Mizoguchi, K., and Yamamoto, M. (2018). Yokukansan, a traditional Japanese medicine, enhances the glutamate transporter GLT-1 function in cultured rat cortical astrocytes. *Evid. Based Complement. Alternat. Med.* 2018:6804017. doi: 10.1155/2018/6804017

Wada, S., Inoguchi, H., Hirayama, T., Matsuoka, Y. J., Uchitomi, Y., Ochiai, H., et al. (2017). Yokukansan for the treatment of preoperative anxiety and postoperative delirium in colorectal cancer patients: a retrospective study. *Jpn. J. Clin. Oncol.* 47, 844–848. doi: 10.1093/jjco/hyx080

Wang, H. L., Li, Y. X., Niu, Y. T., Zheng, J., Wu, J., Shi, G. J., et al. (2015). Observing Anti-inflammatory and Anti-nociceptive Activities of Glycyrrhizin Through Regulating COX-2 and Pro-inflammatory Cytokines Expressions in Mice. *Inflammation* 38, 2269–2278. doi: 10.1007/s10753-015-0212-3

Wang, L., Jing, N., Liu, X., Jiang, G., and Liu, Z. (2020). Nurturing and modulating gut microbiota with jujube powder to enhance anti-PD-L1 efficiency against murine colon cancer. *J. Funct. Foods* 64:103647. doi: 10.1016/j.jff.2019.103647

Wei, H., Ding, L., Wang, X., Yan, Q., Jiang, C., Hu, C., et al. (2021). Astragalus root extract improved average daily gain, immunity, antioxidant status and ruminal microbiota of early weaned yak calves. *J. Sci. Food Agric.* 101, 82–90. doi: 10.1002/jsfa.10617

Wu, C., Shan, J., Feng, J., Wang, J., Qin, C., Nie, G., et al. (2019). Effects of dietary Radix Rehmanniae Preparata polysaccharides on the growth performance, immune response and disease resistance of Luciobarbus capito. *Fish Shellfish Immunol.* 89, 641–646. doi: 10.1016/j.fsi.2019.04.027

Wu, Z., Kong, X., Zhang, T., Ye, J., Fang, Z., and Yang, X. (2014). Pseudoephedrine/ephedrine shows potent anti-inflammatory activity against TNF-α-mediated acute liver failure induced by lipopolysaccharide/D-galactosamine. *Eur. J. Pharmacol.* 724, 112–121. doi: 10.1016/j.ejphar.2013.11.032

Xin, Q., Yuan, R., Shi, W., Zhu, Z., Wang, Y., and Cong, W. (2019). A review for the anti-inflammatory effects of paeoniflorin in inflammatory disorders. *Life Sci.* 237:116925. doi: 10.1016/j.lfs.2019.116925

Xu, Y., Yu, Y., Wang, Q., Li, W., Zhang, S., Liao, X., et al. (2021). Active components of Bupleurum chinense and Angelica biserrata showed analgesic effects in formalin induced pain by acting on Nav1.7. *J. Ethnopharmacol.* 269:113736. doi: 10.1016/j.jep.2020.113736

Yamaguchi, K. (2015). Traditional Japanese herbal medicines for treatment of odontopathy. *Front. Pharmacol.* 6:176. doi: 10.3389/fphar.2015.00176

Yamaguchi, T., Tsujimatsu, A., Kumamoto, H., Izumi, T., Ohmura, Y., Yoshida, T., et al. (2012). Anxiolytic effects of yokukansan, a traditional Japanese medicine, via serotonin 5-HT_{1A} receptors on anxiety-related behaviors in rats experienced aversive stress. *J. Ethnopharmacol.* 143, 533–539. doi: 10.1016/j.jep.2012.07.007

Yamahara, J., Matsuda, H., Huang, Q., Li, Y. U. H. A. O., and Fujimura, H. (1990). Intestinal motility enhancing effect of Atractylodes lancea rhizome. *J. Ethnopharmacol.* 29, 341–344. doi: 10.1016/0378-8741(90)90044-t

Yamakawa, J., Moriya, J., and Kobayashi, J. (2016). Fatigue and Kampo (Japanese herbal) medicines: Hochuekkito and juzentaihoto. *Methods Pharmacol. Toxicol.* 2016, 97–111. doi: 10.3389/fphar.2020.00917

Yamamoto, T., Saito, O., Shono, K., Aoe, T., and Chiba, T. (2003). Anti-mechanical allodynic effect of intrathecal and intracerebroventricular injection of orexin-A in the rat neuropathic pain model. *Neurosci. Lett.* 347, 183–186. doi: 10.1016/s0304-3940(03)00716-x

Yan, Y. H., and Liu, Y. J. Z. (2012). *Yan Shi Ji Sheng Fang (TCM clinical Intangible Cultural Heritage Classic Reader)*, 1st Edn. Tianjin: Chinese Medical Science and Technology Press.

Yano, Y., Yano, H., Takahashi, H., Yoshimoto, K., Tsuda, S., Fujiyama, K., et al. (2017). Goreisan Inhibits Upregulation of Aquaporin 4 and Formation of Cerebral Edema in the Rat Model of Juvenile Hypoxic-Ischemic Encephalopathy. *Evid. Based. Complement. Alternat. Med.* 2017:3209219. doi: 10.1155/2017/3209219

Yin, D., Liu, Y. Y., Wang, T. X., Hu, Z. Z., Qu, W. M., Chen, J. F., et al. (2016). Paeoniflorin exerts analgesic and hypnotic effects via adenosine A1 receptors in a mouse neuropathic pain model. *Psychopharmacology* 233, 281–293. doi: 10.1007/s00213-015-4108-6

Yoshikawa, M., Yamaguchi, S., Kunimi, K., Matsuda, H., Okuno, Y., Yamahara, J., et al. (1994). Stomachic principles in ginger. III. An anti-ulcer principle, 6-gingesulfonic acid, and three monoacyldigalactosylglycerols, gingerglycolipids A, B, and C, from Zingiberis Rhizoma originating in Taiwan. *Chem. Pharm. Bull.* 42, 1226–1230. doi: 10.1248/cpb.42.1226

Yoshimasu, T. (1181). *Hoki*. Available online at: https://rmda.kulib.kyoto-u.ac.jp/item/rb00000733 (accessed August 16, 2021).

Yu, C., Xiong, Y., Chen, D., Li, Y., Xu, B., Lin, Y., et al. (2017). Ameliorative effects of atractylodin on intestinal inflammation and co-occurring dysmotility in both constipation and diarrhea prominent rats. *Kor. J. Physiol. Pharmacol.* 21, 1–9. doi: 10.4196/kjpp.2017.21.1.1

Yu, H. Y., Wang, S. J., Teng, J. L., Ji, X. M., Wu, Z. C., Ma, Q. C., et al. (2012). Effects of Radix aconiti lateralis preparata and Rhizoma zingiberis on energy metabolism and expression of the genes related to metabolism in rats. *Chin. J. Integr. Med.* 18, 23–29. doi: 10.1007/s11655-012-0964-7

Zhang, G., Zeng, X., Han, L., Wei, J. A., and Huang, H. (2010). Diuretic activity and kidney medulla AQP_1, AQP_2, AQP_3, V_2R expression of the aqueous extract of sclerotia of Polyporus umbellatus FRIES in normal rats. *J. Ethnopharmacol.* 128, 433–437. doi: 10.1016/j.jep.2010.01.032

Zhang, S., Tang, X., Tian, J., Li, C., Zhang, G., Jiang, W., et al. (2011). Cardioprotective effect of sulphonated formononetin on acute myocardial infarction in rats. *Basic Clin. Pharmacol. Toxicol.* 108, 390–395. doi: 10.1111/j.1742-7843.2011.00676.x

Zhang, W. J., Zhao, Z. Y., Chang, L. K., Cao, Y., Wang, S., Kang, C. Z., et al. (2021). Atractylodis Rhizoma: A review of its traditional uses, phytochemistry, pharmacology, toxicology and quality control. *J. Ethnopharmacol.* 266:113415. doi: 10.1016/j.jep.2020.113415

Zhang, Y., Qiu, Z., Qiu, Y., Su, T., Qu, P., and Jia, A. (2019). Functional Regulation of Ginsenosides on Myeloid Immunosuppressive Cells in the Tumor Microenvironment. *Integr. Cancer. Ther.* 18:1534735419886655. doi: 10.1177/1534735419886655

Zhang, Z. (1999). *Shang Han Lun: On Cold Damage, Translation & Commentaries*. Taos, NM: Paradigm Publications.

Zhang, Z. (2020). *Essentials from the Golden Cabinet: Translation and Annotation of Jin Gui Yao Lue*. Singapore: World Scientific.

Conflict of Interest: MS received a research grant from Tsumura & Co. (Tokyo, Japan).

The remaining authors declare that the research was conducted in the absence of any commercial or financial relationships that could be construed as a potential conflict of interest.

frontiers in Molecular Neuroscience

ORIGINAL RESEARCH
published: 16 December 2021
doi: 10.3389/fnmol.2021.728128

Selected Thiadiazine-Thione Derivatives Attenuate Neuroinflammation in Chronic Constriction Injury Induced Neuropathy

Sonia Qureshi[1], Gowhar Ali[1,2], Muhammad Idrees[3,4], Tahir Muhammad[5,6], Il-Keun Kong[3,4,7]*, Muzaffar Abbas[8], Muhammad Ishaq Ali Shah[9], Sajjad Ahmad[10], Robert D. E. Sewell[11] and Sami Ullah[1]*

[1] Department of Pharmacy, University of Peshawar, Peshawar, Pakistan, [2] Laboratory of Neurogenomics and Novel Therapies, The Ken and Ruth Davee Department of Neurology, Department of Neurology and Clinical Neurosciences, Feinberg School of Medicine, Northwestern University, Chicago, IL, United States, [3] Division of Applied Life Science (BK21 Four), Gyeongsang National University, Jinju, South Korea, [4] Institute of Agriculture and Life Science, Gyeongsang National University, Jinju, South Korea, [5] Molecular Neuropsychiatry and Development (MiND) Lab, Campbell Family Mental Health Research Institute, Centre for Addiction and Mental Health, Toronto, ON, Canada, [6] Institute of Medical Science, University of Toronto, Toronto, ON, Canada, [7] The Kingkong Co., Ltd., Gyeongsang National University, Jinju, South Korea, [8] Faculty of Pharmacy, Capital University of Science & Technology, Islamabad, Pakistan, [9] Department of Chemistry, Abdul Wali Khan University, Mardan, Pakistan, [10] Department of Health and Biological Sciences, Abasyn University, Peshawar, Pakistan, [11] School of Pharmacy and Pharmaceutical Sciences, Cardiff University, Cardiff, United Kingdom

OPEN ACCESS

Edited by:
Tao Liu,
The First Affiliated Hospital of Nanchang University, China

Reviewed by:
Filipa Pinto-Ribeiro,
University of Minho, Portugal
Cyril Rivat,
Université de Montpellier, France

***Correspondence:**
Gowhar Ali
gowhar.ali@northwestern.edu;
gowhar_ali@uop.edu.pk;
gohar.pharmacist@gmail.com
orcid.org/0000-0002-9749-0645
Il-Keun Kong
ikong7900@gmail.com

Specialty section:
This article was submitted to Pain Mechanisms and Modulators, a section of the journal Frontiers in Molecular Neuroscience

Received: 20 June 2021
Accepted: 17 November 2021
Published: 16 December 2021

Citation:
Qureshi S, Ali G, Idrees M, Muhammad T, Kong I-K, Abbas M, Shah MIA, Ahmad S, Sewell RDE and Ullah S (2021) Selected Thiadiazine-Thione Derivatives Attenuate Neuroinflammation in Chronic Constriction Injury Induced Neuropathy. Front. Mol. Neurosci. 14:728128. doi: 10.3389/fnmol.2021.728128

Neuropathic pain refers to a lesion or disease of peripheral and/or central somatosensory neurons and is an important body response to actual or potential nerve damage. We investigated the therapeutic potential of two thiadiazine-thione [TDT] derivatives, 2-(5-propyl-6-thioxo-1, 3, 5-thiadiazinan-3-yl) acetic acid [TDT1] and 2-(5-propyl-2-thioxo-1, 3, 5-thiadiazinan-3-yl) acetic acid [TDT2] against CCI (chronic constriction injury)-induced neuroinflammation and neuropathic pain. Mice were used for assessment of acute toxicity of TDT derivatives and no major toxic/bizarre responses were observed. Anti-inflammatory activity was assessed using the carrageenan test, and both TDT1 and TDT2 significantly reduced carrageenan-induced inflammation. We also used rats for the induction of CCI and performed allodynia and hyperalgesia-related behavioral tests followed by biochemical and morphological analysis using RT-qPCR, immunoblotting, immunohistochemistry and immunofluorescence. Our findings revealed that CCI induced clear-cut allodynia and hyperalgesia which was reversed by TDT1 and TDT2. To determine the function of TDT1 and TDT2 in glia-mediated neuroinflammation, Iba1 mRNA and protein levels were measured in spinal cord tissue sections from various experimental groups. Interestingly, TDT1 and TDT2 substantially reduced the mRNA expression and protein level of Iba1, implying that TDT1 and TDT2 may mitigate CCI-induced astrogliosis. *In silico* molecular docking studies predicted that both compounds had an effective binding affinity for TNF-α and COX-2. The compounds interactions with the proteins were dominated by both hydrogen

bonding and van der Waals interactions. Overall, these results suggest that TDT1 and TDT2 exert their neuroprotective and analgesic potentials by ameliorating CCI-induced allodynia, hyperalgesia, neuroinflammation and neuronal degeneration in a dose-dependent manner.

Keywords: thiadiazine-thione, neuropathic pain, allodynia/hyperalgesia, astrocyte, tumor necrotic factor-alpha

INTRODUCTION

Neuropathic pain is a condition instigated by a lesion of somatosensory neurons including both the peripheral and/or the central nervous system (Jensen et al., 2011). Neuropathologically, it is an important body response that indicates actual or potential neuronal damage and protects the body from deep injuries. Neuronal damage that leads to neuropathic pain may last for years (Alles and Smith, 2018) and, together with nociceptive pain, represents a fundamental pain condition (Freynhagen et al., 2019). Chronic neuropathic pain usually encompasses both peripheral and central neuropathic pain (Scholz et al., 2019). Often, it is ineffectively controlled clinically, possibly due to its complex etiology regularly characterized by clinical manifestations such as allodynia, paresthesia, stinging pain, numbness, and hyperalgesia that result in generalized discomfort and an altered quality of life (Jensen and Finnerup, 2014; Wu et al., 2019). The exact pathogenesis of neuropathic pain is still largely unknown, however, some evidence indicates that neurotransmitter systems involving ion channels, multiple types of receptor and various peripheral and central nervous system cells interactively contribute to the pathogenesis of neuropathological pain (Descalzi et al., 2015).

An epidemiological survey has shown that quite a high proportion of patients with neuropathic pain do not receive completely appropriate therapy (Kapural et al., 2018). For the treatment of peripheral neuropathy, first-line drugs include tricyclic antidepressants (TCA), anticonvulsants, non-steroidal anti-inflammatory drugs (NSAID), topical lidocaine, and selective serotonin and norepinephrine reuptake inhibitors (SNRI). TCAs are effective for multiple types of neuropathic pain including nerve injury pain, diabetic peripheral neuropathic pain and central post-stroke pain (Xu et al., 2012; Pusan and Abdi, 2018), Moreover, selected anticonvulsants are considered to be the drugs of choice for treatment of peripheral neuropathies (Muthuraman and Singh, 2012) but they are associated with adverse effects including dizziness, hallucinations, confusion, somnolence, and sedation. The second-line treatments for neuropathies include opioid analgesics like tramadol, however, long term use of such analgesics may lead to dependence and a withdrawal syndrome at the end of therapy which may limit their chronic use (Johnson et al., 2015). Thiadiazine-thione derivatives (TDT) have been reported for their promising medicinal properties which include antibacterial, antifungal, anthelminthic, antiprotozoal, tuberculostatic (Avuloğlu-Yılmaz et al., 2017), herbicidal and antioxidant activities (Wang et al., 2019). In addition to antimicrobial activity, these compounds have a place in the treatment of arteriosclerosis and possess anti-fibrinolytic (Ozçelik et al., 2007), cytotoxic (Sever et al., 2016), and antiepileptic activity (Ahmad et al., 2017; Arshad et al., 2018).Thiadiazine-thione derivatives have also been studied as potential components of prodrugs for different biological activities. Thus, antibiotic drugs like ampicillin, amoxicillin, and cephalexin have been incorporated with the thiadiazine-thione nucleus to create prodrugs (Arshad et al., 2018). Despite the disclosure of several multiple pharmaceutical and biological activities of thiadiazine-thione derivatives, to date, these compounds have not been screened against neuropathic pain (Shah M. I. A. et al., 2019).

Both neuroinflammatory and neuropathic pain involves a range of common mediators. These include nuclear factor-κB (NF-κB), activated microglia (ionized calcium-binding adaptor molecule 1 [Iba-1]), pro-inflammatory cytokines including tumor necrotic factor α (TNF-α), interleukin-1/8(Il-1/8) and the neurotrophin nerve growth factor (NGF). A selection of these mediators has been shown to contribute toward the initiation not only of thermal, but also mechanical hyperalgesia (Woolf et al., 1997). In relation to this, antibodies induced in response to TNF-α reduce hyperalgesia which tends to ameliorate rheumatoid arthritis (Bresnihan et al., 1998) and neuropathic pain. In contrast, there is an indication that endogenous IL-6 may mediate certain hypersensitive responses that characterize peripheral neuropathic pain (Murphy et al., 1999).

In our study, we have explored the activity of two specific TDT derived test compounds, i.e., 2-(5-propyl-6-thioxo-1, 3, 5-thiadiazinan-3-yl) acetic acid (TDT1) (**Figure 1A**) and 2-(5-propyl-2-thioxo-1, 3, 5-thiadiazinan-3-yl) acetic acid (TDT2) (**Figure 1B**) in nociceptive and acute inflammation mice models. Then we developed a chronic constriction injury (CCI) rat model of neuropathic pain and examined the potentials of TDT1 and TDT2 against neuropathic pain. During the course of the investigation, we performed behavioral, biochemical and histopathological analyses to appraise the anti-inflammatory and antinociceptive potential of TDT1 and TDT2 against CCI-induced neuropathic pain in rodent models.

MATERIALS AND METHODS

Chemicals and Kits

The following reagents with sources were employed: dimethyl sulfoxide DMSO (Cas No: 67-68-5) (Sigma, United States), Tween 80 (Cas No: 9005-65-6) (Sigma, United States), gabapentin (Cas No. 60142-96-3 (Sigma, United States), xylene (Cas No: 1330-20-7) (Thermo Fisher Scientific, United States),

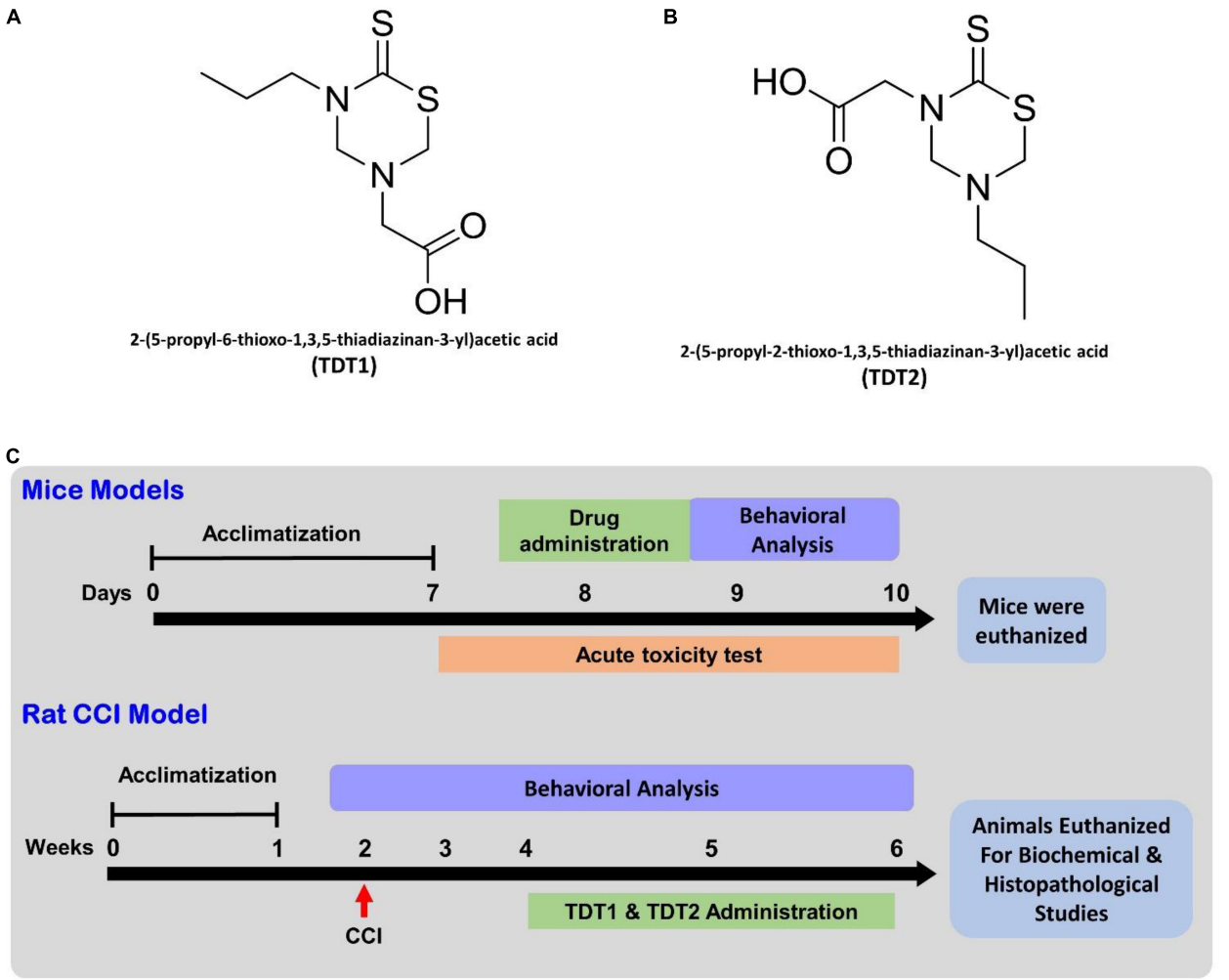

FIGURE 1 | (A,B) Chemical structure of the test compounds 2-(5-propyl-6-thioxo-1, 3, 5-thiadiazinan-3-yl) acetic acid (TDT1) and 2-(5-propyl-2-thioxo-1, 3, 5-thiadiazinan-3-yl) acetic acid (TDT2). **(C)** Representative schematic diagram of the experiment schedule showing CCI-operation, behavioral analysis and treatment plan.

ketamine (Cas No:1867-66-9) (Sigma, United States), 1% acetic acid (Cas No: 64-19-7) (Sigma, United States), naloxone (Cas No: 357-08-4) (Sigma Aldrich, United States), tramadol (Cas No: 36282-47-0) (Sigma, United States), pentylenetetrazol (Cas No: 54-95-5) (Sigma-Aldrich, United States), 1% carrageenan (Cas No: 9000-07-1) (Sigma-Aldrich, United States), hematoxylin (Cas No: 517-28-2) (Sigma-Aldrich, United States), eosin (Cas No: 548-24-3) (Sigma-Aldrich, United States), normal saline (Cas No: 7647-14-5) (Sigma-Aldrich, United States), Aspirin (Cas No: 50-78-2) (Sigma-Aldrich, United States), ELISA Rat TNF-α Kit (Catalog No: E-EL-R0019) (Elabscience), ImunoCruz (Santa Cruz biotechnology. Inc., United States) (Catalog No: CA95060-5706), ab6789 Goat Pab to Ms IgG (Catalog No: GR311326-6) (Santa Cruz biotechnology), COX-2 mouse monoclonal IgM (Catalog No:sc-376861) (Santa Cruz biotechnology United States), p-NFκB p65 mouse monoclonal IgG 2b (Catalog No: sc-136548) Santa Cruz biotechnology, TNF-α IgG1 (Catalog No: sc-52746) (Santa Cruz biotechnology United States), Anti-Iba1 -AIF1 polyclonal antibody (Catalog No: K006764P) (Solarbio Life Sciences).

Animals and Experimental Groups

For hot plate, tail immersion, abdominal constriction, and carrageenan tests Balb-C mice (18–22 g) of both sexes were used and each group contained n = 6–8 animals. Mice were grouped as; (1) WT-vehicle (vehicle: normal saline with 1% tween and 2% DMSO) group, (2) STD group, (3) TDT 1–30 mg/kg, (4) TDT 1–45 mg/kg, (5) TDT 2–30 mg/kg, and (6) TDT 2–45 mg/kg. Sprague Dawley rats (300–450 g) were used for chronic constriction injury model generation. Animals were randomly assigned to separate groups each containing 6–8 rats. The study continued for 30 days and during this time we measured hind paw withdrawal latency. The experimental groups were designated as (1) Sham-operated group; (2) CCI group (vehicle: normal saline with 1% tween and 2% DMSO); (3) CCI + standard drug (STD) group; (4) CCI + TDT 1–30 mg/kg; (5) CCI + TDT

1–45 mg/kg; (6) CCI + TDT 2–30 mg/kg; (7) CCI + TDT 2–45 mg/kg. Both test compounds (TDT1 and TDT2) were dissolved in 2% DMSO plus 1% Tween 80 and vehicle in a ratio of 5:1:94. All chemical solutions were freshly prepared before drug administration. The experimental area was maintained on a12/12 h light/dark cycle at 22 ± 2°C. Rats were bred in the animal house and bioassay laboratory, Department of Pharmacy University of Peshawar. The animals had *ad libitum* access to food and water throughout. The experimental procedures on animals were performed according to United Kingdom Animals (Scientific procedures) Act 1986 and following protocols set by the ethical committee of the Department of Pharmacy, University of Peshawar (registration number: 19/EC/F.LIFE-2020). TDT derivatives were checked for their solubility pattern in different solvents that included dimethyl sulfoxide (DMSO), methanol, distilled water and dimethyl formide (DMF). Test compounds suspensions were made by mixing test compound with normal saline and made soluble by adding 1% tween along with 2% DMSO (Khan et al., 2019).

Experimental Design

Mice were acclimatized in the experimental room for 1 week after which they were used for tests like acute toxicity, hot plate, tail immersion abdominal constrictions and carrageenan tests for determination of antinociceptive and anti-inflammatory activities of TDT1 and TDT2. Next, rats were also acclimatized for 1 week in the experimental room followed by initiating the CCI model. Rats were allowed for 14 days to develop neuropathy. The development of neuropathy was confirmed by behavioral studies starting 1 day before CCI operation and continued on 3rd, 14th, 21st, and 28th day of the experiment. Treatment was started 14 days after the CCI operation and continued for 14 days. Rats were euthanized on day 30th and spinal cord tissue samples were collected for further biochemical and morphological analysis (**Figure 1C**).

Acute Toxicity Analysis

To determine the acute toxicity of either test compound, separate Balb-C mice irrespective of their sex were used in each group injected intraperitoneally with test compounds at doses ranging from Group 1 (250 mg/kg), Group 2 (350 mg/kg), Group 3 (500 mg/kg), Group 4 (650 mg/kg), and Group 5 (control) for each dose $n = 6$. After administering different doses, the behavior of each animal was observed for 2 h and then kept under longer-term observation during the ensuing 24 h period. Responses which included aggressiveness, ataxia, spontaneous locomotor activity, cyanosis, abdominal constriction reflex, catalepsy, tail pinch response and any bizarre behaviors were considered (Kheir et al., 2010; Kamil et al., 2021).

Anti-nociceptive Potential Analysis

Hot-Plate Test

Balb/C mice (18–22 g) were used to perform the hot-plate test. Animals were habituated in the experimental area for 1–2 h before starting each procedure. A hot-plate Analgesiometer (Harvard Apparatus) was pre-heated and maintained at 54 ± 1°C temperature. Responses entailing jumping, licking and hind paw flicking were carefully observed. At each endpoint, mice were removed from hot plate to avoid any tissue damage. Pre-tests were also performed to exclude animals that showed a latency of more than 15 s. A gap of 30 min was kept between pretesting and the test compound trial. After 30 min, standard drug (Tramadol 30 mg/kg), TDT1 or TDT2 was administered intraperitoneally to the allocated animal groups. The hot-plate readings were measured at 30, 60, 90, and 120 min after intraperitoneal injection of compounds. To establish any underlying mechanism or origin of the pain mechanism, naloxone 1mg/kg (NLX) subcutaneously (s.c) or pentylenetetrazol 15 mg/kg (PTZ) intraperitoneally (i.p.) were administered 10 min before dosing with test compound (Akbar et al., 2016). Percentage analgesia was calculated from the formula:

$$\text{Percentage analgesia} = (\text{Test latency} - \text{control latency}) \div (\text{cut off time} - \text{control latency}) \times 100.$$

Tail Immersion Test

To assess the analgesic potential of test compounds, mice were habituated for 2 h in the experimental area. A water bath was maintained at a temperature of 55 ± 5°C and the tail of each animal was immersed in the water bath by gently holding it in a vertical position then carefully immersing the tail. The latency (s) to a tail-flick response was determined and a cut-off time of 15 s was imposed. Pre-drug latency readings were recorded after which animals were given an i.p. injection of standard (STD Tramadol 30 mg/kg), control and test compounds. Post-drug readings were observed at 0, 30, 60, and 120 min after the administration of all drugs (Shahid et al., 2017). Percentage analgesia was calculated according to the following formula:

$$\text{Percentage analgesia} = (\text{post} - \text{drug latency}) - (\text{pre} - \text{drug latency}) \div (\text{cut of time}) - (\text{pre} - \text{drug latency}) \times 100.$$

Abdominal Constriction Test

The abdominal constriction test was performed to assess the mouse abdominal constrictions in peripheral algesia. Intraperitoneal injection of 1% acetic acid (10 ml/kg) was administered to individual mice in each group. Water and food were withheld 2 h before starting the experiment and all treatment groups were given their respective drug/test compound 30 min before administration of 1% acetic acid. Five min after administration of acetic acid, the incidence of abdominal constrictions was counted for 20 min duration which was compared with the standard Aspirin (50 mg/kg) group. Percentage analgesia was calculated by the following formula (Abbas et al., 2011):

$$\text{Percentage protection} = (1 - \text{mean number of constrictions in the drug} - \text{treated group} \div \text{mean number of constrictions in control}) \times 100.$$

Anti-inflammatory Carrageenan Test

To check for any anti-inflammatory propensity of TDT test compounds, the carrageenan test was performed. Each mouse (15–20 g) was given food with free access to water. All test compound groups and standard Aspirin (50 mg/kg) group were given their respective treatments intraperitoneally. After 30 min the same animals of each group were injected with 0.05 ml of 1% carrageenan in the sub plantar area of the right hind paw. The volume of the paw was measured before carrageenan administration, and which were again repeated after administration of carrageenan from 1 to 5 hourly intervals (Fehrenbacher et al., 2012; Zadeh-Ardabili and Rad, 2019). A digital plethysmometer was used to measure the paw volume and relative inflammation was estimated by the following formula:

$$\% \text{ inhibition } = \text{P1} - \text{P/P1} \times 100.$$

"P1" represented the increased paw volume in the carrageenan-treated group.

"P" represented the increased paw volume in the drug-treated group.

Chronic Constriction Injury Model Generation

Neuropathic pain was induced in male rats through the chronic constriction injury (CCI) model by placing loosely constrictive ligatures around the common sciatic nerve (Bennett and Xie, 1988). Each animal was anesthetized with xylene 10 mg/kg and ketamine 100 mg/kg i.p (Medeiros et al., 2020). Each rat was then laid in the prone position on a heat-controlled pad. The left thigh was slightly elevated and the posterior hair was shaved to expose the skin for incision. The skin was then cleaned with topical povidone-iodine 10% w/v solution. The sciatic nerve was exposed by a 3–4 cm incision parallel to the long axis of the femur and down the center of the femoris muscle followed by cutting of connective tissue between the gluteus superficialis and bicep femoris muscle. The gap between the two muscles was opened by a ribbon retractor and up to 10 mm sciatic nerve was exposed and tied with four loose ligature (chromic catgut sutures 4/0, metric 2) with a double knot 1 mm apart from each other. After ligation, the muscle was closed with the help of silk braided 2/0 metric sutures and the skin was then closed up with a surgical skin stapler. There was a sham-operated animal group in which the sciatic nerve was uncovered but not ligated (Gu and Pan, 2015).

Behavioral Analysis

Static Mechanical Allodynia

A consecutive series of 8 von Frey filaments (0.4, 0.7, 1.2, 2.0, 3.0, 5.0, 8.0, and 15.1g) were applied at 90 degrees to mid plantar fasciitis surface of the constricted left leg hind paw to an extent where bending of the von Frey filament occurred up to a cut-off time of 6 s or until the appearance of an animal positive response (paw withdrawal PWD or licking). Paw flinching and lifting on the removal of the filament were recorded as a positive response. The same procedure was repeated four times after the first positive response or five consecutive negative responses. A15.1 g force was selected as a cut-off force after which further force application was terminated (La and Chung, 2017).

Dynamic Mechanical Allodynia

To evaluate dynamic mechanical allodynia, a cotton bud was lightly stroked on the mid plantar surface of the operated rat hind paw, with a cut-off time of 15 s. Licking or withdrawal of the paw was taken as a positive response and the time for this to occur, was considered as the paw withdrawal latency (PWL) (Nakazato-Imasato et al., 2009).

Cold Allodynia

The mid plantar surface of the operated rat hind paw was covered with a 50 μl drop of acetone using a blunt needle without touching the skin. The paw withdrawal response was recorded with an arbitrary minimal value of 0.5 s and a maximum of 15 s (Decosterd and Woolf, 2000).

Thermal Hyperalgesia

To measure the thermal nociceptive threshold following test compound treatment, the hot-plate Analgesiometer method (Harvard Apparatus) was employed at a maintained temperature of 52 ± 2°C. Each animal was placed in a hot-plate chamber surrounded by transparent walls and a lid. The nociceptive response latency to paw licking, flicking or jumping was recorded with cut-off time of 15 s (Su et al., 2017).

Pinprick Test

The mid plantar surface of the operated rat hind paw was touched perpendicularly with a blunt needle applying sufficient force to evoke a pinprick withdrawal response but at an intensity which was insufficient to penetrate the skin. Paw withdrawal duration (PWD) was recorded and compared with the normal value of 0.5 s (Kukkar et al., 2013). Hyperalgesia analysis was performed according to Erichsen and Blackburn-Munro (2002).

Enzyme-Linked Immunosorbent Assay

At the end of the treatment, male rats (n = 3–4) were euthanized by administering xylene (20 mg/ml) and ketamine (50 mg/ml). Spinal cords (lumbar region) were removed carefully and stored at −80°C until further analysis. Spinal cord samples were then homogenized in Tris buffer saline with protease inhibitor mix and 1% Triton X-100. The homogenized spinal cord tissues were then centrifuged at 17,000 × g at 4°C for 30 min. The supernatant was then collected and stored at −80°C to be analyzed later. Spinal cord TNF-α was measured using an ELISA kit (Rat TNF-α Elabscience), according to the manufacturer's instructions (Jung et al., 2017).

RNA Extraction and Reverse Transcription-Quantitative PCR

For RT-qPCR analysis of mRNA expression, spinal cord tissue (lumbar region) samples were used for mRNA isolation using a Dynabeads Direct kit for mRNA (Cat#: 61012, Thermo Fisher Scientific, MA, United States). The mRNA concentration was determined via NanoDrop™ (Cat#: 2000C, Fisher Scientific,

MA, United States). cDNA was synthesized from mRNA by utilizing the iScriptRcDNA Synthesis Kit (Cat#: 1708890, Bio-Rad Laboratories, CA, United States). RT-qPCR primers were designed (**Table 1**) using the online primer blast tool[1], which was used to analyze the transcription level of genes of interest. ASYBR Green Super Mix Kit (cat#: 170-8882, Bio-Rad Laboratories, CA, United States) was used for gene expression analysis of the level of genes of interest via aCFX98 instrument (Ref#:1855195, Bio-Rad Laboratories, CA, United States). Samples were processed in triplicate and the relative gene expression was calculated by employing the threshold $^{\Delta\Delta}$ C(t) method. We used the GAPDH gene as endogenous control and for data standardization (Idrees et al., 2020).

Immunoblotting

Western blot analysis was performed as previously described (Muhammad et al., 2019) with some minor changes. In brief, spinal cord tissue (lumbar region) samples were dissolved in the protein extraction buffer (PRO-PREP, Cat#: 17081, iNtRON Biotechnology, NJ, United States). Samples were homogenized and the lysates were then centrifuged and fractionated on an SDS-PAGE gel. The protein was subsequently transferred to a polyvinylidene fluoride membrane, blocked with 3% BSA for 1 h, washed and incubated with primary antibodies of interest (**Table 1**) overnight at 4°C on a shaker. Afterward, membranes were incubated with secondary HRP conjugated antibody at RT for 2 h and then protein was visualized by using a chemiluminescence detection kit (Pierce^{TM}ECL substrate, Cat# 32109).

Immunohistochemistry

Spinal cord samples (lumbar region) were fixed in 4% paraformaldehyde and embedded in paraffin. The tissue was then sectioned in a cryostat with a microtome blade set at a thickness of 40 μm and the slices were processed for immune-staining by the free-floating method. The spinal cord tissue sections were deparafinised with three absolute xylene washes followed by rehydration with ethyl alcohol (from 100 to 70%). In the next step slides were washed with distilled water and immersed in 0.01 M in PBS for 10 min. The heat method was used for antigen retrieval followed by slide cooling and washing with PBS twice. After the antigen retrieval step, slides were quenched with 3% hydrogen peroxide in methanol for 5–10 min. The sections were then blocked with 5% normal goat serum for 1.5 h at room temperature. Slides were then divided to check different markers. Slides were washed with primary antibodies (**Table 1**) overnight at 4°C. The next day after washing with PBS for 10 min, slides were washed with secondary antibody ab6789 Goat pAb to MsIgG (HRP) and incubated for 2 h at room temperature followed by incubation in ABC complex (Immune Cruz ABC kit) for 1 h. The tissue on slides was then washed with PBS and stained with Dab solution until they appeared brown. Afterward, slides were washed with distilled water and rehydrated in graded ethanol (70, 80, 90, and 100%). Slides were fixed in xylene and covered sliped with mounting media. Images were taken by connecting a light microscope with a digital photomicroscopy system. Four slides were processed for each primary antibody. The quantification of the % area for each primary antibody occupied was carried out using Image J software for all the groups and was expressed as the relative integrated density relative to the sham group (Jia et al., 2015; Shah F. A. et al., 2019).

Confocal Immunofluorescence Analyses

For immunofluorescence staining, the spinal cord tissue samples (lumbar region) were blocked in 4% (v/v) paraformaldehyde in 1 M PBS and stored at 4°C as previously described (Ikram et al., 2019; Ahmad et al., 2020). On the day of staining, tissue samples were washed 2× with 0.3% polyvinyl alcohol in 1× PBS (PBS-PVA). The tissue samples were further permeabilized with 0.1% protein K solution for 5 min then after washing twice with PBS-PVA the samples were incubated in 5% blocking solution (BSA-PBS-PVA) for 90 min. After blocking, TNF-a primary antibody was applied to samples and stored at 4°C overnight. The next day, samples were again washed twice with PBS-PVA for 10 min and samples had secondary antibodies (FITC and TRITC)applied at room temperature for 90 min. Samples were then treated for nuclear staining with 4, 6-diamidino-2-phenylindole (10 μg/ml) for about 5 min. After completing the final staining step, samples were washed with PBS-PVA three times for at least 5 min and final tissue samples were then mounted with a fluorescent mounting medium and covered with a coverslip. To capture the images, a confocal laser scanning microscope (Fluoview FV 1000, Olympus, Japan) was used and the images were analyzed by Image J software (National Institute of Health, Bethesda, MD, United States) for relative integrated density of the signals.

Hematoxylin and Eosin Staining

After completion of the 15 days CCI protocol, rat spinal cord tissue (lumbar region) was collected and subjected to Hematoxylin and eosin (H and E) staining by a well-established method (Fischer et al., 2008). After curing the mounting media, the samples were observed under a light microscope and the lesion area was measured using Image J software. The relative lesion was defined as an inflammatory area divided by the area of the whole longitudinal spinal cord 2 mm from the epicenter of the injury.

Molecular Docking

Molecular docking is useful *in silico* approach widely employed in predicting the binding affinity and binding mode of ligands to a given biomolecule. In this work, our objective was to rank the binding affinities of TDT1 and TDT2 for COX-2 (PDB ID: 3NT1) and TNF-α (PDB ID: 1TNF) to correlate with the experimental findings that these proteins could be potential targets for the compounds. The compound structures were drawn in Chem Draw Ultra 12. 0 (Milne, 2010), and minimized in Chem3D 12.0. Protein minimization was performed in UCSF Chimera 1.15 (Pettersen et al., 2004) through the steepest descent and conjugate gradient algorithm as per the procedure described by the manufacture. All the docking calculations were done using Auto Dock 4.2 (Morris et al., 2009) on a Linux workstation (Ubuntu 20.0) with Intel Core i7-10700 processor

[1]https://www.ncbi.nlm.nih.gov/tools/primer-blast/

TABLE 1 | Details of primers and primary antibodies used in RT-qPCR, WB, IHC, and IF analysis.

Name	Accession no.	Order name	Sequence (5′–3′)	Product size (bp)
Iba1 (Aif1)	NM_017196.3	F	CAGCCTCATCGTCATCTCCC	112
		R	TTCCTGTTGGGCTTTCAGCA	
NF-κB (Rela)	NM_199267.2	F	TGGTCACCAAAGACCCACCT	150
		R	GGTCTCGCTTCTTCACACAC	
TNF-α	NM_012675.3	F	CATCCGTTCTCTACCCAGCC	146
		R	AATTCTGAGCCCGGAGTTGG	
Cox2	S67722.1	F	GTTCCATTTGTGAAGATTCCTGTGT	102
		R	CTCACTGGCTTATGCCGAAA	

Antibody	Host	Application	Concentration	Catalog #
Anti-Iba1 (Aif1)	Rabbit	IHC	1:100	K006764P
Anti-Iba1 (Aif1)	Rabbit	WB	1:1000, 1:800	#17198
Anti-NF-κB (p65)	Mouse	WB, IHC	1:500, 1:100	sc-136548
Anti-TNF-α	Mouse	WB, IF, IHC	1:500, 1:100, 1:100	sc-52746
Anti-Cox2	Mouse	WB, IHC	1:500, 1:100	sc-376861

F, forward; R, reverse; WB, Western blot; IF, Immunofluorescence; IH, immunohistochemistry.

(10th generation) and 32 GB (3,200 MHz). The Graphical User Interface program Auto Dock Tools (ADT) (Huey et al., 2012) was considered to generate pdbqt files for both proteins and compounds as well as creating grid box. Assigning polar hydrogen atoms, solvation parameters, united atom Kollman charges and fragmental volumes to the proteins was carried out using ADT. The grid box was prepared for each protein using AutoGrid. The grid size allowed was to 25 × 25 × 25 along XYZ keeping the grid spacing of 0.375 Å. The grid center dimensions for each protein were as follows: COX-2 (*X*: −42.96 Å, *Y*: −48.29 Å, *Z*: −22.53 Å), TNF-α (*X*: 31.68 Å, *Y*: 56.29 Å, *Z*: 33.64 Å). The grid box parameters addressing information for docking the compounds to the proteins were written in a configuration file. In the docking procedure, the proteins were kept rigid whereas the compounds were treated as flexible. Compound poses were clustered together and the one with lowest energy value in kcal/mol was aligned with the protein(s) for visual examination. Complex visualization and chemical interaction analyses were done in UCSF Chimera 1.15 (Pettersen et al., 2004) and Discovery studio visualizer v.2021, respectively (Studio, 2008).

Statistical Analysis

The data of all behavioral and biochemical data are expressed as Mean ± SEM and are representative of three experiment repeats. The densitometric analysis of immunoblot bands, immunohistochemistry, and confocal images were analyzed by Image J software programs[2]. Differences between the WT vs. Tramadol and Sham vs. CCI groups were analyzed using student's *t*-test and the difference between tramadol and sham vs. other treated groups of were analyzed using One-way analysis of variance (ANOVA) followed by Bonferroni *post hoc* test. For Paw and tail withdrawal latency, allodynia and hyperalgesia where repeated measurement over a period of time was involved, a two-way ANNOVA followed by Bonferroni *post hoc* test was used. All statistical analysis were carried out with Graph-Pad Prism Version-6 software (GraphPad Software Inc., San Diego, CA, United States). Significance: $^{*}p < 0.05$, $^{**}p < 0.01$, $^{\#}p < 0.001$, and $^{\#\#}p < 0.0001$; ns, non-significant.

[2]https://imagej.nih.gov/ij/download.html

RESULTS

Assessment of the Acute Toxicity and Tolerance of TDT1 and TDT2 Test Compounds

For the assessment of a safety profile for TDT derivatives, an acute toxicity test was performed initially monitoring animal behavior and well-being for 2, 4, and 6 h and then up to 24 h after intraperitoneal compound administration. No animals displayed any bizarre or atypical responses like spontaneous activity, ataxia, tail pinch response, catalepsy, abnormal weight loss, abdominal constrictions, convulsions or aggressiveness at doses up to 500 mg/kg. There was no mortality/death seen in any mice treated with both the test compounds below 500 mg/kg dose. The combined results indicated that TDT1 and TDT2 were both safe up to a dose of 500 mg/kg body weight which was considered as a maximum tolerated dose (MTD).

Analgesic Potential of TDT1 and TDT2 Test Compounds in Adult Mice

To evaluate the potential acute antinociceptive effect of the test compounds two way ANOVA test was performed (Bannon and Malmberg, 2007). The two way ANOVA revealed nociception varied significantly between treatment groups [F(Interaction) (10,90) = 1.319, p = ns; F (Group factor) (5,90) = 86.22, $p < 0.0001$; F(Time factor) (2,90) = 1.346. p = ns]. Both TDT1 (30 and 45 mg/kg) and TDT2 (45 mg/kg) were found

to produce an statistically significant antinociceptive effect ($p < 0.05$) 30 min after administration as compared to WT. This effect was sustained after 60 min for both TDT1 and TDT2 (45 mg/kg) doses and after 90 min for TDT1 and TDT2 (45 mg/kg) (**Figure 2A**). The two way ANOVA revealed tail immersion withdrawal varied significantly between experiment groups [F(Interaction) (8,75) = 0.9790, p = ns; F(Group factor) (4,75) = 8.192, $p < 0.0001$; F(Time Factor) (2,75) = 1.166, p = ns]. In the tail immersion test when compared to WT, TDT2 (45 mg/kg), displayed an antinociceptive effect at 30 min while at 60 and 90 min TDT1 and TDT2 (45 mg/kg) showed antinociceptive effect (**Figure 2B**).

To confirm any assumed mechanism of action of our test compounds, animals were co-administered either an opioid or GABA antagonist. The one way ANOVA of naloxone test revealed nociception varied significantly between treatment groups [F(2.346,11.73) = 25.88, $p < 0.0001$]. The antinociceptive activity of tramadol was significantly decreased ($p < 0.05$) by naloxone. Naloxone also reduced the antinociceptive activity of TDT1 and TDT2 significantly ($p < 0.05$) suggesting opioidergic signaling involvement. The one way ANOVA of PTZ test revealed nociception varied significantly between treatment groups [F(2.966,14.83) = 51.25, $p < 0.0001$]. PTZ also reduced the thermal antinociception effects of TDT derivatives suggesting the role of GABAergic signaling (**Figures 2C,D**). The one way ANOVA of abdominal constriction test revealed nociception varied significantly between treatment groups [F(1.768,8.841) = 1.431, p = ns]. In the abdominal constriction test, the incidence of constrictions to intraperitoneal 1% acetic acid, was markedly reduced ($p < 0.0001$) by both doses of TDT1 and TDT2 along with the aspirin (standard positive control – STD) (**Figure 2E**).

Activity of TDT1 and TDT2 on CCI-Induced Allodynia and Hyperalgesia in Adult Rats

Allodynia is potentially useful for rapidly illustrating the analgesic profile of compounds and conducting mechanistic studies. Drug treatment was instigated on protocol day 14 after the development of neuropathy in ligated rats. Two way ANOVA test was performed to analyze the significance of our test compound effect. The treatment had a significant main dose effect on CCI induced static allodynia (**Figure 3A**). The two way ANOVA revealed antiallodynic effect varied significantly between treatment groups [F(Interaction) (24,175) = 3.386, $p < 0.0001$; F(Group factor) (6,175) = 15.98, $p < 0.0001$; F(Time factor) (4,175) = 68.93, $p < 0.0001$]. Daily administration of gabapentin (75 mg/kg, i.p.) (standard positive control – STD) ($p < 0.0001$), and derivatives of TDT1 and TDT2 (30 and 45 mg/kg) ($p < 0.001$) started to reverse the decreased paw withdrawal threshold of CCI (PWT) indicating a decrease on the plantar surface of evoked nociception in the hind paw plantar surface. It was noted that no static mechanical allodynia was observed in the sham-operated control group. The two way ANOVA revealed that there was statistically significant decrease in nociception of treated group as compare to CCI group ($p < 0.0001$).

To evaluate the effect of our test compound on CCI induced dynamic allodynia non-painful stimulus was applied to the mid plantar region of the ligated left hind paw. The two way ANOVA revealed antiallodynic effect varied significantly between treatment groups [F(Interaction) (24,120) = 7.513, $p < 0.0001$; F(Group factor) (6,30) = 35.86, $p < 0.0001$; F(Time factor) (4,20) = 32.83, $p < 0.0001$]. There was a noticeable reduction ($p < 0.0001$) in the PWT in the CCI-operated group as compared to the sham and pre-surgery operated group when a cotton swab was lightly stroked on the mid-plantar foot surface during the last 2 weeks of the study protocol (**Figure 3B**). After treatment with TDT1 and TDT2, there was a significant elevation in CCI-induced reduction at dose of 30 mg/kg ($p < 0.001$) and 45 mg/kg ($p < 0.0001$) in PWT on days 21 and 28. The two way ANOVA revealed PWD varied significantly between experiment groups [F(Interaction) F(24,175) = 17.77, $p < 0.0001$; F(Group factor) (6,175) = 133.0, $p < 0.0001$; F(Time factor) (4,175) = 299.9, $p < 0.0001$]. Moreover, in the cold allodynia test, the paw withdrawal duration (PWD) reflex was significantly prolonged upon acetone drop application to the mid-plantar foot surface of the operated hind paw in the CCI group ($p < 0.0001$) compared to the sham-operated group. This extended PWD was markedly reduced in the TDT1 ($p < 0.0001$), TDT2 ($p < 0.0001$), and standard gabapentin treated groups (**Figure 3C**). A heat hyperalgesia test was performed to assess the anti-nociceptive effect of test compounds against non-painful heat stimuli evoked nociception. The two way ANOVA revealed antiallodynic effect varied significantly between experiment groups [F(Interaction) (24,120) = 1.840, p = ns; F(Group factor) (6,30) = 10.80, $p < 0.0001$; F(Time factor) (4,20) = 29.96, $p < 0.0001$]. After the development of an elevated nociceptive response on day 14 post-surgery, animals were treated with gabapentin, TDT1 or TDT2, respectively. There was a marked elevation of response in the untreated CCI group ($p < 0.001$) compared to the sham-operated animals. The nociceptive thermal sensation in the mid-plantar area was significantly alleviated as indicated by an increased PWL in the gabapentin ($p < 0.001$), TDT1 ($p < 0.05$), and TDT2 ($p < 0.05$), treatment groups (**Figure 3D**).

Subsequently, we evaluated the hyperalgesia induced by pinprick in the mid plantar surface of the operated paw. The two way ANOVA revealed that PWT varied statistically experiment groups [F(Interaction) (24,175) = 15.98, $p < 0.0001$; F(Group factor) (6,175) = 136.8, $p < 0.0001$; F(Time factor) (4,175) = 293.1, $p < 0.0001$]. In consequence, pinprick significantly raised the PWT on day 3 in the CCI-operated group as compared to the sham-operated animals. On the other hand, treatment with gabapentin, TDT1 orTDT2 manifested a significant reduction ($p < 0.0001$), in the PWT compared with CCI-operated rats and this response was evident from protocol day 21 to the final test day (day 28) (**Figure 3E**).

Activity of TDT1 and TDT2 on Carrageenan-Induced Acute Inflammation in Adult Rats

Carrageenan induces acute inflammation and gives rise to other signs related to inflammation such as

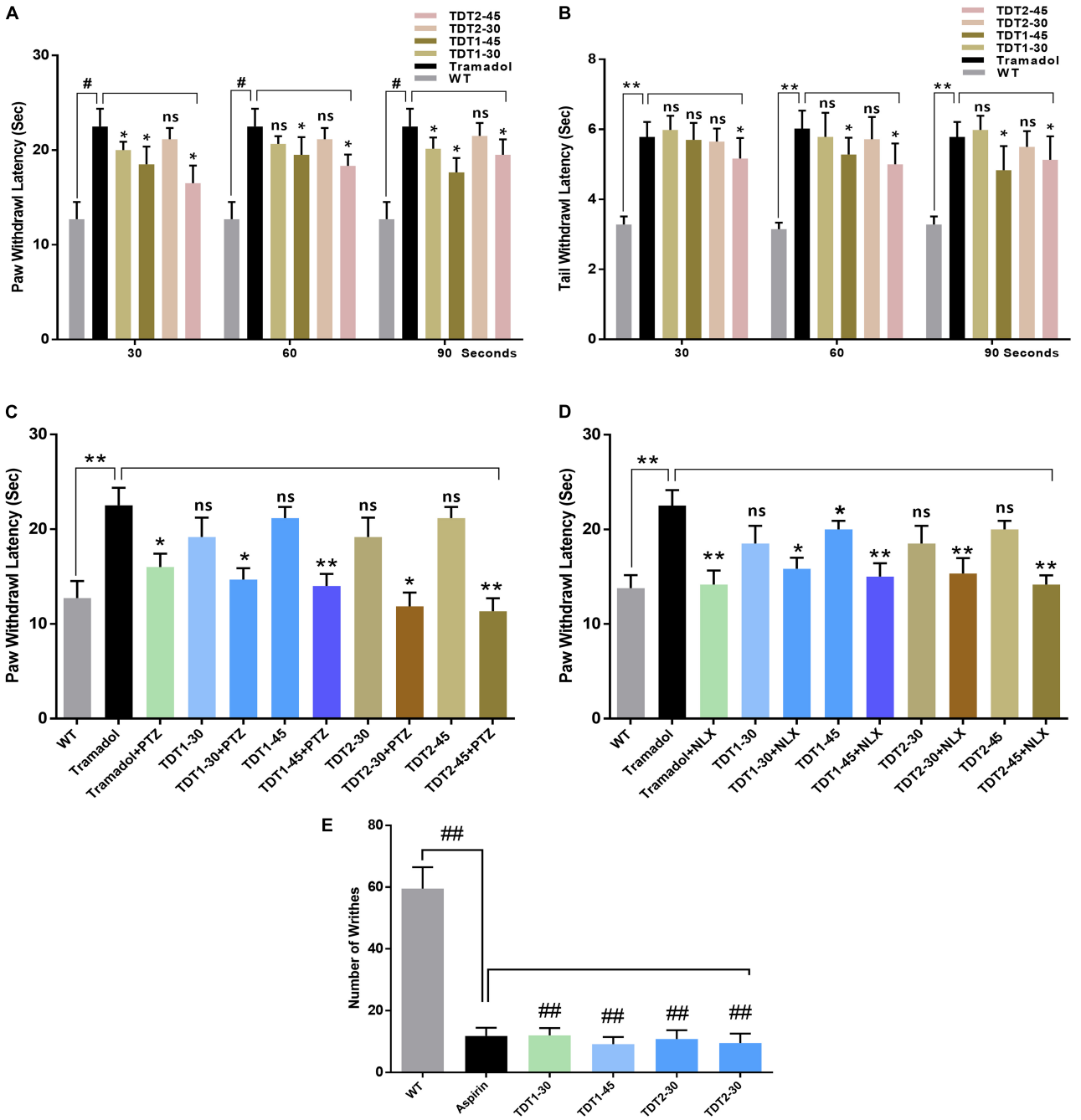

FIGURE 2 | Analgesic effects of tramadol (30 mg/kg) and TDT1 and TDT2 test compounds (30 and 45 mg/kg) on nociception in adult mice. **(A)** Paw withdrawal latency (PWL) in the mouse hot plate test. **(B)** Tail withdrawal response latency of mice in the tail immersion test. **(C,D)** PWL of mice in different experimental groups after administration of pentylenetetrazol (15 mg/kg i.p) (PTZ) or Nalaxone (1 mg/kg s.c.) (NLX) respectively. **(E)** Incidence of abdominal constrictions after the administration of drugs to different animal groups. The data are presented as the mean ± SEM of 6–8 mice per group and representative of three repeats. Data analyses were performed using *t*-test between WT and Tramadol group, and two-way ANOVA followed by Bonferroni *post hoc* test for **(A,B)**, and one-way ANOVA followed by Bonferroni *post hoc* test for **(C–E)** was used for comparative analysis between Tramadol and Tramadol+ treated groups. Significance: $^{*}p < 0.05$, $^{**}p < 0.01$, $^{\#}p < 0.001$, $^{\#\#}p < 0.0001$, and ns = non-significant. WT, wild-type vehicle administered group; TDT1, 2-(5-propyl-6-thioxo-1, 3, 5-thiadiazinan-3-yl) acetic acid; TDT2, 2-(5-propyl-2-thioxo-1, 3, 5-thiadiazinan-3-yl) acetic acid.

hyperalgesia, edema, and erythema (Morris, 2003). Our results demonstrated that carrageenan induced an acute inflammatory response characterized by an increase in paw size, edema, and erythema. In contrast, TDT1 and TDT2 significantly ($p < 0.001$), decreased carrageenan-induced inflammation compared with standard aspirin (50 mg/kg),

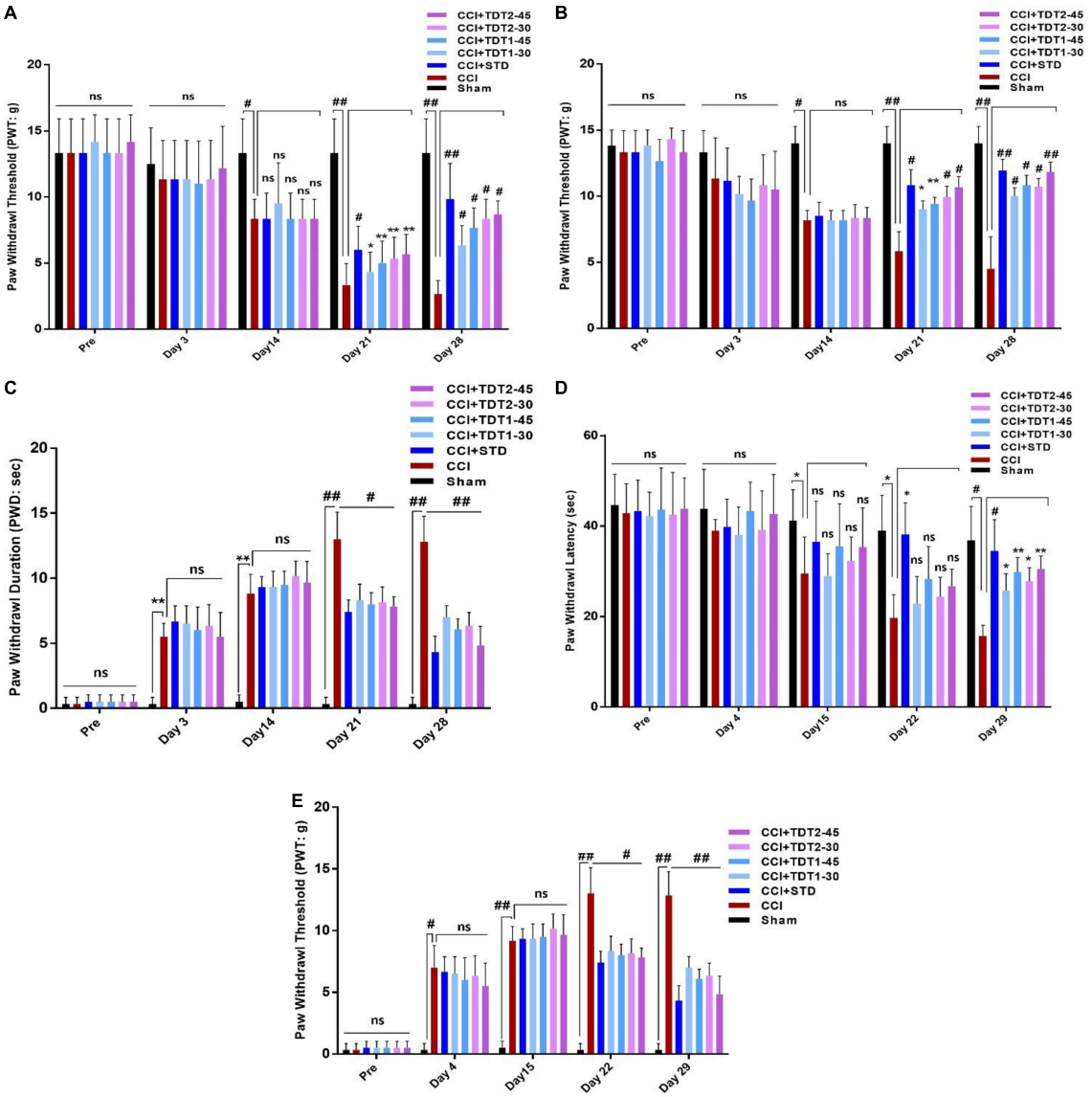

FIGURE 3 | Effects of TDT1 and TDT2 test compounds (30 and 45 mg/kg) versus STD (75 mg/kg) on allodynia and hyperalgesia behavior in rats. **(A,B)** Representative histograms showing the effects of TDT1 and TDT2 on static and dynamic mechanical allodynia. **(C)** Effects of TDT1 and TDT2 on cold allodynia (acetone drop test) in adult rats. **(D,E)** Representative histograms showing the effects of TDT1 and TDT2 on heat-induced and pinprick-induced hyperalgesia behavioral tests. The data are presented as the mean ± SEM of 6–8 rats per group and representative of three repeats. Data analyses were performed using t-test between Sham and CCI group, and Two-way ANOVA followed by Bonferroni *post hoc* test was used for comparative analysis between CCI and CCI+ treated groups. Significance: $^{*}p < 0.05$, $^{**}p < 0.01$, $^{\#}p < 0.001$, $^{\#\#}p < 0.0001$; ns, non-significant. Sham, CCI-operated vehicle administered group; STD, standard (gabapentin) group; TDT1, 2-(5-propyl-6-thioxo-1, 3, 5-thiadiazinan-3-yl) acetic acid; TDT2, 2-(5-propyl-2-thioxo-1, 3, 5-thiadiazinan-3-yl) acetic acid.

reflecting a strong anti-inflammatory effect of the test compounds (**Table 2**).

Thiadiazine-Thione Derivatives Mitigate the Elevated Expression of Chronic Constriction Injury-Induced Microgliosis

Mounting literature suggests that microglia is an important source of various cytokines that contribute toward neuroinflammation, pain, and neuronal apoptosis (Suter et al., 2007; Muhammad et al., 2019). To evaluate the expression of ionized calcium-binding adaptor molecule 1 (Iba1)as a marker of activated microglia (microgliosis), rat spinal cord tissue from different experimental groups was prepared for RT-qPCR. The one way ANOVA revealed the expression of Iba1 varied significantly between experimental groups [$F(6,35) = 14.54$, $p < 0.0001$]. The mRNA expression level of Iba1 was significantly higher in the CCI group ($p < 0.001$) while TDT1 ($p < 0.05$), and TDT2 ($p < 0.05$) at 45 mg/kg dose, both reduced its expression (**Figure 4A**). Similarly, we confirmed this

TABLE 2 | TDT1 and TDT2 activity on carrageenan-Induced inflammatory edema and erythema in rat paw.

Time (hrs)	Control	Carr	Carr+ Asp	% Inhibition	Carr+ TDT1-30	% Inhibition	Carr+ TDT1-45	% Inhibition	Carr+ TDT2-30	% Inhibition	Carr+ TDT2-45	% Inhibition
1	0.0124	0.068$^{\#}$	0.032***	41.8	0.032***	41.6	0.030***	45.3	0.028***	45.6	0.024***	52.8
2	0.0126	0.068$^{\#}$	0.032***	41.8	0.03***	45.5	0.026***	50.4	0.024***	52.1	0.020***	57.0
3	0.0134	0.068$^{\#}$	0.032***	41.8	0.025***	49.7	0.026***	52.1	0.023***	49.6	0.020***	56.2
4	0.0104	0.068$^{\#}$	0.032***	41.8	0.024***	52.5	0.025***	50.45	0.026***	49.7	0.025***	54.1
5	0.0100	0.070$^{\#}$	0.032***	44.3	0.03***	45.45	0.028***	48.2	0.030***	45.4	0.028***	48.2

Results are presented as mean ± SEM of 6–8 mice per group, one-way ANOVA followed by Bonferroni's post hoc analysis was performed. $^{\#}p < 0.0001$ compared to control group, $^{***}p < 0.001$ compared to Carr treated group. Carr, carrageenan; Asp, aspirin.

outcome by western blot analysis and found that the Iba1 protein level was substantially elevated in the CCI group ($p < 0.05$) and that it was markedly reduced by TDT1 ($p < 0.001$) and TDT2 ($p < 0.001$) at 45 mg/kg treatment (**Figures 4B,C**). Furthermore, immunohistochemistry also supported the above results, i.e., the expression of Iba1 was significantly elevated by CCI ($p < 0.05$) while TDT derivative administration reduced ($p < 0.05$) its expression at 45 mg/kg dose (**Figures 4D,E**). These results demonstrate that our TDT1 and TDT2 compounds exerted their neuroprotective activity by lowering the expression of Iba1 in a dose-dependent manner.

Thiadiazine-Thione Derivatives Mitigate Chronic Constriction Injury -Induced Activated Microglia and p-NF-κB Expression

Nuclear factor-kappa B (NF-κB), a key transcription factor, is known to play a critical role in neuropathic pain by regulating several inflammatory genes (Fu et al., 2018). Therefore, we assessed NF-κB mRNA levels in rat spinal cord tissue. The one way ANOVA revealed NF-κB mRNA levels varied significantly between experiment groups [$F(6,35) = 19.32$, $p < 0.0001$]. The RT-qPCR results disclosed that the CCI ($p < 0.05$) procedure resulted in a higher NF-κB level while both TDT1 ($p < 0.05$) and TDT2 ($p < 0.05$) reduced its expression (**Figure 5A**). Moreover, we further validated the effects of TDT derivatives on phosphorylated-NF-κB (p-NF-κB) expression using western blot and immunohistochemistry (**Figures 5B–E**). These results revealed that TDT1 ($p < 0.05$) and TDT2 ($p < 0.05$) significantly reduced the level of the active NF-κB transcription factor that is involved in the regulation of several other neuro-inflammatory cytokines.

Protective Effects of Thiadiazine-Thione Derivatives Against Chronic Constriction Injury-Induced Neuroinflammation

TNF-α is a critical cytokine released by glia and several immune cells which is intrinsic to the pathogenesis of both central and peripheral neuropathic pain (Leung and Cahill, 2010). To evaluate the anti-inflammatory effects of TDT derivatives, we examined the expression of TNF-α protein through Elisa in rat spinal cord tissue. The one way ANOVA revealed TNF-α protein expression varied significantly between experiment groups [$F(6,35) = 19.90$, $p < 0.0001$]. Our findings divulged that CCI significantly enhanced the expression level of TNF-α in CCI group ($p < 0.001$) but in contrast; TDT1 ($p < 0.05$) and TDT2 ($p < 0.05$) reversed this elevated expression of TNF-α (**Figure 6A**). Similarly, we followed this up with RT-qPCR to assess the mRNA level of TNF-α and found that both of our TDT test compounds markedly reduced ($p < 0.05$) TNF-α mRNA expression (**Figure 6B**). Moreover, we performed western blot analysis to examine the protein level of TNF-α in the spinal cord tissue lysates. The protein level of TNF-α was significantly elevated in the CCI group ($p < 0.001$) while it was substantially diminished in the TDT1 ($p < 0.05$) and TDT2 ($p < 0.05$) treated groups (**Figures 6C,D**). To further

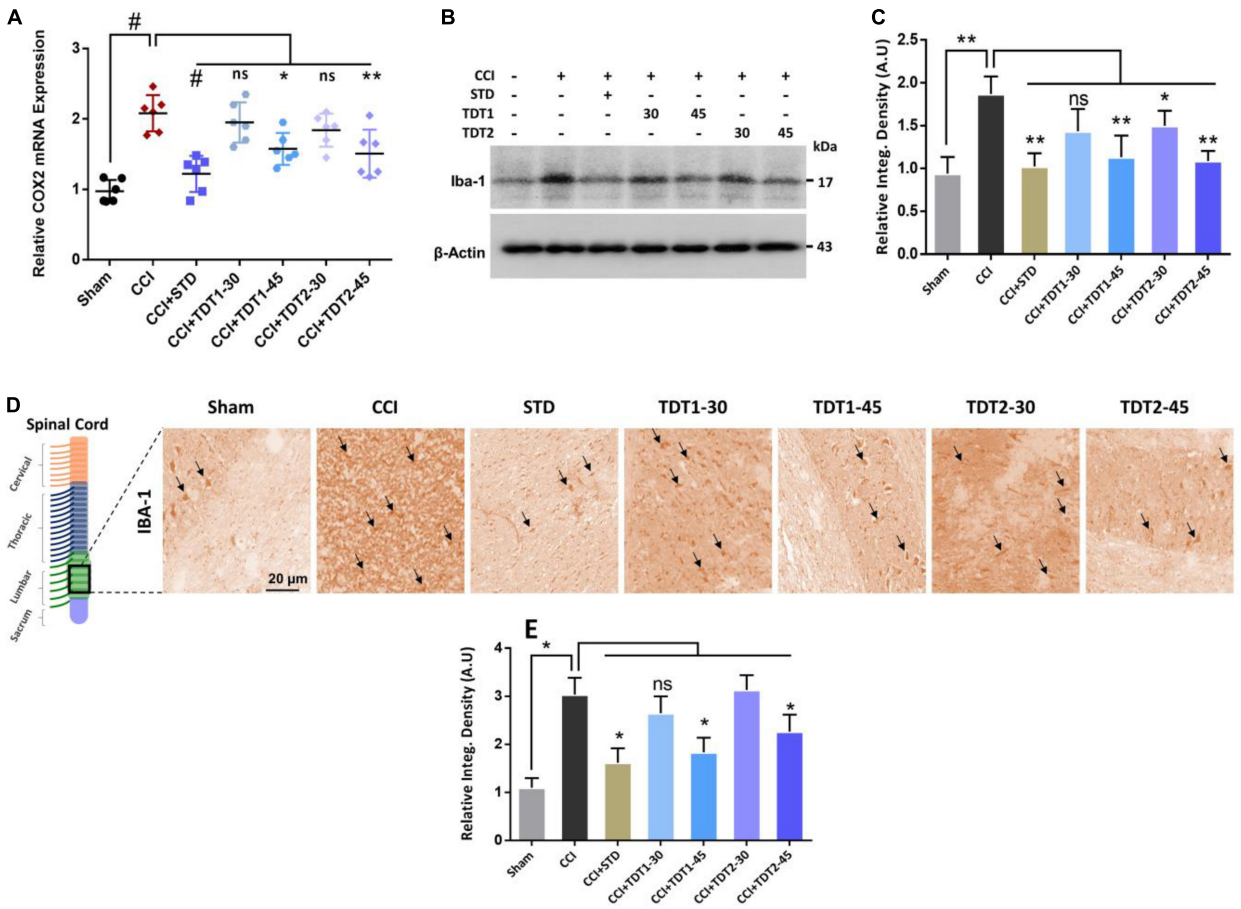

FIGURE 4 | TDT1 and TDT2 (30 and 45 mg/kg) and STD (75 mg/kg) ameliorates the expression of CCI-induced astrogliosis. **(A)** mRNA level of Iba1 gene analyzed via RT-qPCR in rat spinal cord tissue of different experimental groups. **(B,C)** Western blot analysis of Iba1 in the spinal cord tissue lysate of adult rats and representative histograms. **(D,E)** Immunohistochemistry images of Iba1 in the rat spinal cord sections. Scale bar 20 μm, magnification 40×. The data are presented as the mean ± SEM of 3–4 rats per group and representative of three repeats. Data analyses were performed using *t*-test between Sham and CCI group, and One-way ANOVA followed by Bonferroni *post hoc* test was used for comparative analysis between CCI and CCI+ treated groups. Significance: $^{*}p < 0.05$, $^{**}p < 0.01$, $^{\#}p < 0.001$; ns, non-significant. Sham, CCI-operated vehicle administered group; STD, standard (gabapentin) group; TDT1, 2-(5-propyl-6-thioxo-1, 3, 5-thiadiazinan-3-yl) acetic acid; TDT2, 2-(5-propyl-2-thioxo-1, 3, 5-thiadiazinan-3-yl) acetic acid.

support these findings, we performed immunofluorescence confocal microscopy and immunohistochemistry. The results further confirmed that our test compounds significantly reduced ($p < 0.05$) the immunoreactivity of TNF-α antibodies in spinal cord sections in comparison with the CCI group (**Figures 6E–H**).

Activity of Thiadiazine-Thione Derivatives on Cox-2 Expression and Histopathological Changes in the Chronic Constriction Injury-Induced Neuropathic Pain Rat Model

Previous studies have reported that cyclooxygenase-2 (Cox-2) is elevated in invading macrophages in the nervous system of rats and humans. It has also been reported that Cox-2 results in the maintenance of neutral endopeptidase (NeP) in aged rats (Ma et al., 2010). To determine any possible protective effect of our TDT compounds against Cox-2, we evaluated the mRNA expression and protein level of the enzyme in different experimental groups. The one way ANOVA revealed Cox-2 mRNA expression varied significantly between experiment groups [$F(6,35) = 17.95$, $p < 0.0001$]. We found that both Cox-2 mRNA expression and the protein level were higher in CCI-induced neuropathic pain. Conversely, TDT1 ($p < 0.05$) and TDT2 ($p < 0.05$) reduced their levels in a dose-dependent manner (**Figures 7A–C**). In addition, our immunohistochemistry ($p < 0.05$) and western blot ($p < 0.05$) results also supported the notion that TDT1 and TDT2 exerted significant anti-inflammatory effects by reducing the immunoreactivity of the Cox-2 antibody in spinal cord sections of adult rats (**Figures 7D,E**).

To understand the consequences of CCI-induced morphological changes in the neuron in the context of apoptotic necrotic neuronal death, we performed Hematoxylin and Eosin (H and E) staining. The results revealed that CCI induced significant apoptosis and morphological changes characterized

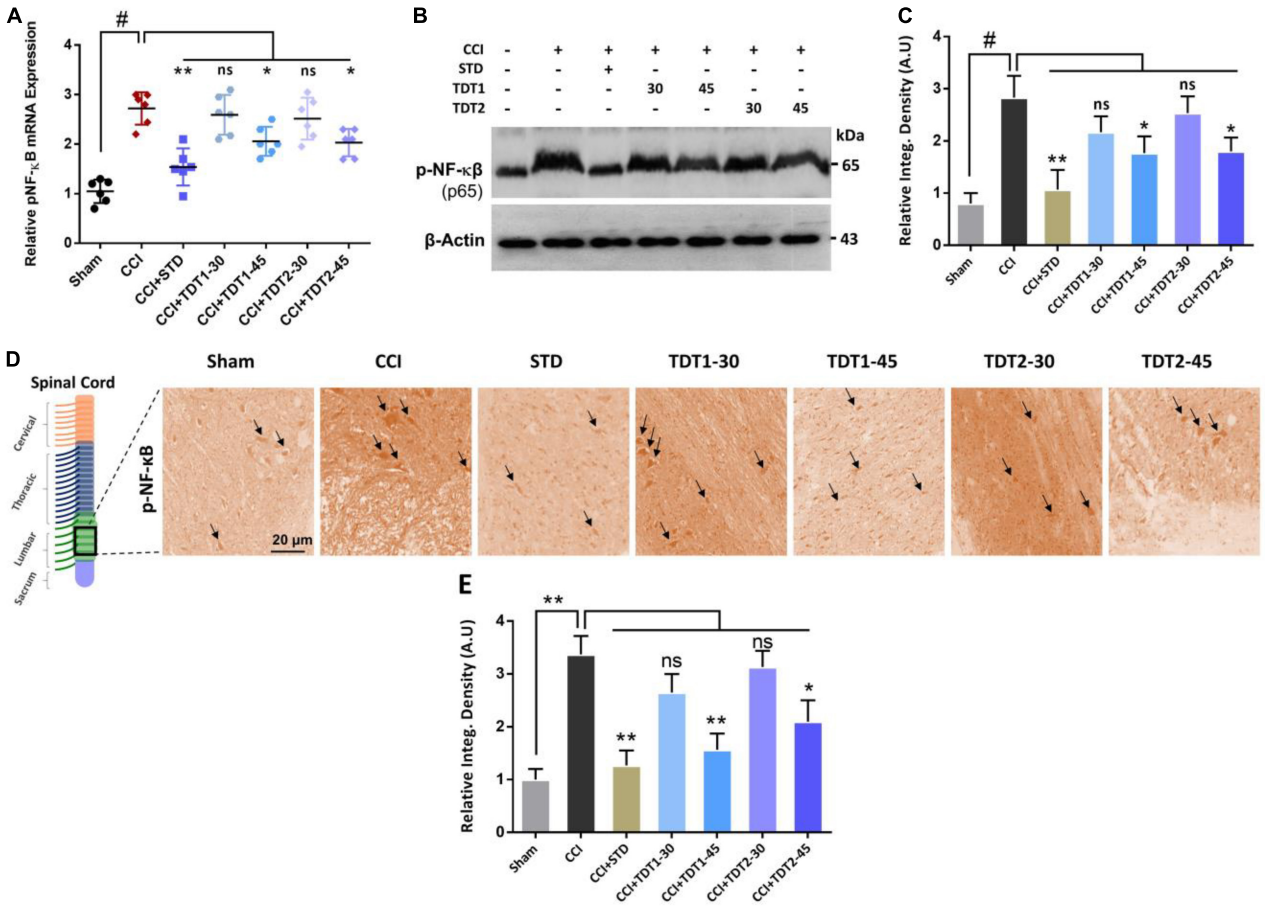

FIGURE 5 | Effects of TDT1 and TDT2 test compounds (30 and 45 mg/kg) and STD (75 mg/kg) on the expression of NF-κB. **(A)** Representative histogram showing the mRNA level of NF-κB gene analyzed via RT-qPCR in the experimental groups. **(B,C)** Western blot analysis of p-NF-κB in the rat spinal cord tissue and its representative histograms. **(D,E)** Immunohistochemistry results of p-NF-κB in spinal cord sections. Scale bar 20 μm, magnification 40×. The data are presented as the mean ± SEM of 3–4 rats per group and representative of three repeats. Data analyses were performed using *t*-test between Sham and CCI group, and One-way ANOVA followed by Bonferroni *post hoc* test was used for comparative analysis between CCI and CCI+ treated groups. Significance: $^{*}p < 0.05$, $^{**}p < 0.01$, $^{\#}p < 0.001$; ns, non-significant. Sham, CCI-operated vehicle administered group; STD, standard (gabapentin) group; TDT1, 2-(5-propyl-6-thioxo-1, 3, 5-thiadiazinan-3-yl) acetic acid; TDT2, 2-(5-propyl-2-thioxo-1, 3, 5-thiadiazinan-3-yl) acetic acid.

by cytoplasmic and nuclear condensation, nuclear budding and fragmentation compared to the sham-operated group. However, histopathologically, the number of dead neuronal cells was significantly reduced in the TDT1 ($p < 0.05$) and TDT2 ($p < 0.05$) treated groups compared to the CCI untreated group (**Figures 7F,G**). Overall, these findings suggest that our TDT derivatives significantly downregulated the expression of apoptosis and other pathophysiological processes and mitigated CCI-induced neuronal degeneration and neuropathic pain.

Molecular Docking Studies Predicting the Binding Modes of TDT1 and TDT2 With Cox-2 and TNF-α

In silico molecular docking studies on both compounds were carried out with two receptors: COX-2 and TNF-α, not only to elucidate their binding affinity and molecular interactions but also to perform a comparative analysis with experimental findings. In comparison, a control (naproxen in case of COX-2 and etanercept in case of TNF- α) was also run in the docking studies. The binding energy score of the compounds is tabulated in **Table 3**. Both compounds displayed good binding energy for the receptors, however, their affinities were predicted as less than the controls used. Moreover, the compounds exhibited similar binding energies suggesting that they had comparable binding strength with the receptors. The compounds were observed to show deep binding with both receptors and established a strong network of hydrophilic and hydrophobic interactions. In the case of COX-2, TDT1 possessed the ability to form hydrogen bonds with Tyr115, Arg120, and Glu524. On the other hand, TDT2 interacted with Arg120, and Glu524 hydrophilically and produced several hydrophobic contacts. The binding mode and interactions of compounds at the docked pocket of COX-2 are presented in **Figure 8**.

In the case of TNF-α, TDT2 appeared to be a more efficient binder than TDT1 mainly because of the prospective formation

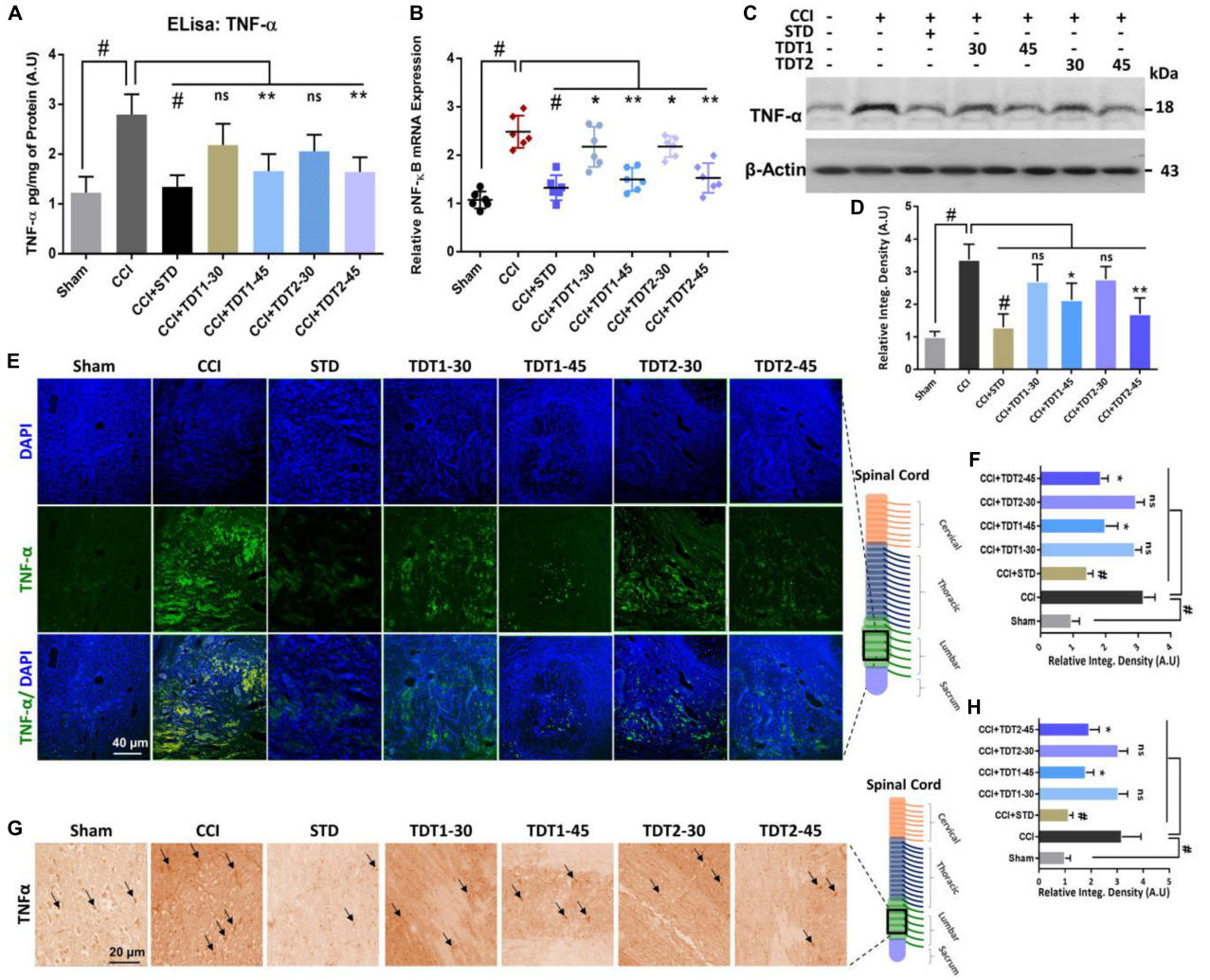

FIGURE 6 | Protective effects of TDT1 and TDT2 (30 and 45 mg/kg) and STD (75 mg/kg) against CCI-induced inflammation. **(A)** TNF-α protein levels measured via Elisa. **(B)** mRNA expression level of the TNF-α gene evaluated by RT-qPCR in rat spinal cord tissue. **(C,D)** Western blot analysis of TNF-α and its representative histograms in spinal cord lysates. **(E,F)** Representative images of anti-TNF-α antibody immunoreactivity in rat spinal cord sections and respective histograms. Scale bar 40 μm, magnification 40×. **(G,H)** Immunohistochemistry results of anti-TNF-α immunoreactivity. Scale bar 20 μm, magnification 40×. The data are presented as the mean ± SEM of 3–4 rats per group and representative of three repeats. Data analyses were performed using *t*-test between Sham and CCI group, and One-way ANOVA followed by Bonferroni *post hoc* test was used for comparative analysis between CCI and CCI+ treated groups. Significance: $^{*}p < 0.05$, $^{**}p < 0.01$, $^{\#}p < 0.001$; ns, non-significant. Sham, CCI-operated vehicle administered group; STD, standard (gabapentin) group; TDT1, 2-(5-propyl-6-thioxo-1, 3, 5-thiadiazinan-3-yl) acetic acid; TDT2, 2-(5-propyl-2-thioxo-1, 3, 5-thiadiazinan-3-yl) acetic acid.

of short distance hydrogen bonds with residues such as Asn92, Ser95, Ser147, and Gln149. TDT1 in contrast was notable in this regard with only two hydrogen bonds: Thr77 and Thr79 (**Figure 9**).

DISCUSSION

Neuropathic pain is highly variable and it develops when neuronal fibers are either damaged or dysfunctional invariably leading to further complications (St John Smith, 2018). Despite the availability of several approved drugs for the management of neuropathic pain, there is a lack of wholly efficacious therapeutic agents with relatively low side effects for chronic neuropathic pain treatment.

Thus, we explored a conceivable therapeutic prospect for our test compounds, TDT1 and TDT2, for antiallodynic, anti-inflammatory, neuro-protective, and analgesic potentials against CCI-induced neuropathic pain. However, chronic constriction injury is a broadly used nerve injury model of chronic neuropathic pain. It evokes chronic neuropathic pain in the rat model resulting from damage to both the peripheral and central nervous systems (Austin et al., 2012). CCI-induced neuropathic pain involves pathological changes observed in both myelinated and non-myelinated neuronal axons. It has also been reported that inflammatory cytokines secreted by glial cells and

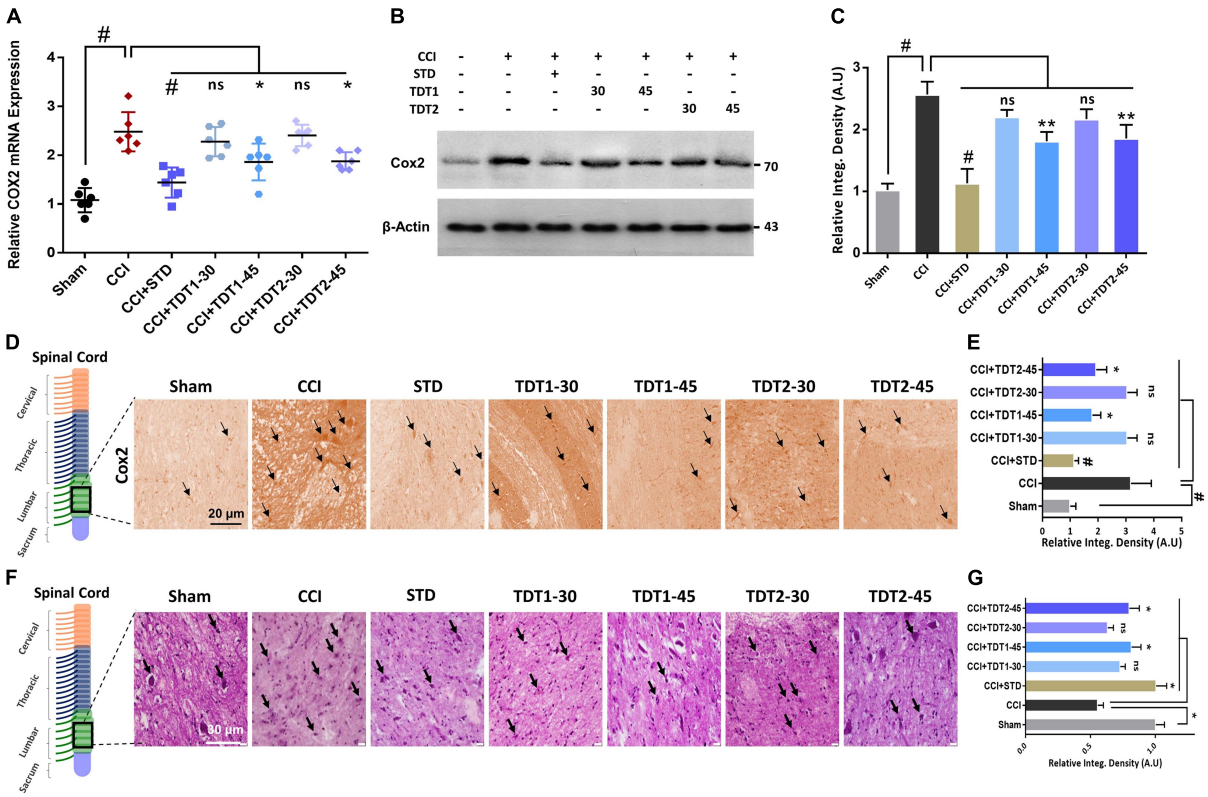

FIGURE 7 | Effects of TDT1 and TDT2 (30 and 45 mg/kg) and STD (75 mg/kg) on CCI-induced COX-2. **(A)** COX-2 mRNA expression level in rat spinal cord tissue examined using RT-qPCR. **(B,C)** COX-2 protein level was assessed by immunoblotting with representative histograms in rat spinal cord tissue lysates of different experimental groups. **(D,E)** Immunohistochemistry images of anti-TNF-α immunoreactivity in spinal cord sections. Scale bar 20 μm, magnification 40×. **(F,G)** Hematoxylin and eosin (H and E) staining showing the neuronal morphology and extent of survival in spinal cord sections of different experimental groups, and representative histograms. Scale bar 20 μm, magnification 40×. The data are presented as the mean ± SEM of 3–4 rats per group and representative of three repeats. Data analyses were performed using *t*-test between Sham and CCI group, and One-way ANOVA followed by Bonferroni *post hoc* test was used for comparative analysis between CCI and CCI+ treated groups. Significance: $^{*}p < 0.05$, $^{**}p < 0.01$, and $^{\#}p < 0.001$; ns, non-significant. Sham, CCI-operated vehicle administered group; STD, standard (gabapentin) group; TDT1, 2-(5-propyl-6-thioxo-1, 3, 5-thiadiazinan-3-yl) acetic acid; TDT2, 2-(5-propyl-2-thioxo-1, 3, 5-thiadiazinan-3-yl) acetic acid.

TABLE 3 | Molecular docking score of compounds and controls with COX-2 and TNF-α.

Target protein	TDT1	TDT2	Control
COX-2	−5.3	−5.3	Naproxen (−8.1)
TNF-α	−4.3	−4.4	Etanercept (−7.1)

injured neurons activate spontaneous activity in non-injured neurons resulting in neuropathic pain behavior (Gabay and Tal, 2004). Additionally, spontaneous mechanical and/or thermal hyperalgesia are frequently associated with neuropathic pain (Huang et al., 2019).

In our study, the safety profile of selected TDT derivatives was evaluated in an acute toxicity test by giving the number of doses from minimum to a maximum of 650 mg/kg. It was found that animals did not show any adverse or bizarre responses such as spontaneous activity, ataxia, tail pinch response, catalepsy, abdominal constrictions, convulsions or aggressiveness upto the dose of 500 mg/kg. After confirming the safety profile of our test compounds, we evaluated the antinociceptive potential of our test compounds of derivative TDT1 and TDT2. In the preliminary hot plate and tail immersion tests, it was found that TDT1 and TDT2 significantly increased the PWL and tail withdrawal latency (**Figures 2A,B**). To determine the possible role of opioidergic and/or GABAergic signaling in the antinociceptive effects of TDT1 and TDT2 derivatives, we co-administered NLX or PTZ as opioid and GABA antagonists respectively. Both NLX and PTZ significantly blocked TDT1 and TDT2 antinociception suggesting the involvement of opioid and GABA signaling (**Figures 2C,D**). Furthermore, we also evaluated the antinociceptive activity of TDT derivatives against the acetic acid-induced peripheral algesia by reducing the number of abdominal constrictions (**Figure 2E**). Hence, taken together, these outcomes suggest that the two TDT derivatives exhibit significant analgesic potentials.

Nerve injury instigates resident immune cells such as macrophages and microglia, which release other nociceptive mediators recruiting additional immune cells and mediators that further exacerbate neuropathic pain (Wen et al., 2018).

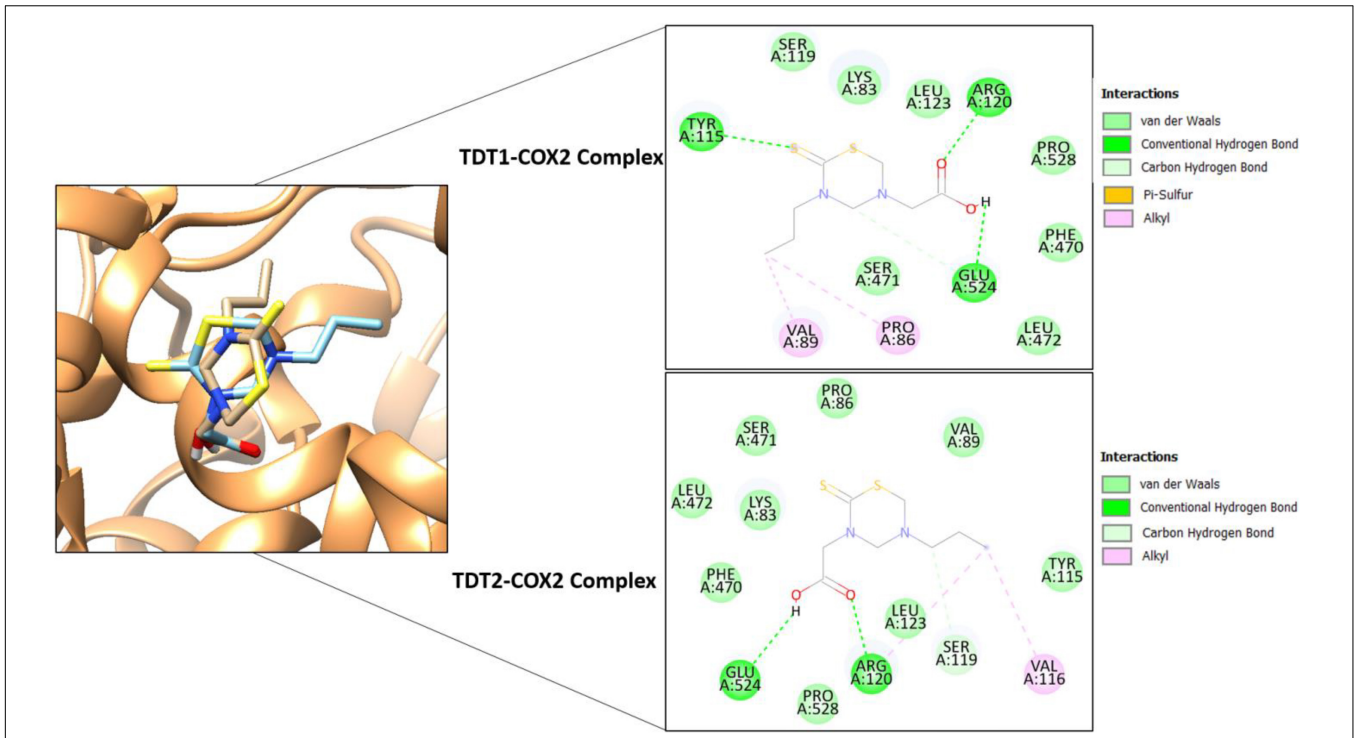

FIGURE 8 | Binding conformation of TDT1 (tan stick) and TDT2 (sky blue stick) in complex with COX-2 receptor (sandy brown cartoon). Different chemical interactions produced by the compounds with the residues of the active pocket.

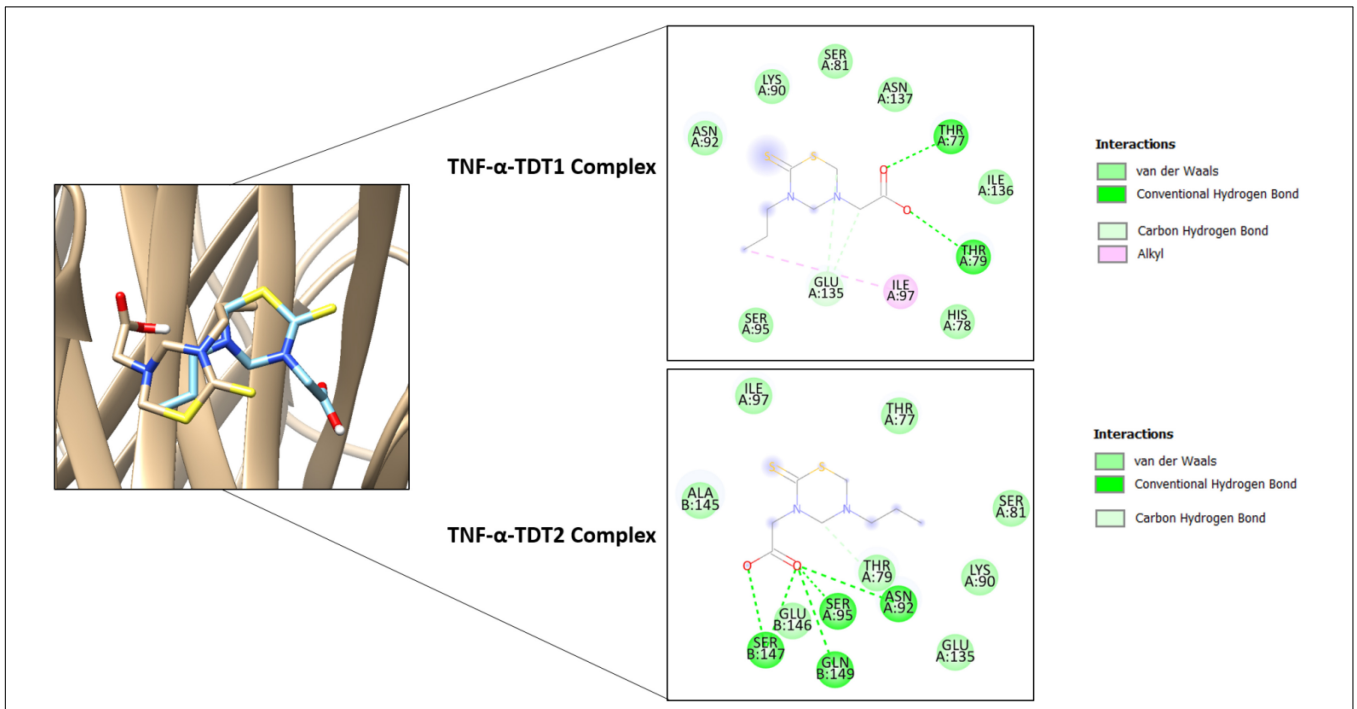

FIGURE 9 | Binding conformation of TDT1 (tan stick) and TDT2 (sky blue stick) in complex with TNF-α (tan cartoon). Different chemical interactions produced by the compounds with the residues of the active side.

Previously, it has been reported that inhibiting glial cells ameliorates allodynia and hyperalgesia in CCI-induced neuropathic pain (Hassel et al., 1992; Tikka and Koistinaho, 2001), in light of this fact we performed a static mechanical allodynia behavioral analysis which disclosed that there was a substantial reduction in nociceptive threshold produced by mechanical Von Frey filament pressure in sciatic nerve ligated left hind paw. Subsequently, a dynamic mechanical allodynia test divulged a notable reduction in the PWL as compared to sham-operated animals when a light stroke of a cotton swab was applied on the mid-plantar foot surface (**Figures 3A,B**). A reduction in PWT was noticeable for succeeding weeks after surgery. However, TDT1 or TDT2 treatment significantly reduced the prolonged PWT in the third and last week of the test protocol as compared to the CCI group. Similarly, an elevated PWD reflex was also observed in the cold allodynia test after CCI sciatic nerve ligation and the administration of TDT1 or TDT2 reduced this prolonged cold allodynia response (**Figure 3C**).

In the heat hyperalgesia test, there was a diminished latency to paw withdrawal in the untreated CCI group compared to the sham-operated controls. Consequently, the nociceptive thermal sensation in the mid-plantar area expressed as the PWL was reduced significantly in the CCI group as compared to the sham group. Hyperalgesia was induced by pinprick in the CCI group versus the sham group while treatment with TDT1or TDT2 reduced this hyperalgesic response to noxious pinprick (**Figures 3D,E**). Subcutaneous injection of carrageenan induces acute inflammation characterized by hyperalgesia, edema plus erythema and the overall response is usually quantified by an increase in the paw size (Morris, 2003; Islam et al., 2017). Both TDT1 and TDT2 reduced carrageenan-induced inflammation as indicated by a reduction in paw volume in the CCI group and this reflected an inherent anti-inflammatory property of these TDT derivatives (**Table 2**).

Microglia, the most common glial cell type in the CNS, play a key role in providing structural and nutrient support and they are also involved in many neural processes. Nerve injury and any noxious stimuli can alter the function and gene expression of reactive gliosis which undergoes morphological, molecular, and functional changes to become reactive microglia in a process termed astrogliosis (Hu et al., 2019; Ji et al., 2019; Li et al., 2019). Mounting evidence proposes that glial cells are vital regulators of CNS diseases including neuro-inflammatory, neurodevelopmental, neuropsychiatric, and neurodegenerative conditions (Wen et al., 2018; Li et al., 2019). In this context, we examined the expression of activated microglia and found that their mRNA expression and the protein level of Iba1 were significantly elevated in CCI animals. Conversely, treatment with TDT1 or TDT2 substantially reversed CCI-induced astrogliosis, activated microglia mRNA expression and the protein level of Iba1 (**Figure 4**). NF-κB, a ubiquitously expressed protein complex, is a key transcription factor that regulates the transcription of several other genes associated with neuroinflammation and chronic pain conditions (Hartung et al., 2015). The mRNA expression level of NF-κB in our study was increased by CCI although at a higher treatment dose, TDT1 or TDT2 both reduced this level of mRNA expression. Phosphorylated-NF-κB (p-NF-κB) using western blot and immunohistochemical analysis suggested that the p-NF-κB protein level was substantially elevated by CCI while TDT1 or TDT2 markedly decreased it (**Figure 5**).

TNF-α is certainly a crucial participant in neuropathic pain as part of the cytokine mediator system which contributes to the pathogenesis of pain either at the peripheral or central level (Leung and Cahill, 2010; Wen et al., 2018). Several lines of study have reported that expressing TNF-α in animal model exacerbates allodynia and hyperalgesia. In addition, intrathecal injection of TNF-α treated astrocytes induces intense allodynia suggesting that the adoptive transfer to reactive astrocytes is sufficient to evoke neuropathic pain (Ji et al., 2019; Li et al., 2019). In our study, evaluation of TNF-α mRNA expression using RT-qPCR revealed an increased expression in the CCI

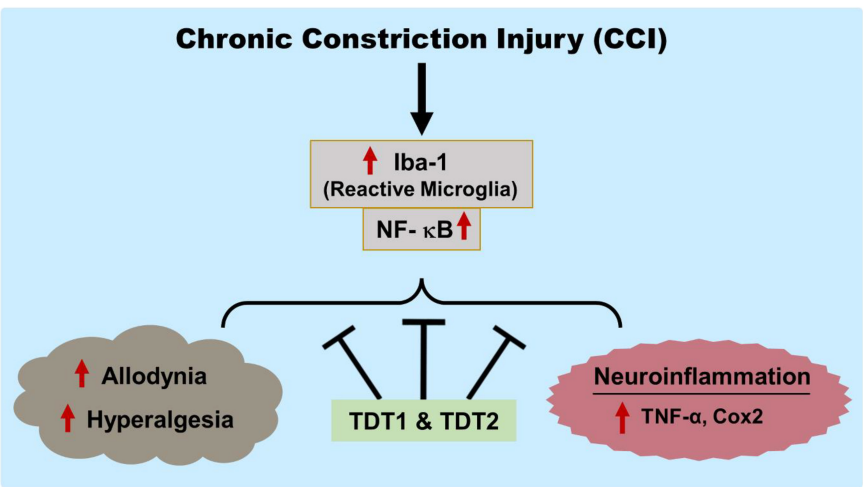

FIGURE 10 | Graphical representation of the study showing the protective effects of TDT1 and TDT2 on CCI-induced allodynia, hyperalgesia and neuroinflammation.

animals while TDT1 and TDT2 both reduced this expression. Elisa assay and western blot analysis also accorded with the above result where by an augmented TNF-α protein level in the CCI group was disclosed, which was then attenuated by TDT1 and TDT2. Likewise, the confocal immunofluorescence and immunohistochemistry experiments confirmed the ameliorative effects of the TDT derivatives against TNF-α (**Figure 6**).

Hence, TNF-α immunoreactivity was high after CCI and both TDT1 and TDT2 markedly reduced anti-TNF-α antibody reactivity. Furthermore, the level of the COX-2 protein has been reported to be elevated after nerve injury, which indicates a contributing role in neuroinflammation and pain. In light of this, inhibition of COX-2 rather than COX-1 using specific enzyme inhibitors has previously been shown to mitigate hyperalgesia in the CCI neuropathic pain model (Jean et al., 2009; Wang and Wang, 2017). Similarly, the protein level and immunoreactivity were also higher after CCI. Furthermore, we performed H and E staining to evaluate the effects of TDT1 and TDT2 on neuronal morphology. It was evident that CCI brought about distinctive morphological changes such as cytoplasmic and nuclear condensation, nuclear budding, and fragmentation in spinal cord tissue (**Figure 7**) which were noticeably slowed down by TDT1 and TDT2. These findings suggest that TDT derivatives exerted substantial anti-inflammatory effects by downregulating Iba1 p-NF-κB, TNF-α, and COX-2 inflammatory markers. Lastly, molecular docking studies were performed to demonstrate the effective binding of TDT1 and TDT2 to COX-2 and TNF-α receptors. The effectual binding of the compounds to the targeted proteins was the outcome of a balanced network of hydrogen bonds and various van der Waals interactions.

Overall, our findings have marked the prospective analgesic activity of the TDT1 and TDT2 test compounds. These compounds exerted protective effects against CCI-induced static and dynamic allodynia as well as hyperalgesia. TDT1 and TDT2 both reduced the expression and protein level of activated microglia (Iba1), p-NF-κB, TNF-α, and COX-2 that were elevated by CCI suggesting a significant anti-inflammatory effect. Furthermore, the TDT test compounds attenuated the histopathological changes associated with nerve injury (**Figure 10**). Additionally, molecular coupling studies were performed that concluded that there was an effective binding of the compounds to COX-2 and TNF-α and that this binding was dominated by strong hydrogen bonds supported by van der Waals interactions.

CONCLUSION

Our findings imply that there may be a potential application of these compounds against inflammation and pain associated with nerve injuries. We aim to conduct further studies in the future to investigate the mechanism of action and any related side effects of these TDT derivatives.

DATA AVAILABILITY STATEMENT

The raw data supporting the conclusions of this article will be made available by the authors, without undue reservation.

ETHICS STATEMENT

The animal study was reviewed and approved by Ethical Committee of the Department of Pharmacy, University of Peshawar (registration number: 19/EC/F.LIFE-2020).

AUTHOR CONTRIBUTIONS

SQ designed and conducted experiments, analyzed the results, and wrote the preliminary manuscript. MI helped in conducting experiments and reviewed and edited the manuscript. TM helped with the study design, experimental analysis, and final manuscript drafting. MS synthesized the test compounds (TDT1 and TDT2), their characterization and analysis. GA, MA, and I-KK helped with study design, supervised and organized, reviewed, and edited the final draft of manuscript. SA performed molecular docking of test compounds. RS and SU had an intellectual input throughout and reviewing and editing the final manuscript draft. All authors reviewed and approved the manuscript.

FUNDING

This study was partially supported by the National Research Foundation of Korea (NRF; MSIT; Grant No. 2020R1A2C2006614) a grant funded by the Korean government, and Korea Institute of Planning, a scholarship from the BK21 Four Program, Ministry of Education, South Korea.

ACKNOWLEDGMENTS

We are thankful to Farah Deeba, Shagufta, Rahim Ullah, and Komal Naeem for their support and help during behavioral and other experimental analysis.

REFERENCES

Abbas, M., Subhan, F., Mohani, N., Rauf, K., Ali, G., and Khan, M. (2011). The involvement of opioidergic mechanisms in the activity of *Bacopa monnieri* extract and its toxicological studies. *Afr. J. Pharm. Pharmacol.* 5, 1120–1124.

Ahmad, A., Varshney, H., Rauf, A., Sherwani, A., and Owais, M. (2017). Synthesis and anticancer activity of long chain substituted 1, 3, 4-oxadiazol-2-thione, 1, 2, 4-triazol-3-thione and 1, 2, 4-triazolo [3, 4-b]-1, 3, 4-thiadiazine derivatives. *Arab. J. Chem.* 10, S3347–S3357.

Ahmad, S. I., Ali, G., Muhammad, T., Ullah, R., Umar, M. N., and Hashmi, A. N. (2020). Synthetic beta-hydroxy ketone derivative inhibits cholinesterases,

rescues oxidative stress and ameliorates cognitive deficits in 5XFAD mice model of AD. *Mol. Biol. Rep.* 47, 9553–9566. doi: 10.1007/s11033-020-05997-0

Akbar, S., Subhan, F., Karim, N., Shahid, M., Ahmad, N., Ali, G., et al. (2016). 6-Methoxyflavanone attenuates mechanical allodynia and vulvodynia in the streptozotocin-induced diabetic neuropathic pain. *Biomed. Pharmacother.* 84, 962–971. doi: 10.1016/j.biopha.2016.10.017

Alles, S. R., and Smith, P. A. (2018). Etiology and pharmacology of neuropathic pain. *Pharmacol. Rev.* 70, 315–347.

Arshad, N., Hashim, J., Minhas, M. A., Aslam, J., Ashraf, T., Hamid, S. Z., et al. (2018). New series of 3, 5-disubstituted tetrahydro-2H-1, 3, 5-thiadiazine thione (THTT) derivatives: synthesis and potent antileishmanial activity. *Bioorgan. Med. Chem. Lett.* 28, 3251–3254. doi: 10.1016/j.bmcl.2018.07.045

Austin, P. J., Wu, A., and Moalem-Taylor, G. (2012). Chronic constriction of the sciatic nerve and pain hypersensitivity testing in rats. *J. Vis. Exp.* 61:e3393. doi: 10.3791/3393

Avuloğlu-Yılmaz, E., Yüzbaşıoğlu, D., Özçelik, A. B., Ersan, S., and Ünal, F. (2017). Evaluation of genotoxic effects of 3-methyl-5-(4-carboxycyclohexylmethyl)-tetrahydro-2H-1, 3, 5-thiadiazine-2-thione on human peripheral lymphocytes. *Pharm. Biol.* 55, 1228–1233. doi: 10.1080/13880209.2017.1296000

Bannon, A. W., and Malmberg, A. B. (2007). Models of nociception: hot-plate, tail-flick, and formalin tests in rodents. *Curr. Protoc. Neurosci.* 41, 8.9.1–8.9.16.

Bennett, G. J., and Xie, Y.-K. (1988). A peripheral mononeuropathy in rat that produces disorders of pain sensation like those seen in man. *Pain* 33, 87–107.

Bresnihan, B., Alvaro-Gracia, J. M., Cobby, M., Doherty, M., Domljan, Z., Emery, P., et al. (1998). Treatment of rheumatoid arthritis with recombinant human interleukin-1 receptor antagonist. *Arthritis Rheum.* 41, 2196–2204.

Decosterd, I., and Woolf, C. J. (2000). Spared nerve injury: an animal model of persistent peripheral neuropathic pain. *Pain* 87, 149–158.

Descalzi, G., Ikegami, D., Ushijima, T., Nestler, E. J., Zachariou, V., and Narita, M. (2015). Epigenetic mechanisms of chronic pain. *Trends Neurosci.* 38, 237–246.

Erichsen, H. K., and Blackburn-Munro, G. (2002). Pharmacological characterisation of the spared nerve injury model of neuropathic pain. *Pain* 98, 151–61. doi: 10.1016/s0304-3959(02)00039-8

Fehrenbacher, J. C., Vasko, M. R., and Duarte, D. B. (2012). Models of inflammation: carrageenan-or complete freund's adjuvant (CFA)–induced edema and hypersensitivity in the rat. *Curr. Protoc. Pharmacol.* 56, 5.4.1–5.4.4.

Fischer, A. H., Jacobson, K. A., Rose, J., and Zeller, R. (2008). Hematoxylin and eosin staining of tissue and cell sections. *Cold Spring Harb. Protoc.* 2008:pdb.rot4986.

Freynhagen, R., Parada, H. A., Calderon-Ospina, C. A., Chen, J., Rakhmawati Emril, D., Fernández-Villacorta, F. J., et al. (2019). Current understanding of the mixed pain concept: a brief narrative review. *Curr. Med. Res. Opin.* 35, 1011–1018. doi: 10.1080/03007995.2018.1552042

Fu, L., Guan, J., Zhang, Y., Ma, P., Zhuang, Y., Bai, J., et al. (2018). Tulobuterol patch alleviates allergic asthmic inflammation by blockade of Syk and NF-kappaB activation in mice. *Oncotarget* 9, 12154–12163. doi: 10.18632/oncotarget.24348

Gabay, E., and Tal, M. (2004). Pain behavior and nerve electrophysiology in the CCI model of neuropathic pain. *Pain* 110, 354–360. doi: 10.1016/j.pain.2004.04.021

Gu, H., and Pan, B. (2015). A four-dimensional neuronal model to describe the complex nonlinear dynamics observed in the firing patterns of a sciatic nerve chronic constriction injury model. *Nonlinear Dyn.* 81, 2107–2126.

Hartung, J. E., Eskew, O., Wong, T., Tchivileva, I. E., Oladosu, F. A., O'Buckley, S. C., et al. (2015). Nuclear factor-kappa B regulates pain and COMT expression in a rodent model of inflammation. *Brain Behav. Immun.* 50, 196–202. doi: 10.1016/j.bbi.2015.07.014

Hassel, B., Paulsen, R. E., Johnsen, A., and Fonnum, F. (1992). Selective inhibition of glial cell metabolism in vivo by fluorocitrate. *Brain Res.* 576, 120–124. doi: 10.1016/0006-8993(92)90616-h

Hu, J.-Z., Rong, Z.-J., Li, M., Li, P., Jiang, L.-Y., Luo, Z.-X., et al. (2019). Silencing of lncRNA PKIA-AS1 attenuates spinal nerve ligation-induced neuropathic pain through epigenetic downregulation of CDK6 expression. *Front. Cell. Neurosci.* 13:50. doi: 10.3389/fncel.2019.00050

Huang, C. P., Lin, Y. W., Lee, D. Y., and Hsieh, C. L. (2019). Electroacupuncture relieves CCI-induced neuropathic pain involving excitatory and inhibitory neurotransmitters. *Evid. Based Complement. Alternat. Med.* 2019:6784735. doi: 10.1155/2019/6784735

Huey, R., Morris, G. M., and Forli, S. (2012). *Using AutoDock 4 and AutoDock Vina with AutoDockTools: A Tutorial*. La Jolla, CA: The Scripps Research Institute, Molecular Graphics Laboratory.

Idrees, M., Kumar, V., Joo, M.-D., Ali, N., Lee, K.-W., and Kong, I.-K. (2020). SHP2 nuclear/cytoplasmic trafficking in granulosa cells is essential for oocyte meiotic resumption and maturation. *Front. Cell Dev. Biol.* 8:611503. doi: 10.3389/fcell.2020.611503

Ikram, M., Muhammad, T., Rehman, S. U., Khan, A., Jo, M. G., Ali, T., et al. (2019). Hesperetin confers neuroprotection by regulating Nrf2/TLR4/NF-kappaB signaling in an Abeta mouse model. *Mol. Neurobiol.* 56, 6293–6309. doi: 10.1007/s12035-019-1512-7

Islam, N. U., Amin, R., Shahid, M., Amin, M., Zaib, S., and Iqbal, J. (2017). A multi-target therapeutic potential of *Prunus domestica* gum stabilized nanoparticles exhibited prospective anticancer, antibacterial, urease-inhibition, anti-inflammatory and analgesic properties. *BMC Complement. Altern. Med.* 17:276. doi: 10.1186/s12906-017-1791-3

Jean, Y. H., Chen, W. F., Sung, C. S., Duh, C. Y., Huang, S. Y., Lin, C. S., et al. (2009). Capnellene, a natural marine compound derived from soft coral, attenuates chronic constriction injury-induced neuropathic pain in rats. *Br. J. Pharmacol.* 158, 713–725. doi: 10.1111/j.1476-5381.2009.00323.x

Jensen, T. S., Baron, R., Haanpää, M., Kalso, E., Loeser, J. D., Rice, A. S., et al. (2011). A new definition of neuropathic pain. *Pain* 152, 2204–2205.

Jensen, T. S., and Finnerup, N. B. (2014). Allodynia and hyperalgesia in neuropathic pain: clinical manifestations and mechanisms. *Lancet Neurol.* 13, 924–935.

Ji, R. R., Donnelly, C. R., and Nedergaard, M. (2019). Astrocytes in chronic pain and itch. *Nat. Rev. Neurosci.* 20, 667–685. doi: 10.1038/s41583-019-0218-1

Jia, Z., Nallasamy, P., Liu, D., Shah, H., Li, J. Z., Chitrakar, R., et al. (2015). Luteolin protects against vascular inflammation in mice and TNF-alpha-induced monocyte adhesion to endothelial cells via suppressing IKBα/NF-κB signaling pathway. *J. Nutr. Biochem.* 26, 293–302. doi: 10.1016/j.jnutbio.2014.11.008

Johnson, S., Ayling, H., Sharma, M., and Goebel, A. (2015). External noninvasive peripheral nerve stimulation treatment of neuropathic pain: a prospective audit. *Neuromodulation* 18, 384–391. doi: 10.1111/ner.12244

Jung, Y., Lee, J. H., Kim, W., Yoon, S. H., and Kim, S. K. (2017). Anti-allodynic effect of Buja in a rat model of oxaliplatin-induced peripheral neuropathy via spinal astrocytes and pro-inflammatory cytokines suppression. *BMC Complement. Altern. Med.* 17:48. doi: 10.1186/s12906-017-1556-z

Kamil, M., Fatima, A., Ullah, S., Ali, G., Khan, R., Ismail, N., et al. (2021). Toxicological evaluation of novel cyclohexenone derivative in an animal model through histopathological and biochemical techniques. *Toxics* 9:119.

Kapural, L., Yu, C., Doust, M., Diabetes, C. N., Schmader, K., Pop-Busui, R., et al. (2018). Pharmacotherapy for neuropathic pain in adults: a systematic review and meta-analysis. *Postgrad. Med.* 130(Suppl. 1), 1–91.

Khan, J., Ali, G., Khan, R., Ullah, R., and Ullah, S. (2019). Attenuation of vincristine-induced neuropathy by synthetic cyclohexenone-functionalized derivative in mice model. *Neurol. Sci.* 40, 1799–1811. doi: 10.1007/s10072-019-03884-6

Kheir, M. M., Wang, Y., Hua, L., Hu, J., Li, L., Lei, F., et al. (2010). Acute toxicity of berberine and its correlation with the blood concentration in mice. *Food Chem. Toxicol.* 48, 1105–1110. doi: 10.1016/j.fct.2010.01.033

Kukkar, A., Singh, N., and Jaggi, A. S. (2013). Neuropathic pain-attenuating potential of aliskiren in chronic constriction injury model in rats. *J. Renin Angiotensin Aldosterone Syst.* 14, 116–123. doi: 10.1177/1470320312460899

La, J.-H., and Chung, J. M. (2017). Peripheral afferents and spinal inhibitory system in dynamic and static mechanical allodynia. *Pain* 158, 2285–2289. doi: 10.1097/j.pain.0000000000001055

Leung, L., and Cahill, C. M. (2010). TNF-alpha and neuropathic pain–a review. *J. Neuroinflammation* 7:27. doi: 10.1186/1742-2094-7-27

Li, T., Chen, X., Zhang, C., Zhang, Y., and Yao, W. (2019). An update on reactive astrocytes in chronic pain. *J. Neuroinflammation* 16:140. doi: 10.1186/s12974-019-1524-2

Ma, W., Chabot, J. G., Vercauteren, F., and Quirion, R. (2010). Injured nerve-derived COX2/PGE2 contributes to the maintenance of neuropathic pain in aged rats. *Neurobiol. Aging* 31, 1227–1237. doi: 10.1016/j.neurobiolaging.2008.08.002

Medeiros, P., de Freitas, R. L., Boccella, S., Iannotta, M., Belardo, C., Mazzitelli, M., et al. (2020). Characterization of the sensory, affective, cognitive, biochemical, and neuronal alterations in a modified chronic constriction injury model of neuropathic pain in mice. *J. Neurosci. Res.* 98, 338–352. doi: 10.1002/jnr.24501

Milne, G. W. (2010). Software review of ChemBioDraw 12.0. *J. Chem. Inf. Model.* 50:2053.

Morris, C. J. (2003). Carrageenan-induced paw edema in the rat and mouse. *Inflamm. Protoc.* 225, 115–121.

Morris, G. M., Huey, R., Lindstrom, W., Sanner, M. F., Belew, R. K., Goodsell, D. S., et al. (2009). AutoDock4 and AutoDockTools4: automated docking with selective receptor flexibility. *J. Comput. Chem.* 30, 2785–2791. doi: 10.1002/jcc.21256

Muhammad, T., Ikram, M., Ullah, R., Rehman, S. U., and Kim, M. O. (2019). Hesperetin, a citrus flavonoid, attenuates LPS-induced neuroinflammation, apoptosis and memory impairments by modulating TLR4/NF-kappaB signaling. *Nutrients* 11:648. doi: 10.3390/nu11030648

Murphy, P., Ramer, M., Borthwick, L., Gauldie, J., Richardson, P., and Bisby, M. (1999). Endogenous interleukin-6 contributes to hypersensitivity to cutaneous stimuli and changes in neuropeptides associated with chronic nerve constriction in mice. *Eur. J. Neurosci.* 11, 2243–2253. doi: 10.1046/j.1460-9568.1999.00641.x

Muthuraman, A., and Singh, N. (2012). Neuroprotective effect of saponin rich extract of *Acorus calamus* L. in rat model of chronic constriction injury (CCI) of sciatic nerve-induced neuropathic pain. *J. Ethnopharmacol.* 142, 723–731. doi: 10.1016/j.jep.2012.05.049

Nakazato-Imasato, E., Tanimoto-Mori, S., and Kurebayashi, Y. (2009). Effect of mexiletine on dynamic allodynia induced by chronic constriction injury of the sciatic nerve in rats. *J. Vet. Med. Sci.* 71, 991–994.

Ozçelik, A. B., Ersan, S., Ural, A. U., Ozkan, S., and Ertan, M. (2007). Synthesis of 3-substituted-5-(4-carb oxycyclohexylmethyl)-tetrahydro-2H-1, 3, 5-thiadiazine-2-thione derivatives as antifibrinolytic and antimicrobial agents. *Arzneimittelforschung* 57, 554–559. doi: 10.1055/s-0031-1296648

Pettersen, E. F., Goddard, T. D., Huang, C. C., Couch, G. S., Greenblatt, D. M., Meng, E. C., et al. (2004). UCSF Chimera—a visualization system for exploratory research and analysis. *J. Comput. Chem.* 25, 1605–1612. doi: 10.1002/jcc.20084

Pusan, S., and Abdi, S. (2018). Treatment of chemotherapy-induced peripheral neuropathy: systematic review and recommendations. *Pain Phys.* 21, 571–592.

Scholz, J., Finnerup, N. B., Attal, N., Aziz, Q., Baron, R., Bennett, M. I., et al. (2019). The IASP classification of chronic pain for ICD-11: chronic neuropathic pain. *Pain* 160, 53–59.

Sever, B., Altıntop, M. D., Kuş, G., Özkurt, M., Özdemir, A., and Kaplancıklı, Z. A. (2016). Indomethacin based new triazolothiadiazine derivatives: synthesis, evaluation of their anticancer effects on T98 human glioma cell line related to COX-2 inhibition and docking studies. *Eur. J. Med. Chem.* 113, 179–186. doi: 10.1016/j.ejmech.2016.02.036

Shah, F. A., Li, T., Kury, L. T. A., Zeb, A., Khatoon, S., Liu, G., et al. (2019). Pathological comparisons of the hippocampal changes in the transient and permanent middle cerebral artery occlusion rat models. *Front. Neurol.* 10:1178. doi: 10.3389/fneur.2019.01178

Shah, M. I. A., Khan, R., Arfan, M., Wadood, A., and Ghufran, M. (2019). Synthesis, in vitro urease inhibitory activity and molecular docking of 3, 5-disubstituted thiadiazine-2-thiones. *J. Heterocycl. Chem.* 56, 3073–3080.

Shahid, M., Subhan, F., Ahmad, N., and Sewell, R. D. (2017). The flavonoid 6-methoxyflavone allays cisplatin-induced neuropathic allodynia and hypoalgesia. *Biomed. Pharmacother.* 95, 1725–1733. doi: 10.1016/j.biopha.2017.09.108

St John Smith, E. (2018). Advances in understanding nociception and neuropathic pain. *J. Neurol.* 265, 231–238. doi: 10.1007/s00415-017-8641-6

Studio, D. J A. (2008). *Discovery Studio.* Waltham, MA: Dassault Systemes.

Su, L., Shu, R., Song, C., Yu, Y., Wang, G., Li, Y., et al. (2017). Downregulations of TRPM8 expression and membrane trafficking in dorsal root ganglion mediate the attenuation of cold hyperalgesia in CCI rats induced by GFRα3 knockdown. *Brain Res. Bull.* 135, 8–24. doi: 10.1016/j.brainresbull.2017.08.002

Suter, M. R., Wen, Y. R., Decosterd, I., and Ji, R. R. (2007). Do glial cells control pain? *Neuron Glia Biol.* 3, 255–268. doi: 10.1017/S1740925X08000100

Tikka, T. M., and Koistinaho, J. E. (2001). Minocycline provides neuroprotection against N-methyl-D-aspartate neurotoxicity by inhibiting microglia. *J. Immunol.* 166, 7527–7533. doi: 10.4049/jimmunol.166.12.7527

Wang, C., and Wang, C. (2017). Anti-nociceptive and anti-inflammatory actions of sulforaphane in chronic constriction injury-induced neuropathic pain mice. *Inflammopharmacology* 25, 99–106. doi: 10.1007/s10787-016-0307-y

Wang, X., Fu, X., Yan, J., Wang, A., Wang, M., Chen, M., et al. (2019). Design and synthesis of novel 2-(6-thioxo-1, 3, 5-thiadiazinan-3-yl)-N′-phenylacethydrazide derivatives as potential fungicides. *Mol. Divers.* 23, 573–583.

Wen, J., Jones, M., Tanaka, M., Selvaraj, P., Symes, A. J., Cox, B., et al. (2018). WWL70 protects against chronic constriction injury-induced neuropathic pain in mice by cannabinoid receptor-independent mechanisms. *J. Neuroinflammation* 15:9. doi: 10.1186/s12974-017-1045-9

Woolf, C., Allchorne, A., Safieh-Garabedian, B., and Poole, S. (1997). Cytokines, nerve growth factor and inflammatory hyperalgesia: the contribution of tumour necrosis factor α. *Br. J. Pharmacol.* 121, 417–424. doi: 10.1038/sj.bjp.0701148

Wu, S., Bono, J., and Tao, Y.-X. (2019). Long noncoding RNA (lncRNA): a target in neuropathic pain. *Exp. Opin. Ther. Targets* 23, 15–20.

Xu, B., Descalzi, G., Ye, H.-R., Zhuo, M., and Wang, Y.-W. (2012). Translational investigation and treatment of neuropathic pain. *Mol. Pain* 8:15.

Zadeh-Ardabili, P. M., and Rad, S. K. (2019). Anti-pain and anti-inflammation like effects of Neptune krill oil and fish oil against carrageenan induced inflammation in mice models: current statues and pilot study. *Biotechnol. Rep.* 22:e00341.

Conflict of Interest: I-KK was employed by The Kingkong Co., Ltd.

The remaining authors declare that the research was conducted in the absence of any commercial or financial relationships that could be construed as a potential conflict of interest.

Publisher's Note: All claims expressed in this article are solely those of the authors and do not necessarily represent those of their affiliated organizations, or those of the publisher, the editors and the reviewers. Any product that may be evaluated in this article, or claim that may be made by its manufacturer, is not guaranteed or endorsed by the publisher.

Advantages of publishing in Frontiers

OPEN ACCESS
Articles are free to read for greatest visibility and readership

FAST PUBLICATION
Around 90 days from submission to decision

HIGH QUALITY PEER-REVIEW
Rigorous, collaborative, and constructive peer-review

TRANSPARENT PEER-REVIEW
Editors and reviewers acknowledged by name on published articles

Frontiers
Avenue du Tribunal-Fédéral 34
1005 Lausanne | Switzerland

Visit us: www.frontiersin.org
Contact us: frontiersin.org/about/contact

REPRODUCIBILITY OF RESEARCH
Support open data and methods to enhance research reproducibility

DIGITAL PUBLISHING
Articles designed for optimal readership across devices

FOLLOW US
@frontiersin

IMPACT METRICS
Advanced article metrics track visibility across digital media

EXTENSIVE PROMOTION
Marketing and promotion of impactful research

LOOP RESEARCH NETWORK
Our network increases your article's readership